70 GODINA ANU BiH АНУ БиХ

50 GODINA 2021

Acta Medica Academica

Journal of Department of Medical Sciences
of Academy of Sciences and Arts of Bosnia and Herzegovina

Special Issue: Diagnostic and Molecular Pathology Advances

ISSN 1840-1848 (Print) Volume 50 ▪ Number 1 ▪ April 2021 ISSN 1840-2879 (Online)

Online First www.ama.ba

Acta Medica Academica

Contents
2021 Vol. 50, No. 1

Acta Medica Academica

www.ama.ba

AIMS AND SCOPE

Acta Medica Academica is a triannual, peer-reviewed journal that publishes: (1) reports of original research, (2) original clinical observations accompanied by analysis and discussion, (3) analysis of philosophical, ethical, or social aspects of the health profession or biomedical sciences, (4) critical reviews, (5) statistical compilations, (6) descriptions of evaluation of methods or procedures, (7) case reports, and (8) images in clinical medicine. The fields covered include basic biomedical research, clinical and laboratory medicine, veterinary medicine, clinical research, epidemiology, phramacology, public health, oral health, and medical information.

EDITORIAL CONTACT INFORMATION

Address of the Editorial Board: *Acta Medica Academica*, Academy of Sciences and Arts of Bosnia and Herzegovina, Bistrik 7, 71000 Sarajevo, Bosnia and Herzegovina, Tel.: 00 387 33 560 718, Fax.: 00 387 33 560 703. Contact person: Nerma Tanović, E-mail: amabih@anubih.ba

SUBSCRIPTION

Acta Medica Academica is published triannually. The annual subscription fee is € 50 outside of Bosnia and Herzegovina.

PUBLISHER CONTACT INFORMATION

Academy of Sciences and Arts of Bosnia and Herzegovina, Sarajevo, Bosnia and Herzegovina. Contact person: Husref Tahirović, E-mail: husref.tahirovic@untz.ba

COVER PHOTO PICTURE

Kornelija Rakić (1879–1952), Austro-Hungarian official female doctor in Bosnia and Herzegovina. With permission of the Historical Archives of the City of Novi Sad.

AUTHOR INFORMATION

Instructions to authors can be found at http://www.ama.ba/forms/AMA-2019-instrukcija.pdf. Home page of the Journal www.ama.ba offers free access to all articles.

EDITORIAL ASSISTANT

Nerma Tanović, Sarajevo, BA.

TECHNICAL EDITOR

Husref Tahirović, Tuzla, BA.

DTP

Narcis Pozderac, Sarajevo, BA.

PRINT

Dobra knjiga, Sarajevo, BA. Printed on acid-free paper.

CIRCULATION

500 copies.

THE JOURNAL IS INDEXED IN

Medline/PubMed; Scopus; Embase; EBSCOhost; Index Copernicus; CAB Abstract/Global Health Databases; IndexScholar.com; DOAJ; CrossRef; InfoBase Index.

Acta Medica Academica (ISSN 1840-1848) is an international peer-reviewed triannual journal which is printed as a continuation of the journal Works of the Academy of Sciences and Arts of Bosnia and Herzegovina, Department of Medical Sciences, founded in 1953. *Acta Medica Academica* Online (ISSN 1840-2879) offers free access to all articles at www.ama.ba.

Editorial
Acta Medica Academica 2021;50(1):1-3
DOI: 10.5644/ama2006-124.321

Advances in Diagnostic and Molecular Pathology

Semir Vranić[1, 2], Ivan Damjanov[3]

[1]College of Medicine, QU Health, Qatar University, Doha, Qatar, [2]Biomedical and Pharmaceutical Research Unit, QU Health, Qatar University, Doha, Qatar, [3]The University of Kansas School of Medicine, Kansas City, Kanas, United States

Correspondence: *semir.vranic@gmail.com* or *svranic@qu.edu.qa* and *idamjano@kumc.edu*; Tel.: + 974 4403 7873; Fax.: + 974 4403 2250

Received: 19 March 2021; **Accepted:** 20 March 2021

Key Words: Pathology ▪ Diagnostics ▪ Molecular Pathology.

Early studies of pathogenesis and classification of human diseases in the late 19th and the first half of the 20th century were primarily based on microscopic examination of hematoxylin and eosin-stained light microscopy slides and autopsy studies. The introduction of immunohistochemistry in the mid-70 enabled further identification and more precise classification of human diseases, particularly cancer diagnostics (1). In the past three decades, advances in molecular biology, genetics, and genomics have dramatically changed the practice of diagnostic pathology worldwide (2). As never before, pathologists are at the crossroads between the traditionally 'visible' morphologic approach and an 'invisible' molecular science.

Given that molecular diagnostics has become widely utilized in histopathologic diagnosis and clinical decision-making, the policymakers had to reframe the process of accreditation and re-accreditation of the modern pathologists in context to the rapid changes taking place in this diagnostic discipline. This has already been the case in most developed countries, while in the developing world, this integration has yet to be fully implemented. In particular, the concept of "precision medicine" (including pathology) is rapidly evolving and becoming a cornerstone of modern cancer management (reviewed here by Vranic and Gatalica and nicely illustrated by a comprehensive case study of Trivedi et al.) (2, 3). Equally important in the digital era are pathology informatics, as nicely reviewed in the paper of Kim et al. (4). Their experience with pathology informatics training and education during the challenging COVID-19 pandemic at the Memorial Sloan Kettering Cancer Center is a good example of how informatics can be useful in solving current worldwide health problems (4).

This special issue of *Acta Medica Academica* highlights the advances in the understanding, diagnostics, and classification of various human cancers. You will note that the authors, all experts in their respective fields, approached their papers on various cancers in different ways. However, all the papers will clearly reflect the authors' strong appreciation for the progress made in the recent decades in diagnostic and molecular pathology. This progress has undoubtedly laid a firm foundation for the future of diagnostic and molecular pathology.

In each of the following reviews (N=12), original, case studies, and images in clinical medicine (N=4), the authors provide recent advances and perspectives that are only achieved by their active involvement in the forwarding paths of progress in diagnostic and molecular pathology. Each of the accepted manuscripts was selected based on their

professional and academic standing and contributions to diagnostic and molecular pathology.

We are happy for contributions from different countries (United States, United Kingdom, Croatia, Slovenia, Serbia, Qatar), including Bosnia and Herzegovina. All of the reviews contain in-depth and up to date information on testicular cancer (5), prostate cancer (6), endocervical adenocarcinoma (7), bladder cancer (8), pleural mesothelioma (9), adult brain tumors (10), and Spitz melanocytic lesions (11). In her review, Dr. Provenzano discussed the most recent advances and challenges in the assessment of breast cancer specimens following neoadjuvant chemotherapy (12). Two hematopathology reviews summarized the advances in this rapidly evolving branch of pathology (13, 14); the first by Perry et al. summed up the critical aspects of diagnosis of the classical Hodgkin lymphoma (13), and the second one by Kurtović-Kozarić et al. explored the recent advances and challenges in the diagnosis of myeloid neoplasms. It is worth noticing that the latter paper's emphasis is on the improved hematopathology diagnostics in Bosnia and Herzegovina, showing that the advances in pathology have no borders (14). The study of Gargano et al. confirmed the clinical utility of ancillary molecular assays in cytologically indeterminate thyroid nodules (15), while Tomita comparatively analyzed the distribution of blood and lymphatic vessels in normal human vs. rhesus monkey samples (using immunohistochemistry on formalin-fixed and frozen section specimens) (16). Two studies (Trivedi et al.) (3) and Ibisevic et al. (17) illustrated the importance of the multidisciplinary approach and the role of (molecular) tumor boards in cancer management.

As the guest editors of this special issue of *Acta Medica Academica*, we would like to thank all the contributors for entrusting their work to this journal. These days, in the midst of the COVID-19 epidemic, we are very proud that we managed to collate AMA's special issue that contains scientific contributions from many parts of the world. Like the former present of US Franklin Roosevelt in his last address to the nation, we would like to quote Thomas Jefferson from more than 200 years ago: "The brotherly spirit of science unites into one family all its votaries of whatever grade, and however, widely dispersed throughout the different quarters of the globe." To this quote, Roosevelt added "If civilization is to survive, we must cultivate the science of human relationships" (18) overcoming national, ethnic, and political differences to forge a better world.

At the end, we would like to express our deepest gratitude to all of the reviewers and the editorial staff of AMA, particularly to Mrs. Nerma Tanović. They have altruistically taken so much of their time to improve others' work and served as guardians of the medical literature. Our thanks also to Professor and Academician Husref Tahirović, who invited us to edit this special issue of AMA. We salute you all!

We hope that the readers of *Acta Medica Academica* will enjoy reading these articles as much as we have!

Conflict of Interest: The authors declare that they have no conflict of interest.

References

1. Gatalica Z, Feldman R, Vranić S, Spetzler D. Immunohistochemistry-enabled Precision Medicine. Cancer Treat Res. 2019;178:111-35.
2. Vranic S, Gatalica Z. The Role of Pathology in the Era of Personalized (Precision) Medicine: A Brief Review. Acta Med Acad. 2021;50(1):47-57.
3. Trivedi H, Hamdani O, Thomas B, Richard J, Shah K, Raskina K, et al. Patient with Lobular Carcinoma of the Breast and Activating AKT1 E17K Variant. Acta Med Acad. 2021;50(1):209-17.
4. Kim D, Hanna MG, Vanderbilt C, Sirintrapun SJ. Pathology Informatics Education during the COVID-19 Pandemic at Memorial Sloan Kettering Cancer Center (MSKCC). Acta Med Acad. 2021;50(1):136-42.
5. Damjanov I. Testicular Germ Cell Tumors: Serological and Immunohistochemical Diagnosis. Acta Med Acad. 2021;50(1):58-70.
6. Krušlin B, Škara L, Vodopić T, Vrhovec B, Murgić J, Štimac G, et al. Genetics of Prostate Carcinoma. Acta Med Acad. 2021;50(1):71-87.
7. Cimic A, Liu-Jarin X. Updated Review on Pathology of Endocervical Adenocarcinoma with Emphasis on Clinically Relevant Findings. Acta Med Acad. 2021;50(1):126-35.

8. Ulamec M, Murgić J, Novosel L, Tomić M, Terlević R, Tomašković I, et al. New insights into the diagnosis, molecular taxonomy, and treatment of bladder cancer. Acta Med Acad. 2021;50(1):143-56.
9. Savic I, Myers J. Update on diagnosing and reporting malignant pleural mesothelioma. Acta Med Acad. 2021;50(1):197-208.
10. Brandner S. Molecular Diagnostics of Adult Gliomas in Neuropathological Practice. Acta Med Acad. 2021;50(1):29-46.
11. Šekoranja D, Pižem J, Luzar B. An update on molecular genetic aberrations in Spitz melanocytic proliferations: Correlation with morphological features and biological behavior. Acta Med Acad. 2021;50(1):157-74.
12. Provenzano E. Neoadjuvant Chemotherapy for Breast Cancer: Moving Beyond Pathological Complete Response in the Molecular Age. Acta Med Acad. 2021;50(1):88-109.
13. Perry AM, Smith LB, Bagg A. Classic Hodgkin Lymphoma – Old Disease, New Directions: An Update on Pathology, Molecular Features and Biological Prognostic Markers. Acta Med Acad. 2021;50(1):110-25.
14. Kurtovic-Kozaric A, Islamagic E, Asic A, Mehinovic-Cavcic L, Besic L, Sahinbegovic H, et al. A review of molecular and genetic diagnostics of myeloid malignancies with emphasis on diagnostics in Bosnia and Herzegovina. Acta Med Acad. 2021;50(1):175-96.
15. Gargano SM, Badjatia N, Nikolaus Y, Peiper SC, Wang Z-X. Characterization and clinical significance of EIF1AX mutations and co-mutations in cytologically indeterminate thyroid nodules: A 5-year retrospective analysis. Acta Med Acad. 2021;50(1):4-12.
16. Tomita T. Immunohistochemical Staining for Lymphatic and Blood Vessels in Normal Tissues: Comparison between Routinely Paraffin-embedded Tissues and Frozen Sections. Acta Med Acad. 2021;50(1):13-28.
17. Ibisevic N, Bajrovic J, Saranovic E, Spiritovic D, Skenderi F, Vranic S. A Giant, Complex Fibroepithelial Tumor of the Breast: Borderline Phyllodes Tumor Combined with Tubular Adenoma – a Rare Clinical Presentation of a Fibroepithelial Tumor of the Breast. Acta Med Acad. 2021;50(1):218-20.
18. Newsday [homepage on the Internet], [cited 2021 Feb 27]. Available from: https://www.newsday.com/opinion/coronavirus/fdr-speech-coronavirus-pandemic-crisis-management-trump-covid-19-1.43836010.

Original Research Study
Acta Medica Academica 2021;50(1):4-12
DOI: 10.5644/ama2006-124.322

Characterization and Clinical Significance of *EIF1AX* Mutations and Co-Mutations in Cytologically Indeterminate Thyroid Nodules: A 5-Year Retrospective Analysis

Stacey M. Gargano, Nitika Badjatia, Yanina Nikolaus, Stephen C. Peiper, Zi-Xuan Wang

Department of Pathology, Anatomy and Cell Biology, Thomas Jefferson University Hospital, Philadelphia, PA, USA

Correspondence: *Stacey.Gargano@jefferson.edu*; Tel.: + 1 215 955 4404; Fax.: + 1 215 923 1969

Received: 3 February 2021; **Accepted:** 8 April 2021

Abstract

Objective. Mutations in the *EIF1AX* gene have been recently detected in a small percentage of benign and malignant thyroid lesions. We sought to investigate the prevalence and clinical significance of *EIF1AX* mutations and co-mutations in cytologically indeterminate thyroid nodules at our institution. **Materials and Methods.** A 5-year retrospective analysis was performed on thyroid nodules with a cytologic diagnosis of Bethesda category III or IV, which had undergone testing by our in-house next generation sequencing panel. Surgically resected nodules with *EIF1AX* mutations were identified, and mutation type and presence of co-mutations were correlated with histopathologic diagnosis. **Results.** 41/904 (4.5%) cases overall and 26/229 (11.4%) surgically resected nodules harbored an *EIF1AX* mutation. The most common histologic diagnoses were follicular thyroid carcinoma and follicular variant of papillary thyroid carcinoma. 11/26 (42.3%) of nodules had isolated *EIF1AX* mutation. Co-mutations were found in *RAS* (12/26; 46.2%), *TERT* (5/26; 19.2%) and *TP53* (2/26; 7.7%). *EIF1AX* mutation alone conferred a 36.4% risk of malignancy (ROM) and 54.5% ROM or noninvasive follicular thyroid neoplasm with papillary-like nuclear features (NIFTP), while the ROM was significantly higher in nodules with concurrent *RAS* (71.4%), *TERT*, *TP53* and *RAS+TERT* (100%) mutations. **Conclusion.** *EIF1AX* mutations occur in benign and malignant follicular thyroid neoplasms. In our cohort, the majority of mutations occurred at the splice acceptor site between exons 5 and 6. Importantly, the coexistence of *EIF1AX* mutations with other driver pathogenic mutations in *RAS*, *TERT* and *TP53* conferred a 100% ROM or NIFTP, indicating that such nodules require surgical removal.

Key Words: *EIF1AX* ▪ Thyroid Nodule ▪ Cytopathology ▪ Next-Generation Sequencing.

Introduction

Up to 30% of biopsied thyroid nodules are classified as either "atypia of undetermined significance (AUS)/follicular lesion of undetermined significance (FLUS)" or "follicular neoplasm (FN)/suspicious for follicular neoplasm (SFN)", Categories III and IV respectively in The Bethesda System for Reporting Thyroid Cytopathology (TBSRTC) (1). Because these diagnoses are not straightforward benign or malignant, and the reported risks of malignancy are highly variable for these categories, clinicians often struggle with the decision of whether or not to recommend surgical removal of these indeterminate nodules. Molecular analysis, via multi-gene sequencing assays and gene expression classifiers, has emerged as an important supplemental tool for evaluating thyroid nodules (1, 2). At our institution, thyroid fine needle aspiration (FNA) specimens with an indeterminate cytologic diagnosis are routinely tested via an in-house next generation sequencing (NGS) panel, in order to provide clinicians with more information that may help with risk stratification and guide clinical management.

The most commonly known mutated genes associated with thyroid malignancies are *BRAF* and *RAS*. The majority of *BRAF* mutations are found in classical papillary thyroid carcinoma (PTC), while *RAS* mutations are seen in follicular variant of papillary thyroid carcinoma (FVPTC) and

other malignant and benign follicular-patterned thyroid lesions (3). More recently, mutations in the *EIF1AX* (Eukaryotic translation initiation factor 1A, X-chromosomal) gene have been detected in a small percentage of various types of thyroid cancer as well as benign thyroid nodules. The likelihood of malignancy in an *EIF1AX*-mutated thyroid nodule is thought to correlate with the presence or absence of co-existing mutations and with the position of the mutations within *EIF1AX* (4).

We sought to investigate the prevalence and clinical significance of *EIF1AX* mutations and co-mutations by examining histologic outcomes of a large cohort of cytologically indeterminate thyroid nodules that underwent molecular testing and subsequent surgical resection.

Materials and Methods

Case Selection and Histopathologic Correlation

A database search was performed to identify all thyroid nodules with a cytologic diagnosis of Bethesda category III or IV, which had undergone testing by our in-house NGS panel over a 5-year period. Samples with *EIF1AX* mutations were identified, and the electronic medical record was searched to determine which nodules had undergone surgical resection. *EIF1AX* mutation type and presence of co-mutations were correlated with final histopathologic diagnosis.

Molecular Specimen Information

At the time of the FNA procedure, a separate needle pass was collected in a vial containing methanol/acetic acid (3:1 ratio). Of the 987 clinical FNA specimens, 904 (91.6%) passed sample quality control and obtained molecular results.

Molecular Analysis

Mutations in *EIF1AX* were identified by NGS with a custom designed Thyroid cancer panel using Illumina's TruSeq Custom Amplicon version 1.5 reagents as previously described (5) or CTL VariantPlex Assay for Illumina Platform (ArcherDx) following the manufacturer's protocol. Besides *EIF1AX* both TruSeq and Archer panels contained primers to amplify targeted regions of interest covering hotspots from additional thyroid cancer-related genes such as *BRAF, GNAS, HRAS, NRAS, PIK3CA, PTEN, RET, TERTpro, TP53* and *TSHR*. Libraries were sequenced on the Illumina MiSeq or NextSeq 500 instrument with paired end 150-bp sequencing. Data analysis was performed as previously described (5) for all TruSeq libraries. For all libraries prepared using Archer VariantPlex methodology, fastq files were generated using a custom script and data analyses were performed using the CTL target region file and Archer analysis software version 6.2. Annotated variants were filtered and reported using an in-house, Web-based reporting application ClinMutReporter (Thomas Jefferson University Hospitals, Philadelphia, Pennsylvania).

Results

Patients

Among the 904 thyroid FNAs with an indeterminate cytopathologic diagnosis (Bethesda Category III or IV) that were characterized by NGS, 41 cases (4.5%) had mutations in the *EIF1AX* gene. Histopathologic confirmation of the diagnosis was available in a surgical follow up specimen in 26 of the 41 cases (63.4%).

Clinical & Pathologic Features

The clinical and pathologic features of the 26 patients with full diagnostic characterization are shown in Table 1. The mean patient age was 64 (range: 43-81 years) and with a female preponderance (female:male ratio=3.3). The mean size of the nodules was 2.8 cm (range: 1.1-6.3 cm). The cytopathologic diagnosis was Bethesda Category III (AUS/FLUS) in 12 (46.2%) and Bethesda Category IV (SFN/FN) in 14 (53.8%). As shown in Table 1 and Figure 1, the histopathologic analysis on follow up excisions included 6 neoplasms with a benign diagnosis (follicular adenoma (FA)), 3 with

Table 1. Summary of All *EIF1AX*-Mutated Surgically Removed Nodules

Case	Age (y)	Gender	Nodule size (cm)	Cytologic diagnosis (Bethesda category)	Histopath-ologic diagnosis	EIF1AX mutation type	Alternate allele frequency (AAF)	EIF1AX mutation location	EIF1AX mutation significance	Co-existing mutation(s), AAF
1	63	F	1.4	3	FA	c.370_371delinsTT; p.G124L	26.6%	Exon 6	Unknown	KRAS p.A59del, 5.6%
2	56	F	4.1	3	FA	c.338-1_338delinsTT; p.?	3.3%	A113_splice site	Pathogenic	-
3	43	F	1.1	3	FA	c.16G>C; p.G6R	9.7%	N terminus	Pathogenic	-
4	75	M	2.7	4	FA	c.338-2A>C; p.?	7.1%	A113_ splice site	Pathogenic	-
5	66	F	2.5	4	FA	c.44G>A; p.G15D	9.7%	N terminus	Pathogenic	-
6	63	F	2.6	4 (Hurthle cell type)	FA	c.338-2A>T; p.?	14.1%	A113_ splice site	Pathogenic	-
7	76	F	5.2	3	NIFTP	c.338-4_355del; p.?	16.5%	A113_ splice site	Pathogenic	-
8	70	F	1.1	4	NIFTP	c.5C>G; p.P2R	4.6%	N terminus	Pathogenic	-
9	59	F	1.5	4	NIFTP	c.210G>C; p.W70C	40.0%	Exon 4	Likely pathogenic	NRAS p.Q61K, 41.9%
10	51	M	1.8	3	FTC	c.338-1G>C; p.?	19.5%	A113_ splice site	Pathogenic	KRAS p.Q61R, 8.7%
11	54	F	1.5	3	FTC	c.338-1G>C; p.?	35.2%	A113_ splice site	Pathogenic	NRAS p.Q61R, 39.2%; TERT c.-146C>T, 39.7%
12	46	F	2.3	3	FTC	c.3_5dup; p.P2dup	4.2%	N terminus	Likely pathogenic	TERT c.-146C>T, 7.3%
13	69	F	2.2	3	FTC	c.28A>G; p.K10E	31.2%	N terminus	Pathogenic	
14	71	M	5.5	4	FTC	c.338-2A>G; p.?	40.6%	A113_ splice site	Pathogenic	HRAS p.Q61R, 20.3%; TERT c.-124C>T, 11.4%
15	57	F	3	4	FTC	c.338-1G>C; p.?	2.1%	A113_ splice site	Pathogenic	NRAS p.Q61K, 2.4%
16	60	F	6.3	4	FTC	c.338-2A>T; p.?	12.7%	A113_ splice site	Pathogenic	KRAS p.Q61R, 12.8%; TERT c.-124C>T, 15.1%
17	69	F	3	4 (Hurthle cell type)	HCC	c.338-1G>C; p.?	26.6%	A113_ splice site	Pathogenic	-
18	81	M	3.7	4 (Hurthle cell type)	HCC	c.338-1G>A; p.?	19.1%	A113_ splice site	Pathogenic	-
19	71	F	3.5	4 (Hurthle cell type)	HCC	c.338-1G>T; p.?	40.3%	A113_ splice site	Pathogenic	TP53 p.H179R, 66.4%
20	63	M	3.1	3	EFVPTC	c.429+1G>A; p.?	39.5%	D143_splice site	Likely pathogenic	-
21	59	F	1.8	3	EFVPTC	c.338-1_339delinsACA; p.?	6.7%	A113_ splice site	Pathogenic	NRAS p.Q61K, 8.2%
22	68	F	1.3	3	EFVPTC	c.338-2A>T; p.?	4.5%	A113_ splice site	Pathogenic	NRAS p.Q61R, 4.3%
23	58	M	4.5	4	EFVPTC	c.338-2A>T; p.?	23.50%	A113_ splice site	Pathogenic	HRAS p.Q61R, 12.7%; TP53 p.Q331Rfs*14, 10.1% & p.S240R, 10.9%
24	65	F	2.7	4	EFVPTC	c.26G>T; p.G9V	22.2%	N terminus	Pathogenic	NRAS p.Q61R, 28.9%
25	68	F	2.6	3	IFVPTC	c.338-8_338-1del; p.?	26.3%	A113_ splice site	Pathogenic	HRAS p.Q61R, 25.5%; TERT c.-124C>T, 21.6%
26	74	F	1.5	4	IFVPTC	c.338-1G>C; p.?	16.7%	A113_ splice site	Pathogenic	YWHAG-BRAF Fusion

EFVPTC=Encapsulated follicular variant of papillary thyroid carcinoma; F=Female, FA=Follicular adenoma, FTC=Follicular thyroid carcinoma; HCC=Hurthle cell carcinoma; IFVPTC=Infiltrative follicular variant of papillary thyroid carcinoma; M=Male, NIFTP=Noninvasive follicular thyroid neoplasm with papillary-like nuclear features.

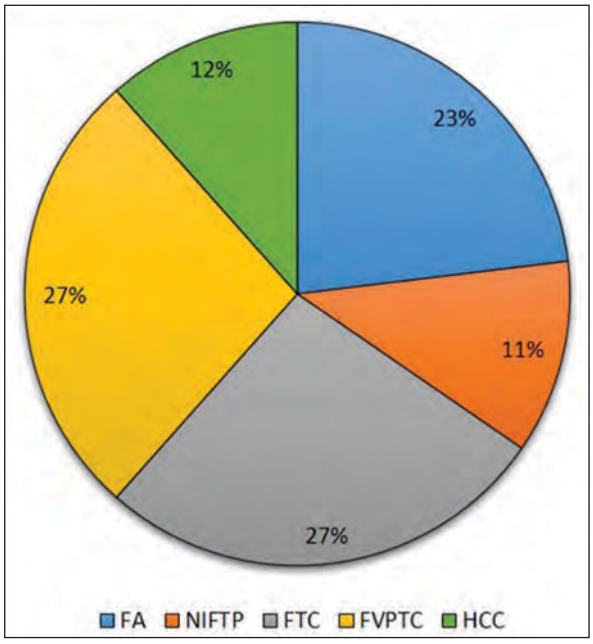

FA=Follicular adenoma; FTC=Follicular thyroid carcinoma; FVPTC=Follicular variant of papillary thyroid carcinoma; HCC=Hurthle cell carcinoma; NIFTP=Noninvasive follicular thyroid neoplasm with papillary-like nuclear features.

Figure 1. Prevalence of histopathologic diagnoses in surgically resected EIF1AX-mutated cytologically indeterminate thyroid nodules (N=26).

a noninvasive follicular thyroid neoplasm with papillary-like nuclear features (NIFTP) diagnosis and 17 with a malignant diagnosis.

Malignant neoplasms included follicular thyroid carcinoma (FTC) (N=7), encapsulated follicular variant of papillary thyroid carcinoma (EFVPTC) with capsular invasion (N=5), Hurthle cell carcinoma (HCC) (N=3), and infiltrative follicular variant of papillary thyroid carcinoma (IFVPTC) (N=2). The Bethesda Category III and IV cytopathologic diagnoses did not distinguish between benign and malignant thyroid neoplasms, as shown in Table 1.

Molecular Characterization

These 26 cases were characterized by mutations in the *EIF1AX* gene. Two distinct types of mutations were observed, as shown in Figure 2 and Table 1. A mutation at the 3' end of the exon 6 splice site was observed in 17 cases and missense mutations in the N-terminal of the protein containing basic amino acids was present in 5 cases. In 4 patients the mutations did not fit neatly into this distribution. A duplication of the proline residue encoded by codon 2 was also detected, but it differs from the missense mutations more commonly seen in the N-terminal. In addition, the p.W70C mutation occurs in a "mini-cluster" of mutations that have been seen in non-thyroid malignancies, but have not been reported in thyroid neoplasia in the COSMIC (6) or cBioPortal (7) databases. The p.G124L and c.429+1G>A mutations have not been previously reported in thyroid malignancies. Single mutations in the exon 6 splice site or the basic amino terminal tail occurred in both benign and malignant thyroid neoplasms. In addition to the abnormal *EIF1AX* gene, mutations in significant tumor-associated genes occurred in 15 of the 26 cases, and 13 of the 15 were detected in malignant neoplasms. The additional mutated genes, shown in Table 1, included *NRAS* (N=6), *HRAS* (N=3), *KRAS* (N=3), the common *TERT* promoter mutation (N=5), and *TP53* (N=2). In 4 cases the *TERT* promoter mutation occurred with a *RAS* gene mutation and in one patient a *TP53* mutation occurred with a mutant *RAS* gene. One case also harbored a novel *YWHAG-BRAF* fusion.

EIF1AX mutation alone conferred a 36.4% (4/11) risk of malignancy (ROM) and 54.5% (6/11) risk of malignancy or NIFTP, while ROM was significantly higher in nodules with concurrent *RAS* (71.4%; 5/7), *TERT*, *TP53* and *RAS+TERT* (100%) mutations (Table 2).

X-axis shows the number of mutations. Green and black circles denote missense and splice site mutations respectively.

Figure 2. Distribution of EIF1AX mutations in surgically resected thyroid nodules (N=26)

Table 2. Summary of Risk of Malignancy (ROM) for All EIF1AX-Mutated Surgically Removed Nodules

Mutation(s)	Number of cases	Percentage	ROM (%)	ROM or NIFTP (%)
EIF1AX alone	11	42.3	36.4	54.5
EIF1AX + RAS	7	26.9	71.4	85.7
EIF1AX + RAS + TERT	4	15.4	100	100
EIF1AX + RAS + TP53	1	3.8	100	100
EIF1AX + BRAF Fusion	1	3.8	100	100
EIF1AX + TERT	1	3.8	100	100
EIF1AX + TP53	1	3.8	100	100
Overall	26	100	65.4	76.9

ROM=Risk of malignancy; NIFTP=Noninvasive follicular thyroid neoplasm with papillary-like nuclear features.

Discussion

EIF1AX encodes the essential, ubiquitously-expressed eukaryotic translation initiation factor EIF1A with 144 amino acids. As a part of the 43S pre-initiation complex (PIC), it binds to the capped mRNA, aids in localizing the start codon and initiates translation. EIF1A protein contains a core RNA binding domain spanning the residues 32-95 which is flanked on either side by highly charged unstructured N- and C-terminus tails (8). Originally identified in uveal melanomas, *EIF1AX* mutations have now also been detected in a variety of other tumor types, including low-grade gliomas, lung adenocarcinoma, endometrial carcinoma, and various neoplastic and nonneoplastic thyroid lesions (4, 9-11). Missense mutations of the first 2-15 amino acids at the N-terminus of *EIFIAX* have been identified in several cancers (9, 12-14). An additional hotspot splice-site mutation (A113_splice) in the C-terminus of the protein is thought to be exclusive to thyroid carcinoma (9, 11, 15).

In our study, 4.5% of cytologically indeterminate thyroid nodules (41 out of 904 total cases) and 11.4% (26 out of 229) of those that were surgically resected harbored an *EIF1AX* mutation. Of these cases, the histopathologic diagnoses were benign neoplasm (FA) in 6/26 (23.1%), NIFTP in 3/26 (11.5%) and malignant neoplasm (FTC, HCC or FVPTC) in 17/26 (65.4%) (Table 3A). Karunamurthy et al. (4) found *EIF1AX* mutations in 27/647 (4.2%) of indeterminate cytology samples, of which 5 had surgical follow-up information (1 EFVPTC, 1 hyperplastic nodule (HN), and 3 FA) yielding an estimated ROM of 20%. Our overall ROM is much higher (65.4%), and even in our nodules with *EIF1AX* mutation alone and no other coexisting mutations, the ROM is 36.4% (4/11) and ROM/NIFTP is 54.5% (6/11) (Table 2). All of our nodules were neoplastic, though other studies have found mutations in one case of HN (4). Of note, the estimated ROM calculated in studies such as this one are overestimations of the actual

ROM, due to the impact of selection bias. Nodules that undergo surgical resection are more likely to have suspicious pre-operative clinical findings (e.g. worrisome radiologic features, interval growth), increasing the likelihood of malignancy regardless of the FNA diagnosis and molecular result.

Similar to other studies, the most common type of *EIF1AX* mutation identified in our study was the A113_splice mutation at the intron 5/exon 6 splice site of *EIF1AX* (17/26), followed by the missense mutations in N-terminus of the protein (5/26). Previous studies have concluded that the A113_splice mutation, especially with co-existing *RAS* mutation, is more frequently observed in thyroid cancer than isolated *EIF1AX* mutations or mutations at the N-terminus hotspot of the gene (4, 11, 14). In our study, 13/17 (76.5%) surgically resected nodules with the A113_splice mutation and 3/5 (60%) nodules with an N-terminal missense mutation were malignant. Of the 13 malignant nodules with the A113_splice mutation, 10 harbored co-mutations (5 harbored one co-mutation and 5 harbored two co-mutations). Of the 3 malignant nodules with N-terminus mutation, 2 harbored co-mutations. Please refer to Table 1 for details.

Four cases harbored *EIF1AX* mutations that did not belong to the 2 common types discussed above. The N-terminal duplication (c.3_5dup, p.P2dup) was not in the COSMIC database, but is likely similar to the missense mutations in the same region. The *EIF1AX* p.W70C identified in the NIFTP case had a concurrent *RAS* mutation. In the COSMIC database, 4 cases with this mutation and 3 additional missense mutations at this amino acid position had been reported in non-thyroid cancer specimens, which makes the p.W70C mutation likely pathogenic. The mutation p. G124L (c.370_371delinsTT), detected in a FA, has been reported once in the COSMIC database, in a small cell carcinoma of the lung. Mutations affecting the same amino acid, p.G124* and p.G124V, were reported in a single thyroid carcinoma specimen (cBioPortal, sample ID TCGA-EM-A3ST-01). Lastly, the mutation c.429+1G>A, exon 6/intron 6 splice site mutation, detected in one of our EFVPTC cases, has never been reported, but 7 malignant cases with mutations affecting the D143_ splice site were documented in the COSMIC database. This mutation most likely affects splicing and hence the function of the protein.

Other studies have reported *EIF1AX* mutations co-occurring with several other driver mutations. Karunamurthy et al. (4) found co-mutations in 3/11 cases (2 with *NRAS* and 1 with *NRAS*, *TP53* and *TERT*), all of which were malignant neoplasms. The TCGA study found co-mutations (*KRAS* and *BRAF*) in one of their 6 cases of *EIF1AX*-mutated PTC (9). Our study showed that *EIF1AX* mutations can co-occur with mutations in *RAS*, *TP53* and *TERT promoter (TERTp)*, and these co-mutations are associated with a very high ROM. Co-existing *EIF1AX* and a hotspot *RAS* mutation conferred an 85.7% ROM and 100% ROM or NIFTP, compared to *EIF1AX* mutation alone that conferred a 36.4% ROM. Malignancy risk was 100% for nodules containing co-mutations in *TERTp*, *TP53*, *RAS+TERTp,* and *BRAF* fusion. Clinicians must be aware of this and should strongly consider surgical intervention, at least a lobectomy, for patients with multiple such mutations in a thyroid nodule.

Key published studies on the *EIF1AX* mutations in thyroid nodules/cancer specimens are summarized in Table 3. The histopathologic diagnoses and ROM for *EIF1AX* mutation positive specimens identified from FNA with indeterminate cytology (Bethesda III and V), including our current study, are shown in Table 3A. The frequencies of the *EIF1AX* mutations in different categories of thyroid nodules from surgically resected specimens are presented in Table 3B.

While *EIF1AX* mutations were identified in HN, FA, and differentiated thyroid cancer (PTC and FTC), the percentage of specimens containing the *EIF1AX* mutations was enriched in advanced thyroid cancer. By combining the case numbers of the studies listed in Table 3B, there were 11 positive specimens for *EIF1AX* mutations in 97 PDTC (11.3%) and 9 positive in 97 ATC cases (9.3%). Additional co-existing mutations in PDTC and ATC include *RAS*, *RAF*, *TERTp*, *TP53* mutations.

Table 3. Prevalence of EIF1AX Mutations in A) Fine Needle Aspirates (FNA) and B) Surgically Removed Nodules, in Present and Previously Published Studies

A. Characterization of EIF1AX Mutation-Positive Fine Needle Aspirates (FNA) with Indeterminate Cytology

Study	EIF1AX-mutated FNA	Surgical pathology follow-up of EIF1AX-mutated FNA						
		Total cases	HN	FA	NIFTP	PTC	FTC	HCC
Karunamurthy et al, 2016 (4)	27/647; 4.2%	5/27	1/5; 20%	3/5; 60%	-	1/5; 20%	-	-
Present Study	41/904; 4.5%	26/41	-	6/26; 23.1%	3/26; 11.5%	7/26; 26.9% (FVPTC)	7/26; 26.9%	3/26; 11.5%

B. Frequency of *EIF1AX* Mutations in Surgically Removed Nodules

Study	HN	FA	Differentiated TC		Undifferentiated TC	
			PTC	FTC	PDTC	ATC
TCGA, 2014 (9)	-	-	6/402; 1.5% (5 FVPTC; 1 mix of follicular & classical variant)	-	-	-
Kunstman et al, 2015 (16)	-	-	-	-	-	3/22; 13.6%
Karunamurthy et al, 2016 (4)	1/80; 1.3%	2/27; 7.4%	2/86; 2.3%	0/53; 0%	0/4; 0%	1/4; 25%
Landa et al, 2016 (11)	-	-	-	-	9/84; 11%	3/33; 9%
Nicolson et al, 2018 (17)	-	-	-	2/39 ; 5.1%	-	-
Pozdeyev et al, 2018 (15)*	-	-	1/89; 1.1%	2/5; 40%	-	2/31; 6.5%
Simoes-Pereira et al, 2019 (14)†	0/7; 0%	-	1/12; 8.3% (FVPTC)		2/9; 22.2%	0/7; 0%

ATC=Anaplastic thyroid cancer; FA=follicular adenoma; FTC=Follicular thyroid carcinoma; HCC=Hurthle cell carcinoma; HN=Hyperplastic nodule; NIFTP=Noninvasive follicular thyroid neoplasm with papillary-like nuclear features; PDTC=Poorly differentiated thyroid carcinoma; PTC=Papillary thyroid carcinoma; TC=Thyroid cancer; *Only those specimens that were sequenced on MSK-IMPACT panels were included in this table since EIF1AX is not tested by the FoundationOne Panels; †9 surgical specimens in this study had distinct histological type and were counted separately based on the histology. Please see the study by Simoes-Pereira et al. (14) for details.

Krishnamoorthy et al. (18) demonstrated *EIF1AX* A113_splice mutation increases protein synthesis globally and cooperates with *RAS* mutations to increase the stability of c-MYC protein to drive thyroid tumorigenesis.

Among the 26 cases carrying the *EIF1AX* mutations in our cohort, 11 cases had *EIF1AX* mutations alone and 15 had co-existing mutations detected by our NGS panel. Within the 15 co-mutation cases, 13 were in the RAS/RAF pathway (including 1 case with a non-hotspot *KRAS* mutation, p.A59del with unknown significance), and 2 cases had a mutation either in the *TERT* promoter or the *TP53* gene. When we compared the alternate allele frequencies (AAF) of the *EIF1AX* and other co-existing mutations, the AAFs for the *EIF1AX* mutations were greater than (N=4) or similar to (N=10) that of other driver mutations (Table 1). In the case with a co-existing *TP53* mutation, the AAF for the *TP53* mutation was 66% and AAF for the *EIF1AX* mutation was 40%. The apparent higher AAF of *TP53* is likely due to a loss of heterozygosity (LOH) event in this case, given the AAF of *TP53* was well over 50%. The high AAFs of *EIF1AX* mutations in comparison to that of co-existing mutations suggests that *EIF1AX* mutations represent an early event, at least in some cases, that promotes initiation of the thyroid tumors and malignant transformation.

Conclusion

EIF1AX mutations can occur in both benign and malignant thyroid neoplasms. The type of *EIF1AX* mutation, and even more importantly, the presence or absence of co-mutations, has an impact on the likelihood of malignancy in an *EIF1AX*-mutat-

ed thyroid nodule. Therefore, in the face of a cytologically indeterminate thyroid nodule with an *EIF1AX* mutation detected upon molecular analysis, a more detailed look at the molecular profile, in conjunction with the clinical and imaging findings, may be helpful in predicting malignancy risk and determining optimal patient care.

What Is Already Known on This Topic:

EIF1AX mutations occur in wide variety of thyroid lesions, including HN, FA, NIFTP, well differentiated carcinomas (FTC and FVPTC) and poorly differentiated carcinomas (PDTC and ATC). Previous studies examining surgically resected nodules have concluded that the A113_ splice mutation, especially with co-existing RAS mutation, is more frequently observed in thyroid cancer than are isolated EIF1AX mutations or mutations at the N-terminus hotspot of the gene. However, there is limited data characterizing EIF1AX mutations in cytology samples from indeterminate thyroid nodules.

What This Study Adds:

The ROM in an EIF1AX-mutated, cytologically indeterminate thyroid nodule may be higher than previously reported, for in our study, 36.4% of thyroid nodules with isolated EIF1AX mutation identified in the FNA sample were diagnosed as malignant neoplasms upon surgical removal. Furthermore, our data suggests that the presence of co-mutations, regardless of the position of the EIF1AX mutation, has a significant influence on malignancy risk. The coexistence of EIF1AX mutations with other pathogenic driver mutations in RAS, TERT and TP53 conferred a 100% ROM or NIFTP in our cohort, indicating that such nodules warrant surgical resection.

Authors' Contributions: Conception and design: SG, YN and ZW; Acquisition, analysis and interpretation of data: SG, NB, YN, SP and ZW; Drafting the article: SG, NB and ZW; Revising it critically for important intellectual content: SP and ZW; Approved final version of the manuscript: SG, NB, YN, SP and ZW.

Conflict of Interest: The authors declare that they have no conflict of interest.

References

1. Rao SN, Bernet V. Indeterminate thyroid nodules in the era of molecular genomics. Mol Genet Genomic Med. 2020;8(9):e1288.
2. Kumar N, Gupta R, Gupta S. Molecular testing in diagnosis of indeterminate thyroid cytology: trends and drivers. Diagn Cytopathol. 2020 Jun 5. doi: 10.1002/dc.24522. Online ahead of print.
3. Yoo SK, Lee S, Kim SJ, Jee HG, Kim BA, Cho H, et al. Comprehensive analysis of the transcriptional and mutational landscape of follicular and papillary thyroid cancers. PLoS Genet. 2016;12(8):e1006239.
4. Karunamurthy A, Panebianco F, Hsiao SJ, Vorhauer J, Nikoforova MN, Chiosea S, et al. Prevalence and phenotypic correlations of EIF1AX mutations in thyroid nodules. Endocr Relat Cancer. 2016;23(4):295-301.
5. Simen BB, Yin L, Goswami CP, Davis KO, Bajaj R, Gong JZ, et al. Validation of a next-generation-sequencing cancer panel for use in the clinical laboratory. Arch Pathol Lab Med. 2015;139(4):508-17.
6. Catalogue of Somatic Mutations in Cancer [database on the Internet]. v92, released Aug 2020 Aug. [Cited 2021 Jan 29]. Available from: http://cancer.sanger.ac.uk/cosmic.
7. cBioPortal for Cancer Genomics [database on the Internet]. [cited 2021 Jan 29]. Available from: http://cbioportal.org.
8. Fekete CA, Applefield DJ, Blakely SA, Shirokikh N, Pestova T, Lorsch JR, et al. The eIF1A C-terminal domain promotes initiation complex assembly, scanning and AUG selection in vivo. EMBO J. 2005;24(20):3588-601.
9. Cancer Genome Atlas Research Network. Integrated genomic characterization of papillary thyroid carcinoma. Cell. 2014;159:676-90.
10. Johnson DB, Roszik J, Shoustari AN, Eroglu Z, Balko JM, Higham C, et al. Comparative analysis of the GNAQ, GNA11, SF3B1, and EIF1AX driver mutations in melanoma and across the cancer spectrum. Pigment Cell Melanoma Res. 2016;29(4):470-3.
11. Landa I, Ibrahimpasic T, Boucai L, Sinha R, Knauf JA, Shah RH, et al. Genomic and transcriptomic hallmarks of poorly differentiated and anaplastic thyroid cancers. J Clin Invest. 2016;126(3):1052-66.
12. Martin M, Masshofer L, Temming P, Rahmann S, Metz C, Bornfeld N, et al. Exome sequencing identifies recurrent somatic mutations in EIF1AX and SF3B1 in uveal melanoma with disomy 3. Nat Genet. 2013;45:933-6.
13. Etemadmoghadam D, Azar WJ, Lei Y, Moujaber T, Garsed DW, Kennedy CJ, et al. EIF1AX and NRAS mutations co-occur and cooperate in low-grade serous ovarian carcinomas. Cancer Res. 2017;77(16):4268-78.
14. Simoes-Pereira J, Moura MM, Marques IJ, Rito M, Cabrera RA, Leite V, et al. The role of EIF1AX in thyroid cancer tumourigenesis and progression. J Endocrinol Invest. 2019;42(3):313-8.
15. Pozdeyev N, Gay LM, Sokol ES, Hartmaier R, Deaver KE, Davis S, et al. Genetic analysis of 779 advanced differentiated and anaplastic thyroid cancers. Clin Cancer Res. 2018;24(13):3059-68. doi 10.1158/1078-0432.CCR-18-0373.
16. Kunstman JW, Juhlin CC, Goh G, Brown TC, Stenman A, Healy JM, et al. Characterization of the mutational landscape of anaplastic thyroid cancer via whole-exome sequencing. Hum Mol Genet. 2015;24(8):2318-29.

17. Nicolson NG, Murtha TD, Dong W, Paulsson JO, Choi J, Barbieri AL, et al. Comprehensive genetic analysis of follicular thyroid carcinoma predicts prognosis independent of histology. J Clin Endocrinol Metab. 2018;103(7):2640-50.

18. Krishnamoorthy GP, Davidson NR, Leach SD, Zhao Z, Lowe SW, Lee G, et al. EIF1AX and RAS mutations cooperate to drive thyroid tumorigenesis through ATF4 and c-MYC. Cancer Discov. 2019;9(2):264-81.

Original Article
Acta Medica Academica 2021;50(1):13-28
DOI: 10.5644/ama2006-124.323

Immunohistochemical Staining for Lymphatic and Blood Vessels in Normal Tissues: Comparison between Routinely Paraffin-Embedded Tissues and Frozen Sections

Tatsuo Tomita

Departments of Integrative Biosciences and Pathology, Oregon Health and Science University, Portland, OR, USA

Correspondence: *tomitat39@gmail.com*; Tel.: + 1 971 470 7252; Fax: + 1 503 4948 311

Received: 18 January 2021; **Accepted:** 17 February 2021

Abstract

Objective. In the current study, we compared the distribution of blood and lymphatic vessels from paraffin-embedded tissues with those of frozen tissues of normal human and rhesus monkey. **Materials and Methods.** We performed immunocytochemical staining for lymphatic and blood vessels using LYVE-1 for lymphatic vessels and von Willebrand factor (F-8) for blood vessels. **Results.** Normal tissues included spleen, lymph node, liver, pancreas, salivary gland, colon, diaphragm, heart, lung, thyroid, adrenal gland, kidney, ovary, endometrium, and prostate. Splenic sinusoids were stained for LYVE-1 and F-8 in the frozen sections, supporting that the sinusoid is a lymphoreticular system and blood vessel in structure and function. In frozen sections, the lymphatic sinusoids were consistently positive for LYVE-1, while hepatic sinusoids were positive for LYVE-1, but not for F-8. Thus, lymphatic and blood vessels were more readily detected in frozen tissue sections than in the paraffin-embedded sections. In the endometrium, lymphatic vessels were not diffusely immunostained in paraffin-embedded sections. However, frozen sections detected cyclic changes of lymphatic vessels, growing from basalis to functionalis in the menstrual cycle. Lymphatic vessels were immunostained in many organs using frozen sections. Small pulmonary blood vessels were not immunostained by F-8 in the periphery of the bronchial vessel tree most likely these smallest blood vessels were not immunostained due to less F-8 attached to their endothelia. **Conclusion.** The present findings illustrate the differences in the immunostaining of blood vessels in sections obtained from paraffin-embedded tissues and those from frozen tissue. These new findings may be relevant for the basic histology and histopathology of lymphatic and blood vessels.

Key Words: Blood Vessels ▪ Lymphatic Vessels ▪ Immunohistochemistry ▪ Factor-8 ▪ LYVE-1.

Introduction

Practically every organ is supplied by lymphatic vessels except the brain, spinal cord, cartilage, bone marrow, eye lens, and others (1-4). However, the presence of lymphatic vessels in each organ is not definitively identified at the histologic levels. Using immunocytochemical staining for lymphatic and blood vessels, we had tried to detect lymphatic and blood vessels using currently available immunocytochemical markers. The currently commercially available markers for lymphatic vessel endothelia include proxy-1 (prospero-related homeobox-1), LYVE-1 (lymphatic vessel endothelial hyaluronic acid factor receptor-1), podoplanin (43 kDa membrane glycoprotein of podocytes), and VEGFR-3 (vascular endothelial growth factor receptor-3) (1-4). LYVE-1 is a transmembrane receptor for hyaluronan, a highly expressed by lymphatic vessels (3-6). A podoplanin is a membrane glycoprotein found on the surface of rat glomerular epithelial cells, podocytes, recognized by the monoclonal antibody, D2-40 (3). These markers bind to their own specific binding sites in different modes, and they all function in diverse ways at different stages of tissue growth and development (2-4). The markers for blood vessels include CD31 (platelet endothelial adhesion molecule PECASM-1, found on endothelial cells), CD34 (single-class

transmembrane sialomucin protein, its antibody is used for hematopoietic progenitor cells, positive for blood vessel endothelium but not lymphatic vessel endothelium), and von Willebrand factor (binds factor-8, F-8, a clotting factor in blood vessel endothelium, platelet aggregation and adhesion to the cell wall of injured vessels), which are pan-vascular endothelial markers (3).

However, there are truly no specific markers for lymphatic vessels and blood vessels, respectively, at present (2, 3, 7-10). We had previously performed such immunocytochemical staining with normal tissues. We found that frozen sections were superior for lymphatic and blood vessels immunostaining than the routinely formalin-fixed and paraffin-embedded sections (11, 12). To anatomic pathologists, it is crucially important to identify the precise presence of lymphatic and blood vessels in the normal organs and the pathological tissue specimens, especially in cancer tissues (11, 12). The classical staining for lymphatic vessels is van Gieson's stain for the lining elastic lamina for distinguishing lymphatic vessels from the small tissue spaces due to the fixation artifacts by buffered formalin-fixation and paraffin embedding. The presence of red blood cells in the endothelium lining vessel lumens supports to identify blood vessels. These two vessel systems supply the organs for lymph fluid and blood and have crucial roles in cancer spread and metastasis.

The aim of the current study was to compare the distribution of blood and lymphatic vessels using paraffin-embedded and frozen tissue samples of normal human and rhesus monkey. We employed mostly LYVE-1 for lymphatic vessels and von Willebrand factor (Factor-8, F-8) for blood vessels stains (13).

Materials and Methods

Normal human tissues were collected from surgically removed organs at the Department of Pathology, University of Kansas Medical Center, Kansas City. These tissues included colon and pancreas. Immunocytochemical staining procedures with paraffin-embedded tissues were previously reported (11, 12). The sources of antibodies used for immunocytochemical staining and each dilution of the antibody for routinely formalin-fixed and paraffin-embedded tissues and frozen sections are as follows (Table 1).

For frozen sections, normal organ tissues from *Macaca mulatta* (rhesus monkey) were procured by necropsy at the laboratory of Drs. Robert Brenner and Ov Slayden, Oregon National Research Center, Beaverton, OR. The frozen tissues were prepared from the liver, spleen, lymph node, diaphragm, heart, lung, thyroid, adrenal gland, kidney, ovary, uterus, and prostate. Additionally, monkey liver and spleen were fixed in a mixture of 1% paraformaldehyde and 1% formalin and were embedded in paraffin. With spleen and liver, double immunocytochemical staining was performed with paraffin sections for LYVE-1 and F-8 using brown color by diaminobenzidine tetrahydrochloride and blue color by Vectastain and Vector SG (Burlingame, CA). For frozen sections, small fresh tissues (1 × 1 × 0.4 cm) were embedded in OCT matrix (Fisher Scientific, Pittsburgh, PA) and were frozen in liquid propane in the liquid nitrogen bath as described before (13-18) and were frozen sectioned at 5-7 microns. Frozen sections were mounted on Super Frost Plus slides (Fisher Scientific), microwaved-irradiated on ice for 3 sec, fixed in 2% paraformaldehyde in phosphate buffer at pH 7.4 for 10 to 15 min at room temperature, and immersed twice for 2 min in 85% ethanol (13). To inhibit endogenous peroxidase activity, sections were incubated with a solution containing glucose oxidase (1 U/ml) and sodium azide (10 mmol/ml) in PBS for 45 min at 25°C (13). Sections were incubated with blocking serum for 20 min. Then,

Table 1. Antibodies that Were Used in the Current Study

Antibody (clone)	Manufacturer	Paraffin sections dilution	Frozen sections dilution
Goat-anti human LYVE-1	R & D System, Minneapolis, MN	1:100	1:1.200
Mouse monoclonal D2-40	Signet Laboratories, Dedham, Mass	1:100	1:100
Rabbit anti-human F-8	Dako System, Carpenteria, CA	1:100	1:800

sections were incubated with each diluted primary antibody solution overnight at 4°C. After rinsing and immersion in blocking serum again, sections were incubated with a second antibody (1: 200 dilution) for 30 min at room temperature. Final visualization was achieved with the ABC kit (Vector Laboratories, Burlingame, CA) and 0.025 diaminobenzidine tetrahydrochloride in Tris-buffer pH 7.6, 0.03% H_2O_2 to induce brown color.

Results

Spleen and Lymph Node (Figure 1)

Frozen sections of the spleen showed diffuse staining in the sinusoidal endothelia and no staining in the central arterioles in the germinal center for LYVE-1, while F-8 staining revealed positive staining in the central arterioles and adjacent larger arteries (Figure 1-A and -B). The positive F-8 staining in the sinusoidal epithelia was only achieved in the frozen section, not in the routinely processed paraffin sections (Figure 1-B and -D). Double staining for LYVE-1 in brown and F-8 in blue (Figure 1-C) and F-8 in brown and LYVE-1 in blue (Figure 1-D), both revealed positive staining in the sinusoidal endothelia for LYVE-1 and central arterioles staining for F-8. There was no F-8 staining sinusoids in the paraffin sections (Figure 1-D). Thus, the red pulp's sinusoidal epithelia were double-positive for LYVE-1 and F-8 only in the frozen section (Figure 1-A and -B). The frozen sections of the lymph node showed a few lymphatic vessels in the cortex. Simultaneously, there were numerous slender or round lymphatic vessels in the medulla and the connective tissue of the hilum (Figure 1-E). There were lymphatic sinusoidal

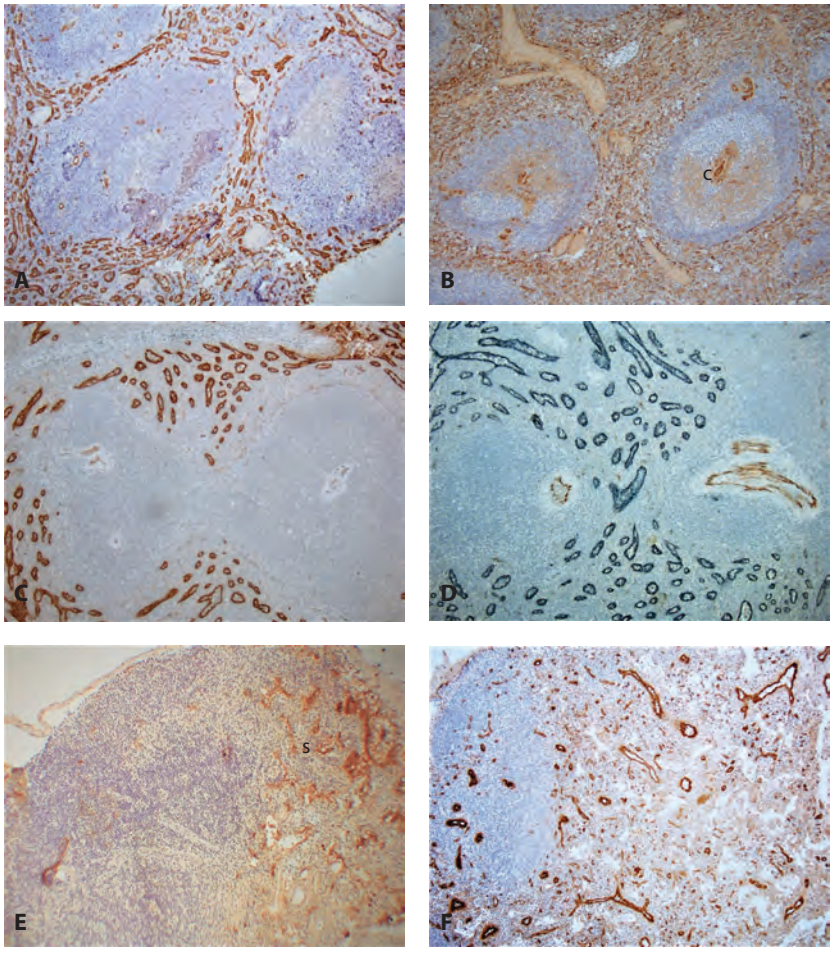

Figure 1. Spleen and Lymph Node. The frozen sections of spleen showed diffuse positive staining in the sinusoids for both LYV-1 and F-8 (A and B), and central arterioles and larger blood vessels were strongly positive for F-8 (B). The paraffin-embedded sections were double stained for LYVE-1 in brown and F-8 in blue, showing positive in sinusoids for LYVE-1 and positive in blood vessels for F-8 (C), and in brown for blood vessels and in blue for sinusoids (D). There was no positive staining for F-8 in the splenic sinusoid in the paraffin-embedded section (D). The frozen sections of lymph node showed LYVE-1 positive staining in lymphatic sinusoids at the subcapsular-medullary junction and linear lymphatic vessels in medulla and hilar connective tissue (E), where abundant F-8 positive blood vessels were present (F). A, B, E and F=Frozen sections; C and D=Paraffin-embedded sections, c: Central artery, s: Lymphatic sinus; A and E=LYVE-1; B and F=F-8, immunostained; C=LYVE-1/F-8; D=F-8/LYVE-1 double-immunostained.

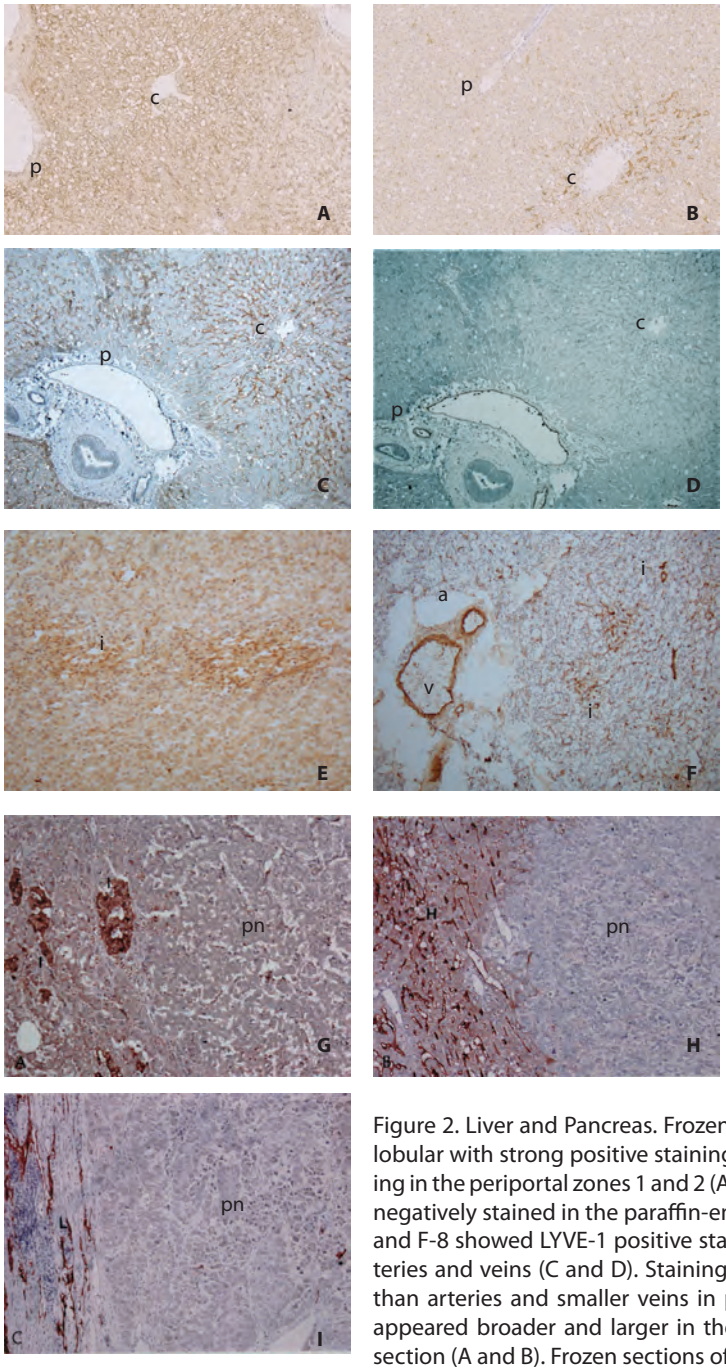

epithelia in the subcapsular (marginal)-medullar junction of the lymph node, strongly positive only for LYVE-1 (Figure 1-E). Mostly round thick-walled arteries were less positively stained for F-8 than thin-walled, dilated veins, which were stronger stained for F-8 with abundant endothelial staining in the small blood vessels in the medulla and large blood vessels in the hilum (Figure 1-F).

Liver and Pancreas (Figure 2)

For LYVE-1 immunostaining, the staining between frozen section and paraffin-embedded section was compared, showing darker staining in the relatively broader liver sheets in the frozen section (Figure 2-A) than the weaker staining in the relatively thinner liver sheets in paraffin-embedded section (Figure 2-B). In the frozen section, pan-lobular sinusoids were diffusely positive for LYVE-1 with stronger pericentral sinusoids than periportal sinusoids. Some periportal sinusoids were barely positive or negative (Figure 2-A). In contrast, the periportal sinusoids were not stained for LYVE-1 in the paraffin-embedded section (Figure 2-B). For F-8 staining, blood

Figure 2. Liver and Pancreas. Frozen section for LYVE-1 staining showed diffuse pan-lobular with strong positive staining in the pericentral zone 3 and less positive staining in the periportal zones 1 and 2 (A) while periportal zone 1 and most of zone 2 were negatively stained in the paraffin-embedded sections (B). Double staining for LYVE-1 and F-8 showed LYVE-1 positive staining in sinusoids and F-8 positive staining in arteries and veins (C and D). Staining for F-8 revealed stronger stained in larger veins than arteries and smaller veins in paraffin-embedded section (D). Liver cell sheets appeared broader and larger in the frozen section than in the paraffin-embedded section (A and B). Frozen sections of pancreas showed barely weakly stained islets by LYVE-1 (E) and F-8 staining showed islets consisting of round baskets of abundant, entangled F-8 positive capillaries (F). Paraffin-sections of pancreas showed strong staining in islets and there was no staining for primary non-functioning Pan-NET (G), metastatic insulinoma in liver (H) and metastatic gastrinoma in lymph node (I). Lymphatic vessels in the pancreatic stroma (G), hepatic sinusoid (H) and lymphatic sinus (I) were positively immunostained for LYVE-1 (G-I), a: Artery, c: Central vein, i: Islet, l: Lymphatic vessel, p: Portal area, pn: Pan-NET, v: Vein. A, E, F=Frozen section; B, C, D, G-I=Paraffin-embedded sections; A, B, E, G-I=LYVE-1, ; C=LYVE-1/F-8 double stained; D=F-8/LYVE-1 double stained; F=F-8 immunostained. Figures G, H and I are from the reference 33 (Tomita T. Pancreas. 2007;35(4):e18-22).

vessels were strongly stained in larger vessels while sinusoids were negative in the paraffin-embedded section (Figure 2-D). Double immunostaining for LYVE-1 and F-8 showed sinusoidal staining endothelial staining in brown for LYVE-1 and weak F-8 staining in arteries and veins in blue (Figure 2-C) and vice versa for brown staining for F-8 and blue staining for LYVE-1 (Figure 2-D).

Frozen section stained for LYVE-1 revealed weakly stained pancreatic islets (Figure 2-E). In contrast, F-8 staining revealed numerous pancreatic islets, consisting of a round basket of abundant, tangled capillaries, and thick-walled arteries and thin-walled veins were moderately and strongly stained, respectively (Figure 2-F). Paraffin-embedded tissues stained strongly for LYVE-1 in pancreatic islets with adjacent lymphatic vessels but no LYVE-1 staining in 23 out of 25 cases of pancreatic neuroendocrine tumors (Pan-NETs) (Figure 2-G), including metastatic insulinoma to the liver (Figure 2-H) and metastatic gastrinoma to lymph node (Figure 2-I). Hepatic and lymphatic sinusoids were positively stained for LYVE-1 in paraffin-embedded sections (Figure 2-H and -I).

Colon, Diaphragm, and Salivary Gland (Figure 3)

In the paraffin-embedded colonic sections, there were numerous slender lymphatic vessels in the submucosa, including lymphoid follicle with a few lymphatic vessels in lamina propria (Figure

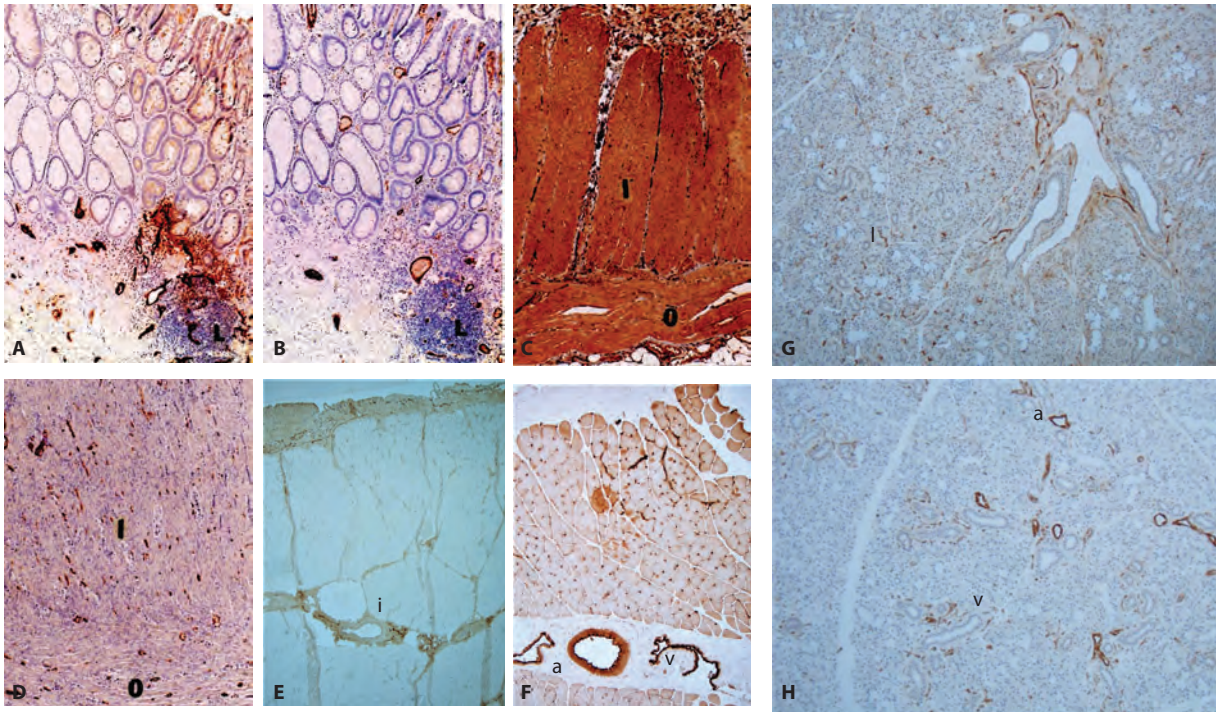

Figure 3. Colon, Diaphragm and Salivary Gland. Paraffin-embedded sections of colon showed a few lymphatic vessels by LYVE-1 staining and numerous round blood vessels by F-8 staining in lamina propria while submucosa contained numerous linear lymphatic vessels and many round blood vessels including the lymphoid follicle (A and B). Lymphatic and blood vessels longitudinally crisscrossed the inner circular and outer longitudinal muscle layer (C and D). Frozen sections of diaphragm contained linear and many small lymphatic vessels in the arterial adventitia of fibrous septa (E) and small capillaries at the outer margins of the striated muscle with many blood vessels in the fibrous septa (F). Frozen sections of salivary gland showed abundant, scattered small linear lymphatic vessels (G) and numerous scattered round blood vessels (H), a: Artery, i: Inner circular muscle, l: Lymphatic vessel, o: Outer longitudinal muscle, v: Vein. A-D=Paraffin-embedded sections; E-H=Frozen sections; A, C and G=LYVE-1; B, D, F, H=F-8; E=D2-40 immunostained; Figures A-D are from the reference 12. Tomita T. Cancer-associated lymphatic and venous vessels in colonic carcinomas. Open J Pathol. 2014;4(2):101-9.

3-A). There were abundant round, dilated veins in the mucosa and submucosa, with some inside the lymphoid follicle (Figure 3-B). Many lymphatic and blood vessels penetrated longitudinally through the two layers of smooth muscles (Figure 3-C and -D). The diaphragm's frozen section was transversely supplied with a scanty, linear network of lymphatic vessels in the thin, fibrous septum and arterial adventitia (Figure 3-E). The striated muscles were diffusely and richly supplied by capillaries at the outer margins of the muscle bundles. On the other hand, abundant thick-walled arteries and thin-walled veins were stained in the endothelia for F-8, with veins stronger stained than arteries (Figure 3-F). The frozen section of the salivary gland revealed many scattered small lymphatic vessels in the periductal and interlobular stroma (Figure 3-G). There were numerous scattered F-8 positive small blood vessels in the inter-lobular stroma, including thick-walled arteries and thin-walled veins in the periductal stroma (Figure 3-H).

Thyroid, Adrenal Gland, and Kidney (Figure 4)

In the thyroid, there were abundant linear lymphatic vessels in interfollicular septa (Figure 4-A). In contrast, more abundant larger thick-walled arteries and thin-walled, plump veins were strongly positive for F-8 in the thyroid septa with veins stronger stained than arteries in the frozen sections (Figure 4-B). The adrenal gland contained numerous small lymphatic vessels and larger, dilated blood vessels in the subcapsular tissue (Figure 4-C and -D). There were few lymphatic vessels in the cortical and medullary septa (Figure 4 -C and -D). In the kidney, there were only a few small linear lymphatic vessels around the glomeruli and very few lymphatic vessels in the cortical stroma (Figure 5-E). Glomerular capillaries were densely and diffusely stained for F-8 with positive staining spreading outside the capillary, suggestive of the leaking endothelia (Figure 5-F). Both thick-walled arteries and thin-walled veins were moderately and strongly stained for F-8, respectively (Figure 5-F).

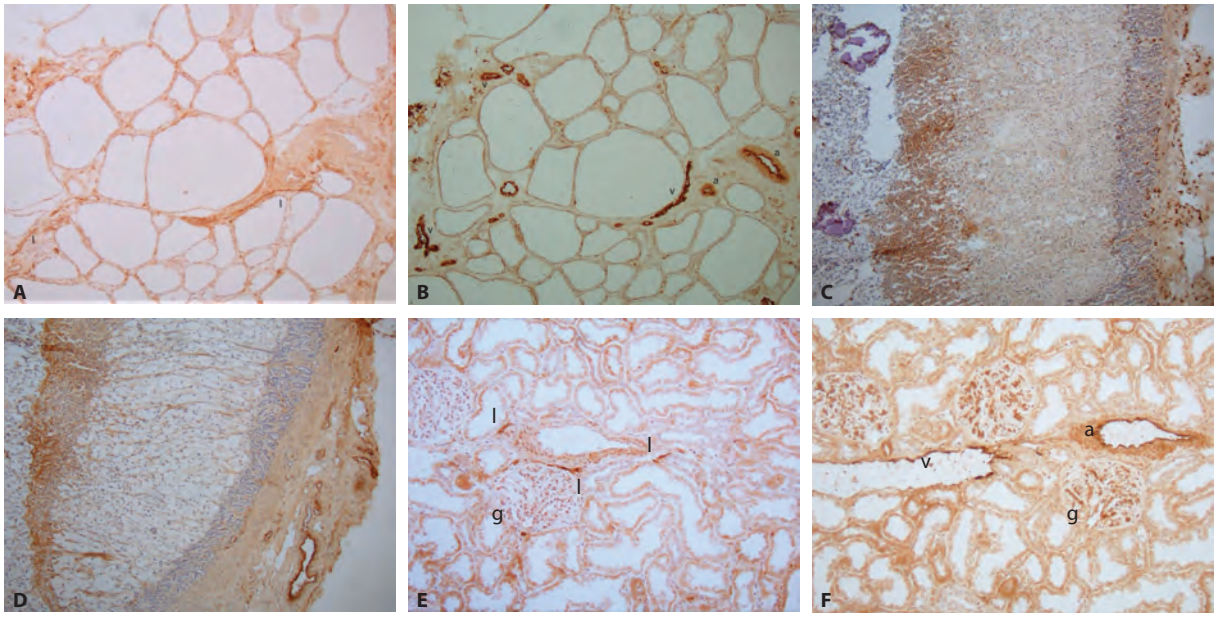

Figure 4. Thyroid, Adrenal Gland and Kidney. Frozen sections of thyroid showed linear and many small lymphatic vessels in fine fibrous septa (A) and more abundant larger, round blood vessels in the septa (B). Adrenal sub-capsular stroma contained numerous small, linear lymphatic vessels (C) and larger round blood vessels (D). There were few lymphatic vessels in the cortex and medulla in kidney. Frozen sections of kidney showed a few small, liner lymphatic vessels around the glomerulus and tubules (E) while glomerular capillaries were densely and diffusely stained for F-8 spreading outside of the capillary, suggestive of leaking blood vessels. There was strong staining for F-8 in larger veins than in arteries (F), a: Artery, g: Glomerulus, l: Lymphatic vessel, v: Vein; A-F=Frozen sections; A, C, E=LYVE-1; B, D, F=F-8 immunostained.

Heart, Lung, Ovary, and Prostate (Figure 5)

Numerous, small, scattered lymphatic vessels were diffusely present in the full thickness of the cardiac ventricle, and much less and a few blood vessels were present in the sections of the ventricle with larger vessels in epicardium than in endocardium (Figure 5A and -B). In the lung, lymphatic vessels were diffusely scattered in the wall of terminal bronchioles, respiratory bronchioles, and alveolar ducts (Figure 5-C). In contrast, fewer blood vessels were revealed by F-8 staining in the wall of mostly terminal bronchioles and respiratory bronchioles (Figure 5-D). Numerous linear lymphatic vessels were present around the ovarian follicle and interstitial stroma, linear with a narrow lumen (Figure 5-E). Likewise, numerous small blood vessels were present around the ovarian follicle in the stroma with plump lumens (Figure 5-F). The prostatic sub-capsule and stroma contained many scattered small, linear lymphatic vessels (Figure 5-G). There were more numerous small blood vessels than lymphatic vessels in the sub-capsule and interlobular stroma than lymphatic vessels (Figure 5-H). There were many nerve fibers in the prostatic sub-capsule (5-G and -H).

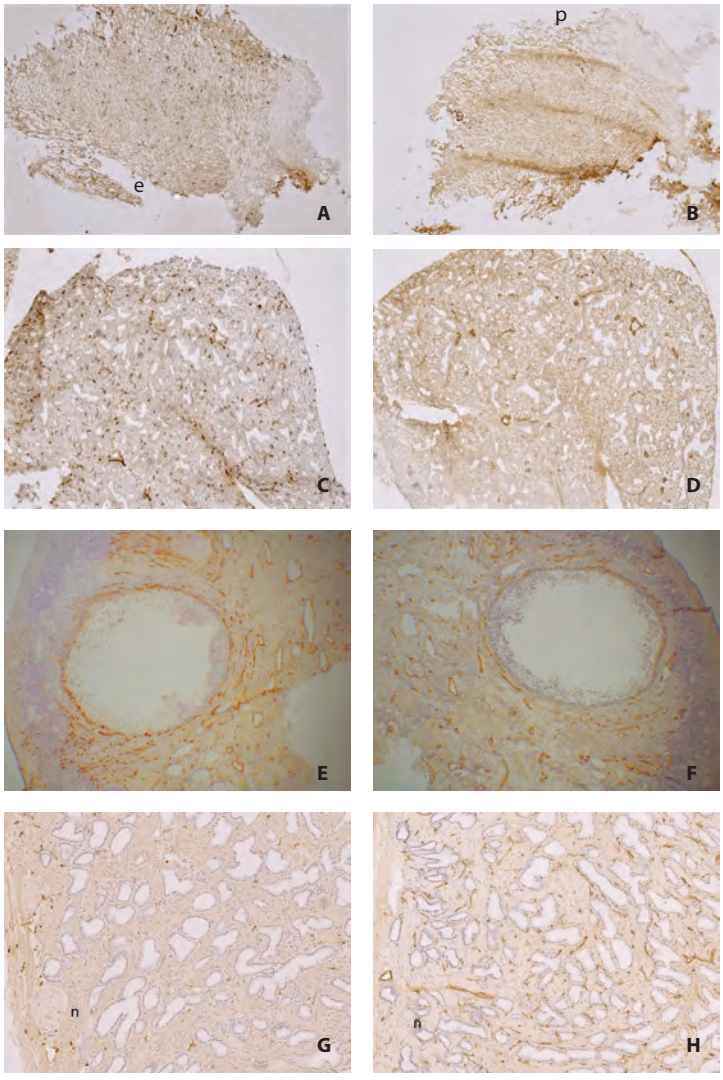

Figure 5. Heart, Lung, Ovary and Prostate. Frozen sections of heart showed numerous scattered small lymphatic vessels (A) and less abundant larger blood vessels with larger caliber in the pericardium (B). There were abundant lymphatic vessels in the wall of terminal bronchioles, respiratory bronchioles, and alveolar ducts (C) while there were less, large blood vessels in in the wall of terminal bronchioles and respiratory bronchioles (D). There was no staining for F-8 in the alveolar capillaries (D). Frozen sections of ovary showed numerous, scattered small lymphatic vessels around the ovarian follicle and interstitial stroma (E), and likewise there were numerous, plump blood vessels in the stroma and around the follicle (F). Prostate showed many small scattered lymphatic vessels in the sub-capsular and interstitial stroma (G) and more numerous small blood vessels in the stroma (H). There were many nerve bundles in the prostatic sub-capsule (G and H), e: Endocardium, n: Nerve, p: Pericardium. A to H=Frozen sections; A, C, E, G=LYVE-1; B, D, G, H=F-8 immunostained.

Macaca mulatta Endometrium, Days 3, 14, and 28 of Menstrual Cycle (Figure 6)

The cyclic endometrium was stained in the frozen sections. The endometrium from the Day 3 of the menstrual cycle showed thin residual basalis, which contained some small lymphatic vessels (Figure 6-A) and numerous dilated blood vessels (Figure 6-B). Day 14 en-

dometrium showed many small lymphatic vessels in the lower stratum functionalis but few lymphatic vessels in the growing upper functionalis (Figure 6-C). Simultaneously, there were numerous blood vessels in both lower and upper functionalis (Figure 6-D). In the endometrium of the 28th day of menstrual cycle, there were small scattered lymphatic vessels in the upper functionalis (Figure 6-E). There were numerous, dilated, densely F-8-stained blood vessels spreading outside of the endothelium, suggestive of leaking blood vessels located perpendicular to the uterine cavity in the upper functionalis (Figure 6-F). There were many perpendicular and transverse lymphatic vessels in the myometrium (Figure 6-A, -B, -D). There were even more numerous larger venous vessels in myometrium than in functionalis and basalis (Figure 6-D).

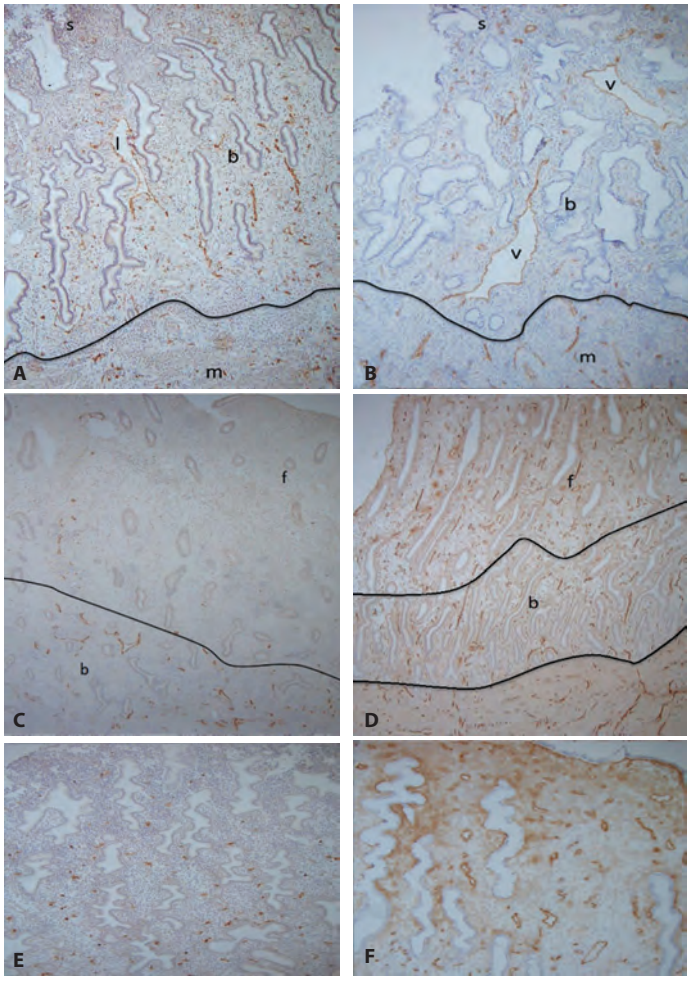

Figure 6. Macaca Mulatta Endometrium, Day 3, 14 and 28 of Menstrual Cycle. Day 3 endometrium of the menstrual cycle showed thin residual basalis, which contained some, small lymphatic vessels (A) and numerous small blood vessels (B). Day 14 endometrium showed a few small, lymphatic vessels (C) and numerous elongating blood vessels in the growing functionalis (D). Day 28 in menstrual cycle, there were several perpendicular small lymphatic vessels in the upper stratum functionalis as compared to numerous small lymphatic vessels in the lower functionalis (E). There were dilated, densely F-8 positive venous vessels, suggestive of leaking blood vessels, which were located perpendicular to the uterine cavity in the upper functionalis (F) as compared to slim elongated blood vessels in the lower functionalis and basalis (D). In myometrium, there were many perpendicular and transverse lymphatic vessels (A, B, D). b: Basalis; f: Functionalis; l: Lymphatic vessel; m: Myometrium; v: Dilated vessel; A-F=Frozen sections; A, C, E=LYVE-1; B, D, F=F-8 immunostained.

Discussion

There are many immunologic and immunohistochemical markers for lymphatic and blood vessels but what we need is just one solely reliable and specific marker for lymphatic vessel and blood vessel, respectively. However, there is none for that purpose at present. The structure-function relationship of lymphatic vasculature has been overshadowed and delayed by a lack of specific markers for lymphatic vessels (1-4). As shown in the dilution of the primary antibody, the frozen sections required a tiny fraction of primary antibodies with much more diluted solutions, especially for the primary LYVE-1 antibody; thus, frozen section immunostaining was much more economical than paraffin-embedded sections since these antibodies were expensive. The hind side of frozen sections is that the frozen tissue preparation is quite cumbersome and labor-intensive. Only small tissue ($1 \times 1 \times 0.4$ cm) may be adequately processed in our method (13-18). During the freezing process, the tissue may crack, the larger tissue tends to crack more often than the smaller tissue, and the freezing process needs to be improved for future study. We used frozen sections of 5-7 μm in thick-

ness, and it was not an easy task to cut thin frozen sections to see a clear view of vascular vessels, and the larger the tissue is, the harder it is to cut good thin sections. Furthermore, frozen sections on the glass slides stored in a deep freezer may degenerate with increasing non-specific staining if kept for more than four weeks. Liver and kidney sections are more prone to degenerate during storage in a deep freezer at -70C°. For the best staining result, the fresh frozen sections are the best for immunocytochemical staining immediately after sectioning. The buffered 10% formalin fixation decreased organ weight by about 10%, but liver sheets were shrunk more than 10% (Figure 2-A and -B).

The clearly different staining pattern was revealed in the spleen, where paraffin-embedded sections revealed LYVE-1 positive sinusoidal epithelia, which were large capillaries and were negative for F-8 (Figure 1-D). Thus, the F-8 positive staining in the splenic sinusoidal epithelia was only positively achieved in the frozen sections (Figure 1-B) but not in the paraffin-embedded sections (Figure 1-D). There were different staining patterns between the frozen section and paraffin-embedded section for splenic sinusoids. In a study using paraffin-embedded sections, splenic sinus was reportedly only patchy positive for F-8 and negative for CD34 (4). The splenic red pulp is lined by distinctive endothelial cells with a partial histologic function called splenic littoral cells, which express endothelial markers like F-8, CD 31, WT1 (Wilms' tumor protein 1), ERG (a member of the erythroblast transformation-specific family), and CD68 (a protein highly expressed by the cells in the monocyte lineage in circulating blood and tissue macrophages) (1-4). Blood is sequestrated in the splenic sinus in the red pulp under the condition of portal hypertension. The sinusoid of larger caliber allows transporting whole blood cells between the capillary wall and the adjacent tissue. Its endothelia increase the attachment of F-8 on the splenic littoral cell surface resulting in strong F-8 staining on the surface (Figure 1-B). Since splenic sinusoidal epithelia are positive for both F-8 and LYVE-1, these epithelia are both venous and lymphatic endothelia, as seen in the frozen sections. They may function as both venous capillaries and lymphatic capillaries. The human spleen's sinusoid is an unusual vessel, which is involved in the removal of damaged erythrocytes and permits the migration of leukocytes from the cords into the circulation (4). This endothelium of the sinusoids is equivalent to other endothelium in their immunoreactivity to F-8 and HLA-DR antigens (4, 19-21). The white splenic pulp, germinal center, consists of central arterioles (Figure 1 A-D), which are surrounded by lymphoid cells, the so-called periarteriolar sheath (PALS), and adjacent outpouchings of nodular lymphoid tissue (3, 4, 19-21). The lymph node sections also showed a different staining pattern for lymphoid sinusoids, positive for LYVE-1 in the frozen sections. Using paraffin-embedded sections, the lymphoid sinus was reportedly positive for CD34 and negative for CD31 (4). The lymphoid sinusoids are located between the subcortical (marginal)-medullary junction (Figure 1-E). Lymph nodes filter protein-rich lymph fluid through lymphatic sinusoids, while the spleen filters blood through splenic sinusoids (3, 4). In lymph nodes, there were abundant arteries and veins in the medullary cord and hilum with small lymphatic vessels in the periarterial stroma (Figure 1-E and -F). Double staining for LYVE-1 and F-8 was possible only with paraffin-embedded sections, and an attempt for double staining with frozen sections was unsuccessful because of too much non-specific background staining, which resulted in too dirty to identify vessels at our hand.

LYVE-1 immunostaining is not restricted to the lymphatic vessels but is expressed in normal hepatic sinusoids, which are downregulated in hepatic cancer and liver cirrhosis (22). The hepatic sinusoids were positively stained for LYVE-1, not entirely in all zones in paraffin-embedded section where oxygen-rich zones 1 (periportal hepatocytes) was negative but oxygen-poor zones 2 and 3 (pericentral hepatocytes) were positive (Figure 2-A and -B). However, all zones 1 to 3 in some tissue areas were positively stained for LYVE-1 in the frozen section. So, zone 3 was stronger stained than zones 1 and 2 (Figure 2-A). There are two types of sinusoidal epithelia in the hepa-

tocytes. Type 1 sinusoidal epithelia are LYVE-1^{-}, CD32^{hi}CD14^{+} hepatocyte in the oxygen-rich zone 1, and type 2 sinusoidal epithelia are LYVE-1^{+}, CD32^{hi}CD14^{+}CD36$^{mid\text{-}lo}$ in the oxygen-poor zone 2 and 3 hepatocytes (Figure 2-A and -B) (22-26). Thus, LYVE-1 staining is mostly stronger stained in the zones 2 and 3 endothelia, which are venous capillaries with more LYVE-1 attached in the endothelia, while zone 1 is arterial capillary with less F-8 attached. Hepatic sinusoids are large capillaries positive for LYVE-1 in zone 3 in the paraffin-embedded section, but not diffusely for F-8 with patchy staining in the literature (3, 4, 24, 25). F-8 immunostaining yielded negatively stained in liver sinusoids, while stronger positive staining was seen in veins with larger caliber vessels (Figure 2-C and -D). In paraffin-embedded sections, zone 1 was positive, and zone 2 was negative for CD34 since CD34 stained stronger for arterioles than venules, supporting that zone 1 is arterial capillary (4, 23). The frozen section for F-8 staining did not yield positive for hepatic sinusoids (25, 26) (Figure not shown). Comparing the sizes of liver sheets, the paraffin-embedded section was smaller than that of frozen sections by more than 10% (Figure 2-A and -B). Veins with larger calibers were stronger stained than those with smaller calibers, and veins were stronger stained than the arteries of the same caliber. This finding may support that larger veins have more F-8 attached on the subendothelial surface than that of smaller veins, and veins with slower blood flow may have more F-8 attached on the endothelia than that of arteries with faster blood flow. Since all undamaged endothelia of veins and arteries are positively stained for F-8 (26), F-8 is not necessarily attached to the damaged vascular endothelia but are attached to the undamaged endothelia as well.

In the three sinusoids containing organs (spleen, lymph nodes, and liver), extramedullary hematopoiesis may occur during fetal development and in hematopoietic malignancies (e.g. chronic myelogenous leukemia and myelofibrosis) (4, 27-30). Extramedullary hematopoiesis is a pathological process in which the differentiation of hematopoietic stem/progenitor cells occurs outside the bone marrow, namely in the sinusoids of spleen, liver and lymph nodes. In the spleen, mesenchymal progenitor-like cells expressing TlX1, an essential transcription factor for spleen organogenesis, are selectively localized in the perifollicular region of the red pulp and are a major source of hematopoietic stem cell factors (31). Thus, many markers of lymphatic and blood vessels may also show diverse immunohistochemical expressions depending on the developmental and hematopoietic neoplastic stages (2-4, 32). Hepatic sinusoidal endothelia separate passenger leukocytes in the sinusoidal lumen from hepatocytes and act as a platform for the adhesion of various liver-resident immune cell populations. Thus, the endothelial cells function as scavengers and pose potent immune function as sentinel cells to detect microbial infection (4, 25). The pancreas showed strikingly different staining patterns between the two staining procedures: frozen sections barely showed LYVE-1 positive pancreatic islets (Figure 2-E) while paraffin sections stained LYVE-1 in islets diffusely and strongly (Figure 2-G). In paraffin-embedded sections, 23 out of 25 cases of Pan-NETs, including non-functioning Pan-NET, metastatic insulinoma in the liver and metastatic gastrinoma in the lymph node, were negative for LYVE-1. Simultaneously, the normal tissues, including pancreatic islets with adjacent lymphatic vessels, hepatic sinusoids, and lymphatic sinusoids, were all positively stained for LYVE-1 (Figure 2-G, -H and -I) (4, 33). In contrast, eight out of 25 Pan-NETs were positively stained for D2-40 (Figure not shown) (34). This strong immunostaining was also observed for staining pancreatic hormones in the paraffin-embedded sections but not in the frozen sections (Figures not shown). LYVE-1 and D2-40 positive staining in islets support that islets are LYVE-1/D2-40 filled endocrine organs, with which islets function as a paracrine endocrine organ in the lymphatic medium since all four pancreatic hormones are interacting with each other by either stimulating or inhibiting the secretion of the other hormones for glucose homeostasis of the whole body. In the paracrine islet system, insulin inhibits glucagon secretion, glucagon stimulates insulin

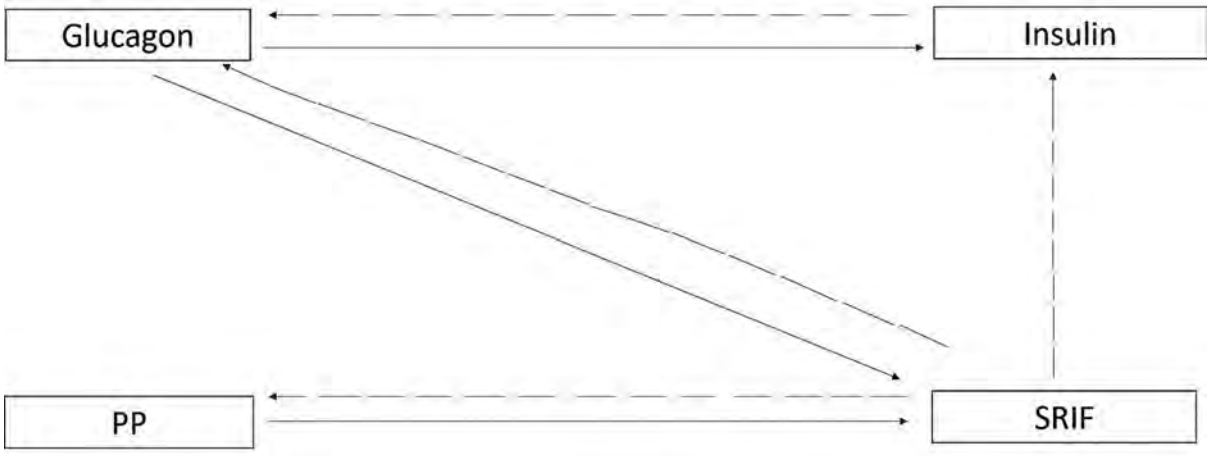

Figure 7. Paracrine System of Four Pancreatic Endocrine Hormones. The solid line with an arrowhead signifies stimulatory effect on the other hormone (s), while the broken line with an arrowhead signifies inhibition on the other hormone (s). For instance, insulin secretion inhibits glucagon secretion while glucagon secretion stimulates insulin secretion. Somatostatin (SRIF) secretion inhibits secretion of the three other hormones secretion and PP secretion inhibits SRIF secretion. From the reference 35 (Tomita, T, Pathol Int. 2002,52(7):425-32).

secretion, somatostatin inhibits insulin, glucagon and pancreatic polypeptide (PP) section, and PP inhibits somatostatin secretion (Figure 7) (35). F-8 immunostaining with frozen sections showed baskets of F-8 positive rich, round capillaries in the islets, showing the presence of numerous, fenestrated capillaries in the endocrine pancreas by this staining (Figure 2-F). Pancreatic islets occupy only 1-2% of the pancreatic tissue volume but receive 10-23% of the entire pancreas' blood supply, which supply rich capillaries in the islets (36, 37).

The intestine was technically difficult to cut good frozen sections, and we used well-fixed paraffin-embedded sections for immunostaining. The colonic sections showed a few lymphatic vessels in lamina propria but showed numerous lymphatic vessels in the submucosa (Figure 3-A). Kennedy et al. reported absent lymphatic vessels in lamina propria of the normal human colon with some lymphatic vessels in most cases with inflammation and neoplasia (12). We believe their negative staining was due to non-optimal preservation of lymphatic vessels in paraffin-embedded colonic tissue. Colon lacks lacteals seen in the small intestine but is well supplied with lymphatic vessels in lamina propria, and the highest densities of lymphatic vessels are found in the submucosa (12). Both lymphatic and blood vessels penetrated longitudinally through the colonic muscle wall to the subserosa (Figure 3-C and -D) (11), through which colonic cancer cells may spread to the pericolonic lymph nodes (38, 39). Blood vessels were abundant in lamina propria and submucosal stroma (Figure 3-B) (12). We observed more non-specific background staining in the routinely paraffin-embedded section than in the frozen sections, as shown in the colonic muscular layers (Figure 3-C and D) (12). Lymphangiogenesis occurs in adult tissue during inflammation, wound healing, and tumorigenesis (2-4). Colonic carcinoma invades through the longitudinal lymphatic vessels through the smooth muscle wall to pericolonic lymph nodes, and some lymphatic vessels are newly formed peritumorous lymphatic vessels (12, 38, 39). The diaphragm prepared longitudinally cut, and the sections showed a few longitudinal LYVE-1 positive lymphatic vessels in the fibrous septum. Simultaneously, there were numerous small capillaries in the outer margin of the striated muscle bundle (Figure 3-E and -F). This rich blood vessel network is thought to be responsible for the hematogenous spread of cancers, especially lung cancers to adrenal glands, which accounts for 40% of metastasis (40). The route of lung cancer metastasizes to the adrenal gland is debated, mainly lymphatic route in the early stage of cancer and mainly hematogenous

spread in the late stage (40). When lung cancer metastasizes through the diaphragm, the hematogenous spread is more likely through the more abundant blood vessels than the less abundant lymphatic vessels (Figure 4-E and -F). Besides, adrenal metastasis is usually in the medulla, not in the adrenal cortex, and is often bilateral. Salivary glands have the highest rate of lymphatic flow per weight of tissues of all regions in the gastrointestinal tract (41) as supported by numerous lymphatic vessels in the gland (Figure 3-G).

The fibrous septum in the thyroid gland contained linear lymphatic vessels and larger round blood vessels (Figure 4-A and -B). These numerous lymphatic vessels and more numerous blood vessels are supported by a classic dye injection study in the dog, in which numerous lymphatic vessels were detected in the fibrous septa (42). The adrenal sub-capsule contains numerous small lymphatic and blood vessels, but few lymphatic vessels in the cortical and medullary parenchymal tissue are described by Merklin (43) (Figure 4-C and -D). The adrenal medulla contains numerous large blood vessels, which emerge from the hilum before forming suprarenal veins and are the site of lung cancer metastasis, bilateral in the rule. When lung cancer metastasizes to the adrenal gland, the cancer cells may reach the medulla via circulating blood through the hilum's blood vessels (44). Kidney and liver tissues showed the most non-specific staining in the frozen sections. The kidney tissue showed a strikingly different distribution of lymphatic vessels and blood vessels: a few lymphatic vessels around the glomeruli and between the tubules (Figure 4-E) (45). Glomerular endothelia were diffusely and densely stained for F-8, suggestive of leaky capillary, while larger blood vessels were stronger stained (Figure 4-F). Thus, we stained fenestrated, leaking glomerular endothelia with F-8 in the frozen sections (Figure 4-F). However, Pusztaszeri et al. reported completely negative staining for F-8 in the glomerular endothelia in the paraffin-embedded sections but were positive for CD31 and CD34 (4). This is one of the major immunostaining differences for F-8 between frozen sections and paraffin-embedded sections. Ishikawa et al. studied formalin-fixed and paraffin-embedded human kidneys fixed and found abundant D2-40 positive lymphatic vessels in the stroma around the interlobular and arcuate arteries few sporadic lymphatic vessels in those around glomeruli and cortical stroma (45). Lymphatic vessels were seldom present in the medulla (45).

The structure and function of cardiac lymphatic vessels are not known. However, the heart's lymphatic vessels consist of terminal lymphatics, of various diameters and lymphatic plexus that drain continuously subendocardial, myocardial and subepicardial areas (46) and regulate lymph transport healing of the infarcted heart (46). There were numerous small, scattered lymphatic vessels and less numerous blood vessels in the ventricular wall in the frozen sections containing pericardial blood vessels (Figure 5-A and -B). Pusztaszeri et al. described capillaries positively stained for CD31 and CD34 with some staining for F-8, but there was no mention of lymphatic vessels in the heart (4). Kambouchner and Bernaudin studied pulmonary lymphatic vessels in the paraffin-embedded human lung using D2-40 as a marker and detected small lymphatic channels within the normal pulmonary lobules, emerging from intralobular stroma, and around small blood vessels constituting the para-alveolar lymphatic vessels (47). With frozen sections, we found numerous lymphatic vessels in the wall of terminal bronchioles, respiratory bronchioles, to alveolar ducts. In contrast, lesser blood vessels were noted in the terminal bronchioles to respiratory bronchioles (Figure 5-C and -D). Adenocarcinomas of the lung arise at the terminal bronchial tree, have easy access to the rich peribronchial lymphatics, and drain into the hilar lymph nodes (48, 49). Alveolar capillaries and arterioles of the lung were reportedly strongly positive for CD31 and CD34 but negative for F-8 (50), reflecting smaller amount of F-8 attached on the subendothelial surface. Small- to large-sized blood vessels were positively stained for F-8 (4). Bronchial arteries supply bronchial trees down to the pulmonary alveolus, however, arterial and venous vessels were not immunostained by F-8 in the periphery of the respiratory bronchioles, likely

due to less amount of F-8 attached in the small vessel and capillary endothelium.

Ovarian sections showed numerous small lymphatic and blood vessels around the Graafian follicle and in the stroma with rich lymphatic vessels and blood vessels (Figure 5-E and -F). Generally, lymphatic vessels were slender while blood vessels were plump with dilated, round lumens (Figure 5-E and -F). The ovaries' lymphatic drainage pathways run via the ovarian and uterine ligaments and ovarian cancer may spread through lymphatic vessels to sentinel nodes, para-aortic and para-internal iliac arteries nodes (51). The prostate showed numerous small lymphatic vessels in the subcapsular and interstitial septa, where there were even more numerous, small blood vessels than lymphatic vessels (Figure 5-G and -H). There were rich nerve fibers in the sub-capsule (Figure 5-G and -H). By double staining for blood vessels and lymphatic vessels, there were numerous CD34 positive blood vessels but only a few LYVE-1 positive lymphatic vessels in the tissues with benign prostatic hyperplasia and prostatic carcinoma, in which the destruction of lymphatic vessels and angiogenesis occurs (52). Peritumoral lymphatic vessels are likely to serve as major conduits for nodal metastasis (53), which spread to the deep branches of internal iliac lymphatic nodes (54). Rich vasculature in the prostate provides access to hematogenous spread of high-grade prostatic cancer, which is found in 35% of autopsy cases, frequently involving bones (90%), lung (46%), and liver (25%) (55).

To study lymphatic vessels in the endometrium is a special technical challenge to pathologists since the definite presence of lymphatic vessels had not been reported using paraffin-embedded tissues: some reported no lymphatic vessels in human endometrium (56-58). Red-Horse et al. used 4% paraformaldehyde-fixed and paraffin-embedded section using LYVE-1 as a lymphatic vessel marker and found no lymphatics in the non-pregnant human uterus (56). Koukourakis et al. studied formalin-fixed and paraffin-embedded human uterus using LYVE-1 and CD31 and found LYVE-1 positive lymphatic vessels in myometrium only (57). Rogers et al. used paraffin-embedded sections of the human endometrium using D2-40, CD31, and F-8 for immunostaining. They reported lymphatic vessels representing 13% of all vessels in functionalis, 43% of basalis, and 28% in the myometrium, respectively, with no difference in staining intensity between functionalis and basalis lymphatic vessels (58). Rogers et al. concluded that lymphatic vessels in functionalis were significantly reduced compared to basalis across the menstrual cycle (58-61). Their photomicrographs showed weakly immunostained lymphatic vessels in the small, limited tissue areas using D2-40 and VEGF-C as lymphatic vessel markers (58-62), which were not to the same degree of staining reported by us using frozen sections (63, 64). These photomicrographs appeared to be taken from the much limited, selectively cherry-picked, positively stained tissue area since there were no large, overview photos of lymphatic vessels at a lower magnification (58-62). Indeed, we had a severe limitation to immunostain lymphatic and blood vessels with routinely processed paraffin-embedded uterine tissues using currently available commercial antibodies. We need better antibodies against these vessels usable for paraffin-embedded tissues of larger than 1 cm^2. The suggestive leaking blood vessels in glomerular capillaries and Day 28 endometrium blood vessels were densely immunostained for F-8 spreading outside the blood vessels. These leaking blood vessels were not observed in the paraffin-embedded sections (58-61). Rogers et al. prompted us to pursue the current study despite the elusiveness of lymphatics presence in the endometrium (58-60). Arterial changes with the menstrual cycle had been well established. However, lymphatic vessels' possible presence remains an enigma, although lymphatic fluid constitutes a few percent of menstrual fluid (58, 62). Using LYVE-1 as a lymphatic vessel marker, we proved that there were also cyclic changes of lymphatic vessels in the endometrium in the menstrual cycle where there were few or no lymphatic vessels in the early proliferative phase functionalis. In contrast, lymphatic vessels proliferated in the later secretory phase, growing from basalis to functionalis, which dilated and burst in

accord with blood vessel bursting during menstruation (63, 64). Thus, the frozen section immunocytochemical staining has validated this method's superiority over paraffin-embedded sections for studying lymphatic and blood vessels. The new findings from frozen sections will eventually shed light on the basic histology and histopathology.

Acknowledgment: I want to express my sincere thanks to Drs. Robert M Brenner and Ov D Slayden who kindly allowed me to use normal organs of rhesus monkey at their research laboratory of the Oregon National Primate Research Center, Beaverton, OR, USA. Their advices and critical comments are highly appreciated, and they prompted me to pursue this study.

Conflict of Interest: The author declares that he has no conflict of interest.

References

1. Kong LL, Yang NZ, Shi LH, Zhao GH, Zhou W, Ding Q, et al. The optimum marker for the detection of lymphatic vessels. Mol Clin Oncol. 2017;7(4):515-20.
2. Müller AM, Hermanns MI, Skrzynski C, Nesslinger M, Müller KM, Kirkpatrick CJ. Expression of the endothelial markers PECAM-1, vWf, and CD34 in vivo and in vitro. Exp Mol Pathol. 2002;72(3):221-9.
3. Scavelli C, Weber E, Aglianò M, Cirulli T, Nico B, Vacca A, et al. Lymphatics at the crossroads of angiogenesis and lymphangiogenesis. J Anat. 2004;204(6):433-49.
4. Pusztaszeri MP, Seelentag W, Bosman FT. Immunohistochemical expression of endothelial markers CD31, CD34, von Willebrand factor, and Fli-1 in normal human tissues. J Histochem Cytochem. 2006;54(4):385-95.
5. Jackson DG, Prevo R, Clasper S, Banerji S. LYVE-1, the lymphatic system and tumor lymphangiogenesis. Trends Immunol. 2001;22(6):317-21.
6. Jackson DG. The lymphatics revisited: new perspectives from the hyaluronan receptor LYVE-1. Trends Cardiovasc Med. 2003;13(1):1-7.
7. Tammela T, Alitalo K. Lymphangiogenesis: Molecular mechanisms and future promise. Cell. 2010;140(4):460-76.
8. Zheng W, Aspelund A, Alitalo K. Lymphangiogenic factors, mechanisms, and applications. J Clin Invest. 2014; 124(3):878-87.
9. Christiansen A, Detmar M. Lymphangiogenesis and cancer. Genes Cancer. 2011;2(12):1146-58.
10. Stacker SA, Williams SP, Karnezis T, Shayan R, Fox SB, Achen MG. Lymphangiogenesis and lymphatic vessel remodelling in cancer. Nat Rev Cancer. 2014;14(3):159-72.
11. Tomita T. Immunocytochemical localization of lymphatic and venous vessels in colonic polyps and adenomas. Dig Dis Sci. 2008;53(7):1880-5.
12. Tomita T. Cancer-associated lymphatic and venous vessels in colonic carcinomas. Open J Pathol. 2014;4(2):101-9.
13. Slayden OD, Koji T, Brenner RM. Microwave stabilization enhances immunocytochemical detection of estrogen receptor in frozen endothelial cells and lymphatic vessels to grow and invade. Cancer Res. 1995;136(6):4012-21.
14. Critchley HO, Kelly RW, Baird DT, Brenner RM. Regulation of human endometrial function: mechanisms relevant to uterine bleeding. Reprod Biol Endocrinol. 2006;4 Suppl 1(Suppl 1):S5.
15. Jabbour HN, Kelly RW, Fraser HM, Critchley HO. Endocrine regulation of menstruation. Endocr Rev. 2006;27(1):17-46.
16. Brenner RM, Slayden OD, Rodgers WH, Critchley HO, Carroll R, Nie XJ, et al. Immunocytochemical assessment of mitotic activity with an antibody to phosphorylated histone H3 in the macaque and human endometrium. Hum Reprod. 2003;18(6):1185-93.
17. Slayden OD, Brenner RM. A critical period of progesterone withdrawal precedes menstruation in macaques. Reprod Biol Endocrinol. 2006;4 Suppl 1(Suppl 1):S6.
18. Cao W, Mah K, Carroll RS, Slayden OD, Brenner RM. Progesterone withdrawal upregulates fibronectin and integrins during menstruation and repair in the rhesus macaque endometrium. Hum Reprod. 2007;22(12):3223-31.
19. Giorno R. Unusual structure of human splenic sinusoids revealed by monoclonal antibodies. Histochemistry. 1984;81(5):505-7.
20. Jønsson V. Comparison and definition of spleen and lymph node: a phylogenetic analysis. J Theor Biol. 1985;117(4):691-9.
21. Borch WR, Aguilera NS, Brissette MD, O'Malley DP, Auerbach A. Practical Applications in Immunohistochemistry: An Immunophenotypic Approach to the Spleen. Arch Pathol Lab Med. 2019;143(9):1093-105.
22. Mouta Carreira C, Nasser SM, di Tomaso E, Padera TP, Boucher Y, Tomarev SI, et al. LYVE-1 is not restricted to the lymph vessels: expression in normal liver blood sinusoids and down-regulation in human liver cancer and cirrhosis. Cancer Res. 2001;61(22):8079-84.
23. Strauss O, Phillips A, Roggiero K, Barlett A. Immunofluorescence identifies distinct subsets of endothelial cells in the human liver. Sci Rep. 2017;17:44356.
24. Do H, Healey JF, Waller EK, Lollar P. Expression of factor VIII by murine liver sinusoidal endothelial cells. J Biol Chem. 1999;274(28):19587-92.
25. Knolle PA, Wohlleber D. Immunological functions of liver sinusoidal endothelial cells. Cell Mol Immunol. 2016;13(3):347-53.
26. Hollestelle MJ, Thinnes T, Crain K, Stiko A, Kruijt JK, van Berkel TJ, et al. Tissue distribution of factor VIII

gene expression in vivo--a closer look. Thromb Haemost. 2001;86(3):855-61.

27. Tsamandas AC, Jain AB, Raikow RB, Demetris AJ, Nalesnik MA, Randhawa PS. Extramedullary hematopoiesis in the allograft liver. Mod Pathol. 1995;8(6):671-4.
28. Kim CH. Homeostatic and pathogenic extramedullary hematopoiesis. J Blood Med. 2010;1:13-9.
29. Yamamoto K, Miwa Y, Abe-Suzuki S, Abe S, Kirimura S, Onishi I, et al. Extramedullary hematopoiesis: Elucidating the function of the hematopoietic stem cell niche (Review). Mol Med Rep. 2016;13(1):587-91.
30. Tefferi A. Primary myelofibrosis: 2013 update on diagnosis, risk-stratification, and management. Am J Hematol. 2013;88(2):141-50.
31. Oda A, Tezuka T, Ueno Y, Hosoda S, Amemiya Y, Notsu C, et al. Niche-induced extramedullary hematopoiesis in the spleen is regulated by the transcription factor Tlx1. Sci Rep. 2018;8(1):8308.
32. Negrini D, Moriondo A. Lymphatic anatomy and biomechanics. J Physiol. 2011;589(Pt 12):2927-34.
33. Tomita T. Lymphatic vessel endothelial hyaluronan receptor 1 immunocytochemical staining for pancreatic islets and pancreatic endocrine tumors. Pancreas. 2007;35(4):e18-22.
34. Tomita T. D2-40 immunocytochemical staining for pancreatic islets and pancreatic endocrine tumors. Pancreas. 2009;38(3):339-40.
35. Tomita T. New markers for pancreatic islets and islet cell tumors. Pathol Int. 2002;52(7):425-32.
36. Jansson L, Barbu A, Bodin B, Drott CJ, Espes D, Gao X, et al. Pancreatic islet blood flow and its measurement. Ups J Med Sci. 2016;121(2):81-95.
37. Diez JA, Arrojo E Drigo R, Zheng X, Stelmashenko OV, Chua M, Rodriguez-Diaz R, et al. Pancreatic Islet Blood Flow Dynamics in Primates. Cell Rep. 2017;20(6):1490-501.
38. Kenney BC, Jain D. Identification of lymphatics within the colonic lamina propria in inflammation and neoplasia using the monoclonal antibody D2-40. Yale J Biol Med. 2008;81(3):103-13.
39. Alexander JS, Ganta VC, Jordan PA, Witte MH. Gastrointestinal lymphatics in health and disease. Pathophysiology. 2010;17(4):315-35.
40. Milovanovic IS, Stjepanovic M, Mitrovic D. Distribution patterns of the metastases of the lung carcinoma in relation to histological type of the primary tumor: An autopsy study. Ann Thorac Med. 2017;12(3):191-8.
41. Gordon SD. Lymphatic system of the thyroid gland. Can Med Assoc J. 1931;25(1):46-8.
42. Aiyama S, Kikuchi K, Takada K, Ikeda R, Sato S, Kuroki J. Immunohistochemical study of the lymphatic vessels in major salivary glands of the rat. Okajimas Folia Anat Jpn. 2011;87(4):177-80.
43. Merklin RJ. Suprarenal gland lymphatic drainage. Am J Anat. 1966;119(3):359-74.
44. Bazhenova L, Newton P, Mason J, Bethel K, Nieva J, Kuhn P. Adrenal metastases in lung cancer: clinical implications of a mathematical model. J Thorac Oncol. 2014;9(4):442-6.
45. Ishikawa Y, Akasaka Y, Kiguchi H, Akishima-Fukasawa Y, Hasegawa T, Ito K, et al. The human renal lymphatics under normal and pathological conditions. Histopathology. 2006;49(3):265-73.
46. Ratajska A, Gula G, Flaht-Zabost A, Czarnowska E, Ciszek E, Jankowska-Steifer E, et al. Comparative and developmental anatomy of cardiac lymphatics. Sci World J. 2014:183170.
47. Huang L-H, Lavine KJ, Randolph GJ. Cardiac lymphatic vessels, transport, and healing of the infarcted heart. JACC Basic Transl Sci. 2017;2(4):477-83.
48. Bennett DE, Sasser WF, Ferguson TB. Adenocarcinoma of the lung in men. A clinicopathologic study of 100 cases. Cancer. 1969;23(2):431-9.
49. Mori M, Andersson CK, Graham GJ, Löfdahl CG, Erjefält JS. Increased number and altered phenotype of lymphatic vessels in peripheral lung compartments of patients with COPD. Respir Res. 2013;14(1):65.
50. Kambouchner M, Bernaudin JF. Intralobular pulmonary lymphatic distribution in normal human lung using D2-40 antipodoplanin immunostaining. J Histochem Cytochem. 2009;57(7):643-8.
51. Kleppe M, Kraima AC, Kruitwagen RF, Van Gorp T, Smit NN, van Munsteren JC, et al. Understanding lymphatic drainage pathways of the ovaries to predict sites for sentinel nodes in ovarian cancer. Int J Gynecol Cancer. 2015;25(8):1405-14.
52. Trojan L, Michel MS, Rensch F, Jackson DG, Alken P, Grobholz R. Lymph and blood vessel architecture in benign and malignant prostatic tissue: lack of lymphangiogenesis in prostate carcinoma assessed with novel lymphatic marker lymphatic vessel endothelial hyaluronan receptor (LYVE-1). J Urol. 2004;172(1):103-7.
53. Zeng Y, Opeskin K, Horvath LG, Sutherland RL, Williams ED. Lymphatic vessel density and lymph node metastasis in prostate cancer. Prostate. 2005;65(3):222-30.
54. Swanson GP, Hubbard JK. A better understanding of lymphatic drainage of the prostate with modern imaging and surgical techniques. Clin Genitourin Cancer. 2013;11(4):431-40.
55. Bubendorf L, Schöpfer A, Wagner U, Sauter G, Moch H, Willi N, et al. Metastatic patterns of prostate cancer: an autopsy study of 1,589 patients. Hum Pathol. 2000;31(5):578-83.
56. Red-Horse K, Rivera J, Schanz A, Zhou Y, Winn V, Kapidzic M, et al. Cytotrophoblast induction of arterial apoptosis and lymphangiogenesis in an in vivo model of human placentation. J Clin Invest. 2006;116(10):2643-52.

57. Koukourakis MI, Giatromanolaki A, Sivridis E, Simopoulos C, Gatter KC, Harris AL, et al. LYVE-1 immunohistochemical assessment of lymphangiogenesis in endometrial and lung cancer. J Clin Pathol. 2005;58(2):202-6.
58. Rogers PA, Donoghue JF, Girling JE. Endometrial lymphangiogensis. Placenta. 2008;29 Suppl A:S48-54.
59. Girling JE, Rogers PA. The endometrial lymphatic vasculature: function and dysfunction. Rev Endocr Metab Disord. 2012;13(4):265-75.
60. Donoghue JF, Lederman FL, Susil BJ, Rogers PA. Lymphangiogenesis of normal endometrium and endometrial adenocarcinoma. Hum Reprod. 2007;22(6):1705-13.
61. Rogers PA, Donoghue JF, Walter LM, Girling JE. Endometrial angiogenesis, vascular maturation, and lymphangiogenesis. Reprod Sci. 2009;16(2):147-51.
62. Critchley HO, Maybin JA. Molecular and cellular causes of abnormal uterine bleeding of endometrial origin. Semin Reprod Med. 2011;29(5):400-9.
63. Tomita T, Mah K. Cyclic changes of lymphatic and venous vessels in human endometrium. Open J Pathol. 2014;4(4):194-205.
64. Tomita, T, Mah, K. Lymphatic vessels in the human endometrium: Are they present or absent? J Clin Exp Pathol 2015;5(4):100241.

Narrative Review
Acta Medica Academica 2021;50(1):29-46
DOI: 10.5644/ama2006-124.324

Molecular Diagnostics of Adult Gliomas in Neuropathological Practice

Sebastian Brandner

Department of Neurodegenerative Disease, UCL Queen Square Institute of Neurology and Division of Neuropathology, the National Hospital for Neurology and Neurosurgery, University College London Hospitals NHS Foundation Trust, London WC1N 3BG, United Kingdom

Correspondence: *s.brandner@ucl.ac.uk*; Tel.: + 44 20 3448 4435

Received: 15 November 2020; **Accepted:** 25 November 2020

Abstract
This review focuses on adult gliomas, highlighting the most relevant biomarkers in the diagnosis of these tumours and the use of DNA methylation arrays to complement conventional molecular diagnostic techniques. The discovery and characterisation of diagnostic and prognostic biomarkers in brain tumours has significantly changed the neuropathological landscape over the last decade. These include mutations in the IDH1 and IDH2 genes in astrocytomas and oligodendrogliomas, histone H3 K27M mutations in midline gliomas, or BRAF mutations in a range of low-grade and high-grade glial and glioneuronal tumours. Other biomarkers of relevance are mutations in the TERT promoter, the ATRX gene, and genomic alterations such as 1p/19q codeletion, EGFR amplification, and chromosome 7 gain and 10 loss. The development of DNA methylation profiling and algorithmic classification of brain tumours has further enhanced the diagnostic abilities of neuropathologists. Methylation profiling is particularly useful for the diagnostic workup of biopsies with an inconclusive molecular test results, small samples, or samples with indistinctive low-grade or high-grade histology. This technology has become indispensable for the risk stratification of ependymal tumours, medulloblastomas and meningiomas. **Conclusion.** This review highlights the importance of an integrated approach to brain tumour diagnostics and gives a balanced view of the relevance and choice of conventional and molecular techniques in the workup of adult gliomas in diagnostic neuropathology practice.

Key Words: DNA Methylation Profiling ▪ Isocitrate Dehydrogenase ▪ TERT Promoter Mutation ▪ EGFR Amplification ▪ 1p/19q Codeletion.

Introduction

The last 10 years have seen a fundamental paradigm shift in brain tumour diagnostics. The most significant discoveries were (i) the identification of mutations in the isocitrate dehydrogenase (IDH) genes 1 and 2 in astrocytomas and oligodendrogliomas (1), (ii) proto-oncogene B-Raf murine sarcoma viral oncogene homolog B (BRAF) mutations in a range of low-grade glial and glioneuronal tumours (2), (iii) histone H3 K27M mutations in pontine gliomas (3) and a subsequent discovery of this mutation in diffuse gliomas along multiple midline locations (4), (iv) the definition of molecular features to diagnose IDH-wildtype glioblastomas, specifically gains of chromosome 7, loss of chromosome 10, epidermal growth factor receptor (EGFR) amplification and telomerase reverse transcriptase (TERT) promoter mutation (5). Also, rarer diagnostic entities were subsequently described, such as histone H3 G34R/V-mutant high-grade gliomas which are clinically and biologically distinct from H3 K27M-mutant tumours (6). The introduction of DNA methylation profiling has led to a further progress in the way neuropathologists approach diagnosis and prognostication of a wide range of adult and paediatric CNS tumours (7-10). This review focuses on biomarker-led classification of gliomas in adults. It is the aim of this review to provide guidance for an evidence-based, practical approach to diagnose intrinsic adult brain tumours using conventional molecular tests and methylation array profiling.

Methodologies for Integrated Histo-Molecular Diagnosis

Immunohistochemical Stainings remain the diagnostic mainstay of histopathology laboratories. Whilst traditionally a range of lineage markers such as glial fibrillary acidic protein (GFAP) (11), S100 (12), synaptophysin (13), cytokeratins (14), or CD (cluster of differentiation) antigens (15) provided helpful guidance to pathologists to determine the lineage of neoplasms, they have not allowed for a refined classification or diagnostic

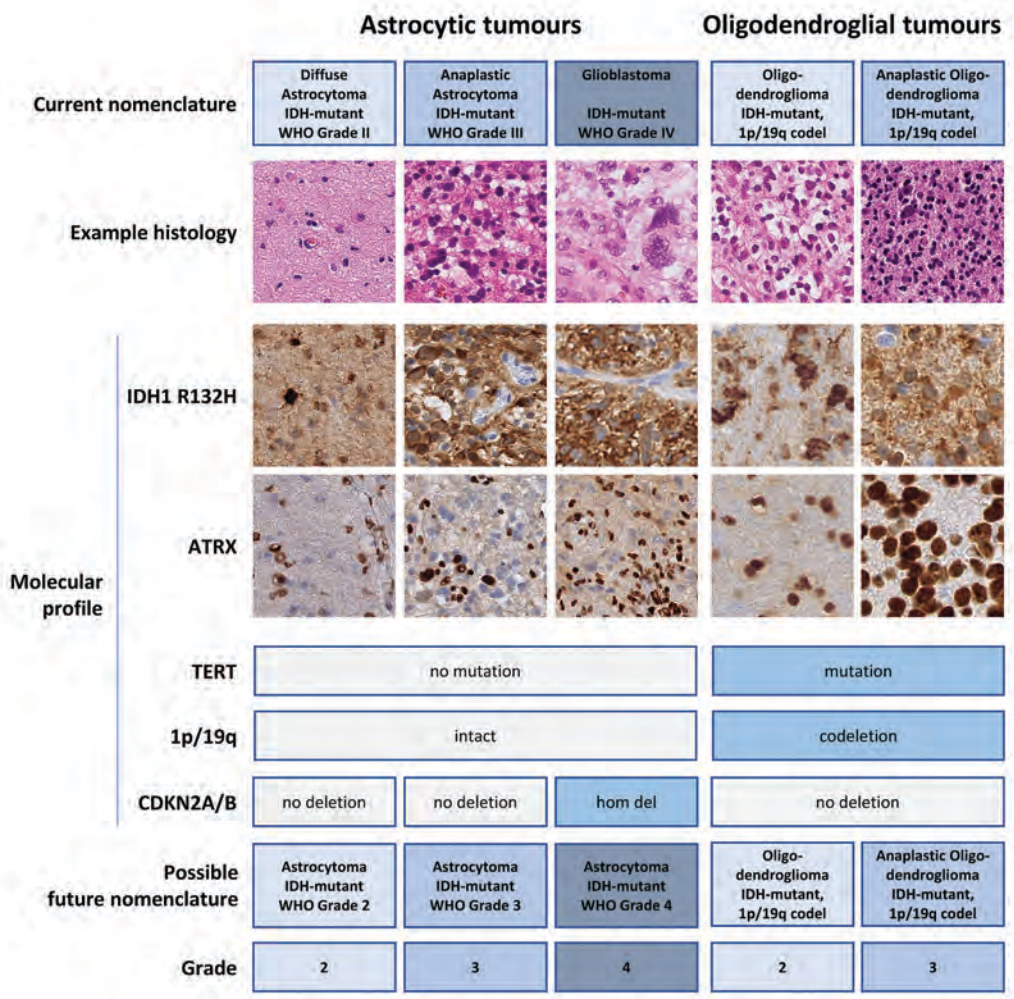

Figure 1. Histology and Molecular Pathology of IDH-mutant Gliomas. The left part of the panel shows the three malignancy grades of IDH-mutant astrocytomas (Grades II, III, IV) and the right part of the two malignancy grades of oligodendrogliomas (Grades II and III). Top row, current nomenclature comprising astrocytoma, anaplastic astrocytoma and glioblastoma, IDH-mutant, and oligodendroglioma and anaplastic oligodendroglioma IDH-mutant and 1p/19q codeleted. The second row shows typical histologies representative of the tumour types and grades. The third row shows the most common IDH mutation (IDH1 R132H) detected by immunostaining. For complete workup however tumours negative for this mutation should be followed up by sequencing. The other relevant diagnostic marker is the expression of ATRX. In most IDH-mutant astrocytic tumours, nuclear ATRX expression is lost in tumour cells but retained in endothelial cells, and non-neoplastic cells of the underlying CNS. The boxes below show the typical molecular profiles. TERT promoter mutation and ATRX mutation are mutually exclusive, thus non-mutant in astrocytomas and mutant in oligodendrogliomas. TERT promoter sequencing can therefore be useful in a small number of IDH-mutant astrocytomas where ATRX protein is retained in tumour cell nuclei despite a gene mutation. 1p/19q is by definition intact in astrocytomas and co-deleted in oligodendrogliomas (28). CDKN2A/B is a prognostically relevant in IDH-mutant astrocytomas (29). Bottom rows: proposed grading and prognostication of IDH-mutant gliomas, adapted from the proposed grading schemes (28, 29, 86).

stratification of tumours arising from progenitors of the central nervous system. For example, GFAP is expressed not only in mature astrocytes but also in a wide range of neural stem and progenitor cells (16). GFAP is expressed in multiple types of glial or glioneuronal tumours (11) and therefore can give only a first indication of the lineage of a tumour but does not allow further prognostication. The discovery of pathogenic and diagnostic point mutations led to the development of mutation-specific antibodies, for example against IDH1 R132H (17), BRAF V600E (18, 19), or histone H3 K27M (4), enabling rapid and reliable identification of these mutations and subsequent classification, grading and thus, prognostication (Figure 1, 4). Other immunostainings to detect diagnostically relevant biomarkers are alpha-thalassemia X-linked mental retardation (ATRX) in a range of tumours of the CNS (Figure 1, 4) and elsewhere, or INI1/SMARCB1 to identify loss of nuclear expression due to an inactivating mutation for example in atypical teratoid/rhabdoid tumour (AT/RT) (20, 21).

Fluorescent or Chromogenic in Situ Hybridisation (FISH, CISH) have been used for several decades to identify copy number changes (such as EGFR amplification, 1p/19q codeletion, MYC amplification) on tissue sections. For that reason, these techniques are popular with pathologists as the sample can be analysed microscopically. Probes are usually expensive and with the decreasing cost of parallel sequencing technologies they gradually become economically less viable, but remain important methods in departments where next generation sequencing is not available.

Sanger Sequencing is an economical and highly informative test for those mutations that cannot be detected with a mutation-specific antibody. For example, the TERT promoter mutation (Figure 1), diagnostically relevant in IDH-mutant oligodendrogliomas, IDH-wildtype glioblastomas (Figure 3) and prognostically relevant in meningiomas, can only be detected by DNA-based methods. Whilst an antibody can be used to detect the most common IDH mutation (IDH1 R132H, Figure 1), the remaining 10% can only be detected with Sanger sequencing of the IDH1 the IDH2 genes.

Multiplex Ligation -Dependent Probe Amplification (MLPA) is a PCR-based technology requiring a thermocycler and capillary electrophoresis equipment and is thus an economical alternative to next-generation sequencing but has the disadvantage of a lack of flexibility. The disadvantage of MLPA assays is that they are pre-developed and require major validation steps following modification.

Next Generation Sequencing **(NGS)** is based on the Sanger sequencing technology and results in single-base readout. It covers millions of fragments in parallel (thus often referred to as (massive) parallel sequencing). The advantage of this technology is the generation of a wealth of information on multiple genes, but it requires infrastructure for data storage and the knowledge to read and interpret the substantial datasets. The generation of NGS data requires expensive equipment in core facilities.

Methylation Arrays interrogate methylation on CpG sites and return datasets that have been used to develop a methylation-based classification tool. DNA methylation is a form of an epigenetic change, which can be considered as surrogate markers for a combination of a cell of origin (reflecting location and time) and a mutation. These methylation profiles can be interrogated by machine learning algorithms and have led to the definition of methylation classes. These methylation classes partly overlap with histological tumour types defined by the WHO classification, but for some tumours, entirely distinct methylation classes have been defined and novel tumour entities have emerged (7-10). This approach will significantly influence the upcoming edition of the WHO 2020/2021 classification. The technology requires commercial micro-array chips (currently Illumina 850k EPIC arrays), a laboratory setup to perform bisulfite conversion of DNA and a relatively expensive chip reader. A widely used analysis platform is hosted by the German Cancer Research Centre (DKFZ) www.molecularneuropathology.org and can currently be accessed free of charge.

IDH-Mutant Gliomas: Oligodendrogliomas and Astrocytic Tumours

Mutations in the IDH1 and IDH2 genes were discovered in the context of a whole-genome sequencing study on glioblastoma (1, 22). Mutations in the IDH1 gene were identified small subgroup of what was known at the time as "secondary GBM", i.e. arising from lower grade astrocytomas. Subsequently, large cohorts of astrocytomas, oligodendrogliomas and the now discontinued oligoastrocytoma were sequenced for the presence of IDH1

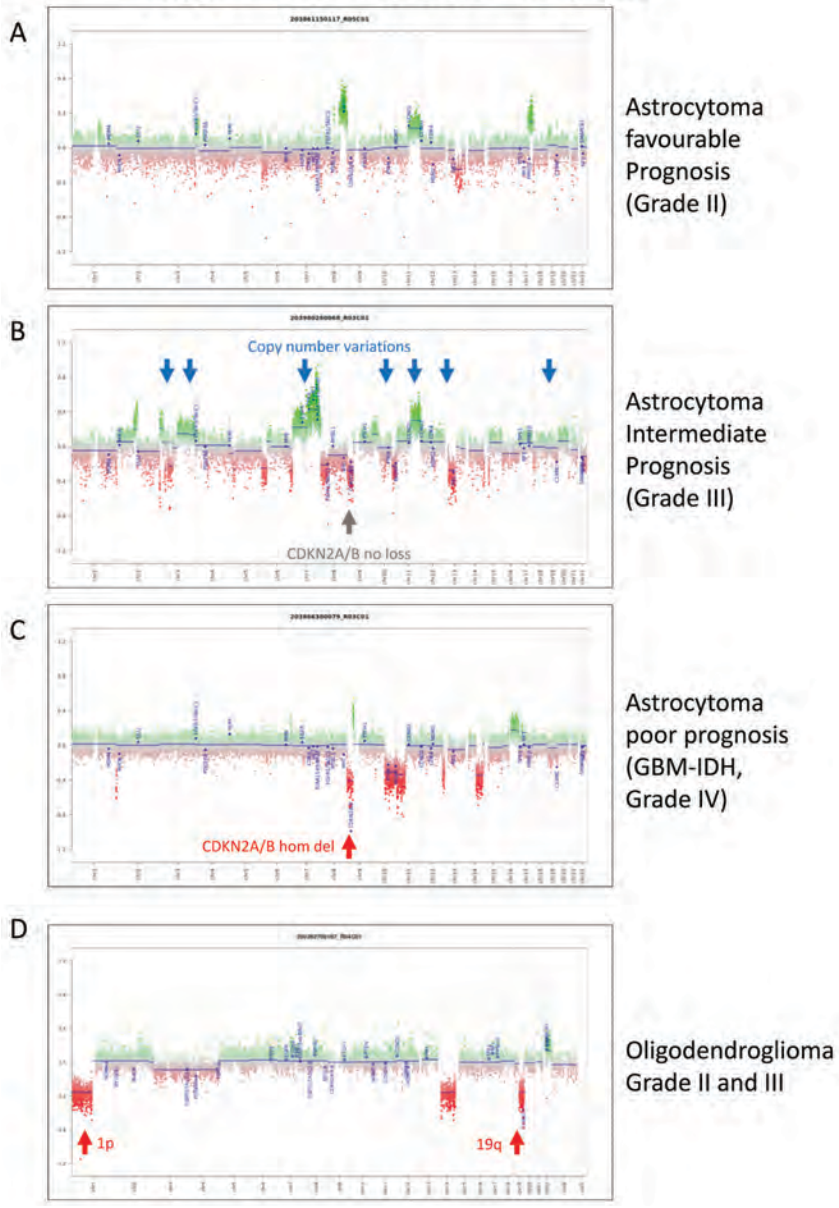

Figure 2. Copy Number Profiles of IDH-mutant Gliomas. A, relatively flat copy number profile of low-grade IDH-mutant astrocytomas. B, multiple copy number changes with multiple gains and losses, but no CDKN2A/B deletion are indicative of a higher recurrence risk (29). C, the presence of a CDKN2A/B homozygous deletion indicates a high recurrence risk, regardless of the presence of microvascular proliferations and necrosis (29). D, Oligodendrogliomas are characterised by the characteristic 1p/19q codeletion. Additional copy number alterations can occur but there is no established molecular profile discriminating grade II from grade III. Currently, oligodendrogliomas are distinguished from anaplastic oligodendroglioma by morphological criteria.

and IDH2 mutations (9, 23). Importantly, it was soon established that 1p/19q-codeleted oligodendrogliomas were invariably IDH-mutant, leading to the subsequent definition of the "oligodendroglioma, IDH-mutant and 1p/19q-codeleted" as diagnostic entity (24) (Figure 1, 2). The remainder of IDH-mutant gliomas had an astrocytic morphology, and it was soon established that the concomitant loss of ATRX expression was a defining feature of astrocytomas (24) (Figure 1). Importantly, the previously known group of oligoastrocytoma could be resolved into either oligodendroglioma or astrocytoma, and thus the diagnosis of oligoastrocytoma has been discontinued (25, 26). As a result, two major IDH-mutant tumour types exist, oligodendroglioma with IDH mutation, 1p/19q codeletion and TERT promoter mutation (27), and the astrocytoma with IDH mutation, ATRX mutation and p53 mutation (28) (Figure 1). The distinction of oligodendroglioma from the anaplastic oligodendroglioma still relies on the identification of morphological features (microvascular proliferations, brisk mitotic activity, necrosis). IDH-mutant astrocytomas can be further stratified not only by histological features but also by the presence of homozygous loss of cyclin-dependent kinase inhibitor 2A/B (CDKN2A/B) (29, 30) (Figure 2). The presence of this mutation is a better predictor of survival than the presence of microvascular proliferations or necrosis. This results in a proposed histo-molecular grading scheme for IDH-mutant astrocytomas ranging from grade II to grade IV. It has been recommended to phase out the term IDH-mutant glioblastoma and to replace it with astrocytoma grade IV to indicate a distinctive biological class of brain tumours (28). Figure 1 illustrates the diagnostic algorithm and grading scheme in IDH-mutant gliomas.

IDH-Wildtype Gliomas: The Spectrum of Glioblastomas and Their Precursors

The glioblastoma multiforme (GBM) is the most common malignant brain tumour in adults. The designation as IDH-wildtype glioblastoma was established in parallel to the distinction of the IDH-mutant counterparts (31). Subsequently, it was discovered that not all glioblastomas present histologically with high-grade features at the time of diagnosis (Figure 3). Instead, it was recognised that many tumours that presented clinically and histologically as diffuse astrocytomas in fact were early forms of glioblastoma (32). This recognition was based on the presence of characteristic diagnostic features such as a combination of a TERT promoter mutation, EGFR amplification, chromosome 7 gain, chromosome 10 loss, in the absence of an IDH mutation (8) (Figure 3). Ultimately, this recognition has led to a recommendation by the cIMPACT-NOW consortium to identify all tumours with some or all of the above features as glioblastoma, IDH-wild-type, regardless of the histological appearance (33).

Histone-Mutant Gliomas

These gliomas are defined by specific mutations, histone H3 K27M or histone H3 G34R. These two mutations are associated with entirely distinct clinical, imaging, histological and molecular features (Figure 4). H3 K27M mutations were described in two large studies (3, 34), which triggered subsequent research into chromatin modifiers in brain tumour pathogenesis (34) and led to the identification of potential therapeutic targets (35, 36). Initially the H3 K27M mutation was identified in diffuse infantile pontine gliomas (DIPG) but with the commercial availability of mutation-specific antibodies (Figure 4A), and the recognition that these tumours are located in midline structures of the central nervous system (spinal cord, pons, thalamus) these tumours were increasingly found also in adults (37). One important recognition is the association of the K27M mutation with midline location and poor clinical outcome, thus mandating a WHO grade IV for H3 K27M midline gliomas (38). However, rarely also other intrinsic tumour types, specifically ependymoma, ganglioglioma or pilocytic astrocytoma can carry an H3 K27M mutation but are explicitly excluded from the grading and typing scheme of H3 K27M-mutant midline gliomas (39-41).

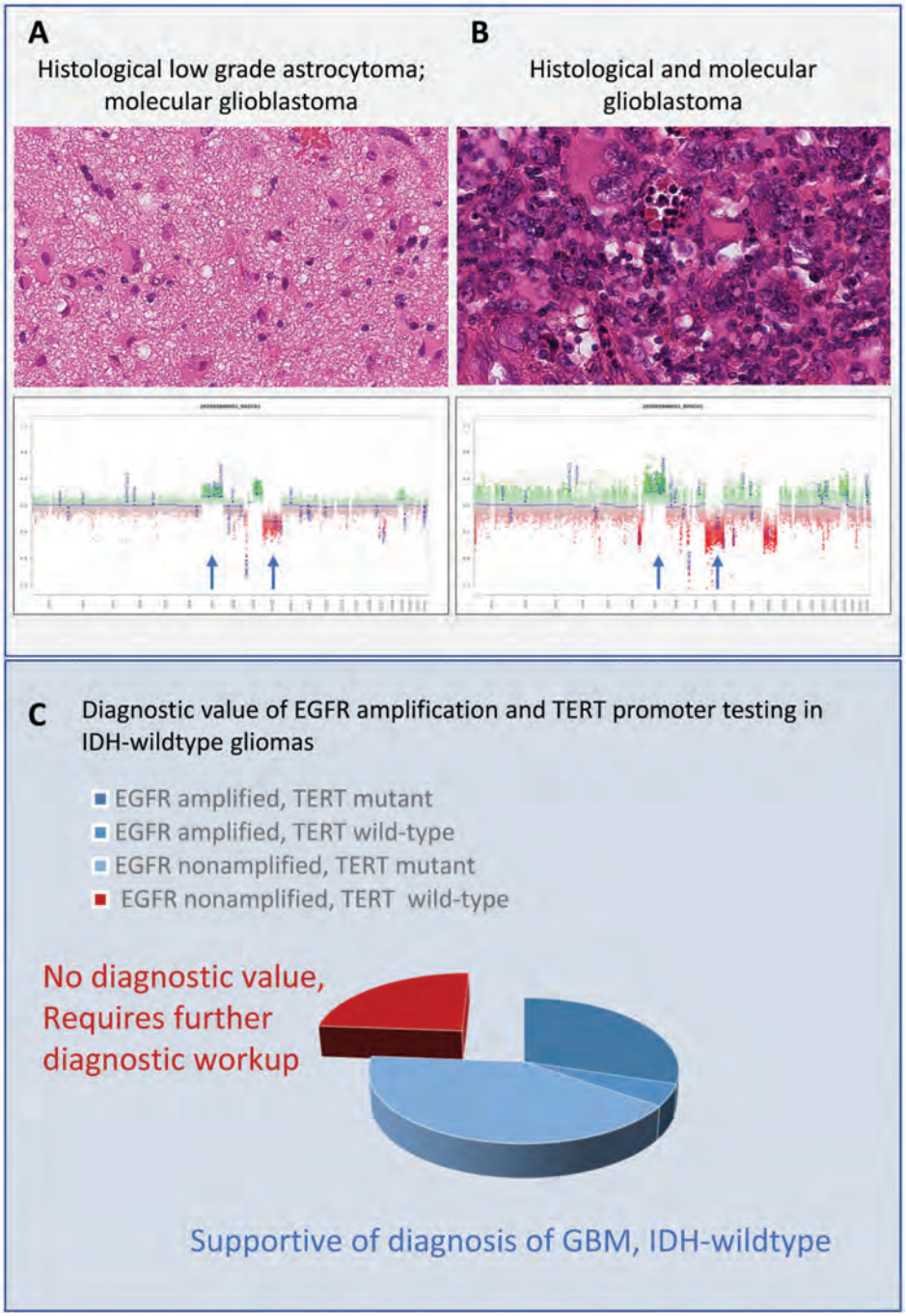

Figure 3. Histological Presentation of IDH-wildtype Glioblastomas Can Vary Significantly. A, in this example the histological features are those of a diffuse low-grade glioma and only molecular testing (for example EGFR amplification, TERT promoter mutation, and/or detection of chromosome 7 gain and chromosome 10 loss) can ascertain the diagnosis of a glioblastoma, IDH-wildtype (33). B, example of glioblastoma with histological high-grade presentation and characteristic copy number changes (7p gain, 10q loss). Both glioblastomas show a CDKN2A/B homozygous deletion which however have no prognostic value in this tumour entity. C, the majority of glioblastomas can be diagnosed by the presence of EGFR amplification and or TERT promoter mutation. If neither TERT promoter mutation nor EGFR amplification can be identified in an IDH-wildtype glioma, further diagnostic tests (copy number profile (A, B), methylation array or next-generation sequencing should be performed in particular for those tumours presenting with histological low-grade features (32).

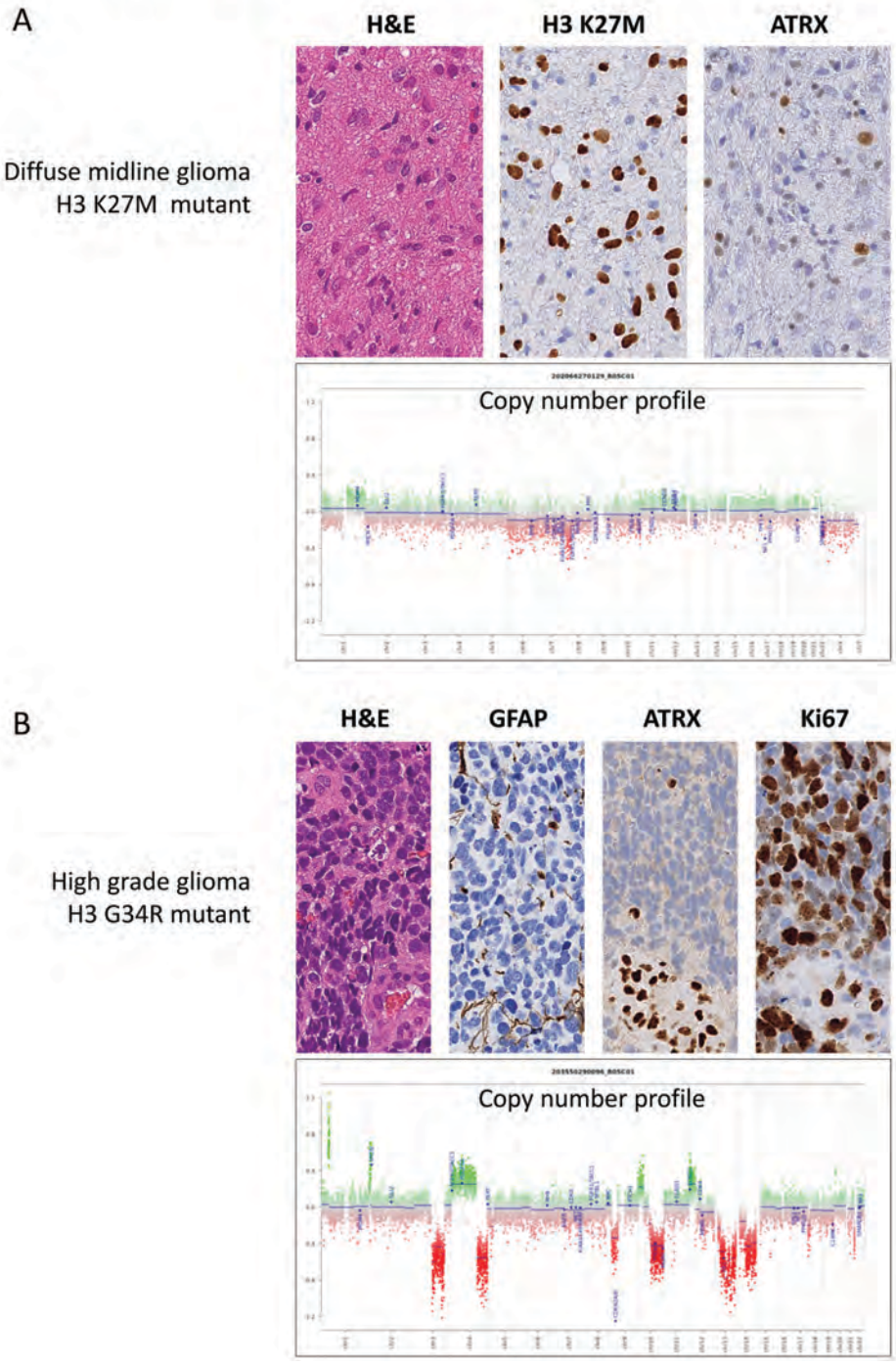

Figure 4. Histone Mutant Gliomas Comprise two Biologically, Clinically and Histologically Distinct Entities. A, the H3 K27M-mutant glioma presents as diffuse astrocytoma, often with no apparent high-grade features. The morphology is that of diffuse glioma but the use of the antibody against the H3 K27M mutation allows reliable diagnosis of these tumours (38). A proportion of these tumours show ATRX loss. Resident endothelial and glial cells show retained ATRX expression. B, the H3 G34R (rarely also G34V) mutant glioma shows a very high cellularity, usually very little or no GFAP expression and a loss of ATRX expression in tumour cells. The remaining positive nuclei are those of endothelial cells. Ki67 labelling indicates the extremely high proliferation of these tumours. In contrast to the K27M-mutant tumours, G34R-mutant gliomas are hemispheric.

Gliomas with H3 G34R/V mutations have discrete clinical presentations (age, location, survival) and molecular features (methylation profiles, expression signatures, and mutational profiles), suggesting that they are arising from a different cell of origin and are essentially distinct diseases (42, 43) (Figure 4B). An important clinical difference to H3 K27M-mutant gliomas is the presentation as hemispheric, often well demarcated primitive tumours (6), but occasionally a diffusely infiltrative hemispheric lesions encompassing multiple lobes, a feature previously referred to as gliomatosis cerebri.

Glial and Glioneuronal Tumours with MAP-Kinase and MYB/MYBL Alterations

The recognition of alterations in the MAP kinase pathway, predominantly through mutations of BRAF, and other MAP kinase pathway members has had some diagnostic benefit, but more importantly also therapeutic implications. The detection of a BRAF mutation is diagnostically helpful, but does not define a specific tumour entity (Figure 5). Approximately 60% of pleomorphic xanthoastrocytoma, 30% of ganglioglioma (a range between 10%-60% has been reported, depending on age and anatomic location of the tumour (44)), and less than 5% of pilocytic astrocytomas carry a BRAF V600E mutation, which therefore is diagnostically neither specific nor is the absence of the mutation informative (Figure 5). Importantly, the detection of a BRAF V600E mutation is also not predictive of the prognosis, as it can occur in a wide range of tumours with low recurrence risk (gangliogliomas), intermediate recurrence risk (pleomorphic xanthoastrocytoma), or high recurrence risk (anaplastic pleomorphic xanthoastrocytoma with CDKN2A/B homozygous deletion which may histologically overlap with the epithelioid GBM).

Gangliogliomas (Figure 5A) often present with a long-standing history of seizures. They grow relatively well demarcated, are occasionally calcified and are composed of dysplastic neuronal and glial cells. Gangliogliomas are characterised by alterations of the MAP kinase pathway showing BRAF, KRAS, RAF1, NF1, FGFR1, or FGFR2 mutations as pathogenic alterations (44, 45). Ganglioglioma correspond to WHO grade I. They can show some morphological overlap with other low-grade glioneuronal tumours, for example pleomorphic xanthoastrocytoma or DNET (46).

Pleomorphic Xanthoastrocytomas (PXA) (Figure 5B) most commonly affect children and young adults, but also can occur in patients in their 40s-60s. These tumours often grow superficially and can form a cyst. Histologically, they may show a highly heterogenous picture with formation of giant astrocytes which can be lipidised (xanthomatous). PXA express GFAP and often also neuronal lineage markers such as neurofilaments and occasionally synaptophysin. The homozygous deletion of CDKN2A/B is a negative prognostic factor associated with more rapid recurrence (47). The detection of the BRAF mutation in PXA (described in up to 60% (2)) is essential to provide guidance to oncologists for treatment options with BRAF antagonists, such as Vemurafinib or Dabrafenib (48, 49).

Pilocytic Astrocytomas (Figure 5C) are most commonly located in the posterior fossa (cerebellum) but hemispheric and midline forms exist. Morphologically, these forms are indistinguishable, but exhibit distinct methylation pattern which can be determined by methylation array analysis. For posterior fossa pilocytic astrocytoma, the most common molecular alteration is the fusion of BRAF with the KIAA 1549 gene (3 common breakpoints KIAA1549:BRAF exons 15:9, 16:11, 16:9 (50) and rarely 15:11 and 17:10 (51)). A large molecular study on more than 100 pilocytic astrocytomas showed additional alterations in other components of the MAP-kinase pathway , such as FGFR1, NTRK2, NF1, KRAS and PTPN11 (52). Amongst the group of pilocytic astrocytomas, there are three molecularly (mostly epigenetic) distinct types, with location in the cerebellum, midline and forebrain hemispheric (53). A separate biological entity with frequent loss of ATRX expression and CDKN2A/B homozygous deletion had previously been termed anaplastic astrocytoma with piloid features (Figure 5E) and the diagnosis of "High-grade astrocytoma with pi-

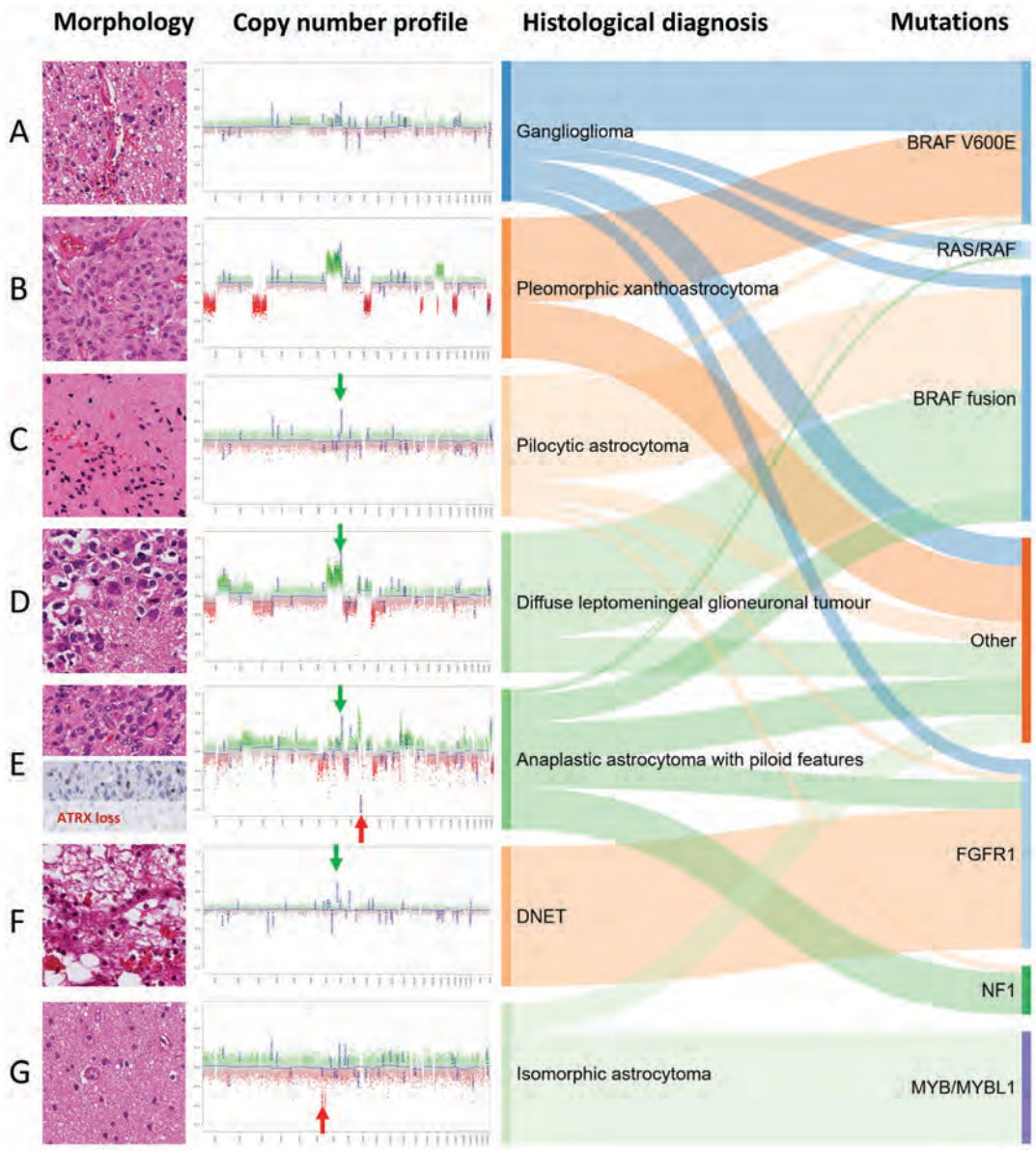

Figure 5. Morphology, Copy Number Profile and Frequently Associated Mutations in a Range of Glial and Glioneuronal Tumours. Tumour location and their association with certain mutations are helpful in the differential diagnosis of these tumour classes. **A**, the ganglioglioma has a characteristic morphology, a flat copy number profile and frequently a BRAF V600E mutation. **B**, the pleomorphic xanthoastrocytoma has a characteristic histology but transitional forms with similarities to gangliogliomas exist and can be resolved by methylation array analysis. The copy number profile typically shows some variability. The majority of PXA has a BRAF V600E mutation. **C**, the pilocytic astrocytoma has a BRAF duplication (fusion) in more than 70% of cases, which can be detected in the copy number profile or with specific fusion tests (50, 61). The remainder of the pilocytic astrocytomas have other MAP kinase pathway alterations. **D**, the rare diffuse leptomeningeal glioneuronal tumour has a BRAF fusion and a 1p deletion, sometimes also 1p/19q codeletion, but strictly without IDH mutation, which discriminates it from the oligodendroglioma. **E**, a relatively recently established tumour class is the anaplastic astrocytoma with piloid features, characterised by BRAF fusion, CDKN2A/B homozygous deletion and frequent ATRX loss (54). **F**, The dysembryoplastic neuroepithelial tumour (DNET) has frequent FGFR fusions and otherwise a flat copy number profile. G, the isomorphic astrocytoma is characterised by mutations of MYB or MYBL which can be detected in copy number profiles (66). All tumours in this figure were confirmed by methylation profiling and tumours showed the corresponding copy number profile.

loid features" has been put forward for the 2021 WHO classification. These tumours are predominantly located in the cerebellum, and form a distinct methylation class (54). These tumours have an unfavourable outcome compared to pilocytic astrocytomas, but better than glioblastoma.

The Diffuse Leptomeningeal Glioneuronal Tumour (DLGNT, Figure 5D) is an entity that is well characterised molecularly but may be less recognised in neuropathological differential diagnosis and thus may be underdiagnosed. Originally described as mostly in leptomeningeal and thus superficial locations, it has been recognised that they can also originate from midline structures and only secondarily spread to hemispheric structures, and other reports suggest isolated hemispheric origin (55). Histologically they appear as "neurocytic" tumours, similar to oligodendroglioma or neurocytoma (56). They can carry microvascular proliferations. All DLGNT carry a 1p loss, often in combination with a BRAF fusion and occasionally with additional 19q loss (57). However, they can be discriminated from 1p/19q-codeleted oligodendrogliomas by their definite absence of IDH mutations. Methylation profiling of a large cohort identified two distinct methylation profiles, separating a predominantly paediatric (DLGNT-MC-1) from an adult subgroup DLGNT-MC-2 (57).

Dysembryoplastic Neuroectodermal Tumours (DNET) (Figure 5F) grows in nodular formations close to the cortical surface. A characteristic feature is the glioneuronal element composed of bundles of glial cells, lined by small neurocytic tumour cells. These structures surround myxoid lakes, containing occasional resident neurons, which are aptly named "floating neurons". A proportion of DNET carry molecular alterations in FGFR (point mutations and fusions) (58) but these are not specific for this tumour entity, as they have been identified in a wider range of low-grade and high-grade glial neoplasms (52, 59-61) . Previous reports of the presence of BRAF V600E mutations in DNET (62-64) may have been based on a diagnostic overlap with gangliogliomas, as discussed in a recent comparative review (46).

Isomorphic Gliomas (Figure 5G) belong to the group of neoplasms with MYB/MYBL mutations and are histogenetically and molecularly unrelated to tumours with MAP kinase pathway alterations (61). Histologically, these tumours have a very low cellular density with a diffuse, compact, fibrillary matrix and lack a distinctive histological pattern (Figure 5G). Sometimes they can be difficult to be discriminated from CNS white matter. Whilst histological features and immunohistochemical profiles are indistinctive, isomorphic gliomas carry diagnostically relevant copy number alteration, fusion or rearrangement on the MYB or MYBL1 loci (65). The methylation profile of these tumours is distinct. (66).

Ependymal Tumours

Ependymomas (Figure 6) were for many years known for their poor correlation between histological appearance, grading and clinical outcome. A wealth of studies with genome-wide profiling of genome, transcriptome and methylome of ependymal tumours have provided a deep insight into the molecular pathogenesis, and at the same time resulted in the discovery of useful biomarkers that can be implemented in standard histological settings. In parallel, the characterisation of methylation profiles has resulted in the identification of 10 biological subclasses ("3+3+4") that can be characterised by a combination of location, molecular profile and to some extent, age of onset (67).

This classification describes 3 supratentorial, 3 infratentorial and 4 spinal forms (Figure 6). In the supratentorial compartment, the 3 molecular types are RELA fusion, YAP fusion and subependymoma. In the infratentorial compartment, the 3 molecular types, ependymoma type A, B, and subependymoma. The four molecular subtypes in the spinal compartment are the classical ependymoma, subependymoma, myxopapillary ependymoma (67) and the recently identified very rare ependymoma with MYCN amplification (68).

The majority of the subclasses show a 100% 5-year survival (Figure 6). The subclasses with poor survival are the supratentorial ependymoma with RELA fusion, the infratentorial ependymoma type A, and the spinal cord ependymoma with MYCN amplification (68-71).

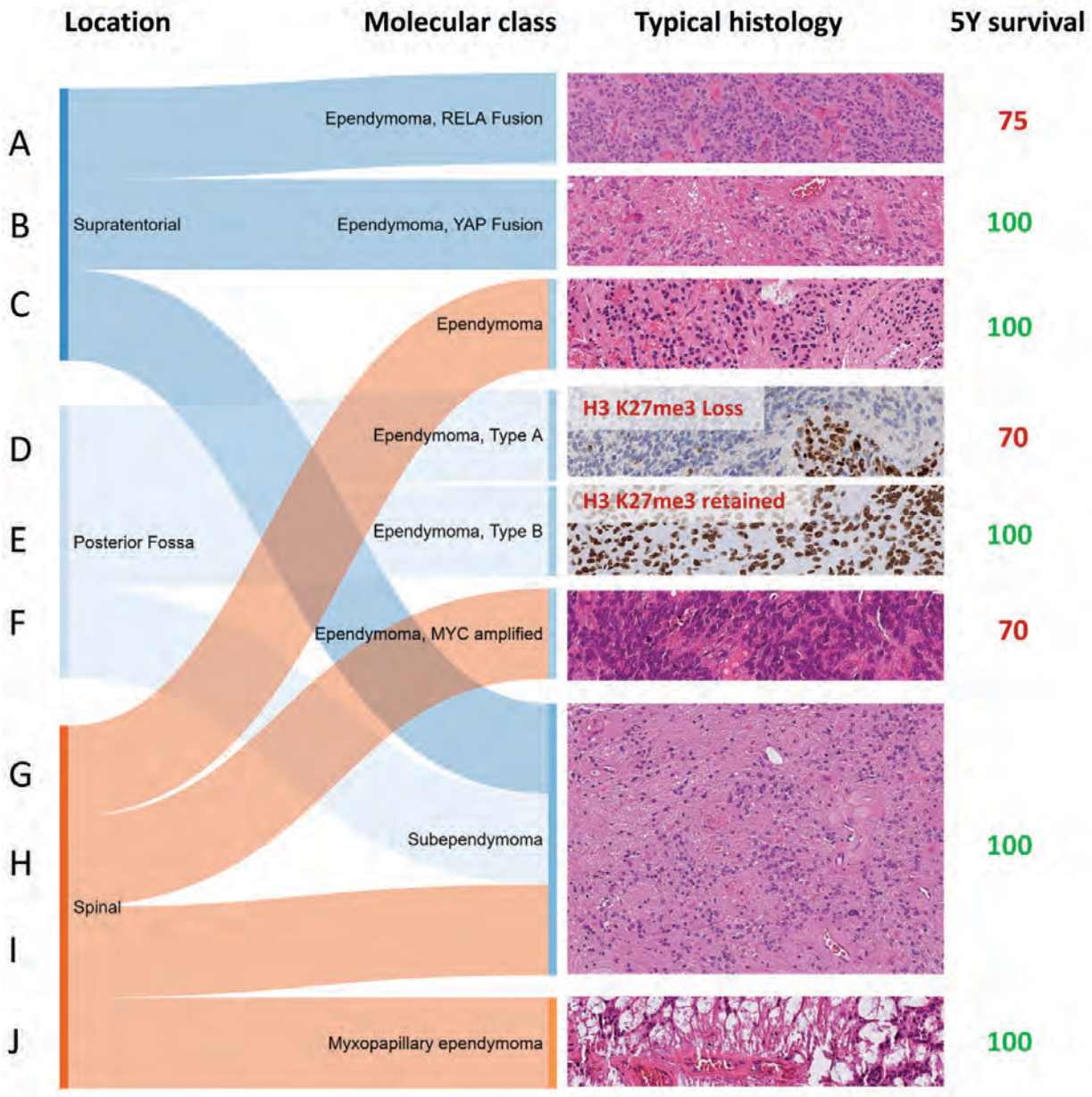

Figure 6. Molecular Classes, Histology and Survival of Ependymomas. 10 distinct molecular groups exist (67, 68, 87). In the supratentorial space (3 groups, A, B, C) ependymoma with RELA (A) or YAP fusion (B) present histologically as high-grade ependymoma. Instead, the subependymoma (C) is histologically benign and histologically indistinguishable, but molecularly distinct between supratentorial (C), infratentorial (F), and spinal (I) locations. In the posterior fossa (3 groups) the ependymoma type A (D) can be diagnosed by the loss of H3 K27me3 expression in tumour cell nuclei (retained expression in tumour vessels) whilst type B (E) has a retained expression of this marker. In the spinal compartment (4 groups), the classic ependymoma (G) appears histologically benign. Instead, the recently identified, rare anaplastic ependymoma with MYC amplification (68) (H) is highly malignant and does not always show the typical ependymal morphology. I, the subependymoma occurs in the cervical spinal cord, and is histologically and clinically benign. J, the myxopapillary ependymoma typically occurs in the cauda equina, and is histologically bland in most instances but a recent study indicates increased recurrence risk (79). The left part of the graph indicates location of the tumour, the centre the molecular class and the associated typical histology. On the right, 5 year survival in percent.

Molecular features and methylation profiles of ependymomas the classification of ependymal tumours not only relies heavily on, but also can be accomplished easily with, methylation arrays (72). The description of methylation classes is formed of acronyms incorporating the tumour type (EPN= ependymoma), location (ST, PF, and SP for supratentorial, posterior fossa and spinal, respectively) and molecular or histological subtype.

In the supratentorial space, the 3 types of ependymoma are the clinically benign subependymomas (EPN_ST_SE) and ependymomas of WHO grades II and III, with either the RELA fusion (EPN_ST_RELA) with a poor 5-year survival or the YAP 1 fusion (EPN_ST_YAP1) with a relatively good 5-year survival (73). Five fusion genes between YAP1-MAMLD1 and YAP1-FAM118B have been described, but the pathogenic mechanism has yet to be determined. More than two-thirds of supratentorial ependymomas contain oncogenic fusions between RELA (effector of canonical NF-κB signalling), and a gene on chromosome 11, C11orf95. C11orf95-RELA fusion proteins translocate to the nucleus and activate NF-κB target genes (74) and this translocation can be detected by immunostaining for the p65 protein (75).

In the posterior fossa there is the clinically benign subependymoma EPN_PF_SE occurring mostly in middle-aged patients, and the ependymomas subtype A (EPN_PF_A) occurring in young children with poor prognosis and the ependymoma subtype B (EPN_PF_B) occurring in older children, teenagers and adults, with a more favourable prognosis (76, 77). An important discovery was the downregulation of the trimethylated form of H3 K27M (H3 K27me3) in EPN_PF_A (H3 K27me3 loss of expression) which enables a diagnostic distinction from EPN_PF_B H3 K27me3 retained expression) (78) (Figure 6 D, E).

Spinal Ependymomas again comprise the benign sub ependymoma (EPN_SP_SE, histologically identical, but molecularly distinct from supratentorial and infratentorial counterparts). This tumour usually occurs in the upper spinal cord in adults. The generally, but not always benign (79) myxopapillary ependymoma (EPN_SP_MPE) is usually located in the cauda equina and occurs in adults. The classical ependymoma (SP_EPN) can occur along the entire spinal cord and an aggressive subtype, molecularly distinct from SP_EPN is the MYCN amplified ependymoma (SP_EPN_MYC).

Despite the significant advances in molecular profiling and classification of ependymal tumours (80), the treatment options have so far not developed at the same pace, and targeted therapies have yet to be developed. Current guidelines recognise molecular subgroups but cannot offer options for personalised treatment (70, 71).

The Use of Methylation Array Profiling in Diagnostic Neuropathology

The use of methylation array profiling to establish the histogenesis, molecular profile, and in some instances prognostication of brain tumours requires a number of considerations to ensure resources are invested adequately, and the outcome meet the expectations of neuropathologists, oncologists, surgeons, and of course, patients.

In previous publications (7, 9) we established 7 broad reasons for using methylation arrays. Over the last 5 years we have analysed over 1500 brain tumour samples with this technology, mostly for diagnostic, and occasionally also for research and quality assurance purposes. Table 1 provides examples for these distinct clinical rationales. Once the rationale for the use is established, there are several different outcomes of the molecular tests, listed in Table 2. The relationship between test rationale and readout/outcome is shown in Figure 7. An important factor for a successful readout of this test is the calibrated score, a "probability" indicator of the match of the profile of a sample to the reference set. In our practice we are using a score of 0.84 as a cut off to rely on the computed methylation class. An important additional information derived from the array chips is the copy number profile that can independently verify certain diagnoses, such as 1p/19q codeletion in oligodendrogliomas, chromosome 7 gain and chromosome 10 loss in IDH-wildtype glioblastoma, BRAF

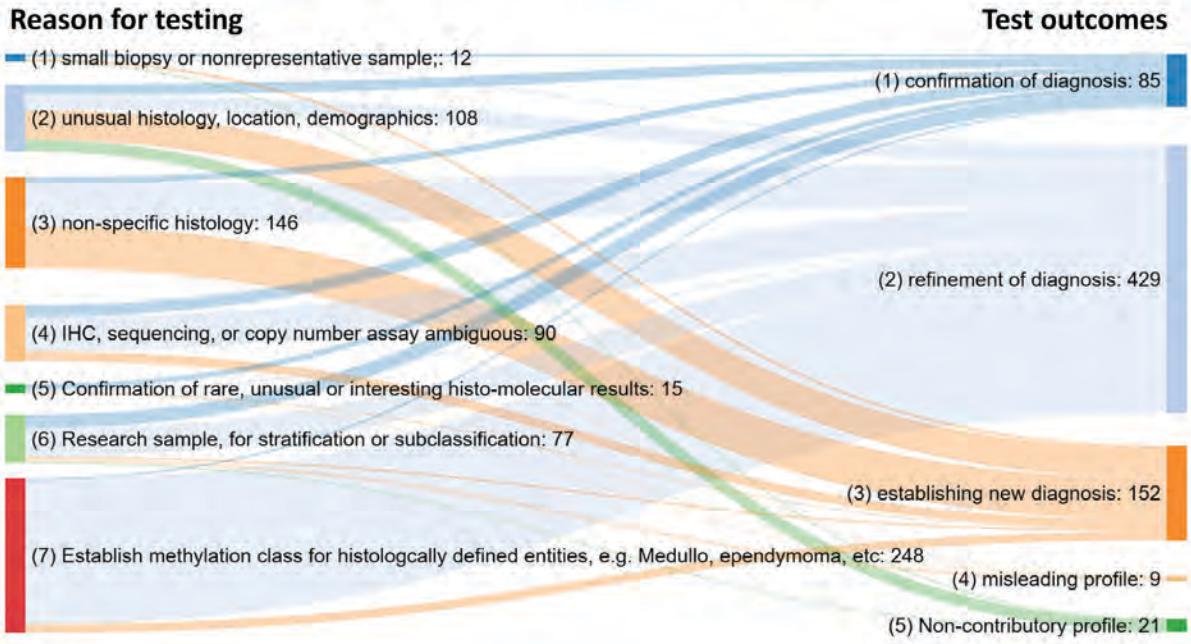

Figure 7. Rationale for Methylation Profiling and Test Outcomes in Our Clinical Practice. Over 1500 tumours were tested between March 2015 and October 2020 for diagnosis, research and quality assurance. Of these, 696 had a calibrated score of 0.84 and higher and are included in this alluvial diagram. The left side shows the reason for testing, as described in table 1. The right side shows the test outcome, as described in table 2. This diagram illustrates that the majority of tumours with a unusual location and demographics (2) or with non-specific histology (3) resulted in a refined or newly established diagnosis. It also shows that the majority of tests performed to establish methylation class of histologically defined entities (7) had a refinement of the diagnosis, whilst a small proportion of tumours with a presumed firm diagnosis returned a (usually unexpected) new diagnosis. This graph also includes research samples where the diagnosis was predominantly confirmed, or refined, but occasionally a new diagnosis was established. The remaining tumours with a calibrated score of lower than 0.84 were not included in the analysis. With a decreasing calibrated score, the proportion of misleading or non-contributory profiles increases.

duplication in pilocytic astrocytomas or DLGNT, SMARCB1 loss in AT/RT.

In our practice the combination of biopsy size, tumour location, treatment options and patient age are factors that determine our threshold to perform methylation arrays. In particular small biopsies (usually from delicate brain regions such as optic tract, pineal gland, brainstem, spinal cord or thalamus) undergo only very limited testing with IHC (context -dependent, for example H3 K27M, IDH, ATRX, INI1), and avoiding stereotypically used stains of often limited diagnostic value such as Ki67, GFAP, synaptophysin, or vimentin to preserve tissue for the far more informative methylation array. We recommend to carefully consider and minimise the use of such markers in particular in small biopsies and encourage to consider referral for methylation arrays.

Table 1. Rationale for the Use of DNA Methylation Profiling for Brain Tumours*

Reason for using classifier		Examples
1	Small biopsy or nonrepresentative sample	Even though it may appear counterintuitive, an important reason for using methylation arrays is a small biopsy. Typically, biopsies in this category are from difficult locations to establish a clinical diagnosis with minimal invasiveness and risk, for example, optic pathway, midline location, brain stem, spinal cord). A minimal number of immunostainings (e.g., IDH R132H, histone K27M, ATRX, SMARCB1) can be performed to preserve tissue for subsequent array analysis. Nearly all small biopsies with indistinctive histology undergo methylation profiling in our practice.
2	Unusual histology, location, demographics	Intrinsic tumours with unusual or distinctive histological patterns, in any age group, which are not diagnostically intuitive. These can turn out to be rare entities (such as hemispheric DLGNT, RELA fusion ependymoma, spindle cell tumours)
3	Non-specific histology	One of the most common indications for the use of methylation arrays: For example, high-grade or low-grade tumours with no distinctive histology, which are negative for common biomarkers (IDH, BRAF, histone, TERT, EGFR). The outcome (methylation profile) of many high-grade tumours with indistinctive histology is however glioblastoma, IDH-wildtype. Typical outcomes in low-grade gliomas are pilocytic astrocytoma, isomorphic glioma, PXA, DNET, or ganglioglioma, but also the histologically low-grade appearing GBM, IDH-wildtype (Figure 3).
4	IHC, sequencing, or copy number assay ambiguous	Ambiguous copy number results include inconclusive 1p/19q codeletion tests, failed sequencing results for IDH, TERT, BRAF, false positive EGFR test results. Methylation arrays provide an independent evaluation of such tumours. This is sometimes the case with tumours with ATRX loss, and no detection of IDH or histone mutations.
5	Confirmation of rare, unusual or interesting histo-molecular results	This is a relatively rare indication, for example a histone K27M-mutant glioma seemingly occurring in a lateral localisation, IDH mutant gliomas in the posterior fossa, rosette-forming glioneuronal tumour in a spinal location, chordoid gliomas, etc.
6	Research sample, for stratification or subclassification	This category is used for research samples. Often such tumours have already undergone a stratification by other means, for example selection of a range of IDH-mutant or IDH-wildtype gliomas in a research study.
7	Establish methylation class for histologically defined entities.	Tumours falling in this category are usually diagnostically relatively straightforward. Typically, these include medulloblastomas, ependymomas, and more recently also meningiomas. The methylation profiling is performed for clinical and treatment stratification. However profiling of such tumours can occasional reveal an incorrect assumption of a tumour type, resulting in "establishing a new diagnosis" (Figure 7).

*The left column indicates the reason for using the classifier (following the categorisation from previous publications (7, 9)) and the right column gives typical examples from clinical practice.

Table 2. Categories of Outcomes from the DNA Methylation Classifier, Following the Definitions from Previous Publications (7, 9)*

Outcome		Examples
1	Confirmation of diagnosis	Confirmation of the differential diagnosis of a histologically diagnosed glioblastoma, pilocytic astrocytoma or low-grade glial or glioneuronal tumours (ganglioglioma, DNET, rosette-forming glioneuronal tumour, etc.).
2	Refinement of diagnosis	Typically these include entities which have been correctly diagnosed but require molecular stratification, such as the molecular subtype of meningioma, ependymoma or medulloblastoma.
3	Establishing new diagnosis	Most commonly these are biopsies of small size or with non-specific histology which have been diagnosed as "diffuse glioma, NOS", classified for example as "ependymoma, RELA fusion", "pilocytic astrocytoma hemispheric type", "ganglioglioma", etc.
4	Misleading profile	Misleading profiles are typically associated with a low calibrated score. They occur in cases which do not correspond to establish methylation classes, or in cases with low DNA content, or poor DNA quality. Figure 7 shows only few such examples as only cases with a calibrated score of 0.84 and higher were included.
5	Non-contributory profile	This can occur in problematic biopsies with low tumour content (classified as CNS tissue), or in samples with significant reactive changes (tumour inflammation), classified as "reactive tumour micro environment". A major proportion of tumours with this outcome were associated with the testing rationale of "unusual histology, location and demographics" (Table 1 and Figure 7). These often result in a low calibrated score due to a mismatch to any of the currently established methylation classes, i.e. may represent new, uncharacterised entities.

*The examples are from our clinical practice and reflect typical outcomes. See Figure 7 for the relationship between testing rationale and outcome.

Summary and Conclusion

This review provides an overview of the state-of-the-art diagnostic approach to gliomas in adults. In particular, the diagnostic and prognostic criteria of IDH-mutant gliomas, the importance of the recognition of precursor forms of the IDH-wildtype glioblastoma and the molecular analytics of a range of low-grade glial and glioneuronal tumours has been outlined. An important area is the molecular stratification of ependymal tumours which benefit from the availability of methylation arrays. Guidelines published by the Royal College of Pathologists provide diagnostic algorithms for an evidence-based, practical approach for the diagnosis of brain tumours https://www.rcpath.org/profession/guidelines/cancer-datasets-and-tissue-pathways.html (accessed December 2020) (81). Further helpful guidance on the use of molecular biomarkers in brain tumour diagnostics is regularly published by the International Collaboration on Cancer Reporting ICCR http://www.iccr-cancer.org/ . Inevitably, this review had to exclude a number of diagnostically important areas in diagnostic neuropathology such as paediatric tumours, meningiomas and metastatic lesions. An excellent review on the application of molecular diagnostic strategies in clinical diagnostics of paediatric tumours has recently been published (82). Meningiomas have over the last few years moved into the focus of advanced molecular diagnostics and clinical decision making algorithms have been published (83-85).

Conflict of Interest: The author declares that he has no conflict of interest.

References

1. Parsons DW, Jones S, Zhang X, Lin JC, Leary RJ, Angenendt P, et al. An integrated genomic analysis of human glioblastoma multiforme. Science. 2008;321(5897):1807-12.
2. Schindler G, Capper D, Meyer J, Janzarik W, Omran H, Herold-Mende C, et al. Analysis of BRAF V600E mutation in 1,320 nervous system tumors reveals high mutation frequencies in pleomorphic xanthoastrocytoma, ganglioglioma and extra-cerebellar pilocytic astrocytoma. Acta Neuropathol. 2011;121(3):397-405.
3. Khuong-Quang DA, Buczkowicz P, Rakopoulos P, Liu XY, Fontebasso AM, Bouffet E, et al. K27M mutation in histone H3.3 defines clinically and biologically distinct subgroups of pediatric diffuse intrinsic pontine gliomas. Acta Neuropathol. 2012;124(3):439-47.
4. Bechet D, Gielen GG, Korshunov A, Pfister SM, Rousso C, Faury D, et al. Specific detection of methionine 27 mutation in histone 3 variants (H3K27M) in fixed tissue from high-grade astrocytomas. Acta Neuropathol. 2014;128(5):733-41.
5. Stichel D, Ebrahimi A, Reuss D, Schrimpf D, Ono T, Shirahata M, et al. Distribution of EGFR amplification, combined chromosome 7 gain and chromosome 10 loss, and TERT promoter mutation in brain tumors and their potential for the reclassification of IDHwt astrocytoma to glioblastoma. Acta Neuropathol. 2018;136(5):793-803.
6. Andreiuolo F, Lisner T, Zlocha J, Kramm C, Koch A, Bison B, et al. H3F3A-G34R mutant high grade neuroepithelial neoplasms with glial and dysplastic ganglion cell components. Acta neuropathologica communications. 2019;7(1):78.
7. Capper D, Jones DTW, Sill M, Hovestadt V, Schrimpf D, Sturm D, et al. DNA methylation-based classification of central nervous system tumours. Nature. 2018;555(7697):469-74.
8. Capper D, Stichel D, Sahm F, Jones DTW, Schrimpf D, Sill M, et al. Practical implementation of DNA methylation and copy-number-based CNS tumor diagnostics: the Heidelberg experience. Acta Neuropathol. 2018;136(2):181-210.
9. Jaunmuktane Z, Capper D, Jones DTW, Schrimpf D, Sill M, Dutt M, et al. Methylation array profiling of adult brain tumours: diagnostic outcomes in a large, single centre. Acta Neuropathol Commun. 2019;7(1):24.
10. Pickles JC, Fairchild AR, Stone TJ, Brownlee L, Merve A, Yasin SA, et al. DNA methylation-based profiling for paediatric CNS tumour diagnosis and treatment: a population-based study. Lancet Child Adolesc Health. 2020;4(2):121-30.
11. Schiffer D, Giordana MT, Mauro A, Migheli A. Glial fibrillary acidic protein (GFAP) in human cerebral tumors. An immunohistochemical study. Tumori. 1983;69(2):95-104.
12. Dhillon AP, Rode J. Immunohistochemical studies of S100 protein and other neural characteristics expressed by granular cell tumour. Diagn Histopathol. 1983;6(1):23-8.
13. Wiedenmann B, Franke WW, Kuhn C, Moll R, Gould VE. Synaptophysin: a marker protein for neuroendocrine cells and neoplasms. Proc Natl Acad Sci U S A. 1986;83(10):3500-4.
14. van Muijen GN, Ruiter DJ, Franke WW, Achtstätter T, Haasnoot WH, Ponec M, et al. Cell type heterogeneity of cytokeratin expression in complex epithelia and carcinomas as demonstrated by monoclonal antibod-

ies specific for cytokeratins nos. 4 and 13. Exp Cell Res. 1986;162(1):97-113.

15. Hans CP, Weisenburger DD, Greiner TC, Gascoyne RD, Delabie J, Ott G, et al. Confirmation of the molecular classification of diffuse large B-cell lymphoma by immunohistochemistry using a tissue microarray. Blood. 2004;103(1):275-82.
16. Garcia-Verdugo JM, Doetsch F, Wichterle H, Lim DA, Alvarez-Buylla A. Architecture and cell types of the adult subventricular zone: in search of the stem cells. J Neurobiol. 1998;36(2):234-48.
17. Capper D, Zentgraf H, Balss J, Hartmann C, von Deimling A. Monoclonal antibody specific for IDH1 R132H mutation. Acta Neuropathol. 2009;118(5):599-601.
18. Capper D, Berghoff AS, Magerle M, Ilhan A, Wohrer A, Hackl M, et al. Immunohistochemical testing of BRAF V600E status in 1,120 tumor tissue samples of patients with brain metastases. Acta Neuropathol. 2012;123(2):223-33.
19. Capper D, Berghoff AS, von Deimling A, Preusser M. Clinical neuropathology practice news 2-2012: BRAF V600E testing. Clin Neuropathol. 2012;31(2):64-6.
20. Versteege I, Sevenet N, Lange J, Rousseau-Merck MF, Ambros P, Handgretinger R, et al. Truncating mutations of hSNF5/INI1 in aggressive paediatric cancer. Nature. 1998;394(6689):203-6.
21. Margol AS, Judkins AR. Pathology and diagnosis of SMARCB1-deficient tumors. Cancer Genet. 2014;207(9): 358-64.
22. Yan H, Parsons DW, Jin G, McLendon R, Rasheed BA, Yuan W, et al. IDH1 and IDH2 mutations in gliomas. N Engl J Med. 2009;360(8):765-73.
23. Hartmann C, Meyer J, Balss J, Capper D, Mueller W, Christians A, et al. Type and frequency of IDH1 and IDH2 mutations are related to astrocytic and oligodendroglial differentiation and age: a study of 1,010 diffuse gliomas. Acta Neuropathol. 2009;118(4):469-74.
24. Reuss DE, Sahm F, Schrimpf D, Wiestler B, Capper D, Koelsche C, et al. ATRX and IDH1-R132H immunohistochemistry with subsequent copy number analysis and IDH sequencing as a basis for an "integrated" diagnostic approach for adult astrocytoma, oligodendroglioma and glioblastoma. Acta Neuropathol. 2015;129(1):133-46.
25. Sahm F, Reuss D, Koelsche C, Capper D, Schittenhelm J, Heim S, et al. Farewell to oligoastrocytoma: in situ molecular genetics favor classification as either oligodendroglioma or astrocytoma. Acta Neuropathol. 2014;128(4):551-9.
26. Sahm F, von Deimling A. Farewell to oligoastrocytoma: response to letters. Acta Neuropathol. 2014.
27. Louis DN, Wesseling P, Paulus W, Giannini C, Batchelor TT, Cairncross JG, et al. cIMPACT-NOW update 1: Not Otherwise Specified (NOS) and Not Elsewhere Classified (NEC). Acta Neuropathol. 2018;135(3):481-4.
28. Brat DJ, Aldape K, Colman H, Figrarella-Branger D, Fuller GN, Giannini C, et al. cIMPACT-NOW update 5: recommended grading criteria and terminologies for IDH-mutant astrocytomas. Acta Nauropathol. 2020:10.1007/s00401-020-2127-9.
29. Shirahata M, Ono T, Stichel D, Schrimpf D, Reuss DE, Sahm F, et al. Novel, improved grading system(s) for IDH-mutant astrocytic gliomas. Acta Neuropathol. 2018;136(1):153-66.
30. von Deimling A, Ono T, Shirahata M, Louis DN. Grading of Diffuse Astrocytic Gliomas: A Review of Studies Before and After the Advent of IDH Testing. Seminars in neurology. 2018;38(1):19-23.
31. Ichimura K, Pearson DM, Kocialkowski S, Backlund LM, Chan R, Jones DT, et al. IDH1 mutations are present in the majority of common adult gliomas but rare in primary glioblastomas. Neuro Oncol. 2009;11(4):341-7.
32. Reuss DE, Kratz A, Sahm F, Capper D, Schrimpf D, Koelsche C, et al. Adult IDH wild type astrocytomas biologically and clinically resolve into other tumor entities. Acta Neuropathol. 2015;130(3):407-17.
33. Brat DJ, Aldape K, Colman H, Holland EC, Louis DN, Jenkins RB, et al. cIMPACT-NOW update 3: recommended diagnostic criteria for "Diffuse astrocytic glioma, IDH-wildtype, with molecular features of glioblastoma, WHO grade IV". Acta Neuropathol. 2018;136(5):805-10.
34. Schwartzentruber J, Korshunov A, Liu XY, Jones DT, Pfaff E, Jacob K, et al. Driver mutations in histone H3.3 and chromatin remodelling genes in paediatric glioblastoma. Nature. 2012;482(7384):226-31.
35. Mohammad F, Weissmann S, Leblanc B, Pandey DP, Hojfeldt JW, Comet I, et al. EZH2 is a potential therapeutic target for H3K27M-mutant pediatric gliomas. Nat Med. 2017;23(4):483-92.
36. Filbin MG, Tirosh I, Hovestadt V, Shaw ML, Escalante LE, Mathewson ND, et al. Developmental and oncogenic programs in H3K27M gliomas dissected by single-cell RNA-seq. Science. 2018;360(6386):331-5.
37. Schreck KC, Ranjan S, Skorupan N, Bettegowda C, Eberhart CG, Ames HM, et al. Incidence and clinicopathologic features of H3 K27M mutations in adults with radiographically-determined midline gliomas. J Neuro-Oncol. 2019;143(1):87-93.
38. Louis DN, Giannini C, Capper D, Paulus W, Figarella-Branger D, Lopes MB, et al. cIMPACT-NOW update 2: diagnostic clarifications for diffuse midline glioma, H3 K27M-mutant and diffuse astrocytoma/anaplastic astrocytoma, IDH-mutant. Acta Neuropathol. 2018;135(4):639-42.
39. Gessi M, Capper D, Sahm F, Huang K, von Deimling A, Tippelt S, et al. Evidence of H3 K27M mutations in posterior fossa ependymomas. Acta Neuropathol. 2016;132(4):635-7.
40. Morita S, Nitta M, Muragaki Y, Komori T, Masui K, Maruyama T, et al. Brainstem pilocytic astrocytoma with H3 K27M mutation: case report. J Neurosurg. 2018;129(3):593-7.

41. Pages M, Beccaria K, Boddaert N, Saffroy R, Besnard A, Castel D, et al. Co-occurrence of histone H3 K27M and BRAF V600E mutations in paediatric midline grade I ganglioglioma. Brain Pathol. 2018;28(1):103-11.
42. Korshunov A, Ryzhova M, Hovestadt V, Bender S, Sturm D, Capper D, et al. Integrated analysis of pediatric glioblastoma reveals a subset of biologically favorable tumors with associated molecular prognostic markers. Acta Neuropathol. 2015;129(5):669-78.
43. Korshunov A, Capper D, Reuss D, Schrimpf D, Ryzhova M, Hovestadt V, et al. Histologically distinct neuroepithelial tumors with histone 3 G34 mutation are molecularly similar and comprise a single nosologic entity. Acta Neuropathol. 2016;131(1):137-46.
44. Pekmezci M, Villanueva-Meyer JE, Goode B, Van Ziffle J, Onodera C, Grenert JP, et al. The genetic landscape of ganglioglioma. Acta Neuropathol Commun. 2018;6(1):47.
45. Koelsche C, Wohrer A, Jeibmann A, Schittenhelm J, Schindler G, Preusser M, et al. Mutant BRAF V600E protein in ganglioglioma is predominantly expressed by neuronal tumor cells. Acta Neuropathol. 2013;125(6):891-900.
46. Blumcke I, Coras R, Wefers AK, Capper D, Aronica E, Becker A, et al. Review: Challenges in the histopathological classification of ganglioglioma and DNT: microscopic agreement studies and a preliminary genotype-phenotype analysis. Neuropathol Appl Neurobiol. 2019;45(2):95-107.
47. Phillips JJ, Gong H, Chen K, Joseph NM, van Ziffle J, Bastian BC, et al. The genetic landscape of anaplastic pleomorphic xanthoastrocytoma. Brain Pathol. 2019;29(1):85-96.
48. Lee EQ, Ruland S, LeBoeuf NR, Wen PY, Santagata S. Successful Treatment of a Progressive BRAF V600E-Mutated Anaplastic Pleomorphic Xanthoastrocytoma With Vemurafenib Monotherapy. J Clin Oncol. 2016;34(10):e87-9.
49. 49. Brown NF, Carter T, Mulholland P. Dabrafenib in BRAFV600-mutated anaplastic pleomorphic xanthoastrocytoma. CNS oncology. 2017;6(1):5-9.
50. Jones DT, Kocialkowski S, Liu L, Pearson DM, Backlund LM, Ichimura K, et al. Tandem duplication producing a novel oncogenic BRAF fusion gene defines the majority of pilocytic astrocytomas. Cancer Res. 2008;68(21):8673-7.
51. Lin A, Rodriguez FJ, Karajannis MA, Williams SC, Legault G, Zagzag D, et al. BRAF alterations in primary glial and glioneuronal neoplasms of the central nervous system with identification of 2 novel KIAA1549:BRAF fusion variants. J Neuropathol Exp Neurol. 2012;71(1):66-72.
52. Jones DT, Hutter B, Jager N, Korshunov A, Kool M, Warnatz HJ, et al. Recurrent somatic alterations of FGFR1 and NTRK2 in pilocytic astrocytoma. Nat Genet. 2013;45(8):927-32.
53. Collins VP, Jones DT, Giannini C. Pilocytic astrocytoma: pathology, molecular mechanisms and markers. Acta Neuropathol. 2015;129(6):775-88.
54. Reinhardt A, Stichel D, Schrimpf D, Sahm F, Korshunov A, Reuss DE, et al. Anaplastic astrocytoma with piloid features, a novel molecular class of IDH wildtype glioma with recurrent MAPK pathway, CDKN2A/B and ATRX alterations. Acta Neuropathol. 2018;136(2):273-91.
55. Appay R, Pages M, Colin C, Jones DTW, Varlet P, Figarella-Branger D. Diffuse leptomeningeal glioneuronal tumor: a double misnomer? A report of two cases. Acta Neuropathol Commun. 2020;8(1):95.
56. 5Gardiman MP, Fassan M, Orvieto E, D'Avella D, Denaro L, Calderone M, et al. Diffuse leptomeningeal glioneuronal tumors: a new entity? Brain Pathol. 2010;20(2):361-6.
57. Deng MY, Sill M, Chiang J, Schittenhelm J, Ebinger M, Schuhmann MU, et al. Molecularly defined diffuse leptomeningeal glioneuronal tumor (DLGNT) comprises two subgroups with distinct clinical and genetic features. Acta Neuropathol. 2018;136(2):239-53.
58. Rivera B, Gayden T, Carrot-Zhang J, Nadaf J, Boshari T, Faury D, et al. Germline and somatic FGFR1 abnormalities in dysembryoplastic neuroepithelial tumors. Acta Neuropathol. 2016;131(6):847-63.
59. Singh D, Chan JM, Zoppoli P, Niola F, Sullivan R, Castano A, et al. Transforming fusions of FGFR and TACC genes in human glioblastoma. Science. 2012;337(6099):1231-5.
60. Gessi M, Moneim YA, Hammes J, Goschzik T, Scholz M, Denkhaus D, et al. FGFR1 mutations in Rosette-forming glioneuronal tumors of the fourth ventricle. J Neuropathol Exp Neurol. 2014;73(6):580-4.
61. Ellison DW, Hawkins C, Jones DTW, Onar-Thomas A, Pfister SM, Reifenberger G, et al. cIMPACT-NOW update 4: diffuse gliomas characterized by MYB, MYBL1, or FGFR1 alterations or BRAF(V600E) mutation. Acta Neuropathol. 2019;137(4):683-7.
62. Thom M, Toma A, An S, Martinian L, Hadjivassiliou G, Ratilal B, et al. One hundred and one dysembryoplastic neuroepithelial tumors: an adult epilepsy series with immunohistochemical, molecular genetic, and clinical correlations and a review of the literature. J Neuropathol Exp Neurol. 2011;70(10):859-78.
63. Chappe C, Padovani L, Scavarda D, Forest F, Nanni-Metellus I, Loundou A, et al. Dysembryoplastic neuroepithelial tumors share with pleomorphic xanthoastrocytomas and gangliogliomas BRAF(V600E) mutation and expression. Brain Pathol. 2013;23(5):574-83.
64. Lee D, Cho YH, Kang SY, Yoon N, Sung CO, Suh YL. BRAF V600E mutations are frequent in dysembryoplastic neuroepithelial tumors and subependymal giant cell astrocytomas. J Surg Oncol. 2014.
65. Qaddoumi I, Orisme W, Wen J, Santiago T, Gupta K, Dalton JD, et al. Genetic alterations in uncommon low-grade neuroepithelial tumors: BRAF, FGFR1, and MYB mutations occur at high frequency and align with morphology. Acta Neuropathol. 2016;131(6):833-45.
66. Wefers AK, Stichel D, Schrimpf D, Coras R, Pages M, Tauziède-Espariat A, et al. Isomorphic diffuse glioma is a morphologically and molecularly distinct tumour entity with

recurrent gene fusions of MYBL1 or MYB and a benign disease course. Acta Neuropathol. 2020;139(1):193-209.

67. Pajtler KW, Witt H, Sill M, Jones DT, Hovestadt V, Kratochwil F, et al. Molecular Classification of Ependymal Tumors across All CNS Compartments, Histopathological Grades, and Age Groups. Cancer Cell. 2015;27(5):728-43.
68. Ghasemi DR, Sill M, Okonechnikov K, Korshunov A, Yip S, Schutz PW, et al. MYCN amplification drives an aggressive form of spinal ependymoma. Acta Neuropathol. 2019.
69. Marinoff AE, Ma C, Guo D, Snuderl M, Wright KD, Manley PE, et al. Rethinking childhood ependymoma: a retrospective, multi-center analysis reveals poor long-term overall survival. J Neurooncol. 2017.
70. Pajtler KW, Mack SC, Ramaswamy V, Smith CA, Witt H, Smith A, et al. The current consensus on the clinical management of intracranial ependymoma and its distinct molecular variants. Acta Neuropathol. 2017;133(1):5-12.
71. Ruda R, Reifenberger G, Frappaz D, Pfister SM, Laprie A, Santarius T, et al. EANO guidelines for the diagnosis and treatment of ependymal tumors. Neuro Oncol. 2018;20(4):445-56.
72. Mack SC, Taylor MD. Put away your microscopes: the ependymoma molecular era has begun. Curr Opin Oncol. 2017.
73. Fukuoka K, Kanemura Y, Shofuda T, Fukushima S, Yamashita S, Narushima D, et al. Significance of molecular classification of ependymomas: C11orf95-RELA fusion-negative supratentorial ependymomas are a heterogeneous group of tumors. Acta Neuropathol Commun. 2018;6(1):134.
74. Parker M, Mohankumar KM, Punchihewa C, Weinlich R, Dalton JD, Li Y, et al. C11orf95-RELA fusions drive oncogenic NF-kappaB signalling in ependymoma. Nature. 2014;506(7489):451-5.
75. Gessi M, Giagnacovo M, Modena P, Elefante G, Gianno F, Buttarelli FR, et al. Role of Immunohistochemistry in the Identification of Supratentorial C11ORF95-RELA Fused Ependymoma in Routine Neuropathology. Am J Surg Pathol. 2019;43(1):56-63.
76. Witt H, Mack SC, Ryzhova M, Bender S, Sill M, Isserlin R, et al. Delineation of two clinically and molecularly distinct subgroups of posterior fossa ependymoma. Cancer Cell. 2011;20(2):143-57.
77. Wani K, Armstrong TS, Vera-Bolanos E, Raghunathan A, Ellison D, Gilbertson R, et al. A prognostic gene expression signature in infratentorial ependymoma. Acta Neuropathol. 2012;123(5):727-38.
78. Panwalkar P, Clark J, Ramaswamy V, Hawes D, Yang F, Dunham C, et al. Immunohistochemical analysis of H3K27me3 demonstrates global reduction in group-A childhood posterior fossa ependymoma and is a powerful predictor of outcome. Acta Neuropathol. 2017.
79. Lee JC, Sharifai N, Dahiya S, Kleinschmidt-DeMasters BK, Rosenblum MK, Reis GF, et al. Clinicopathologic features of anaplastic myxopapillary ependymomas. Brain Pathol. 2019;29(1):75-84.
80. Mack SC, Pajtler KW, Chavez L, Okonechnikov K, Bertrand KC, Wang X, et al. Therapeutic targeting of ependymoma as informed by oncogenic enhancer profiling. Nature. 2018;553(7686):101-5.
81. Brandner S, Hilton DA, Jaunmuktane Z, Thom M, Ansorge O, Roncaroli F, et al. Dataset for tumours of the central nervous system, including the pituitary gland (5th edition). The Royal College of Pathologists. 2019.
82. Pickles JC, Stone TJ, Jacques TS. Methylation-based algorithms for diagnosis: experience from neuro-oncology. J Pathol. 2020;250(5):510-7.
83. Nassiri F, Mamatjan Y, Suppiah S, Badhiwala JH, Mansouri S, Karimi S, et al. DNA methylation profiling to predict recurrence risk in meningioma: development and validation of a nomogram to optimize clinical management. Neuro Oncol. 2019;21(7):901-10.
84. Paramasivam N, Hübschmann D, Toprak UH, Ishaque N, Neidert M, Schrimpf D, et al. Mutational patterns and regulatory networks in epigenetic subgroups of meningioma. Acta Neuropathol. 2019;138(2):295-308.
85. Suppiah S, Nassiri F, Bi WL, Dunn IF, Hanemann CO, Horbinski CM, et al. Molecular and translational advances in meningiomas. Neuro Oncol. 2019;21(Suppl 1):i4-i17.
86. Brandner S, Jaunmuktane Z. IDH mutant astrocytoma: biomarkers for prognostic stratification and the next frontiers. Neuropathol Appl Neurobiol. 2018.
87. Archer TC, Pomeroy SL. Defining the molecular landscape of ependymomas. Cancer Cell. 2015;27(5):613-5.

Narrative Review
Acta Medica Academica 2021;50(1):47-57
DOI: 10.5644/ama2006-124.325

The Role of Pathology in the Era of Personalized (Precision) Medicine: A Brief Review

Semir Vranic[1, 2, *], Zoran Gatalica[3]

[1]College of Medicine, QU Health, Qatar University, Doha, Qatar, [2]Biomedical and Pharmaceutical Research Unit, QU Health, Qatar University, Doha, Qatar, [3]Department of Pathology, Oklahoma University Health Sciences Center, Oklahoma City, OK, United States

Correspondence: *semir.vranic@gmail.com* or *svranic@qu.edu.qa*; Tel.: + 974 4403 7873; Fax.: + 974 4403 2250

Received: 15 December 2020; **Accepted:** 22 December 2020

Abstract
This review provides a brief overview of the state-of-the-art molecular pathology approaches emphasizing the increasingly important pathology role in clinical precision cancer medicine. Recent advances in molecular biology and genetics have tremendously affected the practice of anatomic pathology, gradually transforming it from a morphology-based into a molecular-based discipline. Molecular diagnostics has a long tradition in pathology, especially in clinical pathology. The improvement of methodology for genomic testing in recent years has made it one of the cornerstones of precision cancer medicine. The decisions related to cancer treatments are no longer solely based on the histopathological diagnosis. Various genomic analyses of human cancers are being incorporated into diagnostic and decision-making algorithms. **Conclusion.** The pathologists continue to play an essential role in developing and implementing molecular and genomic tests in practice and communicate the results and their relevance with clinicians. Such activities are of utmost importance for successfully translating scientific advancements into a benefit to patients ("next-generation pathologists").

Key Words: Cancer Therapy ▪ Precision Medicine ▪ Pathology ▪ Diagnostics ▪ Companion Diagnostics.

Introduction

In the early 19th century, diagnostic pathology was predominantly restricted to a postmortem assessment, and description of macroscopic tumor spread in the dissection room (1). However, pathology's principles and practice changed dramatically with the establishment of light microscopy and histopathologic investigations in the second half of the 19th century by the renowned German pathologist Dr. Rudolf Virchow (1821–1902), who is considered the 'father of modern pathology.' Thanks to these advances, it became possible to investigate different microscopic characteristics of various human diseases, including cancer (1).

Microscopic classification of tumors has, over the last 100 years, helped in improving the pathologic diagnosis of neoplastic diseases, predicting tumor behavior and thus formulating the prognosis for each case and thus facilitating clinical decision-making. Traditional cancer classification is based on microscopic evaluations, focusing on various clinicopathological features of tumors, such as tumor morphology (type), grade, surgical margins, vascular/lymphatic invasion, lymph node assessment and routine analysis of biomarkers. Pathologists traditionally utilize frozen sections that enable a rapid gross and microscopic tissue analysis and guide surgeons' hands during surgery (e.g., providing provisional diagnosis, assessing surgical margins, and identifying tissue of origins) (2) (Figure 1). However, none of those mentioned above

*ORCID: http://orcid.org/0000-0001-9743-7265

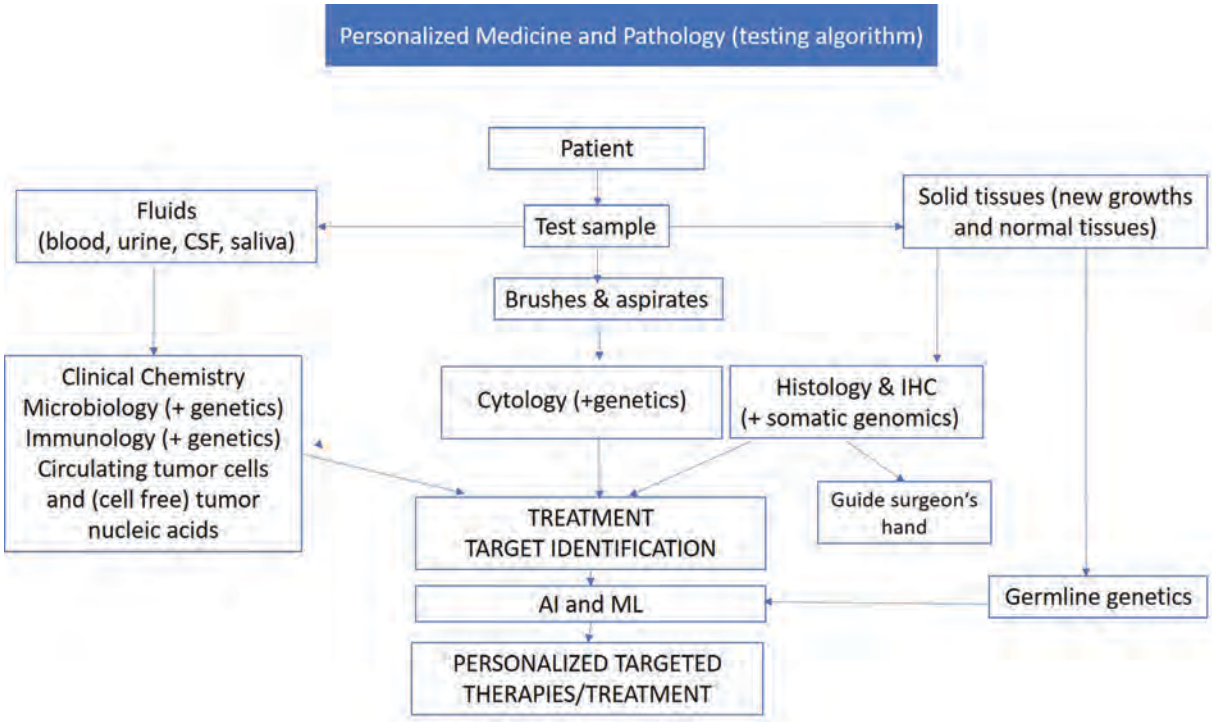

Figure 1. A proposed algorithm for the pathology role in personalized (precision) medicine. CSF=Cerebrospinal fluid; IHC=Immunohistochemistry; AI=Artificial intelligence; ML=Machine learning.

may capture individual cancers' variable clinical courses (heterogeneity).

The underlying basic biology of various cancer and their development and progression are still poorly understood but undoubtedly depend on each tumor's genetic background. The fact that cancer is a genetic disorder was suspected surprisingly early (1914) in the history of cancer research by Dr. Theodor Boveri. He presented a systematic somatic mutation theory of cancer (3). According to Boveri's hypothesis, chromosomal changes caused the transition from normal to the cells' malignant proliferation (3). However, the detailed oncogenesis model was first described by Nowell some 50 years later (4). Dr. Nowell provided evidence that the accumulation of mutations in cancers over time makes them more advanced and aggressive, increasing their metastatic potential. In 2000, Drs. Hanahan and Weinberg elegantly explained detailed cancer evolution in their seminal papers "The hallmarks of cancer" (5, 6). The authors outlined the principal biological characteristics of carcinogenesis ("hallmarks of cancer"). These features include not only cell proliferation/replication, apoptosis, (neo)angiogenesis, down-regulation of growth suppressors, invasion/metastasis (5) but also the altered metabolic properties, genomic instability/mutations, escape from immune surveillance, and tumor-promoting inflammation (6). This evolutionary model of carcinogenesis can efficiently explain the complexity and the marked heterogeneity that characterize the vast majority of human cancers (7). Recent findings from high-throughput, multiplex/massively parallel technologies (assays) added important information about the underlying genomic alterations and human cancers' biological events. These findings provide insights into novel treatment modalities and allow for patient stratifications that impact cancer patients' management (7).

In the previous two decades, with the increasing understanding of human cancer's molecular genomic drivers, the number of novel biomarkers and the subsequent development of targeted pharmaceutical treatments have dramatically increased. These changes have strongly influenced

diagnostic pathology practice, gradually transforming it from morphology-based into molecular-based discipline.

This brief review will discuss and critically assess molecular biology's contributions to diagnostic pathology and precision cancer medicine.

Precision Medicine and Pathology

The concept of personalized medicine stems from the advances in biotechnology, molecular biology, and genetics. It affects the diagnostic tests that may guide the therapeutic options based on individual (specific) characteristics (1). Using massively parallel, high-throughput technologies, these advances enable detecting minute and precise changes at different molecular (DNA, RNA, protein) levels in enormous quantity and variety and at an ever-increasing speed. The methods include DNA/RNA sequencing, mass spectrometry, microarray technologies, comparative genomic hybridization, digital polymerase chain reaction (PCR), each of which generates an enormous quantity of information called "big data" (8, 9).

In the U.S., the Personalized Medicine Coalition defined personalized medicine as the "tailoring of medical treatment to each patient's characteristics. It does not mean that drugs (or medical devices) are developed to be unique to a patient but rather the ability to classify individuals into subpopulations that differ in their susceptibility to a particular disease or their response to a specific treatment. Therefore, the preventive or therapeutic interventions can be concentrated on those who will benefit, sparing expense, and adverse effects for those who will not" (10). On the other hand, the U.S. National Cancer Institute (NCI) defines personalized medicine as "a form of medicine that uses information about a person's genes, proteins, and environment to prevent, diagnose, and treat disease" (11). The key features of personalized medicine include identifying populations (or individual patients) who are candidates for treatment, either by identifying patient/disease characteristics that are likely to benefit or show no improvement/develop adverse effects from treatment (12). Von Hoff and collaborators at TGen and Caris Life Sciences were the pioneers in the precision medicine treatment approach, demonstrating that molecular profiling of patients' tumors is an efficient approach to identifying potential targets and selecting the best treatments for their refractory cancers (13). Since then, numerous studies have confirmed the clinical relevance of molecular profiling and personalized medicine in cancer treatment leading to the paradigm shift in cancer treatment (9).

Even though personalized medicine's potential benefits are already evident (e.g., enhanced therapeutic efficacy and increased safety of targeted drugs), its uptake by health care systems varies across the globe. Generally, it remains limited at this time (14). However, it is anticipated that, as a scientific understanding of cancer progresses at the molecular level, personalized medicine approaches to cancer diagnosis and treatment will become more common. For example, the number of personalized medicine devices that have been commercialized in Europe quadrupled between 2006 and 2011 (10). The development of therapeutic products (devices) that are paired with diagnostic tests is also rapidly increasing. In December 2013, the Food and Drug Administration (FDA) approved the first next-generation sequencer (NGS) (Illumina's MiSeqDx) for commercial use in the United States (15). This platform's approval made possible the dozens of genomic information in clinical practice, and markedly expanded this technology's clinical utility to guide patients' care (15). In 2017, the FDA approved the FoundationOne CDx (Foundation Medicine, Inc.) as the first comprehensive, FDA-approved tissue-based companion diagnostic (CDx) assay that is validated for all solid tumors (16). In August 2020, the FDA granted approval for the first liquid biopsy-based NGS CDx test, The Guardant360 CDx (The Guardant Health, Inc.) (17). The Guardant360 CDx utilizes liquid biopsy and NGS technology to detect 55 different genomic alterations, including *EGFR* gene mutations in patients with NSCLC from circulating cell-free DNA (cfDNA). Besides, several comprehensive NGS-platforms are currently available (e.g., Caris MI profile, Tempus xT assay,

Invitae Multi-Cancer Panel) (18) and are being increasingly used in cancer decision-making and treatment (19) (please refer to the next paragraph for more details). Recently, the European Society of Medical Oncology (ESMO) Precision Medicine Working up came out with their recommendations for the use of NGS testing for patients with metastatic cancers (20). Using the ESMO Scale for Clinical Actionability of molecular Targets (ESCAT), the ESMO group found concrete evidence. It strongly recommended routine NGS testing for patients with metastatic NSCLC, prostate, ovarian cancers, and cholangiocarcinoma. Besides, they recommended NGS testing for several other common cancers such as colorectal cancer, small cell lung cancer (SCLC), endometrial cancer, neuroendocrine tumors, salivary, thyroid, and vulvar cancers (mainly for the tumor mutational burden (TMB) assessment as a predictive biomarker for immune checkpoint inhibitors) (20).

The Concept of Companion Diagnostic Tests (CDx)

The rise of precision medicine in pathology accelerated in the 1980s with the diagnostic use of automated immunohistochemistry (IHC) (21, 22). Since that time, IHC has been substantially improved, standardized, and its clinical utility in cancer diagnostics has been markedly expanded, particularly in recent years (23-27). IHC is an essential tool for cancer diagnostics and tumor typing (Figure 1). However, it has been increasingly used as a reliable and affordable method for precision medicine purposes. The vast majority of diagnostic tests are developed in the individual laboratories and are designated as a laboratory (or in-house) developed tests (LDT). However, several IHC tests are now designated as "companion diagnostic" or "complementary diagnostic" tests to indicate their status concerning the FDA approval/clearance status. Although IHC is a relatively simple and widely utilized method, frequently fully automated in most pathology laboratories, its interpretation is entirely subjective; hence a strict training/validation processes must be applied.

A companion diagnostic device is defined as "an in vitro diagnostic device (IVD) or an imaging tool that provides information that is essential for the safe and effective use of a corresponding therapeutic product" (28). The use of an IVD companion diagnostic test with a specific therapeutic product is stipulated in the instructions for use in the labeling of both the diagnostic device and the corresponding medicinal product and the labeling of any generic or biosimilar equivalents of the therapeutic product. In other words, a CDx test is required before a specific treatment to determine eligibility. On the other hand, although predictive, a complementary diagnostics test is not needed for the drug's prescription. The concept of precision medicine is accompanied by various CDx tests that have become increasingly approved and used for targeted treatment purposes (29) [a full list of companion diagnostic devices that have been approved by the FDA is available at its website (28)].

One of the earliest CDx relied on the identification of *HER2/erbB2* gene amplification (in-situ hybridization) or HER2 protein overexpression (immunohistochemistry) in breast and later in gastric/gastroesophageal junction (GEJ) cancers for the treatment with various anti-HER2 therapeutics such as trastuzumab and pertuzumab (monoclonal antibodies) and lapatinib (a small molecule tyrosine kinase inhibitor that inhibits HER2 specifically) (30-32) (Table 1).

Additional examples of commonly used CDx assays include the assessment of *C-KIT* (CD117) and *PDGFRα* mutations in gastrointestinal stromal tumors (GIST) (33), tyrosine kinase mutations affecting the Epidermal growth factor receptor (*EGFR*) gene, and *EML-ALK* gene rearrangements in non-small cell lung cancer (NSCLC) (34-36), and mutations in the *BRAF* gene in malignant melanoma (37). Notably, most of these genetic alterations have a substantial potential to render tumors susceptible to specific inhibitors mentioned above. In addition to diagnostic PCR or in-situ hybridization-based assays, IHC testing, performed by pathologists, is robust, genomic alteration-specific, cheap, and consequently utilized in a clinical setting. For instance, the ALK 5A4 IHC assay has

Table 1. Some of the Commonly Used Single Diagnostic Tests [Diagnostic Antibodies (Immunohistochemistry) and Probes (in Situ Hybridization)] with an Approved Status As "Companion Diagnostic" Assays

Biomarker/diagnostic assay (manufacturer)	Scoring system	Companion diagnostic (CDx) Thresholds	Indication (cancer subtype)	Drug(s)
Immuno-Oncology (I-O) Biomarkers				
22c3 (DAKO Agilent)	CPS	<1, ≥1, ≥10	Gastric/GEJ carcinoma, cervical carcinoma TNBC	Pembrolizumab
22c3 (DAKO Agilent)	TPS	0, 1-49, ≥50	NSCLC	Pembrolizumab
SP142 (Ventana)	IC scoring	IC ≥1%, IC≥5%	TNBC, Urothelial carcinoma (bladder)	Atezolizumab
Other companion diagnostic (CDx) single tests				
ALK Testing ALK D5F3 Ventana (IHC)	Positive/ negative	Any percentage of positive cancer cells	NSCLC	Crizotinib or ceritinib
Vysis ALK Break Apart FISH Probe Kit (Abbott) (FISH)	-	Identification of *ALK* gene rearrangements with its partners (e.g., *EML4*, *TFG*, *KIF5B*)	NSCLC	Crizotinib or ceritinib
HER2 testing anti-HER2 (4B5) (Ventana) (IHC)	Score 0-3+	Score 3+ in cancer cells	Breast cancer	Trastuzumab, pertuzumab, adotrastuzumab emtansine
INFORM HER2 Dual ISH DNA Probe Cocktail (Ventana) (ISH)	*HER2/CEP*17 ratio	*HER2/CEP*17 ratio ≥2 (positive)	Breast cancer	Trastuzumab, pertuzumab, adotrastuzumab emtansine
DAKO c-Kit PharmDx (IHC)	Positive/ negative	Any expression in cancer cells	GIST	Imatinib mesylate
DAKO EGFR PharmDx (IHC)	Positive/ negative	Any membranous expression in cancer cells	Colorectal cancer	Cetuximab, panatumumab

All the listed assays have been approved by the Food and Drug Administration/FDA/ (28). ALK=Anaplastic lymphoma kinase; CEP17=Centromere of chromosome 17; CPS=Combined positive score is defined as the number of PD-L1 positive cells (cancer cells, lymphocytes, and macrophages) divided by the total number of viable tumor cells, multiplied by 100; EGFR=Epidermal growth factor receptor; FISH=Fluorescent in situ hybridization; GEJ=carcinoma Gastro-esophageal junction carcinoma; GIST=Gastrointestinal stromal tumor; HER2=Human epidermal growth receptor 2; IC (immune cells) score=A proportion of the tumor area occupied by PD-L1 staining of any intensity; IHC=Immunohistochemistry; ISH=In situ hybridization; NSCLC=Non-small cell lung cancer; TC=Tumor cells; TNBC=Triple-negative breast cancer; TPS=Tumor proportion score. Defined as the percentage of viable cancer cells showing a partial or complete membrane staining at any intensity.

been confirmed as a reliable screening diagnostic test for ALK-rearranged NSCLCs and is associated with treatment response and survival (38). Similarly, c-Kit expression using c-Kit PharmDx (Agilent) is indicated in both differential diagnosis of gastrointestinal stromal tumors (GIST) (95% positive) and in selecting the GIST patients that are eligible for treatment with imatinib mesylate (Gleevec). EGFR pharmDxTM is another FDA-approved IHC-based assay that was supposed to identify colorectal cancer patients who are eligible for anti-EGFR-treatment modalities such as cetuximab or panitumumab (Table 1). However, later studies revealed that EGFR protein expression is not a clinically useful predictive biomarker to cetuximab response in patients with CRC (39, 40).

Specific biomarkers can also indicate when patients are less likely to respond to a specific therapy, e.g., *KRAS* or *NRAS* mutations make colorectal cancers unresponsive to anti-epidermal growth factor receptor (anti-EGFR) therapies such as cetuximab or panitumumab (40-42). Similarly, specific *EGFR* gene mutations in NSCLC (e.g., point mutation T790M) are responsible for approximately 50% of acquired resistance to the EGFR tyrosine kinase inhibitors (43).

In contrast to those mentioned above single genomic assays, FoundationOne CDx is the first FDA-approved comprehensive tissue-based CDx

that has been validated in a variety of solid tumors. It includes a broad panel of tested genes (N=324) and two genomic signatures. It has already been utilized in treatment decision-making for various solid cancers, including NSCLC, colorectal, breast, ovarian cancer, and malignant melanoma (44) (Table 2). The test also provides microsatellite instability (MSI) and tumor mutational burden (TMB) status, both of which are essential predictive biomarkers in immuno-oncology (I-O) treatment regardless of the tumor histology ("tumor agnostic approach") (please refer to the next paragraph). The FoundationOne CDx is also a CDx for identifying the neurotrophic receptor tyrosine kinase (NTRK) genes (*NTRK1, NTRK2*, and *NTRK3*) fusions. All the patients whose cancers harbor any of these fusions and regardless of the tumor histotype are eligible for the treatment with an NTRK inhibitor (entrectinib or larotrectinib) (Another "tumor agnostic approach") (45). FoundationOne Liquid CDx is a similar FDA-approved CDx that explores potentially targetable genes using a simple blood sample (liquid biopsy, which is based on peripheral blood analysis of cell-free circulating tumor DNA). It is along with the Guardant360 CDx, the only comprehensive FDA-approved blood-based test that analyzes > 300 genes, making it the most comprehensive FDA-approved liquid biopsy CDx currently available (Table 2). Besides, FoundationOne Liquid CDx provides blood tumor mutational burden (bTMB), MSI, and tumor fraction values. Another FDA-approved comprehensive molecular genomic assay is the MSK-IMPACT™ test developed by the Memorial Sloan Kettering Cancer Center. Memorial Sloan Kettering-Integrated Mutation Profiling of Actionable Cancer Targets (MSK-IMPACT) covers 468 different genes, many of which are potentially targetable with currently available drugs (46). MSK-IMPACT has been shown to reliably profile tumor DNA for somatic mutations in various solid malignancies with high accuracy and sensitivity (47). In contrast to the FoundationOne CDx, this assay is mainly used in the United States.

Immunotherapy, based on immune checkpoint inhibitors against programmed cell death protein 1/programmed death-ligand 1 (PD-1/PD-L1) axis, has dramatically changed the cancer treatment paradigm and improved the outcomes of several common cancers such as melanoma, NSCLC, renal, urothelial, cervical, gastric/gastroesophageal (GEJ), head and neck squamous cell and triple-negative breast carcinomas (TNBC) (48). The therapeutic breakthroughs have been followed by the development of predictive biomarkers of response to immune checkpoint inhibitors. Several of these biomarkers have been validated and achieved a companion diagnostic status, including PD-L1 expression in tumor (T.C.) or immune cells (IC) tested by IHC. Tumor mutational burden (TMB) and microsatellite instability-high (MSI-H) status, determined by NGS-based assays, have also been approved as predictive biomarkers to immune checkpoint blockade (e.g., pembrolizumab) (49) (Table 2). Other potential predictive biomarkers [e.g., PD-1 status, PD-L1 (*CD274* gene) amplification], although extensively studied, have not been fully validated and consequently approved as CDx assays.

Multiple IHC assays with different scoring algorithms have been approved for various immune checkpoint blockade therapies and associated cancers (Table 1). Several of these IHC assays have been approved as CDx, such as VENTANA SP142 assay for selecting NSCLC, bladder, and TNBC patients for the treatment with immune checkpoint inhibitor atezolizumab. DAKO 22C3 pharmDx assay has been approved for testing eligibility of NSCLC, TNBC, gastric/GEJ, cervical, urothelial, head and neck squamous cell (HNSCC), and esophageal squamous cell carcinoma patients for the treatment with pembrolizumab while DAKO 28-8 pharmDx clone is utilized for the selection of NSCLC patients for the combined treatment with two immune checkpoint inhibitors: nivolumab (against PD-1) + ipilimumab (targeting cytotoxic T-lymphocyte-associated protein 4/CTLA-4/) (28). Notably, each of these assays has different scoring algorithms, e.g., tumor proportion score (TPS), combined positive score (CPS), and immune cells (I.C.) score, all of which have different thresholds for positivity. These issues make the current PD-L1 IHC testing landscape very compli-

Table 2. Overview of the Commonly Used and FDA-Approved Comprehensive Companion Diagnostic Tests

Assay*	Technology	Gene panel†	Indications‡	Drugs
FoundationOne CDx§	NGS-based	324 targetable Genes MSI status TMB status	Multiple cancers (NSCLC, colon, breast, ovary, melanoma)	21 FDA-approved targeted therapies
FoundationOne Liquid CDx‖	NGS-based	300 targetable genes MSI status Blood TMB status	Multiple cancers	Multiple targeted drugs
MSK-IMPACT§	NGS-based	468 targetable genes MSI status	Multiple cancers	Multiple targeted drugs
The Guardant360 CDx‖	NGS-based	55 targetable genes, including *EGFR*	NSCLC and other cancers	TAGRISSO (Osimertinib) and other targeted drugs

*Manufacturer; †Predictive biomarkers; ‡Cancer subtypes; §Tissue-based assay; ‖Based on peripheral blood analysis of cell-free circulating tumor DNA (cfDNA) (=liquid biopsy); EGFR=Epidermal Growth Factor Receptor; FDA=Food and Drug Administration; MSI=Microsatellite instability; NGS=Next-generation sequencing; NSCLC=Non-small cell lung cancer; TMB=Tumor mutational burden.

cated. They require pathologists to be specifically trained for each of the proposed assays and their respective scoring systems.

Besides, PD-L1 status in cancer is substantially challenged by its complex regulation within the tumor parenchyma and microenvironment (immune cells), its dynamic clonal and proteomic changes to therapy, heterogeneous host immune defects, and markedly variable standardization among sample preparation and reporting (48). Despite all the advances mentioned above, there is still an unmet need to optimize predictive I-O biomarkers given their limited clinical utility (a low response rate/resistance in most cancers) and highly demanding testing and interpretation algorithms (20).

Challenges Ahead: "Next-Generation Pathologists" and Precision Medicine

Molecular pathology has become one of the cornerstones of precision cancer medicine. This change has required enormous efforts from pathologists to gain and demonstrate expertise and skills in this rapidly evolving era (50). Simultaneously, the paradigm shift allowed for the discipline of pathology to reinvent itself as a leading diagnostic discipline in the precision medicine era. Indeed, this would imply additional and continuous efforts to educate pathologists in using genomic and molecular data and interpret novel diagnostic tests and procedures. Therefore, the dissemination of knowledge on molecular pathology among pathologists by incorporating the courses in postgraduate training programs for trained pathologists and improving pathology residency training programs are critical for the future of diagnostic molecular pathology (51). In this regard, several countries have already taken the necessary measures. Thus, the Dutch Society of Pathology has launched a 2-year training program in molecular pathology, while the Royal College of Pathologists has a fellowship in molecular pathology for clinical scientists. In the United States, the Association of Molecular Pathology has also developed a molecular pathology curriculum for medical laboratory scientists (52). At the same time, the American Board of Pathology offers certification for the pathologist completing at least 12 months of training in an ACGME (The Accreditation Council for Graduate Medical Education) accredited molecular genetic pathology program (53).

Another essential aspect in which the pathologists play a crucial role is developing and implementing molecular tests in clinical practice and communicating the obtained results with other diagnostic disciplines (e.g., microbiology, clinical chemistry, genetics, and immunology) (15, 54-56) and clinicians (Figure 1). Pathologists also play a crucial role in optimizing the samples for molecular profiling. They are also responsible for the proper and selective use of the available specimens

to enhance predictive tests' clinical utility. New, complementary diagnostic methods have also been launched, e.g., the sequence analysis of cell-free tumor DNA isolated from plasma or urine (=liquid biopsy) (Figure 1). Liquid biopsy and the traditional tissue samples (biopsy, cytology) are of utmost importance for identifying biomarkers for personalized medicine. Increased availability of diagnostic tests and a growing emphasis on personalized medicine have been approached by the novel, revolutionary technologies such as machine learning (ML) and artificial intelligence (A.I.), both of which could greatly help in analyzing the "big data" and identifying the proper biomarkers for precision medicine (treatment) and diagnostics ("personalized diagnosis") (57, 58) (Figure 1). Both methods are rapidly evolving and are believed to contribute to precision medicine and other healthcare fields.

All of the activities mentioned above contribute to a successful translation of the scientific advancements into a benefit to patients ("next-generation pathologists"). In this regard, the European Society of Pathology (ESP) and the Royal College of Pathology (RCPath) groups proposed the guidelines for laboratories performing molecular pathology for cancer patients (52). The guideline encompasses all the essential issues related to molecular pathology testing, including preanalytical considerations, sample receipt and handling (fixation and processing), DNA and RNA extraction, selection of appropriate analytical method(s), and quality control (both internal and external) (52). College of American Pathologists (CAP) has also been actively developing numerous evidence-based guidelines about preanalytical and analytical aspects of diagnostic and molecular pathology. These guidelines also include precision medicine biomarkers and CDx assays such as estrogen receptor (ER), progesterone receptor (PR) and HER2 (breast cancer), various predictive biomarkers in NSCLC and CRC, biomarkers for prostate cancer, Human Papillomavirus (HPV) testing in HNSCC, etc. (59). Similar initiatives have been taken by international external quality assurance (EQA) agencies [e.g., UK NEQAS ICC & ISH, NordiQC, and European Molecular Quality Network (EMQN)], who put joint efforts to publish the guidelines for EQA. These guidelines aim to improve molecular tests' performance for precision medicine purposes (60).

Conclusions and Future Directions

The practice of diagnostic pathology has been substantially changed in the previous years due to the advances in molecular diagnostics and targeted treatment (precision medicine). Molecular pathology has become one of the cornerstones of precision cancer medicine. Although "the next-generation pathologists" have already been launched, further and continuous educational efforts must fully implement the paradigm shift into diagnostic molecular pathology practice and reinvent it as a leading diagnostic discipline in the precision medicine era. Most of the approved and validated predictive biomarkers in precision medicine still require further optimization and standardization. There is an unmet need for novel and more reliable predictive tests (biomarkers) given a low response rate and common resistance for most approved targeted treatment modalities.

Acknowledgment: We thank Professor Miroslav Harjacek MD, PhD (College of Medicine and Health Sciences, Al Ain, United Arab Emirates) for his critical reading and valuable comments.

Conflict of Interest: The authors declare that they have no conflict of interest.

References

1. Birner P, Prager G, Streubel B. Molecular pathology of cancer: how to communicate with disease. ESMO Open. 2016;1(5):e000085.
2. Rosai J. Guiding the Surgeon's Hand: The History of American Surgical Pathology. 1st ed. Washington, DC: American Registry of Pathology; 1997.
3. Boveri T. Concerning the origin of malignant tumours by Theodor Boveri. Translated and annotated by Henry Harris. J Cell Sci. 2008;121 Suppl 1:1-84.
4. Nowell PC. The clonal evolution of tumor cell populations. Science. 1976;194(4260):23-8.

5. Hanahan D, Weinberg RA. The hallmarks of cancer. Cell. 2000;100(1):57-70.
6. Hanahan D, Weinberg RA. Hallmarks of cancer: the next generation. Cell. 2011;144(5):646-74.
7. Tsang JYS, Tse GM. Molecular Classification of Breast Cancer. Adv Anat Pathol. 2020;27(1):27-35.
8. Gu J, Taylor CR. Practicing pathology in the era of big data and personalized medicine. Appl Immunohistochem Mol Morphol. 2014;22(1):1-9.
9. El-Deiry WS, Goldberg RM, Lenz HJ, Shields AF, Gibney GT, Tan AR, et al. The current state of molecular testing in the treatment of patients with solid tumors, 2019. CA Cancer J Clin. 2019;69(4):305-43.
10. Personalized Medicine Coalition. [2020 Oct 15]. Available from: http://www.personalizedmedicinecoalition.org/Userfiles/PMC-Corporate/file/pmc_bridgehead_issue_brief_european_reimbursement.pdf.
11. National Cancer Institute. [2020 Oct 15]. Available from: https://www.cancer.gov/publications/dictionaries/cancer-terms/def/personalized-medicine.
12. Food and Drug Administration; [In Vitro Companion Diagnostic Devices]. [2020 Oct 15]. Available from: https://www.fda.gov/regulatory-information/search-fda-guidance-documents/vitro-companion-diagnostic-devices.
13. Von Hoff DD, Stephenson JJ Jr, Rosen P, Loesch DM, Borad MJ, Anthony S, et al. Pilot study using molecular profiling of patients' tumors to find potential targets and select treatments for their refractory cancers. J Clin Oncol. 2010;28(33):4877-83.
14. Chen A, Flaherty K, O'Dwyer PJ, Giantonio B, Marinucci DM, Lee J-W, et al. Tumor Genomic Profiling Practices and Perceptions: A Survey of Physicians Participating in the NCI-MATCH Trial. JCO Precision Oncology. 2020(4):1207-16.
15. Collins FS, Hamburg MA. First FDA authorization for next-generation sequencer. N Engl J Med. 2013;369(25):2369-71.
16. Foundation Medicine; [FoundationOne CDx]. [2020 Oct 15]. Available from: https://www.foundationmedicine.com/test/foundationone-cdx.
17. FDA approves liquid biopsy NGS companion diagnostic test for multiple cancers and biomarkers: Food and Drug Administration; 2020. [2020 Oct 15]. Available from: https://www.fda.gov/drugs/fda-approves-liquid-biopsy-ngs-companion-diagnostic-test-multiple-cancers-and-biomarkers#:~:text=FDA%20approves%20liquid%20biopsy%20NGS%20companion%20diagnostic%20test%20for%20multiple%20cancers%20and%20biomarkers,-Share&text=On%20October%2026%20and%20November,(Foundation%20Medicine%2C%20Inc.).
18. Zeng J, Johnson A, Shufean MA, Kahle M, Yang D, Woodman SE, et al. Operationalization of Next-Generation Sequencing and Decision Support for Precision Oncology. JCO Clin Cancer Inform. 2019(3):1-12.
19. Freedman AN, Klabunde CN, Wiant K, Enewold L, Gray SW, Filipski KK, et al. Use of Next-Generation Sequencing Tests to Guide Cancer Treatment: Results From a Nationally Representative Survey of Oncologists in the United States. JCO Precision Oncology. 2018(2):1-13.
20. Mosele F, Remon J, Mateo J, Westphalen CB, Barlesi F, Lolkema MP, et al. Recommendations for the use of next-generation sequencing (NGS) for patients with metastatic cancers: a report from the ESMO Precision Medicine Working Group. Ann Oncol. 2020;31(11):1491-505.
21. Taylor CR, Burns J. The demonstration of plasma cells and other immunoglobulin-containing cells in formalin-fixed, paraffin-embedded tissues using peroxidase-labelled antibody. J Clin Pathol. 1974;27(1):14-20.
22. Grogan TM. Automated immunohistochemical analysis. Am J Clin Pathol. 1992;98(4 Suppl 1):S35-8.
23. Taylor CR. Milestones in Immunohistochemistry and Molecular Morphology. Appl Immunohistochem Mol Morphol. 2020;28(2):83-94.
24. Taylor CR. Improved and Standardized Approaches to Selection of Control Materials From ISIMM: Announcing a Workshop at the Annual ASCP Meeting, September 6-7, 2017, Sponsored by the International Society for Immunohistochemistry and Molecular Morphology. Appl Immunohistochem Mol Morphol. 2017;25(7):451-2.
25. Torlakovic EE, Cheung CC, D'Arrigo C, Dietel M, Francis GD, Gilks CB, et al. Evolution of Quality Assurance for Clinical Immunohistochemistry in the Era of Precision Medicine. Part 3: Technical Validation of Immunohistochemistry (IHC) Assays in Clinical IHC Laboratories. Appl Immunohistochem Mol Morphol. 2017;25(3):151-9.
26. Torlakovic EE, Cheung CC, D'Arrigo C, Dietel M, Francis GD, Gilks CB, et al. Evolution of Quality Assurance for Clinical Immunohistochemistry in the Era of Precision Medicine - Part 2: Immunohistochemistry Test Performance Characteristics. Appl Immunohistochem Mol Morphol. 2017;25(2):79-85.
27. Cheung CC, D'Arrigo C, Dietel M, Francis GD, Gilks CB, Hall JA, et al. Evolution of Quality Assurance for Clinical Immunohistochemistry in the Era of Precision Medicine: Part 1: Fit-for-Purpose Approach to Classification of Clinical Immunohistochemistry Biomarkers. Appl Immunohistochem Mol Morphol. 2017;25(1):4-11.
28. List of Cleared or Approved Companion Diagnostic Devices (In Vitro and Imaging Tools): Food and Drug Administration. [2020 Oct 15]. Available from: https://www.fda.gov/medical-devices/vitro-diagnostics/list-cleared-or-approved-companion-diagnostic-devices-vitro-and-imaging-tools.
29. Plones T, Engel-Riedel W, Stoelben E, Limmroth C, Schildgen O, Schildgen V. Molecular Pathology and Personalized Medicine: The Dawn of a New Era in Companion

Diagnostics-Practical Considerations about Companion Diagnostics for Non-Small-Cell-Lung-Cancer. J Pers Med. 2016;6(1):3.

30. Geyer CE, Forster J, Lindquist D, Chan S, Romieu CG, Pienkowski T, et al. Lapatinib plus capecitabine for HER2-positive advanced breast cancer. N Engl J Med. 2006;355(26):2733-43.
31. Hortobagyi GN. Trastuzumab in the treatment of breast cancer. N Engl J Med. 2005;353(16):1734-6.
32. Baselga J, Bradbury I, Eidtmann H, Di Cosimo S, de Azambuja E, Aura C, et al. Lapatinib with trastuzumab for HER2-positive early breast cancer (NeoALTTO): a randomised, open-label, multicentre, phase 3 trial. Lancet. 2012;379(9816):633-40.
33. Rubin BP, Heinrich MC, Corless CL. Gastrointestinal stromal tumour. Lancet. 2007;369(9574):1731-41.
34. Lynch TJ, Bell DW, Sordella R, Gurubhagavatula S, Okimoto RA, Brannigan BW, et al. Activating mutations in the epidermal growth factor receptor underlying responsiveness of non-small-cell lung cancer to gefitinib. N Engl J Med. 2004;350(21):2129-39.
35. Maemondo M, Inoue A, Kobayashi K, Sugawara S, Oizumi S, Isobe H, et al. Gefitinib or chemotherapy for non-small-cell lung cancer with mutated EGFR. N Engl J Med. 2010;362(25):2380-8.
36. Soda M, Choi YL, Enomoto M, Takada S, Yamashita Y, Ishikawa S, et al. Identification of the transforming EML4-ALK fusion gene in non-small-cell lung cancer. Nature. 2007;448(7153):561-6.
37. Flaherty KT, Puzanov I, Kim KB, Ribas A, McArthur GA, Sosman JA, et al. Inhibition of mutated, activated BRAF in metastatic melanoma. N Engl J Med. 2010;363(9):809-19.
38. Fiset PO, Labbe C, Young K, Craddock KJ, Smith AC, Tanguay J, et al. Anaplastic lymphoma kinase 5A4 immunohistochemistry as a diagnostic assay in lung cancer: A Canadian reference testing center's results in population-based reflex testing. Cancer. 2019;125(22):4043-51.
39. Licitra L, Storkel S, Kerr KM, Van Cutsem E, Pirker R, Hirsch FR, et al. Predictive value of epidermal growth factor receptor expression for first-line chemotherapy plus cetuximab in patients with head and neck and colorectal cancer: analysis of data from the EXTREME and CRYSTAL studies. Eur J Cancer. 2013;49(6):1161-8.
40. Evaluation of Genomic Applications in Practice and Prevention (EGAPP) Working Group. Recommendations from the EGAPP Working Group: can testing of tumor tissue for mutations in EGFR pathway downstream effector genes in patients with metastatic colorectal cancer improve health outcomes by guiding decisions regarding anti-EGFR therapy? Genet Med. 2013;15(7):517-27.
41. Amado RG, Wolf M, Peeters M, Van Cutsem E, Siena S, Freeman DJ, et al. Wild-type KRAS is required for panitumumab efficacy in patients with metastatic colorectal cancer. J Clin Oncol. 2008;26(10):1626-34.
42. Jimeno A, Messersmith WA, Hirsch FR, Franklin WA, Eckhardt SG. KRAS mutations and sensitivity to epidermal growth factor receptor inhibitors in colorectal cancer: practical application of patient selection. J Clin Oncol. 2009;27(7):1130-6.
43. Gazdar AF. Activating and resistance mutations of EGFR in non-small-cell lung cancer: role in clinical response to EGFR tyrosine kinase inhibitors. Oncogene. 2009;28 Suppl 1:S24-31.
44. FoundationOne CDx - P170019: Food and Drug Administration; 2020. [2020 Oct 15]. Available from: https://www.fda.gov/medical-devices/recently-approved-devices/foundationone-cdx-p170019.
45. FDA Approves Companion Diagnostic to identify NTRK fusions in solid tumors for Vitrakvi: Food and Drug Administration. [2020 Oct 15]. Available from: https://www.fda.gov/drugs/fda-approves-companion-diagnostic-identify-ntrk-fusions-solid-tumors-vitrakvi.
46. MSK-IMPACT: A Targeted Test for Mutations in Both Rare and Common Cancers: Memorial Sloan Kettering Cancer Center. [2020 Oct 15]. Available from: https://www.mskcc.org/msk-impact.
47. Cheng DT, Mitchell TN, Zehir A, Shah RH, Benayed R, Syed A, et al. Memorial Sloan Kettering-Integrated Mutation Profiling of Actionable Cancer Targets (MSK-IMPACT): A Hybridization Capture-Based Next-Generation Sequencing Clinical Assay for Solid Tumor Molecular Oncology. J Mol Diagn. 2015;17(3):251-64.
48. McKean WB, Moser JC, Rimm D, Hu-Lieskovan S. Biomarkers in Precision Cancer Immunotherapy: Promise and Challenges. Am Soc Clin Oncol Educ Book. 2020;40:e275-e91.
49. Nucleic Acid Based Tests: Food and Drug Administration; 2020. [2020 Oct 15]. Available from: https://www.fda.gov/medical-devices/vitro-diagnostics/nucleic-acid-based-tests.
50. Tonellato PJ, Crawford JM, Boguski MS, Saffitz JE. A national agenda for the future of pathology in personalized medicine: report of the proceedings of a meeting at the Banbury Conference Center on genome-era pathology, precision diagnostics, and preemptive care: a stakeholder summit. Am J Clin Pathol. 2011;135(5):668-72.
51. Fassan M. Molecular Diagnostics in Pathology: Time for a Next-Generation Pathologist? Arch Pathol Lab Med. 2018;142(3):313-20.
52. Cree IA, Deans Z, Ligtenberg MJ, Normanno N, Edsjo A, Rouleau E, et al. Guidance for laboratories performing molecular pathology for cancer patients. J Clin Pathol. 2014;67(11):923-31.
53. Molecular Genetic Pathology: The American Board of Pathology. [2020 Oct 15]. Available from: https://www.ab-

path.org/index.php/to-become-certified/requirements-for-certification?id=46.

54. Croxatto A, Prod'hom G, Greub G. Applications of MALDI-TOF mass spectrometry in clinical diagnostic microbiology. FEMS Microbiol Rev. 2012;36(2):380-407.
55. Deurenberg RH, Bathoorn E, Chlebowicz MA, Couto N, Ferdous M, Garcia-Cobos S, et al. Reprint of "Application of next generation sequencing in clinical microbiology and infection prevention". J Biotechnol. 2017;250:2-10.
56. Mellors T, Withers JB, Ameli A, Jones A, Wang M, Zhang L, et al. Clinical Validation of a Blood-Based Predictive Test for Stratification of Response to Tumor Necrosis Factor Inhibitor Therapies in Rheumatoid Arthritis Patients. Network and Systems Medicine. 2020;3(1):91-104.
57. Savage N. How AIis improving cancer diagnostics. Nature. 2020;579(7800):S14-S6.
58. Machine learning in cancer diagnostics. EBioMedicine. 2019;45:1-2.
59. Human Papillomavirus Testing in Head and Neck Carcinomas: College of American Pathologists; 2020. [2020 Oct 15]. Available from: https://www.cap.org/protocols-and-guidelines/cap-guidelines/current-cap-guidelines/human-papillomavirus-testing-in-head-and-neck-carcinomas.
60. Dufraing K, Fenizia F, Torlakovic E, Wolstenholme N, Deans ZC, Rouleau E, et al. Biomarker testing in oncology - Requirements for organizing external quality assessment programs to improve the performance of laboratory testing: revision of an expert opinion paper on behalf of IQNPath ABSL. Virchows Arch. 2020.

Narrative Review
Acta Medica Academica 2021;50(1):58-70
DOI: 10.5644/ama2006-124.326

Testicular Germ Cell Tumors: Serological and Immunohistochemical Diagnosis

Ivan Damjanov*

Department of Pathology and Laboratory Medicine, The University of Kansas School of Medicine, Kansas City, KS 66160, USA

Correspondence: *idamjano@kumc.edu*; Tel.: + 011 267 400 9562; Fax.: + 011 913 588 8780

Received: 21 December 2020; **Accepted:** 25 December 2020

Abstract
This review deals with serologic and immunohistochemical tumor markers used in clinical laboratories for the diagnosis of testicular germ cell tumors. Time tested serologic markers such as alpha-fetoprotein, human chorionic gonadotropin, and lactate dehydrogenase are routinely used in the work-up of patients with testicular tumors. Professional organizations regulating the practice of medicine in most countries worldwide require that the laboratory values for these serologic reactants be included in the pathology reports on testicular tumors as part of the tumor staging process. Immunohistochemical markers of testicular germ have been identified and widely tested during the first two decades of the XXI century. We have selected the most useful immunohistochemical markers from a few of these markers and discussed them in this review. **Conclusion.** Published data show that testicular tumor markers are widely used in routine practice. The study of tumor markers has improved the pathologic and clinical diagnosis of testicular germ cell tumors and has thus contributed to their treatment.

Key Words: Testicular Tumors ▪ Germ Cell Tumors ▪ Serologic Diagnosis ▪ Immunohistochemistry ▪ Tumor Markers.

Introduction

Lecturing for many years to medical students about testicular tumors, I adopted the same principle that the U.S. Navy applied to the design of new weapons in the 1960's. This principle is best known as *KISS*, an acronym, which stands for "keep it simple, stupid" (1).

Using the KISS principle, in these simplified lectures, I would tell my students that testicular tumors are "more than 90 percent tumors":

- More than 90% are malignant;
- More than 90% are of germ cell origin and thus classified as germ cell tumors (GCT);
- More than 90% sporadic (i.e., not related to exogenous or endogenous or genetic factors);
- More than 90% are diagnosed in adult males in the 20-45 years age group and
- More than 90% of patients have long-term survival and most are cured by modern therapeutic approaches.

Even though testicular tumors account for only 1% of malignant neoplasms in males, they have become a poster example of malignant tumors that can be cured by combining surgery, chemotherapy, and, if need be, radiation therapy, as reviewed in several recent publications (2-5). These tumors, which have previously accounted for significant cancer related mortality in adult men, who were in the most productive period of their lives were literally conquered by modern medicine.

The study of serologic and immunohistochemical tumor markers, to be reviewed here, has contributed to diagnosis and treatment of GCT.

Clinicopathologic Classification

Pathology has made significant contributions to this modern medicine paradigmatic success sto-

*ORCID: http://orcid.org/0000-0002-1394-6052

ry. It all began with the groundbreaking study of Friedman and Moore (6), who examined more than 900 testicular tumors diagnosed in soldiers of the U.S. Armed Forces during World War II. The basic tenets of that study were subsequently confirmed and expanded in numerous clinicopathologic studies. Widely accepted worldwide, these classifications were disseminated in the atlases of the Armed forces Institute of Pathology (AFIP) and included in consecutive classifications of the World Health Organization (WHO), the latest of which was published in 2016 (7).

Histopathologic classification of testicular tumors is primarily based on the histogenesis of these tumors. Even though testicular tumors' exact histogenesis has not been fully elucidated, all the data indicate that most neoplasm can be traced to the germ cell line and its early embryonic and fetal precursors (8-11). Subclassification of germ cell tumors is essential, primarily because of the biological and clinical differences between seminoma on one hand side and mixed germ cell tumors, also known clinically as "nonseminomas" or "nonseminomatous germ cell tumors (NSGCT)" on the other (7).

According to the most widely used classification of germ cell tumors, testicular GCT can be classified into three categories, which have distinct features: patients' age, histologic characteristics, and molecular and cellular histogenesis (8, 11). Type I GCT include teratomas and yolk sac tumors of neonates and infants, which do not develop from a preexistent intratubular germ cell neoplasia in situ (GCNIS) (Figure 1). Type II GCT develop from preexistent GCNIS of the testis and include seminomas and mixed (nonseminomatous) germ cell tumors (also known as NSGCT), which develop mostly in adolescents and adults. Type III category of GCT includes only spermatocytic tumors (previously known as spermatocytic seminoma), which develop without a preinvasive GCNIS in older adults. Over 90% of all invasive GCT develop from GCNIS and belong to type II neoplasms.

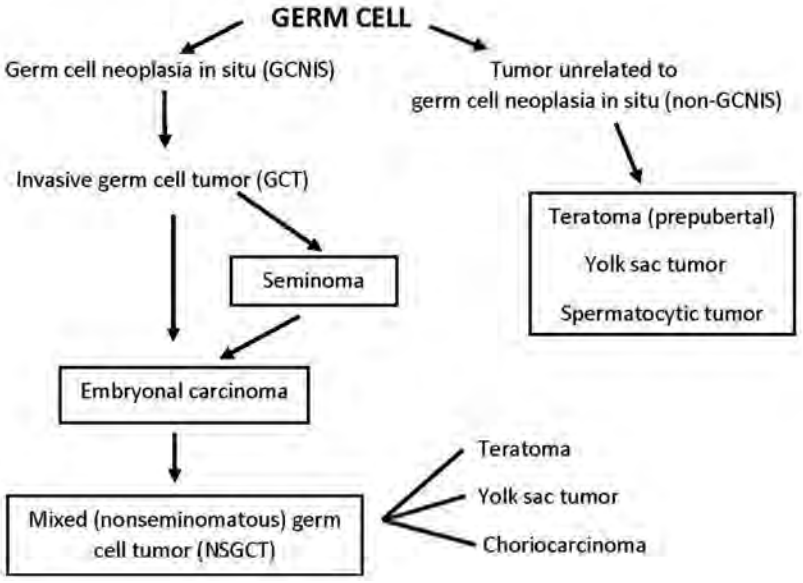

Figure 1. Histogenetic classification of testicular germ cell tumors. Tumors may develop directly from intratubular germ cells or a preinvasive form of intratubular germ cell neoplasia in situ (GCNIS). Tumors that develop directly from germ cells include prepubertal teratoma and childhood yolk sac tumor, and spermatocytic tumor. Most invasive GCTs are classified as type II GCT that develop from GCNIS. GCNIS give rise to invasive malignant stem cells, which may be classified as embryonal carcinoma or seminoma. Seminoma is the most common GCT. The malignancy of seminoma cells may progress, and they become embryonal carcinoma. Embryonal carcinoma cells are the stem cells of mixed (nonseminomatous) germ cell tumors. In addition to their malignant stem cells (embryonal carcinoma), the components of these mixed germ cell tumors include teratoma, yolk sac, and choriocarcinoma. These components may grow clonally and give rise to pure teratoma, yolk sac tumor or choriocarcinoma.

Tumors originating from sex cord lineages or nonspecific stromal cells are less common (12-15). These tumors are mentioned only for the completeness of the presentation and will not be discussed in detail. Tumors originating from testicular adnexa, including rete testis, or tunica vaginalis (mesothelial cells) and some embryonic structures that normally involute during fetal life, such a műllerian ducts, are also quite rare (16-20). Metastatic tumors to the testis and lymphoma are rare but must be considered in the differential diagnosis, especially in elderly patients (21, 22).

Algorithms used by diagnostic pathologists are practice-proven thus straight forward and include the following questions sequentially:

1) Is this testicular lesion a neoplasm or something else?
2) If it is a neoplasm, is it a primary testicular/epididymal tumor or a metastasis?
3) If it is a primary tumor, is it originating from germ cells and their precursors, or from sex cord cells, stromal cells of adnexal structures, or embryonic
4) If the tumor is a GCT, is it a seminoma or NSGCT?
5) If the tumor is an NSGCT, its microscopic components must be identified and listed, such as embryonal carcinoma (EC), teratoma, yolk sac tumor (YST), or choriocarcinoma. For example, it is well known that the extent of embryonal carcinoma in an NSGCT determines the malignancies of such a tumor—the more EC, the more likely the tumor be more malignant. Seminoma elements may be found in 46.9% of mixed germ cell tumors (23), which are otherwise classified as NSGCT. However, the admixture of seminoma to NSGCT does not have any clinical significance.

As stated above, more than 90% of all testicular tumors are of germ cell origin. Accordingly, unless specified otherwise, most clinical and histopathologic problems encountered in the diagnostics and treatment of testicular tumors relate to germ cell tumors. As reported in a large recent study of more than 5 000 testicular tumors from North Rhein-Westphalia, Germany, 93.9% of all tumors were of germ cell origin (23). Approximately 5% of testicular tumors included in cancer registers and national statistics seem to be inadequately documented and cannot be appropriately classified (23). Novel or controversial new testicular tumor entities continuously appear in the literature and are not correctly classified, requiring additional studies (24-28).

Tumor Markers

Tumor markers used in clinical and pathologic practice can be classified as a) serologic markers secreted by or released from the tumor cells and readily detectable in serum, and b) cell-related markers detectable by immunohistochemistry or molecular biologic techniques applied to tumor tissue that was obtained by biopsy or surgical intervention. In this review, we will limit our discussion to tumor markers, which have proven their usefulness for diagnosing testicular tumors.

Serologic Tumor Markers

From the historical point of view, testicular tumors have played an important role in defining tumors markers, such as human chorionic gonadotropin (hCG) (29-31), alpha fetoprotein (AFP) (32-34), placental like alkaline phosphatase (34) and lactate dehydrogenase (LDH) (35). Serologic tumor markers AFP, hCG, and LDH are currently routinely used in testicular tumors' clinical work-up and are included as part of the staging protocol for germ cell tumors (36-41), and are also used for formulating the prognosis after treatment (42).

Human Chorionic Gonadotropin *(*hCG) is produced by placental syncytiotrophoblasts during pregnancy (43). As a tumor marker, it is a reliable marker for choriocarcinoma originating from the placenta, as well as ovarian and testicular choriocarcinomas. Patients with mixed germ cell tumors containing choriocarcinoma elements are also positive for hCG (44).

hCG consist of two chains labeled alpha and beta (43). The alpha subunit of hCG has a molecular weigh,t of approximately 14.5 kD. It is identi-

cal to the alpha subunit of three pituitary trophic hormones: two gonadotropins (FSH and LH) and thyroid-stimulating hormone (TSH). The beta subunit (β-hCG) has a molecular weight of approximately 22.2 kD and is found only in hCG. It is encoded by the *HCGB* gene complex comprising seven *HCGB* genes that form a cluster on the long arm of chromosome 19 (45).

hCG detected in serum can be further subclassified depending on the analytical technique used. To improve the diagnostic value, proposals have been made to selectively look for these subtypes such as β-subunit hCG, β-core fragment hCG, and hyperglycosylated, nicked hCG. However, most laboratories report either regular intact hCG or β-hCG. Hyperglycosylated hCG is the form seen in choriocarcinoma.

β-hCG is measured routinely in the serum of testicular cancer patients. Elevated concentrations of β-hCG found in approximately 50% of patients with NSGCT (41). The serum levels of β-hCG vary depending on the tumor stage and the extent of choriocarcinoma elements in each tumor. Pure choriocarcinomas are always positive.

Immunohistochemistry with polyclonal or monoclonal antibodies to β-hCG is widely used in daily histopathology practice to identify choriocarcinoma cells in the tumor tissue. Since tumor cells secrete β-hCG into the plasma, it will often be seen inside the blood vessels of the tumor and permeating the tissues near the neoplastic choriocarcinoma cells.

Scattered syncytiotrophoblastic multinucleated giant cells can be seen in approximately 20% of seminomas. Patients who have such seminomas have elevated levels of hCG can be elevated in serum, albeit in concentrations that are much lower than those in patients with NSGCT (41).

The half-life of hCG in serum is 2-3 days. Accordingly, one can expect normalization of serum hCG in about 10-15 days (five half-lives) after removing the tumor. However, such a normalization does not exclude metastases composed of embryonal carcinoma cells, which do not produce hCG. Recurrence of NSGCT is associated with rising hCG levels in serum in approximately 25% of cases (41).

Alpha Fetoprotein is a 70kD protein normally found in fetal serum. In the early stages of intrauterine life, it is produced by the yolk sac and, after that by the fetal liver and parts of the gastrointestinal tract (46). The postnatal liver continues to secrete AFP, and therefore the serum levels of AFP remain elevated during infancy and even in early childhood. The *AFP* gene is located on the long arm of chromosome 4 (4q25) (47).

AFP is a widely used tumor marker, most useful in diagnosing hepatocellular carcinoma, NSGCT of the testis, yolk sac tumor of infancy and childhood, extragonadal germ cell tumors, and mixed germ cell tumors of the ovary. AFP is a reliable marker for yolk sac components of germ cell tumors in testicular and ovarian tumors. Overall, AFP is elevated in the serum of 25% of all patients with testicular germ cell tumors (41). In the subgroup of patients with NSGCT, serum AFP levels are elevated in 60% of cases (41).

The half-life of AFP is approximately 5–7 days, and therefore, one could expect the serum AFP to normalize 25–35 days (five half-lives) after orchidectomy for NSGCT (37, 44). False-positive results could result from liver injury related to chemotherapy or even some non-neoplastic liver diseases such as steatohepatitis or chronic viral hepatitis and cirrhosis. In patients receiving chemotherapy, tumor lysis syndrome may include elevated serum AFP levels, even though there are no viable tumor cells in the treated patient's body. Three isoforms of AFP are known to appear in blood: L1 found in the serum of patients with non-neoplastic liver disease, L2 found in patients with yolk sac tumors, and L3 in patients with hepatocellular carcinoma (48). In routine clinical practice, these subtypes are of limited significance.

Immunohistochemistry with polyclonal or monoclonal antibodies is routinely used in the work-up testicular NSGCT, extragonadal germ cell tumors, and yolk sac tumors (49, 50). AFP is a useful marker for most forms of yolk sac tumors, even though some variants, such as parietal yolk sac tumor, are negative. This is important to keep in mind because AFP positive yolk sac rich tumors may undergo clonal evolution and transform into AFP

negative neoplasms (51). It is also important to note that AFP can be elevated in the serum of patients who have adenocarcinomas of the gastrointestinal tract and the upper aerodigestive system (37).

Placental Alkaline Phosphatase also known as Regan isoenzyme, is one of the four alkaline phosphatases (AP) typically found in the human tissues from which they are released into the circulation (52). Functionally, they are all hydrolases that have their optimal enzymatic activity in an alkaline milieu. Each of these four alkaline phosphatases is derived from a different organ and encoded by its gene. In addition to PLAP, other three forms are known as hepatic, bone and kidney AP, intestinal A.P., and placental like AP. *PLAP* is encoded by a gene on the long arm of chromosome 2 (2q37), which also contains the genes for placental-like and intestinal AP (53). *PLAP* gene is usually expressed in trophoblastic cells and fetal primordial germ cells. It is not expressed on normal spermatogenic cells of the adult testis. Monoclonal antibodies to PLAP and those specific for other isoenzymes of AP are available, making their immunohistochemical localization in tissue sections possible (54).

PLAP was initially considered a useful marker for seminoma. However, later on, it became evident that it is also expressed on the cells forming the intratubular GCNIS and embryonal carcinoma cells, yolk sac tumor, and choriocarcinoma. Accordingly, it is a useful tumor marker for testicular and ovarian, and extragonadal GCTs (54-56). Immunohistochemical studies with monoclonal antibodies disclosed that AP of testicular germ cell tumors could be either PLAP or placental-like isoenzyme (54), confounding the issue of specificity of PLAP as a tumor marker. Subsequent studies disclosed PLAP on some non-germ cell tumors. Furthermore, it was detected in the serum of smokers, which reduced its overall utility as a tumor marker (57). Antibodies to PLAP are still used in clinical laboratories but considerably less often than the newer reagents.

Lactate Dehydrogenase (LDH) is a ubiquitous enzyme present in nearly all human tissues, from which it is released into the serum (58). Structurally it is a tetramer composed of four subunits, the most common being LDH-M and LDH-H protein, encoded by two *LDH* genes, called *LDHA* and *LDHB*, respectively (59). Serum LDH and its main isoenzymes are routinely measured in clinical laboratories.

LDH is found inside the cell of most human tumors (60, 61) and is thus often measured in cancer patients. Due to its wide distribution in normal and neoplastic tissues, it cannot be used as a diagnostic tumor marker. Nevertheless, serum LDH values can be used as a valuable laboratory finding, reflecting tumor burden, invasiveness of neoplastic cells, and the extent of tumor spread and metastasis. In patients receiving chemotherapy, serum LDH can be used to monitor the residual total tumor mass and spontaneous and chemotherapy-induced tumor necrosis.

American Joint Committee on Cancer (AJCC) staging system for testicular tumors (39) requires from clinicians to record the serum levels of LDH at the time of diagnosis and periodically monitored them after surgical intervention and chemotherapy. In patients diagnosed with small tumors limited to the testis, serum LDH is within normal limits in 80-90% of cases. As the tumors grow, serum levels of LDH will rise proportionally to the size of the tumor. Patients with metastatic tumors have almost all high LDH serum levels. Likewise, tumor lysis is accompanied by markedly increased levels of serum LDH. Recurrence of tumors is also typically associated with high serum LDH levels.

Stem Cell Markers of Germ Cell Tumors

Testicular tumor stem cell markers have been studied immunohistochemically and by means of molecular biology. These studies' primary aims were to elucidate the histogenesis of germ cell tumors, define the developmental pluripotency of tumor cells and their pluripotentiality, and improve the histopathologic diagnosis of germ cell tumors. The salient data from these studies have been reviewed comprehensively (7-10, 62, 63). The important tumor cell markers identified so far will be briefly discussed here.

Octamer-Binding Transcription Factor 4 (Oct4)

Oct4 (also known as Oct3, Oct3/4, Pouf1, POU5F1, and Otf3) is a member of the POU-domain family of octamer-binding transcription factors expressed in early murine embryonic cells and primordial germ cells (8-10, 57). *OCT4* gene has been localized to chromosome 6p21.3 (64).

OCT4 gene accounts for the stemness and pluripotency of embryonic cells before implanting the embryo and early stages of post-implantation development. If injected into differentiated somatic cells and three other genes (*SOX2, MYC,* and *KLF4*), it may transform them into developmentally pluripotent undifferentiated embryonic stem cells (65). It is also expressed in primordial germ cells in the developing fetus but is not apparent in adult spermatogenic cells. *OCT4* is also expressed in human embryonic stem cells (EST) cultured in vitro. If these cells are injected into immunodeficient mice, they form benign teratoma composed of somatic tissues. These teratoma cells do not express *OCT4* (66). Malignant stem cells produced from EST also express *OCT4* (67). However, if these stem cells are allowed to differentiate into yolk sac cells or somatic tissues, they lose *OCT4* activity.

OCT4 protein is localized in the nucleus. It is resistant to formalin fixation, and thus it can be demonstrated by immunohistochemistry in tissues. As one would expect from these experimental data mentioned above, testicular embryonal carcinoma cells are also Oct4 positive (68, 69). Furthermore, seminomas and intratubular preinvasive germ cell neoplasia in situ cells are also positive. These studies have also shown that Oct4 is not expressed in yolk sac tumor cells, choriocarcinoma and somatic cells forming teratoma components of NSGCT. The cells of the spermatocytic tumor also negative for Oct4 (11). Several malignant tumors may be positive for Oct4, such as carcinoma of the lung or thymus (57).

c-KIT Protooncogene (CD117)

c-KIT proto-oncogene was initially identified as a human equivalent of the animal oncogene of the Hardy-Zuckerman IV feline sarcoma virus (HZ4-FeSV), including its transforming activity (57, 70, 71). The human *c-KIT* gene has been localized to chromosome 4q12 (72).

The human *c-KIT* gene encodes the type III tyrosine kinase receptor, also known as tyrosine-protein kinase KIT, or mast/stem cell growth factor receptor (SCFR). Most pathologists know it as CD117 (73) since it reacts with the antibody to the cluster of differentiation 117 (CD117). It occurs in multiple transcript variants and isoform and is expressed on numerous cells. The c-KIT enzyme plays an important role in many physiological processes such as cell growth and proliferation, melanogenesis, hematopoiesis, angiogenesis and gametogenesis. Dysregulation of c-Kit signaling or gain-of-function mutations of *c-KIT* gene plays a role in the pathogenesis of various neoplasms (71, 72).

In a comprehensive review of normal tissue and tumors, Miettinen and Lasota (73) have found CD117 immunoreactivity on various cell types including mast cells, some hematopoietic stem cells, germ cells, melanocytes, and Cajal cells of the gastrointestinal tract. Other c-KIT-positive normal cells include epithelial cells in skin adnexa, breast, and subsets of cerebellar neurons. c-KIT positivity has been variably reported in sarcomas such as angiosarcoma, Ewing sarcoma, synovial sarcoma, leiomyosarcoma, and malignant fibrous histiocytoma (MFH); results of the last three are controversial. In addition, c-KIT is expressed in pulmonary and other small cell carcinomas, adenoid cystic carcinoma (breast and salivary glands), renal chromophobe carcinoma, thymic, and some ovarian and few breast carcinomas (usually with basal-like and triple-negative phenotype).

c-KIT gene is expressed in normal fetal gonocytes but not in adult spermatogonia and their derivatives (74). It is expressed in intratubular GCNIS and seminoma (75, 76). Approximately 30% of seminomas are positive in the testis, with a higher rate of positivity recorded in bilateral tumors, extragonadal seminomas, and dysgerminomas (77). Embryonal carcinoma cells and other components of NSGCT are negative. Immunohistochemistry with antibodies to c-KIT is useful when trying to distinguish seminoma from embryonal carcinoma cells.

Sall4

Sall4 is a zinc-finger transcription factor originally cloned on sequence homology to Drosophila homeotic genes of the Spalt family (57, 78-80). The human *SALL4* gene is located on chromosome 20q13.2 (80). It interacts with three other genes, *OCT4, NANOG,* and *SOX2* in maintaining the stemness and pluripotency of early embryonic cells and in vitro propagated murine and human embryonic stem cells.

SALL4 gene is expressed on primordial germ cells and weakly several fetal organs during early stages of organogenesis, such as neural tube formation, intestinal differentiation, and hepatogenesis. In the testis, it is weakly expressed in normal spermatogonia, in contrast to intense immunohistochemical staining of the nuclei of GCNIS, embryonal carcinoma, and seminoma. Antibodies to Sall4 are among the rare antibodies that react with some of the cells in spermatocytic tumors (57). It is negative in choriocarcinomas, even though sometimes it may react with cytotrophoblastic cells (57). SALL4 is strongly expressed in yolk sac tumors. In the teratomatous part of the mixed germ cell tumors antibodies to Sall4 react with neural tubes and neural cell precursors, as well as many other immature cells (81, 82).

As stated by Miettinen et al. (83), SALL4 is an excellent marker for germ cell tumors, as long as one keeps in mind that it may be expressed in some immature somatic tissues of teratomas. SALL4 can be expressed in poorly differentiated serous carcinoma of the ovary, high-grade urothelial carcinoma, and gastric adenocarcinoma (especially the intestinal type). SALL4 was only rarely (≤ 5%) expressed in common adenocarcinomas, such as breast, large intestine, and squamous cell carcinomas. Many SALL4-positive carcinomas are poorly differentiated and often show strong immunohistochemical positivity mimicking its expression in GCT. SALL4 is not found in hematopoietic tumors and lymphomas, and most sarcomas, but may be found in rhabdoid tumors of the kidney and extrarenal sites and the Wilms tumor (nephroblastoma).

Sox2

Sox2 protein is encoded by the gene *SOX2,* which belongs to the family of some 20 *SOX* genes (84). The term *SOX* is a contraction for their full designation, including keywords such as SRY (sex-determining region Y) and high mobility group (HMG) box. These proteins' functions range from embryonic development and stem cell maintenance to homeostasis in adult tissues.

SOX2 gene, one of the SOX family members, was discovered and characterized in humans in 1994 and then localized to the chromosome 3q26.3–q27 (85). *SOX2* has a crucial role in stem cell maintenance, lineage fate determination and reprogramming of somatic cells back towards pluripotency. *SOX2* plays a role in the pathogenesis of several forms of cancer, including testicular germ cell neoplasia, usually by interacting with the protein product of the *OCT4* gene (86). During the testis' fetal development and in testicular germ cell tumors, it is reciprocally expressed to Sox17, another protein of this group, encoded by a gene located on the 8q11.23 chromosome (57, 86).

Studies performed *in vitro* on ESC, human embryonal carcinoma cells and TCam-2 cell line that has features of seminoma show that Sox2 interacts with Oct4 and is essential for maintaining the undifferentiated state by activating pluripotency-linked genes (86-88). In contrast to Oct4, which is present in primordial germ cells and fetal gonocytes, suppressing these cells' apoptosis, Sox2 is not found in these cells. These cells contain, however, Sox17. As expected, GCNIS and seminoma cells are positive for Oct4 and Sox17 but negative for Sox2. On the other hand, embryonal carcinoma cells are positive for Sox2 and Oct4 and negative for Sox17. Embryonal carcinoma cell lines and seminoma like TCam-2 cell line cultured *in vitro* reflect the reciprocal expression of Sox2 and Sox17 in germ cell tumors as evidenced immunohistochemically (87, 88).

Immunohistochemical studies of testicular germ cell tumors show that *SOX2* gene is expressed in embryonal carcinoma cells, immature neuroepithelium, and some differentiated somatic tissues in teratomas, such as squamous epithelium

(57, 89, 90). GCNIS and seminoma, yolk sac tumor, and choriocarcinoma, as well as spermatocytic tumor, are negative. *SOX2* gene expression is not limited to GCT, and it may be expressed in several somatic adenocarcinomas, such as those of the ovary, breast, and prostate. Its expression correlates with the invasiveness of these cancers (91).

Other Markers for Embryonal Carcinoma and Seminoma

Several antibodies raised against various human antigens have been found to react selectively with embryonal carcinoma cells or seminoma cells (92). This reactivity cannot be explained now. Nevertheless, some of these antibodies have been adopted in diagnostic histopathology and will be briefly reviewed here.

CD30 is a cytokine receptor that belongs to the tumor necrosis factor superfamily (57). Antibodies to CD30 are used as a diagnostic marker in hematopathology. However, these antibodies also react quite specifically with embryonal carcinoma cells in various GCT (92, 93). Overall, CD30 is considered a useful marker for embryonal carcinomas, especially if there is a need to distinguish embryonal carcinoma from seminoma or yolk sac tumors, which are negative for this marker. CD30 is not expressed in GCNIS either. Some seminomas contain scattered CD30 positive cells; most likely, these cells are nascent embryonal carcinoma cells within those seminomas that are abortively trying to differentiate into embryonal carcinoma (57). Embryonal carcinoma cells surviving chemotherapy often lose CD30, and accordingly, antibodies to CD30 should not be used for identifying embryonal carcinoma cells in post-chemotherapy patients (94).

Podoplanin (PDPN) is a transmembrane sialoglycoprotein found in numerous tissues, most notably lymphatic endothelium (57). Its name relates to the fact that it was identified in glomerular podocytes, but it is also known as M2A (D2-40) antigen and gp36 (aggrus, T1A-2) (95). The best-known commercially available monoclonal antibody reacting with PDPN is D2-40. Antibody D2-40 reacts with fetal gonocytes, but not with spermatogenic cells in the adult seminiferous tubules (95, 96). However, it is positive in GCNIS and seminoma and could be considered an excellent marker for seminomas. However, a certain number of embryonal carcinomas react with D2-40 antibody as well (97). Therefore, Lau et al. (97) warn that D2-40 is not always a reliable antibody for distinguishing seminomas from embryonal carcinoma and recommend using antibodies to CD117 and CD30 instead.

Other Antibodies, usually in the monoclonal form, have been tested on germ cell tumors to identify diagnostic tumor cell markers. Some of these markers have been reviewed in detail by Favilla et al. (92), Preda and Nogales (57), and Oosterhuis and Looijenga (76). Most of these markers have not been adopted for routine usage in diagnostic pathology laboratories, even though they have been extensively tested in investigative studies. Expression of potential tumor markers such as doublesex and mab-3 related transcription factor 1 (encoded by the gene *DMRT1*) has been registered in very rare testicular GCT, such as spermatocytic tumors and mixed germ cell-sex cord Sertoli cell tumors; reagents for such markers will be limited in use to only highly specialized laboratories (98). Some of potentially useful GCT markers including proteins encoded by genes such *as NANOG, LIN28, TCL-1, UTF-1, KLF4, AP-2γ, IMP3* have been reviewed recently (57, 92).

It is worth mentioning that antibodies to some ubiquitous cell components, such as cytokeratins, can be used in the immunohistochemical evaluation of some germ cell tumors (99). However, such antibodies are best used if included in a diagnostic panel with other reagents. Positive or negative results obtained with such antibodies are thus interpreted in the context of other findings. On the other hand, some antibodies considered to be diagnostic for certain pathological entities are occasionally found to react with GCT and could cause a diagnostic pitfall, as in terminal deoxynucleotidyl transferase (TdT), a well-known hematopathologic biomarker (100). Likewise, thyroid transcription factor 1 (encoded by the gene *TTF-1*), a reli-

able marker of the thyroid and pulmonary cancers, may be positive in some yolk sac tumors (101).

Yolk Sac Tumor Markers

Yolk sac tumors (YST) of the infantile testis and the yolk sac components of mixed germ cell tumors react with several antibodies, some of which have proven to be useful in histopathological practice. Since YST presents in various microscopic patterns (101), such tumors' immunohistochemical profile may be quite variable.

Alpha-fetoprotein is a reliable yolk sac marker, discussed above. However, AFP is expressed unevenly in yolk sac tumors, and the interpretation of spotty findings may be problematic. Furthermore, as a secretory protein, it is found in the plasma, and accordingly, the staining of tissue sections may be smudgy. Additional markers have thus been used for immunohistochemical diagnosis of yolk sac tumor, usually to prove their GCT nature and/or early endodermal or hepatoid differentiation.

The most reliable GCT marker for yolk sac tumors is *SALL4. PLAP* is also positive, whereas the tumor cells are negative for *SOX2, OCT4,* and *CD117* (102). YSTs are also positive for *CDX2*, an endodermal and intestinal marker, as well as for glypican 3 and GATA3. Markers for hepatoid differentiation such as HEPAR1, hepatocyte nuclear factor 1 β (103, 104) are also useful markers for YST. Zinc finger and BTB domain containing 16 (*ZBTB16*), a gene expressed during spermatogenesis, is another promising YST marker (105).

Conclusions and Future Directions

Serologic and immunohistochemical markers for GCT have been extensively studied during the last 30 years. Reagents for the most useful markers have been included in the standard sets used in clinical practice. Genetic and molecular biologic profiling of GCT has been performed in numerous laboratories providing genetic underpinning to the clinical and serologic tests. Many of these genetic studies, including those that are still in the experimental stage, have been reviewed in detail in several lengthy articles (106-113), clearly showing that molecular biology will play a pivotal role in future research and many international efforts to refine the diagnosis of testicular GCT. Collaborative initiatives such as Gene Expression Omnibus (GEO), an international public repository that archives and freely distributes microarray and next-generation sequencing (NGS) data, could facilitate the search for novel GCT markers (114).

Conflict of Interest: The author declares that he has no conflict of interest.

References

1. About KISS 2020 [cited 2020 Oct 10]. Available from: https://en.wikipedia.org/wiki/KISS_principle.
2. Bosl GJ, Motzer RJ. Testicular germ-cell cancer. N Engl J Med. 1997;337(4):242-53.
3. Hanna NH, Einhorn LH. Testicular cancer--discoveries and updates. N Engl J Med. 2014;371(21):2005-16.
4. Adra N, Einhorn LH. Testicular cancer update. Clin Adv Hematol Oncol. 2017;15(5):386-96.
5. Chieffi P, De Martino M, Esposito F. New Anti-Cancer Strategies in Testicular Germ Cell Tumors. Recent Pat Anticancer Drug Discov. 2019;14(1):53-9.
6. Friedman NB, Moore RA. Tumors of the testis; a report on 922 cases. Mil Surg. 1946;99(5):573-93.
7. Moch H HP, Ulbright TM, Reuter VE. WHO classification of tumours of the urinary system and male genital organs. 4th ed. Lyon: IARC; 2016.
8. Oosterhuis JW, Looijenga LH. Testicular germ-cell tumours in a broader perspective. Nat Rev Cancer. 2005;5(3):210-22.
9. Looijenga LH, Stoop H, Biermann K. Testicular cancer: biology and biomarkers. Virchows Arch. 2014;464(3):301-13.
10. Oosterhuis JW, Looijenga LHJ. Human germ cell tumours from a developmental perspective. Nat Rev Cancer. 2019;19(9):522-37.
11. Baraban EG, Cooper K. Pathogenesis of Testicular Germ Cell Neoplasia: A Conceptual Approach. Adv Anat Pathol. 2019;26(4):241-5.
12. Fankhauser CD, Grogg JB, Hayoz S, Wettstein MS, Dieckmann KP, Sulser T, et al. Risk Factors and Treatment Outcomes of 1,375 Patients with Testicular Leydig Cell Tumors: Analysis of Published Case Series Data. J Urol. 2020;203(5):949-56.
13. Zhang C, Ulbright TM. Nuclear Localization of beta-Catenin in Sertoli Cell Tumors and Other Sex Cord-

Stromal Tumors of the Testis: An Immunohistochemical Study of 87 Cases. Am J Surg Pathol. 2015;39(10):1390-4.

14. Conlon N, Schultheis AM, Piscuoglio S, Silva A, Guerra E, Tornos C, et al. A survey of DICER1 hotspot mutations in ovarian and testicular sex cord-stromal tumors. Mod Pathol. 2015;28(12):1603-12.
15. Tatsi C, Faucz FR, Blavakis E, Carneiro BA, Lyssikatos C, Belyavskaya E, et al. Somatic PRKAR1A Gene Mutation in a Nonsyndromic Metastatic Large Cell Calcifying Sertoli Cell Tumor. J Endocr Soc. 2019;3(7):1375-82.
16. Al-Obaidy KI, Idrees MT, Grignon DJ, Ulbright TM. Adenocarcinoma of the Rete Testis: Clinicopathologic and Immunohistochemical Characterization of 6 Cases and Review of the Literature. Am J Surg Pathol. 2019;43(5):670-81.
17. Young RH, Scully RE. Testicular and paratesticular tumors and tumor-like lesions of ovarian common epithelial and mullerian types. A report of four cases and review of the literature. Am J Clin Pathol. 1986;86(2):146-52.
18. Lin M, Awalt H, Ayala AG, Ro JY. Clear cell carcinoma of testis: A review. Ann Diagn Pathol. 2019;40:26-9.
19. Butnor KJ, Pavlisko EN, Sporn TA, Roggli VL. Mesothelioma of the tunica vaginalis testis. Hum Pathol. 2019;92:48-58.
20. Drevinskaite M, Patasius A, Kevlicius L, Mickys U, Smailyte G. Malignant mesothelioma of the tunica vaginalis testis: a rare case and review of literature. BMC Cancer. 2020;20(1):162.
21. Ulbright TM, Young RH. Metastatic carcinoma to the testis: a clinicopathologic analysis of 26 nonincidental cases with emphasis on deceptive features. Am J Surg Pathol. 2008;32(11):1683-93.
22. Ghazarian AA, Rusner C, Trabert B, Braunlin M, McGlynn KA, Stang A. Testicular cancer among U.S. men aged 50 years and older. Cancer Epidemiol. 2018;55:68-72.
23. Stang A, Rusner C, Trabert B, Oosterhuis JW, McGlynn KA, Heidinger O. Incidence of testicular tumor subtypes according to the updated WHO classification, North Rhine-Westphalia, Germany, 2008-2013. Andrology. 2019;7(4):402-7.
24. Paluru S, Ulbright TM, Amin M, Montironi R, Epstein JI. The Morphologic Spectrum of Sertoliform Cystadenoma of the Rete Testis: A Series of 15 Cases. Am J Surg Pathol. 2018;42(2):141-9.
25. Gibson WE, Gonzalez RS, Cates JMM, Liu E, Shi C. Hepatic micrometastases are associated with poor prognosis in patients with liver metastases from neuroendocrine tumors of the digestive tract. Hum Pathol. 2018;79:109-15.
26. Michalova K, Michal M Jr, Kazakov DV, Sedivcova M, Hes O, Hadravsky L, et al. Primary signet ring stromal tumor of the testis: a study of 13 cases indicating their phenotypic and genotypic analogy to pancreatic solid pseudopapillary neoplasm. Hum Pathol. 2017;67:85-93.
27. Ulbright TM. Recently Described and Clinically Important Entities in Testis Tumors: A Selective Review of Changes Incorporated Into the 2016 Classification of the World Health Organization. Arch Pathol Lab Med. 2019;143(6):711-21.
28. Michalova K, McKenney JK, Kristiansen G, Steiner P, Grossmann P, Putzova M, et al. Novel insights into the mixed germ cell-sex cord stromal tumor of the testis: detection of chromosomal aneuploidy and further morphological evidence supporting the neoplastic nature of the germ cell component. Virchows Arch. 2020;477(5):615-23.
29. Zondek B. Gonadotropic Hormone in the Diagnosis of Chorionepithelioma. Journal of the American Medical Association. 1937;108(8):607-11.
30. Kirwin TJ. Chorioepithelioma of the Testis, With Report of a Case Showing Extensive Metastasis. J Urol. 1937;38(1):91-9.
31. Abelev GI. Alpha-fetoprotein in ontogenesis and its association with malignant tumors. Adv Cancer Res. 1971;14:295-358.
32. Sell S, Becker FF, Leffert HL, Watabe L. Expression of an oncodevelopmental gene product (alpha-fetoprotein) during fetal development and adult oncogenesis. Cancer Res. 1976;36(11 Pt. 2):4239-49.
33. Damjanov I, Sell S. Yolk sac carcinoma grown from rat egg cylinders. J Natl Cancer Inst. 1977;58(5):1523-5.
34. Lange PH, Millan JL, Stigbrand T, Vessella RL, Ruoslahti E, Fishman WH. Placental alkaline phosphatase as a tumor marker for seminoma. Cancer Res. 1982;42(8):3244-7.
35. Lippert MC, Javadpour N. Lactic dehydrogenase in the monitoring and prognosis of testicular cancer. Cancer. 1981;48(10):2274-8.
36. Lange PH, McIntire KR, Waldmann TA, Hakala TR, Fraley EE. Serum alpha fetoprotein and human chorionic gonadotropin in the diagnosis and management of nonseminomatous germ-cell testicular cancer. N Engl J Med. 1976;295(22):1237-40.
37. Gilligan TD, Seidenfeld J, Basch EM, Einhorn LH, Fancher T, Smith DC, et al. American Society of Clinical Oncology Clinical Practice Guideline on uses of serum tumor markers in adult males with germ cell tumors. J Clin Oncol. 2010;28(20):3388-404.
38. Javadpour N. The role of biologic tumor markers in testicular cancer. Cancer. 1980;45(7 Suppl):1755-61.
39. Amin MB, Edge S, Greene F, Byrd DR, Brookland RK, Washington MK, et al. (editors). AJCC Cancer Staging Handbook. New York: Springer; 2017.
40. Marshall C, Enzerra M, Rahnemai-Azar AA, Ramaiya NH. Serum tumor markers and testicular germ cell tumors: a primer for radiologists. Abdom Radiol (N.Y.). 2019;44(3):1083-90.
41. Dieckmann KP, Simonsen-Richter H, Kulejewski M, Anheuser P, Zecha H, Isbarn H, et al. Serum Tumour Markers in Testicular Germ Cell Tumours: Frequencies of Elevated

Levels and Extents of Marker Elevation Are Significantly Associated with Clinical Parameters and with Response to Treatment. Biomed Res Int. 2019;2019:5030349.

42. Siddiqui BA, Zhang M, Pisters LL, Tu SM. Systemic therapy for primary and extragonadal germ cell tumors: prognosis and nuances of treatment. Transl Androl Urol. 2020;9(Suppl 1):S56-65.
43. Cole LA. Human chorionic gonadotropin and associated molecules. Expert Rev Mol Diagn. 2009;9(1):51-73.
44. Kohli M ZB, Costello BA. Management of germ cell tumors. In: Nogales FF, Jimenez RE, editors. Pathology and Biology of Germ Cell Tumours. Heidelberg: Springer; 2017. p. 181-94.
45. Talmadge K, Boorstein WR, Fiddes JC. The human genome contains seven genes for the beta-subunit of chorionic gonadotropin but only one gene for the beta-subunit of luteinizing hormone. DNA. 1983;2(4):281-9.
46. Tomasi TB, Jr. Structure and function of alpha-fetoprotein. Annu Rev Med. 1977;28:453-65.
47. Yang F, Luna VJ, McAnelly RD, Naberhaus KH, Cupples RL, Bowman BH. Evolutionary and structural relationships among the group-specific component, albumin and alpha-fetoprotein. Nucleic Acids Res. 1985;13(22):8007-17.
48. Tsuchida Y, Kaneko M, Fukui M, Sakaguchi H, Ishiguro T. Three different types of alpha-fetoprotein in the diagnosis of malignant solid tumors: use of a sensitive lectin-affinity immunoelectrophoresis. J Pediatr Surg. 1989;24(4):350-5.
49. Nogales FF, Quinonez E, Lopez-Marin L, Dulcey I, Preda O. A diagnostic immunohistochemical panel for yolk sac (primitive endodermal) tumours based on an immunohistochemical comparison with the human yolk sac. Histopathology. 2014;65(1):51-9.
50. Kinjo T, Taniguchi H, Kushima R, Sekine S, Oda I, Saka M, et al. Histologic and immunohistochemical analyses of alpha-fetoprotein--producing cancer of the stomach. Am J Surg Pathol. 2012;36(1):56-65.
51. Damjanov I, Amenta PS, Zarghami F. Transformation of an AFP-positive yolk sac carcinoma into an AFP-negative neoplasm. Evidence for in vivo cloning of the human parietal yolk sac carcinoma. Cancer. 1984;53(9):1902-7.
52. Fishman WH. Alkaline phosphatase isozymes: recent progress. Clin Biochem. 1990;23(2):99-104.
53. Seargeant LE, Stinson RA. Evidence that three structural genes code for human alkaline phosphatases. Nature. 1979;281(5727):152-4.
54. Paiva J, Damjanov I, Lange PH, Harris H. Immunohistochemical localization of placental-like alkaline phosphatase in testis and germ-cell tumors using monoclonal antibodies. Am J Pathol. 1983;111(2):156-65.
55. Manivel JC, Jessurun J, Wick MR, Dehner LP. Placental alkaline phosphatase immunoreactivity in testicular germ-cell neoplasms. Am J Surg Pathol. 1987;11(1):21-9.
56. Kommoss F, Oliva E, Bittinger F, Kirkpatrick CJ, Amin MB, Bhan AK, et al. Inhibin-alpha CD99, HEA125, PLAP, and chromogranin immunoreactivity in testicular neoplasms and the androgen insensitivity syndrome. Hum Pathol. 2000;31(9):1055-61.
57. Preda O NF. Diagnostic immunopathology of germ cell tumors. In: Nogales FF, Jimenez RE, editors. Pathology and Biology of Germ Cell Tumours. Heidelberg: Springer; 2017. p. 131-80.
58. Glick JH Jr. Serum lactate dehydrogenase isoenzyme and total lactate dehydrogenase values in health and disease, and clinical evaluation of these tests by means of discriminant analysis. Am J Clin Pathol. 1969;52(3):320-8.
59. Lactate dehydrogenase 2020 [cited 2020 Oct 10]. Available from: https://en.wikipedia.org/wiki/Lactate_dehydrogenase.
60. Gallo M, Sapio L, Spina A, Naviglio D, Calogero A, Naviglio S. Lactic dehydrogenase and cancer: an overview. Front Biosci (Landmark Ed). 2015;20:1234-49.
61. Petrelli F, Cabiddu M, Coinu A, Borgonovo K, Ghilardi M, Lonati V, et al. Prognostic role of lactate dehydrogenase in solid tumors: a systematic review and meta-analysis of 76 studies. Acta Oncol. 2015;54(7):961-70.
62. Looijenga LH, Oosterhuis J.W. Pathobiology of germ cell tumors - applying the gossip test! Int J Dev Biol. 2013;57(2-4):289-98.
63. Ulbright TM, Tickoo SK, Berney DM, Srigley JR, Members of the IIiDUPG. Best practices recommendations in the application of immunohistochemistry in testicular tumors: report from the International Society of Urological Pathology consensus conference. Am J Surg Pathol. 2014;38(8):e50-9.
64. Guillaudeux T, Mattei MG, Depetris D, Le Bouteiller P, Pontarotti P. In situ hybridization localizes the human OTF3 to chromosome 6p21.3-->p22 and OTF3L to 12p13. Cytogenet Cell Genet. 1993;63(4):212-4.
65. Takahashi K, Yamanaka S. Induction of pluripotent stem cells from mouse embryonic and adult fibroblast cultures by defined factors. Cell. 2006;126(4):663-76.
66. Damjanov I, Andrews PW. Teratomas produced from human pluripotent stem cells xenografted into immunodeficient mice - a histopathology atlas. Int J Dev Biol. 2016;60(10-11-12):337-419.
67. International Stem Cell Initiative, Adewumi O, Aflatoonian B, Ahrlund-Richter L, Amit M, Andrews PW, et al. Characterization of human embryonic stem cell lines by the International Stem Cell Initiative. Nat Biotechnol. 2007;25(7):803-16.
68. Looijenga LH, Stoop H, de Leeuw HP, de Gouveia Brazao CA, Gillis AJ, van Roozendaal KE, et al. POU5F1 (OCT3/4) identifies cells with pluripotent potential in human germ cell tumors. Cancer Res. 2003;63(9):2244-50.
69. Jones TD, Ulbright TM, Eble JN, Baldridge LA, Cheng L. OCT4 staining in testicular tumors: a sensitive and specific marker for seminoma and embryonal carcinoma. Am J Surg Pathol. 2004;28(7):935-40.

70. Lennartsson J, Jelacic T, Linnekin D, Shivakrupa R. Normal and oncogenic forms of the receptor tyrosine kinase kit. Stem Cells. 2005;23(1):16-43.
71. Wang H, Boussouar A, Mazelin L, Tauszig-Delamasure S, Sun Y, Goldschneider D, et al. The Proto-oncogene c-Kit Inhibits Tumor Growth by Behaving as a Dependence Receptor. Mol Cell. 2018;72(3):413-25.e5.
72. Vandenbark GR, deCastro CM, Taylor H, Dew-Knight S, Kaufman RE. Cloning and structural analysis of the human c-kit gene. Oncogene. 1992;7(7):1259-66.
73. Miettinen M, Lasota J. KIT (CD117): a review on expression in normal and neoplastic tissues, and mutations and their clinicopathologic correlation. Appl Immunohistochem Mol Morphol. 2005;13(3):205-20.
74. Robinson LL, Gaskell TL, Saunders PT, Anderson RA. Germ cell specific expression of c-kit in the human fetal gonad. Mol Hum Reprod. 2001;7(9):845-52.
75. Kemmer K, Corless CL, Fletcher JA, McGreevey L, Haley A, Griffith D, et al. KIT mutations are common in testicular seminomas. Am J Pathol. 2004;164(1):305-13.
76. Oosterhuis JW, Looijenga LHJ. Germ cell tumors from a developmental perspective: Cells of origin, pathogenesis, and molecular biology (emerging patterns). In: Nogales FF, Jimenez RE, editors. Pathology and Biology of Germ Cell Tumours. Heidelberg: Springer; 2017. p. 23-131.
77. Yang J, Chai L, Fowles TC, Alipio Z, Xu D, Fink LM, et al. Genome-wide analysis reveals Sall4 to be a major regulator of pluripotency in murine-embryonic stem cells. Proc Natl Acad Sci U S A. 2008;105(50):19756-61.
78. Tatetsu H, Kong NR, Chong G, Amabile G, Tenen DG, Chai L. SALL4, the missing link between stem cells, development and cancer. Gene. 2016;584(2):111-9.
79. Rao S, Zhen S, Roumiantsev S, McDonald LT, Yuan GC, Orkin SH. Differential roles of Sall4 isoforms in embryonic stem cell pluripotency. Mol Cell Biol. 2010;30(22):5364-80.
80. Cao D, Li J, Guo CC, Allan RW, Humphrey PA. SALL4 is a novel diagnostic marker for testicular germ cell tumors. Am J Surg Pathol. 2009;33(7):1065-77.
81. Wang F, Liu A, Peng Y, Rakheja D, Wei L, Xue D, et al. Diagnostic utility of SALL4 in extragonadal yolk sac tumors: an immunohistochemical study of 59 cases with comparison to placental-like alkaline phosphatase, alpha-fetoprotein, and glypican-3. Am J Surg Pathol. 2009;33(10):1529-39.
82. Liu A, Cheng L, Du J, Peng Y, Allan RW, Wei L, et al. Diagnostic utility of novel stem cell markers SALL4, OCT4, NANOG, SOX2, UTF1, and TCL1 in primary mediastinal germ cell tumors. Am J Surg Pathol. 2010;34(5):697-706.
83. Miettinen M, Wang Z, McCue PA, Sarlomo-Rikala M, Rys J, Biernat W, et al. SALL4 expression in germ cell and non-germ cell tumors: a systematic immunohistochemical study of 3215 cases. Am J Surg Pathol. 2014;38(3):410-20.
84. Novak D, Huser L, Elton JJ, Umansky V, Altevogt P, Utikal J. SOX2 in development and cancer biology. Semin Cancer Biol. 2020;67(Pt 1):74-82.
85. Bass AJ, Watanabe H, Mermel CH, Yu S, Perner S, Verhaak RG, et al. SOX2 is an amplified lineage-survival oncogene in lung and esophageal squamous cell carcinomas. Nat Genet. 2009;41(11):1238-42.
86. de Jong J, Stoop H, Gillis AJ, van Gurp RJ, van de Geijn GJ, Boer M, et al. Differential expression of SOX17 and SOX2 in germ cells and stem cells has biological and clinical implications. J Pathol. 2008;215(1):21-30.
87. Nettersheim D, Heimsoeth A, Jostes S, Schneider S, Fellermeyer M, Hofmann A, et al. SOX2 is essential for in vivo reprogramming of seminoma-like TCam-2 cells to an embryonal carcinoma-like fate. Oncotarget. 2016;7(30):47095-110.
88. Jostes SV, Fellermeyer M, Arevalo L, Merges GE, Kristiansen G, Nettersheim D, et al. Unique and redundant roles of SOX2 and SOX17 in regulating the germ cell tumor fate. Int J Cancer. 2020;146(6):1592-605.
89. Sonne SB, Perrett RM, Nielsen JE, Baxter MA, Kristensen DM, Leffers H, et al. Analysis of SOX2 expression in developing human testis and germ cell neoplasia. Int J Dev Biol. 2010;54(4):755-60.
90. Nonaka D. Differential expression of SOX2 and SOX17 in testicular germ cell tumors. Am J Clin Pathol. 2009;131(5):731-6.
91. Chaudhary S, Islam Z, Mishra V, Rawat S, Ashraf GM, Kolatkar PR. Sox2: A Regulatory Factor in Tumorigenesis and Metastasis. Curr Protein Pept Sci. 2019;20(6):495-504.
92. Favilla V, Cimino S, Madonia M, Morgia G. New advances in clinical biomarkers in testis cancer. Front Biosci (Elite Ed). 2010;2:456-77.
93. Leroy X, Augusto D, Leteurtre E, Gosselin B. CD30 and CD117 (c-kit) used in combination are useful for distinguishing embryonal carcinoma from seminoma. J Histochem Cytochem. 2002;50(2):283-5.
94. Berney DM, Shamash J, Pieroni K, Oliver RT. Loss of CD30 expression in metastatic embryonal carcinoma: the effects of chemotherapy? Histopathology. 2001;39(4):382-5.
95. Sonne SB, Herlihy AS, Hoei-Hansen CE, Nielsen JE, Almstrup K, Skakkebaek NE, et al. Identity of M2A (D2-40) antigen and gp36 (Aggrus, T1A-2, podoplanin) in human developing testis, testicular carcinoma in situ and germ-cell tumours. Virchows Arch. 2006;449(2):200-6.
96. Schacht V, Dadras SS, Johnson LA, Jackson DG, Hong YK, Detmar M. Up-regulation of the lymphatic marker podoplanin, a mucin-type transmembrane glycoprotein, in human squamous cell carcinomas and germ cell tumors. Am J Pathol. 2005;166(3):913-21.
97. Lau SK, Weiss LM, Chu PG. D2-40 immunohistochemistry in the differential diagnosis of seminoma and embryonal carcinoma: a comparative immunohistochemical

study with KIT (CD117) and CD30. Mod Pathol. 2007;20(3):320-5.

98. Roth LM, Michal M, Michal M, Jr., Cheng L. Protein expression of the transcription factors DMRT1, TCLF5, and OCT4 in selected germ cell neoplasms of the testis. Hum Pathol. 2018;82:68-75.
99. Brobeil A, Wagenlehner F, Gattenlohner S. Expression of terminal deoxynucleotidyl transferase (TdT) in classical seminoma: a potential diagnostic pitfall. Virchows Arch. 2018;472(3):433-40.
100. Shojaei H, Hong H, Redline RW. High-level expression of divergent endodermal lineage markers in gonadal and extragonadal yolk sac tumors. Mod Pathol. 2016;29(10):1278-88.
101. Nogales FF, Preda O, Nicolae A. Yolk sac tumours revisited. A review of their many faces and names. Histopathology. 2012;60(7):1023-33.
102. Jimenez RA GS, Herrera-Hernandez LP, Sebo TP. esticular germ cell tumors. In: Nogales FF, Jimenez RE, editors. Pathology and Biology of Germ Cell Tumours. Heidelberg: Springer; 2017. p. 267-326.
103. Rougemont AL, Tille JC. Role of HNF1beta in the differential diagnosis of yolk sac tumor from other germ cell tumors. Hum Pathol. 2018;81:26-36.
104. Gallo A, Fankhauser C, Hermanns T, Beyer J, Christiansen A, Moch H, et al. HNF1beta is a sensitive and specific novel marker for yolk sac tumor: a tissue microarray analysis of 601 testicular germ cell tumors. Mod Pathol. 2020;33(11):2354-60.
105. Xiao GQ, Li F, Unger PD, Katerji H, Yang Q, McMahon L, et al. ZBTB16: a novel sensitive and specific biomarker for yolk sac tumor. Mod Pathol. 2016;29(6):591-8.
106. Murray MJ, Huddart RA, Coleman N. The present and future of serum diagnostic tests for testicular germ cell tumours. Nat Rev Urol. 2016;13(12):715-25.
107. Blanco L, Tirado CA. Testicular Germ Cell Tumors: A Cytogenomic Update. J Assoc Genet Technol. 2018;44(4):128-33.
108. Buljubasic R, Buljubasic M, Bojanac AK, Ulamec M, Vlahovic M, Jezek D, et al. Epigenetics and testicular germ cell tumors. Gene. 2018;661:22-33.
109. Singla N, Lafin JT, Ghandour RA, Kaffenberger S, Amatruda JF, Bagrodia A. Genetics of testicular germ cell tumors. Curr Opin Urol. 2019;29(4):344-9.
110. Chang Y, Wang X, Xu Y, Yang L, Qian Q, Ju S, et al. Comprehensive characterization of cancer-testis genes in testicular germ cell tumor. Cancer Med. 2019;8(7):3511-9.
111. Lobo J, Gillis AJM, Jeronimo C, Henrique R, Looijenga LHJ. Human Germ Cell Tumors are Developmental Cancers: Impact of Epigenetics on Pathobiology and Clinic. Int J Mol Sci. 2019;20(2):258.
112. Dieckmann KP, Radtke A, Geczi L, Matthies C, Anheuser P, Eckardt U, et al. Serum Levels of MicroRNA-371a-3p (M371 Test) as a New Biomarker of Testicular Germ Cell Tumors: Results of a Prospective Multicentric Study. J Clin Oncol. 2019;37(16):1412-23.
113. Raos D, Krasic J, Masic S, Abramovic I, Coric M, Kruslin B, et al. In Search of TGCT Biomarkers: A Comprehensive In Silico and Histopathological Analysis. Dis Markers. 2020;2020:8841880.
114. Batool A, Karimi N, Wu XN, Chen SR, Liu YX. Testicular germ cell tumor: a comprehensive review. Cell Mol Life Sci. 2019;76(9):1713-27.

Narrative Review
Acta Medica Academica 2021;50(1):71-87
DOI: 10.5644/ama2006-124.327

Genetics of Prostate Carcinoma

Božo Krušlin[1, 2], Lucija Škara[3], Tonći Vodopić[4], Borna Vrhovec[5], Jure Murgić[6], Goran Štimac[5], Ana Fröbe[2, 6], Cvjetko Lež[7], Monika Ulamec[1, 2], Koraljka Gall-Trošelj[8]

[1]Ljudevit Jurak Department of Pathology and Cytology, Sestre Milosrdnice University Hospital Centre, Zagreb, Croatia, [2]Department of Pathology, School of Medicine, University of Zagreb, Zagreb, Croatia, [3]University of Zagreb, School of Medicine, Scientific Group for Research on Epigenetic Biomarkers, Zagreb, Croatia, [4]Department of Pathology, Cytology and Forensic Medicine, Varaždin General Hospital, Varaždin, Croatia, [5]Department of Urology, Sestre Milosrdnice University Hospital Centre, Zagreb, Croatia, [6]Department of Oncology, Sestre Milosrdnice University Hospital Centre, Zagreb, Croatia, [7]Department of Pathology and Cytology, Zabok General Hospital, Bračak, Croatia and Josip Juraj Strossmayer University of Osijek, Faculty of Dental Medicine and Health Osijek, Croatia, [8]Laboratory for Epigenomics, Division of Molecular Medicine, Ruđer Bošković Institute, Zagreb, Croatia

Correspondence: *bozo.kruslin@gmail.com*; Tel.: + 385 1 3787 177; Fax.: + 385 1 3787 244

Received: 30 December 2020; **Accepted:** 11 January 2021

Abstract
The aim of this review is to provide a brief overview of some current approaches regarding diagnostics, pathologic features, treatment, and genetics of prostate carcinoma (PCa). Prostate carcinoma is the most common visceral tumor and the second most common cancer-related cause of death in males. Clinical outcomes for patients with localized prostate cancer are excellent, but despite advances in prostate cancer treatments, castrate-resistant prostate cancer and metastatic prostate cancer patients have a poor prognosis. Advanced large-scale genomic studies revealed a large number of genetic alterations in prostate cancer. The meaning of these alterations needs to be validated in the specific prostate cancer molecular subtype context. Along these lines, there is a critical need for establishing genetically engineered mouse models, which would include speckle type BTB/POZ protein and isocitrate Dehydrogenase (NADP (+)) 1 mutant, as well as androgen receptor neuroendocrine subtypes of prostate cancer. Another urgent need is developing highly metastatic prostate cancer models, as only up to 17% of available models display bone metastases and exhibit a less typical neuroendocrine prostate cancer or sarcomatoid carcinoma. Moreover, androgen deprivation and relapse should be mimicked in the genetically engineered mouse models, as androgen independence may yield a better model for metastatic castrate-resistant prostate cancer. The development of such refined animal models should be guided by comparative genomics of primary versus corresponding metastatic tumors. Such an approach will have the potential to illuminate the key genetic events associated with specific molecular prostate cancer subsets and indicate directions for effective therapy. **Conclusion**. Despite excellent results in the treatment of localized prostatic carcinoma, castrate-resistant prostate cancer and metastatic prostate cancer have a poor prognosis. Advanced large-scale genomic studies revealed a large number of genetic alterations in PCa. Experimental models of prostate carcinoma in genetically modified mice could provide new data about the genetic changes in such cancers and help in developing better animal models for treatment resistant prostate carcinomas.

Key Words: Prostate Cancer ▪ Genetic Changes ▪ Molecular Subtypes ▪ Treatment.

Introduction

Prostate cancer (PCa) is the most common visceral tumor in males, with more than 1.1 million newly diagnosed cases each year worldwide. It is the second most common cancer-related cause of death in males due to malignant tumors, with approximately 300,000 deaths per year (1). It usually appears in persons older than 50 years. These days, most PCa are routinely diagnosed in asymptomatic patients by a simple and easily performed procedure that includes prostate-specific antigen (PSA) measurement and needle core biopsy. Such an approach enables adequate and timely treatment, leading to a good prognosis. In the pathogenesis of prostate cancer, various exogenous and endog-

enous factors are involved. The second one include inherited and acquired genetic and epigenetic changes. Understanding role of these factors concerning the occurrence and progression of PCa to a lethal outcome in some patients has a crucial translational impact on the detection, diagnosis, and prognosis of this frequently occurring cancer. Specifically, predicting men at risk for developing a lethal PCa vs. an indolent one is extremely important, but currently unmet clinical need (2, 3). This review will provide a brief overview of some current approaches regarding diagnostics, pathologic features, treatment, and genetics of PCa.

Diagnostics of Prostate Cancer

The suspicion of prostate cancer arises from digitorectal examination (DRE) and/or rising of the PSA levels. Most PCas are located in the peripheral zone and may be detected by DRE in conjunction with PSA value when the volume is >0.2 mL (4, 5). The use of PSA as a serum marker has revolutionized PCa diagnosis (4). This marker may be elevated in benign prostatic hypertrophy, prostatitis, and other non-malignant conditions. As an independent variable, PSA is a better predictor of cancer than either DRE or transrectal ultrasound (TRUS) (5). PSA is a continuous parameter, with higher levels indicating a greater likelihood of PCa. Currently, PSA is a gold-standard marker also used for assessing PCa risk and biochemical recurrence (BRE) (6). With respect to PCa, the PSA sensitivity and specificity of 60% and 79%, respectively, makes it the organ-specific marker but cannot be considered as a tumor-specific marker (7). One should be aware of high false-positive rates in indolent, low-risk localized PCa that may lead to overtreatment of PCa patients. On the other hand, many clinically significant PCa remain undetected until presented in the advanced stage (8).

The need for a better marker has been recognized and addressed timely. As a result, there are many tests currently available. They may be applied before and after taking the biopsy. Blood-based risk assessment tests that reduce unnecessary biopsies by ~ 40% are the Prostate Health Index (PHI) and 4Kscore. The first test relies on total PSA, free PSA, and precursor PSA, while the second one relies on total PSA, free PSA, intact PSA, and human kallikrein2 (7). In the modern era, genomic, epigenetic, and proteomic-based biomarkers are available to augment PSA and reduce unnecessary biopsies. They are all expected to improve diagnostics, staging, and monitoring. Finally, they can contribute to the knowledge needed to understand the basis of tumor aggressiveness and guide therapy decisions. Novel biomarkers are not necessarily restricted to proteins in a specific tissue or the blood. Instead, there may be other types of molecules (micro RNA (mi-RNA), for example) present in various biological specimens (9).

Urine-based noninvasive tests are useful for deciding whom to biopsy (SelectMDx, EndoDX Prostate IntelliScore) while the combination of urine- and tissue-based markers are useful for deciding whom to rebiopsy (SelectMDx, EndoDX Prostate IntelliScore, Progensa PCA3, The Michigan Prostate Score (MiPS), ConfirmMDx). The positive aspect of these tests should be considered for reducing the number of unnecessary biopsies and for improving a discrimination between clinically significant and indolent PCa. They are very useful for avoiding overdiagnosis (7). SelectMDx measures Homeobox C6 (*HOXC)* and Distal-Less Homeobox 1 (*DLX1)* mRNA in urine. In contrast, EndoDX Prostate IntelliScore measures Prostate Cancer-Associated 3 (*PCA3)*, ETS transcription factor *ERG* and SAM Pointed Domain Containing ETS Transcription Factor (*SPDEF)* mRNA in urinary exosomes (7). Progensa PCA3 is a urine-based assay that measures the level of prostate-specific long noncoding *PCA3* and *PSA* transcripts. The PCA3/PSA mRNA ratio is used to aid in repeated biopsy decision-making (10). The Michigan Prostate Score evaluates chimeric transcript Transmembrane Serine Protease 2 – *TMPRSS2:ERG* and *PCA3* mRNA in urine and normalizes it with serum PSA (11). ConfirmMDx, considering that non-tumors cells adjacent to the cancer are epigenetically changed, detects changes in DNA methylation of Glutathione S-Transferase pi1 (*GSTP1*), Ras Association Domain Family

Member 1 (*RASSF1*), and Adenomatous Polyposis Coli (*APC*) genes in histopathologically negative biopsy tissue (7, 12).

Currently, there are four commercially available tests for assessing PCa behavior and guiding therapy decisions for localized disease. ProMark quantifies eight protein markers in biopsy tissue of Gleason score 3+3 and 3+4. It is useful for predicting the risk of PCa aggressive behavior and helpful in the situation when the therapist must decide between active surveillance and active treatment (13). OncotypeDX Genomic Prostate Score determines mRNA levels of 17 genes in biopsy tissue of Gleason score 3+3 and 3+4 to predict aggressiveness, adverse pathology, and biochemical recurrence (7). Decipher measures RNA expression of 22 genes in biopsy or prostatectomy specimens. The test results predict a 5-year risk for clinical metastases and 10-year PCa-specific mortality risk from both specimens. It adds to the accuracy for predicting the existence of a high-grade PCa from the biopsy and is also helpful for making decisions related to therapy protocol (radiation therapy timing and hormone deprivation therapy) (14). Prolaris determines RNA expression of 31 cell cycle progression genes and 15 housekeeping genes in biopsy or prostatectomy specimens to predict cancer aggressiveness, PCa-specific mortality, and therapy decision-making (active surveillance or definitive treatment) (15).

Multiparametric-magnetic resonance imaging (mp-MRI) has shown promising results in diagnosis, localization, risk stratification, and clinically significant prostate cancer (16). Mp-MRI includes high-resolution T2-weighted imaging (T2WI) and at least two functional MRI techniques (17). Suspicious lesions in mp-MRI are graded using the Prostate-Imaging Reporting and Data Scoring System (PIRADS) version 2 (18). PI-RADS™ v2 assessment uses a 5-point scale based on the likelihood that a combination of mp-MRI findings correlates with the presence of a clinically significant cancer for each lesion in the prostate gland. There are five assessment categories (18) ranging from PI-RADS 1 – very low probability (clinically significant cancer is highly unlikely to be present) to PI-RADS 5 – very high probability (clinically significant cancer is highly likely to be present). Three methods based on MRI guidance are available for performing the targeted prostate biopsy: a) Cognitive fusion, in which the ultrasound operator positions the biopsy needle in the prostate area where the prior MRI demonstrated a lesion; b) Direct MRI-guided biopsy, performed within an MRI tube; and c) Software coregistration of stored MRI with real-time ultrasound, using a fusion device (19). Correlation with radical prostatectomy (RP) specimens shows that mp-MRI has good sensitivity for the detection and localization of the International Society of *Urological* Pathology (ISUP) grade > 2 cancers but is less sensitive in identifying PCas *ISUP* grade 1 (20). MRI-TBx (MRI-targeted biopsies) significantly out-performs systematic biopsy to detect ISUP grade > 2 in the repeat-biopsy setting. In biopsy-naïve patients, the difference appears less marked and not significant in all series, but it remains in favor of MRI-TBx in most studies (20).

Although DRE, TRUS, and MR are beneficial, the definitive diagnosis depends on histopathological verification of adenocarcinoma in prostate biopsy cores (20).

Pathology

On gross examination, prostate carcinoma is a gritty and firm, gray-yellow, poorly circumscribed tumor, which can be more easily felt than seen. Accurate identification of prostate cancer by gross inspection is possible in only 63% of cases, with a 19% false-positive rate (21). These days grading is performed according to the World Health Organization (WHO) 2016 recommendations based on the original Gleason grading system. Defined initially by Donald Gleason and published in the 1960s and 1970s (22, 23), the score is based on prostate adenocarcinoma histological patterns. It has been refined over the years and is nowadays the most widely used grading system (23). Grading should include primary and secondary Gleason grade, Gleason score as well as grade group that is determined on the basis of Gleason grades. Different architectural patterns have been as-

signed a number from 1 to 5 (from well to poorly differentiated). Gleason score is a sum of the two most prevalent Gleason grades and ranges from 2 to 10. However, in practice, only scores from 6 to 10 are usually used. There were some other inconsistencies in the Gleason system that led to some modifications and a grade group proposal that has been subsequently validated on a large number of patients (24). Today, grade groups from 1 to 5 and Gleason grading, are used according to WHO 2016 classification (23, 24).

Microscopically, prostate carcinoma is usually composed of small glands. However, medium to large papillary or cribriform glands or solid growth, as well as single cells, can be found. The cytoplasm is usually finely granular but may be clear/foamy due to intracellular lipid accumulation. Bluish luminal mucin and/or crystalloids can be seen in the lumina of neoplastic glands and peritumoral clefting around some glands (23, 25-27). There are nuclear enlargement, hyperchromasia, and prominent nucleoli. Mitotic figures are quite uncommon except in high-grade tumors (21, 25). However, diagnosis is based on at least three criteria, some of which are mentioned earlier. These criteria are favoring but not diagnostic of adenocarcinoma. Some features are associated with false-positive diagnoses, such as atrophic cytoplasm, atypical glands associated with inflammation, adenosis, and many others (21, 25, 26). Certain features are confirmative and diagnostic, including perineural invasion, mucinous fibroplasia, and glomeruloid structures (21, 25, 26). Diagnosis is occasionally difficult and for that reason some immunohistochemical methods should be used such as antibodies to p63, PSA, ERG, high-molecular weight cytokeratin, alpha-methyl CoA racemase (AMACR) and others.

Treatment of PCa

Approaches for managing localized PCa include active surveillance, brachytherapy, external beam radiation, radical prostatectomy and androgen deprivation therapy (28). Radical prostatectomy (as a surgical treatment of PCa) is the gold standard because hormone therapy and chemotherapy are usually not curative. Not all cancer cells can be eradicated consistently by radiation or other physical forms of energy, even if the tumor is localized within the prostate capsule. Moreover, if the prostate gland remains *in situ,* new prostate cancers can develop in the residual prostatic epithelium. There are four different approaches to radical prostatectomy: open perineal, open retropubic, manual laparoscopic, and robot-assisted laparoscopic approaches (29). Radical prostatectomy is indicated for the treatment (with curative intent) of patients in good condition with localized PCa whose life expectancy exceeds ten years (30).

While clinical outcomes for patients with localized PCa are excellent, metastatic PCa patients have a poor prognosis. The treatment of choice for metastatic PCa is androgen deprivation therapy (ADT) and, if ADT fails, cytotoxic chemotherapy. Phase III clinical trials investigating their combination are in progress (31). Hormone-sensitive PCa, even under low-androgen conditions, progress to lethal, castration-resistant PCa (CRPC). Therapy for castration-resistant PCa are androgen receptor (AR) signaling inhibitors and, in case of failure, AR-directed therapy, chemotherapy, Radium-223, poly (ADP-ribose) polymerase (PARP)-inhibitors (if harboring *BRCA1*, *BRCA2*, or *ATM* alterations) and immunotherapy are available (31-33). There are indications that androgen inhibition enhances cell sensitivity to PARP-inhibitors, and several clinical trials based on their combination are currently underway (33). Since the adverse effect of ADT is a decrease in bone mineral density, a combination of ADT and bisphosphonates is recommended but only in documented osteoporosis or androgen-independent prostate cancer with bone metastasis (34). Despite advances in CRPC treatments, it remains lethal. New strategies that would achieve long-term disease remissions are needed. Potentially targetable molecular targets may be p300/CBP, fibroblast growth factor (FGF), Wnt family member 5A (WNT5A)/receptor tyrosine kinase-like orphan receptor 1 (ROR1), tyrosine kinase ACK1, and STEAP1 (Six-transmembrane epithelial antigen of prostate-1).

Bipolar androgen therapy that combines a permanent ADT with high doses of testosterone applied monthly showed promising outcomes, which were even better when combined with checkpoint immunotherapy was applied (31).

Genetics of Prostate Carcinoma

Prostate cancer has an extraordinarily complex genetic makeup containing mutations, DNA copy-number changes, rearrangements, and gene fusions (2, 3, 35). These aberrations are associated with extensive changes in the epigenetic landscape (36). Multiple studies have shown a genetic component to the etiology of prostate cancer, which has been reviewed elsewhere (2, 3, 35-39). Epidemiological studies have shown that a family history of prostate cancer may significantly increase PCa occurrence risk (39). Twin studies have indicated a substantial heritability of prostate cancer (35). Large-scale genome-wide association studies (GWASs) have identified many prostate cancer susceptibility loci (3, 35), including 63 novel risk-associated single-nucleotide polymorphisms (SNPs), among which four SNPs (rs111599055, rs11859370, rs2788524, rs56366063) were shown to be clinically significant (40).

Several large-scale genomic studies in both primary malignant prostate tumors and metastatic castration-resistant prostate cancer (mCRPC) have identified recurrent DNA copy number changes, mutations, rearrangements, and gene fusions such as familial mutations in Homeobox B13 (*HOXB*13) and DNA repair genes, including *BRCA*2, *ATM*, Checkpoint Kinase 2 (*CHEK*2), *BRCA*1, DNA Repair Protein RAD51 Homolog 4 (*RAD*51D), and Partner and Localizer of BRCA2 (*PALB*2) (3, 35). It is known that germline mutations in BRCA genes are associated with increased risk for prostate cancer and a more aggressive phenotype and worse outcomes (3, 35).

Primary prostate tumors and mCRPC exhibit markedly increased genome-wide copy number alterations (35, 38). On the other hand, somatic point mutations are less common in prostate cancer than in most other solid tumors (41). The whole-exome sequencing analysis applied to 333 tumors revealed only 0.94 mutations per megabase (mut/Mb), corresponding to 19 non-synonymous mutations per tumor genome (median; 13–25, 25th, and 75th percentiles respectively) (41). As recently published, this contrasts with, for example, numbers related to small cell lung carcinomas of which 40% (N=122) was shown to contain a high mutation burden, defined as 10 mut/Mb (42). Prior exome sequencing of 112 prostate cancers identified 12 recurrently mutated genes through focused assessment of point mutations and short insertions and deletions (43). Moreover, differences in prostate cancer incidence and outcome have been observed in men from different racial/ethnic groups, with men of African descent having the highest incidence and mortality rates, which may partially be attributed to genetic factors (44). The heritability factor is crucial when mutations are present in DNA-repair genes (45).

Another important factor relates to the activity of the androgen pathway, as the signaling pathway mediated by AR plays a central role in the prostate gland's development and function. Studies using conventional approaches and next-generation sequencing (NGS) have revealed that a majority of primary and metastatic prostate cancers harbors genomic alterations in the androgen signaling pathway, including AR amplification/mutations, gain of AR nuclear receptor coactivator 1/2 (NCOA1/2), and loss of AR nuclear receptor corepressor 1/2 (NCOR1/2) which contributes to castration resistance (46). In addition, AR genomic structural rearrangements are present in one-third of mCRPC tumors, resulting in aberrant expression of diverse AR variant species lacking the ligand-binding domain and resulting in persistent activation of AR signaling, such as AR variant 7 (AR-V7), which appears to drive disease progression (47, 48).

Based on the previously mentioned study (41), it seems that a high proportion of all prostate cancers (74%) can be assigned to one of seven molecular classes based on oncogenic fusions: 1) *ERG*, 2) *ETV1*, 3) *ETV4*, or 4) *FLI1* (46, 8, 4, and 1% respectively), or mutations in 5) *SPOP*, 6) *FOXA1*, or 7) *IDH1* mutations (11, 3, and 1% respectively) (41).

Changes in the Number of Chromosomes and Copy Number Variations of Select Chromosomal Regions

Changes in Chromosomal Number There are few reports on chromosome number changes associated with prostate cancer progression (49-51). Braun et al. were explored 428 PCa, and PCa related specimens (186 localized, 75 lymph node metastasized, 125 lymph node metastases, 42 hormone-refractory distant metastases) and observed a significant increase in aneuploidy with advanced tumor stage (49). An increased expression of the mitotic marker Phosphorylated Histone H3 – PHH3 was significantly associated with aneuploidy and higher pT stage (49). Copy number gains were most commonly present on chromosomes X (26.6%), 21 (22.8%), Y (20.7%), 14 (19.2%), and 8 (17.7%), while the losses of chromosomes 20 (11.0%), 10 (4.1%), and 6 (4.0%) accounted for the most frequent monosomies. However, while overall ploidy status and PHH3 expression in primary tumors indicate advanced disease, a fluorescence in situ hybridization (FISH) – based test for distinct alterations did not seem to be beneficial for diagnostic or prognostic purposes (49). Celep et al. observed numerical aberrations in 41% of 19 analyzed prostate cancer cases (50). The most frequent aberration was a loss of chromosome 9 that was detected in 12 (63%) samples, followed by monosomic chromosomes 8, 7, and 17, which were present in 11 (58%), 9 (47%), and 6 (32%) tumors, respectively. The highest rate for trisomy was observed for chromosome 7 (three tumors, 16%) (50). There were no significant aberrations in benign prostate hyperplasia (BPH) samples. Visakorpi et al. studied 23 prostate cancer and 10 BPH specimens by FISH using pericentromeric repeat-specific probes for 10 chromosomes (51). All BPH specimens were diploid, without apparent chromosomal aberrations, as assessed by flow cytometry and FISH. In prostate carcinoma, flow cytometry and FISH revealed abnormal DNA content in 35% and 74% of tumors, respectively. Aberrant copy number of chromosomes 7, X, and 8 were found in approximately 40% of cases. Simple chromosome losses were uncommon. Still, in DNA tetraploid tumors, relative losses (trisomy or disomy) of several chromosomes were often found, with chromosome Y being most commonly affected, suggesting prostate cancer progression through tetraploidization, followed by losses of selected chromosomes. The most recent data have convincingly shown that, over a median follow-up of 15.3 years, increasing tumor aneuploidy strongly associates with an increased risk of lethal prostate cancer. When comparing the biological behavior of tumors with the same Gleason score, 23% of patients with five or more altered chromosome arms in their tumors had fivefold higher odds of lethal disease compared with those without aneuploidy (52).

Copy Number Alterations Copy number alterations (CNAs) are gains or losses in genetic material that affect a larger fraction of the genome. These alterations are found in nearly 90% of prostate cancers (2). Somatic tumor CNA burden (TCB) and genome-wide CNA patterns were shown to be associated with biochemical recurrence and metastasis in primary prostate cancer, especially in low and intermediate-risk prostate cancer patients (Gleason scores of 7 and less) (53). Tumor CNA burden as a continuous variable was also shown to be significantly associated with prostate cancer-specific death (53) in conservative treatment cohort, independent of Gleason sum score and Cancer of the prostate risk assessment (CAPRA) score (53). Copy number alterations (gains and losses) have an integral role in both the activation of oncogenes and inactivation of tumor suppressor genes. For example, the most common loss of 8p (the minimal region of deletion: 8p21.3-p21.2 harboring NK3 Homeobox 1 (*NKX*3-1)) was found in 304 of 546 (55.7%) and 105 of 116 (90.5%) cases of localized and advanced prostate carcinoma, respectively. Other common deletions in primary tumors were also on chromosomes 13q (13q13-q31.1; loss of RB transcriptional corepressor 1 (*RB*1)), 5q11.2-q23.3, 17p13.3-p11.2, 10q23.2-q26.12, 18q. On the other hand, the gain of chromosome 8q was identified in 114 of 546 (20.9%) and 97 of 116 (83.6%) primary and advanced cases, respectively (54). In metastatic tu-

mors, hundreds of aberrations can be found. This phenomenon may reflect increasing genomic instability, which relates to disease progression.

Recent genetic studies revealed that mCRPCs with neuroendocrine (NE) features commonly are *RB1* and *TP53* deficient and display attenuated AR signaling compared with non-metastatic CRPC (35, 51). On the other hand, castration-resistant metastatic tumors often show amplification of chromosomes X, 7, 8q, and 9q and include genes from the androgen receptor pathway and the *MYC* oncogene. Numerous studies have demonstrated an increase of *MYC* copy number in up to 50% of prostate cancers (55). Overexpression of Myc in mice resulted in prostatic intraepithelial neoplasia (PIN) with progression to invasive carcinoma (56). Besides, Myc functions as a driver in the metastatic Pten/Trp53-deficient Rapid CaP genetically engineered mouse models (GEMM) (57), in which *Myc* activation in combination with phosphatase and tensin homolog (*PTEN*) loss drives genomic instability and contributes to the occurrence of metastatic disease (58, 59).

It is challenging to detect CNAs in the sample obtained by prostatic needle core biopsy. Therefore, it was proposed that their identification should be performed in circulating and disseminated tumor cells from blood and bone marrow, respectively (3). However, the most recent data did not confirm circulating prostate cancer cells in the blood and bone marrow of patients with a localized prostate tumor (60).

Structural Rearrangements

Improper repair of double-stranded DNA breaks can result in both intra- and inter-chromosome rearrangements. The most common prostate cancer genomic alterations are translocations involving androgen-regulated promoters and the ETS family of transcription factors, such as ERG and the E twenty-six family of transcription factors (ETV) genes (61). In the previously mentioned study (41), 53% of tumors were found to have ETS-family gene fusions (*ERG*, *ETV1*, *ETV4*, and *FLI1*). A recurrent gene fusion of the 5' untranslated region of the androgen-responsive *TMPRSS2* to *ERG* (TMPRSS2:ERG) was the first translocation discovered by Tomlins and collaborators (62). This type of fusion is present in ~50% of localized prostate cancers (35). This chimera expression confers an increased risk of disease relapse after treatment for clinically localized prostate cancer due to the growth-promoting activity of the *ERG* oncogene under the control of the regulatory elements of *TMPRSS2* gene. The presence of TMPRSS2:ERG chimera varies concerning ethnicity and is more prevalent (~50%) in Caucasians than in African-Americans (31.3%) and Japanese patients (15.9%) (63). Several other rearrangements have been described in prostate cancer, including *ESRP1:CRAF*, the ETS family, and *RAF* kinase gene fusions (64). ERG-associated rearrangement has been associated with 10q, 17p, and 3p14 deletions (65). On the other hand, those tumors without ERG rearrangement exhibit 6q and 16q deletion and 7q amplification (65). The whole-genome sequencing of primary prostate tumors T2c or greater, and Gleason grade 7 or higher obtained from seven patients showed a median of 90 structural rearrangements (range 43–213) per tumor genome, highlighting the prevalence and complexity of these changes as well as the importance of chromatin structure. Further, in the tumors with *TMPRSS2:ERG*, rearrangement breakpoints were enriched near open chromatin, androgen receptor, and ERG DNA binding sites (66).

Single Nucleotide Polymorphisms and Point Mutations

The mutation rate is a crucial factor in determining a somatic cells risk of malignant transformation. Kan et al. have shown a low number of mutations (0.33 per Mb) in 58 analyzed prostate cancers, associated with a high number of *TMPRSS2–ERG* gene fusion transcripts, which were present in 75% of samples (67). Still, even with such a low mutation rate, there are crucial and clinically important genes for occurrence, development, and biological behavior of prostate carcinoma. It is thought that, on average, less than 20 mutations are likely

to affect protein stability or function. For example, in Kan's research, only three genes (*TP*53, speckle type BTB/POZ protein (*SPOP),* and A-kinase anchoring protein 9 (*AKAP*9) were shown to have a significant prevalence of protein-altering mutations (q-score ≥1.0) (67).

On the other hand, there are genes whose SNPs gained interest concerning PCa occurrence and progression. Some of these polymorphisms were thoroughly analyzed. However, in the *RNASEL (HPC1)* gene (1q25.3), elaC Ribonuclease Z 2 (*ELAC*2 or *HPC*2) (17p12), and macrophage scavenger receptor 1 (*MSR*1) (8p22), none of the polymorphisms analyzed was shown to be a strong prognostic/predictive and independent factor for prostate cancer (68, 69) (Table 1).

However, there is no doubt that prostate cancer is a polygenetic disease that is highly dependent on SNP–based genetic risk score (GRS). The first reported study assessing the association of a polygenic risk score derived from well-established risk-associated SNPs with patient age at PCa diagnosis was published in 2019 (70). The independent PCa risk-associated SNPs discovered through GWAS were defined through three standard criteria (70), which allowed for the profiling of 110 PCa risk-associated SNPs. The paper was shown a significant association of GRS with patient age at PCa diagnosis, especially when combined with family history. The highest risk allele frequency (RAF) value (0.93) was shown for rs12480328. This polymorphism is located in the intron of the activity-dependent neuroprotector homeobox gene (*ADNP*). So far, there are no data related to the importance of this gene in PCa.

Several GWAS have revealed the SNPs rs2292884 (missense mutation in melanophilin, *MLPH*; 2q37.3) and rs902774 in the noncoding region 12q13 (38). A large meta-analysis based on 78 PCa GWAS risk associations within 85 distinct genomic regions was recently published (71). Although numerous data have been published, the final confirmation of some SNPs as *bona fide* prognostic markers is yet to come. For example, the polymorphism rs2735839 in the *PSA* coding gene, kallikrein-related peptidase 3, (*KLK*3*)*, was crucial when estimating the occurrence and biological behavior of PCas in several populations (72, 73). A recently published meta-analysis, including 35,838 patients and 36,369 control subjects, did not find

Table 1. Common Genetic Changes in Prostate Carcinoma

Gene	Genomic alteration	Locus	Function	References
RNASEL (RNS4; PRCA1)	Mutation	1q25.3; HPC1 – hereditary-prostate-cancer (HPC)-predisposition locus; 8 exons	Innate immunity, part of the interferon-regulated 2-5A system	Alvarez-Cubero et al., 2016 (68); Liu et al., 2018 (69); Wallis et al., 2015 (3)
ELAC2 (HPC2; COXPD17)	Missense mutations	17p12; 25 exons	tRNA biosynthesis; interacts with activated Smad Family Member 2 (SMAD2)	Alvarez-Cubero et al., 2016 (68); Liu et al., 2018 (69); Wallis et al., 2015 (3)
MSR1(SRA; SR-A; CD204)	Mutation	8p22; 12 exons	The isoforms type 1 and type 2 mediate the endocytosis of modified low density lipoproteins (LDLs).The isoform 3 inhibits the function of isoforms type 1 and type 2	Alvarez-Cubero et al., 2016 (68); Liu et al., 2018 (69); Wallis et al., 2015 (3)
SPOP (TEF2; BTBD32)	Mutation	17q21.33; 16 exons	Modulation of the transcriptional repression activity of death-associated protein 6	Clark et al., 2020 (75); An et al., 2014 (76); Blattner et al., 2017 (77)
FOX1A (HNF3A; TCF3A)	Mutations	14q21.1; 3 exons	Binding to DNA	Zhou et al., 2020 (78); Adams et al., 2019 (79)
IDH1 (IDH; IDP)	Mutation	2q34; 2 exons	Oxidative decarboxylation	Kang et al., 2009 (80); Ghiam et al., 2012 (81); Dang et al., 2009 (82); Waitkus et al., 2018 (83)

an association between rs2735839 and the risk for PCa. It was, however, shown that there is a strong association between rs1058205 (T>C) and the decreased risk of PCa (74).

SPOP *SPOP* has been found to be mutated in prostate cancer in a range from 4.4% to 28.6% of cases (75). The inability of the mutant SPOP to induce degradation of full-length AR and inhibit AR-mediated gene transcription is of great importance for prostate cancer pathogenesis (76). However, the mutant SPOP (SPOP-F133V) was not confirmed as a strong prostate cancerogenesis driver in a transgenic mouse with prostate-specific conditional expression of the mutant allele, although it was associated with strong PI3K/mTOR signaling. However, when mice expressing mutant SPOP in a conditional *Pten* heterozygous background (Pb-Cre; PtenL/+; R26F133V) was generated, a highly penetrant phenotype with focal areas of high-grade prostatic intraepithelial neoplasia (HG-PIN) by six months of age was observed (77). The validation model presented by human *SPOP* mutant organoids revealed that *SPOP* mutations associate with specific changes, including genomic deletions at 5q21, 6q15, and 2q21 (77). On the other hand, *SPOP* mutant prostate cancers were shown to be exclusively negative for ETS rearrangement. All these facts point to the *SPOP* mutation-positive prostate cancers as a distinct molecular subtype. There is a high similarity in mRNA, copy-number, and methylation profiles in tumors with *FOXA*1 mutations and those with *SPOP* mutations.

Forkhead Box A1 – FOX1A Zhou et al. were recently shown that *FOXA*1 mRNA is consistently the most abundant mRNA in prostate tumors, ranking in the 95th percentile in 492 of 497 prostate tumors deposited in TCGA (78). By analyzing 3086 primary and metastatic prostate cancers, Adams et al. (79) were shown *FOXA1*-related aberrations in 11.4 % of samples. Among them, 3% were genomic amplifications, while 8.4% of tumors had somatic point mutations. Less than 1% of tumors were carrying both types of changes. Over 50% of *FOXA*1 mutations in the cited study were mapped to a specific hotspot in Wing2 of the forkhead (FKHD) DNA-binding domain, mainly between H247 and F266. These mutations were more prevalent in primary locoregional cases. Truncation mutations with consequential loss of the C-terminal transactivating domain were presented with 20% (79). Some functional consequences of these mutations will be explained later.

Isocitrate Dehydrogenase-1 (IDH1) In 2009, Kang et al. were shown the presence of the *IDH1* point mutations (R132H and R132C) in only two out of 75 analyzed prostate cancers (80). This finding was confirmed three years later; identical *IDH1* point mutations in codon 132 were discovered in two out of 158 analyzed prostate cancers (81). IDH1 is a cytoplasmic metabolic enzyme needed for oxidative decarboxylation of isocitrate to 2-oxoglutarate (α-ketoglutarate). When one allele is mutated, abnormally high 2-hydroxyglutarate (2-HG) production associated with an extensive reshape of cellular epigenome occurs (82). Targeting altered IDH1 in various tumors, including select prostate cancer patients, would be of the most significant interest (83). Although mutations in *IDH1* are the most common in gliomas, the first mutant IDH1 blocking drug (ivosidenib) was approved by the FDA in 2019 for treating adults with relapsed or refractory acute myeloid leukemia (AML) with an *IDH*1 mutation. Whether PCa may be targeted in a similar way remains to be seen.

General Epigenetic Landscape in Prostate Cancer and Micro-RNAs

Deregulation of genes controlling epigenetic processes involved in DNA modification (e.g., methylation and hydroxymethylation), histone modification, or nucleosome remodeling has been recognized as a tumorigenesis driver in many cancer types, including prostate cancer. Genomic DNA can be methylated by canonical DNA methyltransferase (DNMT) consisting of DNMT1, DNMT3A, and DNMT3B at the C-5 position of the cytosine within CpG dinucleotides, which are present in CpG islands (CGIs). There is app. 50,000 experimentally supported CGIs (eCGIs) in the human genome (84). Their length varies between 200 bps and 3.6 kbps. DNA methylation in normal cells

ensures that gene expression and gene silencing are adequately regulated. Aberrant level of DNA methylation is a part of disturbing epigenetics found in cancers. In the malignantly transformed cell, DNA is commonly hypermethylated in promoter regions of tumor suppressor genes, leading to decreased activity. Notwithstanding this fact, cancer is a disease of global hypomethylation, which is commonly present in non-coding regions of DNA. In prostate cancer, hypomethylation of noncoding long interspersed nuclear elements (LINE-1), which constitutes approximately 17% of the human genome, was shown in 1999 (85). As recently reviewed by Lam et al., the methylation rate of certain genes in prostate cancer may be considered a valid prognostic parameter for certain disease aspects (86). With respect to methylation, among all explored genes so far, none was shown to be undoubtedly predictive when all studies were taken into consideration (86). The reasons for these findings include diversity in sample type, cohort size, clinical endpoints examined, methylation profiling methodologies, analytical approach, and clinicopathological factors adjusted for in multivariate analyses. The methylation status of the *PITX*2 (paired-like homeodomain transcription factor 2)gene (4q25) seems to be highly conclusive for predicting biochemical recurrence-free survival in prostate cancer patients after radical prostatectomy (RP) (training cohort: hazard ratio (HR) = 1.83 (95 % CI 1.07–3.11), P=0.027; validation cohort: HR=2.56 (95 % CI 1.44–4.54), P=0.001 (87).

The only commercially available epigenetic test, ConfirmMDx, is made for diagnostic purposes. It is set up to produce binary results based on the methylation status of three genes: *APC*, *RASSF*1, and *GSTP1,* to detect cancer in histologically negative biopsies. Methylation-positive test result profiles men who are at increased risk of harboring occult (high-grade) cancer. Methylation negative samples spare the patient from unnecessary repeat biopsy due to the high accuracy of the test (negative predictive value (NPV) between 90% and 96%) (88, 89).

Previously described transcription factor FOXA1 is a "pioneer factor" that can bind to DNA in those segments where the chromatin is compacted. The role of FOXA1 is to contribute to increased accessibility of these regions for other transcription factors to bind (90). Specifically, in prostate tissue, FOXA1 plays a crucial role in AR-mediated gene regulation and signaling. AR chromatin binding is dependent on FOXA1 (91). The molecular basis of this process is not simple. Gao et al. were recently shown that lysine-specific histone demethylase 1A (LSD1) may regulate FOXA1 chromatin binding through directly demethylating its lysine 270, *in vitro* (91). The complexity of this process should be kept in mind when considering LSD1 inhibitors for treating tumors with mutated or highly expressed FOXO1. In prostate cancer, this may be problematic because the loss of FOXA1 can result in transdifferentiation from AR/FOXA1-driven adenocarcinoma to neuroendocrine prostate cancer (NEPC). This aggressive subtype is AR-ligand independent (92, 93).

Micro-RNA and Prostate Cancer Mi-RNAs are a class of small noncoding RNAs (22-25 nucleotides long) that bind to messenger RNA (mRNA). Consequently, they negatively influence protein expression through cleavage of specific target mRNAs or inhibition of their translation (94). Thus, a specific mi-RNA's functional role depends on the role of the specific mRNA, which is a miRNA binding partner (95). If specific mi-RNA targets mRNA originating from a tumor suppressor gene, then it has a strong potential to act as oncogenic mi-RNA (96). If, on the other hand, miRNA targets mRNA originating from an oncogene, it may be considered a tumor-suppressive molecule in a specific tissue. Mi-RNAs are highly promiscuous molecules as one miRNA may bind to and control numerous target mRNAs simultaneously. Currently, 2654 mature human miRNA sequences are known (97). Many miRNAs are located in genetically unstable sites where they are prone to deletion or rearrangement, which occur in cancer (98). Accordingly, the miRNAs located in the chromosomal regions of deletion show the lowest expression level.

In contrast, the miRNAs located in the regions of amplifications show the highest expression levels (99). Many miRNA genes are located next to CpG islands, where they may be prone to epigenetic silencing through methylation. In prostate cancer, this miRNA silencing mechanism was shown in 2014 through analysis of 74 formalin-fixed, paraffin-embedded (FFPE) clinical specimens: 24 normal prostate samples and 50 PCa samples from radical prostatectomies (100). Methylation occurred in 0%, 5%, and 13% of cancers for miR-18b, miR-148a, and miR-450a/542-3p, respectively, while no methylation was present in control samples. The same research study has shown that low levels of miR-132 correlated with a higher rate of metastatic events, lymph node invasion, and shorter recurrence-free time (Table 2). There was a negative correlation of miR-132 expression levels with the overall Gleason score and tumor stage (100). Two years later, Qu et al. demonstrated that decreased miR-132 levels in prostate cancer cells positively regulate the Warburg effect through inhibiting solute carrier family 2 member 1 *SLC*2A1/*GLUT1* expression (101).

In 2007, Porkka et al. published a seminal paper describing miRNA expression in 4 BPHs, 5 untreated prostate carcinomas, and four hormone-refractory prostate carcinomas (99). Their work has shown a unique profile of 51 differentially expressed miRNAs (PCa vs. BPH: 37 and 14 miRNAs downregulated and upregulated, respectively). Among these miRNAs, 22 and 8 were decreased and increased in all carcinoma samples, respectively, whereas 15 and 6 of them were downregulated and upregulated, respectively, only in the hormone-refractory carcinomas compared with BPH samples. These early data pointed out on mi-RNAs as unique molecules, which are mechanistically involved in prostate cancer development. They were confirmed in recent studies.

Table 2. Some miRNAs with confirmed clinical value associated with Prostate Carcinoma

miRNA	Locus	Clinical Significance	Mode of Action	References
miR-132	17p13.3	Downregulated in human PCa tissues; miR-adverse correlation with Gleason score	In vitro: inhibition of TGF-β (transforming growth factor-β)-induced EMT)	Formosa et al., 2013 (100); Qu et al., 2016 (101); Liu et al., 2016 (102)
miRNA -146a	5q33.3	Downregulated in androgen-independent prostate cancer (AIPC) tissue, suppressive role	Regulation of ROCK/Caspase 3 signaling pathway	Xu et al, 2015 (103)
miR-141	12p13.31	Associated with increased risk of biochemical PC recurrence.	In vitro: Suppression of prostate cancer stem cells and metastasis by targeting a cohort of pro-metastasis genes, including Enhancer of Zeste Homologue 2 (EZH2)	Richardsen et al., 2019 (105); Liu et al., 2017 (106)
miR-375-3p	2q35	Prediction of time to progression in mCRPC patients treated with docetaxel or abiraterone	Predicted targets: CCND2, MAP3K2, MXI1, PAFAH1B1, YOD1, ZFYVE26	Zedan et al., 2020 (107); Ciszkowicz et al., 2020 (108)
miR-331-3p	12q22	High expression is associated with advanced PC stage and distant metastases	Suppressive role through targeting NACC1, ERBB-2 expression and androgen receptor signaling. Oncogenic role through stimulation of epithelial-to-mesenchimal transition (EMT)	Epis et al., 2009 (111); Morita et al, 2018 (112); Fujii et al 2016 (113)
miR1792 cluster (miR-17, miR-18a, miR-19a, miR-20a, miR-19b-1 and miR-92a)	13q31.3	Oncogenic role in majority of prostate cancer models.	Specific targeting of SERTAD3 with miR-92a;enhancement of migration and invasion in vitro, attributed to the induction of integrin β-1	Zhang et al 2020 (114); Zhou et al 2016 (115)

For example, the difference between androgen-dependent- (ADPC) and androgen-independent prostate cancer (AIPC) tissues was shown to be dependent on miR-146a and its influence on Rho-associated coiled-coil containing protein kinase 1 (*ROCK*1) kinase (102, 103). The presence of miRNAs in plasma of PCa patients was for the first time described in 2008 (104). The potential discriminatory miRNA was shown to be miR-141, which had the most significant differential expression and could detect individuals with cancer with 60% sensitivity at 100% specificity (104). In PCa tissues (N=535), expression of miR-141 in the epithelial part of the tumor significantly correlates to Gleason score ≥8 (P=0.040) and large tumor size (≥20 mm, P = 0.025). In contrast, its overall expression (defined as both epithelial and stromal expression) strongly relates to Gleason grade (P=0.001) (105). It was recently shown that plasma levels of miR-141-3p and miR-375-3p might predict time to progression in mCRPC patients treated with docetaxel or abiraterone; their high baseline levels were significantly associated with shorter overall survival (OS) in the abiraterone and in docetaxel treated patients (106-108).

There are also efforts to explore the clinical value of mi-RNAs in the urine. A novel logistic regression model based on five urine miRNAs (miR-151a-5p, miR-204-5p, miR-222-3p, miR-23b-3p, and miR-331-3p) and PSA were recently shown as a strong predictor for biochemical recurrence (109).

The crosstalk between miRNAs and molecules belonging to various signaling pathways may be established through strong networks containing transcription factors and various protein kinases. Erb-b2 receptor tyrosine kinase 2, ERBB2 (Her-2/neu), is a tyrosine kinase receptor that is overexpressed in abiraterone-resistant prostate cancer. It was recently shown to be included in the activation of the PI3K/AKT signaling and stabilization of AR protein. Accordingly, it was hypothesized that combination therapy with abiraterone and ERBB2 antagonists might be effective for treating the subset of CRPC with increased ERBB2 activity (110). In 2009, miR-331-3p expression was shown to be reduced in prostate tumors relative to normal adjacent tissue and is inversely correlated with *ERBB*2 mRNA expression (111). Thus, in this specific scenario, miR-331-3p may be considered to be a suppressive molecule (112, 113). At least ten different miRNAs have been found to be involved in apoptosis. In many cases, their way of acting follows a cascade pattern. Up-regulation of the miR-17-92 cluster leads to overexpression of miR-20a, which subsequently targets E2F1-3 transcription factors (114-116). Then, depending on the cell cycle phase, reduced E2F1-3 results either in cellular proliferation or reduced apoptosis via TP53 and caspase activity, thus creating an auto-regulatory feedback loop as E2F1-3 controls miR-20a expression. MiR-21 also contributes to apoptosis through the mechanism, which includes TP53 and is preserved in various malignant tumors (117). In prostate cancer specifically, miR-21 acts as an oncogenic factor, as it targets both *PDCD*4 (programmed cell death 4) (118) and *PTEN* mRNA (119). Numerous biological processes can be significantly affected by mi-RNA molecules. For example, MiR-15a and miR-16-1 are down-regulated in most prostate tumors (120).

Conclusions

Advanced large-scale genomic studies revealed a large number of genetic alterations in PCa. The meaning of these alterations needs to be validated in the context of the specific PCa molecular subtype. Along these lines, there is a critical need for establishing GEMMs, which would include *SPOP* and *IDH*1 mutants and AR−NE− subtypes of PCa. Another urgent need is the development of highly metastatic PCa models, as less than 20% of available models display bone metastases and exhibit a less typical NEPC or sarcomatoid pathology. Moreover, androgen deprivation and relapse should be mimicked in the GEMMs models, as androgen independence may yield a better model for metastatic CRPC. The development of such refined animal models should be guided by comparative genomics of primary PCa and corresponding metastases. Such an approach will potentially illu-

minate the critical genetic events associated with specific molecular Pca subsets and indicate directions for effective therapy.

Acknowledgement: This work is supported in part by the University of Zagreb funds for scientific research (Grant number: 1120056) and by the Croatian Science Foundation Grant number: IP-2016-06-4404; NRF2 at the crossroads of epigenetic remodeling, metabolism and proliferation of cancer cells; KGT—PI.

Conflict of Interest: The authors declare that they have no conflict of interest.

References

1. Torre LA, Bray F, Siegel RL, Ferlay J, Lortet-Tieulent J, Jemal A. Global cancer statistics, 2012. CA Cancer J Clin. 2015;65(2):87-108.
2. Isaacs WB, Xu J. Current progress and questions in germline genetics of prostate cancer. Asian J Urol. 2019;6(1):3-9.
3. Wallis CJ, Nam RK. Prostate Cancer Genetics: A Review. EJIFCC. 2015;26(2):79-91.
4. Stamey TA, Yang N, Hay AR, McNeal JE, Freiha FS, Redwine E. Prostate-specific antigen as a serum marker for adenocarcinoma of the prostate. N Engl J Med. 1987;317(15):909-16.
5. Catalona WJ, Richie JP, Ahmann FR, Hudson MA, Scardino PT, Flanigan RC, et al. Comparison of Digital Rectal Examination and Serum Prostate Specific Antigen in the Early Detection of Prostate Cancer: Results of a Multicenter Clinical Trial of 6,630 Men. J Urol. 2017;197(2S):S200-7.
6. Whitaker H, Tam JO, Connor MJ, Grey A. Prostate cancer biology & genomics. Transl Androl Urol. 2020;9(3):1481-91.
7. Porzycki P, Ciszkowicz E. Modern biomarkers in prostate cancer diagnosis. Cent European J Urol. 2020;73(3):300-6.
8. Bronimann S, Pradere B, Karakiewicz P, Abufaraj M, Briganti A, Shariat SF. An overview of current and emerging diagnostic, staging and prognostic markers for prostate cancer. Expert Rev Mol Diagn. 2020;20(8):841-50.
9. Mollica V, Di Nunno V, Santoni M, Cimadamore A, Scarpelli M, Lopez-Beltran A, et al. An evaluation of current prostate cancer diagnostic approaches with emphasis on liquid biopsies and prostate cancer. Expert Rev Mol Diagn. 2020;20(2):207-17.
10. Duffy MJ. Biomarkers for prostate cancer: prostate-specific antigen and beyond. Clin Chem Lab Med. 2020;58(3): 326-39.
11. Raja N, Russell CM, George AK. Urinary markers aiding in the detection and risk stratification of prostate cancer. Transl Androl Urol. 2018;7(Suppl 4):S436-42.
12. Alford AV, Brito JM, Yadav KK, Yadav SS, Tewari AK, Renzulli J. The Use of Biomarkers in Prostate Cancer Screening and Treatment. Rev Urol. 2017;19(4):221-34.
13. Tonry C, Finn S, Armstrong J, Pennington SR. Clinical proteomics for prostate cancer: understanding prostate cancer pathology and protein biomarkers for improved disease management. Clin Proteomics. 2020;17(1):41.
14. Counago F, Lopez-Campos F, Diaz-Gavela AA, Almagro E, Fenandez-Pascual E, Henriquez I, et al. Clinical Applications of Molecular Biomarkers in Prostate Cancer. Cancers (Basel). 2020;12(6):1550.
15. Vince RA Jr, Tosoian JJ, Jackson WC, Spratt DE, Morgan TM. Tissue-based genomics: which test and when. Curr Opin Urol. 2019;29(6):598-604.
16. Ghai S, Haider MA. Multiparametric-MRI in diagnosis of prostate cancer. Indian J Urol. 2015;31(3):194-201.
17. Barentsz JO, Richenberg J, Clements R, Choyke P, Verma S, Villeirs G, et al. ESUR prostate MR guidelines 2012. Eur Radiol. 2012;22(4):746-57.
18. Weinreb JC, Barentsz JO, Choyke PL, Cornud F, Haider MA, Macura KJ, et al. PI-RADS Prostate Imaging – Reporting and Data System: 2015, Version 2. Eur Urol. 2016;69(1):16-40.
19. Marks L, Young S, Natarajan S. MRI-ultrasound fusion for guidance of targeted prostate biopsy. Curr Opin Urol. 2013;23(1):43-50.
20. Mottet N, Bellmunt J, Bolla M, Briers E, Cumberbatch MG, De Santis M, et al. EAU-ESTRO-SIOG Guidelines on Prostate Cancer. Part 1: Screening, Diagnosis, and Local Treatment with Curative Intent. Eur Urol. 2017;71(4):618-29.
21. Renshaw AA. Correlation of gross morphologic features with histologic features in radical prostatectomy specimens. Am J Clin Pathol. 1998;110(1):38-42.
22. Gleason DF, Mellinger GT. Prediction of prognosis for prostatic adenocarcinoma by combined histologic grading and clinical staging. J Urol. 1974;111(1):58-64.
23. Moch H, Humphrey PA, Ulbright MT, Reuter VE. WHO classification of tumours of the urinary system and male genital organs. Lyon: International Agency for Research on Cancer; 2016.
24. Epstein JI, Zelefsky MJ, Sjoberg DD, Nelson JB, Egevad L, Magi-Galluzzi C, et al. A Contemporary Prostate Cancer Grading System: A Validated Alternative to the Gleason Score. Eur Urol. 2016;69(3):428-35.
25. Iczkowski KA, Torkko KC, Wilson RS, Lucia MS, Bostwick DG. Prostatic atrophy: its spatial proximity to carcinoma and intraepithelial neoplasia based on annotation of digital slides. Hum Pathol. 2014;45(1):54-8.
26. Iczkowski KA, Bostwick DG. Criteria for biopsy diagnosis of minimal volume prostatic adenocarcinoma: analytic comparison with nondiagnostic but suspicious atypical small acinar proliferation. Arch Pathol Lab Med. 2000;124(1):98-107.

27. Kruslin B, Tomas D, Rogatsch H, Novosel I, Cupić H, Belicza M, et al. Periacinar retraction clefting in the prostatic needle core biopsies: an important diagnostic criterion or a simple artifact? Virchows Arch. 2003;443(4):524-7.
28. Taylor JM, Chen VE, Miller RC, Greenberger BA. The Impact of Prostate Cancer Treatment on Quality of Life: A Narrative Review with a Focus on Randomized Data. Res Rep Urol. 2020;12:533-46.
29. Wein AJ KL, Partin AW, Peters AA, Catalona WJ, Han M. Management of localized prostate cancer. In: Wein A, Kavoussi LR, Campbell, MF, Walsh, PC, editors. Campbell-Walsh Urology. 11 ed. Philadelphia, PA: Elsevier; 2016. p. 2614.
30. Reynard J, Brewster S, Biers, S. Oxford handbook of urology. 3rd ed. Oxford: Oxford University Press; 2013.
31. Shore ND. Current and Future Management of Locally Advanced and Metastatic Prostate Cancer. Rev Urol. 2020;22(3):110-23.
32. Chakravarty D, Huang L, Kahn M, Tewari AK. Immunotherapy for Metastatic Prostate Cancer: Current and Emerging Treatment Options. Urol Clin North Am. 2020;47(4):487-510.
33. Powers E, Karachaliou GS, Kao C, Harrison MR, Hoimes CJ, George DJ, et al. Novel therapies are changing treatment paradigms in metastatic prostate cancer. J Hematol Oncol. 2020;13(1):144.
34. Kaler J, Hussain A, Haque A, Naveed H, Patel S. A Comprehensive Review of Pharmaceutical and Surgical Interventions of Prostate Cancer. Cureus. 2020;12(11):e11617.
35. Wang G, Zhao D, Spring DJ, DePinho RA. Genetics and biology of prostate cancer. Genes Dev. 2018;32(17-18):1105-40.
36. Houlahan KE, Shiah YJ, Gusev A, Yuan J, Ahmed M, Shetty A, et al. Genome-wide germline correlates of the epigenetic landscape of prostate cancer. Nat Med. 2019;25(10):1615-26.
37. Goldgar DE, Easton DF, Cannon-Albright LA, Skolnick MH. Systematic population-based assessment of cancer risk in first-degree relatives of cancer probands. J Natl Cancer Inst. 1994;86(21):1600-8.
38. Schumacher FR, Al Olama AA, Berndt SI, Benlloch S, Ahmed M, Saunders EJ, et al. Association analyses of more than 140,000 men identify 63 new prostate cancer susceptibility loci. Nat Genet. 2018;50(7):928-36.
39. Benafif S, Kote-Jarai Z, Eeles RA. A Review of Prostate Cancer Genome-Wide Association Studies (GWAS). Cancer Epidemiol Biomarkers Prev. 2018;27(8):845-57.
40. Schumacher FR, Berndt SI, Siddiq A, Jacobs KB, Wang Z, Lindstrom S, et al. Genome-wide association study identifies new prostate cancer susceptibility loci. Hum Mol Genet. 2011;20(19):3867-75.
41. Network CGAR. The Molecular Taxonomy of Primary Prostate Cancer. Cell. 2015;163(4):1011-25.
42. Shao C, Li G, Huang L, Pruitt S, Castellanos E, Frampton G, et al. Prevalence of High Tumor Mutational Burden and Association With Survival in Patients With Less Common Solid Tumors. JAMA Netw Open. 2020;3(10):e2025109.
43. Barbieri CE, Baca SC, Lawrence MS, Demichelis F, Blattner M, Theurillat JP, et al. Exome sequencing identifies recurrent SPOP, FOXA1 and MED12 mutations in prostate cancer. Nat Genet. 2012;44(6):685-9.
44. Huang FW, Mosquera JM, Garofalo A, Oh C, Baco M, Amin-Mansour A, et al. Exome Sequencing of African-American Prostate Cancer Reveals Loss-of-Function ERF Mutations. Cancer Discov. 2017;7(9):973-83.
45. Pritchard CC, Mateo J, Walsh MF, De Sarkar N, Abida W, Beltran H, et al. Inherited DNA-Repair Gene Mutations in Men with Metastatic Prostate Cancer. N Engl J Med. 2016;375(5):443-53.
46. Pisano C, Tucci M, Di Stefano RF, Turco F, Scagliotti GV, Di Maio M, et al. Interactions between androgen receptor signaling and other molecular pathways in prostate cancer progression: Current and future clinical implications. Crit Rev Oncol Hematol. 2020;157:103185.
47. Henzler C, Li Y, Yang R, McBride T, Ho Y, Sprenger C, et al. Truncation and constitutive activation of the androgen receptor by diverse genomic rearrangements in prostate cancer. Nat Commun. 2016;7:13668.
48. Li Y, Yang R, Henzler CM, Ho Y, Passow C, Auch B, et al. Diverse AR Gene Rearrangements Mediate Resistance to Androgen Receptor Inhibitors in Metastatic Prostate Cancer. Clin Cancer Res. 2020;26(8):1965-76.
49. Braun M, Stomper J, Kirsten R, Shaikhibrahim Z, Vogel W, Böhm D, et al. Landscape of chromosome number changes in prostate cancer progression. World J Urol. 2013;31(6):1489-95.
50. Celep F, Karagüzel A, Ozgür GK, Yildiz K. Detection of chromosomal aberrations in prostate cancer by fluorescence in situ hybridization (FISH). Eur Urol. 2003;44(6):666-71.
51. Visakorpi T, Hyytinen E, Kallioniemi A, Isola J, Kallioniemi OP. Sensitive detection of chromosome copy number aberrations in prostate cancer by fluorescence in situ hybridization. Am J Pathol. 1994;145(3):624-30.
52. Stopsack KH, Whittaker CA, Gerke TA, Loda M, Kantoff PW, Mucci LA, et al. Aneuploidy drives lethal progression in prostate cancer. Proc Natl Acad Sci U S A. 2019;116(23):11390-5.
53. Hieronymus H, Schultz N, Gopalan A, Carver BS, Chang MT, Xiao Y, et al. Copy number alteration burden predicts prostate cancer relapse. Proc Natl Acad Sci U S A. 2014;111(30):11139-44.
54. Williams JL, Greer PA, Squire JA. Recurrent copy number alterations in prostate cancer: an in silico meta-analysis of publicly available genomic data. Cancer Genet. 2014;207(10-12):474-88.

55. Jenkins RB, Qian J, Lieber MM, Bostwick DG. Detection of c-myc oncogene amplification and chromosomal anomalies in metastatic prostatic carcinoma by fluorescence in situ hybridization. Cancer Res. 1997;57(3):524-31.
56. Ellwood-Yen K, Graeber TG, Wongvipat J, Iruela-Arispe ML, Zhang J, Matusik R, et al. Myc-driven murine prostate cancer shares molecular features with human prostate tumors. Cancer Cell. 2003;4(3):223-38.
57. Nowak DG, Cho H, Herzka T, Watrud K, DeMarco DV, Wang VM, et al. MYC Drives Pten/Trp53-Deficient Proliferation and Metastasis due to IL6 Secretion and AKT Suppression via PHLPP2. Cancer Discov. 2015;5(6):636-51.
58. Sumanasuriya S, De Bono J. Treatment of Advanced Prostate Cancer-A Review of Current Therapies and Future Promise. Cold Spring Harb Perspect Med. 2018;8(6):a030635.
59. Hubbard GK, Mutton LN, Khalili M, McMullin RP, Hicks JL, Bianchi-Frias D, et al. Combined MYC Activation and Pten Loss Are Sufficient to Create Genomic Instability and Lethal Metastatic Prostate Cancer. Cancer Res. 2016;76(2):283-92.
60. Chalfin HJ, Glavaris SA, Malihi PD, Sperger JM, Gorin MA, Lu C, et al. Prostate Cancer Disseminated Tumor Cells are Rarely Detected in the Bone Marrow of Patients with Localized Disease Undergoing Radical Prostatectomy across Multiple Rare Cell Detection Platforms. J Urol. 2018;199(6):1494-501.
61. Sizemore GM, Pitarresi JR, Balakrishnan S, Ostrowski MC. The ETS family of oncogenic transcription factors in solid tumours. Nat Rev Cancer. 2017;17(6):337-51.
62. Tomlins SA, Rhodes DR, Perner S, Dhanasekaran SM, Mehra R, Sun XW, et al. Recurrent fusion of TMPRSS2 and ETS transcription factor genes in prostate cancer. Science. 2005;310(5748):644-8.
63. Magi-Galluzzi C, Tsusuki T, Elson P, Simmerman K, LaFargue C, Esgueva R, et al. TMPRSS2-ERG gene fusion prevalence and class are significantly different in prostate cancer of Caucasian, African-American and Japanese patients. Prostate. 2011;71(5):489-97.
64. Palanisamy N, Ateeq B, Kalyana-Sundaram S, Pflueger D, Ramnarayanan K, Shankar S, et al. Rearrangements of the RAF kinase pathway in prostate cancer, gastric cancer and melanoma. Nat Med. 2010;16(7):793-8.
65. Taylor BS, Schultz N, Hieronymus H, Gopalan A, Xiao Y, Carver BS, et al. Integrative genomic profiling of human prostate cancer. Cancer Cell. 2010;18(1):11-22.
66. Berger MF, Lawrence MS, Demichelis F, Drier Y, Cibulskis K, Sivachenko AY, et al. The genomic complexity of primary human prostate cancer. Nature. 2011;470(7333):214-20.
67. Kan Z, Jaiswal BS, Stinson J, Janakiraman V, Bhatt D, Stern HM, et al. Diverse somatic mutation patterns and pathway alterations in human cancers. Nature. 2010;466(7308):869-73.
68. Alvarez-Cubero MJ, Pascual-Geler M, Martinez-Gonzalez LJ, Expósito Ruiz M, Saiz M, Cozar JM, et al. Association between RNASEL, MSR1, and ELAC2 single nucleotide polymorphisms and gene expression in prostate cancer risk. Urol Oncol. 2016;34(10):431.e1-8.
69. Liu X, Zheng D, Lu G, Yang B. The RNASEL -1385G/A polymorphism is associated with risk of prostate cancer in Africans. Onco Targets Ther. 2018;11:97-102.
70. Na R, Labbate C, Yu H, Shi Z, Fantus RJ, Wang CH, et al. Single-Nucleotide Polymorphism-Based Genetic Risk Score and Patient Age at Prostate Cancer Diagnosis. JAMA Netw Open. 2019;2(12):e1918145.
71. Dadaev T, Saunders EJ, Newcombe PJ, Anokian E, Leongamornlert DA, Brook MN, et al. Fine-mapping of prostate cancer susceptibility loci in a large meta-analysis identifies candidate causal variants. Nat Commun. 2018;9(1):2256.
72. Eeles RA, Kote-Jarai Z, Giles GG, Olama AA, Guy M, Jugurnauth SK, et al. Multiple newly identified loci associated with prostate cancer susceptibility. Nat Genet. 2008;40(3):316-21.
73. Motamedi RK, Sarhangi N, Afshari M, Sattari M, Jamaldini SH, Samzadeh M, et al. Kallikarein-related peptidase 3 common genetic variant and the risk of prostate cancer. J Cell Biochem. 2019;120(9):14822-30.
74. Ding WH, Ren KW, Yue C, Zou JG, Zuo L, Zhang LF, et al. Association between three genetic variants in kallikrein 3 and prostate cancer risk. Biosci Rep. 2018;38(6):BSR20181151.
75. Clark A, Burleson M. SPOP and cancer: a systematic review. Am J Cancer Res. 2020;10(3):704-26.
76. An J, Wang C, Deng Y, Yu L, Huang H. Destruction of full-length androgen receptor by wild-type SPOP, but not prostate-cancer-associated mutants. Cell Rep. 2014;6(4):657-69.
77. Blattner M, Liu D, Robinson BD, Huang D, Poliakov A, Gao D, et al. SPOP Mutation Drives Prostate Tumorigenesis In Vivo through Coordinate Regulation of PI3K/mTOR and AR Signaling. Cancer Cell. 2017;31(3):436-51.
78. Zhou S, Hawley JR, Soares F, Grillo G, Teng M, Madani Tonekaboni SA, et al. Noncoding mutations target cis-regulatory elements of the FOXA1 plexus in prostate cancer. Nat Commun. 2020;11(1):441.
79. Adams EJ, Karthaus WR, Hoover E, Liu D, Gruet A, Zhang Z, et al. FOXA1 mutations alter pioneering activity, differentiation and prostate cancer phenotypes. Nature. 2019;571(7765):408-12.
80. Kang MR, Kim MS, Oh JE, Kim YR, Song SY, Seo SI, et al. Mutational analysis of IDH1 codon 132 in glioblastomas and other common cancers. Int J Cancer. 2009;125(2):353-5.
81. Ghiam AF, Cairns RA, Thoms J, Dal Pra A, Ahmed O, Meng A, et al. IDH mutation status in prostate cancer. Oncogene. 2012;31(33):3826.

82. Dang L, White DW, Gross S, Bennett BD, Bittinger MA, Driggers EM, et al. Cancer-associated IDH1 mutations produce 2-hydroxyglutarate. Nature. 2009;462(7274):739-44.
83. Waitkus MS, Diplas BH, Yan H. Biological Role and Therapeutic Potential of IDH Mutations in Cancer. Cancer Cell. 2018;34(2):186-95.
84. Mendizabal I, Yi SV. Whole-genome bisulfite sequencing maps from multiple human tissues reveal novel CpG islands associated with tissue-specific regulation. Hum Mol Genet. 2016;25(1):69-82.
85. Santourlidis S, Florl A, Ackermann R, Wirtz HC, Schulz WA. High frequency of alterations in DNA methylation in adenocarcinoma of the prostate. Prostate. 1999;39(3):166-74.
86. Lam D, Clark S, Stirzaker C, Pidsley R. Advances in Prognostic Methylation Biomarkers for Prostate Cancer. Cancers (Basel). 2020;12(10):2993.
87. Holmes EE, Goltz D, Sailer V, Jung M, Meller S, Uhl B, et al. PITX3 promoter methylation is a prognostic biomarker for biochemical recurrence-free survival in prostate cancer patients after radical prostatectomy. Clin Epigenetics. 2016;8:104.
88. Partin AW, Van Neste L, Klein EA, Marks LS, Gee JR, Troyer DA, et al. Clinical validation of an epigenetic assay to predict negative histopathological results in repeat prostate biopsies. J Urol. 2014;192(4):1081-7.
89. Van Neste L, Partin AW, Stewart GD, Epstein JI, Harrison DJ, Van Criekinge W. Risk score predicts high-grade prostate cancer in DNA-methylation positive, histopathologically negative biopsies. Prostate. 2016;76(12):1078-87.
90. Cirillo LA, Lin FR, Cuesta I, Friedman D, Jarnik M, Zaret KS. Opening of compacted chromatin by early developmental transcription factors HNF3 (FoxA) and GATA-4. Mol Cell. 2002;9(2):279-89.
91. Gao S, Chen S, Han D, Wang Z, Li M, Han W, et al. Chromatin binding of FOXA1 is promoted by LSD1-mediated demethylation in prostate cancer. Nat Genet. 2020;52(10):1011-7.
92. Kim J, Jin H, Zhao JC, Yang YA, Li Y, Yang X, et al. FOXA1 inhibits prostate cancer neuroendocrine differentiation. Oncogene. 2017;36(28):4072-80.
93. Omarjee S, Carroll JS. Targeting LSD1 and FOXA1 in prostate cancer. Nat Genet. 2020;52(10):1002-3.
94. Bartel DP. MicroRNAs: genomics, biogenesis, mechanism, and function. Cell. 2004;116(2):281-97.
95. Watanabe Y, Tomita M, Kanai A. Computational methods for microRNA target prediction. Methods Enzymol. 2007;427:65-86.
96. Dhawan A, Scott JG, Harris AL, Buffa FM. Pan-cancer characterisation of microRNA across cancer hallmarks reveals microRNA-mediated downregulation of tumour suppressors. Nat Commun. 2018;9(1):5228.
97. Kozomara A, Birgaoanu M, Griffiths-Jones S. miRBase: from microRNA sequences to function. Nucleic Acids Res. 2019;47(D1):D155-62.
98. Calin GA, Sevignani C, Dumitru CD, Hyslop T, Noch E, Yendamuri S, et al. Human microRNA genes are frequently located at fragile sites and genomic regions involved in cancers. Proc Natl Acad Sci U S A. 2004;101(9):2999-3004.
99. Porkka KP, Pfeiffer MJ, Waltering KK, Vessella RL, Tammela TL, Visakorpi T. MicroRNA expression profiling in prostate cancer. Cancer Res. 2007;67(13):6130-5.
100. Formosa A, Lena AM, Markert EK, Cortelli S, Miano R, Mauriello A, et al. DNA methylation silences miR-132 in prostate cancer. Oncogene. 2013;32(1):127-34.
101. Qu W, Ding SM, Cao G, Wang SJ, Zheng XH, Li GH. miR-132 mediates a metabolic shift in prostate cancer cells by targeting Glut1. FEBS Open Bio. 2016;6(7):735-41.
102. Liu H, Wu Z, Zhou H, Cai W, Li X, Hu J, et al. MicroRNA-132/212 Upregulation Inhibits TGF-β-Mediated Epithelial-Mesenchymal Transition of Prostate Cancer Cells by Targeting SOX4. Prostate. 2016;76(16):1560-70.
103. Xu B, Huang Y, Niu X, Tao T, Jiang L, Tong N, et al. Hsa-miR-146a-5p modulates androgen-independent prostate cancer cells apoptosis by targeting ROCK1. Prostate. 2015;75(16):1896-903.
104. Mitchell PS, Parkin RK, Kroh EM, Fritz BR, Wyman SK, Pogosova-Agadjanyan EL, et al. Circulating microRNAs as stable blood-based markers for cancer detection. Proc Natl Acad Sci U S A. 2008;105(30):10513-8.
105. Richardsen E, Andersen S, Melbø-Jørgensen C, Rakaee M, Ness N, Al-Saad S, et al. MicroRNA 141 is associated to outcome and aggressive tumor characteristics in prostate cancer. Sci Rep. 2019;9(1):386.
106. Liu C, Liu R, Zhang D, Deng Q, Liu B, Chao HP, et al. MicroRNA-141 suppresses prostate cancer stem cells and metastasis by targeting a cohort of pro-metastasis genes. Nat Commun. 2017;8:14270.
107. Zedan AH, Osther PJS, Assenholt J, Madsen JS, Hansen TF. Circulating miR-141 and miR-375 are associated with treatment outcome in metastatic castration resistant prostate cancer. Sci Rep. 2020;10(1):227.
108. Ciszkowicz E, Porzycki P, Semik M, Kaznowska E, Tyrka M. MiR-93/miR-375: Diagnostic Potential, Aggressiveness Correlation and Common Target Genes in Prostate Cancer Int J Mol Sci. 2020;21(16):5667.
109. Fredsøe J, Rasmussen AKI, Mouritzen P, Borre M, Ørntoft T, Sørensen KD. A five-microRNA model (pCaP) for predicting prostate cancer aggressiveness using cell-free urine. Int J Cancer. 92019;145(9):2558-67.
110. Gao S, Ye H, Gerrin S, Wang H, Sharma A, Chen S, et al. ErbB2 Signaling Increases Androgen Receptor Expression in Abiraterone-Resistant Prostate Cancer. Clin Cancer Res. 2016;22(14):3672-82.
111. Epis MR, Giles KM, Barker A, Kendrick TS, Leedman PJ. miR-331-3p regulates ERBB-2 expression and androgen receptor signaling in prostate cancer. J Biol Chem. 2009;284(37):24696-704.

112. Morita K, Fujii T, Itami H, Uchiyama T, Nakai T, Hatakeyama K et al. NACC1, as a Target of MicroRNA-331-3p, Regulates Cell Proliferation in Urothelial Carcinoma Cells. Cancers (Basel). 2018;10(10):347.

113. Fujii T, Shimada K, Tatsumi Y, Tanaka N, Fujimoto K, Konishi N. Syndecan-1 up-regulates microRNA-331-3p and mediates epithelial-to-mesenchymal transition in prostate cancer. Mol Carcinog. 2016;55(9):1378-86.

114. Zhang S, Yu J, Sun BF, Hou GZ, Yu ZJ, Luo H. MicroRNA-92a Targets SERTAD3 and Regulates the Growth, Invasion, and Migration of Prostate Cancer Cells via the P53 Pathway. Onco Targets Ther. 2020;13:5495-514.

115. Zhou P, Ma L, Zhou J, Jiang M, Rao E, Zhao Y, et al. miR-17-92 plays an oncogenic role and conveys chemoresistance to cisplatin in human prostate cancer cells. Int J Oncol. 2016;48(4):1737-48.

116. Sylvestre Y, De Guire V, Querido E, Mukhopadhyay UK, Bourdeau V, Major F, et al. An E2F/miR-20a autoregulatory feedback loop. J Biol Chem. 2007;282(4):2135-43.

117. Ma X, Choudhury SN, Hua X, Dai Z, Li Y. Interaction of the oncogenic miR-21 microRNA and the p53 tumor suppressor pathway. Carcinogenesis. 2013;34(6):1216-23.

118. Zennami K, Choi SM, Liao R, Li Y, Dinalankara W, Marchionni L, et al. PDCD4 Is an Androgen-Repressed Tumor Suppressor that Regulates Prostate Cancer Growth and Castration Resistance. Mol Cancer Res. 2019;17(2):618-27.

119. Yang Y, Guo JX, Shao ZQ. miR-21 targets and inhibits tumor suppressor gene PTEN to promote prostate cancer cell proliferation and invasion: An experimental study. Asian Pac J Trop Med. 2017;10(1):87-91.

120. Bonci D, Coppola V, Musumeci M, Addario A, Giuffrida R, Memeo L, et al. The miR-15a-miR-16-1 cluster controls prostate cancer by targeting multiple oncogenic activities. Nat Med. 2008;14(11):1271-7.

Narrative Review
Acta Medica Academica 2021;50(1):88-109
DOI: 10.5644/ama2006-124.328

Neoadjuvant Chemotherapy for Breast Cancer: Moving Beyond Pathological Complete Response in the Molecular Age

Elena Provenzano

Department of Histopathology, Addenbrookes Hospital, Cambridge, UK

Correspondence: *elena.provenzano@addenbrookes.nhs.uk*; Tel.: + 44 1223 256154; Fax.: + 44 1223 257003

Received: 14 January 2021; **Accepted:** 2 February 2021

Abstract
This review focuses on neoadjuvant chemotherapy for breast cancer which introduces practical issues for pathologists, including predicting response, optimising specimen handling, size measurement and assessment of residual disease, and recent advances in management of the axilla. The role of neoadjuvant chemotherapy in breast cancer is increasing, and it has become standard of care for high risk Human Epidermal Growth Factor Receptor 2 positive and triple negative breast cancers. The benefits of the neoadjuvant approach extend beyond pathological complete response to tumour downstaging permitting conservative surgical options in the breast and axilla, and assessment of response provides valuable prognostic information to enable escalation and de-escalation of adjuvant therapy to optimise oncological outcomes. Hence histopathologists play a vital role in patient management in the neoadjuvant setting. Optimal patient selection for neoadjuvant chemotherapy requires consideration of pre-treatment histopathological and molecular tumour characteristics. Post chemotherapy, tumour staging can be challenging, and changes in criteria for measurement of primary tumour and metastases in the 7th and 8th editions of the TNM have led to confusion amongst pathologists. This review offers practical guidance on specimen handling and measurement of lesion size. Moving forwards more detailed information on degree of response will be required for adjuvant therapy decision making, and the Residual Cancer Burden is emerging as the preferred method for quantifying residual disease not just within clinical trials but in routine practice. Recent advances in management of the axilla are discussed, including the significance of minimal residual disease in the form of isolated tumour cells and micrometastases which portend a worse prognosis in the neoadjuvant setting.
Conclusion. Neoadjuvant chemotherapy now forms part of routine breast cancer management, and detailed histopathological assessment and an understanding of the importance of molecular tumour biology is essential for clinical decision making.

Key Words: Breast Cancer ▪ Neoadjuvant Therapy ▪ Staging ▪ Grading Response.

Introduction

Neoadjuvant chemotherapy (NACT) has evolved from treatment of locally advanced breast cancer to routine management of biologically aggressive disease, particularly oestrogen receptor negative (ER-) and/ or human epidermal growth factor 2 positive (HER2+) cancers. The neoadjuvant approach shows similar survival outcomes to adjuvant therapy, but offers potential advantages in both standard clinical care and clinical trial settings (1). Firstly, response to neoadjuvant therapy with complete eradication of disease or a reduction of tumour volume enables less aggressive surgical options, with the potential for breast conservation surgery (BCS) in patients that would have required mastectomy pre-treatment (2). There is also a growing body of evidence to support the role of sentinel node biopsy (SLNB) following NACT in both node negative and node positive patients, leading to avoidance of axillary clearance (ALND) following a complete response in the axilla (3-5). Interestingly, in our own multidisciplinary meetings, it is now the surgeons rather than the oncologists driving decisions regarding NACT. Tumour downstaging to enable conservative procedures can reduce surgical morbidity without compromising oncological out-

comes, however NACT is not the correct approach for all cases and careful patient selection based on clinical features and histological and molecular tumour subtypes is essential to optimise results.

Perhaps even more importantly, assessment of response to NACT provides valuable prognostic information that is increasingly used to guide further adjuvant therapy (6). Complete pathological response (pCR) shows an association with survival outcomes across all molecular subtypes, although this is strongest for ER- and/or HER2+ disease (1, 7). As a result, pCR has been approved by the U.S. Food and Drug Administration (FDA) as a surrogate outcome to survival for neoadjuvant clinical trials in high risk breast cancer (8). The neoadjuvant context provides faster results in smaller cohorts of patients, and alongside novel adaptive trial designs such as ISPY provides exciting potential to screen new agents resulting in more rapid introduction of effective drugs into clinical practice (9, 10). Furthermore, patients who experience a pCR may not benefit from further adjuvant therapy, and there are trials looking at de-escalation of adjuvant therapy in complete responders (11). Hence accurate identification of pCR is vital for ongoing patient management, and requires careful and methodical histological assessment beginning with gross specimen handling.

At the other end of the spectrum, patients who show a limited response to NACT have a poor prognosis. Recent trials, including the KATHERINE and CREATE-X trials, have shown improved survival outcomes with additional adjuvant therapy in incomplete responders with HER2+ and triple negative breast cancer (TNBC) respectively (12, 13). However, non-pCR encompasses a wide variation of response from almost complete response with minimal residual disease (MRD), to minimal or absent response with significant residual tumour. Some series have shown similar survival outcomes for patients with MRD to those who undergo a pCR, however the impact of residual disease volume on survival outcomes varies by molecular tumour subtype (14, 15). Assessment of the degree of response beyond pCR will form an integral part of patient care moving forwards.

Tumour staging post NACT also shows a strong association with survival outcomes (16, 17). Measuring residual tumour size can be challenging, particularly when there has been patchy response across the tumour bed. Definitions of size measurements used for staging in both the breast and axillary lymph nodes have evolved across the 6th, 7th and 8th editions of the TNM, leading to confusion amongst pathologists (18-20). Accurate staging is essential not only in determining patient prognosis, but to generate reliable population based data from cancer registries around the world.

Hence, the pathologist plays a key role in determining optimal patient care in the neoadjuvant setting. This review will focus on some of the key practical issues for pathologists, including predictors of response, optimising specimen handling, size measurement and assessment of residual disease, and recent advances in management of the axilla.

Predictors of Response to NACT

Response to NACT, including the likelihood of achieving pCR and its association with prognosis, is strongly linked to tumour biology (1, 21-25). This has important implications for clinical decisions regarding whether to give neoadjuvant versus adjuvant therapy, particularly if the goal is tumour downsizing to enable conservation. Breast cancer is generally divided into 3 broad molecular groups; luminal (ER+/HER2-), HER2+ and TNBC (25). HER2+ and TNBC show the greatest response to NACT, but even these tumour types contain subgroups with different behaviour.

NACT response of HER2+ breast cancers largely depends on ER status. ER+/HER2+ cancers given standard chemotherapy without HER2 targeted agents show a pCR rate of 18%, rising to 31% with the addition of trastuzumab (1). In contrast, ER-/HER2+ tumours have a much higher pCR rate of 30% without trastuzumab and 50% with trastuzumab; the addition of pertuzumab gives pCR rates as high as 80% (26). The association between pCR and survival outcomes is also much stronger for ER-/HER2+ cancers (HR 0.29; 95% CI 0.17-0.50) without trastuzumab and HR 0.08(95% CI 0.03-

0.22) with trastuzumab) than for ER+/HER2+ cancers where it does not reach significance (HR 0.57(95% CI 0.31-1.04) without trastuzumab and HR 0.56 (95% CI 0.23-1.37) with trastuzumab). ER+/HER2+ tumours also show a different pattern of recurrence with late relapses, in comparison to ER-/HER2+ disease where the majority of relapses occur within the first 5 years after diagnosis (27).

Similar differences are seen when clinically defined HER2+ tumours are classified as HER2-Enriched or luminal subtypes by gene expression profiling (28). Within the NOAH trial only 55% of tumours were HER2-Enriched, with 21% luminal, 7% basal and 18% normal-like. The pCR rate was significantly higher in HER2-Enriched compared with luminal HER2+ tumours (53% versus 29% respectively), and there was a larger improvement in event free survival with the addition of trastuzumab indicating greater benefit from HER2 pathway blockade (29). These findings have been confirmed in a meta-analysis of 16 neoadjuvant trials which showed a significant association with HER2-Enriched subtype and pCR in both ER+ and ER- disease (30). Recent reviews suggest intrinsic subtype as defined by PAM50 is a valuable adjunct to clinical receptor status in making decisions about NACT (27, 31). Studies have also suggested a relationship between higher HER2 protein expression, gene copy number >10 and HER2:CEP17 ratio >4.5 and improved pCR rates following NACT with trastuzumab (32-34). Cancers that are HER2 3+ on immunohistochemistry show higher pCR rates than those that are 2+ with *HER2* gene amplification on FISH (35). Presence of intratumoural heterogeneity for HER2, more commonly found in association with equivocal cases and polysomy/ co-amplification of the *HER2* and *CEP17* probe sites, is also associated with lower pCR rates and poorer survival outcomes; in one series 10% of cases showed HER2 heterogeneity of which none went on to pCR (31). Newer drug conjugates which use the HER2 receptor to enter cells and have a bystander effect, such as trastuzumab-deruxtecan, may prove to be an effective treatment option in these difficult cases. Approximately one third of apocrine carcinomas are HER2+; a recent study found androgen receptor (AR) positivity was associated with improved response to NACT with trastuzumab, and better survival outcomes in ER- disease (36). Other tumour features that have been associated with response to NACT in HER2+ disease include higher levels of tumour infiltrating lymphocytes (TILs), and presence of *PIK3CA* alterations has been associated with lower pCR rates and poorer survival (31).

TNBC form an even more heterogeneous group, perhaps unsurprising given they encompass several histological subtypes including salivary type and metaplastic carcinomas. Overall, TNBC show a pCR rate of 34% with a very strong association between pCR and survival outcomes (HR 0.16; 95% CI 0.11-0.25) (1). Modern chemotherapy regimens with inclusion of platinum agents have increased the pCR rate to over 50% (37). Gene expression analysis identified six different subtypes of TNBC which was revised to four subgroups; two basal-like, a mesenchymal, and a luminal AR group (38). The luminal AR group has high expression of genes related to AR signalling, and a response pattern similar to ER+ cancers with a relatively low pCR rate (29%) but better survival outcomes than other TNBC subtypes (39). The basal-like 1 group has a signature enriched for genes involved in proliferation and DNA damage repair and shows the highest pCR rate (49%) with intermediate survival outcomes, whilst the basal-like 2 group driven by growth factor receptor signalling has a low pCR rate (18%) and poor survival.

The original 6 types included an immune modulatory group with a pCR rate of 30% and a relatively good prognosis; this signature is now believed to reflect infiltration with TILs which is associated with chemotherapy response and improved outcomes in TNBC (38, 40). A recent meta-analysis confirmed the relationship between increasing levels of TILs with pCR, disease free survival (DFS) and overall survival (OS) in TNBC (41).

Metaplastic carcinoma is a subtype of TNBC associated with poor response to NACT and adverse survival outcomes. This reflects the difference in molecular profile compared to NST TNBC, with lower levels of genomic instability and a higher

rate of EGFR and PI3K and Wnt signalling abnormalities (42, 43). In one single institution series of 18 patients, 7 showed no response or progressed whilst on treatment, and only 2 had a pCR (44). In another single institution series, there were 29 cases of metaplastic carcinoma that received NACT with a pCR rate of 17% (45). Interestingly, 4 of the 5 cases that had a pCR were matrix-producing metaplastic carcinomas with a pCR rate of 24% for this subtype, although pCR or tumour type were not associated with survival. There are several special types of TNBC associated with good prognosis, including adenoid cystic carcinoma, secretory carcinoma, the recently described tall cell carcinoma with reversed polarity (TCCRP), and low grade adenosquamous and fibromatosis-like variants of metaplastic carcinoma, where systemic therapy is not indicated (Figure 1). These tumours do not have the genomic instability typical of NST type TNBC, with adenoid cystic and secretory carcinomas characterised by translocations of *MYB-NFIB* and *ETV6-NTRK3* genes respectively, and TCCRP with mutations in the *IDH2* gene (46). The important thing is to recognise these cancers on core biopsy to prevent the patient from receiving unnecessary NACT. If the diagnosis is uncertain then primary surgery should be recommended.

Luminal, or ER+, breast cancers are generally associated with low pCR rates of 0-16% (1). In the intrinsic subtype classification, they are divided into luminal A with low proliferation and high expression of ER signalling genes, and luminal B cancers with high proliferation and/ or HER2 positivity (47, 48). Low grade ER+ tumours with low proliferation have a very low pCR rate (2-7%) but retain an excellent prognosis due to their response to endocrine therapy, and do not derive any additional benefit from chemotherapy (1, 48-52). Many invasive lobular cancers fall into the luminal A or low risk subtypes on gene expression profiling, and several studies have shown poor response to NACT with lower pCR rates than grade and ER matched ductal NST cancers, as well lower rates of tumour downstaging and BCS (53-57). In one study, lobular histological type predicted absence of response to NACT (58).

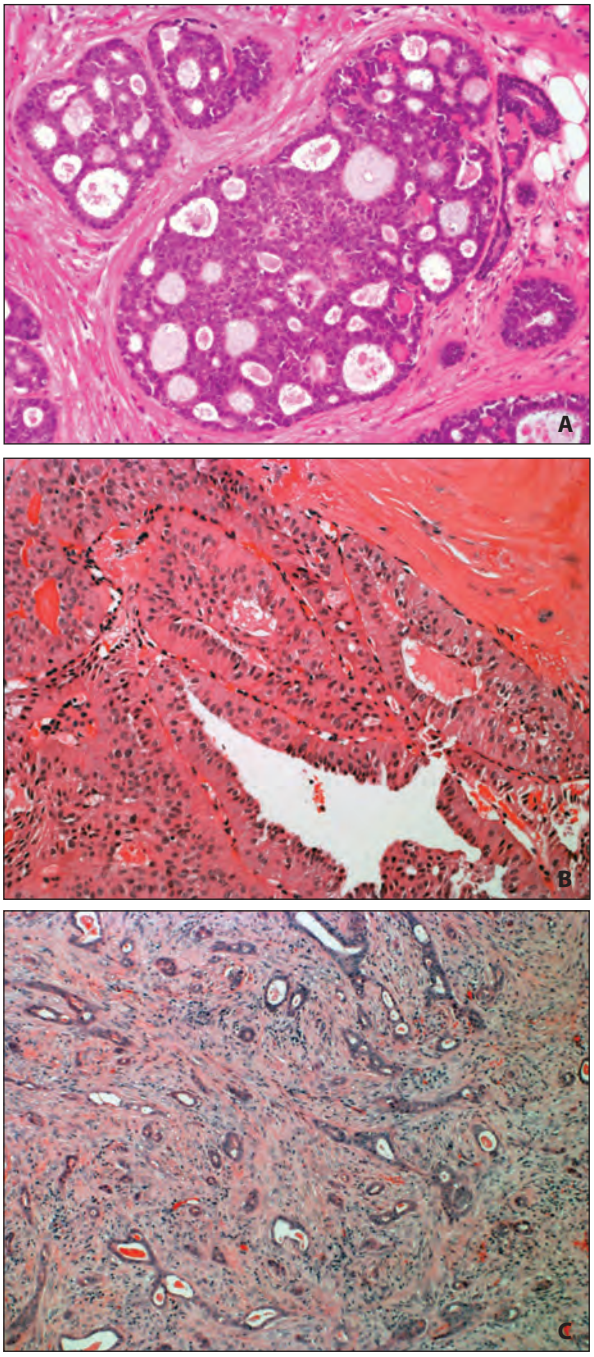

Figure 1. Special types of triple negative breast cancer associated with good prognosis: A) Classical adenoid cystic carcinoma (× 20); B) Tall cell carcinoma with reversed polarity (×10); C) Low grade adenosquamous carcinoma (×20).

However, there is a subset of ER+/HER2- breast cancers with a worse prognosis in which chemotherapy is indicated; features associated with in-

creased responsiveness to NACT include grade 3, PR negativity and a high Ki67 labelling index (55). In the Cortazar analysis, grade 3 ER+ tumours had a pCR rate of 16%, with pCR showing a significant association with improved OS with a HR of 0.29 (95% CI 0.13-0.65) (1). High Ki67 has been shown to predict pCR in ER+/HER2- cancers, however there are difficulties interpreting the literature due to differences in methodology and variation in cut points (59-61). The most recent ASCO-CAP guidelines recognise a Low Positive ER group with nuclear staining in 1-10% of cells, representing less than 5% of ER+ cancers (62); many of these tumours have a basal-like gene expression profile (63, 64). In one trial, 18% of ER+/HER2- cancers were of basal intrinsic subtype, and these tumours had a pCR rate of 32% (65). This reinforces data from HER2+ cancers that intrinsic subtype provides additional information regarding benefit of NACT.

Specimen Handling

Surgical excisions post NACT are becoming increasingly common, and represent the most complex breast specimens handled by histopathology laboratories. Methodical detailed gross specimen handling is essential for accurate determination of pCR, assessment of response and tumour staging. For this to occur, communication between pathologists and the multidisciplinary team, with provision of adequate clinical information on pathology request forms is vital (66). At a minimum, the clinical notes need to state neoadjuvant therapy has been given and it's nature, with a clear description of the number of tumour foci and their location within the breast; a schematic diagram indicating the site of tumour/s is very helpful. Where available, details of tumour size on pre-treatment imaging should also be provided, as sampling should include the area of the original pre-treatment tumour bed, which may extend beyond macroscopically detectable residual disease.

Basic principles of specimen handling also apply in the neoadjuvant setting. Where national guidelines exist these should be followed. Good fixation is vital for subsequent histological interpretation, and specimens should be sliced when fresh if possible to ensure formalin penetration. When delays are likely, one option is to instruct surgeons on how to slice larger specimens such as mastectomies to aid fixation without compromising subsequent pathological evaluation.

Residual tumour is often more ill-defined and softer post NACT, especially if there has been a good response to treatment, making it more challenging to detect on gross assessment. Textural changes may be found on palpation, even if there is no visible tumour bed. Placement of fiducial marker clips at the time of diagnosis is extremely helpful in localising the tumour bed when there is no gross residual lesion, and is recommended even in patients planned for mastectomy to aid localisation of the tumour bed (67). Gel foam or larger metallic clips may be seen on slicing; gel foam clips appear as a cyst filled with gelatinous substance (68). Alternatively, the markers can be identified on x-ray of the specimen slices. Where the tumour was associated with malignant calcification this can also be identified on specimen x-ray, although calcifications can increase or decrease with NACT, and the presence of residual calcification does not show a good correlation with pathological tumour response (69).

As residual tumour is harder to delineate macroscopically, it is typically necessary to take more sections than in the adjuvant setting. Blocks should include any gross residual disease and/ or marker clips, and adjacent uninvolved tissue to encompass the extent of the tumour on pre-treatment imaging (67, 70). For small wide local excision (WLE) specimens it is prudent to submit the entire specimen for histological evaluation. For larger WLE or mastectomy specimens, close clinical-pathological correlation guided by the imaging findings to localise the site of the tumour bed is preferable to exhaustive blind sampling. There is some guidance on the number of blocks required for diagnosis of pCR and assessment of response. The US FDA have recommended taking one block for every cm of tumour size on pre-treatment imaging, or at least 10 tumour blocks, whichever is greater (8). In guid-

ance published in 2015, the international Residual Disease Working Group advised taking blocks representing the full face of the pre-treatment tumour area from every 1-2 cm slice of the specimen, up to a maximum of 25 blocks (70). To determine the Residual Cancer Burden (RCB), described below, five sections representing the maximum cross section of the tumour bed is sufficient to estimate residual tumour cellularity (71). If clip site or tumour bed changes are not present in the initial sections, it may be necessary to review the specimen and take further blocks. Additional routine blocks, such as those for assessment of margins, should also be taken as per the adjuvant setting.

Precise description of where blocks have been taken is essential for reconstruction of the specimen from the glass slides to enable size and cellularity estimates. A visual annotation of the position of blocks on sketched diagrams, photographs of specimen slices, or copies of specimen radiographs is the best way to do this, and is invaluable in subsequent reporting of the microscopic findings. Where available, large tissue cassettes or 'megablocks' are helpful for measurement of lesion size and assessment of margins.

Defining pCR

The ultimate goal of NACT is the attainment of pCR, i.e. the complete eradication of invasive disease. The broadest definition of pCR is the absence of residual invasive disease in the breast and axilla (ypT0 ypN0 and ypTis ypN0 – the y prefix indicating post NACT). The overall rate of pCR decreases according to the stringency of definition used; in a pooled analysis the rate of pCR was 22% for no invasive tumour in breast only, 18% for no invasive tumour in breast and axilla, and only 13% for no invasive tumour or DCIS in the breast and no disease in the axilla (1). Early clinical trials considered pCR in the breast only, however up to 4% of patients who have a pCR in the breast will have residual disease in the axilla (72). Residual disease in the axilla, including the presence of isolated tumour cells (ITCs) and micrometastases, is associated with worse survival outcomes independent of tumour response in the breast. Several series have shown number of involved nodes and size of largest metastasis post NACT to be the strongest determinants of overall survival (72-74). Hence, currently accepted definitions of pCR require absence of residual disease in the axilla also. Importantly, whilst ITCs are staged as ypN0(i+), their presence indicates treatment resistant residual disease and is not regarded as pCR (19).

Whether the presence of residual DCIS should be considered pCR is controversial. A pooled analysis found no difference in survival outcome with residual DCIS alone (1), however in a cumulative analysis of their trials the German Breast Group found residual DCIS was associated with worse DFS but not OS (7). This may be due to increased local recurrence risk with incompletely excised DCIS, although a differential response in DCIS and invasive components has been reported in HER2+ disease (75). The histopathology report should include a comment on the presence of residual DCIS in the breast regardless of the definition of pCR used, along with measurement of its extent and proximity to margins as per the minimum dataset in the adjuvant setting.

A rare but challenging scenario with respect to staging is the presence of lymphovascular invasion (LVI) in the absence of a residual invasive tumour focus. Firstly, ensure that the tumour bed has been adequately sampled and invasive tumour has not been missed. An alternative possibility is invasive disease or DCIS with retraction artefact; immunostaining for a lymphatic marker such as D2-40 (podoplanin) may be helpful in distinguishing the two (Figure 2) (70). When presence of residual LVI alone is confirmed, although this is strictly staged as ypN0, it should not be regarded as pCR, similar to the scenario with ITCs above. If the area of LVI is localised, the LVI itself can be measured and cellularity assessed to quantify residual disease and calculate the RCB. This pattern of residual disease has been associated with poor survival outcomes in small series (76, 77), although one slightly larger study suggested that pre and post treatment nodal involvement are also important (78).

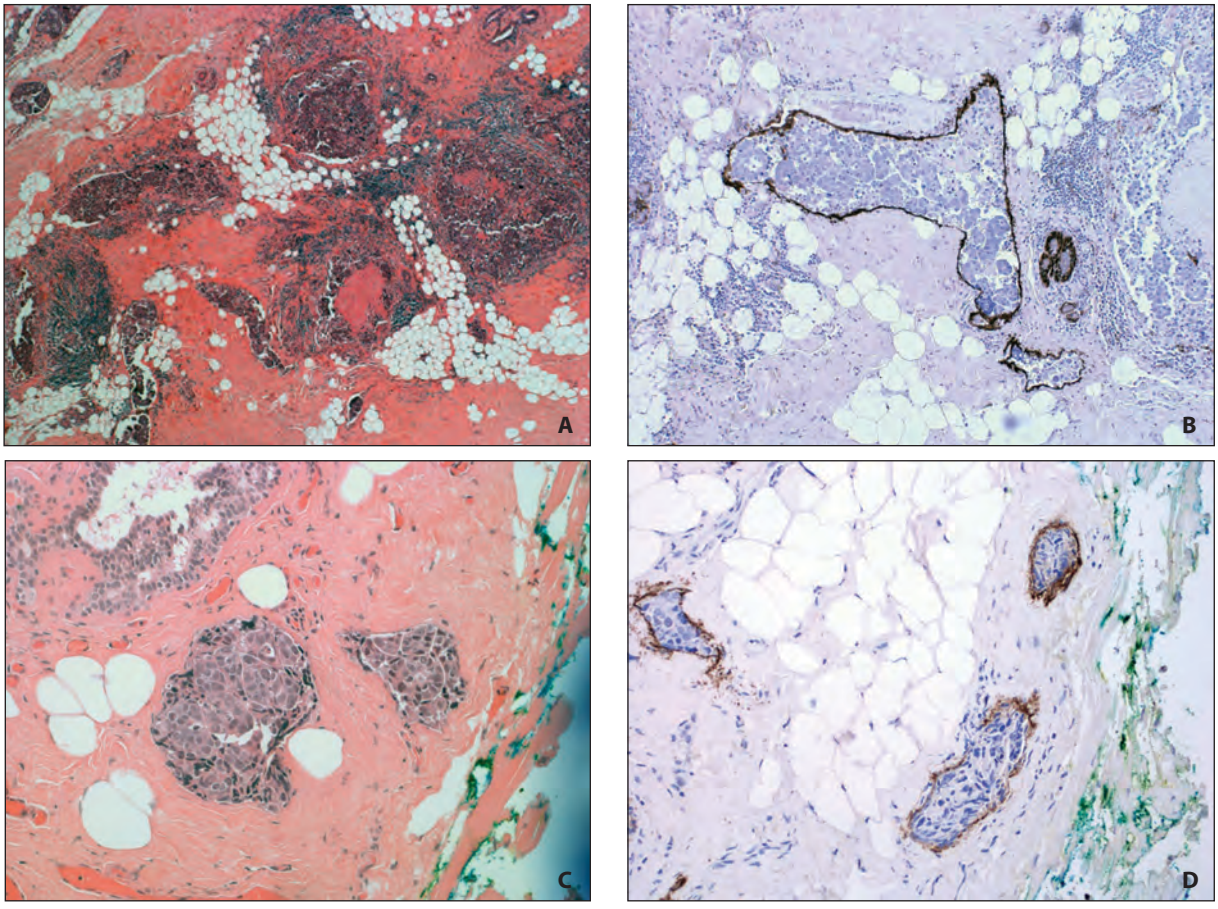

Figure 2. Residual invasive carcinoma predominantly in the form of LVI (A); D2-40 immunohistochemical staining distinguishing tumour in lymphatic spaces from invasive disease (B); Tumour adjacent to a margin confirmed as LVI on D2-40 staining (C+D).

TNM Staging

Traditional staging systems, such as the TNM and Nottingham Prognostic Index (NPI), retain prognostic significance following NACT (16, 79). Pathological TNM staging post NACT is given a y prefix. There have been modifications to how primary invasive tumour and metastases are measured for staging purposes in the 7th and 8th editions (18, 19), which are summarised in Table 1. Although only currently applied following primary surgery, there is emerging evidence that the AJCC prognostic stage incorporating grade and receptor status introduced in the 8th edition is also predictive of outcome post NACT and may provide better discrimination of prognostic groups (17, 80). Future staging systems incorporating both molecular tumour characteristics and tumour response are required.

There are two main patterns of response seen on serial imaging in patients receiving NACT (81, 82). The first is concentric shrinking, where there is a single tumour mass that progressively decreases in size. Measurement of tumour size in this situation is relatively straight forward as there is a single invasive tumour focus. Tumour bed changes may extend beyond the invasive carcinoma, however it is the maximum residual invasive cancer size that is measured; surrounding stroma without invasive tumour is excluded (Figure 3) (66, 70, 71).

The second pattern is the scatter or Swiss cheese pattern, where there is a patchy response with scattered foci of residual enhancement across the tumour bed. This pattern is a reflection of in-

Table 1. Definitions Used for Primary Tumour and Metastasis Measurement in Residual Cancer Burden and Subsequent Editions of the TNM Staging System

Staging system	Size measurement breast	Size measurement nodal metastases
Residual Cancer Burden	Maximum size residual invasive disease in two dimensions. Scattered foci measured as a single lesion including areas of intervening fibrosis.	Maximum dimension metastatic focus including associated fibrosis. ITCs regarded as positive.
AJCC/ UICC 6th edition	Maximum size residual invasive disease in one dimension. Scattered foci measured as a single lesion including areas of intervening fibrosis.	Maximum dimension metastatic focus including associated fibrosis. ITCs regarded as negative.
AJCC/ UICC 7th edition	Measurement largest contiguous tumour focus, with use of (m) classifier if multiple deposits present across the tumour bed	Maximum dimension size of metastatic focus including associated fibrosis. ITCs regarded as negative.
AJCC/ UICC 8th edition	Measurement largest contiguous tumour focus, with use of (m) classifier if multiple deposits present across the tumour bed	Maximum dimension of largest contiguous tumour cell deposit excluding associated fibrosis. ITCs regarded as negative.

ITCs=Isolated tumour cells.

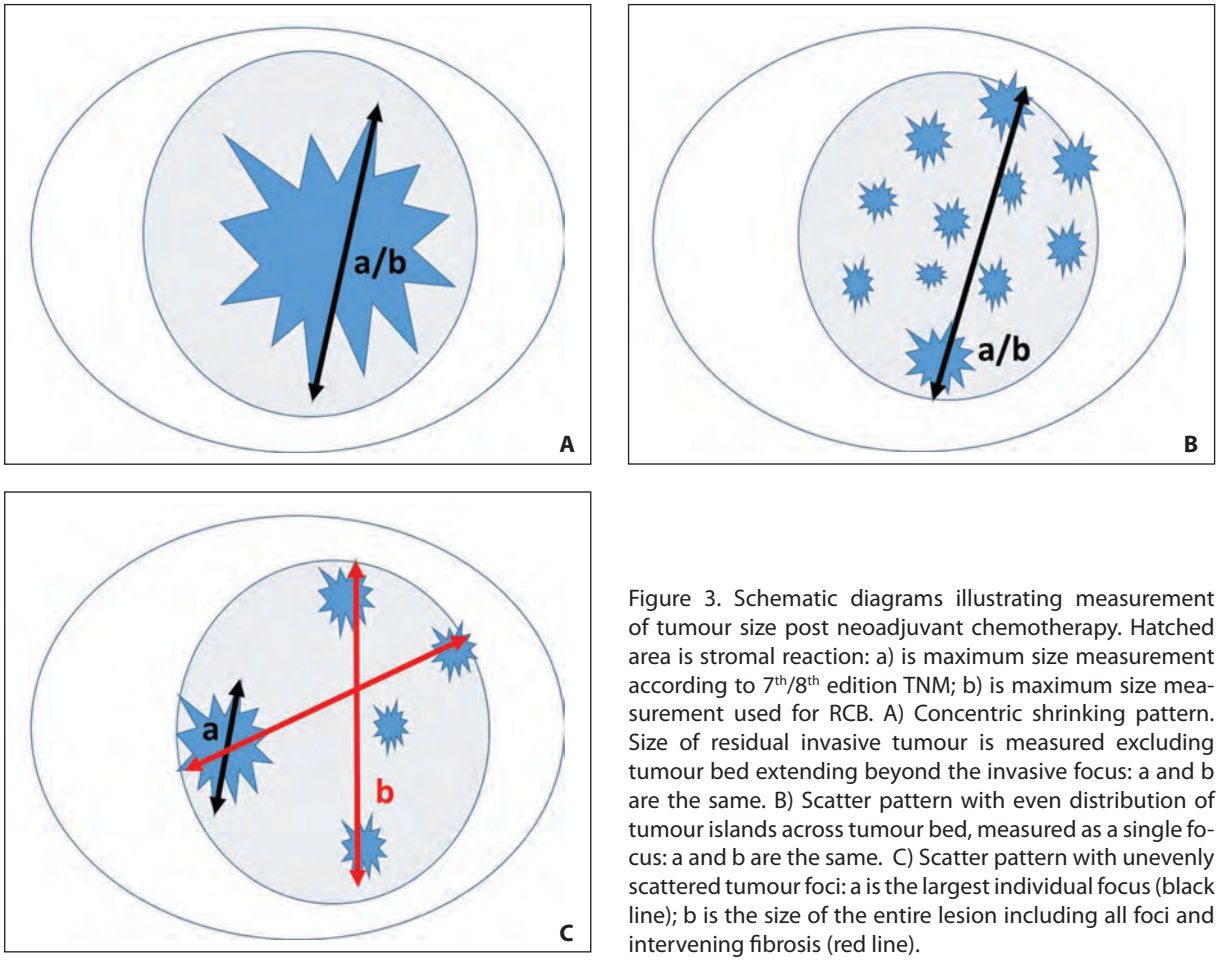

Figure 3. Schematic diagrams illustrating measurement of tumour size post neoadjuvant chemotherapy. Hatched area is stromal reaction: a) is maximum size measurement according to 7th/8th edition TNM; b) is maximum size measurement used for RCB. A) Concentric shrinking pattern. Size of residual invasive tumour is measured excluding tumour bed extending beyond the invasive focus: a and b are the same. B) Scatter pattern with even distribution of tumour islands across tumour bed, measured as a single focus: a and b are the same. C) Scatter pattern with unevenly scattered tumour foci: a is the largest individual focus (black line); b is the size of the entire lesion including all foci and intervening fibrosis (red line).

tratumoural heterogeneity leading to a differential response to NACT. At the histological level, this is seen as separate nests and islands of tumour cells dispersed within an ill-defined background of reactive fibrous stroma (Figure 4).

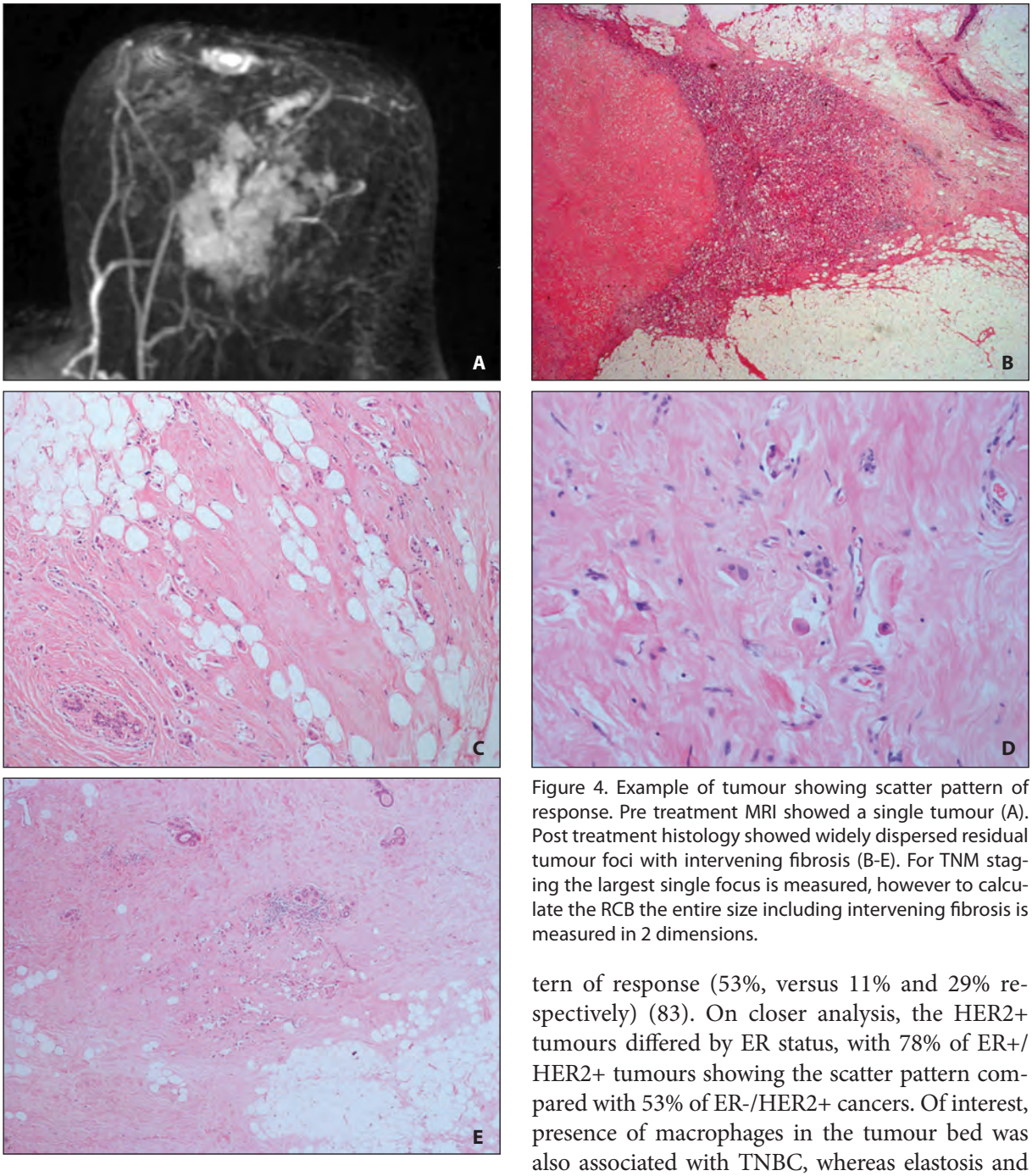

Figure 4. Example of tumour showing scatter pattern of response. Pre treatment MRI showed a single tumour (A). Post treatment histology showed widely dispersed residual tumour foci with intervening fibrosis (B-E). For TNM staging the largest single focus is measured, however to calculate the RCB the entire size including intervening fibrosis is measured in 2 dimensions.

Perhaps unsurprisingly, the pattern of response has been shown to correlate with molecular subtype. In one series looking at histological findings, TNBC was more likely to show the concentric shrinking pattern, whilst ER+/HER2- and HER2+ tumours more commonly showed the scatter pattern of response (53%, versus 11% and 29% respectively) (83). On closer analysis, the HER2+ tumours differed by ER status, with 78% of ER+/HER2+ tumours showing the scatter pattern compared with 53% of ER-/HER2+ cancers. Of interest, presence of macrophages in the tumour bed was also associated with TNBC, whereas elastosis and myxoid change was more common in ER+/HER2- cancers. In contrast, the study of Ballesio et al looked solely at MRI patterns of response and found that ER-/HER2+ showed a concentric pattern, whilst TNBC showed a multinodular pattern (82).

The scatter pattern has been associated with a higher locoregional recurrence (LRR) rate post

breast conservation surgery and increased risk of positive margins. Standard definitions of clear margins as 'tumour at ink' are likely to be inadequate in this context, and if residual invasive tumour lies in close proximity to the margin with transection of the tumour bed consideration should be given to re excision (2). The MD Anderson group identified four features associated with increased risk of LRR post NACT; clinical nodal stage 2/3, residual invasive tumour size >2 cm, scatter/ multifocal pattern of residual disease and presence of LVI (84). A recent study found no difference in LRR rates between a margin <1 mm and wider margins of excision, although numbers were too small for meaningful subset analyses (85). When assessing margin status in BCS specimens post NACT, it is important to comment on the presence of tumour bed at the inked margin, however this is not an indication for further surgery in the absence of invasive tumour or DCIS. When the clip site/ tumour bed is located centrally within the specimen and has been well sampled, then excision is most likely adequate even if tumour bed extends to margins. However, if the clip site/ tumour bed lies at the edge of the specimen this should be noted in the histopathology report, and multidisciplinary discussion is needed to determine if the tumour bed has been accurately targeted and adequately sampled.

Accurate determination of lesion size can be particularly challenging with the scatter pattern, and this is further complicated as the TNM and various national and international guidelines differ in their approach to what is measured (70, 86). The original approach was applied in TNM 6th edition (20). Where there is a single lesion present on pre-treatment imaging and the tumour cells are present within a reactive stromal tumour bed, then the residual disease is treated as a single tumour with the maximum extent being the area involved by all the residual islands of tumour cells including intervening stroma; i.e. residual islands of tumour cells, although separated, are treated as a single lesion and measured together (Figure 3, Table 1). As above, tumour bed beyond the residual invasive foci is not included. This is the tumour size measurement used to calculate the RCB, and adopted by the U.K. Royal College of Pathologists (87, 88), and has been shown to correlate with survival (16).

The method of size measurement was amended in 7th edition TNM, whereby if the residual tumour consists of multiple nests in a fibrotic stroma, the largest contiguous focus of invasive carcinoma is measured and used for ypT staging, with the 'm' modifier to indicate multiple tumour foci are present (18, 19). So in simple terms, the largest single tumour focus is measured and this is used for TNM staging; other foci and the associated stromal background are NOT included. Confusion arises in what precisely is meant by a 'contiguous focus', and an element of practical judgement is required. My approach is to look at the way the residual disease is distributed across the tumour bed; if there are discrete foci situated some distance from each other, I regard them as separate foci and measure them individually. If the tumour foci are distributed relatively evenly across the tumour bed, then I measure it as a single large focus (Figure 3). For this situation, a more detailed descriptive report including both measurements is often best; for example 'Residual invasive carcinoma is present as scattered islands of cells extending across a tumour bed 52 mm by 36 mm, the largest single focus measuring 16 mm in maximum dimension'. This scenario would have a T classification of ypT1b(m). When there were multiple tumours present on pre-treatment imaging, the residual tumour foci are separated by intervening normal breast tissue, or are morphologically distinct with different grade and/ or histological subtype, then they should be regarded as distinct tumour foci and measured independently. Response should be assessed separately for each focus.

Evaluation of nodal metastases can also be more complex post NACT. The number of positive nodes, the size of the largest metastatic deposit measured microscopically and the presence of extracapsular extension should be reported. The presence of fibrosis or evidence of regressed metastatic disease should be documented; metastasis with complete regression has an intermediate prognosis to a true negative axilla, and an estimate of the number of positive nodes pre-treatment will

influence decisions to give adjuvant regional radiotherapy (70). If a node was clipped pre-treatment, then presence of the clip site should be documented and specific comment made as to presence of residual disease and treatment effect in the clipped node. As with the primary tumour, there is a lack of agreement in how to measure disease in this setting that generates confusion amongst pathologists. In the 6th and 7th edition TNM the approach was to measure the size of the entire area involved by metastatic tumour including intervening fibrosis (18, 20); as in the breast, this is the distance between tumour cells, and fibrous tissue extending beyond metastatic tumour cells is excluded. This is also the maximum metastasis size measurement used for calculating the RCB, and has been associated with survival (71, 72, 74). The 8th edition TNM has changed the method of measuring metastases to the size of the largest contiguous focus in the node not including tumour associated fibrosis (19). According to the definition in adjuvant disease, a contiguous focus is tumour cells directly in contact with one another without intervening lymphocytes. When there has been good response to NACT, residual metastatic disease is often present as scattered single cells within a reactive fibrous background and this is now defined as ITCs under the 8th edition (Figure 5). This could potentially downstage nodal involvement in a significant number of patients, and again an element of clinical judgement is required. My personal approach, as with the primary tumour, is to look at

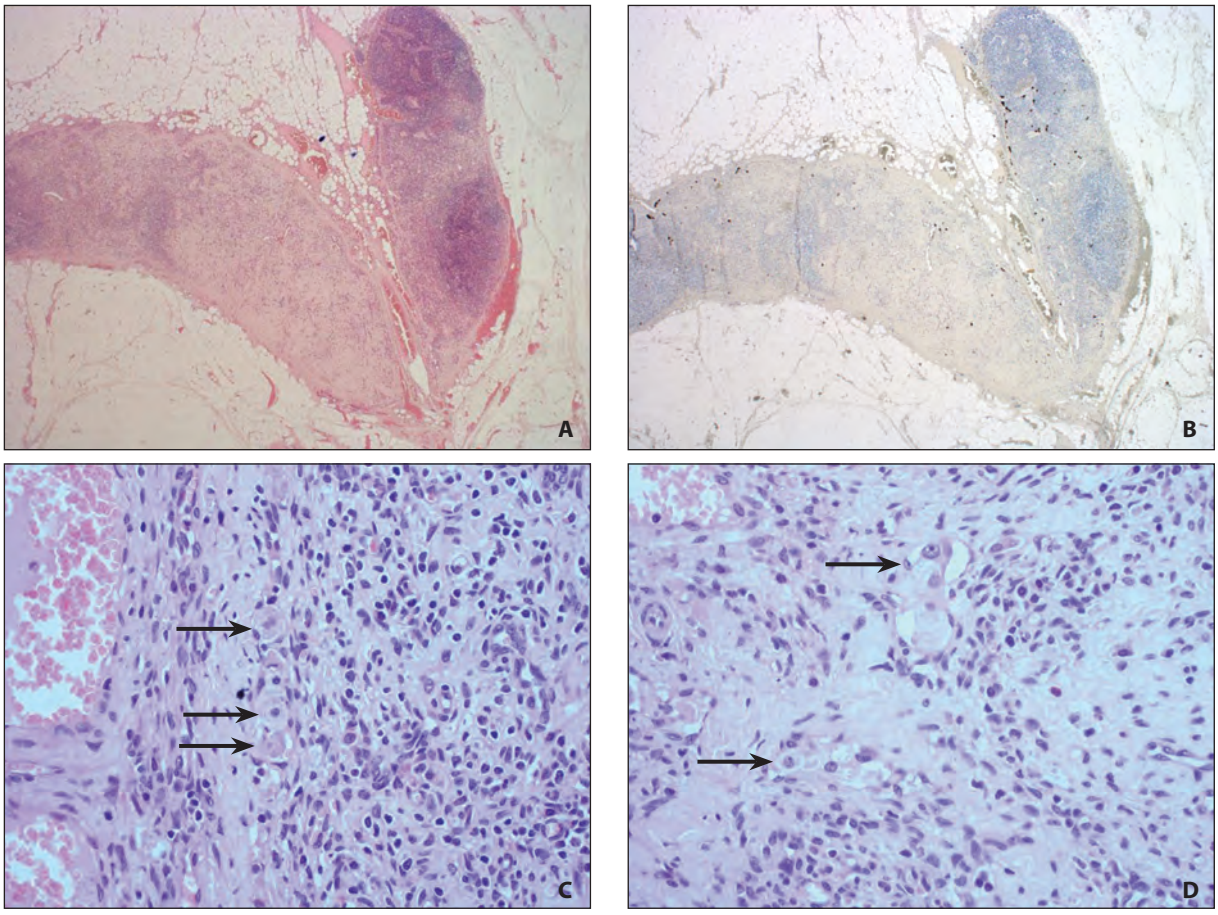

Figure 5. Lymph node post chemotherapy showing an area of fibrosis containing scattered single cells and small clusters, classified as isolated tumour cells in the 8th edition TNM: A) Low power H&E showing area of fibrosis; B) Low power cytokeratin stain highlighting distribution of residual tumour cells; C-D) Higher power images of residual tumour cells (bold arrows) on H&E (×40 magnification).

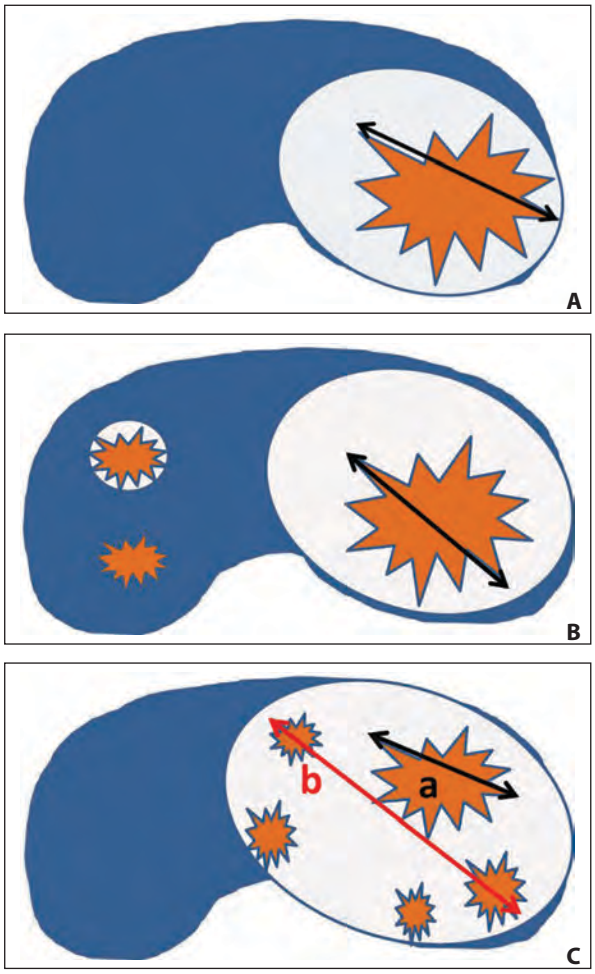

Figure 6. Schematic diagram illustrating measurement of metastases post neoadjuvant chemotherapy. Hatched area represents associated fibrosis. A) Single metastatic focus within area of fibrosis. Measure extent of tumour only, not background fibrosis extending beyond tumour. B) If multiple separate foci of tumour, with or without fibrosis, them measure the largest single focus. C) Scattered metastatic foci in a single area of fibrosis: a) size of largest single contiguous cluster of cells excluding background fibrosis used for TNM staging (black line); b) maximum size including all foci and intervening fibrosis (red line) used to calculate the RCB.

the pattern of spread of the tumour cells across the metastatic deposit; if they form discrete foci a distance apart then these should be measured individually, however if they are evenly dispersed cells/foci across the area of fibrosis I measure the entire lesion as a single deposit (Figure 6).

The interpretation of ITCs is a particular source of controversy in the neoadjuvant setting (70). ITCs are handled the same way as in the adjuvant setting in the TNM Staging System and are classed as node negative [ypN0(i+)] (19), whereas in the UK reporting guidelines nodes containing ITCs should be counted as positive (87). Regardless of whether they are considered positive or negative, ITCs post NACT represent tumour cells that have persisted despite systemic therapy and have different significance to the adjuvant setting and it is agreed they should not be regarded as axillary pCR. There is considerable evidence that the presence of any residual tumour cells in the axillary lymph nodes following NACT, even in the form of ITCs, is associated with worse prognosis (72-74). In a recent series examining a US National Cancer Database (NCD) cohort, ITCs were associated with poorer survival outcomes with 83% 5 year OS compared with 89% for ypN0; this was present in patients that were cN0 and cN1 pre-treatment (66% and 81% increase in mortality respectively), with the greatest impact on TNBC (89).

Assessing Response

Whilst early clinical trials showed a drop in proportion of cases classified as pCR following central histology review compared with local reports (90), our own experience with the ARTEMIS trial showed excellent agreement between source laboratory reports and central review with respect to pCR (91). However, in an audit of local pathology reports as part of the trial, only 45% of reports included an assessment of tumour response in the breast, dropping to 30% for response in the axillary lymph nodes (92). A similar review of external pathology reports is being undertaken as part of the UK multicentre PARTNER trial, and whilst most reports now include a general comment on presence or absence of response in both the primary tumour and axillary nodes, the majority still do not incorporate formal grading of response (unpublished data).

There are two main approaches to assessment of residual disease post NACT. The first examines actual response by comparing tumour cellularity before and after treatment. Response to NACT is

often accompanied by a reduction in tumour cellularity, and this is associated with improved survival outcomes. Comparison between pre and post treatment cellularity forms the basis for several grading systems of response, including the Chevallier, Sataloff, Miller-Payne and Pinder systems (93-96). The second approach is quantification of residual disease post NACT by looking at invasive tumour size and cellularity, the main example of which is the RCB proposed by Symmans et al. (71). Newer systems such as the Neo-Bioscore have been developed that incorporate tumour molecular profile and biomarkers such as Ki67, although these are currently not in widespread use (60, 97, 98). The different systems have advantages and disadvantages and at present there is no one universally agreed system; readers are referred to review articles comparing the different systems (99-101). The important thing for pathologists is to work closely with their oncology colleagues to agree which system to use.

Residual Cancer Burden

The RCB is presently the most widely used system and will be described in more detail; it has been well validated, is simple and reproducible (91, 102, 103), and shows a strong association with survival outcomes across all molecular subtypes. As a result the RCB has been incorporated in the soon to be released International Collaboration on Cancer Reporting (ICCR) minimum dataset for breast pathology reporting post NACT. The RCB website provides detailed instructions on how to assess the RCB score, including macroscopic specimen handling, a visual guide to estimating the percentage of residual tumour cells, and an online calculator that provides both the numerical RCB score and RCB class (88).

The RCB incorporates four variables; maximum invasive tumour size measured in two dimensions, average residual invasive tumour cellularity, number of positive lymph nodes and size of largest metastasis. There are several important things to note when making measurements for the RCB. The website refers to primary tumour bed area; 'tumour bed area' refers to the size of the residual invasive cancer, i.e. the greatest distance between invasive tumour cell foci (Figure 3). Background stromal changes such as reactive fibrosis or DCIS that extends outside the limit of the invasive tumour are not included. It is not necessary to measure the area of stromal change, just the dimensions of the residual invasive disease. Second, the invasive tumour dimension for the RCB includes intervening background stroma, i.e. include fibrosis between invasive tumour cell foci. If there are scattered islands of tumour cells across the tumour bed you measure the total size across all the islands as a single lesion, unless there are multiple separate primary tumours. This is different to the size measurement for TNM staging from the 7th edition onwards, described above (Table 1, Figure 3). Similarly, when evaluating cellularity, the entire tumour area including intervening fields with no tumour should be assessed to calculate the average, not just fields that contain tumour cells.

There are similar caveats in evaluating the nodal disease. The total nodal count includes all nodes that contain tumour cells including nodes with ITCs only, although these are not regarded as positive nodes for TNM staging. As with invasive tumour, the size of the largest metastasis is the greatest distance between tumour cells within a lymph node including background reactive fibrosis between metastatic tumour cell islands, but not fibrosis that extends outside the metastasis. Again, this is different to how metastases are measured according to the 8th edition of the TNM (Table 1, Figure 6)

These values are combined in an algorithm available online that calculates a continuous numerical score, and places residual tumour in 3 classes with class I representing MRD and class III extensive residual disease. Although class I correlates with excellent response and class III with poor response, this system is not strictly a measure of response as cellularity in this case is absolute cellularity post treatment rather than the change in cellularity. Indeed low cellularity post-treatment does not necessarily equate with response as some cancers, e.g. lobular cancers, are hypocellu-

lar to begin with. Cellularity is heavily weighted in the algorithm, so small tumours with a high cellularity will often end up as RCB II, whereas larger tumours with low cellularity can still be RCB I.

As mentioned, both RCB class and the RCB score as a continuous variable show an association with survival outcomes across all molecular subtypes, although the nature of the relationship varies by subtypes (14). Early data suggested for TNBC, patients that achieve RCB I have an excellent prognosis similar to that of pCR. A more recent multicentre pooled analysis with larger numbers has shown a linear relationship between RCB and BCSS, with a small but significant difference between pCR and RCB I (15). In contrast, for ER-/HER2+ patients the curve has a slightly different shape with a steeper rise at low levels of residual disease that plateaus out across higher RCB scores suggesting even small volumes of residual disease has an adverse prognosis for this subtype. ER+/HER2- cancers had the opposite profile with the curve rising slowly across low volumes of residual disease and a steeper rise beginning in RCB II. The relationship between residual disease and survival in ER+/HER2- cancers has been a source of controversy, with these tumours having a relatively favourable prognosis despite low pCR rates and a poorer correlation between residual disease and survival outcomes; this data confirms the prognostic relevance of RCB for this subtype, and molecular type-specific RCB class cut-offs could improve clinical accuracy. This highlights the importance in considering molecular subtype when assessing residual disease, and the future need for a combined system including anatomical residual disease extent and tumour biological characteristics.

Whilst ypAJCC and RCB staging both provide a quantitative assessment of residual disease and show an association with survival outcomes, an analysis of cases from the I-SPY-1 trial showed a discrepancy in classification in up to one third of cases using 7th edition TNM (104). Of 55 discrepant cases, 36 had a higher RCB class, and 19 had a higher ypAJCC stage. The source of discrepancy was weighting of lymph node involvement and tumour cellularity in the RCB. For example, a small tumour with high cellularity will be low AJCC stage but RCB class II, and conversely a large tumour with low cellularity will have a higher stage but a relatively low RCB score. For discrepant cases, if residual disease was RCB or ypAJCC stage 3 there was a poor outcome suggesting the two systems are complementary.

Management of the Axilla

In patients that are axillary node negative pretreatment, the safety and accuracy of SLNB post NACT has now been established in several large series with identification (IR) and false negative rates (FNR) comparable to the adjuvant setting. A meta-analysis found IR of 93-97%, a FNR of 6% and axillary recurrence rates of 2% (105). In patients with proven positive axillary lymph nodes pre-NACT surgical management of the axilla is still subject to debate. Early series showed huge variation in results, with one meta-analysis finding an IR of 68-100% with a pooled FNR of 11%, although the FNR was as high as 33% in individual studies (106). However, the reliability of SLNB in node positive patients has now been examined in several prospective clinical trials, and with better patient selection and the evolution of targeted axillary sampling techniques is yielding more promising results.

Early evidence came from the NSABP-B27 trial, where a subset of 428 patients underwent SLNB followed by ALND; the SLN was positive in 36%, and in 56% was the only positive node (107). The FNR was 12% for patients that were cN1-2, and in patients with breast pCR this fell to 2%. Subsequently, the ACOSOG Z1071 trial specifically addressed the question of post NACT SLNB in patients with biopsy proven axillary metastases with no prior axillary surgery (108). Patients underwent SLNB followed by completion ALND; the overall nodal pCR rate was 41%, rising to 49% in TNBC and 65% for HER2+ disease, and in 21% residual nodal disease was confined to the SLN. The overall FNR was 12.6% which fell short of the study target of 10%, however if dual mapping with blue dye and radioisotope was used the FNR fell

to 11%, and if 3 or more nodes were sampled the FNR was only 9% compared with 21% for 2 nodes and 31% if one node was removed. The SN FNAC study looked at SLNB in node positive patients, with immunohistochemistry (IHC) undertaken on all negative nodes; the FNR was 13%, which fell to 8% when nodes with ITCs were regarded as positive (109). A subset analysis of Z1071 utilizing IHC found a similar FNR of 9%.

The Europe-based SENTINA study had a more complex design including both cN0 and cN1 disease. Patients that were cN1 proceeded directly to post NACT SLNB, with an IR of 80% and a FNR of 14%. cN0 patients had a pre chemotherapy SLNB, and if positive had a second attempt at SLNB post NACT with ALND (110). The second line SLNB had an IR of 60% and a FNR of 52%, showing repeat SLNB has a poor success rate.

Within Z1071, a substudy of 170 patients examined the role of clipping the biopsied node and identifying the clip at the time of SLNB. The clip was present in a SLN in 76% of cases with a FNR of 7%, however in the remaining 24% where the clip was in a non-SLN the FNR was 19% (111). In 41% the clipped node was the only positive node. This has led to the evolution of targeted axillary sampling techniques, where the biopsied node is clipped or otherwise labelled and localised at the time of surgery and/ or at least 3 SLN are removed following dual localisation, achieving acceptably low FNR.

In a series of 12 patients, Caudle et al. clipped the positive biopsied node then placed a radioactive 125I seed before surgery to localise the clipped node; five underwent SLN, which included the clipped node in 4 patients (112). A total of 9 patients including the SLN group had an ALND; 4 had residual metastatic disease and the clipped node was positive in all cases. In a larger follow up series, removing the clipped node gave a FNR of 4%, which fell to 2% when combined with SLNB (113). In a similar approach, a Dutch group used 125I seed to label the positive node at the time of diagnosis, termed the MARI procedure (Marking the Axillary lymph node with Radioactive I) then removed the labelled node alone with a FNR of 7% (114).

The Mayo Clinic group reported 38 SLNB after clipping the biopsied node; 25 had a 125I seed placed in the clipped node, 9 had no preoperative localisation of the clip, and 4 had no documentation (115). In the 25 patients with the 125I seed, the labelled node was successfully identified preoperatively in 20; in the remaining 14 where the seed was not localised or localisation was not attempted, the clipped node was found in 11. Overall, the IR for the clip was 78% with a FNR of 3%. The same group had trialled using HydroMARK gel clips to mark the biopsied node but found these were no longer visible following NACT, however in the Spanish ILINA trial placement of HydroMARK clips with intraoperative US successfully localised the clipped node in 96% of cases, with a 4% FNR when combined with SLNB; in all cases the clipped node was positive except one false negative case where both clipped node and SLN were negative (116).

In a separate single institution series of 630 cN1 patients without clipping of the positive node, 91% converted to cN0 post NACT and proceeded to SLNB (117, 118). Three or more SLNs were mapped in 93% of cases, regarded as adequate mapping, with 7% having less than 3 nodes identified and complete failure in 2%. Unsuccessful mapping was associated with high body mass index and presence of LVI. In patients with successful mapping, 41% had nodal pCR and were able to avoid ALND, by molecular subtype 20% of HR+/HER2-, 44% of TNBC, 55% of HR+/HER2+ and 78% of HR-/HER2+. Of note, 43% of patients with unsuccessful mapping also achieved an axillary pCR. Other predictors for avoiding ALND included ductal or apocrine histological subtype (44% and 50% versus 17% for lobular cancers), grade 3 cancers (54% versus 24% for grade 2 and 14% for grade 1) and absence of LVI (78% versus 22%). Grade 3, molecular subtype and presence of LVI remained significant predictors of ALND on multivariate analysis. This supports the conclusion from an earlier study that clipping the biopsied node is not required if there is thorough SLN technique with dual labelling and removal of 3 or more nodes at the time of SLNB (119).

The ISPY-2 trial group have published guidance on surgical management of the axilla for use in clinical trials that is generalizable to routine practice (3). For cN0 patients, SLN with removal of at least 2 nodes is advised. For proven node positive patients, the biopsied node should be marked at the time of diagnosis with SLN or ALND after completion of NACT. Where SLN is performed, dual tracer mapping of the SLN is required with identification and removal of the clipped node. If the node was not clipped, a minimum of 2 SLNs must be removed. If the SLN is positive ALND is advised but not mandated; however, if RCB calculation is part of the trial then completion ALND is needed to determine the RCB score. In multidisciplinary UK guidelines, in patients with a positive axilla SLN may be considered post NACT but dual mapping with removal of four nodes is advised (120). If any residual disease including ITCs is identified then ALND is recommended.

Of note, a recent review of the US NCD has shown an increase in adoption of SLNB for cN+ patients post NACT from 32% in 2012 to 49% in 2015, with SLNB more frequent in younger patients, TNBC or HER2+ disease, and following BCS (5). Of concern, follow up ALND was not performed for 37% of patients with ITCs (21% in 2012 increasing to 49% in 2015), 24% with micrometastases (19% in 2012 to 31% in 2015) and 13% with ypN1 macrometastases. This is despite clinical guidelines recommending ALND for any residual nodal disease including ITCs post NACT due to a lack of clinical evidence on safety of omission of ALND. Studies post NACT show higher FNR with additional non-SLN positivity in 17% of cases with ITCs, 64% with micrometastases and 62% with macrometastases (121). There is evidence showing worse DFS for ypN0(i+) and ypN1(mic) (1.9 and 2.2 times increased mortality respectively); this was true for both cN0 and cN1 disease, with the greatest impact of low volume residual nodal disease in TNBC and HER2+ cancers (89). Using NCD data, Almahariq et al. showed inferior survival outcomes in ypN1 patients that underwent SLNB alone with regional nodal irradiation, with 71% 5 year OS compared with 77% in those that had ALND (122). There is still limited data on LRR rates in patients who achieve axillary pCR post NACT. The study of Pitilin et al. found 17 LRR in 602 patients after 34 months of follow up, 3 in patients that were ypN0; of interest none of the 9 patients with ITCs had a LRR (123).

Results of two ongoing clinical trials are awaited. The NSABP B-51/RTOG 1304 trial is looking at the oncological safety of SLNB alone in node positive patients that revert to node negative post NACT, and is randomising patients to regional nodal irradiation versus no further axillary therapy. In contrast, the Alliance 11202 trial will examine the group of women with positive SLNB post NACT and randomise them to nodal radiotherapy versus ALND. Of note, both trials regard women with ITCs as node negative so will not provide direct evidence as to the need for further axillary therapy in this important subset of patients.

A rare clinical scenario is presentation with axillary nodal disease and no identifiable primary breast tumour. A recent study looking at 28 women with occult primary breast cancer found a pCR rate of 80%, 93% in those with cN1 disease, suggesting that SLN alone post NACT may be an option for these patients (124). Interestingly, looking at the molecular subtypes the pCR rate was 50% in ER+/HER2- tumours, 88% for TNBC and 100% for HER2+ disease, higher than for women with an identifiable breast primary in most series. One proposed theory is this represents a subset of tumours that invoke a strong immune response with regression of the primary disease, and immune therapies may be a future treatment option for these patients.

Conclusion

In conclusion, NACT is now routine breast cancer management. Assessment of response is becoming increasingly important in adjuvant therapy decisions, and more than ever the pathologist plays a vital role in patient care. Management of the axilla remains controversial but there is growing evidence supporting the safety of SLNB in previously node positive patients, however even minimal re-

sidual nodal involvement in the form of ITCs and micrometastases has adverse prognostic significance and clinical evidence for the safety of omitting ALND in these patients is currently lacking.

Conflict of Interest: The author declares that she has no conflict of interest.

Acknowledgement: This research was supported by the NIHR Cambridge Biomedical Research Centre (BRC-1215-20014). The views expressed are those of the authors and not necessarily those of the NIHR or the Department of Health and Social Care

References

1. Cortazar P, Zhang L, Untch M, Mehta K, Costantino JP, Wolmark N, et al. Pathological complete response and long-term clinical benefit in breast cancer: the CTNeoBC pooled analysis. Lancet. 2014;384(9938):164-72.
2. King TA, Morrow M. Surgical issues in patients with breast cancer receiving neoadjuvant chemotherapy. Nat Rev Clin Oncol. 2015;12(6):335-43.
3. Boughey JC, Alvarado MD, Lancaster RB, Fraser Symmans W, Mukhtar R, Wong JM, et al. Surgical Standards for Management of the Axilla in Breast Cancer Clinical Trials with Pathological Complete Response Endpoint. NPJ Breast Cancer. 2018;4:26.
4. Morrow M, Dang CT. Sentinel node biopsy after neoadjuvant chemotherapy: a new standard for patients with axillary metastases? JAMA. 2013;310(14):1449-50.
5. Wong SM, Weiss A, Mittendorf EA, King TA, Golshan M. Surgical Management of the Axilla in Clinically Node-Positive Patients Receiving Neoadjuvant Chemotherapy: A National Cancer Database Analysis. Ann Surg Oncol. 2019;26(11):3517-25.
6. Pelizzari G, Gerratana L, Basile D, Fanotto V, Bartoletti M, Liguori A, et al. Post-neoadjuvant strategies in breast cancer: From risk assessment to treatment escalation. Cancer Treat Rev. 2019;72:7-14.
7. von Minckwitz G, Untch M, Blohmer JU, Costa SD, Eidtmann H, Fasching PA, et al. Definition and impact of pathologic complete response on prognosis after neoadjuvant chemotherapy in various intrinsic breast cancer subtypes. J Clin Oncol. 2012;30(15):1796-804.
8. U.S. Food and Drug Administration. Guidance for Industry: Pathological Complete Response in Neoadjuvant Treatment of High-Risk Early-Stage Breast Cancer: Use as an Endpoint to Support Accelerated Approval. [cited 2020 Dec 26] Available from: http://www.fda.gov/downloads/Drugs/GuidanceComplianceRegulatoryInformation/Guidances/UCM305501.pdf2014. Add a date of citation in the red parentheses
9. Barker AD, Sigman CC, Kelloff GJ, Hylton NM, Berry DA, Esserman LJ. I-SPY 2: an adaptive breast cancer trial design in the setting of neoadjuvant chemotherapy. Clin Pharmacol Ther. 2009;86(1):97-100.
10. Esserman LJ, Woodcock J. Accelerating identification and regulatory approval of investigational cancer drugs. JAMA. 2011;306(23):2608-9.
11. File D, Curigliano G, Carey LA. Escalating and De-escalating Therapy for Early-Stage HER2-Positive Breast Cancer. Am Soc Clin Oncol Educ Book. 2020;40:1-11.
12. Masuda N, Lee SJ, Ohtani S, Im YH, Lee ES, Yokota I, et al. Adjuvant Capecitabine for Breast Cancer after Preoperative Chemotherapy. N Engl J Med. 2017;376(22):2147-59.
13. von Minckwitz G, Huang CS, Mano MS, Loibl S, Mamounas EP, Untch M, et al. Trastuzumab Emtansine for Residual Invasive HER2-Positive Breast Cancer. N Engl J Med. 2019;380(7):617-28.
14. Symmans WF, Wei C, Gould R, Yu X, Zhang Y, Liu M, et al. Long-Term Prognostic Risk After Neoadjuvant Chemotherapy Associated With Residual Cancer Burden and Breast Cancer Subtype. J Clin Oncol. 2017;35(10):1049-60.
15. Yau C, Van der Noordaa M, Wei J, Osdoit M, Reyal F, Hamy AS, et al. Residual cancer burden after neoadjuvant therapy and long-term survival outcomes in breast cancer: A multi-center pooled analysis. Cancer Res. 2020;80(4 Suppl):GS5-01. doi: 10.1158/1538-7445.SABCS19-GS5-01.
16. Carey LA, Metzger R, Dees EC, Collichio F, Sartor CI, Ollila DW, et al. American Joint Committee on Cancer tumor-node-metastasis stage after neoadjuvant chemotherapy and breast cancer outcome. J Natl Cancer Inst. 2005;97(15):1137-42.
17. Kantor O, Bao J, Jaskowiak N, Yao K, Tseng J. The Prognostic Value of the AJCC 8th Edition Staging System for Patients Undergoing Neoadjuvant Chemotherapy for Breast Cancer. Ann Surg Oncol. 2020;27(2):352-8.
18. Edge SB, Byrd DR, Compton CC, Fritz AG, Greene FL, Trotti I, editors. Cancer Staging Handbook From the AJCC Cancer Staging Manual. 7th ed. New York: Springer-Verlag; 2010.
19. Hortobagyi GN, Connolly JL, D'Orsi CJ, Edge SB, Mittendorf EA, Rugo H, et al. Breast. AJCC Cancer Staging Manual. 8th ed. New York: Springer; 2017. p. 589-628.
20. Greene FL, Page DL, Fleming ID, Fritz AG, Balch CM, Haller DG, et al., editors. AJCC Cancer Staging Manual. 6th ed. New York: Springer; 2002.
21. Boughey JC, Ballman KV, McCall LM, Mittendorf EA, Symmans WF, Julian TB, et al. Tumor Biology and Response to Chemotherapy Impact Breast Cancer-specific Survival in Node-positive Breast Cancer Patients Treated With Neoadjuvant Chemotherapy: Long-term Follow-up From ACOSOG Z1071 (Alliance). Ann Surg. 2017;266(4):667-76.

22. Hayashi N, Takahashi Y, Matsuda N, Tsunoda H, Yoshida A, Suzuki K, et al. The Prognostic Effect of Changes in Tumor Stage and Nodal Status After Neoadjuvant Chemotherapy in Each Primary Breast Cancer Subtype. Clin Breast Cancer. 2018;18(2):e219-29.
23. Hieken TJ, Murphy BL, Boughey JC, Degnim AC, Glazebrook KN, Hoskin TL. Influence of Biologic Subtype of Inflammatory Breast Cancer on Response to Neoadjuvant Therapy and Cancer Outcomes. Clin Breast Cancer. 2018;18(4):e501-6.
24. Houssami N, Macaskill P, von Minckwitz G, Marinovich ML, Mamounas E. Meta-analysis of the association of breast cancer subtype and pathologic complete response to neoadjuvant chemotherapy. Eur J Cancer. 2012;48(18):3342-54.
25. Prat A, Fan C, Fernandez A, Hoadley KA, Martinello R, Vidal M, et al. Response and survival of breast cancer intrinsic subtypes following multi-agent neoadjuvant chemotherapy. BMC Med. 2015;13:303.
26. Foldi J, Mougalian S, Silber A, Lannin D, Killelea B, Chagpar A, et al. Single-arm, neoadjuvant, phase II trial of pertuzumab and trastuzumab administered concomitantly with weekly paclitaxel followed by 5-fluoruracil, epirubicin, and cyclophosphamide (FEC) for stage I-III HER2-positive breast cancer. Breast Cancer Res Treat. 2018;169(2):333-40.
27. Brandao M, Caparica R, Malorni L, Prat A, Carey LA, Piccart M. What Is the Real Impact of Estrogen Receptor Status on the Prognosis and Treatment of HER2-Positive Early Breast Cancer? Clin Cancer Res. 2020;26(12):2783-8.
28. Prat A, Carey LA, Adamo B, Vidal M, Tabernero J, Cortes J, et al. Molecular features and survival outcomes of the intrinsic subtypes within HER2-positive breast cancer. J Natl Cancer Inst. 2014;106(8):dju152.
29. Prat A, Bianchini G, Thomas M, Belousov A, Cheang MC, Koehler A, et al. Research-based PAM50 subtype predictor identifies higher responses and improved survival outcomes in HER2-positive breast cancer in the NOAH study. Clin Cancer Res. 2014;20(2):511-21.
30. Schettini F, Pascual T, Conte B, Chic N, Braso-Maristany F, Galvan P, et al. HER2-enriched subtype and pathological complete response in HER2-positive breast cancer: A systematic review and meta-analysis. Cancer Treat Rev. 2020;84:101965.
31. Pernas S, Tolaney SM. Targeting HER2 heterogeneity in early-stage breast cancer. Curr Opin Oncol. 2020;32(6):545-54.
32. Guiu S, Gauthier M, Coudert B, Bonnetain F, Favier L, Ladoire S, et al. Pathological complete response and survival according to the level of HER-2 amplification after trastuzumab-based neoadjuvant therapy for breast cancer. Br J Cancer. 2010;103(9):1335-42.
33. Wu Z, Xu S, Zhou L, Yin W, Lin Y, Du Y, et al. Clinical significance of quantitative HER2 gene amplification as related to its predictive value in breast cancer patients in neoadjuvant setting. Onco Targets Ther. 2018;11:801-8.
34. Bianchini G, Kiermaier A, Bianchi GV, Im YH, Pienkowski T, Liu MC, et al. Biomarker analysis of the NeoSphere study: pertuzumab, trastuzumab, and docetaxel versus trastuzumab plus docetaxel, pertuzumab plus trastuzumab, or pertuzumab plus docetaxel for the neoadjuvant treatment of HER2-positive breast cancer. Breast Cancer Res. 2017;19(1):16.
35. Krystel-Whittemore M, Xu J, Brogi E, Ventura K, Patil S, Ross DS, et al. Pathologic complete response rate according to HER2 detection methods in HER2-positive breast cancer treated with neoadjuvant systemic therapy. Breast Cancer Res Treat. 2019;177(1):61-6.
36. Akashi M, Yamaguchi R, Kusano H, Ogasawara S, Abe E, Obara H, et al. Androgen receptor expression is useful to predict the therapeutic effect in HER2-positive breast carcinoma. Breast Cancer Res Treat. 2020;184(2):277-85.
37. Sharma P, Connolly RM, Roussos Torres ET, Thompson A. Best Foot Forward: Neoadjuvant Systemic Therapy as Standard of Care in Triple-Negative and HER2-Positive Breast Cancer. Am Soc Clin Oncol Educ Book. 2020;40:1-16.
38. Lehmann BD, Jovanovic B, Chen X, Estrada MV, Johnson KN, Shyr Y, et al. Refinement of Triple-Negative Breast Cancer Molecular Subtypes: Implications for Neoadjuvant Chemotherapy Selection. PLoS One. 2016;11(6):e0157368.
39. Masuda H, Baggerly KA, Wang Y, Zhang Y, Gonzalez-Angulo AM, Meric-Bernstam F, et al. Differential response to neoadjuvant chemotherapy among 7 triple-negative breast cancer molecular subtypes. Clin Cancer Res. 2013;19(19):5533-40.
40. Lehmann BD, Pietenpol JA, Tan AR. Triple-negative breast cancer: molecular subtypes and new targets for therapy. Am Soc Clin Oncol Educ Book. 2015:e31-9.
41. Gao G, Wang Z, Qu X, Zhang Z. Prognostic value of tumor-infiltrating lymphocytes in patients with triple-negative breast cancer: a systematic review and meta-analysis. BMC Cancer. 2020;20(1):179.
42. Gonzalez-Martinez S, Perez-Mies B, Carretero-Barrio I, Palacios-Berraquero ML, Perez-Garcia J, Cortes J, et al. Molecular Features of Metaplastic Breast Carcinoma: An Infrequent Subtype of Triple Negative Breast Carcinoma. Cancers (Basel). 2020;12(7):1832.
43. Reddy TP, Rosato RR, Li X, Moulder S, Piwnica-Worms H, Chang JC. A comprehensive overview of metaplastic breast cancer: clinical features and molecular aberrations. Breast Cancer Res. 2020;22(1):121.
44. Al-Hilli Z, Choong G, Keeney MG, Visscher DW, Ingle JN, Goetz MP, et al. Metaplastic breast cancer has a poor response to neoadjuvant systemic therapy. Breast Cancer Res Treat. 2019;176(3):709-16.
45. Han M, Salamat A, Zhu L, Zhang H, Clark BZ, Dabbs DJ, et al. Metaplastic breast carcinoma: a clinical-pathologic

study of 97 cases with subset analysis of response to neoadjuvant chemotherapy. Mod Pathol. 2019;32(6):807-16.

46. Pareja F, Weigelt B, Reis-Filho JS. Problematic breast tumors reassessed in light of novel molecular data. Mod Pathol. Epub 2020 Oct 6.
47. Cheang MC, Martin M, Nielsen TO, Prat A, Voduc D, Rodriguez-Lescure A, et al. Defining breast cancer intrinsic subtypes by quantitative receptor expression. Oncologist. 2015;20(5):474-82.
48. Sorlie T, Perou CM, Tibshirani R, Aas T, Geisler S, Johnsen H, et al. Gene expression patterns of breast carcinomas distinguish tumor subclasses with clinical implications. Proc Natl Acad Sci U S A. 2001;98(19):10869-74.
49. Sparano JA, Gray RJ, Makower DF, Pritchard KI, Albain KS, Hayes DF, et al. Prospective Validation of a 21-Gene Expression Assay in Breast Cancer. N Engl J Med. 2015;373(21):2005-14.
50. Esserman LJ, Berry DA, Cheang MC, Yau C, Perou CM, Carey L, et al. Chemotherapy response and recurrence-free survival in neoadjuvant breast cancer depends on biomarker profiles: results from the I-SPY 1 TRIAL (CALGB 150007/150012; ACRIN 6657). Breast Cancer Res Treat. 2012;132(3):1049-62.
51. Ohnstad HO, Borgen E, Falk RS, Lien TG, Aaserud M, Sveli MAT, et al. Prognostic value of PAM50 and risk of recurrence score in patients with early-stage breast cancer with long-term follow-up. Breast Cancer Res. 2017;19(1):120.
52. Ribnikar D, Cardoso F. Tailoring Chemotherapy in Early-Stage Breast Cancer: Based on Tumor Biology or Tumor Burden? Am Soc Clin Oncol Educ Book. 2016;35:e31-8.
53. Boughey JC, Wagner J, Garrett BJ, Harker L, Middleton LP, Babiera GV, et al. Neoadjuvant chemotherapy in invasive lobular carcinoma may not improve rates of breast conservation. Ann Surg Oncol. 2009;16(6):1606-11.
54. Guiu S, Wolfer A, Jacot W, Fumoleau P, Romieu G, Bonnetain F, et al. Invasive lobular breast cancer and its variants: how special are they for systemic therapy decisions? Crit Rev Oncol Hematol. 2014;92(3):235-57.
55. Petruolo OA, Pilewskie M, Patil S, Barrio AV, Stempel M, Wen HY, et al. Standard Pathologic Features Can Be Used to Identify a Subset of Estrogen Receptor-Positive, HER2 Negative Patients Likely to Benefit from Neoadjuvant Chemotherapy. Ann Surg Oncol. 2017;24(9):2556-62.
56. Truin W, Vugts G, Roumen RM, Maaskant-Braat AJ, Nieuwenhuijzen GA, van der Heiden-van der Loo M, et al. Differences in Response and Surgical Management with Neoadjuvant Chemotherapy in Invasive Lobular Versus Ductal Breast Cancer. Ann Surg Oncol. 2016;23(1):51-7.
57. Delpech Y, Coutant C, Hsu L, Barranger E, Iwamoto T, Barcenas CH, et al. Clinical benefit from neoadjuvant chemotherapy in oestrogen receptor-positive invasive ductal and lobular carcinomas. Br J Cancer. 2013;108(2):285-91.
58. Balmativola D, Marchio C, Maule M, Chiusa L, Annaratone L, Maletta F, et al. Pathological non-response to chemotherapy in a neoadjuvant setting of breast cancer: an inter-institutional study. Breast Cancer Res Treat. 2014;148(3):511-23.
59. Denkert C, Loibl S, Muller BM, Eidtmann H, Schmitt WD, Eiermann W, et al. Ki67 levels as predictive and prognostic parameters in pretherapeutic breast cancer core biopsies: a translational investigation in the neoadjuvant GeparTrio trial. Ann Oncol. 2013;24(11):2786-93.
60. Jones RL, Salter J, A'Hern R, Nerurkar A, Parton M, Reis-Filho JS, et al. The prognostic significance of Ki67 before and after neoadjuvant chemotherapy in breast cancer. Breast Cancer Res Treat. 2009;116(1):53-68.
61. von Minckwitz G, Schmitt WD, Loibl S, Muller BM, Blohmer JU, Sinn BV, et al. Ki67 measured after neoadjuvant chemotherapy for primary breast cancer. Clin Cancer Res. 2013;19(16):4521-31.
62. Allison KH, Hammond MEH, Dowsett M, McKernin SE, Carey LA, Fitzgibbons PL, et al. Estrogen and Progesterone Receptor Testing in Breast Cancer: ASCO/CAP Guideline Update. J Clin Oncol. 2020;38(12):1346-66.
63. Deyarmin B, Kane JL, Valente AL, van Laar R, Gallagher C, Shriver CD, et al. Effect of ASCO/CAP guidelines for determining ER status on molecular subtype. Ann Surg Oncol. 2013;20(1):87-93.
64. Iwamoto T, Booser D, Valero V, Murray JL, Koenig K, Esteva FJ, et al. Estrogen receptor (ER) mRNA and ER-related gene expression in breast cancers that are 1% to 10% ER-positive by immunohistochemistry. J Clin Oncol. 2012;30(7):729-34.
65. Whitworth P, Beitsch P, Mislowsky A, Pellicane JV, Nash C, Murray M, et al. Chemosensitivity and Endocrine Sensitivity in Clinical Luminal Breast Cancer Patients in the Prospective Neoadjuvant Breast Registry Symphony Trial (NBRST) Predicted by Molecular Subtyping. Ann Surg Oncol. 2017;24(3):669-75.
66. Bossuyt V, Provenzano E, Symmans WF, Boughey JC, Coles C, Curigliano G, et al. Recommendations for standardized pathological characterization of residual disease for neoadjuvant clinical trials of breast cancer by the BIG-NABCG collaboration. Ann Oncol. 2015;26(7):1280-91.
67. Bossuyt V, Spring L. Pathologic evaluation of response to neoadjuvant therapy drives treatment changes and improves long-term outcomes for breast cancer patients. Breast J. 2020;26(6):1189-98.
68. Carmon M, Zilber S, Gekhtman D, Olsha O, Hadar T, Golomb E. Hygroscopic sonographically detectable clips form characteristic breast and lymph node pseudocysts. Mod Pathol. 2018;31(1):62-7.
69. Weiss A, Lee KC, Romero Y, Ward E, Kim Y, Ojeda-Fournier H, et al. Calcifications on mammogram do not correlate with tumor size after neoadjuvant chemotherapy. Ann Surg Oncol. 2014;21(10):3310-6.

70. Provenzano E, Bossuyt V, Viale G, Cameron D, Badve S, Denkert C, et al. Standardization of pathologic evaluation and reporting of postneoadjuvant specimens in clinical trials of breast cancer: recommendations from an international working group. Mod Pathol. 2015;28(9):1185-201.
71. Symmans WF, Peintinger F, Hatzis C, Rajan R, Kuerer H, Valero V, et al. Measurement of residual breast cancer burden to predict survival after neoadjuvant chemotherapy. J Clin Oncol. 2007;25(28):4414-22.
72. Hennessy BT, Hortobagyi GN, Rouzier R, Kuerer H, Sneige N, Buzdar AU, et al. Outcome after pathologic complete eradication of cytologically proven breast cancer axillary node metastases following primary chemotherapy. J Clin Oncol. 2005;23(36):9304-11.
73. Cure H, Amat S, Penault-Llorca F, le Bouedec G, Ferriere JP, Mouret-Reynier MA, et al. Prognostic value of residual node involvement in operable breast cancer after induction chemotherapy. Breast Cancer Res Treat. 2002;76(1):37-45.
74. Klauber-DeMore N, Ollila DW, Moore DT, Livasy C, Calvo BF, Kim HJ, et al. Size of residual lymph node metastasis after neoadjuvant chemotherapy in locally advanced breast cancer patients is prognostic. Ann Surg Oncol. 2006;13(5):685-91.
75. von Minckwitz G, Darb-Esfahani S, Loibl S, Huober J, Tesch H, Solbach C, et al. Responsiveness of adjacent ductal carcinoma in situ and changes in HER2 status after neoadjuvant chemotherapy/trastuzumab treatment in early breast cancer--results from the GeparQuattro study (GBG 40). Breast Cancer Res Treat. 2012;132(3):863-70.
76. Cheng E, Ko D, Nguyen M, Moo TA, Andreopoulou E, Hoda SA, et al. Residual Pure Intralymphatic Breast Carcinoma Following Neoadjuvant Chemotherapy Is Indicative of Poor Clinical Outcome, Even in Node-Negative Patients. Am J Surg Pathol. 2017;41(9):1275-82.
77. Rabban JT, Glidden D, Kwan ML, Chen YY. Pure and predominantly pure intralymphatic breast carcinoma after neoadjuvant chemotherapy: an unusual and adverse pattern of residual disease. Am J Surg Pathol. 2009;33(2):256-63.
78. Guilbert MC, Overmoyer B, Lester SC. Pure Intralymphatic Invasion in the Absence of Stromal Invasion After Neoadjuvant Therapy: A Rare Pattern of Residual Breast Carcinoma. Am J Surg Pathol. 2018;42(5):679-86.
79. Abdel-Fatah TM, Ball G, Lee AH, Pinder S, MacMilan RD, Cornford E, et al. Nottingham Clinico-Pathological Response Index (NPRI) after neoadjuvant chemotherapy (Neo-ACT) accurately predicts clinical outcome in locally advanced breast cancer. Clin Cancer Res. 2015;21(5):1052-62.
80. Yi M, Lin H, Bedrosian I, Shen Y, Hunt KK, Chavez-MacGregor M, et al. Staging for Breast Cancer Patients Receiving Neoadjuvant Chemotherapy: Utility of Incorporating Biologic Factors. Ann Surg Oncol. 2020;27(2):359-66.
81. Murata Y, Kubota K, Hamada N, Miyatake K, Tadokoro M, Nakatani K, et al. Diffusion-weighted magnetic resonance imaging for assessment after neoadjuvant chemotherapy in breast cancer, based on morphological concepts. Oncol Lett. 2010;1(2):293-8.
82. Ballesio L, Gigli S, Di Pastena F, Giraldi G, Manganaro L, Anastasi E, et al. Magnetic resonance imaging tumor regression shrinkage patterns after neoadjuvant chemotherapy in patients with locally advanced breast cancer: Correlation with tumor biological subtypes and pathological response after therapy. Tumour Biol. 2017;39(3):1010428317694540.
83. Pastorello RG, Laws A, Grossmith S, King C, McGrath M, Mittendorf EA, et al. Clinico-pathologic predictors of patterns of residual disease following neoadjuvant chemotherapy for breast cancer. Mod Pathol. 2020. doi: 10.1038/s41379-020-00714-5. Online ahead of print.
84. Akay CL, Meric-Bernstam F, Hunt KK, Grubbs EG, Bedrosian I, Tucker SL, et al. Evaluation of the MD Anderson Prognostic Index for local-regional recurrence after breast conserving therapy in patients receiving neoadjuvant chemotherapy. Ann Surg Oncol. 2012;19(3):901-7.
85. Choi J, Laws A, Hu J, Barry W, Golshan M, King T. Margins in Breast-Conserving Surgery After Neoadjuvant Therapy. Ann Surg Oncol. 2018;25(12):3541-7.
86. Apple SK, Suthar F. How do we measure a residual tumor size in histopathology (the gold standard) after neoadjuvant chemotherapy? Breast. 2006;15(3):370-6.
87. Ellis IO, Carder P, Hales S, Lee AH, Pinder S, Rakha EA, et al. Pathology reporting of breast disease in surgical excision specimens incorporating the dataset for histological reporting of breast cancer. London: The Royal College of Pathologists; 2016.
88. Guide for Measuring Cancer Cellularity, Examples of Gross & Microscopic Evaluation, Pathology Protocol for Macroscopic and Microscopic Assessment of RCB [cited 2020 Dec 26] Available from: http://www3.mdanderson.org/app/medcalc/index.cfm?pagename=jsconvert3
89. Wong SM, Almana N, Choi J, Hu J, Gagnon H, Natsuhara K, et al. Prognostic Significance of Residual Axillary Nodal Micrometastases and Isolated Tumor Cells After Neoadjuvant Chemotherapy for Breast Cancer. Ann Surg Oncol. 2019;26(11):3502-9.
90. Dieras V, Fumoleau P, Romieu G, Tubiana-Hulin M, Namer M, Mauriac L, et al. Randomized parallel study of doxorubicin plus paclitaxel and doxorubicin plus cyclophosphamide as neoadjuvant treatment of patients with breast cancer. J Clin Oncol. 2004;22(24):4958-65.
91. Thomas JSJ, Provenzano E, Hiller L, Dunn J, Blenkinsop C, Grybowicz L, et al. Central pathology review with two-stage quality assurance for pathological response after neoadjuvant chemotherapy in the ARTemis Trial. Mod Pathol. 2017;30(8):1069-77.
92. Provenzano E, Vallier AL, Champ R, Walland K, Bowden S, Grier A, et al. A central review of histopathology reports after breast cancer neoadjuvant chemotherapy in the neo-tango trial. Br J Cancer. 2013;108(4):866-72.

93. Chevallier B, Roche H, Olivier JP, Chollet P, Hurteloup P. Inflammatory breast cancer. Pilot study of intensive induction chemotherapy (FEC-HD) results in a high histologic response rate. Am J Clin Oncol. 1993;16(3):223-8.
94. Ogston KN, Miller ID, Payne S, Hutcheon AW, Sarkar TK, Smith I, et al. A new histological grading system to assess response of breast cancers to primary chemotherapy: prognostic significance and survival. Breast. 2003;12(5):320-7.
95. Pinder SE, Provenzano E, Earl H, Ellis IO. Laboratory handling and histology reporting of breast specimens from patients who have received neoadjuvant chemotherapy. Histopathology. 2007;50(4):409-17.
96. Sataloff DM, Mason BA, Prestipino AJ, Seinige UL, Lieber CP, Baloch Z. Pathologic response to induction chemotherapy in locally advanced carcinoma of the breast: a determinant of outcome. J Am Coll Surg. 1995;180(3):297-306.
97. Mittendorf EA, Jeruss JS, Tucker SL, Kolli A, Newman LA, Gonzalez-Angulo AM, et al. Validation of a novel staging system for disease-specific survival in patients with breast cancer treated with neoadjuvant chemotherapy. J Clin Oncol. 2011;29(15):1956-62.
98. Mittendorf EA, Vila J, Tucker SL, Chavez-MacGregor M, Smith BD, Symmans WF, et al. The Neo-Bioscore Update for Staging Breast Cancer Treated With Neoadjuvant Chemotherapy: Incorporation of Prognostic Biologic Factors Into Staging After Treatment. JAMA Oncol. 2016;2(7):929-36.
99. Mrkonjic M, Berman HK, Done SJ, Youngson B, Mulligan AM. Breast specimen handling and reporting in the post-neoadjuvant setting: challenges and advances. J Clin Pathol. 2019;72(2):120-32.
100. Penault-Llorca F, Radosevic-Robin N. Biomarkers of residual disease after neoadjuvant therapy for breast cancer. Nat Rev Clin Oncol. 2016;13(8):487-503.
101. Provenzano E, Brown JP, Pinder SE. Pathological controversies in breast cancer: classification of ductal carcinoma in situ, sentinel lymph nodes and low volume metastatic disease and reporting of neoadjuvant chemotherapy specimens. Clin Oncol (R Coll Radiol). 2013;25(2):80-92.
102. Peintinger F, Sinn B, Hatzis C, Albarracin C, Downs-Kelly E, Morkowski J, et al. Reproducibility of residual cancer burden for prognostic assessment of breast cancer after neoadjuvant chemotherapy. Mod Pathol. 2015;28(7):913-20.
103. Naidoo K, Parham DM, Pinder SE. An audit of residual cancer burden reproducibility in a UK context. Histopathology. 2017;70(2):217-22.
104. Campbell JI, Yau C, Krass P, Moore D, Carey LA, Au A, et al. Comparison of residual cancer burden, American Joint Committee on Cancer staging and pathologic complete response in breast cancer after neoadjuvant chemotherapy: results from the I-SPY 1 TRIAL (CALGB 150007/150012; ACRIN 6657). Breast Cancer Res Treat. 2017;165(1):181-91.
105. Hunt KK, Yi M, Mittendorf EA, Guerrero C, Babiera GV, Bedrosian I, et al. Sentinel lymph node surgery after neoadjuvant chemotherapy is accurate and reduces the need for axillary dissection in breast cancer patients. Ann Surg. 2009;250(4):558-66.
106. Straver ME, Rutgers EJ, Russell NS, Oldenburg HS, Rodenhuis S, Wesseling J, et al. Towards rational axillary treatment in relation to neoadjuvant therapy in breast cancer. Eur J Cancer. 2009;45(13):2284-92.
107. Mamounas EP, Brown A, Anderson S, Smith R, Julian T, Miller B, et al. Sentinel node biopsy after neoadjuvant chemotherapy in breast cancer: results from National Surgical Adjuvant Breast and Bowel Project Protocol B-27. J Clin Oncol. 2005;23(12):2694-702.
108. Boughey JC, Suman VJ, Mittendorf EA, Ahrendt GM, Wilke LG, Taback B, et al. Sentinel lymph node surgery after neoadjuvant chemotherapy in patients with node-positive breast cancer: the ACOSOG Z1071 (Alliance) clinical trial. JAMA. 2013;310(14):1455-61.
109. Boileau JF, Poirier B, Basik M, Holloway CM, Gaboury L, Sideris L, et al. Sentinel node biopsy after neoadjuvant chemotherapy in biopsy-proven node-positive breast cancer: the SN FNAC study. J Clin Oncol. 2015;33(3):258-64.
110. Kuehn T, Bauerfeind I, Fehm T, Fleige B, Hausschild M, Helms G, et al. Sentinel-lymph-node biopsy in patients with breast cancer before and after neoadjuvant chemotherapy (SENTINA): a prospective, multicentre cohort study. Lancet Oncol. 2013;14(7):609-18.
111. Boughey JC, Ballman KV, Le-Petross HT, McCall LM, Mittendorf EA, Ahrendt GM, et al. Identification and Resection of Clipped Node Decreases the False-negative Rate of Sentinel Lymph Node Surgery in Patients Presenting With Node-positive Breast Cancer (T0-T4, N1-N2) Who Receive Neoadjuvant Chemotherapy: Results From ACOSOG Z1071 (Alliance). Ann Surg. 2016;263(4):802-7.
112. Caudle AS, Yang WT, Mittendorf EA, Black DM, Hwang R, Hobbs B, et al. Selective surgical localization of axillary lymph nodes containing metastases in patients with breast cancer: a prospective feasibility trial. JAMA Surg. 2015;150(2):137-43.
113. Caudle AS, Yang WT, Krishnamurthy S, Mittendorf EA, Black DM, Gilcrease MZ, et al. Improved Axillary Evaluation Following Neoadjuvant Therapy for Patients With Node-Positive Breast Cancer Using Selective Evaluation of Clipped Nodes: Implementation of Targeted Axillary Dissection. J Clin Oncol. 2016;34(10):1072-8.
114. Donker M, Straver ME, Wesseling J, Loo CE, Schot M, Drukker CA, et al. Marking axillary lymph nodes with radioactive iodine seeds for axillary staging after neoadjuvant systemic treatment in breast cancer patients: the MARI procedure. Ann Surg. 2015;261(2):378-82.
115. Nguyen TT, Hieken TJ, Glazebrook KN, Boughey JC. Localizing the Clipped Node in Patients with Node-Positive

Breast Cancer Treated with Neoadjuvant Chemotherapy: Early Learning Experience and Challenges. Ann Surg Oncol. 2017;24(10):3011-6.

116. Siso C, de Torres J, Esgueva-Colmenarejo A, Espinosa-Bravo M, Rus N, Cordoba O, et al. Intraoperative Ultrasound-Guided Excision of Axillary Clip in Patients with Node-Positive Breast Cancer Treated with Neoadjuvant Therapy (ILINA Trial) : A New Tool to Guide the Excision of the Clipped Node After Neoadjuvant Treatment. Ann Surg Oncol. 2018;25(3):784-91.
117. Montagna G, Mamtani A, Knezevic A, Brogi E, Barrio AV, Morrow M. Selecting Node-Positive Patients for Axillary Downstaging with Neoadjuvant Chemotherapy. Ann Surg Oncol. 2020;27(11):4515-22.
118. Montagna G, Morrow M. ASO Author Reflections: Axillary Staging in Node-Positive Breast Cancer Patients Treated with Neoadjuvant Chemotherapy-Beyond Clinical Trials. Ann Surg Oncol. 2020;27(11):4523-4.
119. Barrio AV, Mamtani A, Edelweiss M, Eaton A, Stempel M, Murray MP, et al. How Often Is Treatment Effect Identified in Axillary Nodes with a Pathologic Complete Response After Neoadjuvant Chemotherapy? Ann Surg Oncol. 2016;23(11):3475-80.
120. Gandhi A, Coles C, Makris A, Provenzano E, Goyal A, Maxwell AJ, et al. Axillary Surgery Following Neoadjuvant Chemotherapy - Multidisciplinary Guidance From the Association of Breast Surgery, Faculty of Clinical Oncology of the Royal College of Radiologists, UK Breast Cancer Group, National Coordinating Committee for Breast Pathology and British Society of Breast Radiology. Clin Oncol (R Coll Radiol). 2019;31(9):664-8.
121. Moo TA, Edelweiss M, Hajiyeva S, Stempel M, Raiss M, Zabor EC, et al. Is Low-Volume Disease in the Sentinel Node After Neoadjuvant Chemotherapy an Indication for Axillary Dissection? Ann Surg Oncol. 2018;25(6):1488-94.
122. Almahariq MF, Levitin R, Quinn TJ, Chen PY, Dekhne N, Kiran S, et al. Omission of Axillary Lymph Node Dissection is Associated with Inferior Survival in Breast Cancer Patients with Residual N1 Nodal Disease Following Neoadjuvant Chemotherapy. Ann Surg Oncol. Epub 2020 Jul 25.
123. Piltin MA, Hoskin TL, Day CN, Davis J Jr, Boughey JC. Oncologic Outcomes of Sentinel Lymph Node Surgery After Neoadjuvant Chemotherapy for Node-Positive Breast Cancer. Ann Surg Oncol. 2020;27(12):4795-801.
124. Botty Van den Bruele A, Lavery J, Plitas G, Pilewskie ML. Axillary Downstaging in Occult Primary Breast Cancer After Neoadjuvant Chemotherapy. Ann Surg Oncol. Epub 2020 Aug 19.

Narrative Review
Acta Medica Academica 2021;50(1):110-125
DOI: 10.5644/ama2006-124.329

Classic Hodgkin Lymphoma – Old Disease, New Directions: An Update on Pathology, Molecular Features and Biological Prognostic Markers

Anamarija M. Perry[1], Lauren B. Smith[1], Adam Bagg[2]

[1]Department of Pathology, University of Michigan, Ann Arbor, MI, USA, [2]Department of Pathology and Laboratory Medicine, Perelman School of Medicine, University of Pennsylvania, Philadelphia, PA, USA

Correspondence: *anaperry@med.umich.edu*; Tel.: + 734 232 5376; Fax.: + 734 232 5360

Received: 18 January 2021; **Accepted:** 19 February 2021

Abstract
The aim of this paper is to review morphologic, immunophenotypic, and molecular features of classic Hodgkin lymphoma, as well as different prognostic markers in this neoplasm. Classic Hodgkin lymphoma (CHL) accounts for 15-25% of all lymphomas in the Western world. The hallmark of this disease is the neoplastic Hodgkin/Reed-Sternberg (HRS) cell, which is favored to be derived from germinal center B-cells but has lost many of the B-cell markers. HRS cells are scattered within a dense inflammatory infiltrate, and through a network of cytokines and chemokines they shape their microenvironment, evade immune response, survive, and grow. In the last two decades multiple prognostic markers related to HRS cells, the microenvironment or both, have been evaluated in patients with CHL. They include clinical, immunohistochemical, cytogenetic, and molecular markers that can predict survival and identify high-risk patients who will likely relapse after therapy. More recently, circulating tumor DNA analysis by next-generation sequencing has opened new avenues for diagnosis and disease monitoring after therapy. The increased understanding of molecular mechanisms underlying CHL pathogenesis has led to successful implementation of novel therapies, such as anti-PD-1 antibodies, which are becoming a mainstay of treatment in relapsed/refractory patients. **Conclusion.** Currently, pathologic prognostic markers are not routinely assessed at initial diagnosis of CHL. However, as more therapies become available, it will be important to identify patients with high-risk disease who may benefit from more intense or targeted therapy upfront.

Key Words: Classic Hodgkin Lymphoma ▪ Prognostic Markers ▪ Immunohistochemical Markers ▪ Tumor Microenvironment ▪ Epstein-Barr Virus.

Introduction

Hodgkin lymphoma is a common lymphoma in the Western world accounting for 15-25% of all lymphomas. This group is comprised of two morphologically and immunophenotypically distinct entities – classic Hodgkin lymphoma (CHL) which accounts for over 90% of cases and nodular lymphocyte predominant Hodgkin lymphoma (1, 2). Although "Hodgkin's disease" was first reported nearly 200 years ago and Hodgkin/Reed-Sternberg (HRS) cells were described at the turn of the 20th century, the nature of this disease (i.e. neoplastic vs. infectious/inflammatory) remained a mystery for a long time (3, 4). The B-cell origin of HRS cells was finally elucidated in the 1990s and the new terminology "Hodgkin lymphoma" was included in the Revised European American Lymphoma (REAL) Classification (5-7). Since then, CHL has been a focus of extensive research which paved the way for better risk stratification and novel therapies.

Classic Hodgkin lymphoma has a bimodal age distribution, with the first peak from 15 to 35 years of and the second after 55 years of age. In resource-poor countries, however, the first peak occurs earlier in childhood. The overall male-to-female ratio is 1.5:1, but females have higher incidence of nodular sclerosis subtype of CHL (2, 8-10). Clini-

cally, CHL mainly involves lymph nodes, most frequently above the diaphragm with cervical, mediastinal, axillary, and supraclavicular lymph node chains being most commonly affected. In a subset of patients, extranodal tissues are involved, such as spleen, lungs and liver (2, 10). Bone marrow involvement is uncommon, occurring in approximately 5% of patients and is more common in the elderly and HIV positive patients (11). So-called "B-symptoms" such as fever, weight loss and night sweats are seen in 30-40% of patients (10). Modern therapy of CHL is based on risk stratification with a goal of curing the patient while minimizing acute toxicity and long-term complications, the most feared being malignancy such as acute leukemia and myelodysplastic syndrome (12). Imaging studies, specifically fluorodeoxyglucose positive emission tomography (FDG-PET) is used in staging as well as during treatment to assess response to chemotherapy and plan further treatment (13). For early stage CHL, the standard treatment includes ABVD (doxorubicin, bleomycin, vinblastine, dacarbazine) chemotherapy with or without involved-field radiation therapy. Even though, compared to many lymphomas, CHL has a very good prognosis and high cure rates, 10-30% of patients will experience relapse and 5-10% are refractory to initial treatment. The management of these patients is challenging and includes high-dose chemotherapy, autologous stem cell transplant, as well as anti-CD30 antibody brentuximab vedotin, and more recently anti-PD-1 antibodies, such as pembrolizumab and nivolumab (12, 14-16).

The current World Health Organization (WHO) Classification requires integration of all available information – morphology, immunophenotype, genetic, and molecular information, as well as clinical features, in order to properly classify lymphomas. Moreover, additional studies to assess prognostic markers are frequently performed, particularly in non-Hodgkin lymphomas, as they help guide clinicians in choosing the most appropriate course of therapy (2). Prognostic markers in CHL are currently not routinely assessed by pathologists, but as more therapies become available, there will likely be a push to identify patients with more aggressive disease who would benefit from more intense or combined therapy upfront. Prognostic markers in CHL include clinical markers, which differ for early and advanced stage disease. The presence of a bulky mediastinal mass, involvement of multiple nodal sites, extranodal involvement, massive splenic disease, age ≥50 years, and elevated sedimentation rate are predictors of poorer outcome in early stage CHL (17). For advanced disease, the International Prognostic Score (IPS) that incorporates seven clinical variables is used (18, 19). The most frequently used pathologic prognostic markers are immunohistochemical markers, due to their wide availability, relatively easy interpretation and low price compared to other methods. Molecular methods used in prognostication most frequently include high-resolution array comparative genomic hybridization (aCGH), gene expression profiling (GEP) and next generation sequencing (NGS). These methods are still not widely available as they require substantial expertise and are relatively expensive. Over the past two decades, numerous studies in the literature have addressed prognostic markers in CHL.

This review will summarize the most relevant pathologically-determined prognostic markers.

Histopathologic Characteristics and Immunophenotype

Classic Hodgkin lymphoma is histologically characterized by HRS cell and its variants, that usually comprise less than 1% of cellular infiltrate, scattered in a mixed inflammatory background. Hodgkin/Reed-Sternberg cell has two or multiple nuclei with open chromatin, accentuated nuclear membrane, and prominent eosinophilic nucleoli. Morphologic variants of HRS cells include mononuclear Hodgkin cells, degenerated mummified cells and lacunar cells, which show shrinkage artifact (i.e. lacunae) in the formalin-fixed tissue. WHO classification recognized four morphologically distinct subtypes of CHL – nodular sclerosis (50-80% of cases), mixed cellularity (20-30% of cases), lymphocyte-rich (5% of cases), and lymphocyte-depleted (1% of cases). These subtypes are associated with different clini-

cal presentations and are differently represented among varied age groups (2, 10).

Nodular sclerosis CHL, the most common subtype in the Western world, typically presents as a mediastinal mass in young adults. Histologically, lymph nodes show nodular pattern of effacement with cellular nodules surrounded by thick fibrotic bands. The infiltrate is composed of scattered lacunar cells (as well as other HRS variants), which sometimes form clusters and sheets, in a mixed inflammatory background composed of small lymphocytes, plasma cells, histiocytes, eosinophils, and neutrophils (Figure 1A and 1B). Mixed cellularity CHL is more commonly seen in the elderly population, among patients with HIV infection, as well as in the pediatric population in developing countries. Notably, around 75% of cases are associated with Epstein-Barr virus (EBV). Histologically, lymph node shows diffuse effacement by infiltrate composed of scattered HRS cells in an inflammatory background (Figure 1C and 1D). Lymphocyte-rich subtype is relatively rare and patients frequently present in early clinical stages. Lymph node is effaced in nodular, or less frequently diffuse pattern, and HRS cells are seen in a background composed mainly of small lymphocytes, hence the term "lymphocyte-rich". In the nodular pattern, small/regressed germinal centers are usually seen in the nodules with HRS cells/variants in the expanded mantle zones (Figure 1E and 1F). Lymphocyte-depleted subtype, the rarest of all, is associated with aggressive clinical behavior, and often with HIV infection. Histologically, it is characterized by sheets of neoplastic cells, sometimes with prominent fibrosis, with scarce inflammatory cells in the background (2, 20).

Table 1. Immunohistochemical Profile of Classic Hodgkin Lymphoma

Positive markers	Negative or rarely positive markers
CD30	CD19
CD15	CD79A
PAX5 (dim)	PU.1
CD20	OCT-2
MUM1	BOB.1
Fascin	CD10
LMO2	BCL6
HGAL	CD45
CD25	CD43
Vimentin	EMA
-	ALK
-	Cytokeratin

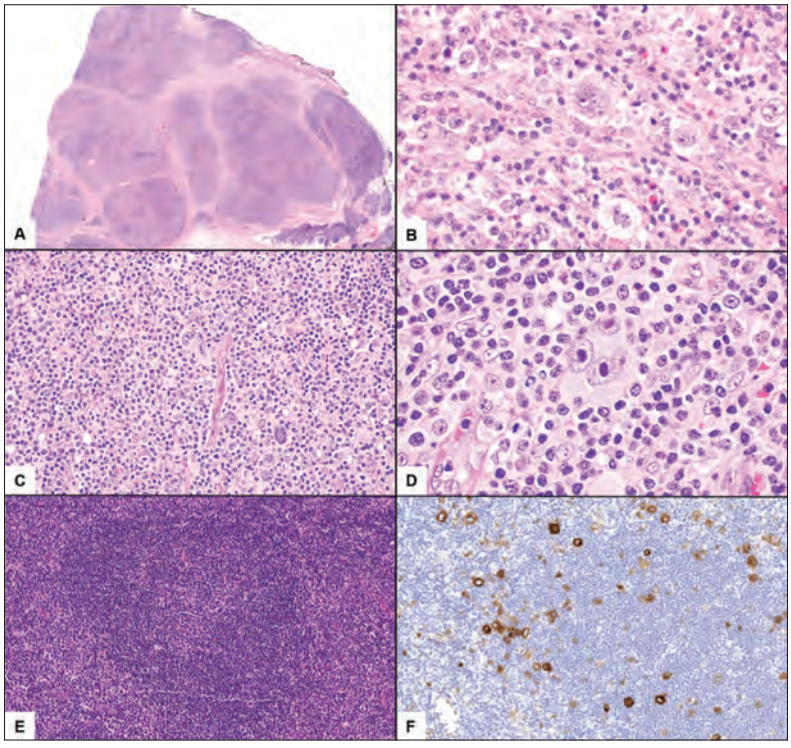

Figure 1. Nodular sclerosis subtype of classic Hodgkin lymphoma showing lymph node effacement by cellular nodules surrounded by thick fibrotic bands (A); infiltrate is composed of scattered lacunar cells in the inflammatory background (B). In mixed cellularity subtype of classic Hodgkin lymphoma there is a diffuse infiltrate composed of scattered RS cells in the inflammatory background (C, D). Lymphocyte-rich subtype of CHL showing neoplastic nodule composed almost entirely of small lymphocytes (E); CD30 immunohistochemical staining highlights scattered RS cells. (A-H&E, original magnification ×10; B and D-H&E, original magnification 400; C-H&E, original magnification ×200; E-H&E, original magnification ×100; F-CD30 immunohistochemical stain, original magnification ×200).

Molecular and Cytogenetic Features

Hodgkin/Reed-Sternberg cells likely originate from germinal center B-cells and show monoclonal immunoglobulin heavy-chain gene rearrangements. In some cases, there is "crippling" somatic hypermutation of this gene that would typically lead to the death of the cell by apoptosis; such cells are rescued by oncogenic mutations and/or EBV. Another mechanism contributing to the survival of these cells that are otherwise destined to die is the loss of most B-cell surface proteins, as well a B-cell transcription factors PU.1, OCT-2 and BOB.1 (5, 7, 29, 34-36). This loss of B-cell phenotype is due to epigenetic silencing of B-cell program regulators, promoter hypermethylation, and upregulation of *ID2* and *NOTCH1*, which are transcriptional antagonists (37-40). Given these unique molecular features of neoplastic HRS cells, including loss of B-cell receptor (BCR) which normally leads to apoptosis in mature B cells, they are dependent on multiple alternate pathways for survival. Major genetic alterations in CHL are summarized in Table 2. Constitutive activation of NF-κB and JAK-STAT signaling pathways are the main genetic features of CHL. Canonical and non-canonical NF-κB pathways are activated through several mechanisms, including mutations in negative regulators (*TNFAIP3, NFKBIE, NFKB1A*) as well as amplifications, chromosomal gains and structural rearrangements that affect gene loci for *MAP3K14, REL,* and *BCL3* and lead to increased activity (41-46). The JAK-STAT pathway is most commonly activated by amplification of *JAK2* gene (9p24.1) and mutations and deletions in negative regulators (*SOCS1* and *PTPN11*). Activation leads to increased phosphorylation of STATs, including STAT3, STAT5 and STAT6 and increased transcription of downstream targets (47-52). Other important deregulated pathways in CHL include NOTCH and PI3K-AKT (53). More recent genomic studies showed that cases of refractory CHL show *TP53* mutations, as well as mutations of epigenetic regulators *EP300* and *CREBBP* (54-56).

Table 2. Major Genetic Alterations in Classic Hodgkin Lymphoma

NF-κB
Mutation – loss of function
TNFAIP3
NFKBIE
NFKB1A
Amplification
MAP3K14
REL
BCL3
JAK-STAT
JAK2 (amplification – 9p24.1)
Mutation – gain of function
JAK1
JAK3
STAT3
STAT5B
STAT6
Mutation – loss of function
SOCS1
PTPN11
Immune Escape (evasion)
PDL-1/2 (amplification – 9p24.1)
Mutation – loss of function
TNFRSF14
CD58
B2M
CIITA (translocation)
NOTCH
NOTCH 1
NOTCH 2
FBXW7
SPEN
PI3K-AKT
GNA13
ITPKB

Tumor Microenvironment and Immune Evasion by Reed-Sternberg Cells

Malignant HRS cells are embedded in a dense reactive microenvironment composed of lymphocytes, plasma cells, macrophages, eosinophils,

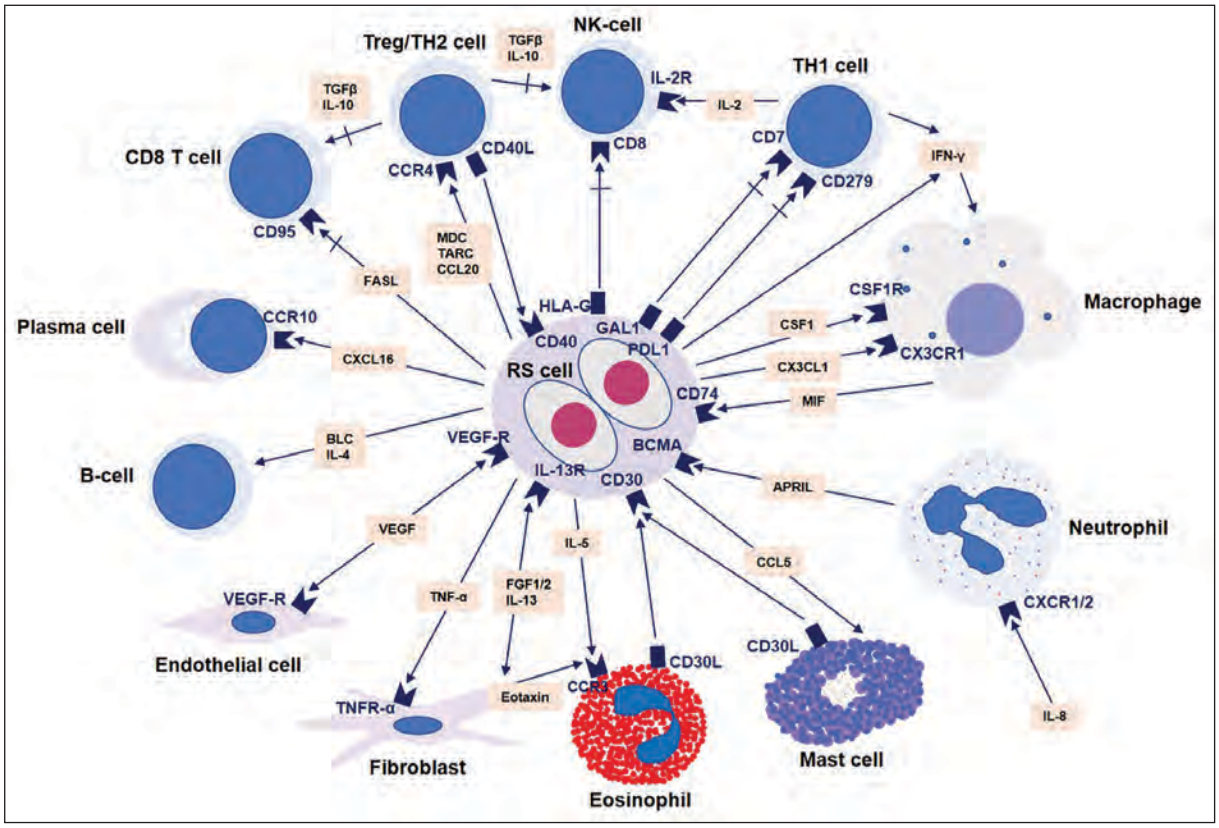

Figure 2. Complex interaction between neoplastic HRS cells and their microenvironment, mediated by cytokines and chemokines. APRIL, a proliferation-inducing ligand; BCL, B lymphocyte chemoattractant; BCMA, B-cell maturation antigen; CC, chemokine (C-C motif); CSF-1, colony stimulating factor-1; CXC, chemokine (C-X-C motif); FASL, Fas ligand; FGF, fibroblast growth factor; Gal-1, galectin-1; IFN-γ, interferon-γ; IL, interleukin; MDC, macrophage-derived chemokine; MIF, macrophage migration inhibitory factor; PDL1, programmed cell death 1 ligand; TARC, thymus and activation-related chemokine; TGF-β, transforming growth factor-β; TH, T helper cell; TNF, tumor necrosis factor; TNFR, tumor necrosis factor receptor; Treg, T regulatory cell; VEGF, vascular endothelial growth factor

neutrophils, mast cells, and stromal cells. Through very complex interaction with their microenvironment, mediated by cytokines and chemokines, HRS cells evade immune response, survive and grow (Figure 2) (57-60). The most abundant cells in the microenvironment are CD4+ T cells, mainly T helper 2 (TH2) and T regulatory (Treg) cells that express CCR4 receptor; however, the dominance of TH2 cells has recently been questioned and TH1 cells may be more important. Several chemokines, such as thymus and activation-related chemokine (TARC) and macrophage-derived chemokine (MDC), as well as CCL5 are secreted by HRS cells and attract TH2 and Treg cells via CCR4 receptor (59, 61-64). Macrophages are another very important cell subset in CHL microenvironment and were found to be prognostically relevant. The major cytokines produced by HRS cells that attract macrophages and enhance their function are interferon gamma, CSF1 and CXCL13. Macrophages, on the other hand, secrete macrophage migration inhibitory factor (MIF), which contributes to proliferation of RS cells (59, 65-67).

So-called "immune evasion" of HRS cells occurs through multiple mechanisms. Programmed death protein-1 (PD-1) is expressed in on activated T cells, B cells, macrophages, NK cells, Tregs and follicular T cells. Malignant cells of CHL highly express programmed death ligand-1 (PD-L1) and programmed death ligand-2 (PD-L2). PD-1/PD-L1 binding leads to crosslinking of the antigen-T-cell receptor (TCR) complex with PD-1

which results in attenuation of TCR-associated downstream signaling, decreased cytokine production, and inhibition of T-cell proliferation. In CHL, copy number gains in *PD-L1* and *PD-L2* (9p24.1) are the main mechanisms for increase in PD-1 protein expression on malignant HRS cells. This leads to T-cell exhaustion (i.e. reduced T-cell activation, suppression of T-cell proliferation and cytokine production) in tumor microenvironment and contributes to immune escape (51, 68-74). Furthermore, amplification of 9p24.1 also results in *JAK2* copy gain, increased JAK-STAT signaling, and increase in PD-1 ligand expression (51). Anti-PD-1 blocking antibodies have been successful in prolonging survival of patients with relapsed/refractory CHL (12, 15, 16). Other genetic lesions that contribute to immune evasion of RS cells include translocations of the MHC class II transactivator (*CIITA*) gene, which result in gene inactivation, and downregulation of HLA class II molecules, as well as increased surface expression of PD-L1/L2 (75). Moreover, inactivating mutations of beta2-microglobulin (*B2M*) gene result in downregulation of HLA class I molecules (76).

Cytogenetic Studies

Classic Hodgkin lymphoma shows recurrent cytogenetic abnormalities, including copy number changes and translocations. Among the most frequent are amplifications of 9p24.1 locus, affecting *JAK2, PD-L1* and *PD-L2* genes, as outlined above. Other copy number changes include gains of 2p, 12q, 14q, 16p, 17p, 17 q, 19q, and 20q; and losses of 4q, 6q, 11q, and 13q (45, 77, 78). Translocations involving immunoglobulin loci (*IG*) are common and can be seen in approximately 20% of cases. The partners were identified in a subset of cases and included *REL* (2p16), *BCL6* (3q27), *MYC* (8q24), and *BCL3/RELB* (19q13.2) (79).

Molecular Prognostic Models

Several studies proposed molecular prognostic models in CHL patients with clinically advanced disease by combining expression of multiple genes (80-82). Sanchez-Espiridion et al. (80) applied reverse-transcription polymerase chain reaction (RT-PCR) assay to 282 formalin-fixed paraffin-embedded (FFPE) tissue samples of CHL patients with clinical stage III and IV, as well as stage IIB with bulky disease. They evaluated expression of 30 genes, including genes expressed by malignant cells and microenvironment and integrated best predictor genes into an 11-gene model. The model included four functional pathways – cell cycle, apoptosis, macrophage activation, and interferon regulatory factor 4, and was able to identify a group of high-risk patients with significantly worse 5-year failure free survival (FFS; 44.1% for high-risk vs. 74% for low-risk). Moreover, when combined with clinical stage IV this model identified a group of patients with particularly poor outcome. Scott et al. (81) evaluated expression levels of 259 genes (including genes associated with microenvironment and the cellular processes associated with outcomes in CHL) by NanoString platform on pretreatment FFPE tissue samples from 290 CHL patients with locally extensive or advanced stage disease. Using penalized Cox regression, they created a prognostic model for overall survival (OS) comprising 23 genes. The model separated the patients into low- and high-risk groups (94% vs. 75% 5-year OS) and was validated in an independent CHL cohort. Furthermore, this prognostic model was superior to IPS in the multivariate analysis. Chan et al. (82) constructed an interesting 30 gene model (so-called "RHL30") using FFPE CHL biopsies taken at disease relapse that predicted outcome post-autologous stem-cell transplantation (ASCT). Gene expression profiling was performed by using NanoString platform and the model included 18 outcome-associated and 12 housekeeping genes and included B-cell, macrophage, RS-cell, neutrophil and natural killer-cell signatures, as well as drug resistance signature. The model identified a group of patients with significantly lower 5-year post-ASCT OS (27.8% for high-risk vs. 85.4% for low-risk) and FFS (23.8% for high-risk vs. 77.5% for low-risk). In summary, these prognostic models are robust and conveniently performed on FFPE tissue samples. However, they

require considerable technical and bioinformatics expertise and are unlikely to become routinely used in the near future.

Immunohistochemical Prognostic Markers

A number of immunohistochemical markers expressed on HRS cells, single or in combination, have been evaluated as prognosticators in CHL. Immunohistochemistry is widely available and relatively inexpensive; however, immunohistochemical studies frequently suffer from poor reproducibility due to differences in tissue fixation and processing, different antibody clones used, and significant interobserver variability (83). More commonly reported immunohistochemical prognostic markers are outlined in Table 3 (30, 84-97).

The most convincing findings appear to be the poorer prognosis associated with BCL2 and T-cell antigen expression by HRS cells (84, 87, 88, 91, 94, 95). Other reported markers associated with decreased survival and refractory disease are MAL and ABCC1 (89, 92). Studies that assessed expression of CD20 showed conflicting results and prognostic significance of CD20 expression in CHL is uncertain (85, 86, 88, 91). Interestingly, studies that assessed prognostic significance of PD-L1 also showed controversial results, including more favorable outcome and poorer prognosis. Ozturk et al. (97) reported poorer prognosis of PD-L1 positive patients. This study also found that overexpression of PD-1 in tumor microenvironment, together with positivity for EBV on RS cells, portends particularly unfavorable prognosis.

Table 3. Immunohistochemical Prognostic Markers Expressed on Hodgkin/Reed-Sternberg Cells in Classic Hodgkin Lymphoma

Prognostic marker	Prognosis	Reference
CD20	CD20+ - no prognostic significance	Rassidakis et al. (2002)
	CD20+ - decreased OS and FFS	Portlock et al. (2004)
	CD20+ - no prognostic significance	Asano et al. (2006)
	Decreased CD20 expression – associated with refractory disease or early relapse	Canioni et al. (2009)
BCL2	BCL2+ - decreased FFS	Rassidakis et al. (2002)
	BCL2+ - decreased OS and FFS	Sup et al. (2005)
	BCL2+ - associated with refractory disease or early relapse	Canioni et al. (2009)
	BCL2+ - no prognostic significance	Koh et al. (2013)
PD-L1	PD-L1+ - increased FFS	Roemer et al. (2018)*
	PD-L1+ - associated with advanced disease; when combined with PD-1+ in microenvironment and EBV+ HRS cells – very high-risk disease	Ozturk et al. (2020)
MHC class I and II	MHC class I+ - no prognostic significance	Roemer et al. (2018)*
	MHC class II+ - increased FFS	
	MHC class II+ - increased FFS	Diepstra et al. (2007)
HGAL	HGAL+ - improved OS and FFS	Natkunam et al. (2007)
MAL	MAL+ - decreased OS and FFS	Hsi et al. (2006)
ABCC1	ABCC1+ - associated with refractory disease and decreased FFS	Greaves et al. (2013)
T-cell markers	CD3, CD4, CD8, CD45RO, TIA-1, granzyme B – decreased OS	Asano et al. (2006)†
	CD3, CD4, CD8, CD5, CD2, CD7 – decreased OS and FFS	Venkataraman et al. (2013)‡
	CD2, CD3, CD4, CD5, CD7, TIA-1 – no prognostic significance	Nguyen et al. (2016)

EBV=Epstein-Barr virus; FFS=Failure free survival; OS=Overall survival; HRS=Hodgkin/Reed-Sternberg; *Immunohistochemical markers were correlated with clinical responses and progression-free survival after anti PD-1 therapy (nivolumab); †27 cases in the study expressed different combinations of T-cell markers; ‡50 cases in the study expressed different combinations of T-cell markers, most commonly CD4 and CD2.

Prognostic Markers Associated with Tumor Microenvironment

The prognostic significance of the inflammatory microenvironment in CHL has been a topic of numerous studies. Tumor-associated macrophages and different T-cell subsets have been most studied, but also other cells such as B cells, plasma cells, and mast cells have also been investigated (Table 4) (91, 95, 98-109). Steidl et al. (103) analyzed 130 CHL samples using GEP, which identified a gene signature of tumor-associated macrophages that was associated with poorer prognosis. Numerous immunohistochemical studies have examined prognostic significance of macrophages in CHL microenvironment using CD68 and CD163 antibodies. The results of these studies vary, with some studies showing worse outcome with increased number of macrophages, while others found no impact on survival, suggesting that GEP results from the Steidl et al. (103) study are not consistently reproducible by immunohistochemistry. Guo et al. (107) performed a meta-analysis of 22 studies (2959 patients) that showed high-density of macrophages to be associated with decreased overall and failure-free survival. T-cells in the microenvironment were also found to be important prognostic marker, with increased number of T regulatory cells being associated with better prognosis, while increased number of cytotoxic T cells portends worse prognosis (91, 95, 98-102, 104).

MicroRNA Signature

MicroRNAs (miRNAs) are small non-coding RNA molecules that regulate important biologic processes such as proliferation and differentiation. Furthermore, they can act as oncogenes (on-

Table 4. Prognostic Markers Associated with Cells in Tumor Microenvironment of Classic Hodgkin Lymphoma

Prognostic marker	Prognosis	Reference
Tumor-associated macrophages IHC for CD68+/- CD163	High-density of CD68+ TAMs – decreased OS and FFS; poor DSS; High-density of CD163+ TAMs – decreased OS and FFS	Guo et al. (2016)*
T-cells Regulatory T cells (FOXP3 IHC)	Increased number – increased OS and FFS	Tzankov et al. (2008)
	Increased number – increased EFS	Chettaile et al. (2009)
	Increased number – increased OS	Greaves et al. (2013)
	Increased number (anergic signature) – decreased FFS	Hollander et al. (2018)
Cytotoxic T cells (TIA-1 or granzyme B IHC)	Increased number – decreased FFS	Oudejans et al. (1997)
	Increased number – decreased OS and EFS	Alvaro-Naranjo et al. (2005)
	Increased number - associated with refractory disease or early relapse	Canioni et al. (2009)
	Increased number – decreased OS	Chettaile et al. (2009)
	Increased number – decreased OS	Nguyen et al. (2016)
Ratio of regulatory T cells to cytotoxic T cells	Ratio ≤1 – decreased OS and FFS	Kelley et al. (2007)
B-cells (CD20 IHC)	Increased number – increased OS and EFS	Chettaile et al. (2009)
	Increased density - increased OS	Greaves et al. (2013)
	Increased number – increased OS and improved FFS	Panico et al. (2015)
Plasma cells (CD138 IHC)	High proportion of plasma cells – decreased OS and EFS; presence of B-symptoms and advanced stage (IIB-IVB)	Gholika et al. (2019)
Mast cells (tryptase or CD117 IHC)	Increased number - associated with refractory disease or early relapse	Canioni et al. (2009)
	High number in CHL-MC – decreased OS and EFS†	Andersen et al. (2016)

CHL-MC=Classic Hodgkin lymphoma, mixed cellularity; DSS=Disease-specific survival; EFS=event-free survival; FFS=failure-free survival; IHC=Immunohistochemistry; OS=Overall survival; TAM=Tumor-associated macrophage; *Meta-analysis of 22 studies with 2959 patients; some studies in the literature showed no impact on survival; †Degree of mast cell infiltration not prognostic in classic Hodgkin lymphoma, nodular sclerosis subtype.

comirs) and tumor suppressor genes and have an important role in carcinogenesis, including lymphoma development (110-112). Sanchez-Espiridion et al. (113) performed miRNA microarray hybridization to define HRS and microenvironment miRNA signatures on frozen tissue samples from 29 CHL patients with advanced clinical stage. They identified CHL-miRNA signature with 234 differentially expressed miRNAs, a subset of which was prognostic. Quantitative polymerase chain reaction (Q-PCR) was performed to evaluate expression of miRNA associated with clinical outcome in an independent cohort of 168 FFPE CHL samples. Ultimately, a miRNA signature that included *MIR21, MIR30E, MIR30D*, and *MIR92B** stratified patients into two risk groups with significantly different 5-year FFS (35.7% for high-risk vs. 81% for low-risk).

Peripheral Blood Prognostic Markers and Circulating Tumor DNA

Several papers have investigated the role of peripheral blood prognostic markers in CHL; some of these markers are novel and can be used to assess the response to therapy. Poratta et al. (114) reported that peripheral blood lymphocyte/monocyte ratio ≥1.1 was associated with increased OS and PFS. Koh and al. (115) found that patients with absolute neutrophil count/absolute lymphocyte count ≥4.3 had decreased OS. Galectin-1, a carbohydrate-binding protein that plays an important role in immune response and fosters immune escape by tumor, was found to be expressed on HRS cells in CHL (116). Subsequently, Ouyang et al. (117) found that serum levels of galectin-1 are higher in CHL patients that in normal controls. Moreover, higher levels correlated with advanced clinical stage and higher IPS. Hsi et al. (118) analyzed levels of serum soluble chemokines/cytokines produced by HRS cells including TARC, MDC, interleukin-10 (IL-10) and soluble CD163 (sCD163). None of the markers were associated with outcome at diagnosis/baseline. At the time of interim PET study, increased levels of sCD163 were associated with favorable PFS. Furthermore, increased levels of TARC, MDC and IL-10 at the end of therapy were associated with shorter survival, making these markers useful in potentially identifying the patients at higher risk for relapse.

Circulating tumor (ct) DNA analysis by NGS is a particularly attractive approach in CHL and it could become complementary method to tissue biopsy in the near future. There are several possible applications of ctDNA analysis in CHL, including making diagnosis (especially in cases where tumor mass is difficult to biopsy and when biopsy is scant), evaluating response to treatment including minimal residual disease, as well as in prognostication to identify patients who are likely to experience disease relapse (55, 119-122). Several studies showed that mutations detected by analyzing ctDNA mirrored mutations in the corresponding tissue biopsies (55, 119). Higher plasma ctDNA levels at diagnosis were associated with unfavorable clinical characteristics (120). Moreover, in patients who responded well to chemotherapy and had negative PET staging ctDNA became undetectable, while in patients with partial response or refractory disease ctDNA remained detectable (119-122). These findings are important and indicate that ctDNA could be routinely used in disease monitoring after therapy and potentially decrease exposure to radiation from imaging techniques, as well as decrease the need for invasive tissue biopsies.

Epstein-Barr Virus (EBV) – Role in Pathogenesis

Epstein-Barr virus, a member of herpes virus family (a.k.a. Human herpesvirus 4), is an important etiological factor in number of human neoplasms, and is of particular interest in the field of lymphoma pathology (2). Epstein-Barr virus is detected in approximately 20-25% of CHL cases, with viral genomes in monoclonal form. Current "gold standard" for its detection in pathology practice is the EBV-encoded small RNA EBER1. Among the four histologic subtypes, EBV is most consistently and most frequently seen in mixed cellularity subtype (123, 124). The epidemiology of EBV-positive CHL

shows distinct patterns of distribution depending on age, as well as geographic and racial differences. Distribution of EBV-positive CHL cases varies around the world and is generally higher in the resource-poor countries, and more prevalent among Asians and Hispanics, compared to whites and Blacks. As for age, EBV+ cases are common in childhood, uncommon in young adults, and again common among older patients (123, 125). The reasons for these differences are not entirely clear, but are likely multifactorial and related to age of first exposure to EBV, genetic background, and changes in immune system related to disease and aging (so-called immunosenescence) (124, 126). People with a history of infectious mononucleosis have several times increased risk of EBV-positive CHL (127). Also, majority of CHL cases in HIV-positive individuals are EBV-positive (128).

Epstein-Barr virus contributes directly to CHL pathogenesis, via its EBV-encoded proteins, including nuclear antigens (EBNAs), latent membrane proteins (LMP1, LMP2A, and LMP2B), noncoding Epstein-Barr-encoded RNAs (EBER1 and EBER2) as well as miRNAs expressed in infected RS cells. Classic Hodgkin lymphoma is characterized by so-called type II latency pattern, which includes expression of EBNA-1, LMP-1, LMP-2, EBERs, and BART miRNAs (129-131). LMP-1 is similar to constitutively activated CD40 receptor, which leads to induction of JAK/STAT, NF-κB, and PI3K-AKT signaling pathways (132-138). LMP1 also induces PD-L1 expression, contributing to immune evasion (139). EBNA1 contributes to pathogenesis of CHL in several ways, such as inhibiting TGFβ signaling and upregulation of chemokine CCL20 in RS cells, which promotes migration of regulatory T cells (140-142). LMP2 mimics BCR, which allows for B-cell development in the absence of normal BCR signaling. LMP activates cellular pathways required for B-cell survival and can immortalize BCR-negative germinal center B-cells (143-145). The tumor microenvironment in EBV-positive CHL cases is characterized by increased numbers of cytotoxic T cells and significantly higher number of macrophages, compared to EBV-negative cases (98, 102, 146). Prognosis of EBV-positive CHL in elderly population is worse than EBV-negative cases. The choice of treatment for this group of patients are PD-1 inhibitors, which are showing very promising results (147, 148).

Conclusions

Over the past two decades numerous studies have contributed to our understanding of molecular mechanisms of CHL pathogenesis and complex interactions between HRS cells and their inflammatory microenvironment. These discoveries opened many avenues for targeted therapies, some of which are already in routine use in CHL management. The prognosis of CHL is overall favorable with modern therapies, however, up to 30% of patients will experience disease relapse and a small subset is refractory to treatment (12). A number of biological prognostic models and single markers have been proposed to improve risk stratification of CHL patients. Most of these prognostic markers are not routinely implemented at initial diagnosis of CHL, but this will likely change in the future as the goals of CHL therapy, like in other neoplasms, are to achieve sustainable remission, prevent relapse, and minimize toxicity. In the era of personalized medicine "one size does not fit all", and CHL is a prime example of this concept.

Conflict of Interest: The authors declare that they have no conflict of interest.

References

1. Laurent C, Do C, Gourraud PA, de Paiva GR, Valmary S, Brousset P. Prevalence of Common Non-Hodgkin Lymphomas and Subtypes of Hodgkin Lymphoma by Nodal Site of Involvement: A Systematic Retrospective Review of 938 Cases. Medicine (Baltimore). 2015;94(25):e987.
2. Swerdlow SH, Campo E, Harris NL, Jaffe ES, Pileri SA, Stein H, et al. WHO Classification of Tumours of Haematopoietic and Lymphoid Tissues. Lyon: IARC; 2017.
3. Hodgkin. On some Morbid Appearances of the Absorbent Glands and Spleen. Med Chir Trans. 1832;17:68-114.
4. Reed. On the Pathological Changes in Hodgkin's Disease, with Special Reference to Its Relation to Tuberculosis. Johns Hopkins Hosp Rep. 1902;10:133-96.

5. Kuppers R, Rajewsky K, Zhao M, Simons G, Laumann R, Fischer R, et al. Hodgkin disease: Hodgkin and Reed-Sternberg cells picked from histological sections show clonal immunoglobulin gene rearrangements and appear to be derived from B cells at various stages of development. Proc Natl Acad Sci U S A. 1994;91(23):10962-6.
6. Pileri SA, Leoncini L, Falini B. Revised European-American Lymphoma Classification. Curr Opin Oncol. 1995;7(5):401-7.
7. Kanzler H, Kuppers R, Hansmann ML, Rajewsky K. Hodgkin and Reed-Sternberg cells in Hodgkin's disease represent the outgrowth of a dominant tumor clone derived from (crippled) germinal center B cells. J Exp Med. 1996;184(4):1495-505.
8. Glaser SL, Jarrett RF. The epidemiology of Hodgkin's disease. Baillieres Clin Haematol. 1996;9(3):401-16.
9. Siegel R, Naishadham D, Jemal A. Cancer statistics, 2013. CA Cancer J Clin. 2013;63(1):11-30.
10. Jaffe ES, Arber DA, Campo E, Harris NL, Quintanilla-Martinez L. Hematopathology. 2nd ed. Philadelphia, PA: Elsevier; 2017.
11. Munker R, Hasenclever D, Brosteanu O, Hiller E, Diehl V. Bone marrow involvement in Hodgkin's disease: an analysis of 135 consecutive cases. German Hodgkin's Lymphoma Study Group. J Clin Oncol. 1995;13(2):403-9.
12. Ansell SM. Hodgkin lymphoma: A 2020 update on diagnosis, risk-stratification, and management. Am J Hematol. 2020;95(8):978-89.
13. Jerusalem G, Beguin Y, Fassotte MF, Najjar F, Paulus P, Rigo P, et al. Whole-body positron emission tomography using 18F-fluorodeoxyglucose for posttreatment evaluation in Hodgkin's disease and non-Hodgkin's lymphoma has higher diagnostic and prognostic value than classical computed tomography scan imaging. Blood. 1999;94(2):429-33.
14. Younes A, Gopal AK, Smith SE, Ansell SM, Rosenblatt JD, Savage KJ, et al. Results of a pivotal phase II study of brentuximab vedotin for patients with relapsed or refractory Hodgkin's lymphoma. J Clin Oncol. 2012;30(18):2183-9.
15. Armand P, Engert A, Younes A, Fanale M, Santoro A, Zinzani PL, et al. Nivolumab for Relapsed/Refractory Classic Hodgkin Lymphoma After Failure of Autologous Hematopoietic Cell Transplantation: Extended Follow-Up of the Multicohort Single-Arm Phase II CheckMate 205 Trial. J Clin Oncol. 2018;36(14):1428-39.
16. Chen R, Zinzani PL, Lee HJ, Armand P, Johnson NA, Brice P, et al. Pembrolizumab in relapsed or refractory Hodgkin lymphoma: 2-year follow-up of KEYNOTE-087. Blood. 2019;134(14):1144-53.
17. Diehl V, Stein H, Hummel M, Zollinger R, Connors JM. Hodgkin's lymphoma: biology and treatment strategies for primary, refractory, and relapsed disease. Hematology Am Soc Hematol Educ Program. 2003:225-47.
18. Hasenclever D, Diehl V. A prognostic score for advanced Hodgkin's disease. International Prognostic Factors Project on Advanced Hodgkin's Disease. N Engl J Med. 1998;339(21):1506-14.
19. Moccia AA, Donaldson J, Chhanabhai M, Hoskins PJ, Klasa RJ, Savage KJ, et al. International Prognostic Score in advanced-stage Hodgkin's lymphoma: altered utility in the modern era. J Clin Oncol. 2012;30(27):3383-8.
20. Shiels MS, Koritzinsky EH, Clarke CA, Suneja G, Morton LM, Engels EA. Prevalence of HIV Infection among U.S. Hodgkin lymphoma cases. Cancer Epidemiol Biomarkers Prev. 2014;23(2):274-81.
21. Pinkus GS, Thomas P, Said JW. Leu-M1--a marker for Reed-Sternberg cells in Hodgkin's disease. An immunoperoxidase study of paraffin-embedded tissues. Am J Pathol. 1985;119(2):244-52.
22. Dorfman RF, Gatter KC, Pulford KA, Mason DY. An evaluation of the utility of anti-granulocyte and anti-leukocyte monoclonal antibodies in the diagnosis of Hodgkin's disease. Am J Pathol. 1986;123(3):508-19.
23. Schwarting R, Gerdes J, Durkop H, Falini B, Pileri S, Stein H. BER-H2: a new anti-Ki-1 (CD30) monoclonal antibody directed at a formol-resistant epitope. Blood. 1989;74(5):1678-89.
24. Said JW. The immunohistochemistry of Hodgkin's disease. Semin Diagn Pathol. 1992;9(4):265-71.
25. von Wasielewski R, Mengel M, Fischer R, Hansmann ML, Hubner K, Franklin J, et al. Classical Hodgkin's disease. Clinical impact of the immunophenotype. Am J Pathol. 1997;151(4):1123-30.
26. Browne P, Petrosyan K, Hernandez A, Chan JA. The B-cell transcription factors BSAP, Oct-2, and BOB.1 and the pan-B-cell markers CD20, CD22, and CD79a are useful in the differential diagnosis of classic Hodgkin lymphoma. Am J Clin Pathol. 2003;120(5):767-77.
27. Schmid C, Pan L, Diss T, Isaacson PG. Expression of B-cell antigens by Hodgkin's and Reed-Sternberg cells. Am J Pathol. 1991;139(4):701-7.
28. Zukerberg LR, Collins AB, Ferry JA, Harris NL. Coexpression of CD15 and CD20 by Reed-Sternberg cells in Hodgkin's disease. Am J Pathol. 1991;139(3):475-83.
29. McCune RC, Syrbu SI, Vasef MA. Expression profiling of transcription factors Pax-5, Oct-1, Oct-2, BOB.1, and PU.1 in Hodgkin's and non-Hodgkin's lymphomas: a comparative study using high throughput tissue microarrays. Mod Pathol. 2006;19(7):1010-8.
30. Natkunam Y, Hsi ED, Aoun P, Zhao S, Elson P, Pohlman B, et al. Expression of the human germinal center-associated lymphoma (HGAL) protein identifies a subset of classic Hodgkin lymphoma of germinal center derivation and improved survival. Blood. 2007;109(1):298-305.
31. Agostinelli C, Paterson JC, Gupta R, Righi S, Sandri F, Piccaluga PP, et al. Detection of LIM domain only 2 (LMO2) in normal human tissues and haematopoietic and non-

haematopoietic tumours using a newly developed rabbit monoclonal antibody. Histopathology. 2012;61(1):33-46.

32. Menter T, Gasser A, Juskevicius D, Dirnhofer S, Tzankov A. Diagnostic Utility of the Germinal Center-associated Markers GCET1, HGAL, and LMO2 in Hematolymphoid Neoplasms. Appl Immunohistochem Mol Morphol. 2015;23(7):491-8.
33. Aladily TN, Mansour A, Alsughayer A, Sughayer M, Medeiros LJ. The utility of CD83, fascin and CD23 in the differential diagnosis of primary mediastinal large B-cell lymphoma versus classic Hodgkin lymphoma. Ann Diagn Pathol. 2019;40:72-6.
34. Marafioti T, Hummel M, Foss HD, Laumen H, Korbjuhn P, Anagnostopoulos I, et al. Hodgkin and reed-sternberg cells represent an expansion of a single clone originating from a germinal center B-cell with functional immunoglobulin gene rearrangements but defective immunoglobulin transcription. Blood. 2000;95(4):1443-50.
35. Schwering I, Brauninger A, Klein U, Jungnickel B, Tinguely M, Diehl V, et al. Loss of the B-lineage-specific gene expression program in Hodgkin and Reed-Sternberg cells of Hodgkin lymphoma. Blood. 2003;101(4):1505-12.
36. Mathas S, Hartmann S, Kuppers R. Hodgkin lymphoma: Pathology and biology. Semin Hematol. 2016;53(3):139-47.
37. Renne C, Martin-Subero JI, Eickernjager M, Hansmann ML, Kuppers R, Siebert R, et al. Aberrant expression of ID2, a suppressor of B-cell-specific gene expression, in Hodgkin's lymphoma. Am J Pathol. 2006;169(2):655-64.
38. Ushmorov A, Leithauser F, Sakk O, Weinhausel A, Popov SW, Moller P, et al. Epigenetic processes play a major role in B-cell-specific gene silencing in classical Hodgkin lymphoma. Blood. 2006;107(6):2493-500.
39. Jundt F, Acikgoz O, Kwon SH, Schwarzer R, Anagnostopoulos I, Wiesner B, et al. Aberrant expression of Notch1 interferes with the B-lymphoid phenotype of neoplastic B cells in classical Hodgkin lymphoma. Leukemia. 2008;22(8):1587-94.
40. Mottok A, Steidl C. Biology of classical Hodgkin lymphoma: implications for prognosis and novel therapies. Blood. 2018;131(15):1654-65.
41. Jungnickel B, Staratschek-Jox A, Brauninger A, Spieker T, Wolf J, Diehl V, et al. Clonal deleterious mutations in the IkappaBalpha gene in the malignant cells in Hodgkin's lymphoma. J Exp Med. 2000;191(2):395-402.
42. Barth TF, Martin-Subero JI, Joos S, Menz CK, Hasel C, Mechtersheimer G, et al. Gains of 2p involving the REL locus correlate with nuclear c-Rel protein accumulation in neoplastic cells of classical Hodgkin lymphoma. Blood. 2003;101(9):3681-6.
43. Martin-Subero JI, Wlodarska I, Bastard C, Picquenot JM, Hoppner J, Giefing M, et al. Chromosomal rearrangements involving the BCL3 locus are recurrent in classical Hodgkin and peripheral T-cell lymphoma. Blood. 2006;108(1):401-2; author reply 2-3.
44. Schmitz R, Hansmann ML, Bohle V, Martin-Subero JI, Hartmann S, Mechtersheimer G, et al. TNFAIP3 (A20) is a tumor suppressor gene in Hodgkin lymphoma and primary mediastinal B cell lymphoma. J Exp Med. 2009;206(5):981-9.
45. Steidl C, Telenius A, Shah SP, Farinha P, Barclay L, Boyle M, et al. Genome-wide copy number analysis of Hodgkin Reed-Sternberg cells identifies recurrent imbalances with correlations to treatment outcome. Blood. 2010;116(3):418-27.
46. Mansouri L, Noerenberg D, Young E, Mylonas E, Abdulla M, Frick M, et al. Frequent NFKBIE deletions are associated with poor outcome in primary mediastinal B-cell lymphoma. Blood. 2016;128(23):2666-70.
47. Joos S, Kupper M, Ohl S, von Bonin F, Mechtersheimer G, Bentz M, et al. Genomic imbalances including amplification of the tyrosine kinase gene JAK2 in CD30+ Hodgkin cells. Cancer Res. 2000;60(3):549-52.
48. Hinz M, Lemke P, Anagnostopoulos I, Hacker C, Krappmann D, Mathas S, et al. Nuclear factor kappaB-dependent gene expression profiling of Hodgkin's disease tumor cells, pathogenetic significance, and link to constitutive signal transducer and activator of transcription 5a activity. J Exp Med. 2002;196(5):605-17.
49. Skinnider BF, Elia AJ, Gascoyne RD, Patterson B, Trumper L, Kapp U, et al. Signal transducer and activator of transcription 6 is frequently activated in Hodgkin and Reed-Sternberg cells of Hodgkin lymphoma. Blood. 2002;99(2):618-26.
50. Weniger MA, Melzner I, Menz CK, Wegener S, Bucur AJ, Dorsch K, et al. Mutations of the tumor suppressor gene SOCS-1 in classical Hodgkin lymphoma are frequent and associated with nuclear phospho-STAT5 accumulation. Oncogene. 2006;25(18):2679-84.
51. Green MR, Monti S, Rodig SJ, Juszczynski P, Currie T, O'Donnell E, et al. Integrative analysis reveals selective 9p24.1 amplification, increased PD-1 ligand expression, and further induction via JAK2 in nodular sclerosing Hodgkin lymphoma and primary mediastinal large B-cell lymphoma. Blood. 2010;116(17):3268-77.
52. Gunawardana J, Chan FC, Telenius A, Woolcock B, Kridel R, Tan KL, et al. Recurrent somatic mutations of PTPN1 in primary mediastinal B cell lymphoma and Hodgkin lymphoma. Nat Genet. 2014;46(4):329-35.
53. Kuppers R, Engert A, Hansmann ML. Hodgkin lymphoma. J Clin Invest. 2012;122(10):3439-47.
54. Mata E, Diaz-Lopez A, Martin-Moreno AM, Sanchez-Beato M, Varela I, Mestre MJ, et al. Analysis of the mutational landscape of classic Hodgkin lymphoma identifies disease heterogeneity and potential therapeutic targets. Oncotarget. 2017;8(67):111386-95.
55. Liang WS, Vergilio JA, Salhia B, Huang HJ, Oki Y, Garrido-Laguna I, et al. Comprehensive Genomic Profiling of Hodgkin Lymphoma Reveals Recurrently Mutated

Genes and Increased Mutation Burden. Oncologist. 2019;24(2):219-28.
56. Mata E, Fernandez S, Astudillo A, Fernandez R, Garcia-Cosio M, Sanchez-Beato M, et al. Genomic analyses of microdissected Hodgkin and Reed-Sternberg cells: mutations in epigenetic regulators and p53 are frequent in refractory classic Hodgkin lymphoma. Blood Cancer J. 2019;9(3):34.
57. Teruya-Feldstein J, Tosato G, Jaffe ES. The role of chemokines in Hodgkin's disease. Leuk Lymphoma. 2000;38(3-4):363-71.
58. Skinnider BF, Mak TW. The role of cytokines in classical Hodgkin lymphoma. Blood. 2002;99(12):4283-97.
59. Steidl C, Connors JM, Gascoyne RD. Molecular pathogenesis of Hodgkin's lymphoma: increasing evidence of the importance of the microenvironment. J Clin Oncol. 2011;29(14):1812-26.
60. King RL, Howard MT, Bagg A. Hodgkin lymphoma: pathology, pathogenesis, and a plethora of potential prognostic predictors. Adv Anat Pathol. 2014;21(1):12-25.
61. van den Berg A, Visser L, Poppema S. High expression of the CC chemokine TARC in Reed-Sternberg cells. A possible explanation for the characteristic T-cell infiltratein Hodgkin's lymphoma. Am J Pathol. 1999;154(6):1685-91.
62. Peh SC, Kim LH, Poppema S. TARC, a CC chemokine, is frequently expressed in classic Hodgkin's lymphoma but not in NLP Hodgkin's lymphoma, T-cell-rich B-cell lymphoma, and most cases of anaplastic large cell lymphoma. Am J Surg Pathol. 2001;25(7):925-9.
63. Ohshima K, Tutiya T, Yamaguchi T, Suzuki K, Suzumiya J, Kawasaki C, et al. Infiltration of Th1 and Th2 lymphocytes around Hodgkin and Reed-Sternberg (H&RS) cells in Hodgkin disease: Relation with expression of CXC and CC chemokines on H&RS cells. Int J Cancer. 2002;98(4):567-72.
64. Fischer M, Juremalm M, Olsson N, Backlin C, Sundstrom C, Nilsson K, et al. Expression of CCL5/RANTES by Hodgkin and Reed-Sternberg cells and its possible role in the recruitment of mast cells into lymphomatous tissue. Int J Cancer. 2003;107(2):197-201.
65. Gerdes J, Kretschmer C, Zahn G, Ernst M, Jones DB, Flad HD. Immunoenzymatic assessment of interferon-gamma in Hodgkin and Sternberg-Reed cells. Cytokine. 1990;2(4):307-10.
66. Hsu PL, Lin YC, Hsu SM. Expression of macrophage colony-stimulating factor (M-CSF) in two Hodgkin's Reed-Sternberg (H-RS) cell lines, HDLM-1 and KM-H2, and in H-RS cells in tissues. Int J Hematol. 1991;54(4):315-26.
67. Truman LA, Ford CA, Pasikowska M, Pound JD, Wilkinson SJ, Dumitriu IE, et al. CX3CL1/fractalkine is released from apoptotic lymphocytes to stimulate macrophage chemotaxis. Blood. 2008;112(13):5026-36.
68. Keir ME, Butte MJ, Freeman GJ, Sharpe AH. PD-1 and its ligands in tolerance and immunity. Annu Rev Immunol. 2008;26:677-704.
69. Chen L, Flies DB. Molecular mechanisms of T cell co-stimulation and co-inhibition. Nat Rev Immunol. 2013;13(4):227-42.
70. Baumeister SH, Freeman GJ, Dranoff G, Sharpe AH. Coinhibitory Pathways in Immunotherapy for Cancer. Annu Rev Immunol. 2016;34:539-73.
71. Boussiotis VA. Molecular and Biochemical Aspects of the PD-1 Checkpoint Pathway. N Engl J Med. 2016;375(18):1767-78.
72. Zou W, Wolchok JD, Chen L. PD-L1 (B7-H1) and PD-1 pathway blockade for cancer therapy: Mechanisms, response biomarkers, and combinations. Sci Transl Med. 2016;8(328):328rv4.
73. Gordon SR, Maute RL, Dulken BW, Hutter G, George BM, McCracken MN, et al. PD-1 expression by tumour-associated macrophages inhibits phagocytosis and tumour immunity. Nature. 2017;545(7655):495-9.
74. Liu WR, Shipp MA. Signaling pathways and immune evasion mechanisms in classical Hodgkin lymphoma. Blood. 2017;130(21):2265-70.
75. Steidl C, Shah SP, Woolcock BW, Rui L, Kawahara M, Farinha P, et al. MHC class II transactivator CIITA is a recurrent gene fusion partner in lymphoid cancers. Nature. 2011;471(7338):377-81.
76. Reichel J, Chadburn A, Rubinstein PG, Giulino-Roth L, Tam W, Liu Y, et al. Flow sorting and exome sequencing reveal the oncogenome of primary Hodgkin and Reed-Sternberg cells. Blood. 2015;125(7):1061-72.
77. Joos S, Menz CK, Wrobel G, Siebert R, Gesk S, Ohl S, et al. Classical Hodgkin lymphoma is characterized by recurrent copy number gains of the short arm of chromosome 2. Blood. 2002;99(4):1381-7.
78. Borchmann S, Engert A. The genetics of Hodgkin lymphoma: an overview and clinical implications. Curr Opin Oncol. 2017;29(5):307-14.
79. Martin-Subero JI, Klapper W, Sotnikova A, Callet-Bauchu E, Harder L, Bastard C, et al. Chromosomal breakpoints affecting immunoglobulin loci are recurrent in Hodgkin and Reed-Sternberg cells of classical Hodgkin lymphoma. Cancer Res. 2006;66(21):10332-8.
80. Sanchez-Espiridion B, Montalban C, Lopez A, Menarguez J, Sabin P, Ruiz-Marcellan C, et al. A molecular risk score based on 4 functional pathways for advanced classical Hodgkin lymphoma. Blood. 2010;116(8):e12-7.
81. Scott DW, Chan FC, Hong F, Rogic S, Tan KL, Meissner B, et al. Gene expression-based model using formalin-fixed paraffin-embedded biopsies predicts overall survival in advanced-stage classical Hodgkin lymphoma. J Clin Oncol. 2013;31(6):692-700.
82. Chan FC, Mottok A, Gerrie AS, Power M, Nijland M, Diepstra A, et al. Prognostic Model to Predict Post-Autologous Stem-Cell Transplantation Outcomes in Classical Hodgkin Lymphoma. J Clin Oncol. 2017;35(32):3722-33.

83. de Jong D, Rosenwald A, Chhanabhai M, Gaulard P, Klapper W, Lee A, et al. Immunohistochemical prognostic markers in diffuse large B-cell lymphoma: validation of tissue microarray as a prerequisite for broad clinical applications--a study from the Lunenburg Lymphoma Biomarker Consortium. J Clin Oncol. 2007;25(7):805-12.
84. Rassidakis GZ, Medeiros LJ, Vassilakopoulos TP, Viviani S, Bonfante V, Nadali G, et al. BCL-2 expression in Hodgkin and Reed-Sternberg cells of classical Hodgkin disease predicts a poorer prognosis in patients treated with ABVD or equivalent regimens. Blood. 2002;100(12):3935-41.
85. Rassidakis GZ, Medeiros LJ, Viviani S, Bonfante V, Nadali GP, Vassilakopoulos TP, et al. CD20 expression in Hodgkin and Reed-Sternberg cells of classical Hodgkin's disease: associations with presenting features and clinical outcome. J Clin Oncol. 2002;20(5):1278-87.
86. Portlock CS, Donnelly GB, Qin J, Straus D, Yahalom J, Zelenetz A, et al. Adverse prognostic significance of CD20 positive Reed-Sternberg cells in classical Hodgkin's disease. Br J Haematol. 2004;125(6):701-8.
87. Sup SJ, Alemany CA, Pohlman B, Elson P, Malhi S, Thakkar S, et al. Expression of bcl-2 in classical Hodgkin's lymphoma: an independent predictor of poor outcome. J Clin Oncol. 2005;23(16):3773-9.
88. Asano N, Oshiro A, Matsuo K, Kagami Y, Ishida F, Suzuki R, et al. Prognostic significance of T-cell or cytotoxic molecules phenotype in classical Hodgkin's lymphoma: a clinicopathologic study. J Clin Oncol. 2006;24(28):4626-33.
89. Hsi ED, Sup SJ, Alemany C, Tso E, Skacel M, Elson P, et al. MAL is expressed in a subset of Hodgkin lymphoma and identifies a population of patients with poor prognosis. Am J Clin Pathol. 2006;125(5):776-82.
90. Diepstra A, van Imhoff GW, Karim-Kos HE, van den Berg A, te Meerman GJ, Niens M, et al. HLA class II expression by Hodgkin Reed-Sternberg cells is an independent prognostic factor in classical Hodgkin's lymphoma. J Clin Oncol. 2007;25(21):3101-8.
91. Canioni D, Deau-Fischer B, Taupin P, Ribrag V, Delarue R, Bosq J, et al. Prognostic significance of new immunohistochemical markers in refractory classical Hodgkin lymphoma: a study of 59 cases. PLoS One. 2009;4(7):e6341.
92. Greaves W, Xiao L, Sanchez-Espiridion B, Kunkalla K, Dave KS, Liang CS, et al. Detection of ABCC1 expression in classical Hodgkin lymphoma is associated with increased risk of treatment failure using standard chemotherapy protocols. J Hematol Oncol. 2012;5:47.
93. Koh YW, Park C, Yoon DH, Suh C, Huh J. Prognostic significance of COX-2 expression and correlation with Bcl-2 and VEGF expression, microvessel density, and clinical variables in classical Hodgkin lymphoma. Am J Surg Pathol. 2013;37(8):1242-51.
94. Venkataraman G, Song JY, Tzankov A, Dirnhofer S, Heinze G, Kohl M, et al. Aberrant T-cell antigen expression in classical Hodgkin lymphoma is associated with decreased event-free survival and overall survival. Blood. 2013;121(10):1795-804.
95. Nguyen TT, Frater JL, Klein J, Chen L, Bartlett NL, Foyil KV, et al. Expression of TIA1 and PAX5 in Classical Hodgkin Lymphoma at Initial Diagnosis May Predict Clinical Outcome. Appl Immunohistochem Mol Morphol. 2016;24(6):383-91.
96. Roemer MGM, Redd RA, Cader FZ, Pak CJ, Abdelrahman S, Ouyang J, et al. Major Histocompatibility Complex Class II and Programmed Death Ligand 1 Expression Predict Outcome After Programmed Death 1 Blockade in Classic Hodgkin Lymphoma. J Clin Oncol. 2018;36(10):942-50.
97. Ozturk V, Yikilmaz AS, Kilicarslan A, Bakanay SM, Akinci S, Dilek I. The Triple Positivity for EBV, PD-1, and PD-L1 Identifies a Very High Risk Classical Hodgkin Lymphoma. Clin Lymphoma Myeloma Leuk. 2020;20(7):e375-81.
98. Oudejans JJ, Jiwa NM, Kummer JA, Ossenkoppele GJ, van Heerde P, Baars JW, et al. Activated cytotoxic T cells as prognostic marker in Hodgkin's disease. Blood. 1997;89(4):1376-82.
99. Alvaro-Naranjo T, Lejeune M, Salvado-Usach MT, Bosch-Princep R, Reverter-Branchat G, Jaen-Martinez J, et al. Tumor-infiltrating cells as a prognostic factor in Hodgkin's lymphoma: a quantitative tissue microarray study in a large retrospective cohort of 267 patients. Leuk Lymphoma. 2005;46(11):1581-91.
100. Kelley TW, Pohlman B, Elson P, Hsi ED. The ratio of FOXP3+ regulatory T cells to granzyme B+ cytotoxic T/NK cells predicts prognosis in classical Hodgkin lymphoma and is independent of bcl-2 and MAL expression. Am J Clin Pathol. 2007;128(6):958-65.
101. Tzankov A, Meier C, Hirschmann P, Went P, Pileri SA, Dirnhofer S. Correlation of high numbers of intratumoral FOXP3+ regulatory T cells with improved survival in germinal center-like diffuse large B-cell lymphoma, follicular lymphoma and classical Hodgkin's lymphoma. Haematologica. 2008;93(2):193-200.
102. Chetaille B, Bertucci F, Finetti P, Esterni B, Stamatoullas A, Picquenot JM, et al. Molecular profiling of classical Hodgkin lymphoma tissues uncovers variations in the tumor microenvironment and correlations with EBV infection and outcome. Blood. 2009;113(12):2765-3775.
103. Steidl C, Lee T, Shah SP, Farinha P, Han G, Nayar T, et al. Tumor-associated macrophages and survival in classic Hodgkin's lymphoma. N Engl J Med. 2010;362(10):875-85.
104. Greaves P, Clear A, Coutinho R, Wilson A, Matthews J, Owen A, et al. Expression of FOXP3, CD68, and CD20 at diagnosis in the microenvironment of classical Hodgkin lymphoma is predictive of outcome. J Clin Oncol. 2013;31(2):256-62.
105. Panico L, Tenneriello V, Ronconi F, Lepore M, Cantore N, Dell'Angelo AC, et al. High CD20+ background cells

predict a favorable outcome in classical Hodgkin lymphoma and antagonize CD68+ macrophages. Leuk Lymphoma. 2015;56(6):1636-42.

106. Andersen MD, Kamper P, Nielsen PS, Bendix K, Riber-Hansen R, Steiniche T, et al. Tumour-associated mast cells in classical Hodgkin's lymphoma: correlation with histological subtype, other tumour-infiltrating inflammatory cell subsets and outcome. Eur J Haematol. 2016;96(3):252-9.
107. Guo B, Cen H, Tan X, Ke Q. Meta-analysis of the prognostic and clinical value of tumor-associated macrophages in adult classical Hodgkin lymphoma. BMC Med. 2016;14(1):159.
108. Hollander P, Rostgaard K, Smedby KE, Molin D, Loskog A, de Nully Brown P, et al. An anergic immune signature in the tumor microenvironment of classical Hodgkin lymphoma is associated with inferior outcome. Eur J Haematol. 2018;100(1):88-97.
109. Gholiha AR, Hollander P, Hedstrom G, Sundstrom C, Molin D, Smedby KE, et al. High tumour plasma cell infiltration reflects an important microenvironmental component in classic Hodgkin lymphoma linked to presence of B-symptoms. Br J Haematol. 2019;184(2):192-201.
110. Esquela-Kerscher A, Slack FJ. Oncomirs - microRNAs with a role in cancer. Nat Rev Cancer. 2006;6(4):259-69.
111. Arribas AJ, Campos-Martin Y, Gomez-Abad C, Algara P, Sanchez-Beato M, Rodriguez-Pinilla MS, et al. Nodal marginal zone lymphoma: gene expression and miRNA profiling identify diagnostic markers and potential therapeutic targets. Blood. 2012;119(3):e9-21.
112. Wang W, Corrigan-Cummins M, Hudson J, Maric I, Simakova O, Neelapu SS, et al. MicroRNA profiling of follicular lymphoma identifies microRNAs related to cell proliferation and tumor response. Haematologica. 2012;97(4):586-94.
113. Sanchez-Espiridion B, Martin-Moreno AM, Montalban C, Figueroa V, Vega F, Younes A, et al. MicroRNA signatures and treatment response in patients with advanced classical Hodgkin lymphoma. Br J Haematol. 2013;162(3):336-47.
114. Porrata LF, Ristow K, Colgan JP, Habermann TM, Witzig TE, Inwards DJ, et al. Peripheral blood lymphocyte/monocyte ratio at diagnosis and survival in classical Hodgkin's lymphoma. Haematologica. 2012;97(2):262-9.
115. Koh YW, Kang HJ, Park C, Yoon DH, Kim S, Suh C, et al. Prognostic significance of the ratio of absolute neutrophil count to absolute lymphocyte count in classic Hodgkin lymphoma. Am J Clin Pathol. 2012;138(6):846-54.
116. Juszczynski P, Ouyang J, Monti S, Rodig SJ, Takeyama K, Abramson J, et al. The AP1-dependent secretion of galectin-1 by Reed Sternberg cells fosters immune privilege in classical Hodgkin lymphoma. Proc Natl Acad Sci U S A. 2007;104(32):13134-9.
117. Ouyang J, Plutschow A, Pogge von Strandmann E, Reiners KS, Ponader S, Rabinovich GA, et al. Galectin-1 serum levels reflect tumor burden and adverse clinical features in classical Hodgkin lymphoma. Blood. 2013;121(17):3431-3.
118. Hsi ED, Li H, Nixon AB, Schoder H, Bartlett NL, LeBlanc M, et al. Serum levels of TARC, MDC, IL-10, and soluble CD163 in Hodgkin lymphoma: a SWOG S0816 correlative study. Blood. 2019;133(16):1762-5.
119. Spina V, Bruscaggin A, Cuccaro A, Martini M, Di Trani M, Forestieri G, et al. Circulating tumor DNA reveals genetics, clonal evolution, and residual disease in classical Hodgkin lymphoma. Blood. 2018;131(22):2413-25.
120. Camus V, Viennot M, Lequesne J, Viailly PJ, Bohers E, Bessi L, et al. Targeted genotyping of circulating tumor DNA for classical Hodgkin lymphoma monitoring: a prospective study. Haematologica. 2020;106(1):154-62.
121. Desch AK, Hartung K, Botzen A, Brobeil A, Rummel M, Kurch L, et al. Genotyping circulating tumor DNA of pediatric Hodgkin lymphoma. Leukemia. 2020;34(1):151-66.
122. Shi Y, Su H, Song Y, Jiang W, Sun X, Qian W, et al. Circulating tumor DNA predicts response in Chinese patients with relapsed or refractory classical hodgkin lymphoma treated with sintilimab. EBioMedicine. 2020;54:102731.
123. Glaser SL, Lin RJ, Stewart SL, Ambinder RF, Jarrett RF, Brousset P, et al. Epstein-Barr virus-associated Hodgkin's disease: epidemiologic characteristics in international data. Int J Cancer. 1997;70(4):375-82.
124. Kapatai G, Murray P. Contribution of the Epstein Barr virus to the molecular pathogenesis of Hodgkin lymphoma. J Clin Pathol. 2007;60(12):1342-9.
125. Jarrett RF, Gallagher A, Jones DB, Alexander FE, Krajewski AS, Kelsey A, et al. Detection of Epstein-Barr virus genomes in Hodgkin's disease: relation to age. J Clin Pathol. 1991;44(10):844-8.
126. Mancuso S, Carlisi M, Santoro M, Napolitano M, Raso S, Siragusa S. Immunosenescence and lymphomagenesis. Immun Ageing. 2018;15:22.
127. Hjalgrim H, Smedby KE, Rostgaard K, Molin D, Hamilton-Dutoit S, Chang ET, et al. Infectious mononucleosis, childhood social environment, and risk of Hodgkin lymphoma. Cancer Res. 2007;67(5):2382-8.
128. Uccini S, Monardo F, Stoppacciaro A, Gradilone A, Agliano AM, Faggioni A, et al. High frequency of Epstein-Barr virus genome detection in Hodgkin's disease of HIV-positive patients. Int J Cancer. 1990;46(4):581-5.
129. Carbone A, Gloghini A. Epstein Barr Virus-Associated Hodgkin Lymphoma. Cancers (Basel). 2018;10(6):163.
130. Vrzalikova K, Sunmonu T, Reynolds G, Murray P. Contribution of Epstein(-)Barr Virus Latent Proteins to the Pathogenesis of Classical Hodgkin Lymphoma. Pathogens. 2018;7(3):59.

131. Murray PG, Young LS. An etiological role for the Epstein-Barr virus in the pathogenesis of classical Hodgkin lymphoma. Blood. 2019;134(7):591-6.
132. Henderson S, Rowe M, Gregory C, Croom-Carter D, Wang F, Longnecker R, et al. Induction of bcl-2 expression by Epstein-Barr virus latent membrane protein 1 protects infected B cells from programmed cell death. Cell. 1991;65(7):1107-15.
133. Laherty CD, Hu HM, Opipari AW, Wang F, Dixit VM. The Epstein-Barr virus LMP1 gene product induces A20 zinc finger protein expression by activating nuclear factor kappa B. J Biol Chem. 1992;267(34):24157-60.
134. Eliopoulos AG, Young LS. Activation of the cJun N-terminal kinase (JNK) pathway by the Epstein-Barr virus-encoded latent membrane protein 1 (LMP1). Oncogene. 1998;16(13):1731-42.
135. Kilger E, Kieser A, Baumann M, Hammerschmidt W. Epstein-Barr virus-mediated B-cell proliferation is dependent upon latent membrane protein 1, which simulates an activated CD40 receptor. EMBO J. 1998;17(6):1700-9.
136. Gires O, Kohlhuber F, Kilger E, Baumann M, Kieser A, Kaiser C, et al. Latent membrane protein 1 of Epstein-Barr virus interacts with JAK3 and activates STAT proteins. EMBO J. 1999;18(11):3064-73.
137. Cahir-McFarland ED, Carter K, Rosenwald A, Giltnane JM, Henrickson SE, Staudt LM, et al. Role of NF-kappa B in cell survival and transcription of latent membrane protein 1-expressing or Epstein-Barr virus latency III-infected cells. J Virol. 2004;78(8):4108-19.
138. Vockerodt M, Morgan SL, Kuo M, Wei W, Chukwuma MB, Arrand JR, et al. The Epstein-Barr virus oncoprotein, latent membrane protein-1, reprograms germinal centre B cells towards a Hodgkin's Reed-Sternberg-like phenotype. J Pathol. 2008;216(1):83-92.
139. Green MR, Rodig S, Juszczynski P, Ouyang J, Sinha P, O'Donnell E, et al. Constitutive AP-1 activity and EBV infection induce PD-L1 in Hodgkin lymphomas and post-transplant lymphoproliferative disorders: implications for targeted therapy. Clin Cancer Res. 2012;18(6):1611-8.
140. Wood VH, O'Neil JD, Wei W, Stewart SE, Dawson CW, Young LS. Epstein-Barr virus-encoded EBNA1 regulates cellular gene transcription and modulates the STAT1 and TGFbeta signaling pathways. Oncogene. 2007;26(28):4135-47.
141. Baumforth KR, Birgersdotter A, Reynolds GM, Wei W, Kapatai G, Flavell JR, et al. Expression of the Epstein-Barr virus-encoded Epstein-Barr virus nuclear antigen 1 in Hodgkin's lymphoma cells mediates Up-regulation of CCL20 and the migration of regulatory T cells. Am J Pathol. 2008;173(1):195-204.
142. Flavell JR, Baumforth KR, Wood VH, Davies GL, Wei W, Reynolds GM, et al. Down-regulation of the TGF-beta target gene, PTPRK, by the Epstein-Barr virus encoded EBNA1 contributes to the growth and survival of Hodgkin lymphoma cells. Blood. 2008;111(1):292-301.
143. Caldwell RG, Wilson JB, Anderson SJ, Longnecker R. Epstein-Barr virus LMP2A drives B cell development and survival in the absence of normal B cell receptor signals. Immunity. 1998;9(3):405-11.
144. Bechtel D, Kurth J, Unkel C, Kuppers R. Transformation of BCR-deficient germinal-center B cells by EBV supports a major role of the virus in the pathogenesis of Hodgkin and posttransplantation lymphomas. Blood. 2005;106(13):4345-50.
145. Chaganti S, Bell AI, Pastor NB, Milner AE, Drayson M, Gordon J, et al. Epstein-Barr virus infection in vitro can rescue germinal center B cells with inactivated immunoglobulin genes. Blood. 2005;106(13):4249-52.
146. Oudejans JJ, Jiwa NM, Kummer JA, Horstman A, Vos W, Baak JP, et al. Analysis of major histocompatibility complex class I expression on Reed-Sternberg cells in relation to the cytotoxic T-cell response in Epstein-Barr virus-positive and -negative Hodgkin's disease. Blood. 1996;87(9):3844-51.
147. Ansell SM, Lesokhin AM, Borrello I, Halwani A, Scott EC, Gutierrez M, et al. PD-1 blockade with nivolumab in relapsed or refractory Hodgkin's lymphoma. N Engl J Med. 2015;372(4):311-9.
148. Meti N, Esfahani K, Johnson NA. The Role of Immune Checkpoint Inhibitors in Classical Hodgkin Lymphoma. Cancers (Basel). 2018;10(6):204.

Narrative Review
Acta Medica Academica 2021;50(1):126-135
DOI: 10.5644/ama2006-124.330

Updated Review on Pathology of Endocervical Adenocarcinoma with Emphasis on Clinically Relevant Findings

Adela Cimic, Xiaolin Liu-Jarin

Department of Pathology and Cell Biology, Columbia University Irving Medical Center, New York, NY, United States

Correspondence: *ac4620@cumc.columbia.edu*; Tel.: + 1 212 342 3013; Fax.: + 1 212 305 1295

Received: 13 January 2021; **Accepted**: 18 February 2021

Abstract
In the present review, we summarize and critically appraise recent advances in the pathology of endocervical adenocarcinoma. In recent years, the diagnosis of endocervical adenocarcinoma has shifted from morphologic criteria classification in 2014 World Health Organization (WHO) to etiology- based classification of International endocervical adenocarcinoma criteria and classification (IECC). IECC recommends classifying endocervical adenocarcinoma into Human Papillomavirus (HPV)-associated and non-HPV-associated. Ultimately, this approach may lead to different treatment options based on molecular pathways rather than purely based on the tumor's grade and stage. Recently, the College of American Pathologists (CAP) has incorporated stromal invasion patterns as an optional data set in the synoptic report. The pattern of invasion classification is a valuable prognostic tool in excision specimens. Conclusion: IECC is a simple classification system that recognizes and classifies endocervical tumors based on pathogenesis and association to HPV. The pathologists should also be familiar with the pattern-based classification of endocervical adenocarcinoma.

Key Words: Endocervical Adenocarcinoma ▪ HPV ▪ Classification ▪ Silva Patterns.

Introduction

Endocervical adenocarcinoma is a relatively rare disease but still accounts for approximately 25% of all cervical carcinomas (1). The most recent World Health Organization (WHO) classification (2014) classifies in the cervical adenocarcinomas based on morphologic findings (2). There are multiple recent advancements in cervical pathology to recognize and to keep in mind for practicing pathologists. In this review article, we will review the most recent changes in cervical pathology to keep the reader up to date.

In the first part, the article will focus on a relatively new classification. It is common knowledge that the high-risk human papillomavirus (HPV) is a primary culprit in developing endocervical adenocarcinoma. International endocervical adenocarcinoma criteria and classification (IECC) classifies endocervical adenocarcinomas into two major subtypes: 1. HPV-associated 2. Non-HPV-associated subtype. This classification incorporates etiology but also coincides with distinctive morphologic patterns and clinical findings (3). The second part will focus on morphologic and stromal invasion patterns and their clinical significance. Proposal for the Silva system for endocervical carcinoma was published in 2013, but it was recently integrated as an optional data set in the College of American Pathologists (CAP) synoptic report.

Lastly, we will briefly comment on changes implemented in the International Federation of Gynecology and Obstetrics (FIGO) staging classification system.

International Endocervical Adenocarcinoma Criteria and Classification (IECC): HPV-Associated Endocervical Adenocarcinoma

HPV-associated endocervical adenocarcinoma has similar risk factors as cervical squamous cell carcinomas, including multiple sexual partners, young age at first intercourse, obesity, smoking etc. Most endocervical adenocarcinomas are HPV-associated and encompass about 85-90% of all endocervical adenocarcinomas (2). Three subtypes HPV 16, 18, and 45, appear to be the most prevalent and accounted for 94% of the cases (4). HPV-associated endocervical adenocarcinoma presents in the younger age (<50 years), and most of them develop in the transformation zone similarly to cervical squamous cell carcinoma. The future treatments based on this classification may be etiology driven and may have better outcomes. The current treatment approach is that all endocervical adenocarcinomas are treated the same, stage by stage, with no specific treatment strategy based on genetic signature or etiology.

Usual Type HPV-Associated Endocervical Adenocarcinoma

Relatively good news is that most endocervical adenocarcinomas are easily recognizable as usual-type endocervical adenocarcinoma. The glands may have papillary, micropapillary, cribriform and single-cell pattern, but the distinctive cytologic features are at least focally present. Those features include pseudostratified, elongated, and enlarged nuclei with eosinophilic cytoplasm and many apical "floating" mitotic figures. Numerous apoptotic bodies are also easily identifiable (Figure 1). The principal differential diagnosis for usual-type endocervical adenocarcinoma is endometrioid adenocarcinoma. Immunohistochemistry (IHC) is very helpful in differentiating the two. While endocervical adenocarcinoma is HPV-associated and p16 strongly and diffusely positive, endometrioid adenocarcinoma is patchy positive for p16 with a high estrogen (ER) and progesterone (PR)

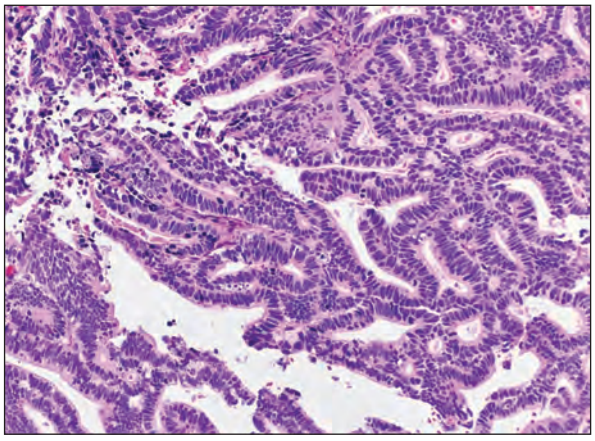

Figure 1. HPV-associated endocervical adenocarcinoma with numerous "floating mitosis" and apoptotic bodies. (Olympus BX43, 20×).

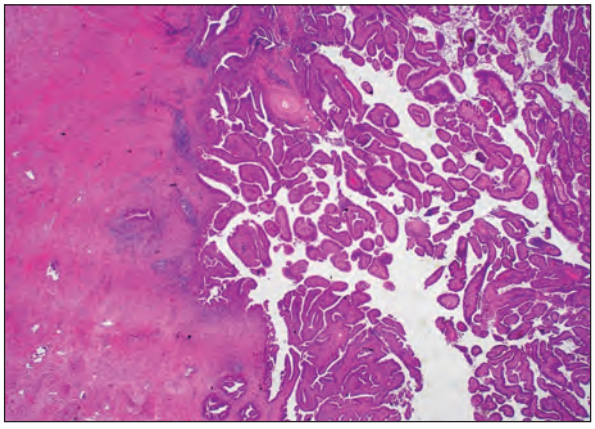

Figure 2. Villoglandular variant of endocervical adenocarcinoma in a 32-year-old woman. Clinically, a large mass with only superficial invasion. Please note that the invasive portion of the tumor is glandular. Eight years later, the patient is well without metastases or recurrence. (Olympus BX43, 2×).

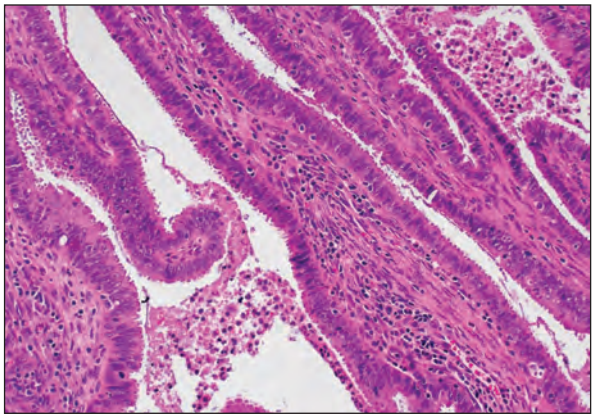

Figure 3. A high-power view reveals classical cytologic features of villoglandular endocervical adenocarcinoma. (Olympus BX43, 20×).

receptor and vimentin positivity (5). While primary endometrioid adenocarcinoma may arise in endometriosis of the cervix, it is exceedingly rare. Preoperative communication with the clinical team and review of radiologic findings will help distinguish these two primary sites.

A rare but distinctive pattern worth mentioning is primary villoglandular endocervical adenocarcinoma. This subtype is recognized by long, thin exophytic papillae with cytologic features of usual-type endocervical adenocarcinoma (Figures 2 and 3). Invasion, if present, is usually superficial. Deeper components/invasive tumor will have glands rather than papillae. This variant is rarely associated with lymphovascular space invasion or lymph node metastasis and therefore carries a better prognosis (6, 7). A gynecologist can grossly visualize the tumors. They may present as a higher stage by the International Federation of Gynecology and Obstetrics (FIGO) staging, which would be treated with hysterectomy. However, if the biopsy suggests this variant, a cone biopsy may be an excellent initial treatment option to evaluate for stromal invasion. The cone excisional biopsy would be sufficient therapy for no or minimal invasion in this subtype of endocervical adenocarcinoma despite the clinical appearance of a larger tumor. This treatment modality should be considered for fertility preservation in young patients.

Additionally, a distinctive pattern is a micropapillary pattern. Microscopically it is characterized by small, cohesive papillary groups of neoplastic cells surrounded by stromal clefting. It is often associated with lymphovascular space invasion and lymph node metastasis (8, 9). The prognosis of this subtype is worse than pure usual type of endocervical adenocarcinoma. It is considered histology of aggressive behavior, and it can be associated with other subtypes (10).

Mucinous Type HPV-Associated Endocervical Adenocarcinoma

Mucinous endocervical adenocarcinomas are a diverse group of tumors. They are defined by the presence of intracellular mucin. The IACC classification recognizes 1. Mucinous adenocarcinoma, not otherwise specified (NOS) 2. Intestinal type, and 3. Signet ring-type. To be classified as such, the tumors have to have >50% of a tumor cell with intracytoplasmic mucin, intestinal goblet cell morphology, or signet cells, respectively. To be classified as HPV-associated, all mucinous types have at least a small morphologic component of usual type endocervical adenocarcinoma (3).

Another distinctive subtype and a relatively newly described entity is invasive stratified mucinous endocervical adenocarcinoma (iSMILE) (11). Histologic features are characteristic invasive nests of stratified columnar epithelium with hyperchromatic nuclei and variable amounts of intracytoplasmic mucin (Figures 4-5). Intracytoplasmic mucin may range from large intracellular droplets

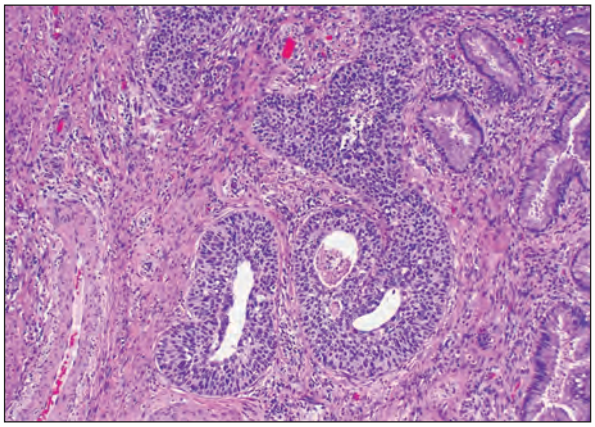

Figure 4. iSMILE nests of neoplastic cells lined with palisading cells at the periphery. (Olympus BX43, 10×).

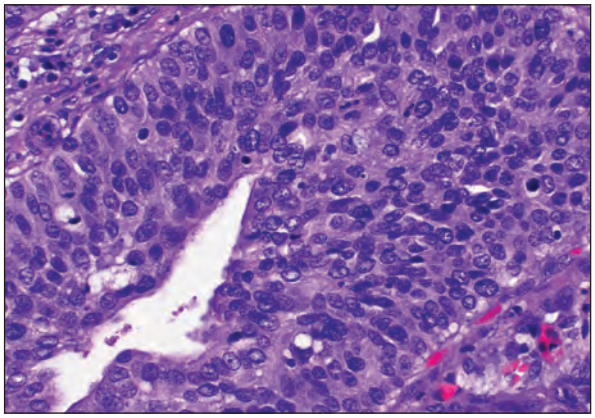

Figure 5. iSMILE mucin-poor variant can be difficult to distinguish on the biopsy material from glandular involvement. (Olympus BX43, 40×).

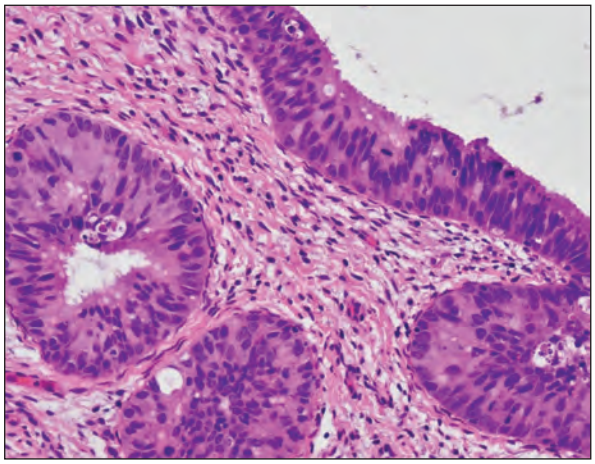

Figure 6. The very classical look of SMILE lesion with intracellular mucin in this stratified epithelium. Mitotic figures are readily identified. This entity is often coupled with endocervical adenocarcinoma in situ or squamous intraepithelial lesion. (Olympus BX43, 40×).

to almost entirely mucin depleted lesions. The nests at the periphery are lined by palisading cells that tend to be positive for p40 and p63. The tumor has a lower prevalence for PAX8 immunostaining with frequent nuclear expression of p53 by immunohistochemistry. The mucin-poor variant may be difficult to recognize, but the large nests with the characteristic immunohistochemistry support the diagnosis. This lesion often arises or is associated with histologically distinct intraepithelial lesion-stratified mucinous intraepithelial lesion (SMILE) (Figure 6). This distinct entity is readily recognizable by multi-layered and stratified epithelium similar to the squamous intraepithelial lesion but intracytoplasmic mucin vacuoles. The lesion is positive for p16 by immunohistochemistry. The previously recognized adenosquamous carcinoma should be only diagnosed in the presence of unequivocal adenocarcinoma and squamous cell carcinoma component (12).

International Endocervical Adenocarcinoma Criteria and Classification (IECC): Non-HPV-Associated Endocervical Adenocarcinoma

Non-HPV-associated endocervical adenocarcinoma has four subtypes. The most common is a gastric subtype, followed by clear cell, endometrioid, and mesonephric adenocarcinoma.

Gastric Type Endocervical Adenocarcinoma

Gastric type endocervical adenocarcinoma is a spectrum of lesions that ranges from well-differentiated to poorly differentiated adenocarcinomas (Figures 7-9). This type of adenocarcinoma usually occurs in older patients. It usually presents as a larger lesion and often with no history of positive HPV test or abnormal Pap test. Lobular cervical glandular hyperplasia (LCGH) has been suggested to be a precursor lesion. This adenocarcinoma has pale cytoplasm, distinct cytoplasmic borders, deep invasion, glands near blood vessels, and often pools of mucin. Gastric type mucin can be easily identified using Alcian blue/PAS stain or MUC6 immunohistochemistry staining (13). The pathogenesis is via HPV independent pathways driven by *TP53, SDK 11, GNAS*, and *KRAS* mutations (14). Immunohistochemistry profile is not specific, and many times the cells are positive for only for CK7. MUC6 and p53 immunoreactivity can be seen in almost half of the cases. PAX8 is frequently negative. Genetically, the associations have been made with Lynch (Hereditary non-polyposis colorectal cancer syndrome) and Peutz-Jeghers syndromes (15, 16).

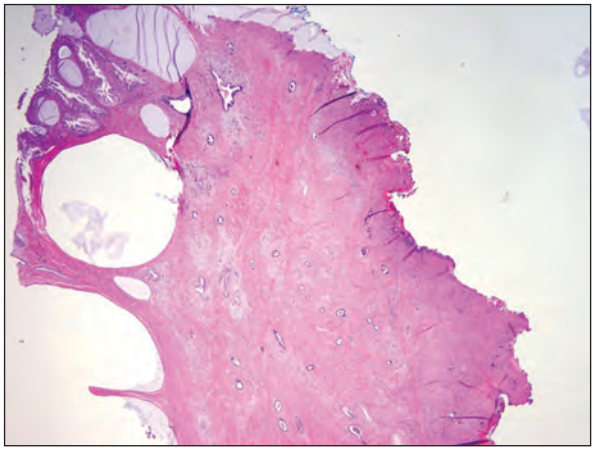

Figure 7. Gastric type endocervical adenocarcinoma. The low-power view reveals deep, destructive growth. (Olympus BX43, 2×).

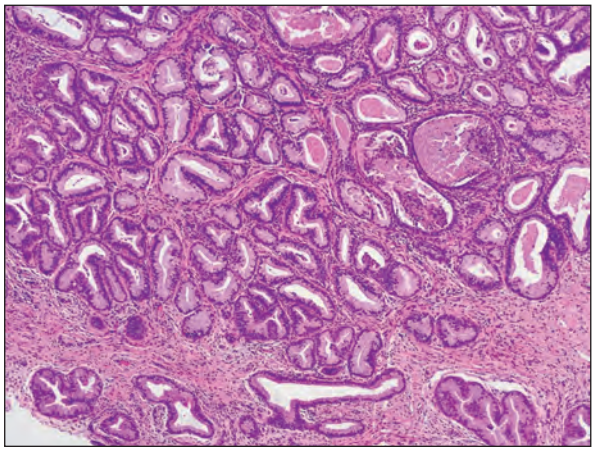

Figure 8. Complex glandular growth in gastric-type endocervical adenocarcinoma. Most cells are mucinous. (Olympus BX43, 10×).

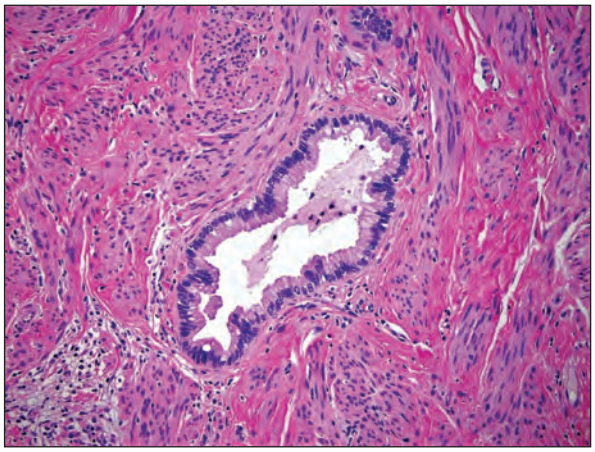

Figure 9. The glands may appear deceivingly bland and can be easily missed on the biopsy material. (Olympus BX43, 20×).

Clear Cell Type Endocervical Carcinoma

Clear cell carcinoma of the lower genital tract has been historically connected with exposure to the diethylstilbestrol. Nowadays, this association is almost never seen. In current milieu of endocervical carcinomas, clear cell carcinoma is rather rare and usually presents in older patients. It is important to emphasize that it is not unheard of to see a younger patient present with clear cell carcinoma (Figure 10). The studies have shown that this carcinoma is not HPV-associated, and despite that about one-third of the cases have been reported to be p16 strongly positive. Positivity for p16 in these cases is seen as a result of aberrant *Retinoblastoma (Rb)* pathway rather than the HPV infection (17). Diagnosis is best achieved on morphologic criteria: large clear cells with abundant cytoplasm and hyalinized background. The nuclei are high-grade with prominent nucleoli. Immunohistochemistry is not particularly useful, but it is essential to mention that the cells are usually positive for HNF-1B, Napsin-A, MUC6 with sometimes aberrant p53 staining. The differential diagnosis in young patients includes pregnancy-related changes (Arias-Stella reaction) and exuberant microglandular hyperplasia (Figure 11) (18, 19). These benign glands are usually strongly positive for ER and PR, while clear cell carcinoma cells are usually negative.

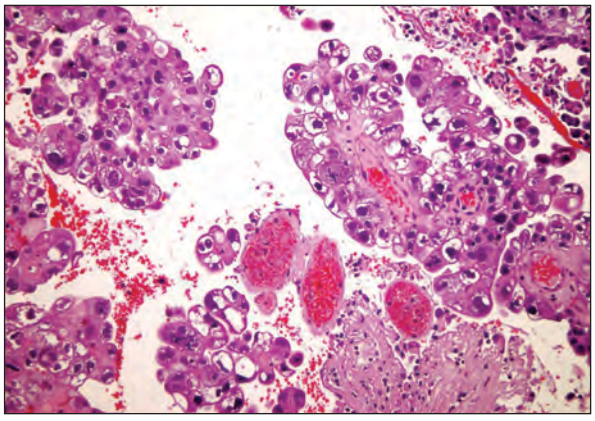

Figure 10. Large cervical mass in a young patient. The histologic finding of clear cell carcinoma. No history of exposure to the diethylstilbestrol. (Olympus BX43, 20×).

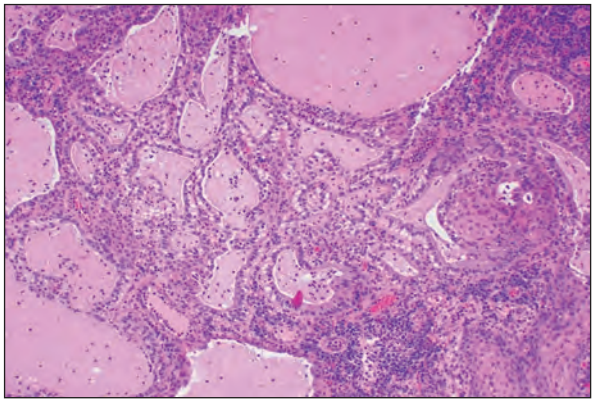

Figure 11. Microglandular adenosis/hyperplasia may look rather complex with cytoplasmic clearing. Nuclear features are low-grade with little variation in size. Mitoses are rare. (Olympus BX43, 10×).

Endometrioid Adenocarcinoma of Endocervix

Endometrial adenocarcinoma of the cervix is a difficult entity to diagnose and the terminology may be confused with endometrial adenocarcinoma. Cervical primary tumor is associated with cervical endometriosis. Histologically, it exhibits endometrioid morphology, columnar pseudostratified cells with squamous morules with predominantly intermediate nuclear grade. This particular type of endocervical adenocarcinoma is rare and not HPV-associated (Figure 12). The primary consideration has to be given to the possibility of endometrial adenocarcinoma extending from the uterus. The best way to differentiate the two would be on hysterectomy specimens where the tumor must be extensively sampled, and the bulk of the tumor is arising from the cervix (13). Immunohistochemistry findings are similar to immunohistochemistry findings in classical endometrioid type adenocarcinoma with patchy p16 positivity, variable positivity for estrogen (ER) and progesterone (PR), and a consistent vimentin positivity.

Mesonephric-Type Adenocarcinoma

This extremely rare tumor usually arises from mesonephric remnants. Mesonephric adenocarcinoma usually displays various growth patterns: ducts, tubules, papillary formations, and slit-like glands. One pattern can be dominant or solitary in the tumor. Cytologically, mesonephric carcinomas reveal bland tumor cells with scant cytoplasm with tubular structures with luminal eosinophilic secretions (Figure 13). Immunohistochemistry findings are extremely helpful in establishing the diagnosis. The tumors are usually negative for ER and PR but are GATA3, calretinin, CD10, and TTF-1 positive (20, 21). The molecular studies have shown alterations in *KRAS* and *NRAS* genes and chromatin remodeling gene mutations such as *ARID1A, ARID1B*, and *SMARCA4* (22). The primary differential diagnosis is a florid type mesonephric hyperplasia (Figure 14).

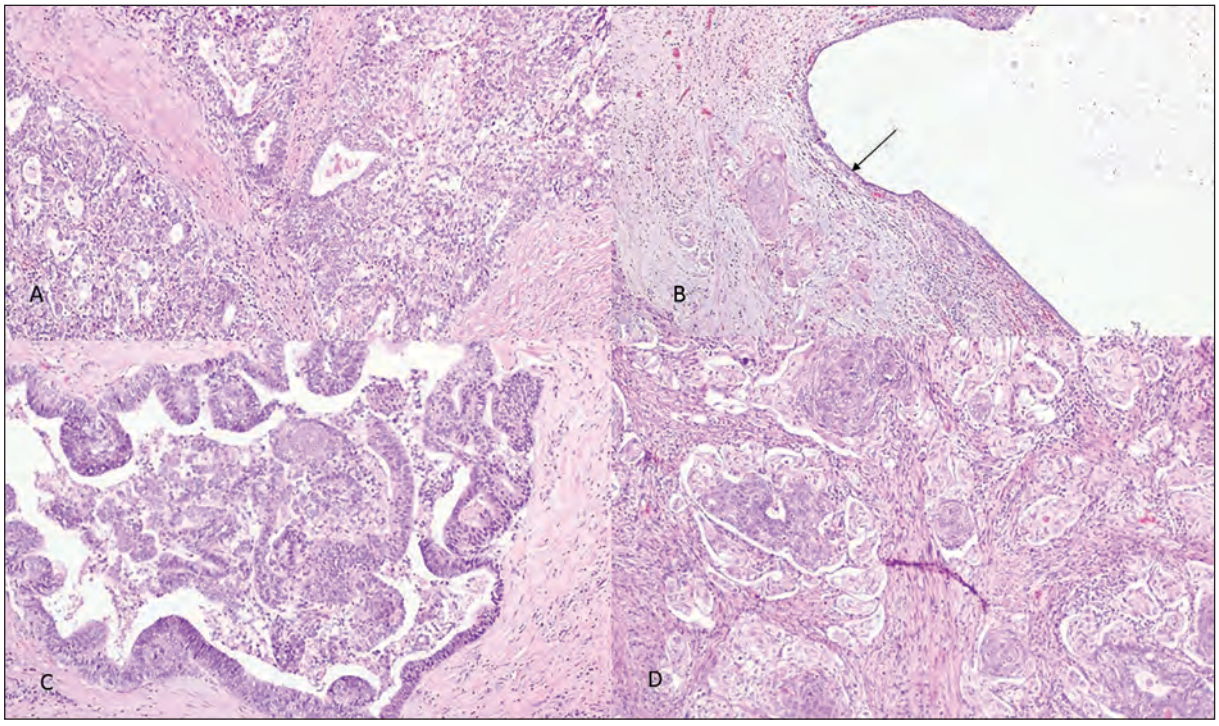

Figure 12A-D. A. Endometrioid adenocarcinoma of the uterine cervix with back to back glands B. Foci of endometriosis C. Focally more classical endometrioid cytologic features D. Prominent squamous morules. (Olympus BX43, A-10×, B-4×, C-20×, D-20×).

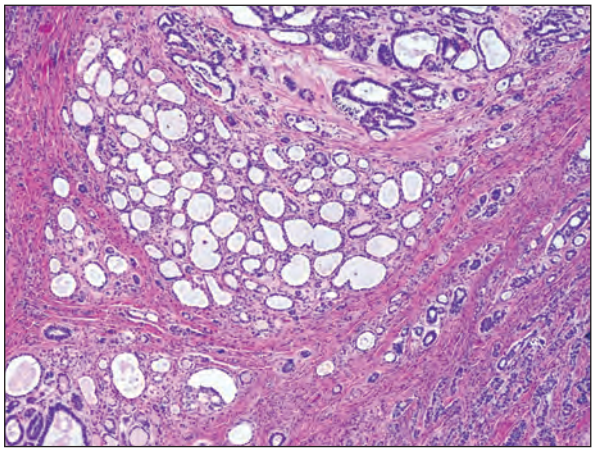

Figure 13. Mesonephric carcinoma of the cervix with infiltrative growth pattern composed of small tubes lined by cuboidal cells with scant cytoplasm. (Olympus BX43, 4×).

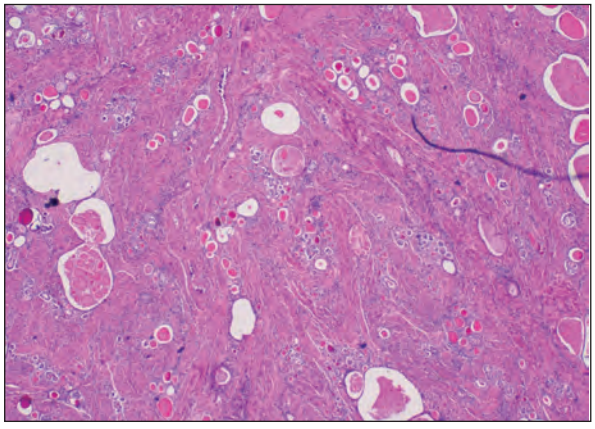

Figure 14. Florid mesonephric hyperplasia retains lobular architecture with associated ducts. No glandular crowding, solid growth, or nuclear atypia. (Olympus BX43, 4×).

Pattern Based Classification of Endocervical Adenocarcinoma

The pattern-based classification of endocervical adenocarcinoma (Silva pattern of invasion) was first recognized and published several years ago (23-26). Recently, the College of American Pathologists (CAP) included this classification as optional data into a synoptic report. Measuring the depth of invasion for endocervical adenocarcinoma can be problematic since it is difficult to estimate from which endocervical gland the invasion originates. Besides, there are no provided guidelines for measurements of the depth of invasion. Sometimes, endocervical adenocarcinoma grows exophytically, and it may be difficult to subtract exuberant exophytic growth from a true invasion. This may lead to an over-estimate of the depth of invasion, consequently causing overtreatment. The pattern-based classification approach has been proven to have quite good interobserver variability and an excellent prognostic value (23). It is important to mention that the system applies only to HVP-associated usual type endocervical adenocarcinoma. The entire tumor has to be examined microscopically to assign the appropriate group. This three-tier system essentially provides risk stratification analysis for the patients (24). The invasion and pattern-based classification was developed in 2013, and the system was validated in subsequent studies, including the assessment of interobserver variability (25-28).

Pattern A can be assigned to the tumors composed of glands with rounded contours, frequently forming groups, and cribriform structures. Papillary growth is acceptable. No destructive stromal invasion, no single cells, or lymphovascular invasion should be seen in this pattern. The solid growth is not acceptable (Figures 15-16) (26, 27).

Pattern B can show focal destructive stromal invasion mostly from the pattern A appearing glands with small groups of tumor cells within desmoplastic stroma or inflammation. Invasion foci can be single, multiple, or linear at the tumor base. The lymphovascular invasion may be present. Solid growth is not acceptable (Figure 17) (26).

Pattern C is easily recognized as a destructive stromal invasion with infiltrating angulated and open glands or solid growth pattern. It is important to remember that the solid growth pattern is considered a high-grade pattern, and nuclear grade can be disregarded. The extensive desmoplastic response is frequently present (Figures 18-20). The lymphovascular invasion may be present.

It is important to emphasize that quantitative criteria for pattern C classification is a linear focus of destructive invasion at the base or advancing front of the tumor filling the diameter of 4X field (5 millimeters or more). This guideline is provided to give some quantitative guidelines to better distinction distinguish pattern B from pattern C classification (26).

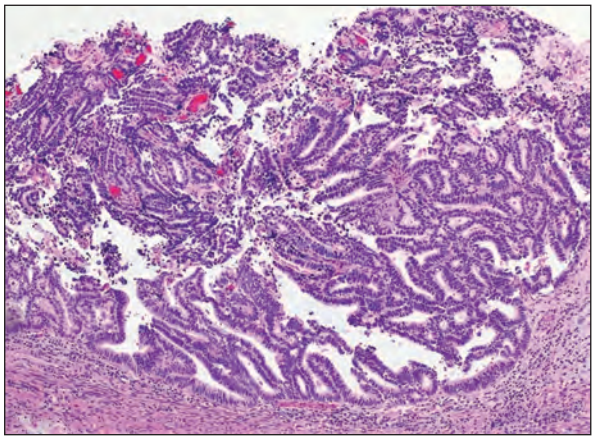

Figure 15. Back to back glands with rounded contours. This exuberant architectural complexity differentiates it from in-situ adenocarcinoma. No infiltrative or solid growth. The findings are compatible with pattern A tumor. (Olympus BX43, 10×).

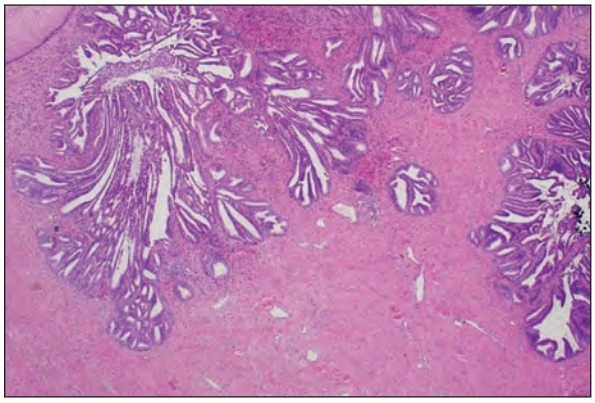

Figure 16. Low power view of pattern A tumor; deeper portions of the tumor do not elicit a stromal response. (Olympus BX43, 4×).

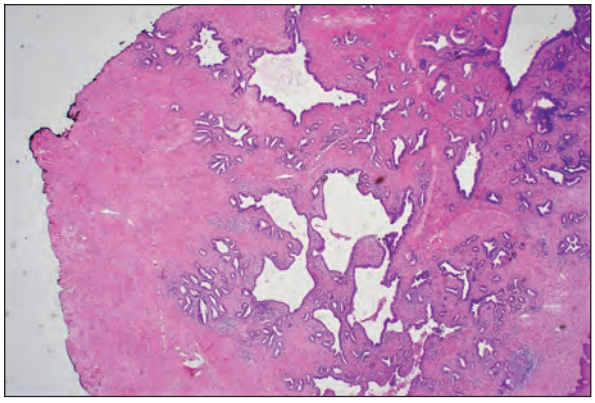

Figure 17. Pattern B shows predominately pattern A glands with foci of destructive growth. This emphasizes the importance of examining the entire specimen before assigning the pattern. (Olympus BX43, 4×).

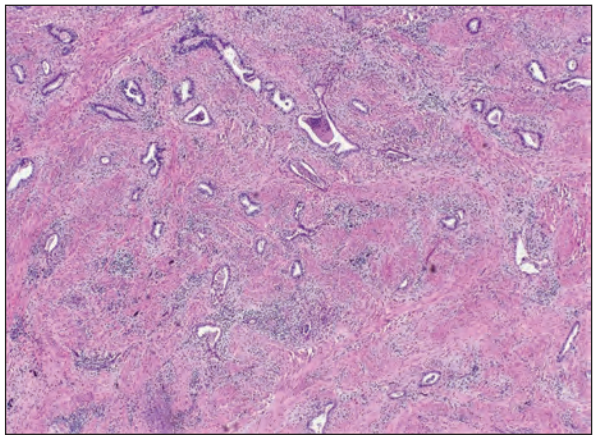

Figure 18. This tumor was assigned pattern C with deep invasion and infiltrative growth. (Olympus BX43, 4×).

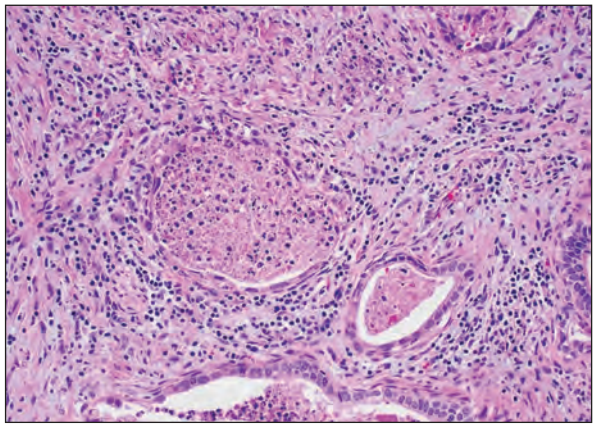

Figure 19. High-power view of desmoplastic response and inflammation around every gland. (Olympus BX43, 40×).

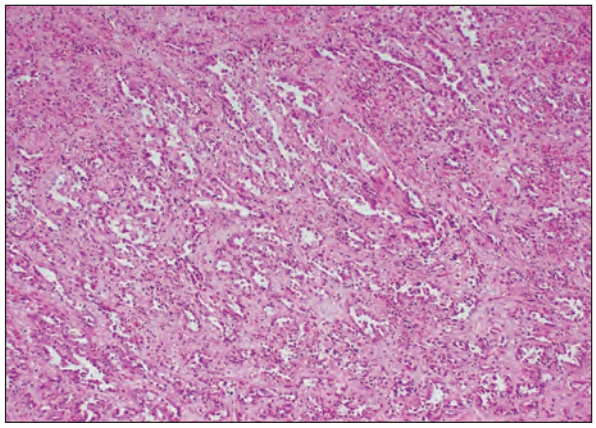

Figure 20. Another pattern C destructive growth and maze-like glands. (Olympus BX43, 20×).

Risk Stratification and Clinical Outcomes

Tumors classified as pattern A are not associated with a risk of lymph node metastasis. They are limited to stage one, and they do not recur. Pattern B tumors also frequently present as stage one. However, given the allowed presence of lymphovascular space invasion, some tumors are at risk for lymph node metastasis. The studies have shown that the pattern C tumors frequently present at the higher stage, and 22% of tumors present with lymph node metastasis. Additionally, about 20% of the cases show a local recurrence of the tumor (28). The classification is useful and reproducible only in excision procedures, and it has limited potential in biopsy material, particularly in pattern A tumors. However, based on the presence of lymphovascular space invasion or solid growth pattern in the biopsy material, the patient may undergo treatment with a more aggressive deeper excision instead of a superficial loop electrosurgical excision procedure (LEEP) (29, 30).

FIGO Staging

The International Federation of Gynecology and Obstetrics (FIGO) staging system is based on the presence or absence of a clinically visible or palpable lesion. The clinically visible mass implies at least stage FIGO IB1. If the tumor is not clinically visible, the staging relies on microscopic measurements. IA1 includes ≤3 mm depth, whereas IA2 includes >3 mm but <5 mm depth. Horizontal extent is now an optional data point in CAP synoptic report. It is no longer used in the AJCC staging update of the 2018 FIGO classification (31). However, the pathologists are encouraged to report horizontal spread in smaller tumors since it is still a valuable data point for future research.

Conclusions

In conclusion, International Endocervical Adenocarcinoma Criteria and Classification (IECC) is a simple classification system that recognizes and classifies endocervical tumors based on pathogenesis and association to HPV. This may facilitate better treatment options based on the natural history of this cancer. The pathologists should also be familiar with the pattern-based classification of endocervical adenocarcinoma. If excisional biopsies show pattern A or B, the entire tumor should be submitted. Future treatments can be based on this classification system, given an excellent interobserver variability. Lastly, FIGO staging does not include horizontal extent, but the pathologists are encouraged to provide this optional data point for future research purposes.

Conflict of Interest: The authors declare that they have no conflict of interest.

References

1. Wilbur DC, Colgan TJ, Ferenczy AS, Hirschowitz L, Loening T, McCluggage WG, et al. Tumors of the uterine cervix - glandular tumors and precursors. In: Kurman RJ, Carcangiu ML, Herrington CS, Young RH, editors. WHO classification of tumours of female reproductive organs. 4th edition. Lyon: International Agency for Research on Cancer; 2014. p. 183-94.
2. Kurman RJ, Carcangiu ML, Herrington CS, Young RH, editors. WHO classification of tumors of female reproductive organs. 4th edition. Lyon: International Agency for Research on Cancer; 2014.
3. Stolnicu S, Barsan I, Hoang L, Patel P, Terinte C, Pesci A, et al. International Endocervical Adenocarcinoma Criteria and Classification (IECC): A New Pathogenetic Classification for Invasive Adenocarcinomas of the Endocervix. Am J Surg Pathol. 2018;42(2):214-26.
4. Pirog EC, Lloveras B, Molijn A, Tous S, Guimerà N, Alejo M, et al. HPV prevalence and genotypes in different histological subtypes of cervical adenocarcinoma, a worldwide analysis of 760 cases. Mod Pathol. 2014;27(12):1559-67.
5. Stolnicu S, Hoang L, Soslow RA. Recent advances in invasive adenocarcinoma of the cervix. Virchows Arch. 2019;475(5):537-49.
6. Korach J, Machtinger R, Perri T, Vicus D, Segal J, Fridman E, et al. Villoglandular papillary adenocarcinoma of the uterine cervix: a diagnostic challenge. Acta Obstet Gynecol Scand. 2009;88(3):355-8.
7. Jones MW, Silverberg SG, Kurman RJ. Well-differentiated villoglandular adenocarcinoma of the uterine cervix: a clinicopathological study of 24 cases. Int J Gynecol Pathol. 1993;12(1):1-7.
8. Stewart CJR, Koay MHE, Leslie C, Acott N, Leung YC. Cervical carcinomas with a micropapillary component: a

clinicopathological study of eight cases. Histopathology. 2018;72(4):626-33.

9. Toyoda S, Kita T, Sugiura A, Itani Y, Okada H, Nakamura S, et al. Cervical adenocarcinoma with stromal micropapillary pattern. Diagn Cytopathol. 2016;44(2):133-6.
10. Alvarado-Cabrero I, McCluggage WG, Estevez-Castro R, Pérez-Montiel D, Stolnicu S, Ganesan R, et al. Micropapillary Cervical Adenocarcinoma: A Clinicopathologic Study of 44 Cases. Am J Surg Pathol. 2019;43(6):802-9.
11. Lastra RR, Park KJ, Schoolmeester JK. Invasive Stratified Mucin-producing Carcinoma and Stratified Mucin-producing Intraepithelial Lesion (SMILE): 15 Cases Presenting a Spectrum of Cervical Neoplasia With Description of a Distinctive Variant of Invasive Adenocarcinoma. Am J Surg Pathol. 2016;40(2):262-9.
12. Stolnicu S, Hoang L, Hanko-Bauer O, Barsan I, Terinte C, Pesci A, et al. Cervical adenosquamous carcinoma: detailed analysis of morphology, immunohistochemical profile, and clinical outcomes in 59 cases. Mod Pathol. 2019;32(2):269-79.
13. Stolnicu S, Hoang L, Soslow RA. Recent advances in invasive adenocarcinoma of the cervix. Virchows Arch. 2019;75(5):537-49.
14. Park E, Kim SW, Kim S, Kim HS, Lee JY, Kim YT, et al. Genetic characteristics of gastric-type mucinous carcinoma of the uterine cervix. Mod Pathol. 2020 Jul 8. doi: 10.1038/s41379-020-0614-0. Epub ahead of print.
15. Moat M, O'Donnell RL, McCluggage WG, Ralte A, Edmondson RJ. Gastric-type adenocarcinoma of the cervix in a patient with Lynch syndrome: A case report. Gynecol Oncol Rep. 2014;10:41-3.
16. Ito M, Minamiguchi S, Mikami Y, Ueda Y, Sekiyama K, Yamamoto T, et al. Peutz-Jeghers syndrome-associated atypical mucinous proliferation of the uterine cervix: a case of minimal deviation adenocarcinoma ('adenoma malignum') in situ. Pathol Res Pract. 2012;208(10):623-7.
17. Stolnicu S, Barsan I, Hoang L, Patel P, Chiriboga L, Terinte C, et al. Diagnostic Algorithmic Proposal Based on Comprehensive Immunohistochemical Evaluation of 297 Invasive Endocervical Adenocarcinomas. Am J Surg Pathol. 2018;42(8):989-1000.
18. Nucci MR, Young RH. Arias-Stella reaction of the endocervix: a report of 18 cases with emphasis on its varied histology and differential diagnosis. Am J Surg Pathol. 2004;28(5):608-12.
19. Nucci, M. Pseudoneoplastic Glandular Lesions of the Uterine Cervix: A Selective Review. Int J Gynecol Pathol. 2014;33(4):330-8.
20. Silver SA, Devouassoux-Shisheboran M, Mezzetti TP, Tavassoli FA. Mesonephric adenocarcinomas of the uterine cervix: a study of 11 cases with immunohistochemical findings. Am J Surg Pathol. 2001;25(3):379-87.
21. Kenny SL, McBride HA, Jamison J, McCluggage WG. Mesonephric adenocarcinomas of the uterine cervix and corpus: HPV-negative neoplasms that are commonly PAX8, CA125, and HMGA2 positive and that may be immunoreactive with TTF1 and hepatocyte nuclear factor 1-β. Am J Surg Pathol. 2012;36(6):799-807.
22. Mirkovic J, Sholl LM, Garcia E, Lindeman N, MacConaill L, Hirsch M, et al. Targeted genomic profiling reveals recurrent KRAS mutations and gain of chromosome 1q in mesonephric carcinomas of the female genital tract. Mod Pathol. 2015;28(11):1504-14.
23. Rutgers JK, Roma AA, Park KJ, Zaino RJ, Johnson A, Alvarado I, et al. Pattern classification of endocervical adenocarcinoma: reproducibility and review of criteria. Mod Pathol. 2016;29(9):1083-94.
24. Turashvili G, Park KJ. Cervical Glandular Neoplasia: Classification and Staging. Surg Pathol Clin. 2019;12(2):281-313.
25. Diaz De Vivar A, Roma AA, Park KJ, Alvarado-Cabrero I, Rasty G, Chanona-Vilchis JG, et al. Invasive endocervical adenocarcinoma: proposal for a new pattern-based classification system with significant clinical implications: a multi-institutional study. Int J Gynecol Pathol. 2013;32(6):592-601
26. Roma AA, Diaz De Vivar A, Park KJ, Alvarado-Cabrero I, Rasty G, Chanona-Vilchis JG, et al. Invasive endocervical adenocarcinoma: a new pattern-based classification system with important clinical significance. Am J Surg Pathol. 2015;39(5):67-72.
27. Paquette C, Jeffus SK, Quick CM, Conaway MR, Stoler MH, Atkins KA. Interobserver variability in the application of a proposed histologic subclassification of endocervical adenocarcinoma. Am J Surg Pathol. 2015;39(1):93-100.
28. Roma AA, Park KJ, Xie H, De Vivar AD, Alvarado-Cabrero I, Rutgers JKL, et al. Role of Lymphovascular Invasion in Pattern C Invasive Endocervical Adenocarcinoma. Am J Surg Pathol. 2017;41(9):1205-11.
29. Roma AA, Mistretta TA, Diaz De Vivar A, Park KJ, Alvarado-Cabrero I, Rasty G, et al. New pattern-based personalized risk stratification system for endocervical adenocarcinoma with important clinical implications and surgical outcome. Gynecol Oncol. 2016;141(1):36-42.
30. Roma AA, Diaz De Vivar A, Park KJ, Alvarado-Cabrero I, Rasty G, Chanona-Vilchis JG, et al. Invasive endocervical adenocarcinoma: a new pattern-based classification system with important clinical significance. Am J Surg Pathol. 2015;39(5):667-72.
31. Bhatla N, Berek JS, Cuello Fredes M, Denny LA, Grenman S, Karunaratne K, et al. Revised FIGO staging for carcinoma of the cervix uteri. Int J Gynaecol Obstet. 2019;145(1):129-35.

Narrative Review
Acta Medica Academica 2021;50(1):136-142
DOI: 10.5644/ama2006-124.331

Pathology Informatics Education during the COVID-19 Pandemic at Memorial Sloan Kettering Cancer Center (MSKCC)

David Kim[1], Matthew G. Hanna[2], Chad Vanderbilt[2], S. Joseph Sirintrapun[2]

[1]Department of Pathology and Laboratory Medicine, Weill Cornell Medicine, New York, NY, United States, [2]Department of Pathology and Warren Alpert Center for Computational and Digital Pathology, Memorial Sloan Kettering Cancer Center, New York, NY, United States

Correspondence: *dak9117@nyp.org*; Tel.: + 1 212 746 2832; Fax: + 1 212 746 8545

Received: 20 January 2021; **Accepted:** 22 February 2021

Abstract
This review details the development and structure of a four-week rotation in pathology informatics for a resident trainee at Memorial Sloan Kettering Cancer Center (MSKCC) in New York City so that other programs interested in such a rotation can refer to. The role of pathology informatics is exponentially increasing in research and clinical practice. With an ever-expanding role, training in pathology informatics is paramount as pathology training programs and training accreditation bodies recognize the need for pathology informatics in training future pathologists. However, due to its novelty, many training programs are unfamiliar with implementing pathology informatics training. The rotation incorporates educational resources for pathology informatics, guidance in the development, and general topics relevant to pathology informatics training. Informatics topics include anatomic pathology related aspects such as whole slide imaging, laboratory information systems, image analysis, and molecular pathology associated issues such as the bioinformatics pipeline and data processing. Additionally, we highlight how the rotation pivoted to meet the department's informatics needs while still providing an educational experience during the onset of the COVID-19 pandemic. **Conclusion.** As pathology informatics continues to grow and integrate itself into practice, informatics education must also grow to meet the future needs of pathology. As informatics programs develop across institutions, such as the one detailed in this paper, these programs will better equip future pathologists with informatics to approach disease and pathology.

Key Words: Informatics Education ▪ Residency ▪ Digital Pathology ▪ Whole Slide Imaging ▪ Molecular and Genomic Pathology Education.

Introduction

Informatics in medicine and pathology has a long history. Medical informatics began in the 1950s as the "science of information" with pathology informatics introduced as a field a few decades later in the 1990s. Many pathologist informaticians argue however, that technology and information management has been a part of pathology since its inception (1). Pathology at its core involves the identification, collection, and interpretation of data, information, and knowledge in order to diagnose, predict disease behavior, and guide treatment. The College of American Pathology (CAP) identifies informatics as the application of information management in healthcare to promote safe, efficient, effective, personalized, and responsive care (2). The recent advent of electronic health records and the digitization of medical information pushed medical informatics into the forefront as a critical and necessary aspect for education and practice. Similarly, in recent years, pathology informatics is placed in the lead with exponential and broad integration of advancements in molecular pathology, genomics, digital imaging, and artificial intelligence. Therefore, education in pathology informatics is crucial now more than

ever for future clinical practice in pathology. The current gap, however, is the limited amount of online pathology informatics training resources and the few "hands-on" experiences in pathology informatics. Online pathology informatics training resources are evolving, and pathology residencies still need training frameworks to keep up with the rapid advancements and ever shifting landscape of informatics education. Only a handful of articles guideline pathology informatics education (3-6). Moreover, the few "hands-on" opportunities include a few U.S. academic centers and pathology informatics fellowships where the focus is more towards pathology informatics such as laboratory information systems (LIS) maintenance, whole slide imaging (WSI), and bioinformatics compared to the more general field of medical informatics (7).

In our review, we detail the pathology informatics rotation in New York City at Memorial Sloan Kettering Cancer Center (MSKCC), as a "hands-on" experience that supplements existing pathology informatics training resources. We detail the rotation's construction, development, and implementation at the trainee (e.g. resident/fellow) level, and also how the implementation of the rotation adapted because of the COVID-19 pandemic in early 2020 to support remote pathologists and clinical services. We provide our review as an example of a successful framework for a pathology informatics rotation so that other institutions, formulating informatics curricula for their trainees, can leverage. Highlighted in this review are the online pathology informatics training resources available to use by any institution for their trainees. Such broad integration of pathology informatics training assures the dissemination of necessary knowledge and empowerment of informatics to the future pathologist community.

Construction and Development of the Pathology Informatics Rotation

The setting for the pathology informatics rotation was in the pathology department of MSKCC which has the experience of attendings who have completed pathology informatics training or have engaged in pathology informatics activities. Through input from these attendings, construction of the rotation began with the objective of maximizing the exposure of the resident to pathology informatics related aspects in a four-week period. MSKCC, as an institution, also has many well-developed pathology informatics resources such as WSI and molecular bioinformatics, combined with clinical and research initiatives to abundantly supplement a well-rounded experience in pathology informatics for the trainee.

An outline of general goals and objectives, though not necessary, is highly recommended in developing an educational curriculum for the trainee. An outline allows the trainee and faculty to gauge the experience and address specific benchmarks throughout the rotation. Our outline of the rotation goals and objectives of the four-week rotation is shown in Table 1. The authors recognize that not every training environment has access to such resources. Two accessible, free and comprehensive online pathology informatics training resources formed the starting point for the rotation and is recommended for training programs with and without resources. The two resources (Table 2) are the Pathology Informatics Essentials for Residents (PIER) curriculum (3) and Training Residents in Genomics (TRIG) (4). Both online curricula provide interactive modules and recorded lectures but also serve as helpful guides for content and structure to approach and teach the material during the rotation.

PIER is an online informatics curriculum, developed by informatics experts, and focused towards residents in helping meet the Accreditation Council for Graduate Medication Education (ACGME) milestones in resident education/training in pathology informatics. Developed in cooperation by the College of American Pathologists (CAP), Association of Pathology Chairs (APC), and Association for Pathology Informatics (API), PIER details essential topics in informatics that are essential for future pathologists. Topics and objectives addressed by PIER include fundamental principles of databases, data and communication standards, digital imaging, laboratory information systems, and the health care information ecosystem to more advanced

Table 1. The Listed Goals and Objectives to Be Met by the Resident Throughout the Rotation*

General Goals and Objectives
Informatics Knowledge:
Handling and management of medical data storage
Familiarity with basic information system terminology
Familiarity with different data structures and database architecture
Data analysis fundamentals
Digital imaging fundamentals
Whole slide imaging fundamentals
Information Systems:
User interface design
Familiarity of pathology workflows and processes
Structure of laboratory information systems and electronic medical/health record (EMR/EHR) systems
Familiarity of how data is stored, transferred, and accessed for information systems
Interpretation and analysis of molecular/genomic data of bioinformatics pipelines
Management:
Management of laboratory information systems and electronic medical/health record (EMR/EHR) systems
Management of operations and flow in pathology practice
Laboratory finance principles
Professionalism:
Proficiency in communicating with and presenting to clinicians and pathologists about informatics related matters
Education:
Prepare a 30-minute informatics based presentation to be presented at the Weill Cornell Clinical Pathology Resident Lecture

*Having such an outline allows the resident and faculty involved in the rotation to have a clear goal as to the goals of the rotation. Therefore, by the end of the rotation the trainee is able to concretely identify what they have gained through the experience.

Table 2. Easily accessible pathology informatics online curricula with their respective URL links

Henricks et al. (3)	https://apc.memberclicks.net/index.php?option=com_content&view=article&id=152:pier&catid=20:site-content&Itemid=156Many
Haspel RL. (4)	https://www.pathologylearning.org/trig

concepts like project management, clinical decision support, image analysis, and artificial intelligence. In addition, participatory interactions with pathology informatics attendings at MSKCC helped solidify the didactic content of PIER through actual "hands-on" practice in the rotation.

Similarly, TRIG is an online curriculum, developed by an expert group in medical education, molecular pathology, and clinical genetics, that promotes genomic pathology education in molecular testing approaches and scenarios. TRIG is a unique collaborative effort with major pathology organizations and representatives from the National Society of Genetic Counselors and the American College of Medical Genetics and Genomics. Through continual grant support from the National Cancer Institute, the TRIG working group holds workshops and courses at annual meetings of major pathology and oncology organizations. This four-week rotation was constructed and developed for anatomic pathology related informatics objectives. Clinical pathology related aspects were not highlighted in the curriculum except for molecular and genomic pathology. Laboratory medicine related informatics activities in clinical chemistry, microbiology, and blood banking were

not highlighted in the curriculum, because of the limited four-week time constraint, which was insufficient to encompass those activities adequately. More time would have unlocked even more potential for learning opportunities in these laboratory medicine related areas in informatics as millions of data points are generated and interpreted for patient care. The focus on anatomic pathology informatics as well as molecular genomic pathology likewise fit the rotating residents' interests. Given the time constraint and the diversity of pathology informatics rotations in informatics training can be tailored to the trainee or pathologists' interests.

Each week in the four-week rotation was devoted to a rotations/topic shown in Table 3. The first and last weeks were situated so the trainee would work with whole slide imaging in the WSI scanner facilities to understand concepts, challenges, the processes of digitizing diagnostic slides and their utilization. In addition, the first and last weeks were set up so that the trainee would also be integrated with the anatomic pathology laboratory information system (AP-LIS) team. In this instance, MSKCC utilizes Cerner CoPathPlus for its AP-LIS. In these weeks the aspects of WSI, AP-LIS support, automation of lab processes in anatomic pathology, computer vision/artificial intelligence (AI) for WSI were addressed; further solidifying the didactic concepts serving as an adjunct to PIER.

The second week was dedicated to informatics in molecular and genomic pathology including the bioinformatics pipeline and scripting. Understanding how sequencing data is processed and analyzed is integral to the future of pathology practice as molecular and genomic pathology expands in testing and complexity. At MSKCC there is a robust and well-integrated molecular/genomics bioinformatics service within the department of pathology. This service allowed for an environment in which a trainee could easily integrate themselves and identify individuals to enrich their experience in molecular bioinformatics. This second week exposes the trainee to how informatics aids in the organization and interpretation of molecular/genomic data and its practical role in clinical care and patient treatments. Through the integration of the bioinformatics pipeline, training includes the understanding of the strengths and weaknesses of molecular/genomic testing.

During this second week, the resident would attend molecular/genomic sign outs, rotate with the bioinformatics group, and attend quality assurance (QA)/quality control (QC) molecular/genomic meetings. MSKCC molecular/genomic sign out is held with a bioinformatician, a molecular fellow, and a molecular attending. In reviewing molecular/genomic reports and the associated molecular/genomic data output, a fluid dynamic dialogue exists as any QA/QC issues are addressed at the time of sign out. This fosters a learning environment to how data is extracted as well as issues that may arise in the process. Additionally, the weekly QA/QC meetings allows the trainee to see how the molecular/genomic data output from molecular platforms are filtered and analyzed computationally as well as the challenges and pitfalls. Also scheduled for the resident during this second week, was one-on-one didactics with a molecular/genomics attending. These didactic sessions further delved into the bioinformatics pipeline by going over the code and architecture in further detail. Didactic topics included next generation sequencing (NGS)

Table 3. The Rotations and Topics Addressed for Each Week of the Rotation*

Week	Rotations/Topics
Week 1	AP-LIS support and automation, WSI, computer vision/AI
Week 2	Molecular and genomic informatics including bioinformatics pipeline and scripting
Week 3	Rotations in Machine Learning Labs and Pathology Imaging Labs
Week 4	AP-LIS, WSI, Surgical Pathology Informatics, and Previous Rotations of Interest

*Didactic lectures in pathology informatics by attending were performed throughout all the weeks. Any informatics related meetings were also attended to when possible throughout the weeks (i.e., QA/QC meetings, molecular sign out, lab meetings, and vendor meetings).

file formats, QA pitfalls, filtering variants, and introductions to using the programming language R for analyzing data.

The third week was designed as an anatomic pathology informatics research week in which the trainee would rotate through the Thomas Fuchs Lab and the Yukako Yagi Lab. The Fuchs Lab is focused on computer vision and AI applications to either WSI, tissue-micro arrays, and medical imaging. The Yagi Lab investigates novel innovative approaches to tissue processing and imaging such as 3D tissue imaging, multispectral image enhancement, and telepathology. During this third week, the trainee would attend lab meetings and team up with research scientists to help on their projects. Experience in both labs immerses the trainee in innovative approaches for pathology and in fostering inspiration in academic pursuits in pathology informatics.

The entire four-week rotation was overseen by multiple pathology informatics attendings. Integrated throughout the four-week rotation is practice experience supplemented by individual one on one didactic lectures with informatics attendings on various informatics topics, informatics research projects, vendor meetings, and hospital wide informatics meetings. Two specific informatics projects were slated for involvement by the trainee during the four-week rotation. The first project was the validation of the Leica Aperio LV1 for remote frozen section diagnosis. The Leica Aperio LV1 (Leica Biosystems, Buffalo Grove, IL) is a small footprint (e.g. 4 slide) hybrid robotic microscope/whole slide scanner providing both WSI capabilities and dynamic robotic telepathology ideal for frozen sections (5). The second project was analyzing component differences across different WSI platforms to further investigate high power field quantification in digital pathology (6).

Implementation and Adaptation of the Rotation to the Covid-19 Pandemic

In December of 2019, cases of an unknown viral pneumonia were reported in Wuhan, China, later identified as SARS-CoV-2 or COVID-19. On January 20th 2020, the first reported case of COVID-19 infection was identified in the United States (8). On March 20th 2020, stay at home orders were placed in New York City with strict gathering and social distancing measures in order to hinder the spread of COVID-19 (9). By early April 2020, hospitals in New York City were overwhelmed, as intensive care units were expanded and healthcare workers redeployed to meet the increasing number of individuals infected with COVID-19. Pathology departments in New York City also faced difficulties in moving forward safely with clinical operations.

Though carefully developed and planned prior, the informatics rotation began right as COVID-19 hit New York City. By the second week of the rotation, all research labs had suspended in person activity with individuals working from home to decrease exposure. At the same time discussions as to how pathology informatics could help in not only data collection and investigation of COVID-19 but also remote sign out of WSI were discussed. MSKCC had in place a robust WSI lab and operation that was situated to aid pathology workflow in a safe manner (10, 11). The focus of the trainee's rotation adjusted towards testing and validation of operational processes adapted for pathologists to review and sign-out pathology specimens remotely through WSI. Accomplishing such an endeavor meant promoting the safety of individuals in the lab and digital scanning, as well as pathologists, while continuing clinical operations and responsibilities. The adaptation of the rotation during the pandemic highlights the flexibility as well as the wide applicability of pathology informatics for training.

Testing and Validation of Remote Sign out Through WSI

MSKCC has numerous WSI technologies, digital scanning staffing, and existing processes to pilot a larger WSI operation for remote sign out. Incorporating WSI at scale during the pandemic for remote sign out became the priority, though many operational questions remained that required tremendous efforts by the trainee in testing and validation in real time. In addition to these testing

and validation efforts, one on one didactic lectures with informatics attendings continued via web conferencing platforms (e.g. WebEx, Zoom Microsoft Teams) on informatics topics such as molecular/genomic bioinformatics, WSI, and laboratory information systems.

For the validation, the Leica Aperio GT450 and Philips UltraFast Scanner were selected as high throughput instruments to pilot remote sign out of surgical pathology specimens. Initially, a select group of attendings began a remote sign out pilot using WSI for one specialty. Shortly after the initial pilot, a study protocol was developed to encompass all surgical pathology subspecialties on randomly selected service days (11). WSI was then expanded to other services/specialties and attendings with the eventual intent to scale operations to all glass slides produced by the lab and all slides of cases received as consultations. The trainee worked as part of the team including digital imaging staff and operational directors to test and address issues that arose. As there was no precedent, the trainee was actively involved in developing process frameworks for slide scanning operations and workflows, addressing slide-reading errors; continual optimization of slide scanning workflows were addressed firsthand without guidance from prior established examples. Additionally, how digital slides were viewed and how to best optimize the required components for WSI viewing, were also addressed directly without guidance from prior established examples.

Regulatory considerations were addressed in the validation for remote WSI sign out. With the need for WSI remote sign out during COVID-19, Centers for Medicare and Medicaid Services (CMS) temporarily used their enforcement discretion to allow remote sites meeting specific criteria to not require dedicated CLIA certifications; in order for pathologists to work remotely (12). Other regulatory bodies in other countries also followed suit (13-15). The FDA also further provided guidance with a temporary enforcement discretion on the use of non-510(k) cleared devices, with validation prior to use (16).

In New York State (NYS), the NYS Department of Health is the CLIA-deemed entity that requires all CLIA-certified laboratories in NYS to have approval for laboratory developed testing (LDT). LDT validation documentation was required for submission and approval, in order to perform remote sign out using WSI. The application for validation by NYS was written and submitted during the validation process and eventually granted approval. By developing the process for remote WSI sign out along with participation in testing, validation, and handling regulation around remote WSI sign out, the education of the trainee was greatly enhanced. Familiarity with all the nuances around digitization of glass slides, the steps required, and the regulations of government and professional societies, brought unforeseen practical experience that would not have occurred without the pandemic forcing adaptions by MSKCC.

Conclusions

Pathology informatics continues to evolve with process-driven technological solutions for an increasingly complex healthcare field. Advances in WSI, computer vision/AI, and digital imaging innovations allow pathologists to not only work efficiently, but also yield new approaches to disease diagnostics and management. Likewise, informatics in molecular and genomic pathology plays a key role in disease diagnostics and management with generations of insights through breakthroughs in data analysis. Future pathologists need to know these aspects of informatics in in their practice. Therefore, training pathology residents and fellows in pathology informatics concepts are essential for the future pathologist workforce. Such essential training is acknowledged by the ACGME and CAP by their efforts to bolster informatics education for trainees. The pathology informatics rotation constructed, developed, and implemented at MSKCC serves as a guide and example in structuring a resident/fellow pathology informatics rotation. While the general goals, objectives, and designed activities pivoted to fit the needs of the department during the COVID-19 pandemic for remote WSI sign out, the rotation still yielded valuable experience in learning about informatics

processes and core concepts. Having clear and well thought out objectives prior to the rotation as well as dedicated mentors and attendings enhanced the education experience.

Conflict of Interest: David Kim, - None; Chad Vanderbilt, - DocDoc Pte. Ltd. (Provision of Services) and Paige.AI, Inc. (Ownership / Equity Interests; Provision of Services); Matthew Hanna, - Paige.AI, Inc. (Provision of Services) and PathPresenter (Provision of Services - uncompensated); S. Joseph Sirintrapun, - None.

References

1. Park S, Parwani AV, Aller RD, Banach L, Becich MJ, Borkenfeld S, et al. The history of pathology informatics: A global perspective. J Pathol Inform. 2013;4:7. doi: 10.4103/2153-3539.112689.
2. College of American Pathologists. Clinical Informatics Resources. Published 2020. [cited 2020 Nov 5]. Available from: https://www.cap.org/member-resources/councils-committees/informatics-committee/.
3. Henricks WH, Karcher DS, Harrison JH, Sinard JH, Riben MW, Boyer PJ, et al. Pathology Informatics Essentials for Residents: A flexible informatics curriculum linked to Accreditation Council for Graduate Medical Education milestones. J Pathol Inform. 2016;7:27. doi: 10.4103/2153-3539.185673.
4. Haspel RL. Teaching Residents Genomic Pathology. Adv Anat Pathol. 2013;20(2):125-9. doi:10.1097/PAP.0b013e31828629b2
5. Leica Biosystems. LEICA BIOSYSTEMS APERIO LV1 IVD APPROVED FOR REMOTE FROZEN SECTION AND TELEPATHOLOGY. 2018. [cited 2020 Nov 5]. Available from: https://www.leicabiosystems.com/news-events/news-details/article/leica-biosystems-aperio-lv1-ivd-approved-for-remote-frozen-section-and-telepathology/News/detail/.
6. Hanna M, Pantanowitz L. Redefining the high power field when counting mitoses using digital pathology. Mod Pathol. 2017;30(S2):396A.
7. American Medical Informatics Association. Clinical Informatics Fellowship Programs. [cited 2020 Nov 5]. Available from: https://amia.org/membership/academic-forum/clinical-informatics-fellowships.
8. World Health Organization. WHO Timeline - COVID-19. [cited 2020 Nov 5]. Available from: https://www.who.int/news/item/27-04-2020-who-timeline---covid-19. Published 2020.
9. New York State. New York State on PAUSE. 2020. [cited 2020 Nov 6]. Available from: https://coronavirus.health.ny.gov/new-york-state-pause.
10. Hanna MG, Reuter VE, Hameed MR, Tan LK, Chiang S, Sigel C, et al. Whole slide imaging equivalency and efficiency study: experience at a large academic center. Mod Pathol. 2019;32(7):916-28. doi:10.1038/s41379-019-0205-0
11. Hanna MG, Reuter VE, Ardon O, Kim D, Sirintrapun SJ, Schüffler PJ, et al. Validation of a digital pathology system including remote review during the COVID-19 pandemic. Mod Pathol. Published online June 2020. doi:10.1038/s41379-020-0601-5
12. Centers for Medicare & Medicaid Services. Centers for Medicare & Medicaid Services Memorandum, Clinical Laboratory Improvement Amendments (CLIA) Laboratory Guidance During COVID-19 Public Health Emergency. [cited 2020 Nov 5]. Available from: https://www.cms.gov/medicareprovider-enrollment-and-certificationsurveycertificationgeninfopolicy-and-memos-states-and/clinical-laboratory-improvement-amendments-clia-laboratory-guidance-during-covid-19-public-health. Published 2020.
13. Williams BJ, Brettle D, Aslam M, Barrett P, Bryson G, Cross S, et al. Guidance for Remote Reporting of Digital Pathology Slides During Periods of Exceptional Service Pressure: An Emergency Response from the UK Royal College of Pathologists. J Pathol Inform. 2020;11:12. doi: 10.4103/jpi.jpi_23_20.
14. College of American Pathologists. COVID-19 - Remote Sign-Out Guidance. [cited 2020 Jan 12]. Available from: https://documents.cap.org/documents/COVID19-%0ARemote-Sign-Out-Guidance-vFNL.pdf. Published 2020.
15. College of American Pathologists. Remote Sign-Out FAQs. [cited 2020 Dec 1]. Available from: https://documents.cap.org/documents/Remote-Sign-Out-FAQs-42.%0AFINAL.pdf. Published 2020.
16. Food and Drug Administration. Enforcement Policy for Remote Digital Pathology Devices During the Coronavirus Disease 2019 (COVID19) Public Health Emergency. Guidance for Industry, Clinical Laboratories, Healthcare Facilities, Pathologists, and Food and Drug Administration Staff. [cited 2020 Nov 23]. Available from: https://www.fda.gov/media/137307/download.

Narrative Review
Acta Medica Academica 2021;50(1):143-156
DOI: 10.5644/ama2006-124.332

New Insights into the Diagnosis, Molecular Taxonomy, and Treatment of Bladder Cancer

Monika Ulamec[1, 2, 3, 4], Jure Murgić[5], Luka Novosel[6], Miroslav Tomić[7], Robert Terlević[8], Igor Tomašković[7, 9], Marijana Jazvić[5], Ana Froebe[3, 5], Božo Krušlin[1, 2, 4]

[1]Department of Pathology and Cytology "Ljudevit Jurak", University Hospital Center "Sestre milosrdnice", Zagreb, Croatia, [2]School of Medicine, University of Zagreb, Zagreb, Croatia, [3]School of Dental Medicine, University of Zagreb, Zagreb, Croatia, [4]Scientific Group for Research on Epigenetic Biomarkers, University of Zagreb, Croatia, [5]Department of Oncology and Nuclear Medicine, University Hospital Center "Sestre milosrdnice", Zagreb, Croatia, [6]Department of Radiology, University Hospital Center "Sestre milosrdnice", Zagreb, Croatia, [7]Department of Urology, University Hospital Center "Sestre milosrdnice", Zagreb, Croatia, [8]Department of Pathology and Cytology, Pula General Hospital, Pula, Croatia, [9]Faculty of Medicine, J.J. Strossmayer University of Osijek, Osijek, Croatia

Correspondence: *monika.ulamec@gmail.com*; Tel.: + 385 91 442 49 49; Fax.: + 385 13 787 442

Received: 11 February 2021; **Accepted:** 4 March 2021

Abstract
This review aims to emphasize new insights into the diagnosis, classification, and therapy of bladder cancer (BC). Bladder cancer is a heterogeneous, complex disease on a morphological, molecular, diagnostic, and prognostic level. Cancer stage is still the most important attribute for prognosis and treatment, while early detection with optimal and rapid individual therapeutic and surveillance approach is crucial. The vast majority of patients have a superficial, non-muscle-invasive tumor associated with a good prognosis after resection and adjuvant intravesical maintenance immuno or chemotherapy if needed. On the other hand, muscle-invasive bladder cancer is a highly aggressive disease with high morbidity and mortality. However, it has become a model for oncology success over the last five years with many available targeted therapeutic modalities. Metastatic BC is now amenable to multimodal treatment combining cystectomy and neoadjuvant chemotherapy and immunotherapy and is a target for precision medicine. **Conclusion**. A new molecular taxonomy for bladder cancer has been proposed and provided insight into BC's carcinogenesis, with some possible effects on therapy decisions. However, this classification is still not applicable in routine clinical practice. It opens new questions regarding the interplay between tumor genetic signature, intratumoral heterogeneity, therapy implications, and tumor progression.

Key Words: Bladder Cancer Pathology ▪ Bladder Cancer Therapy ▪ Bladder Cancer Genetics.

Introduction

Bladder cancer (BC) accounts for 3% of global cancer with higher frequency in the developed countries. According to the GLOBCAN data in 2020, the incidence was 9.5 (men) and 2.4 (women) per 100 000 with mortality rates of 1.9/100 000. It is the fourth most common cancer in men, 11th in women, and the ninth most common cause of cancer deaths in Europe. Sixty-five years is the median age at diagnosis, and the average 5-year survival is about 75% in developed countries. Five-year survival for metastatic disease is up to 5%. Smoking is the strongest risk factor related to BC. Schistosomiasis infection with persistent chronic inflammation in Africa and the Middle East is a critical tropical pathogen in BC carcinogenesis (1, 2).

Although BC is a heterogeneous disease in many ways, which is confirmed with new techniques such as next-generation sequencing, at the morphological level, urothelial carcinoma of the usual subtype (UC) comprises 90% of BC. Among these, up to 85% of patients will have disease confined to the mucosa (non-invasive BC; pTa) or

submucosa (non-muscle invasive BC; pT1), which were formerly called "superficial" bladder cancer. Muscle invasive BC (≥pT2) is a high-grade, aggressive disease, which requires early detection with optimal and rapid therapeutic and surveillance approaches (1, 3).

For the sake of clarity, in this review, we will use the following terminology: NMIBC (non-muscle invasive BC) and MIBC (muscle-invasive BC). Whereas the tumor stage primarily determines BC's prognosis and therapy, other aspects of this malignancy also have considerable clinical significance. These clinically important data on the diagnosis, classification, and therapy of BC will be discussed in this review.

Clinical Presentation, Screening, and Diagnosis

The most common symptom of bladder tumors (recorded in up to 85% of BC) is painless hematuria. Macrohematuria is usually associated with higher-stage disease. BC may also present with lower urinary tract symptoms (hesitancy, poor and intermittent stream, straining, prolonged micturition, incomplete bladder emptying, dribbling, frequency, urge incontinence, and nocturia, lower urinary tract symptoms and especially irritative voiding, commonly seen with in situ carcinoma (CIS) (4).

After excluding urinary tract infection, clinical examination of the abdomen, external genitalia, urethra, and prostate is required. Ultrasound (US) of the kidneys and bladder, followed by cystoscopy using a flexible, fiberoptic cystoscope, is standard of care. In case of negative cystoscopy findings, further steps are urine cytology, computed tomography (CT) or urography/intravenous urography if CT is not available (5). Positive urine cytology is a sign of UC anywhere in the urinary tract. However, negative cytology does not exclude its presence since the false-negative rate is up to 20% in high-grade UC. In high-grade tumors, urine cytology with cystoscopy has high sensitivity, up to 84%. In low-grade tumors, sensitivity is very low, up to 16%. Although cytological interpretation is user-dependent, the test's specificity can be up to 90% in experienced centers (5, 6). In 2016 the Paris Working Group redefined the diagnostic categories for urine cytology, suggesting the diagnostic reports to be classified into the following diagnostic categories: a) Negative for high-grade urothelial carcinoma (Negative); b) Atypical urothelial cells (AUC); c) Suspicious for high-grade urothelial carcinoma (Suspicious); d) High-grade urothelial carcinoma (HGUC); and e) Low-grade urothelial neoplasia (LGUN) (7).

In the last decade, urine and cytology samples are being adopted as promising and suitable sources to develop non-invasive, accurate, and cost-beneficial tests to diagnose and monitor BC patients, particularly for early low-grade tumors (8). Such tests include panels of markers related to gene expression and epigenetic changes such as DNA methylation patterns and post-translational histone modifications. In addition to cellular DNA or RNA, in urine samples, cell-free DNA (cfDNA), referring to degraded tumor DNA fragments, is valuable for detecting genetic and epigenetic alterations (9). The most useful panels for BC are those searching for *TERT* promoter mutations and *FGFR3* mutations. Some studies have shown these changes months before the clinical manifestation of BC (10). In addition to cfDNA assays for urine, some promising plasma cfDNA diagnostic platforms show good detection of genetic changes in patients with NMIBC and invasive and metastatic disease (11).

Imaging of Bladder Cancer

In the initial diagnosis of BC, imaging plays an important role. The US is the first-line evaluation for patients with hematuria due to its availability. It can be used for staging, particularly in patients with renal insufficiency or contrast allergy; however, it may underestimate the local depth of invasion. Newer US contrast involving microbubbles has enabled the developing of a novel imaging technique called contrast-enhanced ultrasound (CEUS), which is promising in predicting the grade of BC and T-stage. US is still the most im-

portant imaging method for the initial evaluation of hematuria and follow-up of early-stage NMIBC after resection (12).

Computed tomography is the primary imaging modality for assessing the extent of the tumor. The National Comprehensive Cancer Network's current recommendations for the staging of MIBC include CT of the chest, abdomen, and pelvis. Magnetic resonance imaging (MRI) of the abdomen and pelvis with additional non-contrast chest CT in patients with contrast allergies is required (13). Recent improvements in CT cancer imaging, including multidetector acquisition with higher image quality and radiation exposure reduction, have solidified its role as the primary imaging modality, despite the rise and availability of more complex and modern methods. Studies show that CT's specificity and sensitivity in bladder cancer detection are 79-89% and 91-94%, respectively (14, 15). One of the main diagnostic goals is to assess extravesical transmural spread. CT urography has almost wholly replaced intravenous urography for the diagnosis and surveillance of localized bladder carcinoma. However, it lacks the resolution to be used in primary tumor staging as it cannot distinguish between different layers of the bladder wall, and it can miss lesions smaller than 1 cm in size (16, 17). If CT is used to analyze and follow-up changes after transurethral resection of bladder cancer, its accuracy can be further reduced due to inflammatory changes, which can be mistaken for BC (17, 18).

Despite its relatively low cost, rapid turnover, wide availability, and new low dose protocols, CT is still less advantageous than MRI or PET scan for local and distal lymph node involvement, with specificity ranging between 68-100% (16). A new imaging approach called dual-energy CT (DECT) uses software to merge 2 CT scans and create a split-dose CT urography in which 1/3 of the total contrast dose is given 8 minutes before the scan and the other 2/3 of the dose 2 minutes before the scan. With additional subtraction of contrast from initial CT scans, a virtual non-contrast CT is also recreated. The results in an artificially created triple-phase exam (non-contrast, venous, and delayed urographic) are completed in one scan acquisition at 1/3 of the radiation dose since the delay non-contrast pass is not needed. The main benefit is reduced radiation exposure (17). When compared to MRI, CT is faster and more cost-effective. Downsides include ionizing radiation, high interobserver variability, and the inability to differentiate the bladder's muscle layers and distinguish T1 from T2 disease. Specificity and sensitivity of CT imaging are low for extravesical extension of locally advanced BC and small metastatic lesions, compared with MRI (17-20).

MRI is used for preoperative staging in T2 and advanced disease and staging after cystoscopy. Transurethral resection (TUR) is considered the most accurate technique for staging invasive and non-muscle invasive tumors. However, it can still underestimate this cancer by 42%. MRI provides extensive soft-tissue resolution with the ability to detect T3 and T4 diseases. MRI is superior to CT in distinguishing T2a from T2b stage. Diffusion-weighted MRI are shown to be an excellent tool for differentiating benign and malignant bladder lesions, tumor staging, and assessment after chemo-radiotherapy treatment (19, 20).

Multiparametric MRI (mpMRI) is a new combination of MRI sequences composed of T1W-MRI, T2W-MRI, and functional MRI methods, including DCE-MRI and DW-MRI. It showed potential for detection, and staging assessment, particularly for assessing muscular invasion depth (21). MRI-PET was approved in 2011. It combines the advantages of two complex scans providing superior sensitivity and specificity for bladder cancer detection and characterization; however, there are not enough clearly defined and large prospective studies to validate these findings (22).

Histopathological Diagnosis

Histological confirmation of BC diagnosis is based on TUR sample analysis in most cases. The most common histological subtype is urothelial carcinoma, constituting approximately 90% of all bladder cancers (in some institutions, the term transitional cell carcinoma is still used). The diagnosis is

Table 1. Bladder Cancer Histological Types*

Urothelial Carcinoma, Pure or Mixed With Other Type
Squamous differentiation
Glandular differentiaton
Sarcomatoid differentiaton
Trophoblastic differentiation
Nested variant
Micropapillary variant
Microcystic variant
Lymphoepitelioma like carcinoma
Giant cell variant
Clear cell variant
Lipid cell variant
Neuroendocrine (Carcinoid, Small cell/large cell carcinoma)

*Moch et al. WHO classification of tumours of the urinary system and male genital organs, 2016.

based on architectural and cytological characteristics. Architecturally, BC shows papillary, infiltrative-solid, or mixed growth patterns (3) (Table 1).

Grade

In NMIBC, grade is still the most important finding for therapy and follow-up decisions. In the WHO 2004 classification, a two-tiered grading system was recommended and confirmed in the WHO 2016 classification of UC (3). Low-grade UC is characterized by papillary architecture and distinct but low-grade cytologic abnormality, with increased crowding and layering of the atypical cells, which are relatively uniform in size and without significant nuclear pleomorphism. Mitoses are mostly rare but sometimes easily visible and placed at the basal tumor layers (3, 23) (Figure 1).

High-grade UC shows prominent architectural and cytologic abnormalities with anastomosing papillae and confluence on low-power examination. Cells show dyscohesion, nuclear pleomorphism and anaplasia, prominent nucleoli, and irregularly clustered disorganized cells. Mitotic figures are numerous and atypical and occupy the full thickness of the epithelial layer. Frequently in situ urothelial carcinoma is found close to high-grade UC (3, 23).

A three-tiered grading system is still used in some institutions (Grade 1: Well-differentiated; Grade 2: Moderately differentiated; and Grade 3: Poorly differentiated UC) but is mostly abandoned due to low interobserver concordance. To convert to a two-tiered system, grade I and II are defined as low grade and grade III as high grade. The grade is of particular importance in NMIBC due to differences in the therapeutic approach. With rare exceptions, MIBC are high-grade tumors (23, 24) (Figure 1).

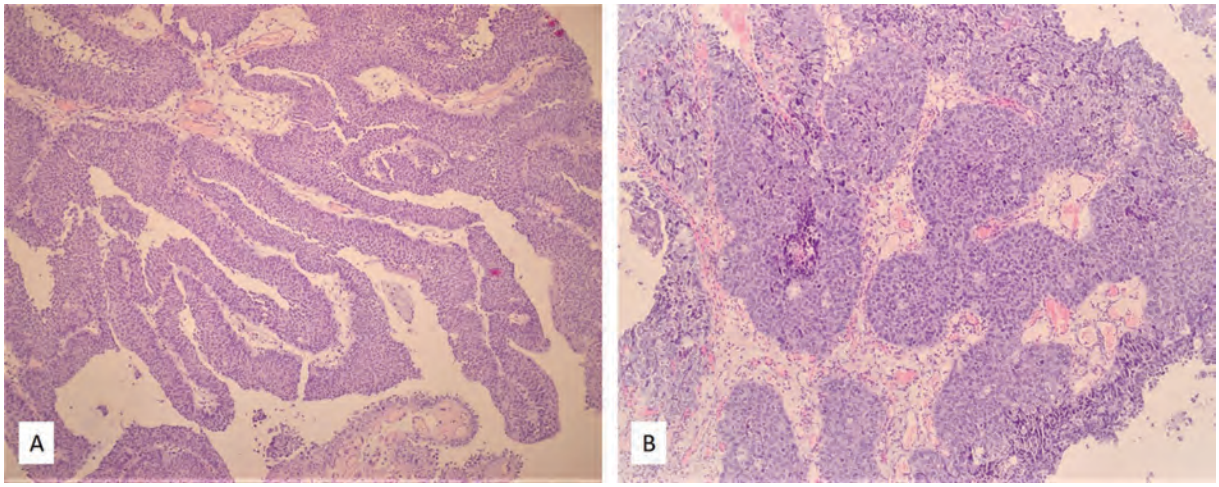

Figure 1. A. Low grade papillary urothelial carcinoma, ×100; B. High-grade urothelial carcinoma, ×100 (Hematoxylin and Eosin stain).

Staging

Tumor-node-metastasis (TNM) staging system is used in histopathological reports for exophytic and endophytic growth patterns. The tumor stage is determined by the depth of tumor invasion into the bladder wall's layers, whose anatomy and histology are variable and can sometimes be confusing even for pathologists. Despite some limitations in sample adequacy and provided data in TUR specimens, it is still obligatory to determine the depth of invasion, defined as the highest pT stage in a given case. Clinical TNM and staging include not only pTNM but also other diagnostic findings (25).

In NMIBC, it is most important to determine the basal lamina's integrity and distinguish between CIS and non-invasive UC. The 2017 American Joint Committee on Cancer TNM recommended pT1 substaging and put the cut-off for microinvasion at 0.5 mm. In the invasive growth pattern (invasion through basal lamina), the absence or presence of muscularis propria and its invasion is of the highest importance. It assigns a pT2 stage category and is an indicator of TUR adequacy. In MIBC, the stage is still the most important prognostic factor. In TUR specimens, muscularis propria may be mimicked by hyperplastic muscle bundles in the lamina propria, leading to overstaging. It is crucial to distinguish these two muscle types morphologically and immunohistochemically. All MIBC tumors are classified as pT2 tumors when confined to the bladder and pT3 tumors when the perivesical fat invasion is found (24-26).

It may be difficult to demarcate the irregular muscularis propria at the perivesical soft tissue junction in cystectomy specimens. Studies have shown significantly poorer outcomes in pT3b compared with pT3a tumors. Proper gross assessment of perivesical soft tissue invasion is of utmost importance for the proper staging of pT3 tumors (25, 26).

Molecular Classification of Urothelial Carcinoma

All malignant tumors are composed of different cell clones, which harbor different genetic makeup and gene expression changes, including molecular characteristics between primary and metastatic tumors (27). UC is well known for its heterogeneity at the morphological and molecular levels, with various subclones developing during tumor progression, metastatic spread, and therapy-induced changes. Identification of lethal tumor subclones and their molecular signature is crucial for precision medicine and patients' survival with MIBC and metastatic BC. In BC, it is also essential to identify NMIBC with the potential for aggressive behavior and progression to MIBC (28, 29).

The main drivers in UC carcinogenesis are changes in DNA. Comprehensive wide genome multiplatform analyses by the TCGA (The Cancer Genome Atlas) group showed various DNA mutations in UC patients. It provided a strong base for future classification of UC based on molecular taxonomy (30). DNA changes included mutations in multiple genes involved in cell-cycle regulation, chromatin remodeling, kinase receptor signaling, transcription, and DNA repair. These findings are in line with melanoma and lung cancer profiles, which are malignancies with most genetic alterations. The most frequently mutated gene in UC was *TP53*, found in half of the samples, and it was mutually exclusive with the amplification/overexpression of mouse double minute 2 homolog (*MDM2*). Another frequently mutated gene was mixed-lineage leukemia 2 (*MLL2*), essential for chromatin remodeling and epigenetic regulation. *RB1* mutation was mutually exclusive with *CDKN2A* deletion. Recurrent hotspot mutations in the *TERT* promoter regions are also common in UC regardless of grade, stage, or histological subtype. Other mutated genes essential for cell proliferation and differentiation were FAT atypical cadherin 1 (*FAT1*), CREB-binding protein (*CREBBP*), *ERBB2/HER2*, spectrin alpha non-erythrocytic 1 *(SPTAN1*), hotspot activating receptor tyrosine kinases mutations, and gene fusions of *FGFR3*, *PIK3CA*, lysine (K)–specific methyltransferase 2C (*KMT2C*), ataxia-telangiectasia mutation (*ATM*), and lysine (K)–specific methyltransferase 2A 700 Arch (*KMT2A*) (30, 31).

Only a few alterations are retained from primary tumors in respective metastases. Molecular/genetic changes are more expressed over time and due to therapy. Early tumor forms in UC are characterized by *FGFR3, AFDN,* and *H3F3A* mutations, which are not found in invasive subclones. Mutations in *KDM6A, TP53, PIK3CA*, and *FGFR3* genes are also characteristics of primary UC clones, while *TP53, MLL3, FBXW7,* and *SETD2* mutations are more commonly seen in metastatic clones (29). Most experts agree that high tumor mutation burden (TMB) reflects frequent mutations and their accumulation over time in bladder cancer. MIBC has TMB >7 mutations per Mb and changes in genomic and transcriptional levels, which are not easy to frame. The DNA-editing enzyme apolipoprotein B mRNA catalytic polypeptide-like (APOBEC3) family is believed to be responsible for high TMB in UC. Chemotherapy may affect APOBEC3 expression, further influencing the genetic signature in UC clones (32, 33). Several molecular subclassification systems have been proposed based on different gene expression. These efforts may be limited by intratumoral heterogeneity, which may be seen morphologically in distinct BC subtypes within the same tumor (31-35). Recently blood and/or urine-based liquid biopsy platforms have been rapidly developing and may be a useful tool for capturing the fast changes in BC's molecular signatures (34). Therefore, a new classification of UC based on histopathological findings and molecular characteristics is needed and proposed during the last five years.

There is strong evidence for the existence of two pathways of bladder carcinogenesis. The first pathway comprises 80% of NMIBC with papillary architecture and precursor lesions in the form of urothelial dysplasia (36). These are locally recurrent tumors without risk of invasive growth. The second pathway is related to urothelial carcinoma in situ and shows high-grade tumor characteristics with infiltrative growth (MIBC). Up to 15% of low-grade papillary tumors progress to high-grade lesions and invasive carcinomas with time.

Urothelial dysplasia and low-grade papillary tumors are characterized by activating fibroblast growth factor receptor 3 (*FGFR3*) mutations, which activate the *RAS* gene (36). In situ UC shows inactivation of *TP53* and *RB1* pathways with SV40 large T antigen. Activation of the phosphoinositide 3-kinase/protein kinase B (PI3K/AKT/mTOR) pathway, resulting from deletions or mutations of tumor suppressor genes, promotes invasive growth. Additionally, loss of phosphatase/tensin homolog (*PTEN*) is well known to be associated with invasive growth and high-grade tumors, which presumes PI3K/AKT/mTOR pathway as the driver of the invasive phenotype. Downregulation of *TP53* and *RB1* is essential in urothelial carcinoma's invasive phenotype (35-37).

An important question is which cells harbor the mentioned mutations, and are the cell of origin for BC development? The multilayered urothelium comprises three cell types; basal cells, which sit on the basal membrane, an intermediate cell layer, and umbrella surface cells. These cells express different cell membrane markers, which may be an essential clue to track the tumor cell of origin. In UC, this cell of origin is believed to come from the basal cell layer (37, 38).

Non-Muscle Invasive Bladder Cancer

The molecular diversity of UC is responsible for the different clinical behavior, progression, and response to conventional and targeted therapies. Different studies are currently trying to gather all the morphological, molecular, and clinical information needed to define the molecular subgroups of UC to simplify therapy selection and improve clinical response and prognosis of the disease. In 2012, Sjödahl et al. (38) analyzed gene expression profiles of NMIBC. They described three major molecular subtypes: urothelial-like (which expressed FGFR3 and cyclin D1 and showed loss of 9p21), genomically unstable, which expressed Forkhead box M1 [*FOXM1*], with loss of *RB1*, and basal/squamous cell carcinoma-like (which expressed cytokeratins CK5 and CK14). The authors showed prognostic differences: urothelial-like had a good prognosis, genomically unstable intermediate prognosis, and basal-like showed the worst outcome. For the first

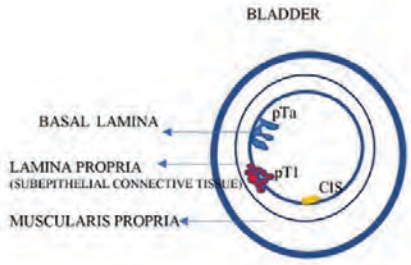

SUBTYPE	MUTATION	PROGNOSIS
I.	FGFR3 (uroplakin expression)	GOOD
II.	TP53 ERCC2 (luminal like signature; epithelial-mesenhimal transition signiture)	HIGH RISK NMIBC
III.	FGFR3 (basal like signature)	BETTER THAN II.

Figure 2. NMIBC molecular subgroups. FGFR3 – Fibroblast growth factor receptor 3, ERCC2 – Excision repair cross complementing repair 2.

time, an immunohistochemical staining panel distinguishing those subtypes was described (39). A comprehensive transcriptional analysis was done, and finally, three different molecular subgroups of NMIBC were found. The first group harbors FGFR3 mutation, expresses uroplakins, and is correlated with a good prognosis. The second group shows luminal-like differentiation with *TP53* and *ERCC2* mutations and is associated with high-risk NMIBC. The third group harbors *FGFR3* mutations and expresses KRT5 and KRT15 as markers of undifferentiated or basal cells (40, 41) (Figure 2).

Muscle Invasive Bladder Cancer

Different molecular subclassifications for MIBC were described as well. Guo et al. (31), based on whole-genome mRNA expression, proposed three subtypes of MIBC: basal, luminal, and p53-like. An immunohistochemical profile was proposed to differentiate these three groups. The basal subtype morphologically showed squamous or sarcomatoid differentiation and expressed CK5/6, CK14, and p63. The luminal subtype was characterized by uroplakins, CK18, CK20, GATA-3 expression, papillary architecture, *FGFR3* mutation, and *ERBB2* amplification. p53-like was described as a subtype of luminal tumors resistant to chemotherapy. The basal subtype showed aggressive behavior with an excellent response to cisplatin-based therapy (31). The following year, Robertson et al. (30) proposed five distinct molecular subtypes based on clinicopathological findings and mRNA expression. These included luminal-papillary, luminal-infiltrated, luminal, basal squamous, and neuronal. Luminal-papillary was related to the FGFR3 pathway (overexpression, amplification, or mutation), papillary architecture, low-grade morphology, and low progression risk. The luminal infiltrating showed strong stromal reaction and myofibroblastic proliferation with dense intratumoral and peritumoral lymphocytic infiltration and revealed the importance of the microenvironment for tumor growth and progression. In this subtype, immune checkpoint markers were highly expressed [programmed death ligand-1 (PD-L1), cytotoxic T lymphocyte-associated protein (CTLA-4)], tagging this subtype as a right candidate for immunotherapy with immune checkpoint inhibitors. The basal/squamous subtype showed squamous differentiation and expression of basal markers (CD44, CK5, CK6A, CK14) as well as transglutaminase 1 (TGM1), desmocollin 3 (DSC3), PI3, and occasionally immune checkpoint markers. This subtype also showed a good response to both cisplatin-based chemotherapy and immune checkpoint therapy. The neuronal subtype was characterized by neuroendocrine marker expression but did not always show morphological features of neuroendocrine tumors, and it was correlated with the worst clinical outcome (36, 42). MIBC with luminal features is likely to progress from pre-existing superficial papillary tumors, while basal tumors develop from flat in situ lesions.

Despite the plurality of molecular taxonomies of UC, the most comprehensive one seems to be presented by the Lund University group and the TCGA group. Recently, the Bladder Cancer Molecular Taxonomy Group issued its recommendations based on cohorts and studies proposing different classifications trying to assimilate and harmonize

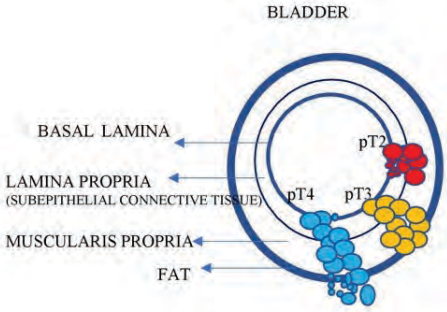

SUBTYPE	MUTATION	PROGNOSIS
I. (luminal papillary)	FGFR3 KDM6A	• least aggressive subtype • younger patients • benefit from FGFR3 inhibitors
II. (luminal nonspecified)	ELF3	• micropapillary variants • associated with CIS
III. (luminal unstable)	P53 ERCC2 APOBEC (increased) high TBM genomicaly unstable	• Sensitivity to chemotherapy
IV. (stroma-rich)	.	• prominent fibroblasts and myofibroblasts • enriched with T and B cell markers • immune checkpoint therapy
V. (basal/squamous)	P53 RB1 EGFR	• squamous differentiation • agressive/ poor prognosis
VI. (neuroendocrine-like)	P53 RB1	• express neuroendocrine markers • agressive/poor survival

Figure 3. MIBC molecular subgroups. FGFR3 – Fibroblast growth factor receptor 3, KDM6A – Lysine demethylase 6A, ELF3 – ETS like transcription factor 3, ERCC2- excision repair cross-complementing repair 2, APOBEC3 – Apolipoprotein B mRNA catalytic polypeptide-like enzyme, RB1 – RB transcriptional corepressor 1.

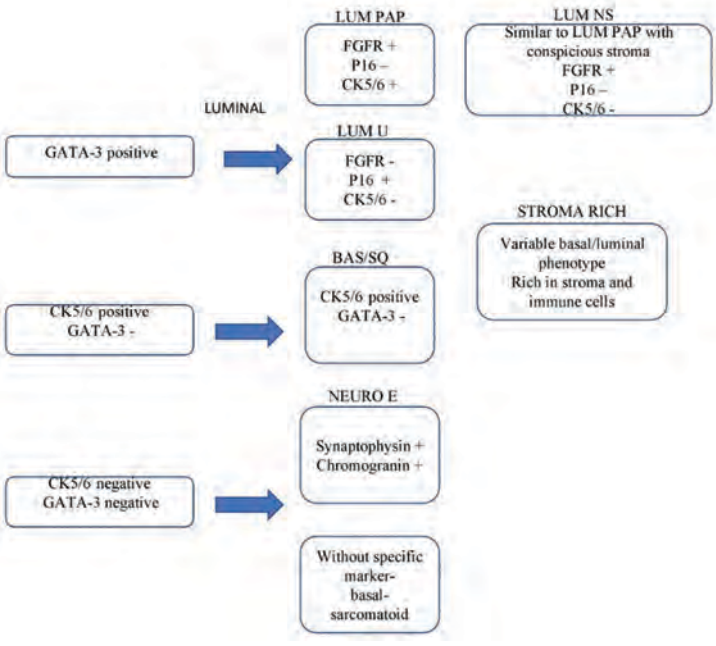

Figure 4. Proposed immunohistochemical panel for bladder cancer subtyping. LumPap – luminal papillary, LumNS – luminal nonspecified, LumU – luminal unstable, Ba/Sq – basal/squamous, and Neuro E – neuroendocrine-like.

the terminology for these subtypes and provide a robust classification system of clinical relevance. Their proposed consensus classification includes six molecular types: luminal papillary (LumP), luminal nonspecified (LumNS), luminal unstable (LumU), stroma-rich, basal/squamous (Ba/Sq), and neuroendocrine-like (NE-like). All luminal tumors show urothelial differentiation, *FGFR3* genetic changes, and active *PPARG* and *GATA3* regulons. LumP shows the least aggressive behavior and frequently harbors *TP53* wild type. LumNS is strongly related to micropapillary morphology and CIS. LumU tumors are characterized by enrichment in genomic instability and mutations in the genes encoding

for the APOBEC protein family and the highest levels of *TP53* and *ERCC2* mutations, associated with sensitivity to chemotherapeutic agents (41-44). Stroma-rich tumors show high expression of endothelial and myofibroblastic gene signatures, T, and B cell markers. Ba/Sq and NE-like subtypes were confirmed as very aggressive with the worst prognosis (45) (Figure 3). To ease every-day histopathological evaluation of BC and enable the best molecular classification in routine pathologists' work, immunohistochemical algorithms for molecular BC subtyping have been proposed (Figure 4) (43).

Molecular subtypes and BC classification are based on different underlying oncogenic mechanisms, genetic and epigenetic alterations, changes in the microenvironment and non-tumor cells, infiltration by immune cells, histologic patterns, and clinical outcomes. Still, some unresolved questions about different histological subtypes of BC are an ongoing topic of research and discussion. Currently, there is not enough evidence about the connection between molecular features and chemotherapy response.

Therapy

Non-Muscle Invasive Bladder Cancer

NMIBC of low-grade is subject to monitoring and early detection protocols, which can be improved with the above-mentioned multigene assays from urine to detect recurrent tumors and search for markers of NMIBC with increased risk of progression into the invasive high-grade tumor (8). NMIBC of high-grade is treated with locally applied chemotherapy (intravesical chemotherapy), which is very effective, together with TUR, in reducing a local recurrence. Mitomycin C, epirubicin, thiotepa, gemcitabine, and doxorubicin are the most commonly used cytotoxic agents (46). BC has been for decades the paradigm of immune-responsive disease. For NMIBC, the standard treatment is still local instillation of Bacillus Calmette-Guérin (BCG), which acts as an immunomodulatory agent eliciting a cell-mediated immune response. This therapy reduces recurrence and progression. It is a good maintenance therapy for patients at intermediate risk and high risk of NMIBC (47).

Muscle Invasive Bladder Cancer

Radical cystectomy with pelvic lymph node dissection as the sole treatment modality offers a chance for a cure only in a minority of patients with MIBC. Occult distant metastases are common even in patients that present with localized MIBC. Moreover, after radical surgery, 50% of patients experience metastatic relapse with a median time to distant failure around one year post-cystectomy. Strategies undertaken to address such high distant failure rates include the use of perioperative chemotherapy. While perioperative chemotherapy implies the use of chemotherapy before or after cystectomy, several distinct features make neoadjuvant chemotherapy specifically an appealing option for the curative treatment of MIBC (48, 49).

***Neoadjuvant chemotherapy* (NAC)** (3 cycles of methotrexate, vinblastine, doxorubicin, cisplatin (MVAC)) followed by radical cystectomy can confront a lower burden micrometastatic disease. The in-vivo therapeutic effect of chemotherapy is observed, and before tolerate chemotherapy better before surgery (decline in performance status, deterioration in kidney function, postoperative morbidity). In patients who respond to NAC, downstaging is possible, optimally resulting in pathologic complete response and clear surgical margins. Despite the level I evidence, NAC's uptake was relatively weak across different healthcare settings and hardly reached 25% of eligible MIBC patients (50-52). There are several possible explanations. Up to 50% of patients with MIBC have significant renal function impairment, which precludes the use of cisplatin-based chemotherapy (kidney filtration rate <60 mg/minute/1.73 m^2 threshold), which leaves them out of the window of opportunity to benefit from NAC (53). Moreover, MIBC patients are often older, frail, and have a high comorbidities burden (primarily cardiovascular, including heart failure). Around half of all patients with MIBC are ineligible to receive cisplatin (54) from the outset.

Apart from eligibility issues, there is a fear of delaying cystectomy due to toxic chemotherapy given to frail patients, which is truly effective only in the minority of patients (25-35% of patients experience tumor downstaging or pathologic complete response). A delay in cystectomy beyond 12 weeks was associated with inferior survival outcomes only when no NAC was given. However, most of the neoadjuvant regimens can be completed within this period, causing no surgery delay. Reassuringly, there was no difference in radical cystectomy rates between the patients randomized to NAC and patients treated with radical cystectomy alone in landmark SWOG 8710 randomized trial (82% vs. 81%) (55, 56).

Standard-dose MVAC regimen has significant toxicity. A novel approach to shorten the duration of treatment and decrease toxicity is the development of a dose-dense (ddMVAC) 2-week regimen with the support of granulocyte–colony-stimulating factors. The observed complete pathologic response after 3 or 4 cycles of ddMVAC is 26% and 38%, respectively. The time from initiation of NAC to cystectomy was well within the optimal 12 weeks window (9.7 weeks). The most common toxicity was manageable myelosuppression and mucositis, with no severe and life-threatening side effects and no cystectomy cancellation (56-58). NAC is standard of care for patients with MIBC fit for cisplatin and is supported by European Association of Urology and National Comprehensive Cancer Network guidelines (50, 51).

Adjuvant chemotherapy for high-risk bladder cancer is based on an actual assessment of pathological risk factors after radical surgery to tailor treatment based on the individualized risk of relapse. This approach would overcome NAC's main shortcoming: unselective treatment with high toxicity in a difficult-to-treat population with a small margin of benefit. However, only a few patients with high-risk pathological features following cystectomy (node-positive patients, pT3-4 disease, positive surgical margins, and extracapsular extension) can receive cisplatin-based adjuvant chemotherapy. This is secondary to several reasons: radical cystectomy is a major and highly morbid surgical procedure with a long recovery and many hospital re-admissions; frailty, poor kidney function, and malnutrition are significant problems that frequently preclude timely receipt of chemotherapy (58, 59).

Treatment of metastatic disease Metastatic bladder cancer is an incurable disease, and current data still support cisplatin-based combination chemotherapy as a standard approach for patients who can tolerate cisplatin. The expected response rate with first-line cisplatin combinations is in the range of 40-60%, with a median survival of 13-16 months (60). Available chemotherapy regimens in metastatic settings include standard MVAC, gemcitabine-cisplatin, and ddMVAC, which are considered standard first-line treatment options for metastatic bladder cancer (61). It was mentioned above how in NMIBC, the use of intravesical BCG activates the immune response. In the era of tumor molecular insights, the discovery of a high tumor somatic mutation load in BC, typical for environmentally caused cancers, as well as a peritumoral cell response, the use of immune checkpoint inhibitor (ICI) therapy became an option in metastatic BC (62). Although it came relatively late in bladder cancer therapy, the first report of the prognostic role of programmed death (PD) PD-1/PD/L1 blockade was published in 2007 by Sharma et al. (63). Phase I testing of the activity of anti-PD-L1 in metastatic bladder cancer was published in 2014, which completely transformed the therapeutic landscape of BC. Over the last few years, five ICI agents were approved for second-line treatment of advanced BC after prior platinum-based chemotherapy progression. Those agents include atezolizumab, pembrolizumab, nivolumab, durvalumab, and avelumab. Two ICI agents were approved for first-line treatment of advanced bladder cancer in patients ineligible for cisplatin with positive PD-L1 status (atezolizumab, pembrolizumab) (64-67). Dual ICI is also being tested as an upfront treatment for advanced urothelial cancer. Current data indicate that avelumab maintenance will become the standard option following induction chemotherapy in patients with advanced disease (68). Recently the selective tyrosine kinase inhibi-

tor erdafitinib has obtained FDA approval to treat *FGFR3* mutated metastatic UC resistant to first-line chemotherapy (15-20% of the cases). Erdafitinib represents the first approved targeted therapy for BC (69, 70). Although BC has been considered a grim disease in the not-so-distant past, it has now become a model for oncology success with many available therapeutic options over the last five years. Several ongoing clinical trials will have definitive results that will define the role and optimal use of ICI and targeted treatments, hopefully further revolutionizing advanced bladder cancer management.

Biomarkers of Response to Chemotherapy

The main drawback of chemotherapy is its unselective nature associated with an absence of validated response biomarkers. More precisely, only a minority of patients exhibit clinical benefit while exposed to toxic treatment. To overcome these issues, an effort has been made to develop single gene-based assays, gene expression, and transcriptome panels to characterize MIBC molecularly. These efforts aim to develop both prognostic and predictive biomarkers, as was previously mentioned. Using gene expression patterns, investigators could dichotomize MIBC in basal and luminal cancers, similar to previous breast cancer efforts, which had a significant clinical impact.

Currently, six biologically relevant consensus molecular classes have been described: luminal papillary, luminal nonspecified, luminal unstable, stroma-rich, basal/squamous, and neuroendocrine-like. The use of immunohistochemistry to reveal the molecular profile is an appealing strategy, given its potential applicability in routine pathology practice. However, this approach is not clinically validated (39-45). Despite some progress in unraveling the molecular complexities of MIBC over the last decade, there is still no readily available molecular biomarker of neoadjuvant chemotherapy response. Moreover, clinicians should be extremely cautious when making clinical decisions based on presumed molecular subtypes. Data supporting neoadjuvant chemotherapy sensitivity in basal tumors are retrospective and require prospective validation (49, 50).

Conclusions

Bladder cancer is a genetically heterogeneous disease. Recent advances have uncovered some aspects of bladder cancer development and progression, which have led to a unified molecular classification of this disease. It was hoped these efforts would lead to clinically relevant subtyping of bladder cancer similar to breast cancer. This goal, however, is yet to be achieved. Some expected benefits include a selection of patients for chemotherapy and immunotherapy. Immunotherapy is an emerging treatment modality in advanced bladder cancer and soon is expected to become the standard of care. In summary, the outlook for bladder cancer patients is substantially improving, with new theranostic and therapeutic options expected to become available in the following years.

Conflict of Interest: The authors declare that they have no conflict of interest.

References

1. GLOBCANBladder-fact-sheet.pdf. [cited 2020 Dec 4]. Available from: https://gco.iarc.fr/today/fact-sheets-cancers.
2. Saginala K, Barsouk A, Aluru JS, Rawla P, Padala SA, Barsouk A. Epidemiology of Bladder Cancer. Med Sci (Basel). 2020:13;8(1):15.
3. Moch H, Humphrey PA, Ulbright TM, Reuter VE. Tumours of the urinary tract. In: World Health Organization classification of tumours of the urinary system and male genital organs. 4th ed. Lyon, France: IARC Press; 2016. p. 77-133.
4. Dobruch J, Daneshmand S, Fisch M, Lotan Y, Noon AP, Resnick MJ, et al. Gender and Bladder Cancer: A Collaborative Review of Etiology, Biology, and Outcomes. Eur Urol. 2016;69(2):300-10.
5. National Collaborating Centre for Cancer (UK). Bladder Cancer: Diagnosis and Management. London: National Institute for Health and Care Excellence (UK); 2015. PMID: 26180884.
6. Yafi FA, Brimo F, Steinberg J, Aprikian AG, Tanguay S, Kassouf W. Prospective analysis of sensitivity and specificity of urinary cytology and other urinary biomarkers for bladder cancer. Urol Oncol. 2015;33(2):66.e25-31.

7. Cowan ML, Rosenthal DL, Van den Bussche CJ. Improved risk stratification for patients with high-grade urothelial carcinoma following application of the Paris System for Reporting Urinary Cytology. Cancer Cytopathol. 2017;125(6):427-34.
8. Batista R, Vinagre N, Meireles S, Vinagre J, Prazeres H, Leão R, et al. Biomarkers for Bladder Cancer Diagnosis and Surveillance: A Comprehensive Review. Diagnostics (Basel). 2020;10(1):39.
9. Lodewijk I, Dueñas M, Rubio C, Munera-Maravilla E, Segovia C, Bernardini A, et al. Liquid Biopsy Biomarkers in Bladder Cancer: A Current Need for Patient Diagnosis and Monitoring. Int J Mol Sci. 2018;19(9):2514.
10. Ward DG, Baxter L, Gordon NS, Ott S, Savage RS, Beggs AD, et al. Multiplex PCR and Next Generation Sequencing for the Non-Invasive Detection of Bladder Cancer. PLoS One. 2016;11:e0149756.
11. Christensen E, Nordentoft I, Vang S, Birkenkamp-Demtröder K, Jensen JB, Agerbæk M, et al. Optimized targeted sequencing of cell-free plasma DNA from bladder cancer patients. Sci Rep. 2018;8(1):1917.
12. Guo S, Xu P, Zhou A, Wang G, Chen W, Mei J, et al. Contrast-Enhanced Ultrasound Differentiation Between Low- and High- Grade Bladder Urothelial Carcinoma and Correlation With Tumor Microvessel Density. J Ultrasound Med. 2017;36(11):2287-97.
13. Galgano SJ, Porter KK, Burgan C, Rais-Bahrami S. The Role of Imaging in Bladder Cancer Diagnosis and Staging. Diagnostics (Basel). 2020;10(9):703.
14. Hugen CM, Duddalwar V, Daneshmand S. Preoperative Imaging for Clinical Staging Prior to Radical Cystectomy. Curr Urol Rep. 2016;17(9):62.
15. Trinh TW, Glazer DI, Sadow CA, Sahni VA, Geller NL, Silverman SG. Bladder cancer diagnosis with CT urography: test characteristics and reasons for false-positive and false-negative results. Abdom Radiol (NY). 2018;43(3):663-71.
16. Rais-Bahrami S, Pietryga JA, Nix JW. Contemporary role of advanced imaging for bladder cancer staging. Urol Oncol. 2016;34(3):124-33.
17. Lee CH, Tan CH, Faria SC, Kundra V. Role of Imaging in the Local Staging of Urothelial Carcinoma of the Bladder. AJR Am J Roentgenol. 2017;208(6):1193-205.
18. Srivastava A, Douglass LM, Chernyak V, Watts KL. Advances in Imaging in Prostate and Bladder Cancer. Curr Urol Rep. 2017;18(9):69.
19. Wang HJ, Pui MH, Guo Y, Yang D, Pan BT, Zhou XH. Diffusion-weighted MRI in bladder carcinoma: the differentiation between tumor recurrence and benign changes after resection. Abdom Imaging. 2014;39(1):135-41.
20. Panebianco V, Narumi Y, Altun E, Bochner BH, Efstathiou JA, Hafeez S, et al. Multiparametric Magnetic Resonance Imaging for Bladder Cancer: Development of VI-RADS (Vesical Imaging-Reporting And Data System). Eur Urol. 2018;74(3):294-306.
21. Öztürk H. Comparing RECIST with EORTC criteria in metastatic bladder cancer. J Cancer Res Clin Oncol. 2016;142(1):187-94.
22. Civelek A, Apolo A, Agarwal P, Evers R, Bluemke D, Malayeri A. 18F-FDG PET-MRI in the management of muscle invasive bladder cancer: Challenges in imaging and solutions. Journal of nuclear medicine: official publication. Soc Nucl Med. 2016;57(suppl 2) abstr 1292.
23. Kirkali Z, Chan T, Manoharan M, Algaba F, Busch C, Cheng L, et al. Bladder cancer: epidemiology, staging and grading, and diagnosis. Urology. 2005;66(6 Suppl 1):4-34.
24. Jordan B, Meeks JJ. T1 bladder cancer: current considerations for diagnosis and management. Nat Rev Urol. 2019;16(1):23-34.
25. Amin MB, Edge S, Greene F, Byrd DR, Brookland RK, Washington MK, et al. AJCC Cancer Staging Manual. 8th ed. Chicago, USA: Springer International Publishing; 2017. p. 727-35.
26. Paner GP, Montironi R, Amin MB. Challenges in Pathologic Staging of Bladder Cancer: Proposals for Fresh Approaches of Assessing Pathologic Stage in Light of Recent Studies and Observations Pertaining to Bladder Histoanatomic Variances. Adv Anat Pathol. 2017;24(3):113-27.
27. McGranahan N, Swanton C. Clonal Heterogeneity and Tumor Evolution: Past, Present, and the Future. Cell. 2017;168(4):613-28.
28. Liu D, Abbosh P, Keliher D, Reardon B, Miao D, Mouw K, et al. Mutational patterns in chemotherapy resistant muscle-invasive bladder cancer. Nat Commun. 2017;8(1):2193.
29. Nordentoft I, Lamy P, Birkenkamp-Demtröder K, Shumansky K, Vang S, Hornshøj H, et al. Mutational context and diverse clonal development in early and late bladder cancer. Cell Rep. 2014;7(5):1649-63.
30. Robertson AG, Kim J, Al-Ahmadie H, Bellmunt J, Guo G, Cherniack AD, et al. Comprehensive molecular characterization of muscle- invasive bladder cancer. Cell. 2017;171(3):540-56.e25.
31. Guo CC, Czerniak B. Bladder Cancer in the Genomic Era. Arch Pathol Lab Med. 2019;143(6):695-704.
32. Law EK, Sieuwerts AM, LaPara K, Leonard B, Starrett GJ, Molan AM, et al. The DNA cytosine deaminase APOBEC3B promotes tamoxifen resistance in ER-positive breast cancer. Sci Adv. 2016;2(10):e1601737.
33. Christensen E, Birkenkamp-Demtröder K, Sethi H, Shchegrova S, Salari R, Nordentoft I, et al. Early detection of metastatic relapse and monitoring of therapeutic efficacy by ultra- deep sequencing of plasma cell- free DNA in patients with urothelial bladder carcinoma. J Clin Oncol. 2019;37(18):1547-57.
34. Hedegaard J, Lamy P, Nordentoft I, Algaba F, Høyer S, Ulhøi BP, et al. Comprehensive transcriptional analy-

sis of early- stage urothelial carcinoma. Cancer Cell. 2016;30(1):27-42.

35. Kamat AM, Hahn NM, Efstathiou JA, Lerner SP, Malmström PU, Choi W, et al. Bladder cancer. Lancet. 2016;388(10061):2796-810.
36. Meeks JJ, Al-Ahmadie H, Faltas BM, Taylor 3rd JA, Flaig TW, DeGraff DJ, et al. Genomic heterogeneity in bladder cancer: challenges and possible solutions to improve outcomes. Nat Rev Urol. 2020;17(5):259-70.
37. Czerniak B, Dinney C, McConkey D. Origins of bladder cancer. Annu Rev Pathol. 2016;11:149-74.
38. Sjodahl G, Lauss M, Lovgren K, Chebil G, Gudjonsson S, Veerla S, et al. A molecular taxonomy for urothelial carcinoma. Clin Cancer Res. 2012;18(12):3377-86.
39. Hedegaard, Lamy P, Nordentoft I, Algaba F, Høyer S, Ulhøi BP, et al. Comprehensive transcriptional analysis of early-stage urothelial carcinoma. Cancer Cell. 2016;30(1):27-42.
40. Stroggilos R, Mokou M, Latosinska A, Makridakis M, Lygirou V, Mavrogeorgis E, et al. Proteome-based classification of nonmuscle invasive bladder cancer. Int. J. Cancer. 2020;146(1):281-94.
41. Rodriguez-Vida A, Lerner SP, Bellmunt J. The Cancer Genome Atlas Project in Bladder Cancer. Cancer Treat Res. 2018;175:259-71.
42. Al-Ahmadie H, Netto GJ. Updates on the Genomics of Bladder Cancer and Novel Molecular Taxonomy. Adv Anat Pathol. 2020;27(1):36-43.
43. Marzouka NA, Eriksson P, Rovira C, Liedberg F, Sjödahl G, Höglund M. A validation and extended description of the Lund taxonomy for urothelial carcinoma using the TCGA cohort. Sci Rep. 2018;8:3737.
44. Tran L, Xiao JF, Agarwal N, Duex JE, Theodorescu D. Advances in bladder cancer biology and therapy. Nat Rev Cancer. 2021;21(2):104-21. doi: 10.1038/s41568-020-00313-1.
45. Kamoun A, de Reyniès A, Allory Y, Sjödahl G, Robertson AG, Seiler R, et al. Bladder Cancer Molecular Taxonomy Group. A Consensus Molecular Classification of Muscle-invasive Bladder Cancer. Eur Urol. 2020;77(4):420-33.
46. Babjuk M, Burger M, Compérat EM, Gontero P, Mostafid AH, Palou J, et al. European Association of Urology Guidelines on Non-muscle-invasive Bladder Cancer (TaT1 and Carcinoma In Situ) - 2019 Update. Eur Urol. 2019;76(5):639-57.
47. Peyton CC, Chipollini J, Azizi M, Kamat AM, Gilbert SM, Spiess PE. Updates on the use of intravesical therapies for non-muscle invasive bladder cancer: how, when and what. World J Urol. 2019;37(10):2017-29.
48. Aminoltejari K, Black PC. Radical cystectomy: a review of techniques, developments and controversies. Transl Androl Urol. 2020;9(6):3073-81.
49. Witjes JA, Bruins HM, Cathomas R, Compérat EM, Cowan NC, Gakis G, et al. European Association of Urology Guidelines on Muscle-invasive and Metastatic Bladder Cancer: Summary of the 2020 Guidelines. Eur Urol. 2021;79(1):82-104.
50. Flaig TW, Spiess PE, Agarwal N, Bangs R, Boorjian SA, Buyyounouski MK, et al. Bladder Cancer, Version 3.2020, NCCN Clinical Practice Guidelines in Oncology. J Natl Compr Canc Netw. 2020;18(3):329-54.
51. Booth CM. Perioperative chemotherapy for muscle-invasive bladder cancer: Closing the gap between evidence and practice. J Can Urol Assoc. 2016;10(1-2):31-2.
52. Koshkin VS, Barata PC, Rybicki LA, Zahoor H, Almassi N, Redden AM, et al. Feasibility of Cisplatin-Based Neoadjuvant Chemotherapy in Muscle-Invasive Bladder Cancer Patients With Diminished Renal Function. Clinical Genitourinary Cancer. Clin Genitourin Cancer. 2018;16(4):e879-92.
53. Thompson RH, Boorjian SA, Kim SP, Cheville JC, Thapa P, Tarrel R, et al. Eligibility for neoadjuvant/adjuvant cisplatin-based chemotherapy among radical cystectomy patients. BJU Int. 2014;113(5b):E17-21.
54. Niegisch G. Should we spare neoadjuvant chemotherapy in low-risk muscle-invasive bladder cancer patients scheduled for radical cystectomy? Transl Androl Urol. 2019 Jul;8(Suppl 3):S283-6.
55. Chu AT, Holt SK, Wright JL, Ramos JD, Grivas P, Yu EY, et l. Delays in radical cystectomy for muscle-invasive bladder cancer. Cancer. 2019;125(12):2011-7.
56. Choueiri TK, Jacobus S, Bellmunt J, Qu A, Appleman LJ, Tretter C, et al. Neoadjuvant dose-dense methotrexate, vinblastine, doxorubicin, and cisplatin with pegfilgrastim support in muscle-invasive urothelial cancer: Pathologic, radiologic, and biomarker correlates. J Clin Oncol. 2014;32(18):1889-94.
57. Plimack ER, Hoffman-Censits JH, Viterbo R, Trabulsi EJ, Ross EA, Greenberg RE, et al. Accelerated methotrexate, vinblastine, doxorubicin, and cisplatin is safe, effective, and efficient neoadjuvant treatment for muscle-invasive bladder cancer: Results of a multicenter phase II study with molecular correlates of response and toxicity J Clin Oncol. 2014;32(18):1895-901.
58. Peyton CC, Tang D, Reich RR, Azizi M, Chipollini J, Pow-Sang JM, et al. Downstaging and Survival Outcomes Associated with Neoadjuvant Chemotherapy Regimens among Patients Treated with Cystectomy for Muscle-Invasive Bladder Cancer. JAMA Oncol. 2018;4(11):1535-42.
59. Harraz AM, Osman Y, El-Halwagy S, Laymon M, Mosbah A, Abol-Enein H, et al. Risk factors of hospital readmission after radical cystectomy and urinary diversion: Analysis of a large contemporary series. BJU Int. 2015;115(1):94-100.
60. Kaufman D, Raghavan D, Carducci M, Levine EG, Murphy B, Aisner J, et al. Phase II trial of gemcitabine plus cisplatin in patients with metastatic urothelial cancer. J Clin Oncol. 2000;18(9):1921-7.

61. Koufopoulou M, Miranda PAP, Kazmierska P, Deshpande S, Gaitonde P. Clinical evidence for the first-line treatment of advanced urothelial carcinoma: Current paradigms and emerging treatment options. Cancer Treat Rev. 2020;89:102072.
62. Powles T, Eder JP, Fine GD, Braiteh FS, Loriot Y, Cruz C, et al. MPDL3280A (anti-PD-L1) treatment leads to clinical activity in metastatic bladder cancer. Nature. 2014;515(7528):558-62.
63. Sharma P, Shen Y, Wen S, Yamada S, Jungbluth AA, Gnjatic S, et al. CD8 tumor-infiltrating lymphocytes are predictive of survival in muscle-invasive urothelial carcinoma. Proc Natl Acad Sci U S A. 2007;104(10):3967-72.
64. Powles T, Durán I, van der Heijden MS, Loriot Y, Vogelzang NJ, de Giorgi U, et al. Atezolizumab versus chemotherapy in patients with platinum-treated locally advanced or metastatic urothelial carcinoma (IMvigor211): a multicentre, open-label, phase 3 randomised controlled trial. Lancet. 2018;391(10122):748-57.
65. Bellmunt J, de Wit R, Vaughn DJ, Fradet Y, Lee J-L, Fong L, et al. Pembrolizumab as Second-Line Therapy for Advanced Urothelial Carcinoma. N Engl J Med. 2017;376(11):1015-26.
66. Balar AV, Castellano D, O'Donnell PH, Grivas P, Vuky J, Powles T, et al. First-line pembrolizumab in cisplatin-ineligible patients with locally advanced and unresectable or metastatic urothelial cancer (KEYNOTE-052): a multicentre, single-arm, phase 2 study. Lancet Oncol. 2017;18(11):1483-92.
67. Powles T, Park SH, Voog E, Caserta C, Valderrama BP, Gurney H, et al. Avelumab Maintenance Therapy for Advanced or Metastatic Urothelial Carcinoma. N Engl J Med. 2020;383(13):1218-30.
68. Mo Q, Nikolos F, Chen F, Tramel Z, Lee YC, Hayashi K, et al. Prognostic Power of a Tumor Differentiation Gene Signature for Bladder Urothelial Carcinomas. Natl Cancer Inst. 2019;111(11):1236.
69. Siefker-Radtke AO, Currie G, Abella E, Vaena DA, Rezazadeh Kalebasty A, Curigliano G, et al. FIERCE-22: Clinical activity of vofatamab (V) a FGFR3 selective inhibitor in combination with pembrolizumab (P) in WT metastatic urothelial carcinoma, preliminary analysis. J Clin Oncol. 37(15 Suppl):4511-4511.
70. Montazeri K, Bellmunt J. Erdafitinib for the treatment of metastatic bladder cancer. Expert Rev Clin Pharmacol. 2020;13(1):1-6.

Narrative Review
Acta Medica Academica 2021;50(1):157-174
DOI: 10.5644/ama2006-124.333

An Update on Molecular Genetic Aberrations in Spitz Melanocytic Proliferations: Correlation with Morphological Features and Biological Behavior

Daja Šekoranja, Jože Pižem, Boštjan Luzar

Institute of Pathology, Faculty of Medicine, University of Ljubljana, Korytkova 2, 1000 Ljubljana, Slovenia

Correspondence: *bostjan.luzar@mf.uni-lj.si;* Tel.: + 386 1 543 7130; Fax.: + 386 1 543 7101

Received: 14 February 2021; **Accepted:** 15 March 2021

Abstract
The aim of the paper is to give an update on molecular genetic aberrations in Spitz melanocytic proliferations with special emphasis on their correlation with morphological features and biological behavior. The Spitz group of melanocytic proliferations is defined by a combination of distinctive morphological features and driver molecular genetic events. Morphologically, these neoplasms are characterized by large, oval, polygonal, or spindled melanocytes with abundant eosinophilic cytoplasm, vesicular nuclei with prominent nucleoli, often in association with epidermal hyperplasia. Molecular aberrations in Spitz melanocytic proliferations can be divided into two main groups, according to the driver genetic change: 1) 11p amplification/*HRAS* mutation, present in about 20% of cases, and 2) kinase fusions, present in about 50%, further subdivided into tyrosine kinase fusions (*ALK*, *ROS1*, *NTRK1*, *NTRK3*, *MET*, *RET*) or serine-threonine kinase fusions (*MAP3K8*, *BRAF*). Driver genetic aberrations can be detected along the whole biological spectrum of Spitz melanocytic proliferations, and are mutually exclusive. Although driver genetic aberrations enable proliferation of melanocytes, additional genetic events (often biallelic inactivation of *CDKN2A* and *TERT* promoter mutations) are necessary for the development of overt Spitz malignancy. **Conclusions**. Recent studies have demonstrated that certain driver genetic aberrations are more often associated with the benign spectrum of Spitz melanocytic proliferations and indolent biological behavior (11p amplification/*HRAS* mutation, tyrosine kinase fusions). In contrast, some driver aberrations are more frequent in the atypical/malignant spectrum of Spitz melanocytic proliferations with a potential for aggressive biological behavior (serine-threonine kinase fusions). In addition, certain driver aberrations are often associated with distinctive morphological features. However, none of the morphological features is entirely specific for any of these driver genetic aberrations. Immunohistochemistry for ALK, ROS1, and pan-TRK can be used for screening purposes to detect corresponding fusion proteins.

Key Words: Spitz Melanocytic Proliferations ▪ Kinase Fusions ▪ 11p Amplification/HRAS Mutation ▪ Morphology ▪ Clinical Behavior.

Introduction

According to the most recent 4th WHO Classification of Skin Tumours, the Spitz group of melanocytic proliferations is defined by a combination of morphological characteristics and driver molecular genetic abnormalities (1). Spitz melanocytic proliferations are characterized morphologically by a proliferation of large, oval, polygonal epithelioid or spindled melanocytes with abundant eosinophilic cytoplasm, vesicular nuclei with prominent nucleoli, often in association with epidermal hyperplasia (1). They encompass the whole biological spectrum of melanocytic proliferations, including Spitz nevi, atypical Spitz tumors, and Spitz melanomas, also referred to as malignant Spitz tumors (1). Based on the underlying genetic aberrations, Spitz melanocytic proliferations can be divided into four distinct groups: 1) 11p amplified/*HRAS* mutated proliferations, 2) proliferations with tyrosine kinase fusions (*ALK, ROS1, NTRK1, NTRK3, MET, RET*), 3) proliferations with serine/threonine kinase fusions (*MAP3K8, BRAF*) and 4) proliferations with Spitz morphology but lack-

ing an 11p/*HRAS* mutation, kinase fusions, *BRAF, NRAS, GNAQ, GNA11* mutations and other driver genetic changes characteristic of other defined melanocytic subgroups (1). The last group is at present poorly defined and will not be discussed further in this review. Importantly, driver genetic events are mutually exclusive in a particular Spitz melanocytic proliferation and are by themselves insufficient for the development of overt malignancy, generally characterized by the development of distant metastases and aggressive biological behavior (2, 3).

As has been demonstrated by recent studies, such a combined morphological/genetic classification better correlates with the biological behavior of different groups of Spitz melanocytic proliferations. The vast majority of Spitz melanomas resulting in distant metastatic spread harbor serine/threonine kinase fusions (4-11). Furthermore, since several biological drugs are available to treat melanocytic proliferations with aggressive clinical behavior, the characterization of particular driver genetic events and additional genetic abnormalities is becoming increasingly important.

Herein, we review recent advances in the molecular genetics of Spitz melanocytic proliferations. Special emphasis is given to the correlation of molecular genetic aberrations with morphological features and with the biological behavior of Spitz melanocytic proliferations. Immunohistochemistry can be a reliable surrogate tool for certain molecular abnormalities to molecular genetic testing, as discussed further in this review (for practical purposes, the list of antibodies reflecting possible kinase fusions the authors are using routinely is summarized in the Table 1. Also, at the end of each section, a table is presented with short summary of key data for each particular Spitz group of melanocytic proliferations).

Table 1. The List of Antibodies Reflecting Possible Kinase Fusions Used Routinely by the Authors of the Current Review

Antigen	Clone	Manufacturer	Dilution
ALK	5A4	Leica Biosystems, Wetzlar, Germany	1:10
ROS1	SP384	Ventana, Roche, Tucson, USA	RTU (Ready To Use)
panTRK	EPR17341	Abcam, Cambridge, UK	1:50

11p Amplified and/or *HRAS* Mutated Spitz Melanocytic Proliferations

The first recurrent genetic alterations discovered in Spitz melanocytic proliferations were 11p amplification and *HRAS* mutation. They were also the first genetic alterations associated with a specific morphologic phenotype in this group of melanocytic neoplasms (12, 13). Both 11p amplification and *HRAS* mutation can appear exclusively or simultaneously in a single lesion and are most commonly associated with a desmoplastic Spitz nevus morphology (13, 14). *HRAS* (Harvey rat **s**arcoma viral oncogene homolog) resides on 11p chromosome arm (11p15.5) and belongs to the Ras family of oncogenes, encoding a GTPase that is involved in cellular signaling (the MAP kinase-signaling pathway) (15, 16). Mutations in *HRAS* lead to constitutive activation of an altered protein that impacts the expression of various transcription factors involved in cell cycle progression, thus stimulating cell growth and differentiation (16). *HRAS* mutations have also been detected in urothelial and squamous cell carcinomas, adenocarcinomas of various origins, leukemias, and myelodysplastic syndromes (17-19). *HRAS* mutations in Spitz melanocytic proliferations are most commonly missense mutations involving codons 61 and 13, with the three most commonly reported mutations being *Q61L* (2, 6, 14, 20), *Q61R* (14, 20-23), and *G13R* (6, 21, 24-28).

The prototypic 11p amplified/*HRAS* mutated Spitz nevus is a symmetrical, predominantly dermal, relatively hypocellular proliferation composed of large, epithelioid and spindled melanocytes with desmoplastic stromal reaction (i.e., thickened collagen fibers between single neoplastic cells) and an infiltrative base (Figure 1) (2, 13, 14). Melanocytes have abundant eosinophilic or amphophilic cytoplasm, vesicular nuclei, and mild to moderate nuclear pleomorphism (2, 13, 14). The proliferation rate is usually low, although

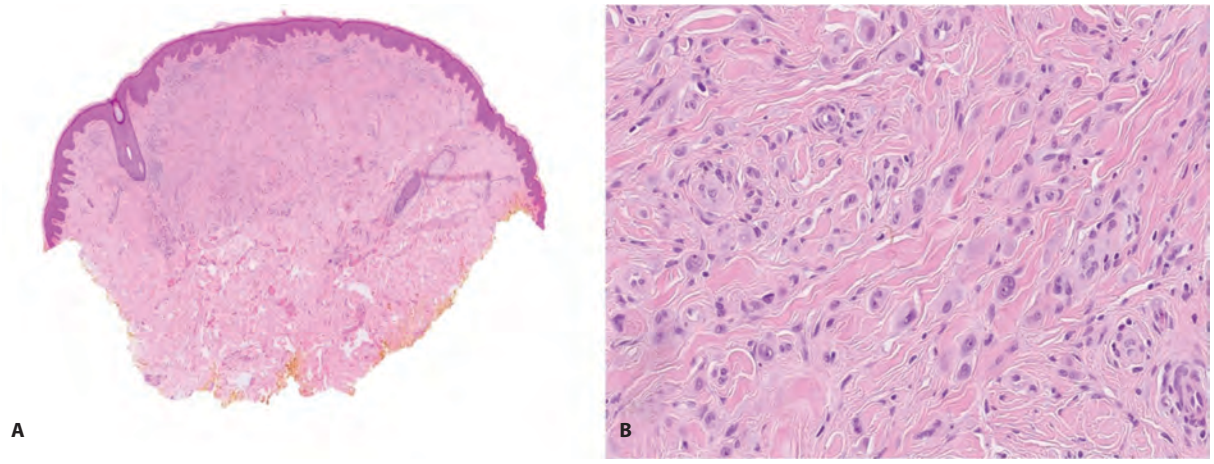

Figure 1. Desmoplastic Spitz nevus. A. Low power magnification reveals a fairly symmetrical intradermal proliferation with infiltrative growth pattern and a desmoplastic stromal reaction. B. Dense collagenous stroma containing epithelioid melanocytes with abundant eosinophilic cytoplasm with darkly stained nuclei and prominent nucleoli is typical for the entity.

isolated deep mitoses and, in rare instances, multiple mitoses may be present and are not associated with malignancy (2, 13, 14, 29). Atypical mitoses are generally absent.

In addition to solitary lesions with typical desmoplastic Spitz nevus morphology, other melanocytic proliferations with *HRAS* mutations and/or 11p gain have also been described, including agminated Spitz nevi with or without associated nevus spilus (25-28), recurrent Spitz nevi (30), melanocytic nevi with deep penetrating nevus-like morphology (21), pseudogranulomatous Spitz nevi (31) and a combination of syringocystadenoma papilliferum, tubular adenoma and a Spitz nevus (24). Moreover, the desmoplastic Spitz nevus phenotype is not restricted to *HRAS* mutated lesions since rare Spitz nevi harboring *ROS1*, *ALK* or even a *BRAF* fusion exhibiting a desmoplastic Spitz nevus morphology have been described (2, 32).

Even though the vast majority of Spitz proliferations with *HRAS* mutations are essentially associated with benign clinical behavior (14, 29, 33), there are occasional reports of *HRAS* mutated Spitz melanomas (6, 23). Recently, Raghavan et al. published a series of Spitz melanomas, two of which harbored *HRAS* hotspot mutations (23). Both lesions were associated with additional genetic aberrations, namely a loss of chromosome 9 (accompanied by negative p16 immunohistochemical reaction) in a case of a 50-year-old female, and a three-codon deletion in *MAP2K1* (p.102_104del), a hemizygous mutation in *ARID1A*, homozygous deletion of *CDKN2A* and *NOTCH2* amplification in a case of a 75-year-old female (23). Unfortunately, clinical follow-up was not available in either of the two cases (23). Lazova et al. also reported two melanomas with *HRAS* mutations in their series (6). One case was of a 73-year-old male diagnosed with Spitz melanoma that harbored an *HRAS Q61L* mutation, which developed metastases two years later, but he was still alive at a 4-year follow-up (6). The second case was a 60-year-old male diagnosed with conventional melanoma that

Table 2. Spitz Melanocytic Proliferations with 11p Amplification/*HRAS* Mutation

Morphological features	• Symmetrical, predominantly intradermal, infiltrative base • Epithelioid and spindled melanocytes – Large – Abundant cytoplasm – Mild to moderate pleomorphism – Mitoses rare, can be deep – Low proliferation rate • Desmoplastic stromal reaction
Biological behavior	Generally benign
Confirmatory test	Next generation sequencing Fluorescence *in situ* hybridization (for 11p amplification) Comparative genomic hybridization (for 11p amplification)

harbored an *HRAS G13R* mutation, who developed metastases two years later, and died at the age of 63 (6).

Spitz Melanocytic Proliferations with Tyrosine Kinase Fusions

ALK Fusions

The **a**naplastic **l**ymphoma **k**inase (*ALK*) gene resides on chromosome 2p23 and encodes a tyrosine kinase receptor, a transmembrane protein that belongs to the insulin receptor family (34). Genetic alterations of the *ALK* gene include point mutations, gene fusions, *ALK* locus amplification, alternative transcription, and small deletions (35) and influence cell proliferation and survival via constitutive activation of the RAS-ERK, JAK3-STAT3, and PI3K-AKT-mTOR pathways (36-38). Fusions involving the *ALK* gene have been discovered in diverse cutaneous neoplasms, including primary cutaneous anaplastic large cell lymphoma (39), epithelioid fibrous histiocytoma (40), acral melanomas (41, 42), and Spitz melanocytic proliferations (2, 43-50).

In Spitz melanocytic proliferations, various different fusion partners have been identified, including *TPM3* (2, 11, 45, 51-54), *DCTN1* (2, 23, 45, 50, 54), *MLPH* (9, 44, 45, 55), *KANK1* (9, 45), *CLIP1* (50), *DDX3Y* (9), *EEF2* (45), *GTF3C2* (50), *MYO5A* (45), *NPM1* (47), *PPFIBP1* (9), *SPTAN1* (9) and *TPR* (50), in descending order of frequency. Lesions from the whole biological spectrum ranging from Spitz nevi, atypical Spitz tumors to Spitz melanomas have been distributed fairly equally among different fusion partners (2, 9, 11, 23, 44, 45, 47, 50-52, 54-56). Although different fusions in Spitz melanocytic proliferations are generally believed to be mutually exclusive with BRAF mutations, a few examples (two Spitz melanomas, one atypical Spitz tumor, and an acral melanoma) with concurrent *ALK* fusion and a *BRAF* mutation have been reported in the literature (41, 54, 57). Such a combination of *ALK* fusion and *BRAF* mutation is, nevertheless, exceptionally rare.

Spitz melanocytic proliferations with *ALK* fusions have the largest average diameter among all Spitz melanocytic proliferations (43). The vast majority of Spitz proliferations with *ALK* fusion are polypoid/dome and/or wedge-shaped solitary lesions with a bulbous and/or infiltrative base. They are composed of plexiform and intersecting fascicles of fairly large, fusiform/spindle cell or mixed spindle and epithelioid cell melanocytes with amphophilic cytoplasm and vesicular nuclei with prominent nucleoli (Figure 2) (2, 23, 43-46, 49, 50, 54, 55, 58). Nuclear pleomorphism is usually mild and occasionally moderate. Melanocytes may appear discohesive with clefts or small vesicle-like spaces in between (23, 50, 55, 59). Ulceration may be present, as may be dermal (even deep) mitoses and perineural invasion, but Kamino bodies are rare (23, 43, 45, 47, 50, 58). Melanin pigment is typically lacking or presents in limited amounts in the cytoplasm of melanocytes. Focal mucin deposits have been described (45). Proliferations with abundant myxoid areas with ALK+/SOX10+/MelanA- spindle cells underneath the superficial nevoid or Spitzoid component have been termed melanocytic myxoid spindle cell tumors with *ALK* rearrangement (MMySTAR) (56). They have been shown to harbor *ALK* fusions with different fusion partners, namely *FBXO28*, *NPAS2*, *PPFIBP1,* and *TPM3* (56). Interestingly, a single example of a desmoplastic Spitz nevus harboring a *TPM3-ALK* fusion has also been reported (2).

ALK immunohistochemistry is a reliable surrogate marker for molecular genetic techniques in cases with diffuse and strong immunopositivity in most melanocytes (Figure 2c) (2, 43-46, 50). In contrast, weak and focal or heterogeneous ALK staining has been demonstrated in non-Spitz melanocytic proliferations with ALK overexpression due to other molecular mechanisms (e.g., alternative transcription initiation that leads to the expression of a novel ALK isoform ALK^{ATI} (60, 61) or in cases with chromosome 2p23 gain (62)), in rare cases of cellular blue nevi and in a single case of deep penetrating nevus (63).

Exceptionally rare examples of Spitz melanocytic proliferations with *ALK* fusion have har-

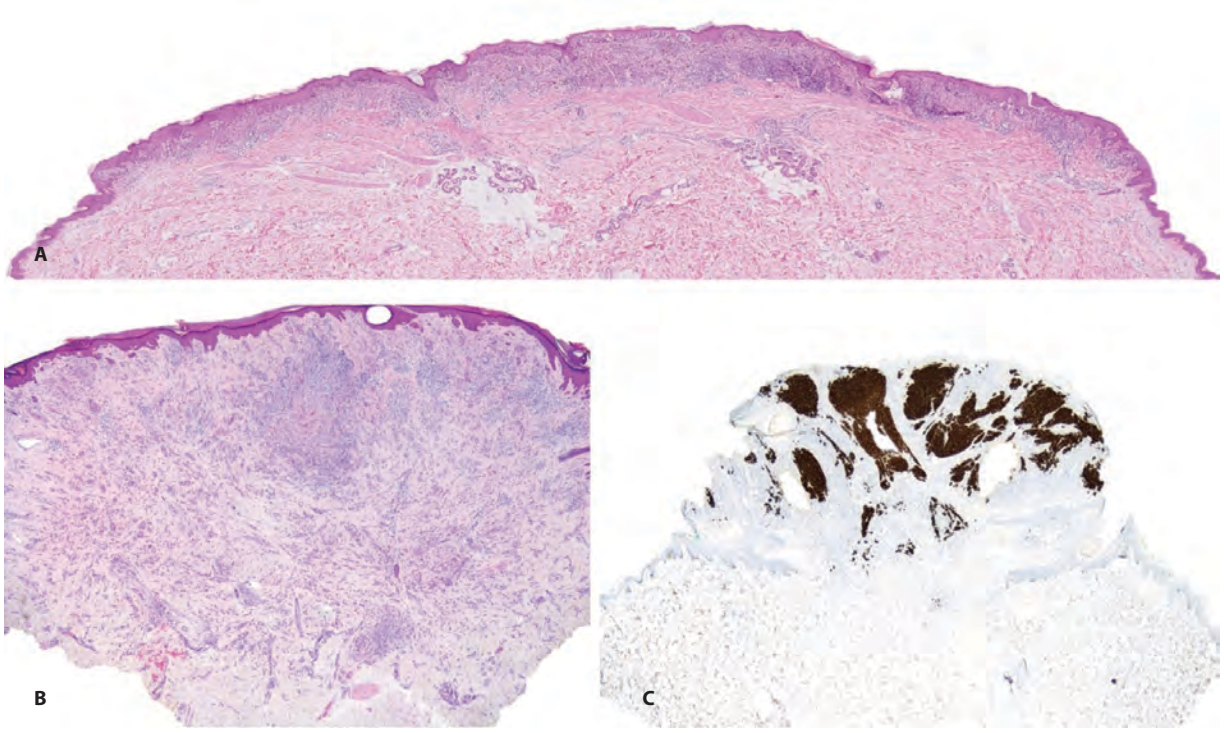

Figure 2. Spitz nevus with *ALK* fusion. A. A large diameter of the proliferation is a characteristic feature of *ALK*-fused melanocytic proliferations. B. A plexiform growth pattern with deep extension of melanocytes is also frequently observed. C. ALK immunohistochemistry.

Table 3. Spitz Melanocytic Proliferations with *ALK* Fusions

Morphological features	• Symmetrical, polypoid/dome and/or wedge-shaped • Large diameter • Plexiform growth pattern • Epithelioid and spindled melanocytes – Mild to moderate pleomorphism – Mitoses rare – Pigmentation absent or scant – Low proliferation rate • Ulceration rare • Kamino bodies usually absent
Biological behavior	Generally favorable (benign) Regional lymph node deposits uncommon No distant metastases or death from the disease
Confirmatory test	• Immunohistochemistry • Next generation sequencing • Fluorescence *in situ* hybridization

bored additional molecular changes, i.e., homozygous 9p21 (*CDKN2A*) deletion in combination with 6p25 (*RREB1*) gain in two cases (49) and a hotspot *TERT*-promoter mutation (C228T) in one case (45), which had no effect on the biological behavior of the proliferation. Only two cases of Spitz melanocytic proliferations with *ALK* fusion and with deposits in lymph nodes have been described, one of which had an additional homozygous 9p21 deletion (49, 55). Importantly, however, none of the cases of Spitz melanocytic proliferations with *ALK* fusion and with available follow-up data were found to be associated with systemic metastases or death from the disease.

ROS1 Fusions

ROS1 protooncogene resides on chromosome 6q22.1 and, like *ALK*, encodes a protein receptor tyrosine kinase that is part of the intracellular signaling pathways Ras-Raf-MEK-ERK, JAK3-STAT3, and PI3K-AKT-mTOR. (64) *ROS1* fusions have been found in a variety of tumors, including non-small cell lung carcinomas, glioblastomas, pediatric gliomas, cholangiocarcinomas, inflamma-

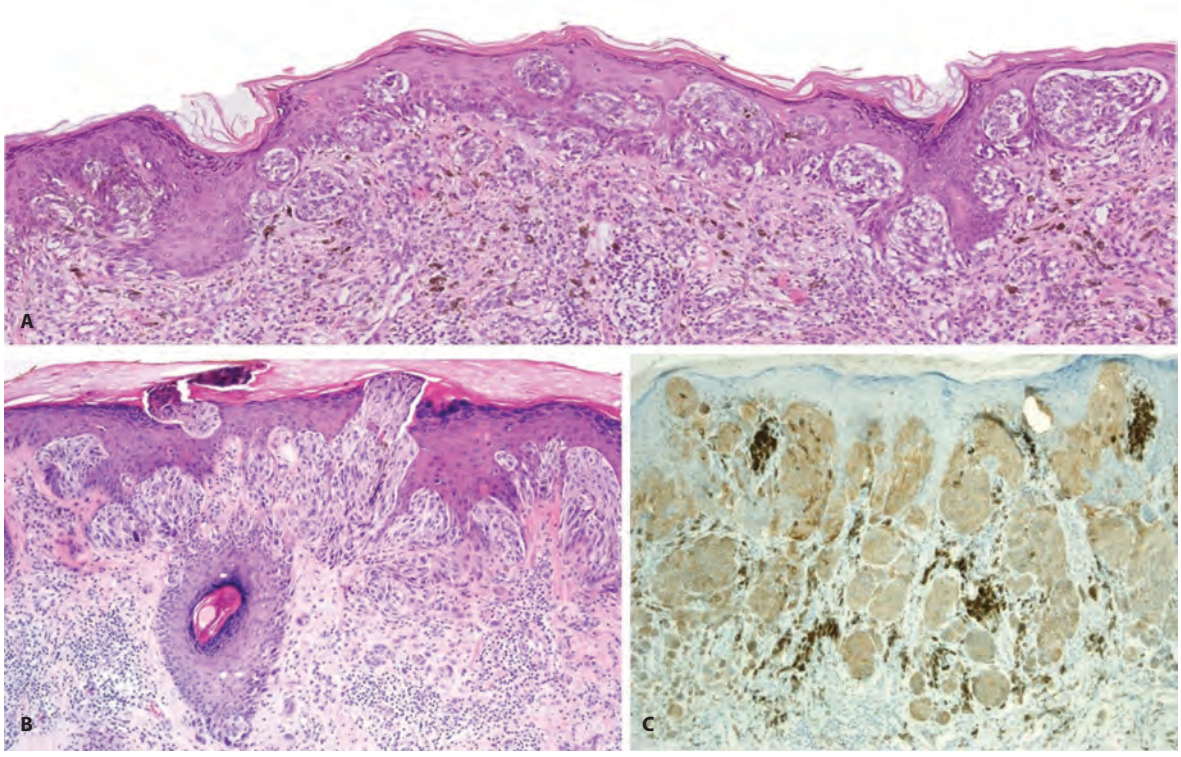

Figure 3. Spitz nevus with *ROS1* fusion. A. *ROS1*-fused melanocytic proliferations often display a prominent junctional component. B. The junctional component consists of melanocytic nests with transepidermal elimination and colonization of the adnexal epithelium. C. ROS1 immunohistochemistry.

tory myofibroblastic tumors, etc (64). *ROS1* fusions are present in up to 17% of Spitz melanocytic proliferations (2). Thirteen different fusion partners have been reported: *PWWP2A, TPM3, PPFIBP1, CAPRIN1, MYO5A, PPFIBP1, CLIP1, ERC1, FIP1L1, HLA-A, KIAA1598, MYH9,* and *ZCCHC8,* in descending order of frequency (2, 23, 32, 65).

Although ROS1-fused Spitz proliferations lack unique identifying morphological features, most *ROS1*-fused melanocytic proliferations are compound, composed either of spindle cells or of a combination of spindle and epithelioid cells with mild to moderate cytological atypia and with limited pigmentation of melanocytes (2, 32, 65). The junctional melanocytic component is frequently prominent, with floating nests or trans-epidermal elimination of melanocytic nests, often colonizing the epithelium of skin adnexa (Figure 3) (32, 65). Kamino bodies seem to be more frequently present in *ROS1* fused Spitz melanocytic proliferations, along with signs of maturation, lack of high-grade cytological atypia, lack of large cells, and fewer mitoses - all statistically significant features differing between *ROS1* and non-*ROS1* Spitz neoplasms in a study by Gerami et al. (32). Nonetheless, large cells were described in 9 of 11 *ROS1* fused Spitz neoplasms in a study by Wiesner et al. (2), and up to 8 mitoses per square millimeter were reported in a study of such proliferations by Donati et al. (65)

Immunohistochemistry for ROS1 protein is a reliable surrogate for molecular testing (Figure 3c). Studies have confirmed that the vast majority (97.4%) of Spitz melanocytic proliferations harboring *ROS1* fusions display ROS1 cytoplasmic positivity on immunohistochemistry (2, 32). It is important to note, though, that immunohistochemical staining is often weak yet diffuse.

The vast majority of hitherto reported Spitz neoplasms with *ROS1* fusion in the literature were classified as either Spitz nevi or atypical Spitz tumors (2, 23, 32, 47, 65-67). Three lesions were of desmoplastic Spitz nevus phenotype (2, 32), four

Table 4. Spitz Melanocytic Proliferations with *ROS1* Fusions

Morphological features	• Junctional component prominent – Transepidermal elimination of nests – Adnexal involvement • Epithelioid and spindled melanocytes – Mild to moderate pleomorphism – Mitoses rare – Pigmentation limited – Low proliferation rate – Maturation present
Biological behavior	Generally favorable (benign) Regional lymph node deposits uncommon No distant metastases or death from the disease
Confirmatory test	• Immunohistochemistry – Staining can be faint • Next generation sequencing *(preferred)* • Fluorescence *in situ* hybridization

were pigmented spindle cell nevi or Reed nevi (2, 67), and one was an eruptive Spitz nevus (48). The last was reported in a 49-year old female, who developed over 100 similar lesions over four years. Further molecular characterization of the proliferation revealed identical *TPM3-ROS1* fusions in the three analyzed lesions (48). Only five Spitz melanomas with *ROS1* fusion have been described, and none of them resulted in distant metastases or death from the disease (2, 47).

NTRK Fusions

Neurotrophic tyrosine kinase receptor genes *NTRK1, NTRK2* and *NTRK3,* are oncogenes encoding the Trk family of tyrosine kinase receptors (TrkA, TrkB, and TrkC, respectively) (68). These tyrosine kinase receptors are all single-pass transmembrane enzymes that stimulate different pathways once activated, namely the MAPK/ERK, PI3K-AKT-mTOR, and phospholipase C-γ pathways (3, 68). In most *NTRK* fusions identified, the 3' portion encoding the kinase domain is retained, and the 5' portion encoding dimerization domains is provided by the fusion partner. The resultant chimeric Trk protein is an oncogenic, constitutively active tyrosine kinase (69).

In Spitz melanocytic proliferations, *NTRK1* fusions predominate over *NTRK3* fusions, the latter being more common in the pigmented spindle cell nevus of Reed, a special subtype of Spitz nevus (2, 9, 11, 23, 43, 46, 47, 67, 69-74). Only a single case of superficial spreading melanoma with an *TRAF2-NTRK2* fusion has been reported so far (7).

The *NTRK1* fusion partners in Spitz melanocytic proliferations include *LMNA* (2, 9, 72), *TPM3* (11, 23, 47, 72), *TP53* (2, 72), and *KHDRBS1* (9, 72), in descending order of frequency. Even though the number of cases for each particular known *NTRK1* fusion partner is relatively low (*LMNA* was identified in 16 cases, while *TP53* and *KHDRBS1* in two cases each), 4 of 5 Spitz melanocytic proliferations with *TPM3-NTRK1* fusion were diagnosed as Spitz melanomas, all with several additional chromosomal aberrations, including (most commonly) homozygous deletions of *CDKN2A* (11, 23, 47, 72). Furthermore, Spitz melanoma was also diagnosed in one of the two reported cases with an *KHDRBS1-NTRK1* fusion (9, 72).

Four different fusion partners have been identified so far for *NTRK3* fusions, namely *MYO5A* (67, 69, 70, 73), *ETV6* (67, 70, 73), *MYH9* (70, 73), and *SQSTM1* (9), in descending order of frequency. While no *NTRK1* fusions have been identified in Reed nevi, they harbor *NTRK3* fusions (with *MYO5A* and rarely *ETV6* fusion partners) in up to 57% of cases (67). In addition to pigmented spindle cell nevi of Reed, Spitz proliferations with *NTRK3* fusions are usually diagnosed as Spitz nevi or atypical Spitz tumors and much less frequently as Spitz melanomas (9, 67, 69, 70, 73).

NTRK1 and *NTRK3* fusions are also occasionally detected in non-Spitz melanocytic proliferations, e.g., pigmented epithelioid melanocytomas (75, 76), acral melanomas (42), and in a wide variety of non-melanocytic tumors, e.g., infantile fibrosarcoma, secretory carcinoma of the breast, secretory carcinoma of the salivary gland, congenital mesoblastic nephroma, lung carcinoma, thyroid papillary carcinoma and high grade gliomas (77).

Histologically, *NTRK1*-fused Spitz melanocytic proliferations are characterized by filigree-like rete ridges (elongated, thin rete ridges), lobulated dermal melanocytic nests (composed of smaller nests inside the larger ones), and by the formation of

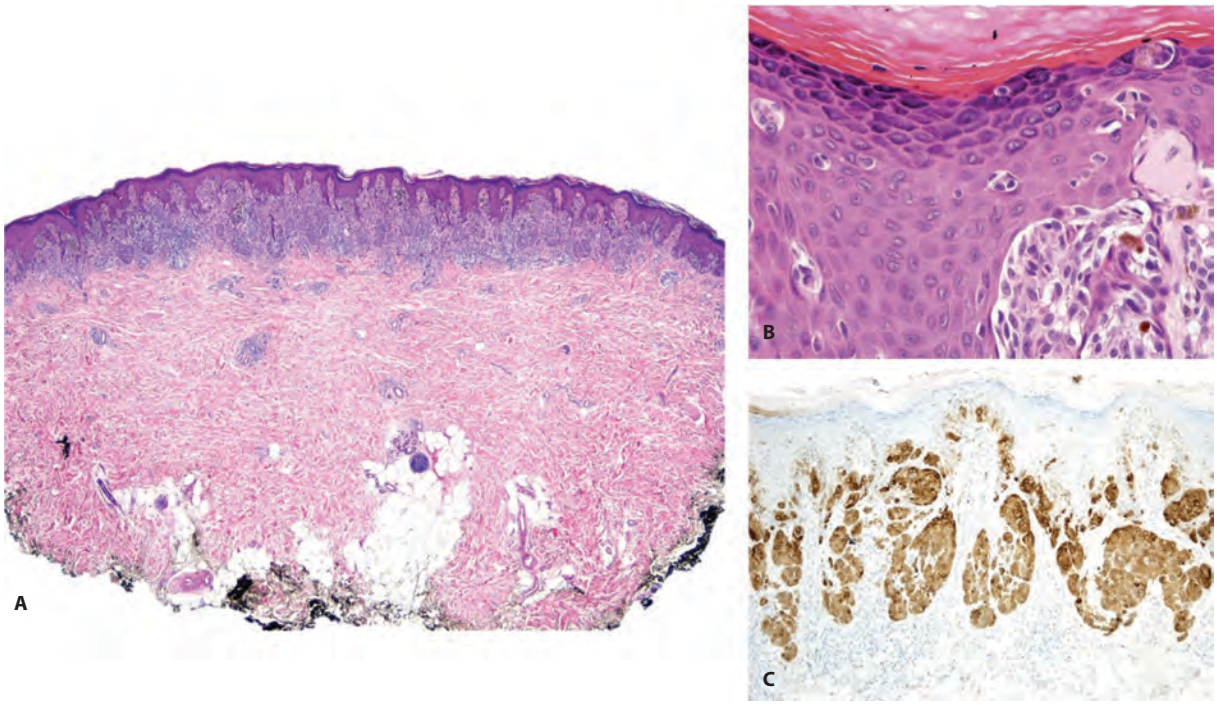

Figure 4. Spitz nevus with *NTRK* fusion. A. A symmetrical compound melanocytic proliferation associated with hyperplasia of the epidermis is depicted in this photo. B. Kamino bodies are often numerous in *NTRK1*-fused Spitz melanocytic proliferations. C. pan-TRK immunohistochemistry.

pseudorosettes (23, 43, 72). Exaggerated maturation of spindled and/or epithelioid melanocytes displaying mild to moderate nuclear pleomorphism is also a characteristic finding (23, 43, 72). Mild to moderate and sometimes even marked lymphocytic infiltrate is often present (2, 46, 72). While the pagetoid spread of melanocytes has been observed in up to 25% of cases, Kamino bodies are variably present (Figure 4) (2, 43, 46, 72). *NTRK1* fused Spitz melanocytic proliferations can occasionally resemble those with *ALK* fusions, exhibiting an intersecting fascicular growth pattern in the dermis (46).

Pigmented spindle cell nevus of Reed is a prototype of Spitz melanocytic proliferation harboring an *NTRK3* fusion (67). While *MYO5A-NTRK3* fusions are the most common driver genetic aberrations in this subgroup of Spitz nevi, *NTRK1* fusions are generally absent (67). It has been recently demonstrated that various *NTRK3* fusion partners have different intracellular localizations, ultimately determining the morphological characteristics of the Spitz melanocytes (62). For example, *MYO5A-NTRK3* chimeric protein is localized to cell dendritic processes and is associated with a fusiform/spindled morphology of melanocytes with a fascicular or sometimes plexiform or syncytial growth pattern (70). Besides, the formation of pseudo-Verocay bodies or pseudorosettes is associated with a more neuroid appearance of these proliferations (70). In contrast, the *ETV6-NTRK3* chimeric protein is localized to both the nucleus and cytoplasm of melanocytes and is linked to an epithelioid morphology with well-defined cell borders. Melanocytes have abundant, glassy cytoplasm and somewhat large, pleomorphic nuclei. They are arranged in large coalescing and also lobulated nests. Signs of maturation are fairly discrete (70). Finally, Spitz melanocytic proliferations with *MYH9-NTRK3* fusion are distinguished by fibrotic stroma and peripheral collagen trapping (70).

Immunohistochemistry with pan-TRK antibody can be used to detect the fusion protein (Figure 4c). Both available clones, clone A7H6R (Cell Signaling Technology) and EPR17341 (Abcam/Ventana) are highly sensitive and specific,

EPR17341 being slightly superior in terms of specificity (78). The staining pattern can hint at the presence of the *NTRK* fusion subtype. However, most pan-TRK immunohistochemistry studies in different *NTRK* fusion subtypes were performed on mostly non-Spitz *NTRK*-fused tumors (79, 80). Pan-TRK immunohistochemical staining is more intense and cytoplasmic in *NTRK1*-fused tumors, with additional nuclear accentuation in cases with an *LMNA-NTRK1* fusion (79, 80). On the other hand, up to 50% of tumors with an *NTRK3* fusion exhibit a cytoplasmic and nuclear pan-TRK immunohistochemical reaction (79, 80). However, a study by de la Fouchardière et al., which included only *NTRK3*-fused Spitz melanocytic proliferations, demonstrated that more intense nuclear and less intense cytoplasmic immunoreactivity is indicative of an *ETV6-NTRK3* fusion. At the same time, linear staining along dendritic processes can point to the presence of an *MYO5A-NTRK3* fusion (70).

Exceptional cases of non-Spitz ('spitzoid') melanomas with *NTRK* fusions have been reported resulting in widespread hematogenous metastases (7). In contrast, Spitz melanomas with *NTRK* fusions do not carry a dismal prognosis since only rare metastases to lymph nodes, but not beyond, have been described (47, 71). At present, no examples of Spitz melanocytic proliferations with *NTRK* fusions and with distant metastases or death from the disease have been reported. In the unlikely event of an *NTRK*-fused metastatic Spitz melanoma, specific therapy with TRK inhibitors is available (81, 82).

Table 5. Spitz Melanocytic Proliferations with *NTRK1* Fusions

Morphological features	• Filigree-like rete ridges • Lobulated melanocytic nests • Rosette-like structures • Extreme maturation • Epithelioid and spindled melanocytes – Mild to moderate pleomorphism – Mitoses rare – Kamino bodies frequent
Biological behavior	Generally favorable Regional lymph node deposits uncommon No distant metastases or death from the disease in proliferations classified as Spitz melanomas
Confirmatory test	• Immunohistochemistry with pan-TRK antibody • Next generation sequencing *(preferred)* • Fluorescence *in situ* hybridization

RET Fusions

The *RET* protooncogene resides on chromosome 10q11.21 and encodes a protein receptor tyrosine kinase involved in the MAPK/ERK, PI3K/AKT/mTOR and phospholipase C-γ1 intracellular signaling pathways (2). Only a handful of Spitz melanocytic proliferations with *RET* fusions have been reported (2, 9, 43, 67, 83). Four different fusion partners have been identified: *CCDC6* (9), *GOLGA5* (2), *KIF5B* (2), and *MYO5A* (67). Similar fusions have also been detected in thyroid cancer (84) and lung adenocarcinomas (85).

RET fusions have been reported in the whole biological spectrum of Spitz melanocytic proliferations, including ordinary Spitz nevi and pigmented spindle cell nevus of Reed, atypical Spitz tumors, and Spitz melanomas (2, 9, 43, 67, 83). Although the morphologic features of *RET* fused Spitz melanocytic proliferations lack specificity, such proliferations are often well-circumscribed, symmetrical, compound melanocytic proliferations with a plaque-like silhouette, a nested growth pattern of small to intermediate-sized epithelioid and spindled melanocytes with only mild cytological atypia (2, 43, 67).

RET-fused Spitz melanocytic proliferations generally follow an indolent clinical course (2, 9, 43, 67, 83). At present, no Spitz melanomas with *RET* fusion and a dismal outcome have been reported in the literature (2, 9, 43, 67, 83). Nevertheless, in the unlikely event of aggressive clinical behavior, potential therapy with RET inhibitors is available (2).

MET Fusions

The *MET* protooncogene is localized on chromosome 7q31.2 and encodes a tyrosine kinase receptor with high affinity for hepatocyte growth factor

(86). Only eight Spitz melanocytic proliferations, including a Spitz nevus, five atypical Spitz tumors, and two Spitz melanomas with *MET* fusions, have been reported (74, 83, 86). The largest series of six Spitz neoplasms with *MET* fusions demonstrated a breakpoint in intron 14 in all of the cases (86). The breakpoint event is localized upstream of the kinase domain-encoding exons 15 to 21, which are fully retained. In contrast, the auto-inhibitory domain encoded in exon 14 is absent in the chimeric protein (86). The N-terminal fusion partners identified in their series were *ZKSCAN1, PPFIBP1, TRIM4, LRRFIP1, EPS15,* and *DCTN1* (86).

MET fusions result in constitutive activation of tyrosine kinase with subsequent activation of the MAPK/ERK, PI3K/AKT/mTOR, and phospholipase C-γ1 pathways, which can be inhibited by cabozantinib (inhibitor of c-MET and VEGFR2) or PF-04217903 (c-MET inhibitor) (86). The number of reported Spitz melanocytic proliferations with *MET* fusions is too small to conclude specific morphologic features and prognosis. However, none of the cases with available follow-up resulted in aggressive clinical behavior (86).

Spitz Melanocytic Proliferations with Serine/Threonine Kinase Fusions

The largest proportion of Spitz melanocytic proliferations with serine/threonine kinase fusions involves the *MAP3K8* or *BRAF* genes. Nevertheless, other serine/threonine kinase fusions involving the *RAF1, PRKCA/B,* and *ARAF* genes have exceptionally been reported in a few examples of atypical Spitz tumors and Spitz melanomas (9, 83). Notably, the vast majority of Spitz melanocytic proliferations with serine/threonine kinase fusions are classified as atypical Spitz tumors or Spitz melanomas and are infrequently detected in Spitz nevi.

MAP3K8 Fusions

Mitogen-activated protein kinase kinase kinase 8 (MAP3K8), also known as Tpl-2 and COT, is an enzyme belonging to the group of serine/threonine protein kinases (87, 88) and is encoded by the *MAP3K8* gene that resides on chromosome 10p11. The enzyme consists of a kinase domain encoded by exons 1-8 of the *MAP3K8* gene and an inhibitory C-terminal domain encoded by exon 9 of the *MAP3K8* gene. The inhibitory C-terminal domain covers the kinase domain in its inactive state, preventing it from phosphorylating MEK proteins. The inhibitory C-terminal domain is also essential for targeting the MAP3K8 enzyme for proteolytic degradation. Fusions involving the *MAP3K8* gene and truncation of the *MAP3K8* gene follow the same basic mechanism, resulting in a fusion/truncated transcript including the intact kinase domain while lacking the inhibitory C-terminal domain. Consequently, kinase activity is unopposed by the C-terminal inhibitory action and, at the same time, the MAP3K8 is not targeted for proteolytic degradation, resulting in significant MAP3K8 overexpression and increased phosphorylation of MEK proteins, which in turn phosphorylate and activate ERK1/2 proteins that influence cell proliferation, division and differentiation (88-90). Similarly, one of the MEK proteins (MAP2K1, also called MEK1) has an autoinhibitory domain in amino acids 98 to 104, and deletions in this region (e.g., p.I103_K104del of MAP2K1) also result in constitutive activation of downstream ERK1/2 proteins (91).

A number of different *MAP3K8* fusion partners have been identified, including *SVIL* (9, 23, 92, 93), *DIP2C* (53, 83, 91, 92), *UBL3* (9, 83, 92), *SPECC1* (9, 92), *STX7* (9, 92), *ATP2A2* (91), *CCNY* (92), *CDC42EP3* (92), *CUBN* (92), *GNG2* (9), *LINC00703* (92), *MIR3681HG* (92), *PCDH7* (91), *PIP4K2A* (92), *PRKACB* (9), *SFMBT2* (92), *SLC4A4* (92), *SUBN* (9) and *ZFP36L1* (23).

MAP3K8 fusions and truncations have also been identified in ovarian, lung, and breast carcinomas, mesotheliomas, cutaneous myxoinflammatory fibroblastic sarcoma, squamous cell carcinomas, and melanocytic tumors – in rare acral melanomas and Spitz neoplasms (9, 23, 53, 83, 92-97).

Morphologically, Spitz proliferations with a *MAP3K8* fusion are often ulcerated tumors (more than 50%) with predominantly epithelioid mor-

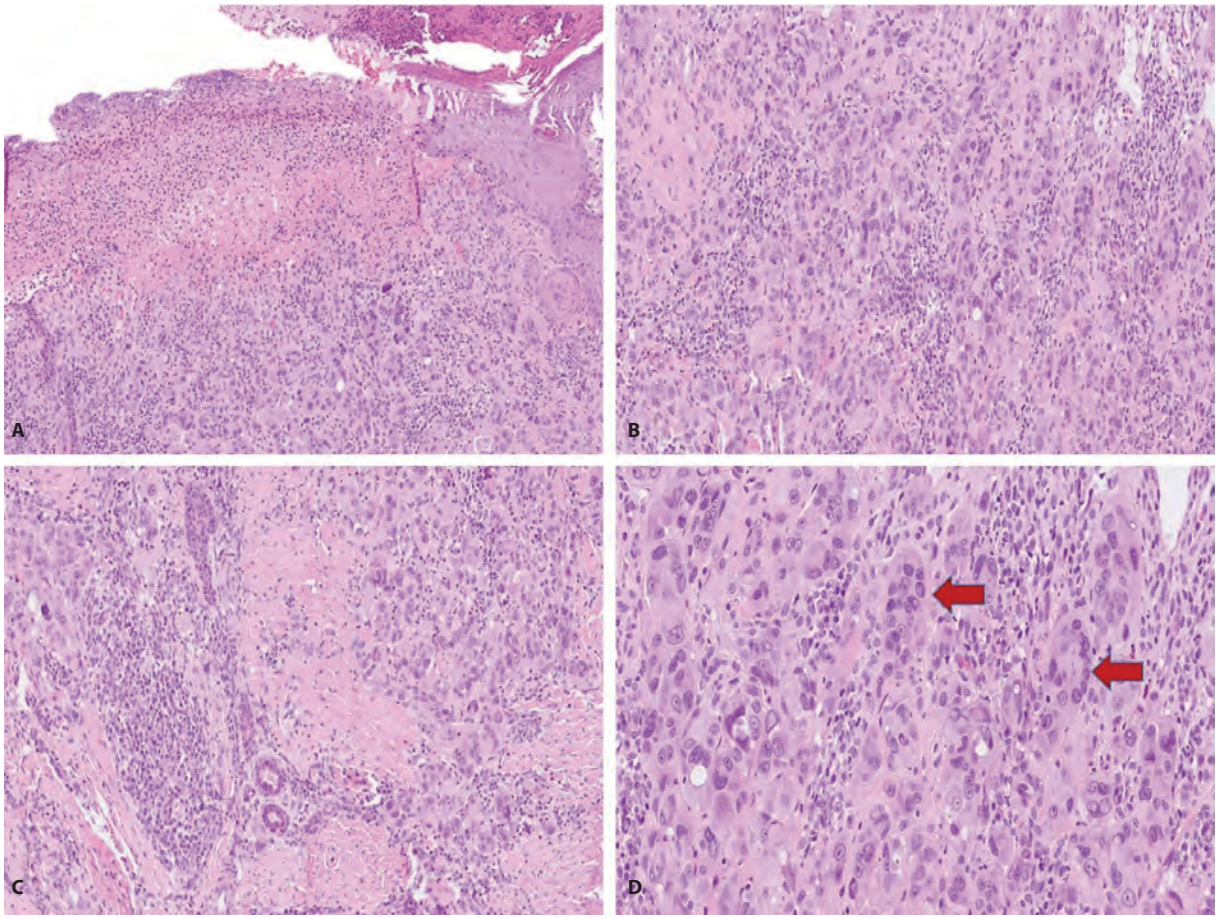

Figure 5. Atypical Spitz tumor. A. This is an example of an ulcerated Spitz melanocytic tumor. B. The lesion is composed of epithelioid melanocytes with moderate cytological atypia. C. No maturation is present. D. Large multinucleated giant melanocytes (arrows) can be a morphological clue for the presence of *MAP3K8* fusion.

phology, moderate to pronounced cytological atypia, and generally lack maturation (Figure 5). Additional characteristic features include focal hyperpigmented dermal clones and giant multinucleated melanocytes. Deep mitotic activity is not uncommon (9, 23, 53, 91, 92). Furthermore, desmoplastic stromal reaction and focal pagetoid scatter can be seen in 73% and 45% of cases, respectively (92).

A literature review revealed that most Spitz proliferations with *MAP3K8* fusion or truncations, a *MAP3K3* fusion, and a *MAP2K1* p.I103_K104del were classified either as atypical Spitz tumors or Spitz melanomas (40% and 52%, respectively). In comparison, Spitz nevi represented only a small portion (8%) of cases in this Spitz subgroup (23, 53, 91, 92, 98). Houlier et al. reported the largest series of 33 cases of Spitz melanocytic proliferations with *MAP3K8* fusions, of which 13 (40%) were classified as atypical Spitz tumors and 15 (45%) as Spitz melanomas (92). Moreover, 77% of these atypical Spitz tumors and Spitz melanomas harbored CDKN2A (92) inactivation, which was also reported as one of the most common secondary genetic events in some other series (23, 83, 91). The biological behavior of Spitz melanocytic proliferations with a *MAP3K8* fusion is variable; it appears that the prognosis depends on the presence of these additional genetic aberrations. Biallelic inactivation of *CDKN2A,* demonstrated either by p16 immunohistochemistry (with focal or diffuse complete loss of p16 expression) or molecular ge-

Table 6. Spitz Melanocytic Proliferations with *MAP3K8* Fusions

Morphological features	• Ulceration common • Epithelioid morphology – Moderate to high grade cytological atypia – Lack of maturation – Mitoses not uncommon • Giant multinucleated melanocytes • Focal hyperpigmented dermal clones
Biological behavior	Mostly in atypical Spitz tumors and Spitz melanomas
Confirmatory test	• Next generation sequencing • Fluorescence *in situ* hybridization

netic techniques, has been detected in about 35% of all reported cases of this *MAP3K8* fused Spitz subgroup of melanocytic proliferation (23, 83, 91, 92), followed by *TERT* promotor mutations and a complex *TERT* structural rearrangement, albeit less frequently (9, 83).

A single case has been reported that resulted in the death of an 11-year old boy, who was diagnosed as having a Spitz melanoma with *MAP3K8-GNG2* fusion, additional complex structural rearrangement in the *TERT* gene, and a homozygous *CDKN2A/B* deletion (9). Three other Spitz melanomas with *MAP3K8* fusions, all three with additional biallelic *CDKN2A* inactivation, demonstrated tumor cells' deposits in at least one lymph node. However, none of these cases resulted in widespread metastatic disease during the 6 to 18 months follow up period (91, 92). Two atypical Spitz tumors with *MAP3K8* fusions locally recurred, with otherwise no signs of distant metastases (83, 91).

BRAF Fusions

The *BRAF* gene encoding a serine-threonine protein kinase is composed of three highly conserved regions (CRs) (99, 100). CR1 contains N-terminal RAS-binding and cysteine-rich domains, while CR2 contains serine-threonine-rich domains, and both CR1 and CR2 act as auto inhibitors of CR3, the kinase domain (99, 100). In *BRAF* fusions, the resulting chimeric protein retains only the intact kinase domain (CR3) of the *BRAF* gene. The loss of autoinhibitory domains results in increased kinase activity, evidenced by increased phosphorylation and activation of downstream MEK1/2 and ERK1/2 proteins (4, 5).

Numerous fusion partners have been identified: *AKAP9* (9, 10, 101), *AGK* (10, 102), *CLIP2* (102, 103), *BAIAP2L1* (11, 47), *CEP89* (2), *CUX1* (10), *DYNC1*/2 (10), *EML4* (11, 47), *LSM14A* (2), *MAD1L1* (9), *MLANA* (102), *MYO5A* (102), *MZT1* (10), *NRF1* (23), *SKAP2* (102), *SLC12A7* (10), *SOX6* (23), *TRIM24* (10) and *ZKSCAN1* (10). In non-Spitz melanoma subtypes, additional fusion partners have been identified, such as *KIAA1549* in a case of an acral melanoma (8), *ZNF767* in two cases of mucosal melanomas (5, 10), *PPFIBP2* in a case of superficial spreading melanoma (8), *GTF2I* in a metastatic melanoma of unknown primary origin (10), *AGAP3*, *CCDC91*, *CDC27*, *PAPSS1*, *RAD18* and *TAX1BP1* in melanomas either classified as non-Spitz (spitzoid) or unclassified (4, 10).

Similar to the *MAP3K8* fused Spitz subgroup of melanocytic proliferations, the vast majority of Spitz melanocytic proliferations with *BRAF* fusion cluster towards the malignant end of the biological spectrum, with roughly 45% of published Spitz melanocytic proliferations with *BRAF* fusion belonging to atypical Spitz tumor, 41% to Spitz melanoma and only 14% to Spitz nevi (2, 9-11, 23, 43, 47, 71, 74, 83, 101-103).

BRAF fusions are present in various tumors, including gliomas, thyroid, and pancreatic carcinomas, non-small cell lung adenocarcinomas, and colorectal carcinomas (10).

Secondary genetic alterations in *BRAF* fused Spitz melanocytic proliferations were similar to those in other Spitz subgroups. The most common secondary changes were the homozygous deletion of 9p21, *TERT* promoter mutations, 6p25 gains, and, in single cases, *MDM2* amplification and *ARID2* p.Q720 mutation (11, 43, 47, 101-103).

Histologically, *BRAF* fused Spitz melanocytic proliferations are predominantly dermal tumors composed of epithelioid or mixed, epithelioid and spindled melanocytes with vesicular nuclei and prominent nucleoli, with moderate to high-grade cytological atypia and somewhat amphophilic

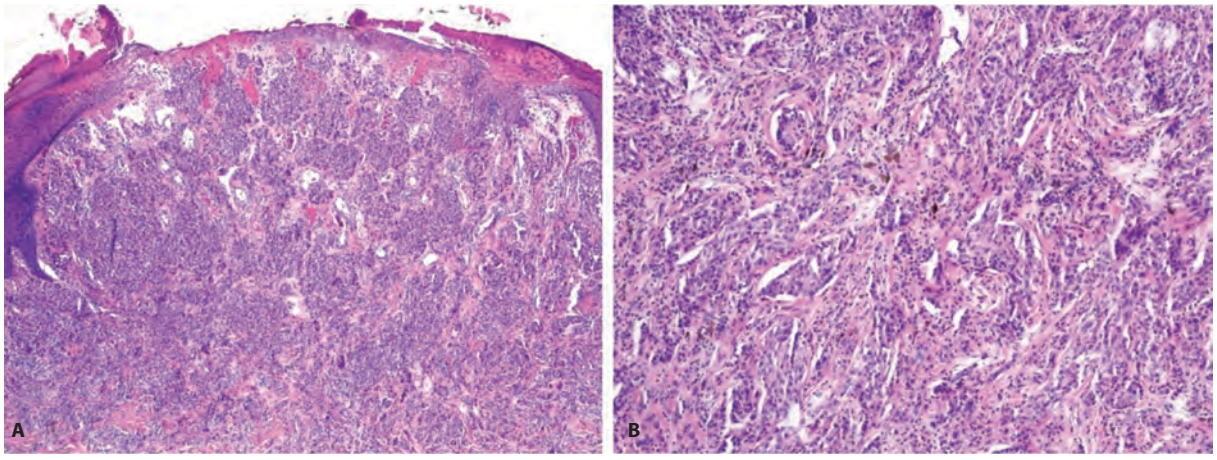

Figure 6. Atypical Spitz tumor. A. Low power magnification depicting an ulcerated melanocytic proliferation composed of epithelioid melanocytes. B. Epithelioid melanocytes with desmoplastic stromal reaction. Although such morphological changes can be seen in *BRAF*-fused Spitz melanocytic proliferations, they lack specificity.

Table 7. Spitz Melanocytic Proliferations with *BRAF* Fusions

Morphological features	• Epithelioid morphology – Moderate to high grade cytological atypia – Lack of maturation – Mitoses not uncommon • Desmoplasia at base
Biological behavior	Mostly in atypical Spitz tumors and Spitz melanomas
Confirmatory test	• Next generation sequencing • Fluorescence *in situ* hybridization

cytoplasm (11, 23, 43, 101-103). Interestingly, some authors have described a common, distinct growth pattern comprising of densely cellular sheet-like proliferation in the superficial part of the lesion, overlying a less cellular, desmoplastic base with prominent dermal sclerosis (Figure 6) (2, 43, 101, 102).

Widespread metastatic disease (i.e., metastases beyond the sentinel lymph node) has been described in 19 patients with melanomas with *BRAF* fusion (4, 5, 8, 10, 11, 47), ten of which were called Spitz melanomas (10, 11, 47). One case of non-Spitz metastasizing melanoma in a 54-year-old male harbored a *BRAF V600E* mutation and an *AGAP3-BRAF* fusion (10). Another case reported as a Spitz melanoma harbored concurrent *BRAF* fusion, *NRAS* mutation, and a *TERT* promoter mutation (83).

Conclusion

Spitz melanocytic proliferations are defined by distinctive morphological and molecular genetic features. They encompass the whole biological spectrum of proliferations ranging from Spitz nevi, atypical Spitz tumors to Spitz melanomas. While most Spitz nevi can be reliably diagnosed on morphological grounds alone, additional molecular genetic testing is generally necessary to classify atypical Spitz tumors and Spitz melanomas and, significantly, to predict their biological behavior. The proposed algorithm of how to approach Spitz melanocytic proliferations is summarized in Figure 7. Molecular testing includes the detection of different driver fusions and additional genetic events associated with biologic behavior. In addition, since several biological drugs are available to treat melanocytic proliferations with aggressive clinical behavior, characterization of particular driver genetic events and additional genetic abnormalities is becoming increasingly important.

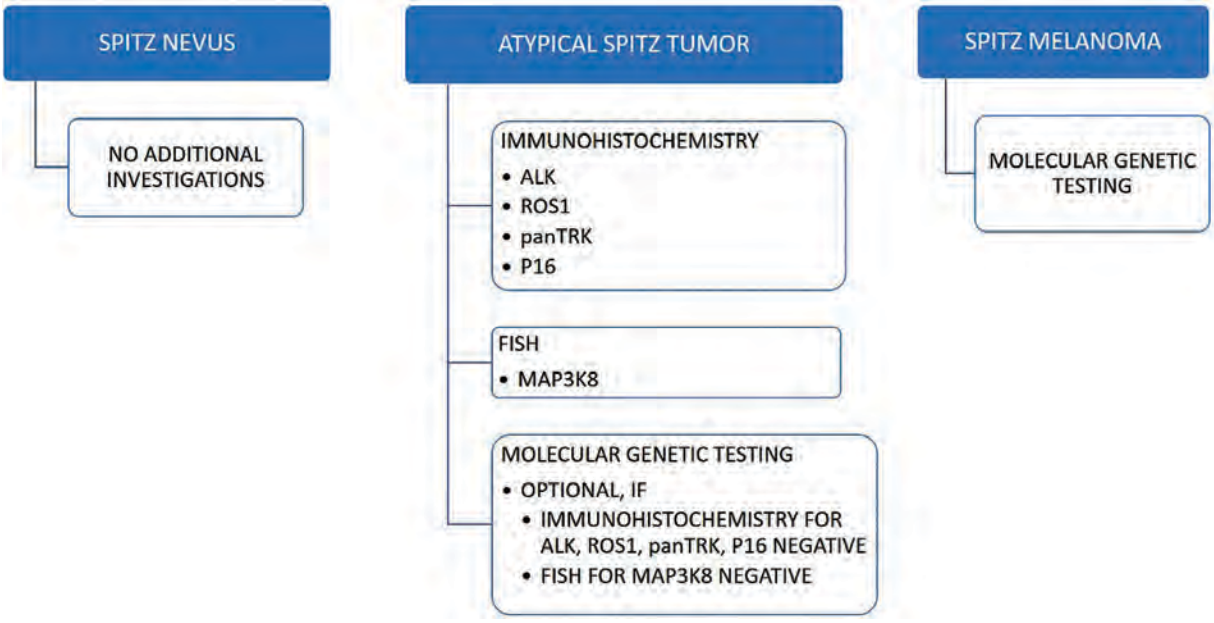

Figure 7. Proposed algorithm for diagnostic work-up of Spitz melanocytic proliferations.

Conflict of Interest: The authors declare that they have no conflict of interest.

References

1. Elder DE, Massi D, Scolyer RA, Willemze R, editors. WHO Classification of Skin Tumours. 4th ed. Lyon: International Agency for Research on Cancer; 2018.
2. Wiesner T, He J, Yelensky R, Esteve-Puig R, Botton T, Yeh I, et al. Kinase fusions are frequent in Spitz tumours and spitzoid melanomas. Nat Commun. 2014;5:3116.
3. Wiesner T, Kutzner H, Cerroni L, Mihm MC Jr, Busam KJ, Murali R. Genomic aberrations in spitzoid melanocytic tumours and their implications for diagnosis, prognosis and therapy. Pathology. 2016;48(2):113-31.
4. Hutchinson KE, Lipson D, Stephens PJ, Otto G, Lehmann BD, Lyle PL, et al. BRAF fusions define a distinct molecular subset of melanomas with potential sensitivity to MEK inhibition. Clin Cancer Res. 2013;19(24):6696-702.
5. Kim HS, Jung M, Kang HN, Kim H, Park CW, Kim SM, et al. Oncogenic BRAF fusions in mucosal melanomas activate the MAPK pathway and are sensitive to MEK/PI3K inhibition or MEK/CDK4/6 inhibition. Oncogene. 2017;36(23):3334-45.
6. Lazova R, Pornputtapong N, Halaban R, Bosenberg M, Bai Y, Chai H, et al. Spitz nevi and Spitzoid melanomas: exome sequencing and comparison with conventional melanocytic nevi and melanomas. Mod Pathol. 2017;30(5):640-9.
7. Lezcano C, Shoushtari AN, Ariyan C, Hollmann TJ, Busam KJ. Primary and Metastatic Melanoma With NTRK Fusions. Am J Surg Pathol. 2018;42(8):1052-8.
8. Menzies AM, Yeh I, Botton T, Bastian BC, Scolyer RA, Long GV. Clinical activity of the MEK inhibitor trametinib in metastatic melanoma containing BRAF kinase fusion. Pigment Cell Melanoma Res. 2015;28(5):607-10.
9. Newman S, Fan L, Pribnow A, Silkov A, Rice SV, Lee S, et al. Clinical genome sequencing uncovers potentially targetable truncations and fusions of MAP3K8 in spitzoid and other melanomas. Nat Med. 2019;25(4):597-602.
10. Ross JS, Wang K, Chmielecki J, Gay L, Johnson A, Chudnovsky J, et al. The distribution of BRAF gene fusions in solid tumors and response to targeted therapy. Int J Cancer. 2016;138(4):881-90.
11. Wu G, Barnhill RL, Lee S, Li Y, Shao Y, Easton J, et al. The landscape of fusion transcripts in spitzoid melanoma and biologically indeterminate spitzoid tumors by RNA sequencing. Mod Pathol. 2016;29(4):359-69.
12. Bastian BC, Wesselmann U, Pinkel D, Leboit PE. Molecular cytogenetic analysis of Spitz nevi shows clear differences to melanoma. J Invest Dermatol. 1999;113(6):1065-9.
13. Bastian BC, LeBoit PE, Pinkel D. Mutations and copy number increase of HRAS in Spitz nevi with distinctive histopathological features. Am J Pathol. 2000;157(3):967-72.
14. van Engen-van Grunsven AC, van Dijk MC, Ruiter DJ, Klaasen A, Mooi WJ, Blokx WA. HRAS-mutated Spitz tumors: A subtype of Spitz tumors with distinct features. Am J Surg Pathol. 2010;34(10):1436-41.

15. Maldonado JL, Timmerman L, Fridlyand J, Bastian BC. Mechanisms of cell-cycle arrest in Spitz nevi with constitutive activation of the MAP-kinase pathway. Am J Pathol. 2004;164(5):1783-7.
16. Ross AL, Sanchez MI, Grichnik JM. Molecular nevogenesis. Dermatol Res Pract. 2011;2011:463184.
17. Bos JL. ras oncogenes in human cancer: a review. Cancer Res. 1989;49(17):4682-9.
18. Hand PH, Vilasi V, Thor A, Ohuchi N, Schlom J. Quantitation of Harvey ras p21 enhanced expression in human breast and colon carcinomas. J Natl Cancer Inst. 1987;79(1):59-65.
19. Riou G, Barrois M, Sheng ZM, Duvillard P, Lhomme C. Somatic deletions and mutations of c-Ha-ras gene in human cervical cancers. Oncogene. 1988;3(3):329-33.
20. van Dijk MC, Bernsen MR, Ruiter DJ. Analysis of mutations in B-RAF, N-RAS, and H-RAS genes in the differential diagnosis of Spitz nevus and spitzoid melanoma. Am J Surg Pathol. 2005;29(9):1145-51.
21. Bender RP, McGinniss MJ, Esmay P, Velazquez EF, Reimann JD. Identification of HRAS mutations and absence of GNAQ or GNA11 mutations in deep penetrating nevi. Mod Pathol. 2013;26(10):1320-8.
22. Kiyohara T, Takata M, Itoh H, Kawami K, Yasuta M, Hayakawa K, et al. HRAS-mutated Spitz nevus on the cheek in a middle-aged man. Acta Derm Venereol. 2012;92(3):326-7.
23. Raghavan SS, Peternel S, Mully TW, North JP, Pincus LB, LeBoit PE, et al. Spitz melanoma is a distinct subset of spitzoid melanoma. Mod Pathol. 2020;33(6):1122-34.
24. Li JY, Berger MF, Marghoob A, Bhanot UK, Toyohara JP, Pulitzer MP. Combined melanocytic and sweat gland neoplasm: cell subsets harbor an identical HRAS mutation in phacomatosis pigmentokeratotica. J Cutan Pathol. 2014;41(8):663-71.
25. Nemeth K, Szabo S, Cottrell CE, McNulty SM, Segura A, Sokumbi O, et al. Mosaic pathogenic HRAS variant in a patient with nevus spilus with agminated Spitz nevi and parametrial-uterine rhabdomyosarcoma. Br J Dermatol. 2018;178(3):804-6.
26. Pontoizeau J, Stefan A, Comoz F, Houlier A, Haddad V, Pissaloux D, et al. Agminated Spitz nevus arising in normal skin with redundant HRAS mutation. Eur J Dermatol. 2017;27(1):73-4.
27. Porubsky C, Teer JK, Zhang Y, Deschaine M, Sondak VK, Messina JL. Genomic analysis of a case of agminated Spitz nevi and congenital-pattern nevi arising in extensive nevus spilus. J Cutan Pathol. 2018;45(2):180-3.
28. Sarin KY, Sun BK, Bangs CD, Cherry A, Swetter SM, Kim J, et al. Activating HRAS mutation in agminated Spitz nevi arising in a nevus spilus. JAMA Dermatol. 2013;149(9):1077-81.
29. Da Forno PD, Pringle JH, Fletcher A, Bamford M, Su L, Potter L, et al. BRAF, NRAS and HRAS mutations in spitzoid tumours and their possible pathogenetic significance. Br J Dermatol. 2009;161(2):364-72.
30. Harvell JD, Bastian BC, LeBoit PE. Persistent (recurrent) Spitz nevi: a histopathologic, immunohistochemical, and molecular pathologic study of 22 cases. Am J Surg Pathol. 2002;26(5):654-61.
31. Sabater Marco V, Escutia Muñoz B, Morera Faet A, Mata Roig M, Botella Estrada R. Pseudogranulomatous Spitz nevus: a variant of Spitz nevus with heavy inflammatory infiltrate mimicking a granulomatous dermatitis. J Cutan Pathol. 2013;40(3):330-5.
32. Gerami P, Kim D, Compres EV, Zhang B, Khan AU, Sunshine JC, et al. Clinical, morphologic, and genomic findings in ROS1 fusion Spitz neoplasms. Mod Pathol. 2020.
33. Roh MR, Eliades P, Gupta S, Tsao H. Genetics of melanocytic nevi. Pigment Cell Melanoma Res. 2015;28(6):661-72.
34. Iwahara T, Fujimoto J, Wen D, Cupples R, Bucay N, Arakawa T, et al. Molecular characterization of ALK, a receptor tyrosine kinase expressed specifically in the nervous system. Oncogene. 1997;14(4):439-49.
35. Hallberg B, Palmer RH. Mechanistic insight into ALK receptor tyrosine kinase in human cancer biology. Nat Rev Cancer. 2013;13(10):685-700.
36. Pulford K, Morris SW, Turturro F. Anaplastic lymphoma kinase proteins in growth control and cancer. J Cell Physiol. 2004;199(3):330-58.
37. Slupianek A, Nieborowska-Skorska M, Hoser G, Morrione A, Majewski M, Xue L, et al. Role of phosphatidylinositol 3-kinase-Akt pathway in nucleophosmin/anaplastic lymphoma kinase-mediated lymphomagenesis. Cancer Res. 2001;61(5):2194-9.
38. Zamo A, Chiarle R, Piva R, Howes J, Fan Y, Chilosi M, et al. Anaplastic lymphoma kinase (ALK) activates Stat3 and protects hematopoietic cells from cell death. Oncogene. 2002;21(7):1038-47.
39. Falini B, Bigerna B, Fizzotti M, Pulford K, Pileri SA, Delsol G, et al. ALK expression defines a distinct group of T/null lymphomas ("ALK lymphomas") with a wide morphological spectrum. Am J Pathol. 1998;153(3):875-86.
40. Doyle LA, Mariño-Enriquez A, Fletcher CD, Hornick JL. ALK rearrangement and overexpression in epithelioid fibrous histiocytoma. Mod Pathol. 2015;28(7):904-12.
41. Niu HT, Zhou QM, Wang F, Shao Q, Guan YX, Wen XZ, et al. Identification of anaplastic lymphoma kinase break points and oncogenic mutation profiles in acral/mucosal melanomas. Pigment Cell Melanoma Res. 2013;26(5):646-53.
42. Yeh I, Jorgenson E, Shen L, Xu M, North JP, Shain AH, et al. Targeted Genomic Profiling of Acral Melanoma. J Natl Cancer Inst. 2019;111(10):1068-77.
43. Amin SM, Haugh AM, Lee CY, Zhang B, Bubley JA, Merkel EA, et al. A Comparison of Morphologic and Mo-

lecular Features of BRAF, ALK, and NTRK1 Fusion Spitzoid Neoplasms. Am J Surg Pathol. 2017;41(4):491-8.

44. Chung CT, Marrano P, Swanson D, Dickson BC, Thorner PS. Fusion of ALK to the melanophilin gene MLPH in pediatric Spitz nevi. Hum Pathol. 2019;87:57-64.
45. Kastnerova L, Martinek P, Grossmann P, Steiner P, Vanecek T, Kyclova J, et al. A Clinicopathological Study of 29 Spitzoid Melanocytic Lesions With ALK Fusions, Including Novel Fusion Variants, Accompanied by Fluorescence In Situ Hybridization Analysis for Chromosomal Copy Number Changes, and Both TERT Promoter and Next-Generation Sequencing Mutation Analysis. Am J Dermatopathol. 2020;42(8):578-92.
46. Kiuru M, Jungbluth A, Kutzner H, Wiesner T, Busam KJ. Spitz Tumors: Comparison of Histological Features in Relationship to Immunohistochemical Staining for ALK and NTRK1. Int J Surg Pathol. 2016;24(3):200-6.
47. Lee S, Barnhill RL, Dummer R, Dalton J, Wu J, Pappo A, et al. TERT Promoter Mutations Are Predictive of Aggressive Clinical Behavior in Patients with Spitzoid Melanocytic Neoplasms. Sci Rep. 2015;5:11200.
48. Raghavan SS, Kapler ES, Dinges MM, Bastian BC, Yeh I. Eruptive Spitz nevus, a striking example of benign metastasis. Sci Rep. 2020;10(1):16216.
49. Rand AJ, Flejter WL, Dowling CA, Brooke LM, Boland GM, Kroshinsky D, et al. Atypical ALK-positive Spitz tumors with 9p21 homozygous deletion: Report of two cases and review of the literature. J Cutan Pathol. 2018;45(2):136-40.
50. Yeh I, de la Fouchardiere A, Pissaloux D, Mully TW, Garrido MC, Vemula SS, et al. Clinical, histopathologic, and genomic features of Spitz tumors with ALK fusions. Am J Surg Pathol. 2015;39(5):581-91.
51. Busam KJ, Kutzner H, Cerroni L, Wiesner T. Clinical and pathologic findings of Spitz nevi and atypical Spitz tumors with ALK fusions. Am J Surg Pathol. 2014;38(7):925-33.
52. Melchers RC, Willemze R, van Doorn R, Jansen PM, Cleven AHG, Solleveld N, et al. Corresponding anaplastic lymphoma kinase-tropomyosin 3 (ALK-TPM3) fusion in a patient with a primary cutaneous anaplastic large-cell lymphoma and a Spitz nevus. JAAD Case Rep. 2019;5(11):970-2.
53. Newman S, Pappo A, Raimondi S, Zhang J, Barnhill R, Bahrami A. Pathologic Characteristics of Spitz Melanoma With MAP3K8 Fusion or Truncation in a Pediatric Cohort. Am J Surg Pathol. 2019;43(12):1631-7.
54. Saraggi D, Salmaso R, Zamuner C, Munari G, Lanza C, Alaibac MS, et al. Prevalence of ALK gene alterations among the spectrum of plexiform spitzoid lesions. J Am Acad Dermatol. 2018;79(4):728-35.
55. Fujimoto M, Togashi Y, Matsuzaki I, Baba S, Takeuchi K, Inaba Y, et al. A case report of atypical Spitz tumor harboring a novel MLPH-ALK gene fusion with discordant ALK immunohistochemistry results. Hum Pathol. 2018;80:99-103.
56. Perron E, Pissaloux D, Charon Barra C, Karanian M, Lamant L, Parfait S, et al. Melanocytic Myxoid Spindle Cell Tumor With ALK Rearrangement (MMySTAR): Report of 4 Cases of a Nevus Variant With Potential Diagnostic Challenge. Am J Surg Pathol. 2018;42(5):595-603.
57. Rousi EK, Koskivuo IO, Juteau SM, Talve LAI, Hernberg MM, Vihinen PP, et al. Different expression of BRAFV600E, ALK and PD-L1 in melanoma in children and adolescents: a nationwide retrospective study in Finland in 1990-2014. Acta Oncol. 2021;60(2):165-72. Epub 2020 Aug 20.
58. Brown RA, Wang JY, Raghavan SS, Zhang J, Wan DC, Born D, et al. ALK-positive compound Spitz nevus with extensive perineural and intraneural neurotropism. J Cutan Pathol. 2021;48(1):154-9. Epub 2020 Nov 8.
59. Ogawa K, Fukumoto T, Azukizawa H, Takeda M, Asada H. First Japanese case report of atypical Spitz tumor with an ALK rearrangement. J Dermatol. 2017;44(12):e342-3.
60. Busam KJ, Vilain RE, Lum T, Busam JA, Hollmann TJ, Saw RP, et al. Primary and Metastatic Cutaneous Melanomas Express ALK Through Alternative Transcriptional Initiation. Am J Surg Pathol. 2016;40(6):786-95.
61. Wiesner T, Lee W, Obenauf AC, Ran L, Murali R, Zhang QF, et al. Alternative transcription initiation leads to expression of a novel ALK isoform in cancer. Nature. 2015;526(7573):453-7.
62. Farah M, Nagarajan P, Curry JL, Tang Z, Kim TB, Aung PP, et al. Spitzoid melanoma with histopathological features of ALK gene rearrangement exhibiting ALK copy number gain: a novel mechanism of ALK activation in spitzoid neoplasia. Br J Dermatol. 2019;180(2):404-8.
63. Dunn ALJ, Gardner JM, Kaley JR, Bellamy W, Shalin SC. ALK Rearrangements Are Infrequent in Cellular Blue Nevus and Deep Penetrating Nevus. Am J Dermatopathol. 2018;40(7):469-78.
64. Drilon A, Jenkins C, Iyer S, Schoenfeld A, Keddy C, Davare MA. ROS1-dependent cancers - biology, diagnostics and therapeutics. Nat Rev Clin Oncol. 2020.
65. Donati M, Kastnerova L, Martinek P, Grossmann P, Sticová E, Hadravský L, et al. Spitz Tumors With ROS1 Fusions: A Clinicopathological Study of 6 Cases, Including FISH for Chromosomal Copy Number Alterations and Mutation Analysis Using Next-Generation Sequencing. Am J Dermatopathol. 2020;42(2):92-102.
66. Mitsui Y, Ogawa K, Takeda M, Nakanishi T, Azukizawa H, Asada H. First Japanese case of atypical Spitz tumor exhibiting ROS1 rearrangement. J Dermatol. 2018;45(9):e248-9.
67. VandenBoom T, Quan VL, Zhang B, Garfield EM, Kong BY, Isales MC, et al. Genomic Fusions in Pigmented Spindle Cell Nevus of Reed. Am J Surg Pathol. 2018;42(8):1042-51.

68. Rubin JB, Segal RA. Growth, survival and migration: the Trk to cancer. Cancer Treat Res. 2003;115:1-18.
69. Wang L, Busam KJ, Benayed R, Cimera R, Wang J, Denley R, et al. Identification of NTRK3 Fusions in Childhood Melanocytic Neoplasms. J Mol Diagn. 2017;19(3):387-96.
70. de la Fouchardière A, Tee MK, Peternel S, Valdebran M, Pissaloux D, Tirode F, et al. Fusion partners of NTRK3 affect subcellular localization of the fusion kinase and cytomorphology of melanocytes. Mod Pathol. Epub 2020 Sep 23.
71. Lee CY, Sholl LM, Zhang B, Merkel EA, Amin SM, Guitart J, et al. Atypical Spitzoid Neoplasms in Childhood: A Molecular and Outcome Study. Am J Dermatopathol. 2017;39(3):181-6.
72. Yeh I, Busam KJ, McCalmont TH, LeBoit PE, Pissaloux D, Alberti L, et al. Filigree-like Rete Ridges, Lobulated Nests, Rosette-like Structures, and Exaggerated Maturation Characterize Spitz Tumors With NTRK1 Fusion. Am J Surg Pathol. 2019;43(6):737-46.
73. Yeh I, Tee MK, Botton T, Shain AH, Sparatta AJ, Gagnon A, et al. NTRK3 kinase fusions in Spitz tumours. J Pathol. 2016;240(3):282-90.
74. Zarabi SK, Azzato EM, Tu ZJ, Ni Y, Billings SD, Arbesman J, et al. Targeted next generation sequencing (NGS) to classify melanocytic neoplasms. J Cutan Pathol. 2020;47(8):691-704.
75. Friedman BJ, Hernandez S, Fidai C, Jiang A, Shwayder TA, Carskadon S, et al. A pediatric case of pigmented epithelioid melanocytoma with chromosomal copy number alterations in 15q and 17q and a novel NTRK3-SCAPER gene fusion. J Cutan Pathol. 2020;47(1):70-5.
76. Isales MC, Haugh AM, Bubley J, Verzì AE, Zhang B, Kudalkar E, et al. Genomic Assessment of Blitz Nevi Suggests Classification as a Subset of Blue Nevus Rather Than Spitz Nevus: Clinical, Histopathologic, and Molecular Analysis of 18 Cases. Am J Dermatopathol. 2018;40(2):118-24.
77. Cocco E, Scaltriti M, Drilon A. NTRK fusion-positive cancers and TRK inhibitor therapy. Nat Rev Clin Oncol. 2018;15(12):731-47.
78. Uguen A. Spitz Tumors With NTRK1 Fusions: TRK-A and pan-TRK Immunohistochemistry as Ancillary Diagnostic Tools. Am J Surg Pathol. 2019;43(10):1438-9.
79. Gatalica Z, Xiu J, Swensen J, Vranic S. Molecular characterization of cancers with NTRK gene fusions. Mod Pathol. 2019;32(1):147-53.
80. Hechtman JF, Benayed R, Hyman DM, Drilon A, Zehir A, Frosina D, et al. Pan-Trk Immunohistochemistry Is an Efficient and Reliable Screen for the Detection of NTRK Fusions. Am J Surg Pathol. 2017;41(11):1547-51.
81. Drilon A, Laetsch TW, Kummar S, DuBois SG, Lassen UN, Demetri GD, et al. Efficacy of Larotrectinib in TRK Fusion-Positive Cancers in Adults and Children. N Engl J Med. 2018;378(8):731-9.
82. Forschner A, Forchhammer S, Bonzheim I. NTRK gene fusions in melanoma: detection, prevalence and potential therapeutic implications. J Dtsch Dermatol Ges. 2020;18(12):1387-92.
83. Quan VL, Zhang B, Zhang Y, Mohan LS, Shi K, Wagner A, et al. Integrating Next-Generation Sequencing with Morphology Improves Prognostic and Biologic Classification of Spitz Neoplasms. J Invest Dermatol. 2020;140(8):1599-608.
84. Rabes HM, Demidchik EP, Sidorow JD, Lengfelder E, Beimfohr C, Hoelzel D, et al. Pattern of radiation-induced RET and NTRK1 rearrangements in 191 post-chernobyl papillary thyroid carcinomas: biological, phenotypic, and clinical implications. Clin Cancer Res. 2000;6(3):1093-103.
85. Lipson D, Capelletti M, Yelensky R, Otto G, Parker A, Jarosz M, et al. Identification of new ALK and RET gene fusions from colorectal and lung cancer biopsies. Nat Med. 2012;18(3):382-4.
86. Yeh I, Botton T, Talevich E, Shain AH, Sparatta AJ, de la Fouchardiere A, et al. Activating MET kinase rearrangements in melanoma and Spitz tumours. Nat Commun. 2015;6:7174.
87. Hagemann D, Troppmair J, Rapp UR. Cot protooncoprotein activates the dual specificity kinases MEK-1 and SEK-1 and induces differentiation of PC12 cells. Oncogene. 1999;18(7):1391-400.
88. Salmeron A, Ahmad TB, Carlile GW, Pappin D, Narsimhan RP, Ley SC. Activation of MEK-1 and SEK-1 by Tpl-2 proto-oncoprotein, a novel MAP kinase kinase kinase. Embo j. 1996;15(4):817-26.
89. Ceci JD, Patriotis CP, Tsatsanis C, Makris AM, Kovatch R, Swing DA, et al. Tpl-2 is an oncogenic kinase that is activated by carboxy-terminal truncation. Genes Dev. 1997;11(6):688-700.
90. Gándara ML, López P, Hernando R, Castaño JG, Alemany S. The COOH-terminal domain of wild-type Cot regulates its stability and kinase specific activity. Mol Cell Biol. 2003;23(20):7377-90.
91. Quan VL, Zhang B, Mohan LS, Shi K, Isales MC, Panah E, et al. Activating Structural Alterations in MAPK Genes Are Distinct Genetic Drivers in a Unique Subgroup Of Spitzoid Neoplasms. Am J Surg Pathol. 2019;43(4):538-48.
92. Houlier A, Pissaloux D, Masse I, Tirode F, Karanian M, Pincus LB, et al. Melanocytic tumors with MAP3K8 fusions: report of 33 cases with morphological-genetic correlations. Mod Pathol. 2020;33(5):846-57.
93. Quan VL, Panah E, Zhang B, Shi K, Mohan LS, Gerami P. The role of gene fusions in melanocytic neoplasms. J Cutan Pathol. 2019;46(11):878-87.
94. Clark AM, Reynolds SH, Anderson M, Wiest JS. Mutational activation of the MAP3K8 protooncogene in lung cancer. Genes Chromosomes Cancer. 2004;41(2):99-108.

95. Gruosso T, Garnier C, Abelanet S, Kieffer Y, Lemesre V, Bellanger D, et al. MAP3K8/TPL-2/COT is a potential predictive marker for MEK inhibitor treatment in high-grade serous ovarian carcinomas. Nat Commun. 2015;6:8583.
96. Lee JH, Lee JH, Lee SH, Do SI, Cho SD, Forslund O, et al. TPL2 Is an Oncogenic Driver in Keratocanthoma and Squamous Cell Carcinoma. Cancer Res. 2016;76(22):6712-22.
97. Sourvinos G, Tsatsanis C, Spandidos DA. Overexpression of the Tpl-2/Cot oncogene in human breast cancer. Oncogene. 1999;18(35):4968-73.
98. Kim D, Khan AU, Compres EV, Zhang B, Sunshine JC, Quan VL, et al. BRAF Fusion Spitz Neoplasms, Clinical, Morphologic and Genomic Findings in 6 Cases. J Cutan Pathol. 2020;47(12):1132-42.
99. Aramini JM, Vorobiev SM, Tuberty LM, Janjua H, Campbell ET, Seetharaman J, et al. The RAS-Binding Domain of Human BRAF Protein Serine/Threonine Kinase Exhibits Allosteric Conformational Changes upon Binding HRAS. Structure. 2015;23(8):1382-93.
100. Richtig G, Hoeller C, Kashofer K, Aigelsreiter A, Heinemann A, Kwong LN, et al. Beyond the BRAF(V)(600E) hotspot: biology and clinical implications of rare BRAF gene mutations in melanoma patients. Br J Dermatol. 2017;177(4):936-44.
101. Perron E, Pissaloux D, Neub A, Hohl D, Tartar MD, Mortier L, et al. Unclassified sclerosing malignant melanomas with AKAP9-BRAF gene fusion: a report of two cases and review of BRAF fusions in melanocytic tumors. Virchows Arch. 2018;472(3):469-76.
102. Kim D, Khan AU, Compres EV, Zhang B, Sunshine JC, Quan VL, et al. BRAF fusion Spitz neoplasms; clinical morphological, and genomic findings in six cases. J Cutan Pathol. 2020;47(12):1132-42.
103. Donati M, Kastnerova L, Ptakova N, Michal M, Kazakov DV. Polypoid Atypical Spitz Tumor With a Fibrosclerotic Stroma, CLIP2-BRAF Fusion, and Homozygous Loss of 9p21. Am J Dermatopathol. 2020;42(3):204-7.

Narrative Review
Acta Medica Academica 2021;50(1):175-196
DOI: 10.5644/ama2006-124.334

A Review of Molecular and Genetic Diagnostics of Myeloid Malignancies with Emphasis on Diagnostics in Bosnia and Herzegovina

Amina Kurtovic-Kozaric[1, 2, 3], Erna Islamagic[2], Adna Asic[3], Lejla Mehinovic-Cavcic[2], Larisa Besic[3], Hana Sahinbegovic[4, 5, 6], Hana Komic[7], Sabira Kurtovic[8], Lejla Burazerovic[8]

[1]Department of Clinical Pathology, Cytology and Human Genetics, Clinical Center of the University of Sarajevo, Sarajevo, Bosnia and Herzegovina, [2]Faculty of Science, University of Sarajevo, Sarajevo, Bosnia and Herzegovina, [3]Department of Genetics and Bioengineering, International Burch University, Sarajevo, Bosnia and Herzegovina, [4]Department of Hematooncology, University Hospital Ostrava, Ostrava, Czech Republic, [5]Faculty of Medicine, University of Ostrava, Ostrava, Czech Republic, [6]Faculty of Science, University of Ostrava, Ostrava, Czech Republic, [7]TIMM Laboratory, Sahlgrenska Center for Cancer Research, University of Gothenburg, Gothenburg, Sweden, [8]Hematology Clinic, Clinical Center of the University of Sarajevo, Sarajevo, Bosnia and Herzegovina

Correspondence: *amina.kozaric@kcus.ba*; Tel.: + 387 33 298 752; Fax.: + 387 33 297 826

Received: 6 March 2021; **Accepted:** 2 April 2021

Abstract
Here we describe the major genetic and genomic aberrations found in myeloid malignancies and how those markers are used in patients' diagnosis, prognosis, and targeted treatment. In Bosnia and Herzegovina, cytogenetic and molecular diagnostics for myeloid malignancies have been established and continually improved since 2005. We report the current state of available diagnostic tools for myeloid malignancies in Bosnia and Herzegovina. Myeloid malignancies are a heterogeneous group of clonal blood diseases characterized by defects in hematopoietic stem cells and myeloid progenitors that lead to abnormal proliferation, differentiation, localization, and self-renewal. Most common myeloid malignancies include myeloproliferative neoplasms (MPNs), myelodysplastic syndrome (MDS), and acute myeloid leukemia (AML). Molecular diagnostics of myeloid malignancies have significantly expanded in the last decade with new genetic and genomic markers for diagnosis, prognosis, and treatment. **Conclusion.** In the last decade, several new genomic markers important for patient diagnosis, prognosis, and therapy have been discovered that need to be implemented in routine molecular diagnostics not only in developed nations but also in developing nations such as Bosnia and Herzegovina.

Key Words: Myeloid Neoplasms ▪ Molecular Diagnostics ▪ Myeloproliferative Neoplasms ▪ Myelodysplastic Syndrome ▪ Acute Myeloid Leukemia.

Introduction and Classification

Myeloid malignancies are a heterogeneous group of clonal diseases where hematopoietic stem or progenitor cells (HSPCs) are disrupted concerning their self-renewal, proliferation, and differentiation capacity as a result of genetic and epigenetic changes (1, 2). The World Health Organization (WHO) classification of myeloid neoplasms was last updated in 2016 (3). According to this classification, myeloid neoplasms include myeloproliferative neoplasms (MPN), mastocytosis, myeloid/lymphoid neoplasms with eosinophilia and gene rearrangement, myelodysplastic/myeloproliferative neoplasms (MDS/MPN), myelodysplastic syndromes (MDS), myeloid neoplasms with germline predisposition, acute myeloid leukemia and related neoplasms (AML), blastic plasmacytoid dendritic cell neoplasm, and acute leukemias of ambiguous lineage (3).

In this review, molecular and genetic diagnostics of more common myeloid malignancies such as MPN, MDS, and AML will be covered.

Myeloproliferative Neoplasms (MPNs)

MPNs are acquired blood malignancies that arise from clonal hematopoiesis through the overproduction of either one or more types of myeloid cell lines. MPNs are classified based on the presence of *BCR-ABL1* gene fusion. Chronic myelogenous leukemia (CML) is therefore classified as a Philadelphia-positive MPN, while polycythemia vera (PV), essential thrombocythemia (ET), and primary myelofibrosis (PMF) are classified as Philadelphia-negative MPNs (4-6).

Philadelphia-Negative MPNs: Polycythemia Vera (PV)

PV is characterized by erythrocytosis, which is often accompanied by leukocytosis and thrombocytosis. The 2016 revision of WHO classification defines three major and one minor criterion for the PV diagnosis. Major criteria are: (1) In men, hemoglobin level >16.5 g/dL or hematocrit >49%; in women, hemoglobin level >16.0 g/dL or hematocrit level >48%, or increased red cell mass; (2) Hypercellular bone marrow with panmyelosis; (3) Detection of *JAK2*^{V617F} mutation or *JAK2* mutation within exon 12. The minor criterion is subnormal erythropoietin level in the patients' serum. PV diagnosis requires confirmation of all three major criteria, or the first two major criteria + minor criterion (3). Treatment includes phlebotomy, hydroxyurea, and interferon-α (4-6).

Philadelphia-Negative MPNs: Essential Thrombocythemia (ET)

ET is characterized by megakaryocytic hyperplasia and thrombocytosis, which elevated granulocyte levels and splenomegaly may accompany. According to the last revision of the WHO classification, four major and one minor criterion are determined for ET diagnosis. Major criteria are (1) Thrombocyte count ≥450x10^9/L; (2) Prominent proliferation of the megakaryocyte lineage, with mature, enlarged megakaryocytes; (3) Not meeting criteria for PV, PMF, MDS, *BCR-ABL*1$^+$ CML, or other myeloid neoplasms; (4) Detection of the *JAK2*, *CALR*, or *MPL* mutations. Minor criterion implies the absence of the reactive thrombocytosis and presence of a clonal marker. ET diagnosis requires meeting four major criteria, or three major criteria and minor criterion (3). Treatment involves salicylic acid and hydroxyurea (4-6).

Philadelphia-Negative MPNs: Primary Myelofibrosis (PMF)

The main characteristics of PMF include abnormal megakaryocytopoiesis, aberrant blood count, elevated myeloid cell proliferation, fibroblast proliferation, as well as the release of reticulin and collagen which leads to bone marrow fibrosis, extramedullary hematopoiesis, and splenomegaly (4-6). Three major criteria for PMF diagnosis are: (1) Megakaryocytic proliferation and atypia, granulocytic proliferation, decreased erythropoiesis, and absence of reticulin fibrosis > 1st grade; (2) Not meeting criteria for PV, ET, MDS, *BCR-ABL1*$^+$ CML, or other myeloid neoplasms; (3) Detection of the *JAK2*, *CALR*, or *MPL* mutations, or presence of another clonal marker. Minor criteria are (1) Palpable splenomegaly; (2) High activity of LDH; (3) Leukocytosis; (4) Anemia. PMF diagnosis can be confirmed if all three major criteria and one minor criterion are met (3).

Philadelphia-Positive MPN: Chronic Myelogenous Leukemia (CML)

CML is a Philadelphia chromosome-positive (Ph$^+$) myeloproliferative disease. The main cause of CML is a reciprocal translocation between chromosomes 9 and 22 in the bone marrow stem cells, which leads to the formation of the *BCR-ABL1* fusion gene. BCR-ABL1 protein conditionally activates several key signal transduction pathways responsible for the proliferation, survival, and dissemination of the malignant myeloid clone (7-13). Bone marrow biopsy at diagnosis is necessary for: a) determination of blast cell percentage, b) assessment of basophils proportion, c) the presence of *BCR-ABL1* translocation by cytogenetic analysis

(karyotyping or FISH) or polymerase chain reaction (PCR) (14). The detection of *BCR-ABL1* clone at diagnosis and every three months after the initiation of treatment is required for each CML patient. Disease monitoring consists of measuring *BCR-ABL1* transcripts by real-time quantitative PCR. Hasford and EUTOS scores were used to predict patients' survival and response to the TKI therapy; however, the new EUTOS Long Term Survival (ELTS) score is more adequate to predict the probability of leukemia-related deaths since the vast majority of CML patients die from the other causes than leukemia (15). A revolutionary advancement in the CML treatment was achieved with a tyrosine kinase inhibitor, such as imatinib mesylate, a drug that specifically blocks the enzymatic activity of the BCR-ABL1 fusion protein (16).

Myelodysplastic Syndrome (MDS)

MDS is a clonal disorder of hematopoietic stem cells (HSCs) characterized by aberrations in both morphology and maturation of cell precursors of one or several lineages and cytopenia with a tendency of progression to acute myeloid leukemia (17, 18). This is a heterogeneous group of malignancies with aberrant proliferation, differentiation, and maturation of HSCs, all of which are evident as morphological changes in myeloid cells. Clinical manifestation includes bone marrow failure, while pathological manifestation includes dysplastic morphology in one or several blood cell lineages in the bone marrow or the peripheral blood. The majority of patients suffer from cytopenia, anemia and require blood transfusions. Less common symptoms include neutropenia and/or thrombocytopenia (17).

Acute Myeloid Leukemia (AML)

AML is characterized by the clonal proliferation of abnormal, immature myeloid cells. The term acute refers to a disease that develops faster and leads to fatal outcomes in as little as a few months if left untreated (19). It arises due to genetic changes in the DNA of myeloid precursors. It is characterized by an obstruction in differentiation and a continuous division of immature myeloid cells, more precisely leukemic blasts, which impair normal hematopoiesis (20). AML primarily forms in the bone marrow, but in most cases, blasts are also found within the peripheral blood. More precisely, AML is defined as a disease characterized by over 20% of blasts in the bone marrow or peripheral blood. This may also spread to other parts of the body, such as lymph nodes, spleen, liver, central nervous system, or testicles (21).

Molecular Markers

Genetic Markers of AML

Genetic markers, both molecular and cytogenetic, have their diagnostic, prognostic, and therapeutic role. As a part of a diagnostic workup, each AML patient requires both cytogenetic and molecular testing. Regarding molecular markers, studies have identified an overwhelming number of mutations in AML genomes. On average, one AML genome shows five mutations. Nine gene categories relevant for AML pathogenesis have been identified, namely gene fusions, *NPM1* mutations, tumor-suppressor genes, DNA methylation genes, signaling genes, chromatin-modifying genes, myeloid transcription factors, cohesin complex genes, and spliceosomal members (Table 1). The most commonly mutated genes in AML are *FLT3* (32% of all cases), *NPM1* (25%), and *DNMT3A* (20%), with the possibility that they are concomitant in the same sample.

FLT3 (Fms-like tyrosine kinase 3) is a gene that encodes a class III receptor tyrosine kinase present in both humans and mice (Figure 1). When a ligand binds to FLT3, it gets dimerized and autophosphorylated, leading to the activation of PI3K/AKT and RAS/MAPK pathways (22). Increased expression levels have been seen in 70% to 100% of AML cases; thus, it was hypothesized that *FLT3* expression plays a role in the survival and proliferation of leukemic blasts (23). The most commonly seen mutation in the *FLT3* gene in AML is internal tandem duplication (24), while the second most

Table 1. AML Risk Stratification and Genomic Classification. Risk Stratification Is Based on Molecular and Cytogenetic Abnormalities and Is Used for Therapeutical Strategies*

AML risk stratification	Molecular markers	Cytogenetics
Favorable	*NPM1* mutated	t(8;21)(q22;q22.1); *RUNX1-RUNX1T1*
	FLT3 wild type	t(15;17)(q24;q21), *PML-RARA*
	CEBPA biallelic mutation	inv(16) or t(16;16); *CBFB-MYH11*
Intermediate	*NPM1* mutated & *FLT3*-ITD mutated	t(9;11)(p21.3;q23.3); *MLLT3-KMT2A*
	NPM1 wild type & *FLT3* wild type	t(6;9)(p23;q34.1); *DEK-NUP214*
	–	Cytogenetic abnormalities not classified as favorable or adverse
Adverse	*NPM1* wild type & *FLT3*-ITD mutated	t(v;11q23.3); *KMT2A* (MLL) rearrangement
	RUNX1 mutated	t(9;22)(q34.1;q11.2); *BCR-ABL1*
	ASXL1 mutated	inv(3)(q21.3q26.2) or t(3;3)(q21.3;q26.2); *GATA2,MECOM(EVI1)*
	TP53 mutated	–5 or del(5q); –7; –17/del(17p)
	–	Complex karyotype, monosomy
AML Genomic Classification		
Classes of AML	Frequency of all AML (%)	Additional mutated genes
NPM1 mutant	30	*DNMT3A* (50%), *FLT3* (40%), Cohesin (15%), *NRAS* (15%), IDH (15%), *TET2* (15%)
Chromatin-spliceosome	13	*RUNX1* (40%), *MLL* (20%), *ASXL1* (20%), *DNMT3A* (20%), *SRSF2* (20%), *FLT3* (15%),
t(15;17)	13	*FLT3* (35%), *WT1* (15%)
TP53/chromosomal aneuploidy	10	–
t(8;21)	7	*KIT* (25%), *NRAS* (20%), Cohesin (20%), *ASXL1* (20%)
inv(16)	5	*NRAS* (40%), *KIT* (35%), *FLT3* (20%)
t(v;11q23)	4	*KRAS* (20%), *NRAS* (20%)
biCEPBA	4	*GATA2* (30%), *NRAS* (30%)
t(9;22)	1	–
t(6;9)	1	*FLT3* (70%)
t(5;11)	1	*FLT3* (80%)
inv(3)	1	–
Other translocations	1	–
IDH2 R172	1	–

*AML genomic classification presents classes of AML based on genomic and cytogenetic abnormalities; Cohesin = RAD21; SMC1A, SMC3 wild type = not mutated, normal.

common one is *FLT3* activation loop point mutation. Internal tandem duplications (ITD) in *FLT3* account for 24%, while the activation loop mutations are seen in 7% of AML patients. Therefore, 30% of AML patients have acquired mutations in the *FLT3* gene, making it the most mutated gene in AML (25). Mutations in the *FLT3* gene result in cellular proliferation, resistance to apoptosis, and DNA defective repair (26). The identification of *FLT3* mutations is essential because of the availability of FLT3 inhibitors, which are part of the standard treatment of AML.

CEBPA (CCAAT/enhancer-binding protein α) encodes transcriptional factor with leucine zipper

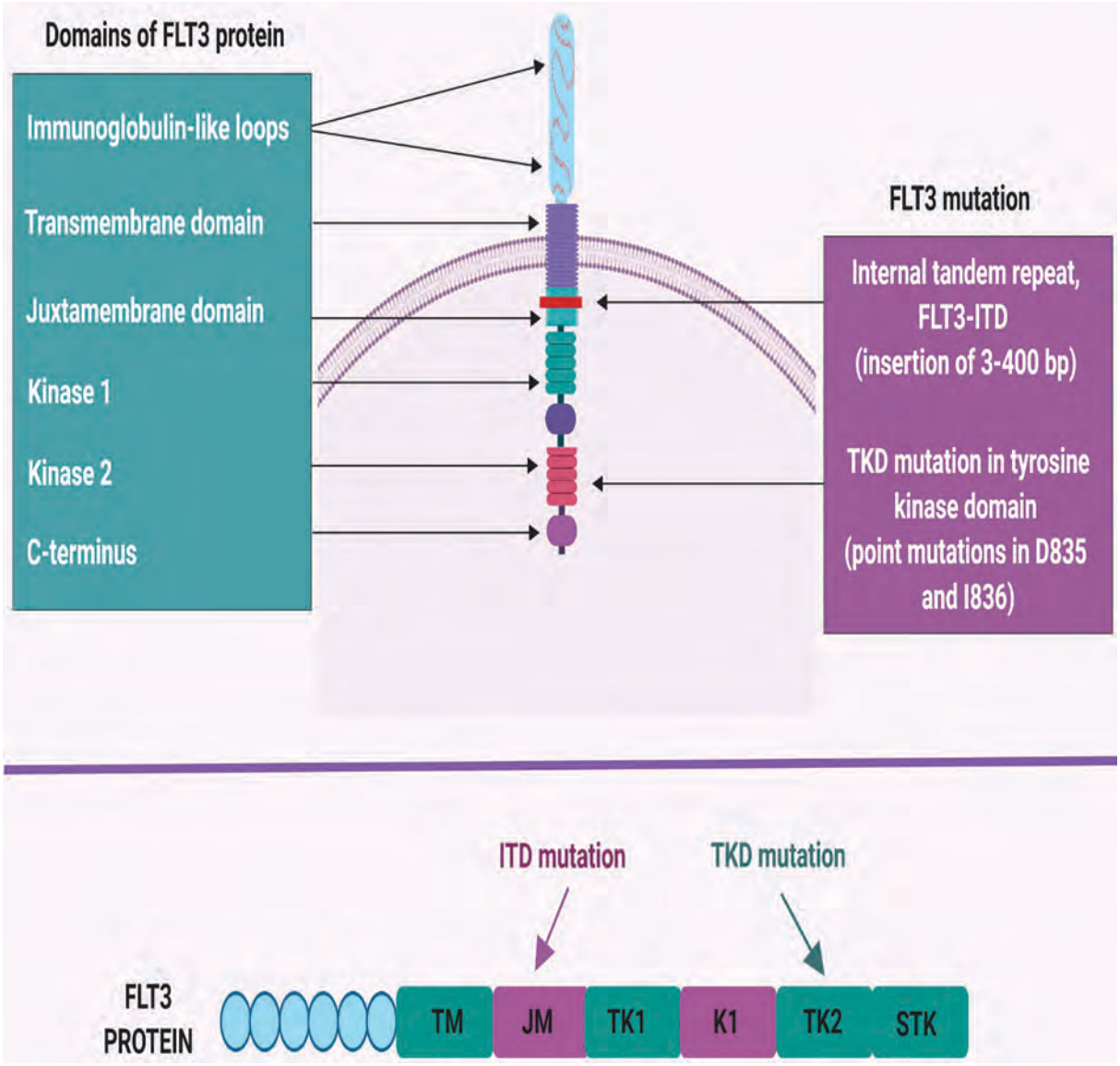

Figure 1. *FLT3* mutations are among the most common mutations in AML patients. Two types of mutations have been identified: internal tandem duplication (ITD) mutation and TKD (tyrosine kinase domain) mutations. ITD mutations are more common than TKD mutations. ITD mutations lead to 3-400 bp insertions in the JM domain, while TKD mutations (D835 and I836) are point mutations in the TK2 domain. Created in Biorender.

domain involved in cell cycle regulation (27, 28), proliferation, and differentiation of the myeloid lineage (28). Nonsense and frameshift mutations are frequent in the N-terminal region, while in-frame indels are typical for the C-terminal region of the protein (27). In general, 5-15% of AML patients have single- or double-mutated *CEBPA*. Double-mutated *CEBPA* (*CEBPA*dm) is related to the characteristic gene expression profile that defines a specific subgroup of AML patients with a more favorable prognosis (3, 29). Coexisting mutations in genes *ASXL1*, *RUNX1*, *NPM1*, and *FLT3-ITD,* are more frequently present in *CEBPA*sm (single-mutated) cases (30).

NPM1 (Nucleophosmin 1) is a gene that encodes multifunctional NPM1 protein, primarily localized in the nucleolus. It functions as a molecular chaperone that transports ribosomal proteins

through the nuclear membrane (31). Mutations in *NPM1* have been linked to tumorigenesis, as *NPM1* was found to be frequently overexpressed in diverse solid tumors and involved in different translocations and deletions (32). It was shown that *NPM1* is mutated in 25% of AML patients, making it one of the most frequently mutated genes in this type of cancer (33). Four-base insertions in exon 12 of *NPM1* are seen in 75-80% of cases (34). All mutations in exon 12 are frameshift mutations, causing changes in the C-terminal region, resulting in the loss of two tryptophan residues and creating a new nuclear export sequence (NES) domain. Consequently, mutant NPM1 (called NPM1c) protein is exported to the cytoplasm instead of in the nucleus.

KIT, a proto-oncogene type III tyrosine kinase, is a receptor for stem cell factors expressed on the surface of the leukemic blast (35). Mutations in this gene are seen either in exon 8 or in codon 816, the latter resulting in a formation of the activation loop. 20-30% of AML patients with t(8;21) and inv(16)/t(16;16) carry mutations in *KIT* (36). They cause the activation of MAPK and PI3K/AKT pathway and STAT3/STAT5 signaling that aid in cancer development (37).

RAS protein family is a diverse group of proteins that activate various receptors, which further trigger downstream effector pathways. These control cell proliferation, differentiation, and survival (38). Guanine nucleotide-binding proteins, which include NRAS, KRAS, and HRAS, are involved in hematopoiesis. RAS activation may result from either a mutation in *RAS* itself or *FLT3* or *KIT*; *NRAS* and *KRAS* mutations are seen in about 15% to 25% of AML patients. *RAS* mutations activate PI3K/Akt/mTOR and the RAF/MEK/ERK proproliferative signaling pathways (38).

DNMT3A (DNA methyltransferase 3A) catalyzes methylation of 5-methylcytosines and is important for differentiation of the embryo and hematopoietic stem cells. There are three active DNA methyltransferases in mammals – DNMT1, DNMT3A, and DNMT3B. They are primarily involved in DNA methylation but also in genetic imprinting, differentiation, X-chromosome inactivation, proliferation, and apoptosis (39). Mutations in *DNMT3A* occur in more than 30% of AML patients with normal karyotype (40). Loss-of-function mutations in *DNMT3A* halt the hematopoietic cell differentiation and are among the first events in leukemogenesis. Mutated *DNMT3A* preleukemic cells represent storage for further progression of the disease if additional mutations occur. The most common mutation seen in *DNMT3A* is at the R882 arginine residue, disrupting the methyltransferase activity. *DNMT3A* mutations in combination with *FLT3* or *NPM1* mutations are linked to adverse prognosis (41).

TET2 (a member of the TET family of dioxygenase proteins) mutations occur in 10-25% of AML (41). TET2 converts 5-methylcytosine to 5-hydroxymethylcytosine, encouraging DNA demethylation. Mutations in *TET2* do not promote AML by themselves but instead disrupt the function of the TET2 enzyme, which leads to the clonal expansion of pre-leukemic stem cells. These cells may override normal hematopoiesis with time and favor the accumulation of mutations leading to AML development (42).

IDH1 and IDH2 are NADP-dependent enzymes involved in the KREBS cycle, as IDH1 (isocitrate dehydrogenase 1) and IDH2 (isocitrate dehydrogenase 2) catalyze the oxidative decarboxylation of isocitrate to alpha-ketoglutarate. *IDH1* and *IDH2* mutations occur in 20% of AML patients and are heterozygous (43). The most common mutations are IDH1 R132, IDH2 R140, and IDH2 R172, which have different prognostic value. *IDH* mutations lead to the formation of a neomorphic enzyme and abnormal accumulation of an oncometabolite, 2-hydroxyglutarate (44, 45). Accumulated 2-hydroxyglutarate initiates potentially oncogenic events: it inhibits jumonji-C domain containing proteins involved in histone demethylation, TET2 protein, prolyl/lysyl hydroxylases, and cytochrome C in the electron-transport chain (41). IDH inhibitors such as enasidenib and ivosidenib were approved in 2018 to treat relapsed/refractory AML.

Regarding cytogenetic markers, recurrent cytogenetic aberrations are found in about 50% of

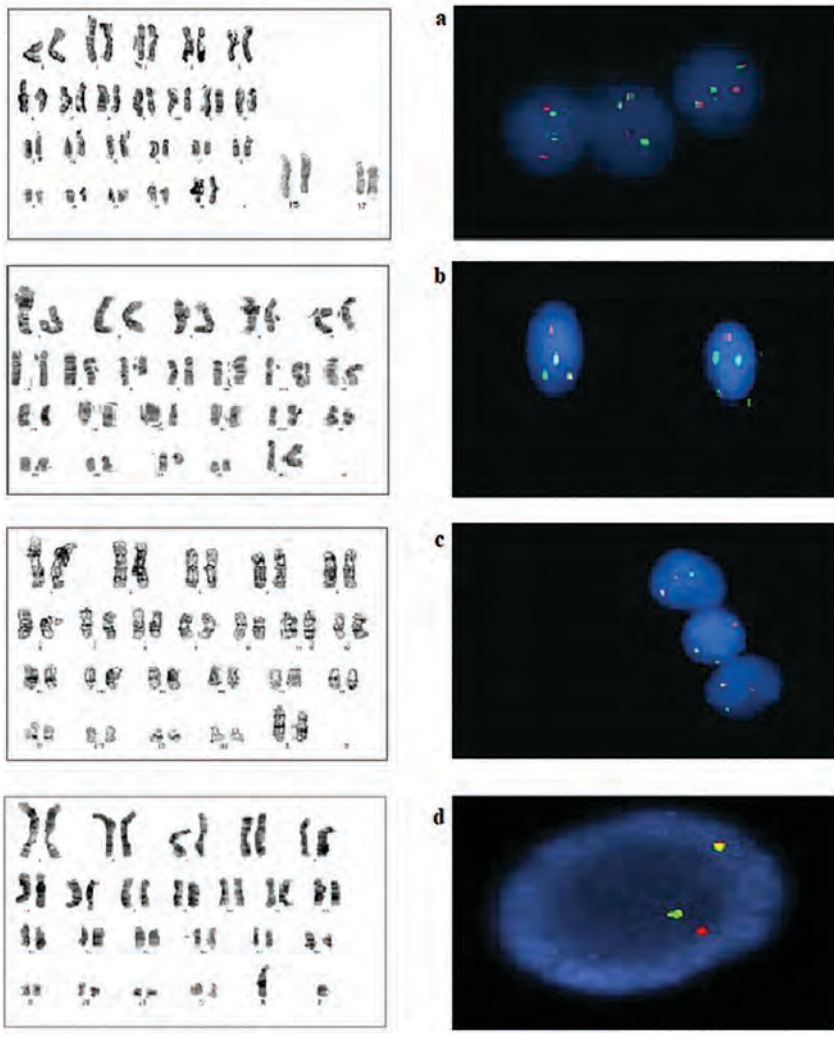

Figure 2. (A) 46,XX,t(15;17)(q22;q21.1) Abnormal female karyotype with translocation between chromosomes 15 and 17. (a) FISH analysis for *PML/RARA* on two hundred interphase nuclei with 1R1G2F positive signal pattern (1 red signal, 1 green signal, and 2 fusions; Abbott, Abbott Park, Illinois, USA). (B) 46,XX,t(8;21)(q22;q22) Abnormal female karyotype with translocation between chromosomes 8 and 21. (b) Dual color dual fusion translocation FISH probe for *RUNX1/RUNX1T1* (Abbott, Abbott Park, Illinois, USA) with abnormal 1R1G2F (1 red signal, 1 green signal, and 2 fusions) pattern. (C) 46,XX,t(9;11)(p23;q23) Abnormal female karyotype with translocation between chromosomes 9 and 11. (c) *MLL* break a part FISH probe with 1R1G1F (1 red signal, 1 green signal, and 1 fusion) abnormal pattern. (D) 46,XY,inv(16)(p13;q22) Abnormal male karyotype with chromosome 16 inversion. (d) Break apart FISH probe for *CBFB* with abnormal pattern *1R1G1F* (1 red signal, 1 green signal, and 1 fusion).

all AML patients, where the most common ones are t(15;17), t(8;21), inv(16), t(9;11), inv(3), and t(6;9) (Figure 2). These balanced translocations and inversions are classified as "AML with recurrent genetic abnormalities" in the WHO classification (3). It is worth noting that besides mentioned cytogenetic aberrations, additional abnormalities including complex karyotype (3 or more chromosomal abnormalities), such as −5 or del(5q), −7 or del(7q), i(17q) or t(17p), −13 or del(13q), del(11q), t(2;11)(p21;q23.3), t(3;21)(q26.2;q22.1), t(1;3)(p36.3;q21.2), t(5;12)(q32;p13.2), t(11;16)(q23.3;p13.3), t(5;7)(q32;q11.2),t(5;17)(q32;p13.2),t(5;10)(q32;q21.2),and t(3;5)(q25.3;q35.1). These are sufficient to establish the diagnosis of "AML with myelodysplasia-related changes" if the bone marrow has ≥20% blasts (27). Around 50% of AML patients have normal karyotype without recurrent genetic abnormalities.

The most commonly found abnormalities can be found on the Atlas of Genetics Oncology website. Here we describe two examples: *PML-RARA* and *MLL* translocations. *PML-RARA* translocation, t(15;17)(q22;q12), involves *PML* (promyelocytic leukemia protein) and *RARA* (retinoic acid receptor alpha) genes, whereby PML N-terminus is fused with the C-terminal RARA receptor region (Figure 3). PML-RARA fusion protein acts as an irregular retinoic acid receptor with modified DNA-binding and transcription-regulation properties. Different protein isoforms are possible, each resulting in a different clinical description of the disease. At the molecular level, this translocation causes inhibition of myeloid differentiation due to inactive RARA protein and blockage in for-

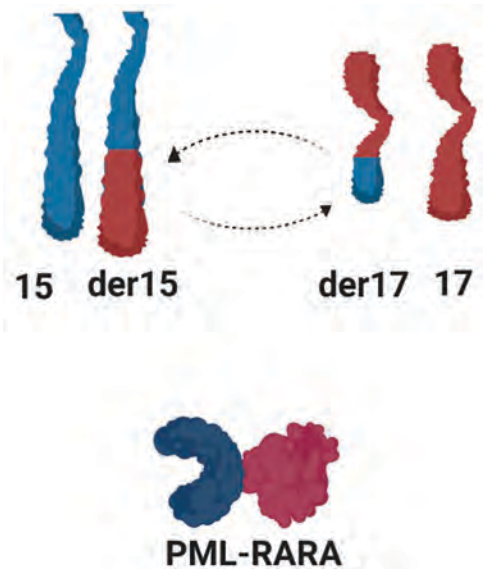

Figure 3. *PML-RARα* results from the translocation between chromosomes 15 and 17 in *PML* and *RARA* genes, respectively, leading to the PML-RARα fusion protein.

mation of nuclear bodies, necessary for the proper functioning of the p53-related pathway. Molecular and cytogenetic diagnostics are essential for the fast determination of the presence of *PML-RARA* translocation in a blood or bone marrow sample because of the need for urgent clinical action. Fast FISH assay or RT-PCR are used to detect this translocation within 2-4 hours.

MLL, coding for a methyltransferase, can harbor gene rearrangement that has been among the first to be associated with unfavorable patient prognosis (46). Translocations and partial tandem duplications in *MLL* are seen in 8-10% of AML. MLL translocates with over 50 different genes, causing the expression of chimeric proteins (47). However, MLL rearrangements show a very low number of potentially cooperating mutations thus indicating that MLL-rearranged leukemias are mostly driven through epigenetic dysregulation (48). Duplication regions are found between exon 5 and 11 and between exon 5 and 12 and are strongly associated with trisomy 11 but have also been noted for karyotypically normal AML (49). *MLL* rearrangements in AML usually result in the overexpression of BCL2 protein, leading to drug resistance (46).

NCCN and ELN risk stratification of AML is based on the presence of molecular and cytogenetic mutations (Table 1) (27, 50). Each AML is categorized as favorable, intermediate, and adverse. The stratification is crucial for treatment strategy and is an integral part of patient evaluation. Even if a genetic mutation may not be included as a prognostic marker, its presence may provide a target for new therapies as with IDH1, IDH2, and KMT2A.

Genetic Markers of CML

CML's main cause is the reciprocal translocation between chromosomes 9 and 22 in bone marrow stem cells, leading to clonal proliferation of mature granulocytes and their precursors. Translocation t(9;22)(q34;q11) with characteristic Philadelphia chromosome (shortened as 22q-) is found in 95% of all CML cases (Figure 4). Depending on exact breakage and rejoining sites, several different BCR-ABL1 proteins might result from this translocation. Protein size can be 210 (p210) or 190 (p190) kDa, depending on the number of amino acids in the BCR primary sequence. p190 is mostly found in acute lymphocytic leukemia (ALL) cases, while p210 is found in both ALL and CML.

The presence of *SETBP1* and *ETNK1* mutations and the absence of t(9;22) translocation and mutations in genes associated with MPN characterize atypical CML (aCML), also called *BCR-ABL*1-CML. Mutations in *CSF3R* are infrequent, present in less than 10% of aCML cases. Patients with advanced CML exhibit numerous genetic abnormalities, including duplicated Philadelphia chromosome, isochromosome 17(p) resulting in *TP53* disturbance, and rarely deletion of p15 and p16 tumor-suppressor genes and *RUNX1-EV11* fusion. In addition, gene expression is likely to be deregulated in advanced diseases. This includes both increase in expression (nuclear genes, mitochondrial genes, RNA-binding genes, genes involved in protein synthesis), as well as a decrease (structural integrity and adhesion genes, inflammation, immune response modulators). Finally, several proto-oncogenes and tumor-suppressor genes can be differentially expressed, including *N-RAS*, *H-RAS*, *FLT3*, *WT1*, *BCL-2,* and *PTPN11*.

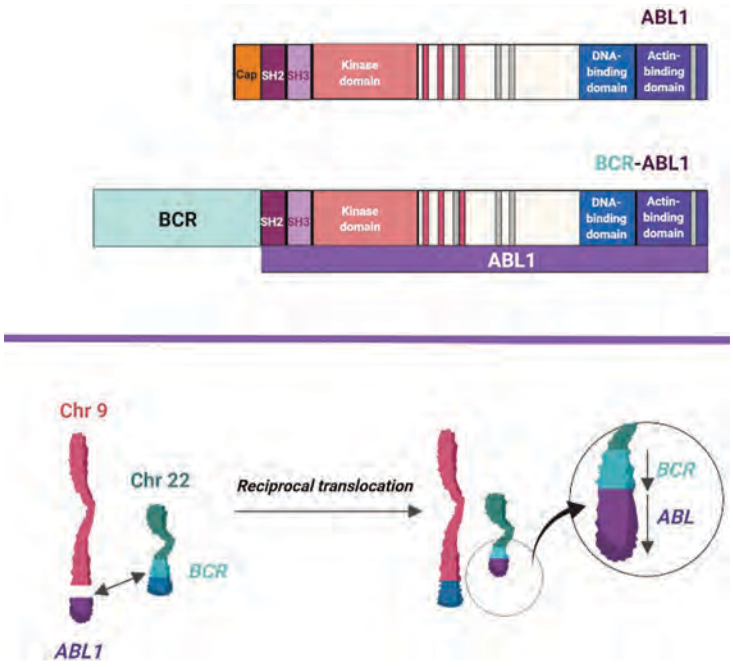

Figure 4. *BCR-ABL1* gene fusion results from a reciprocal translocation between long arms of chromosomes 9 and 22, leading to the BCR-ABL1 fusion protein (depicted at the top). Created in Biorender.

Genetic Markers of MPNs

Over 95% of patients suffering from Philadelphia-negative MPNs harbor either *JAK2*, *CALR*, or *MPL* driver gene mutations. The fourth phenotype driver gene is *CSF3R*, and mutation in any of these genes is mutually exclusive with the other three. A common characteristic of MPNs is increased JAK-STAT signaling. Besides, *TET2, DNMT3A, ASXL1, IDH1/2, EZH2, SF3B1, SRSF2, TP53, NRAS,* and *KRAS* mutations were also reported, mainly in so-called triple-negative patients. These mutations can also appear before or after phenotypic driver mutations, in which case they modify or amplify the effect of those drivers (5, 51). Other DNA sequence variants or mutations found in a fraction of MPN patients are *TP53*, *CUX1*, *IKZF1*, *NF-E2* (transcriptional regulation), *ASXL1, IDH1*, *IDH2*, *TET2*, *EZH2*, *DNMT3A* (epigenetic regulation), *SRSF2*, *U2AF1*, and *SF3B1* (RNA splicing). It has been reported that *TP53*, *IDH2*, and *SRSF2* mutations are over-represented in blast-phase MPN (52). Similarly, *ASXL1*, *EZH2*, and *SRSF2* mutations in PMF patients are associated with leukemic transformation and poor prognosis.

The three most commonly mutated genes in MPN (*JAK2*, *MPL* and *CALR*) are a part of the MPN diagnostic algorithm. *JAK2* (Janus kinase 2) V617F mutation in exon 14 is most abundantly found in the Philadelphia-negative MPNs, namely PV (in around 95% of cases), ET (around 55% of cases), and PMF (around 65% of the cases). This mutation leads to the growth-factor independence in affected cells due to constitutive tyrosine phosphorylation and consequential JAK2 protein activation (5, 6, 51-56). *MPL* (MPL proto-oncogene) gene encodes thrombopoietin receptor, and its mutations are found in around 4% of ET and 10% of PMF patients, but not in PV patients. Mutations are mostly found in residue W515 in exon 10, including W515L, which results in constitutive activation of downstream signaling pathway even in the absence of thrombopoietin. Other MPL mutations in MPNs are W515S, W515A, S505N, A506T, and A519T. Calreticulin (CALR) is a multifunctional chaperone protein involved in various cellular processes, including cell adhesion (57-60). Recent studies have found *CALR* mutations in exon 9 in MPN patients who lack the *JAK2* or *MPL* mutations. *CALR* mutations were reported in ET and PMF patients at a frequency between 20% and 30% and accounted for approximately 70% of *JAK2*/*MPL*-nonmutated ET and around 85% of *JAK2*/*MPL*-nonmutated PMF. They were not reported in PV patients (57-60). Over 36 different frameshift insertions or deletions were reported, all of which results in a novel C-terminal amino acid sequence in the mutated calreticulin, which leads to malfunctioning in calcium-binding and cell growth. The most prominent two mutations are the type 1 and type 2 mutations, which account for over 80% of the *CALR* exon 9 mutations. The type 1 mutation (L367fs*46) is a 52-base pair deletion, while type 2 mutation (K385fs*47) is a 5-base pair TTGTC

insertion, both of which lead to a frameshift. Both mutations induce a change in the subcellular localization signal by leading to a loss of negatively charged amino acids in the protein C-domain (57-60).

Genetic Markers of MDS

MDS is associated with two types of mutations: chromosomal aberrations and somatic gene mutations. Common chromosomal aberrations that are associated with MDS are -5/5q-, -7/7q-, +8, 20q-, +21, 12p-, 13q- and 17p- (Figure 5, Table 2). Their prognostic values are shown in Table 3. They are detected in 40-60% of primary MDS patients and more than 80% of therapy-associated MDSs (61) (Table 1). These aberrations are best detected with karyotyping or microarrays. The affected chromosomal regions often involve tumor-suppressor genes. While these changes are encountered at diagnosis, additional or evolved clones can be found during the clinical progression of the disease and are associated with a poor prognosis.

Table 2. Cytogenetic Abnormalities Found in MDS and Therapy-Related MDS*

MDS cytogenetics	Abnormality	MDS (%)	t-MDS (%)
Unbalanced	+8*	10	-
	-7 or del(7q)	10	50
	-5 or del(5q)	10	40
	del(20q)*	5-8	-
	-Y*	5	-
	i(17q) or t(17p)	3-5	-
	-13 or del(13q)	3	-
	del(11q)	3	-
	del(12p) or t(12p)	3	-
Balanced	t(11;16)(q23;p13.3)	-	3
	t(3;21)(q26.2;q22.1)	-	2
	t(1;3)(p36.3;q21.2)	1	-
	t(2;11)(p21;q23)	1	-
	inv(3)(q21q26.2)	1	-
	t(6;9)(q23;q34)	1	-

*Table adapted from reference (61); MDS=Myelodysplastic syndrome; t-MDS=Therapy related MDS.

Table 3. Genomic/Molecular Abnormalities in MDS and AML*

Gene	Frequency in MDS (%)	Prognosis	Comment
RNA splicing			
SF3B1	20-30	Favorable	MDS-rS and MDS-MLD, associated with ring sideroblasts, fewer mutations in other genes
SRSF2	15	Unfavorable	CMML phenotype
U2AF1	10	Unfavorable	Often with del(20q)
ZRSR2	5	Unknown	On X-chromosome, more common in males
Epigenetic regulators			
TET2	20-30	Unknown	Normal karyotype, more frequent in CMML
DNMT3A	10-15	Unfavorable	-
IDH1 and IDH2	5	Unknown	-
ASXL1	15-20	Unfavorable	-
EZH2	5	Unfavorable	More common in CMML
Transcription and signaling pathways			
TP53	8	Unfavorable	Associated with complex karyotype and high risk disease, few mutations in other genes
RUNX1	5-10	Unfavorable	Thrombocytopenia, excess blasts
NRAS/KRAS	5-10	Unfavorable	Thrombocytopenia, excess blasts, more common in CMML
JAK2	5	Unknown	50% of RARS-T, often subclonal

*Table adapted from reference (68).

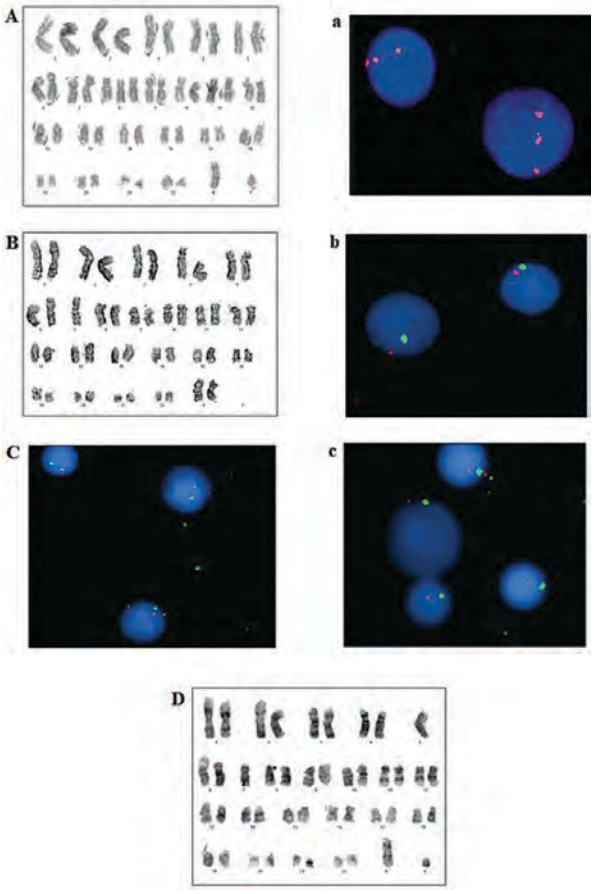

Figure 5. (A) 47,XY,+8 Abnormal male karyotype with chromosome 8 trisomy. (a) FISH for centromere of chromosome 8 (Abbott, Abbott Park, Illinois, USA). Trisomy 8 is shown (3 red signals). (B) 45,XX,-7 Abnormal female karyotype with a chromosome 7 monosomy. (b) FISH dual color probes for chromosome 7 centromere and D7S522 locus at 7q31 (Abbott, Abbott Park, Illinois, USA). Monosomy 7 is shown with an abnormal signal pattern 1R1G (1 red and 1 green signal). (C-c) FISH analysis for chromosomes 5 and 7 was performed on a patient sample. (C) Dual color probes for loci at 5p15.2 and 5q31. Deletion is shown with a positive 1R2G scheme (1 red and 2 green signals). (c) Dual color probe for chromosome 7 centromere and D7S522 locus at 7q31. Monosomy of chromosome 7 is shown. (D) 44,XY,-5,-7 Abnormal male karyotype with monosomies of chromosomes 5 and 7 was determined in the analyzed cells.

Regarding somatic mutations, almost half of MDS patients have two or more genes simultaneously mutated (Figure 6). The most efficient method for the simultaneous detection of mutations in several genes is a next-generation sequencing (NGS). Affected genes are involved in RNA splicing, transcription, signaling pathways, and epigenetic regulation. Their prognostic values are presented in Table 2. Mutations in *SF3B1* (splicing factor 3b subunit 1) are found in one-third of MDS patients). Other spliceosome-associated genes mutated in MDS include *SRSF2*, *U2AF1,* and *PRPF8*. Among the most significant epigenetic factors that mutate in MDS patients are *TET2* and *DNMT3A*. *TET2* mutations are found in up to 30% of all MDS patients and up to 60% of CMML patients. The most common *DNMT3A* mutation is R882, and patients with this mutation have an increased chance of AML progression. *ASXL1* encodes a polycomb protein involved in histone methylation. Mutations in this gene are found in 15-20 % of MDS patients, usually frameshift or nonsense mutations in exon 12.

Mutations associated with the progression of MDS to secondary AML include *SRSF2, SF3B1, U2AF1, ZRSR2, ASXL1, EZH2, BCOR*, and *STAG2*. These mutations occur in MDS and continue through sAML. Mutations in *IDH1* and *IDH2* are found at frequencies around 5%, with a high occurrence in high-risk MDS (around 23%). Most mutations are missense, including R132 in IDH1 and R172K in IDH2 (Table 2) (43, 62-68). The detection of the mutations mentioned above leads to clonal expansion. However, it is worth noting that those mutations can also be detected, particularly *TET2*, *ASXL1, DNMT3A*, and *TP53*, in healthy aging populations, a phenomenon called clonal hematopoiesis of indeterminate potential (CHIP) (53-55). CHIP is defined as the presence of at least 2% of a somatic mutation in peripheral blood and the absence of malignant hematological disease. Currently, somatic mutations are not a part of the clinical diagnosis of MDS. CHIP likely transitions to MDS through a complex interaction of several factors within HSC and bone marrow microenvironment.

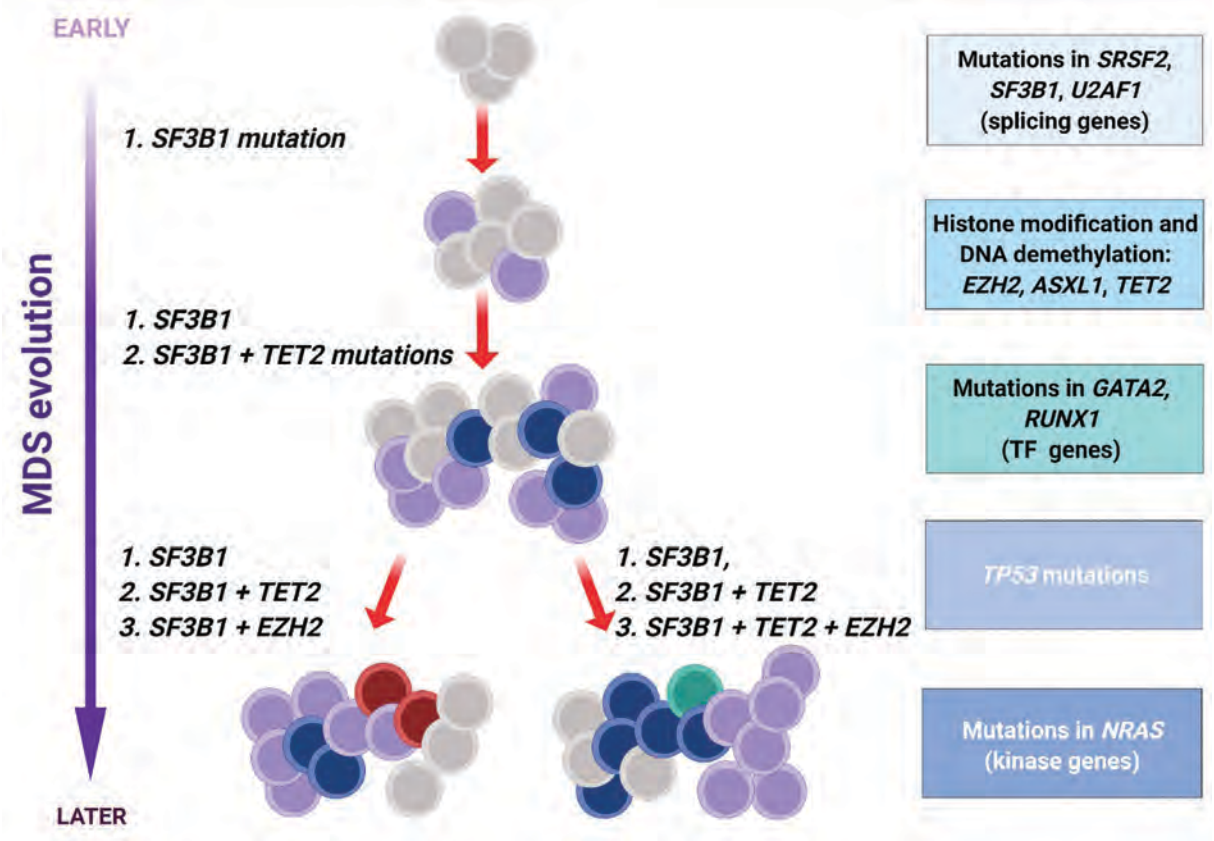

Figure 6. Clonal evolution of MDS. Initial clones develop mutations in splicing factors such as *SF3B*1, *SRSF2*, or *U2AF1*. Later events typically involve *TP53* and *NRAS* mutations, leading to several different clones in MDS patients. Created in Biorender.

Molecular and Genetic Techniques

Cytogenetics

Cytogenetic analysis of peripheral blood and bone marrow aspirates is the golden diagnostic standard for myeloid malignancies. AML, MDS, MPN, CML, and other myeloid malignancies rely on cytogenetic analysis for both diagnosis and prognosis. Conventional cytogenetic analysis is mandatory in the diagnostic evaluation of AML. Standard cytogenetic analysis refers to karyotyping, where 20 metaphases are screened for chromosomal abnormalities such as translocations, deletions, duplications, inversions, trisomies, monosomies, and other abnormalities. The karyotype is considered complex if it consists of three or more abnormalities. Reporting abnormalities is standardized through ISCN (International System for Human Cytogenetic Nomenclature), which contains guidelines on cytogenetic formulations. Clonality, or the presence of one or more clones with unique abnormalities, can easily be deduced from cytogenetic formulas (56). If cytogenetic analysis cannot be obtained, fluorescence in situ hybridization is used to detect specific translocations or deletions, such as t(8;21), inv(16), t(15;17), del 5q, del7q, and del17p.

Cytogenetic abnormalities have diagnostic and prognostic values. The presence of t(9;22) in a myeloid patient is diagnostic of chronic myeloid leukemia when taken in the context of clinical parameters (one should also be aware of the AML with t(9;22)). Similarly, other translocations such as t(15;17), t(11;?), and t(6;9) are essential to detect in AML patients because of therapy management and prognosis. All these abnormalities are part of the WHO classification of tumors of hematopoi-

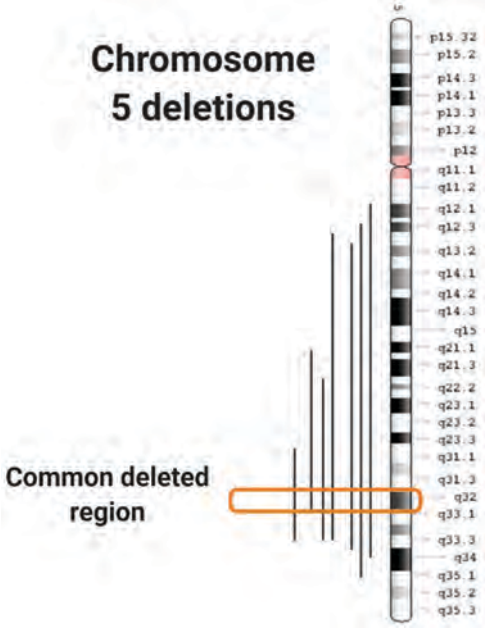

Figure 7. Deletions of the long arm of chromosome 5 are defined as del5q syndrome, a subtype of MDS with a more indolent disease course. Deletions can be larger or smaller, where the common deleted region is in 5q32. Created in Biorender.

etic and lymphoid tissues. Furthermore, deletion of the long arm of chromosome 5, or del5q, is a unique subset of MDS, referred to as del5q syndrome (Figure 7). Classical prognostic markers for MDS are deletion del7q, monosomy of 7, or trisomy 8, which carry a worse prognosis. Complex karyotypes are generally considered unfavorable prognostic markers (56).

The urgent karyotype is typically requested for AML or other hematological malignancies such as ALL or Burkitt lymphoma and can be signed out within 3-7 days. Once the bone marrow aspirate or peripheral blood are received, mononuclear cells are counted and the appropriate number placed in liquid media for 24-72 h. Once the cells have divided and proliferated, they are harvested, cytoplasm removed, fixed, dropped onto slides, and stained with trypsin and Giemsa (GTG banding). The analysis is conducted on 20 metaphases using a light microscope.

After *BCR-ABL1* is confirmed by qualitative or quantitative PCR in CML patients, karyotyping is the next step to demonstrate additional chromosomal abnormalities besides the Ph chromosome; if the Ph chromosome is not found, FISH analysis is necessary to detect variant translocations (69-70). Karyotyping is also an optimal method for analyzing additional chromosomal abnormalities (ACA), previously divided as major and minor route ACA (69). The current classification includes low-risk and high-risk ACA (additional Ph, additional 19 chromosome, trisomy 8, isochromosome 17q, deletion -7/7q) (69). The presence of high-risk ACA is related to a worse prognosis in the CML patients, who are accordingly classified as high-risk patients, and they usually show resistance to the TKI therapy (70-73).

Polymerase Chain Reaction - PCR

Endpoint polymerase chain reaction (PCR) used to amplify DNA segments of interest is applied in all branches of molecular studies, including molecular diagnostics of myeloid malignancies. The method has shown better sensitivity than the direct sequencing of PCR-amplified DNA (detecting mutations with variant allele fractions between 1 and 3%). The major drawback of this method is that many of the protocols are designed in a manner that only the mutant sequence will be amplified if present (such as the protocol designed for the *JAK2*V617F mutation), which may potentially lead to false-negative results, but also prevents differentiation between heterozygous and wild-type mutated samples (74-79). Jeong et al. (2016) developed an AS-PCR-based system for *CALR* type 1 (L367fs*46) and type 2 (K385fs*47) mutation screening (80).

Amplification refractory mutations system (ARMS)-PCR is often used to detect single base variations or minor deletions. This screening method allows for the amplification of mutant and wild-type alleles in a single reaction with the addition of a second pair of primers. The primary deployment of ARMS-PCR is the detection of single nucleotide polymorphisms (SNPs), which makes it ideal for *JAK2* variant screening. Today, the method has been optimized to detect the mutation with as little as a 0.05% variant allele fraction. A

drawback of the method is the lack of quantification of wild type-mutant allele ratios (74, 81, 82). The *JAK2*V617F ARMS-PCR primers designed by Jones et al. (2005) involves two outer control primers (FO and RO) which are complementary to the region flanking exon 14 of the *JAK2* gene, while the inner primers are complementary to the region flanking the G (in case of a wild-type sequence) or the T (in case of a mutation) (83).

Allele-specific oligonucleotide-polymerase chain reaction (ASO-PCR), also recommended to detect specific frequent mutations in the BCR-ABL1 kinase domain, is a more sensitive method compared to Sanger sequencing (84). The mechanism for TKI resistance and a main cause of suboptimal response in CML patients is the presence of mutations in the *BCR-ABL*1 kinase domain (85, 86). However, the detection of mutations is more efficient and sensitive using next-generation sequencing (NGS) (87-90).

Real-Time Quantitative PCR

Real-time PCR enables simultaneous amplification, quantification, and analysis of the variants of interest via fluorescent molecules' detection by fluorescent excitation based on the change in fluorescence during amplification. The combination of real-time PCR and DNA-melting curve analysis is a time- and cost-effective system. Its high sensitivity and specificity make it the best alternative to direct sequencing. Besides, due to its quantification property, this method allows for detecting wild type-mutant allele ratios (76).

Type of *BCR-ABL1* transcript (e13a3/b2a2, e14a3/b3a2, or atypical) in the peripheral blood should be identified by qualitative RT-PCR (nested PCR) at diagnosis and optionally during the follow-up of the patient to assess the response to therapy (91). A quantitative PCR (qPCR) is used to evaluate *BCR-ABL*1 transcript level. It is not required at the diagnosis; however, it is mandatory to perform qPCR every three months during follow-up to track patients' molecular response to TKI (11).

The molecular response is defined as the ratio of *BCR-ABL*1 transcripts and ABL transcripts/GUSB transcripts, according to the International Scale (IS), and it should be reported as a percentage on the log scale. Values 1% (2 log), 0.1% (3 log), 0.01% (4 log), 0.0032% (4.5 log), and 0.001% (5 log) are below the baseline defined in the IRIS study (92-95). Complete cytogenetic response (CCyR) is defined as ≤1% *BCR-ABL*1 transcript level. Major molecular response (MMR, MR^3) is equivalent to ≤0.1% *BCR-ABL*1 transcript level; deep molecular response is determined by MR^4 (≤0.01%) and MR^5 (≤0.001%) (92, 93). It is recommended to use the term "molecularly undetectable leukemia" with the reported number of ABL1/GUSB transcripts instead of "complete molecular response" (94). Monitoring of *BCR-ABL*1 transcript level (time point at 3, 6, and 12 months of follow-up) is important in determining patient's response to TKI therapy (optimal, warning, or failure). Achievement of MMR is crucial to assess eligibility for TKI continuation. At 12 months, optimal response is defined as ≤0.1 % *BCR-ABL*1 transcript (TKI treatment should be continued), warning as ≤0.1-1% *BCR-ABL*1 transcript level (considering the treatment change), and failure as ≤1 % *BCR-ABL*1 transcript (TKI should be changed) (92-97).

Sanger Sequencing

Sanger sequencing is a molecular method for determining nucleotide sequence in a DNA molecule based on *in vitro* DNA replication, most widely performed to detect the single-nucleotide variants (SNVs) and small indels (98). Sanger (conventional) sequencing has been the golden standard for the detection of SNVs because of the high-level of accuracy (99.99%), longer read length (1000 bp), and cost-effectiveness for a smaller number of samples compared to the next-generation sequencing (NGS) (99). Thus, Sanger sequencing helps discriminate true genetic alterations from errors caused by NGS (99-101). However, below a threshold of 20%, the mosaic allele's detection is not possible.

In Ph^- MPN patients negative for *JAK2* and *CALR* mutations, Sanger sequencing can be used for detection and discrimination of

W515L (type 1, 1544G>T) and W515K (type 2, 1543_1544TG>AA) mutations in MPL gene (exon 10) (102). This method is performed for the sequencing of the *BCR-ABL1* gene and detection of the most common *BCR-ABL*1 kinase domain mutations related to the TKI resistance (like T315I, E255K, E255V, Y253H, Y253F) in Ph^+ CML and ALL patients, and it is less sensitive compared to the ASO-PCR (103). In the MDS and AML subclones, the vast majority of alterations in the DNA sequence are precisely detected at the lower allele fractions, which cannot be reported using Sanger sequencing due to its limitations regarding sensitivity (100, 101).

Next-Generation Sequencing (NGS)

Next-generation sequencing (NGS) allows identifying mutations with variant allele fractions of a minimum of 1% or lower variant allele fractions, leading to discoveries of rare mutations. The detection of rare mutations provides a better understanding of the disease complexity and prognostic relevance. Discoveries of rare variants have also led to the classification of novel subsets of hematologic diseases, enabling new targeted therapies. Furthermore, NGS is used to quantify variant allele fraction, which is of great importance as it was reported that mutational burden is connected to prognosis in clonal hematopoiesis (104-107).

NGS is a fast, massively parallel/deep sequencing technology, with higher error rates (~0.1–15%) and generally shorter read lengths than Sanger sequencing. Two main NGS applications are short-read and long-read sequencing. While short-read sequencing is cheaper, more accurate, and generally used for clinical variant discovery, the long-read approach is more suitable for full-length sequencing isoforms and *de novo* genome assembly applications.

There are two main types of short-read NGS technologies: sequencing by ligation (SBL) and sequencing by synthesis (SBS). SBL approaches use a fluorophore-bound probe sequence that hybridizes to a DNA fragment and ligates to an adjacent oligonucleotide for imaging purposes. The base(s) identity complementary to positions within the probes are identified by the emission spectrum of the fluorophore. SBS approach is polymerase-dependent, and nucleotide incorporation into an elongating strand is detected by special signals (fluorophores or a change in ionic concentration). In most short-read sequencing cases, DNA is clonally amplified on a solid surface, and the signal is distinguished from the background noise by placing identical copies of DNA fragments into a well-defined area. To ensure massive parallelization of the process, millions of individual SBL or SBS reaction centers are formed, each with its clonal DNA template. A sequencing platform collects information from these reaction centers simultaneously, providing parallel sequencing of many millions of DNA molecules. SBS can be further classified into cyclic reversible termination (CRT) and single-nucleotide addition (SNA). CRT method is characterized by the use of terminator molecules, similar to Sanger sequencing. In contrast, the SNA method uses a single signal to detect the dNTP addition to an elongating strand. Long repetitive elements, copy number alterations, and structural variations important for disease onset, development, or prognosis are not captured by short-read paired-end technologies. Long-read technology can provide continuous sequences from 10 kilobases to several megabases directly from native DNA. Long reads help transcriptomic research, as they can capture the entire mRNA transcripts, allowing the identification of precise exon junctions and gene isoforms. There are two main types of long-read technologies: single-molecule real-time sequencing (SMRT) and synthetic approach. The SMRT method does not require chemical cycling for added dNTPs. It does not rely on a clonal population of amplified DNA fragments to generate a detectable signal, in contrast to short-read approaches (108). Synthetic long-read technology relies on existing reads sequenced by short-read technology to construct longer reads in silico using barcodes' power.

Some of the NGS applications are *de novo* sequencing (sequencing and construction of new genome or transcriptome), resequencing, target-

ed resequencing, metagenomics and meta-transcriptomics, DNA- and RNA-protein interactions (ChIP-seq), methylation sequencing, and transcriptome or RNA sequencing (mRNA, miRNA, snRNA). Among many different NGS myeloid panels available, two Illumina sequencing panels (TruSight and AmpliSeq) target the most relevant genes in AML, MPN, MDS, CMML, CML, and JMML (juvenile myelomonocytic leukemia). TruSight Myeloid sequencing panel provides an assessment of 15 full and 39 partial genes (tumor suppressor genes and oncogenic spots). AmpliSeq Myeloid sequencing panel enables analysis of both DNA and RNA in a single assay, with 40 key DNA target genes and 29 RNA fusion driver genes. It allows the detection of SNVs, indels, and gene fusions.

The challenges of NGS in the diagnostics of myeloid malignancies are reviewed by Bacher et al. (90). They reviewed bioinformatics tools to discriminate leukemia-initiating mutations from incidental passenger germline mutations vs. somatic mutations and somatic vs. CHIP mutations. A recent study by Duncavage et al. (2021) tested and streamlined the whole-genome sequencing (WGS) approach (ChromoSeq) for diagnosis and prognosis of AML and MDS patients (109). ChromoSeq provides comprehensive genomic profiling of clinically relevant AML/MDS mutations. Genomic profiling of 263 patients (including 235 that had previously undergone cytogenetic analysis) by WGS detected all 91 copy-number alterations and 40 recurrent translocations previously identified by cytogenetics. Furthermore, it provided new genetic information for 40 out of 235 patients (17%) that had not been detected by conventional cytogenetic analysis. New copy-number alterations were identified in 14 patients with conclusive and in 13 patients either inconclusive or ambiguous cytogenetic results. Additionally, new structural variants were found in 13 patients. By using prospective sequencing of samples from 117 consecutive patients, WGS provided new genetic information for 29 patients (24.8%), and 19 of them (16.2%) were reclassified into risk groups. WGS also allowed stratification of Patients with inconclusive cytogenetic analysis results into risk groups. In conclusion, ChromoSeq provided a greater diagnostic yield and more efficient risk stratification based on standard risk categories, and could potentially be a good replacement for conventional cytogenetic analysis (109).

Molecular Diagnostics of Myeloid Malignancies in Bosnia and Herzegovina

Hematological malignancies have increased significantly in the last 20 years in Bosnia and Herzegovina compared to European data (110, 111). The possible causes of the increase in the number of patients have not yet been clarified. Cytogenetic tools, i.e., karyotyping, have been established in 2005 at the University Clinical Center Tuzla (UKCT), in 2007 at the Clinical Center of the University of Sarajevo (KCUS), and later in University Clinical Center of Republic of Srpska in Banja Luka (UKCBL).

The largest cytogenetic laboratory is in KCUS, Sarajevo, which receives patient samples from all cantons of the Federation of Bosnia and Herzegovina except Tuzla. FISH (hematological and tissue) is only performed in KCUS, with a wide variety of panels for myeloid malignancies, including MDS panel (del5, del/mono 7, trisomy 8), AML (t(15;17), t(8;21), inv(16), MLL, etc.). A molecular test for CML, quantitative *BCR-ABL1*, is performed in Sarajevo and Tuzla, where Sarajevo conducts about 70 samples every three months for current CML patients. Other CML tests include karyotype, FISH, qualitative nested PCR, and the detection of the most common *BCR-ABL1* kinase domain mutations using ASO-PCR. For MPN, *JAK2* is detected by real-time PCR using qualitative and quantitative assays. *CALR* mutations type 1 and type 2 are detected by ASO-PCR. *MPL* mutations are detected by Sanger sequencing. For AML, Invivoscribe can detect *FLT3* mutations on the capillary sequencer and *NPM1* mutations on real-time PCR. The Myeloid panel on NGS is currently in development.

In order to understand the state of diagnostics of myeloid malignancies, we conducted a retro-

spective study on myeloid neoplasms from the Sarajevo Canton in the period from 1995 to 2015. We found 268 patients, including AML N=64), Ph(-) MPN N=102), Ph(+)MPN (CML) N=47), MDS N=51), MDS/MPN N=4) (unpublished data, 111). The unique issue with CML patients in Bosnia and Herzegovina was that many of them had to wait for the start of treatment with tyrosine kinase inhibitors. We have analyzed the effects of delayed treatment in detail previously, are be summarized below. In Bosnia and Herzegovina, TKI therapy has been available since 2005. First frontline TKI therapy was imatinib (Glivec, first-generation TKI); however, due to lack of insurance cover, patients received therapy on a first-come-first-served basis (112). In resource-poor countries like Bosnia and Herzegovina, TKI therapy's availability and monitoring of the disease are limited (113-115). Until 2013, when generic formulations of imatinib were introduced, a certain number of CML patients had to wait for the TKI therapy for an extended period. These patients had worse responses to the therapy, progression or transformation of the disease, and lower survival rate (112). It was shown that generic versions of imatinib in Bosnia and Herzegovina (Anzovip, Meaxin, Plivatinib) are cost-effective, and response to the therapy was similar to the response to Glivec (115-117). In 2011, nilotinib (Tasigna, Novartis, second-generation TKI) became available as front- or second-line therapy, and it was designed to overcome specific *BCR-ABL*1 mutations in imatinib-resistant patients (85, 87, 118-121). Our previous studies showed that nilotinib might be a more potent TKI therapy than imatinib for treating CML patients with a delayed start of therapy (both Glivec and generic alternatives) (112, 116). In addition, several international studies showed the superiority of 2GTKI over 1GTKI in terms of efficacy (72, 120-122). Besides standard TKI therapies, novel therapies for CML have emerged, specifically for T315I-mutated CML. Asciminib is a Specifically Targeting the ABL Myristoyl Pocket (STAMP) inhibitor capable of blocking BCR-ABL1 activity via allosteric binding to the myristoyl residue distinct to the BCR-ABL1 kinase domain (KD) (123). Asciminib blocks both, wild-type and mutated BCR-ABL1 fusion protein, and has potential to overcome resistence to the frontline 1GTKI or 2GTKI (124).

Conclusions

Myeloid malignancies are a heterogeneous group of blood disorders in which myeloid cells show aberrant proliferation, differentiation, and localization. In the last decade, several new discoveries regarding the genetic makeup of these diseases have led to the expansion of molecular genetic and genomic testing needed for diagnosis, prognosis, and therapy. Molecular diagnostics is required for determining the most suitable treatment, such as *FLT3* or IDH inhibitors in AML. It is presumed that myeloid gene panels will soon be incorporated in disease guidelines and will become a routine molecular test needed for patient diagnosis and prognosis.

Conflict of Interest: The authors declare that they have no conflict of interest.

References

1. Murati A, Brecqueville M, Devillier R, Mozziconacci MJ, Gelsi-Boyer V, Birnbaum D. Myeloid malignancies: mutations, models and management. BMC Cancer. 2012;12:304.
2. Zeidner JF, Roy D, Perl A, Gojo I. Myeloid Malignancies. The American Cancer Society's Oncology in Practice: Clinical Management. 1st ed. New Jersey, US: Wiley-Blackwell; 2018. p. 397-421.
3. Arber DA, Orazi A, Hasserjian R, Thiele J, Borowitz MJ, Le Beau MM, et al. The 2016 revision to the World Health Organization classification of myeloid neoplasms and acute leukemia. Blood. 2016;127(20):2391-405.
4. Boissinot M, Vilaine M, Hermouet S. The Hepatocyte Growth Factor (HGF)/Met Axis: A Neglected Target in the Treatment of Chronic Myeloproliferative Neoplasms?. Cancers (Basel). 2014;6(3):1631-69.
5. Choi CW, Bang SM, Jang S, Jung CW, Kim HJ, Kim HY, et al. Guidelines for the management of myeloproliferative neoplasms. Korean J Intern Med. 2015;30(6):771-88.
6. Furtado LV, Betz BL. Diagnostic Molecular Pathology. Cambridge, MA: Academic Press; 2016.
7. Thompson PA, Kantarjian HM, Cortes JE. Diagnosis and Treatment of Chronic Myeloid Leukemia in 2015. Mayo Clin Proc. 2015;90(10):1440-54.

8. Jabbour E, Kantarjian H. Chronic myeloid leukemia: 2018 update on diagnosis, therapy and monitoring. Am J Hematol. 2018;93(3):442-59.
9. Eden RE, Coviello JM. Chronic Myelogenous Leukemia. In: StatPearls. Treasure Island (FL): StatPearls Publishing; 2020.
10. Pasternak G, Hochhaus A, Schultheis B, Hehlmann R. Chronic myelogenous leukemia: molecular and cellular aspects. J Cancer Res Clin Oncol. 1998;124(12):643-60.
11. Baccarani M, Cortes J, Pane F, Niederwieser D, Saglio G, Apperley J, et al. Chronic myeloid leukemia: an update of concepts and management recommendations of European LeukemiaNet. J Clin Oncol. 2009;27(35):6041-51.
12. Baccarani M, Deininger MW, Rosti G, Hochhaus A, Soverini S, Apperley JF, et al. European LeukemiaNet recommendations for the management of chronic myeloid leukemia: 2013. Blood. 2013;122(6):872-84.
13. Baccarani M, Saglio G, Goldman J, Hochhaus A, Simonsson B, Appelbaum F, et al. Evolving concepts in the management of chronic myeloid leukemia: recommendations from an expert panel on behalf of the European LeukemiaNet. Blood. 2006;108(6):1809-20.
14. Khoury HJ, Williams LA, Atallah E, Hehlmann R. Chronic myeloid leukemia: what every practitioner needs to know in 2017. Am Soc Clin Oncol Educ Book. 2017;37:468-79.
15. Pfirrmann M, Baccarani M, Saussele S, Guilhot J, Cervantes F, Ossenkoppele G, et al. Prognosis of long-term survival considering disease-specific death in patients with chronic myeloid leukemia. Leukemia. 2016;30(1):48-56.
16. An X, Tiwari AK, Sun Y, Ding PR, Ashby CR Jr, Chen ZS. BCR-ABL tyrosine kinase inhibitors in the treatment of Philadelphia chromosome positive chronic myeloid leukemia: a review. Leuk Res. 2010;34(10):1255-68.
17. Greenberg PL, Young NS, Gattermann N. Myelodysplastic syndromes. Hematology Am Soc Hematol Educ Program. 2002;136-61.
18. Sperling AS, Gibson CJ, Ebert BL. The genetics of myelodysplastic syndrome: from clonal haematopoiesis to secondary leukaemia. Nat Rev Cancer. 2017;17(1):5-19.
19. Robak T, Wierzbowska A. Current and emerging therapies for acute myeloid leukemia. Clin Ther. 2009;31(2):2349-70.
20. Agarwal A, Bolosky WJ, Wilson DB, Eide CA, Olson SB, Fan G, et al. Differentiation of leukemic blasts is not completely blocked in acute myeloid leukemia. Proc Natl Acad Sci U S A. 2019;116(49):24593-9.
21. Dunphy CH, O'Malley DP, Perkins SL, Chang CC. Analysis of immunohistochemical markers in bone marrow sections to evaluate for myelodysplastic syndromes and acute myeloid leukemias. Appl Immunohistochem Mol Morphol. 2007;15(2):154-9.
22. Leung AYH, Man C, Kwong Y. FLT3 inhibition : a moving and evolving target in acute myeloid leukaemia. Leukemia. 2012;27(2):260-8.
23. Birg BF, Courcoul M, Rosnet O, Bardin F, Pebusque M, Marchetto S, et al. Expression of the FMS/KIT-like gene FLT3 in human acute leukemias of the myeloid and lymphoid lineages. Blood. 1992;80(10):2584-93.
24. Kiyoi H, Naoe T, Yokota S, Nakao M, Minami S, Kuriyama K, et al. Internal tandem duplication of FLT3 associated with leukocytosis in acute promyelocytic leukemia. Leukemia. 1997;11(9):1447-52.
25. Gilliland G, Griffin J. The roles of FLT3 in hematopoiesis and leukemia. Blood. 2002;100(5):1532-42.
26. Small D. Targeting FLT3 for the Treatment of Leukemia. Semin Hematol. 2008;45(2):S17-21.
27. Dohner H, Estey E, Grimwade D, Amadori S, Appelbaum FR, Buchner T, et al. Diagnosis and management of AML in adults: 2017 ELN recommendations from an international expert panel. Blood. 2017;129(4):424-47.
28. Zhang Y, Wang F, Chen X, Zhang Y, Wang M, Liu H, et al. Companion gene mutations and their clinical significance in AML with double mutant CEBPA. Cancer Gene Ther. 2020;27(7-8):599-606.
29. Wouters BJ, Löwenberg B, Erpelinck-Verschueren CA, van Putten WL, Valk PJ, Delwel R. Double CEBPA mutations, but not single CEBPA mutations, define a subgroup of acute myeloid leukemia with a distinctive gene expression profile that is uniquely associated with a favorable outcome. Blood. 2009;113(13):3088-91.
30. Fasan A, Haferlach C, Alpermann T, Jeromin S, Grossmann V, Eder C, et al. The role of different genetic subtypes of CEBPA mutated AML. Leukemia. 2014;28(4):794-803.
31. Borer RA, Nigg EA, Francisco S. Major Nucleolar Proteins Shuttle between Nucleus and Cytoplasm. Cell. 1989;56(3):379-90.
32. Grisendi S, Mecucci C, Falini B, Pandolfi PP. Nucleophosmin and cancer. Nature. 2006;6(7):493-505.
33. Falini B, Mecucci C, Tiacci E, Alcalay M, Rosati R, Pasqualucci L, et al. Cytoplasmic Nucleophosmin in Acute Myelogenous Leukemia with a Normal Karyotype. N Engl J Med. 2005;352(3):254-66.
34. Falini B, Martelli MP, Sportoletti P, Liso A, Tiacci E. Acute myeloid leukemia with mutated nucleophosmin (NPM1): is it a distinct entity? Blood. 2011;117(4):1109-21.
35. Meyer SC, Levine RL. Translational implications of somatic genomics in acute myeloid leukaemia. Lancet Oncol. 2014;15(9):e382-94.
36. Paschka P, Marcucci G, Ruppert AS, Mro K, Chen H, Kittles RA, et al. Adverse Prognostic Significance of KIT Mutations in Adult Acute Myeloid Leukemia With inv(16) and t(8;21): A Cancer and Leukemia Group B Study. J Clin Oncol. 2015;24(24):3904-11.
37. Kindler T, Breitenbuecher F, Marx A, Beck J, Hess G, Weinkauf B, et al. Efficacy and safety of imatinib in adult patients with c-kit – positive acute myeloid leukemia. Blood. 2004;103(10):3644-55.

38. Schubbert S, Shannon K, Bollag G. Hyperactive Ras in developmental disorders and cancer. Nat Rev Cancer. 2007;7(4):295-308.
39. Jurkowska RZ, Jurkowski TP, Jeltsch A. Structure and Function of Mammalian DNA Methyltransferases. ChemBioChem. 2011;12(2):206-22.
40. Nebbioso A, Benedetti R, Conte M, Iside C, Altucci L. Genetic mutations in epigenetic modifiers as therapeutic targets in acute myeloid leukemia. Expert Opin Ther Targets. 2015;19(9):1187-202.
41. Falini B, Sportoletti P, Brunetti L, Martelli MP. Perspectives for therapeutic targeting of gene mutations in acute myeloid leukaemia with normal cytogenetics. Br J Haematol. 2015;170(3):305-22.
42. Nakajima H, Kunimoto H. TET2 as an epigenetic master regulator for normal and malignant hematopoiesis. Cancer Sci. 2014;105(9):1093-9.
43. Marcucci G, Maharry K, Wu Y, Radmacher MD, Mro K, Holland KB, et al. IDH1 and IDH2 Gene Mutations Identify Novel Molecular Subsets Within De Novo Cytogenetically Normal Acute Myeloid Leukemia : A Cancer and Leukemia Group B Study. J Clin Oncol. 2010;28(14):2348-55.
44. Ward PS, Patel J, Wise DR, Abdel-Wahab O, Bennett BD, Coller HA, et al. The Common Feature of Leukemia-Associated IDH1 and IDH2 Mutations Is a Neomorphic Enzyme Activity Converting a -Ketoglutarate to 2-Hydroxyglutarate. Cancer Cell. 2010;17(3):225-34.
45. Gross S, Cairns RA, Minden MD, Driggers EM, Bittinger MA, Jang HG, et al. Cancer-associated metabolite 2-hydroxyglutarate accumulates in acute myelogenous leukemia with isocitrate dehydrogenase 1 and 2 mutations. J Exp Med. 2010;207(2):3-8.
46. Sakamoto KM, Grant S, Saleiro D, Crispino JD, Hijiya N, Giles F, et al. Targeting novel signaling pathways for resistant acute myeloid leukemia. Mol Genet Metab. 2015;114(3):397-402.
47. Muntean AG, Hess JL. The pathogenesis of mixed-lineage leukemia. Annu Rev Pathol. 2012;7:283-301.
48. Dobbins S, Sherborne A, Ma Y, Bardini M, Biondi A, Cazzaniga G, et al. The Silent Mutational Landscape of Infant MLL-AF4 pro-B Acute Lymphoblastic Leukemia. Genes, Chromosom Cancer. 2013;52(10):954-60.
49. Schnittger S, Kinkelin U, Schoch C, Heinecke A, Haase D, Haferlach T, et al. Screening for MLL tandem duplication in 387 unselected patients with AML identify a prognostically unfavorable subset of AML. Leukemia. 2000;14(5):796-804.
50. Tallman MS, Wang ES, Altman JK, Appelbaum FR, Bhatt VR, Bixby D, et al. Acute Myeloid Leukemia, Version 3.2019, NCCN Clinical Practice Guidelines in Oncology. J Natl Compr Canc Netw. 2019;17(6):721-49.
51. Mead AJ, Mullally A. Myeloproliferative neoplasm stem cells. Blood. 2017;129(12):1607-16.
52. Tefferi A, Thiele J, Vardiman JW. The 2008 World Health Organization classification system for myeloproliferative neoplasms: order out of chaos. Cancer. 2009;115(17):3842-7.
53. Bowman RL, Busque L, Levine RL. Clonal Hematopoiesis and Evolution to Hematopoietic Malignancies. Cell Stem Cell. 2018;22(2):157-70.
54. Gibson CJ, Steensma DP. New Insights from Studies of Clonal Hematopoiesis. Clin Cancer Res. 2018;24(19):4633-42.
55. Jaiswal S, Natarajan P, Silver AJ, Gibson CJ, Bick AG, Shvartz E, et al. Clonal Hematopoiesis and Risk of Atherosclerotic Cardiovascular Disease. N Engl J Med. 2017;377(2):111-21.
56. McGowan-Jordan J, Simons A, Schmid M. An International System for Human Cytogenomic Nomenclature (2016). Basel, Switzerland: Karger Publishers; 2016.
57. Klampfl T, Gisslinger H, Harutyunyan AS, Nivarthi H, Rumi E, Milosevic JD, et al. Somatic mutations of calreticulin in myeloproliferative neoplasms. N Engl J Med. 2013;369(25):2379-90.
58. Michalak M, Corbett EF, Mesaeli N, Nakamura K, Opas M. Calreticulin: one protein, one gene, many functions. Biochem J. 1999;344(2):281-92.
59. Nangalia J, Massie CE, Baxter EJ, Nice FL, Gundem G, Wedge DC, et al. Somatic CALR mutations in myeloproliferative neoplasms with nonmutated JAK2. N Engl J Med. 2013;369(25):2391-405.
60. Tefferi A, Wassie EA, Guglielmelli P, Gangat N, Belachew AA, Lasho TL, et al. Type 1 versus Type 2 calreticulin mutations in essential thrombocythemia: a collaborative study of 1027 patients. Am J Hematol. 2014;89(8):E121-4.
61. Visconte V, Tiu RV, Rogers HJ. Pathogenesis of myelodysplastic syndromes: an overview of molecular and non-molecular aspects of the disease. Blood Res. 2014;49(4);216-27.
62. DiNardo CD, Propert KJ, Loren AW, Paietta E, Sun Z, Levine RL, et al. Serum 2-hydroxyglutarate levels predict isocitrate dehydrogenase mutations and clinical outcome in acute myeloid leukemia. Blood. 2013;121(24):4917-24.
63. Figueroa ME, Abdel-Wahab O, Lu C, Ward PS, Patel J, Shih A, et al. Leukemic IDH1 and IDH2 mutations result in a hypermethylation phenotype, disrupt TET2 function, and impair hematopoietic differentiation. Cancer Cell. 2010;18(6):553-67.
64. Kosmider O, Gelsi-Boyer V, Slama L, Dreyfus F, Beyne-Rauzy O, Quesnel B, et al. Mutations of IDH1 and IDH2 genes in early and accelerated phases of myelodysplastic syndromes and MDS/myeloproliferative neoplasms. Leukemia. 2010;24(5):1094-6.
65. Medeiros BC, Fathi AT, DiNardo CD, Pollyea DA, Chan SM, Swords R. Isocitrate dehydrogenase mutations in myeloid malignancies. Leukemia. 2017;31(2):272-81.
66. Mondesir J, Willekens C, Touat M, de Botton S. IDH1 and IDH2 mutations as novel therapeutic targets: current perspectives. J Blood Med. 2016;7:171-80.

67. Patel JP, Gönen M, Figueroa ME, Fernandez H, Sun Z, Racevskis J, et al. Prognostic relevance of integrated genetic profiling in acute myeloid leukemia. N Engl J Med. 2012;366(12):1079-89.
68. Bejar R. Clinical and genetic predictors of prognosis in myelodysplastic syndromes. Haematologica. 2014;99(6);956-64.
69. Wang W, Cortes JE, Tang G, Khoury JD, Wang S, Bueso-Ramos CE, et al. Risk stratification of chromosomal abnormalities in chronic myelogenous leukemia in the era of tyrosine kinase inhibitor therapy. Blood. 2016;127(22):2742-50.
70. Zhang Z, Chen Z, Jiang M, Liu S, Guo Y, Wan L, et al. Heterogeneous BCR-ABL1 signal patterns identified by fluorescence in situ hybridization are associated with leukemic clonal evolution and poorer prognosis in BCR-ABL1 positive leukemia. BMC Cancer. 2019;19(1):935.
71. Hehlmann R, Voskanyan A, Lauseker M, Pfirrmann M, Kalmanti L, Rinaldetti S, et al. High-risk additional chromosomal abnormalities in CML herald death by blast crisis already at low blast levels. Blood. 2019;134(Suppl 1):666.
72. Hochhaus A, Saglio G, Hughes TP, Larson RA, Kim DW, Issaragrisil S, et al. Long-term benefits and risks of frontline nilotinib vs imatinib for chronic myeloid leukemia in chronic phase: 5-year update of the randomized ENESTnd trial. Leukemia. 2016;30(5):1044-54.
73. Hochhaus A, Larson RA, Guilhot F, Radich JP, Branford S, Hughes TP, et al. Long-term outcomes of imatinib treatment for chronic myeloid leukemia. N Engl J Med. 2017;376(10):917-27.
74. Chen Q, Lu P, Jones AV, Cross NC, Silver RT, Wang YL. Amplification refractory mutation system, a highly sensitive and simple polymerase chain reaction assay, for the detection of JAK2 V617F mutation in chronic myeloproliferative disorders. J Mol Diagn. 2007;9(2):272-6.
75. Darawi MN, Ai-Vyrn C, Ramasamy K, Hua PPJ, Pin TM, Kamaruzzaman SB, et al. Allele-specific polymerase chain reaction for the detection of Alzheimer's disease-related single nucleotide polymorphisms. BMC Med Genet. 2013;14:27.
76. Gaudet M, Fara AG, Beritognolo I, Sabatti M. Single Nucleotide Polymorphisms. New York, NY: Humana Press; 2009.
77. Heim M, Meyer UA. Genotyping of poor metabolisers of debrisoquine by allele-specific PCR amplification. Lancet. 1990;336(8714):529-32.
78. Steensma DP. JAK2 V617F in myeloid disorders: molecular diagnostic techniques and their clinical utility: a paper from the 2005 William Beaumont Hospital Symposium on Molecular Pathology. J Mol Diagn. 2006;8(4):397-526.
79. Ugozzoli L, Wallace RB. Allele-specific polymerase chain reaction. Methods. 1991;2(1):42-8.
80. Jeong JH, Lee HT, Seo JY, Seo YH, Kim KH, Kim MJ, et al. Screening PCR Versus Sanger Sequencing: Detection of CALR Mutations in Patients With Thrombocytosis. Ann Lab Med. 2016;36(4):291-9.
81. McLornan D, Percy M, McMullin MF. JAK2 V617F: a single mutation in the myeloproliferative group of disorders. Ulster Med J. 2006;75(2):112-9.
82. Vannucchi AM, Pancrazzi A, Bogani C, Antonioli E, Guglielmelli P. A quantitative assay for JAK2(V617F) mutation in myeloproliferative disorders by ARMS-PCR and capillary electrophoresis. Leukemia. 2006;20(6):1055-60.
83. Jones AV, Kreil S, Zoi K, Waghorn K, Curtis C, Zhang L, et al. Widespread occurrence of the JAK2 V617F mutation in chronic myeloproliferative disorders. Blood. 2005;106(6):2162-8.
84. Kang HY, Hwang JY, Kim SH, Goh HG, Kim M, Kim DW. Comparison of allele specific oligonucleotide-polymerase chain reaction and direct sequencing for high throughput screening of ABL kinase domain mutations in chronic myeloid leukemia resistant to imatinib. Haematologica. 2006;91(5):659-62.
85. Branford S, Rudzki Z, Walsh S, Parkinson I, Grigg A, Szer J, et al. Detection of BCR-ABL mutations in patients with CML treated with imatinib is virtually always accompanied by clinical resistance, and mutations in the ATP phosphate-binding loop (P-loop) are associated with a poor prognosis. Blood. 2003;102(1):276-83.
86. Parker WT, Yeoman AL, Jamison BA, Yeung DT, Scott HS, Hughes TP, et al. BCR-ABL1 kinase domain mutations may persist at very low levels for many years and lead to subsequent TKI resistance. Br J Cancer. 2013;109(6):1593-8.
87. Soverini S, Abruzzese E, Bocchia M, Bonifacio M, Galimberti S, Gozzini A, et al. Next-generation sequencing for BCR-ABL1 kinase domain mutation testing in patients with chronic myeloid leukemia: a position paper. J Hematol Oncol. 2019;12(1):131.
88. Berenstein R, Blau IW, Kar A, Cay R, Sindram A, Seide C, et al. Comparative examination of various PCR-based methods for DNMT3A and IDH1/2 mutations identification in acute myeloid leukemia. J Exp Clin Cancer Res. 2014;33(1):44.
89. Levine RL, Valk PJM. Next-generation sequencing in the diagnosis and minimal residual disease assessment of acute myeloid leukemia. Haematologica. 2019;104(5):868-71.
90. Bacher U, Shumilov E, Flach J, Porret N, Joncourt R, Wiedemann G, et al. Challenges in the introduction of next-generation sequencing (NGS) for diagnostics of myeloid malignancies into clinical routine use. Blood Cancer J. 2018;8(11):113.
91. Baccarani M, Castagnetti F, Gugliotta G, Rosti G, Soverini S, Albeer A, et al. The proportion of different BCR-ABL1 transcript types in chronic myeloid leukemia. An international overview. Leukemia. 2019;33(5):1173-83.

92. Branford S, Fletcher L, Cross NC, Müller MC, Hochhaus A, Kim DW, et al. Desirable performance characteristics for BCRABL measurement on an international reporting scale to allow consistent interpretation of individual patient response and comparison of response rates between clinical trials. Blood. 2008;112(8):3330-8.
93. Cross NC, White HE, Müller MC, Saglio G, Hochhaus A. Standardized definitions of molecular response in chronic myeloid leukemia. Leukemia. 2012;26(10):2172-5.
94. Cross NC, White HE, Colomer D, Ehrencrona H, Foroni L, Gottardi E, et al. Laboratory recommendations for scoring deep molecular responses following treatment for chronic myeloid leukemia. Leukemia. 2015;29(5):999-1003.
95. Guilhot J, Preudhomme C, Mahon FX, Guilhot F. Analyzing molecular response in chronic myeloid leukemia clinical trials: pitfalls and golden rules. Cancer. 2015;121(4):490-7.
96. Hochhaus A, Baccarani M, Silver RT, Schiffer C, Apperley JF, Cervantes F, et al. European LeukemiaNet 2020 recommendations for treating chronic myeloid leukemia. Leukemia. 2020;34(4):966-84.
97. Lauseker M, Hanfstein B, Haferlach C, Schnittger S, Pfirrmann M, Fabarius A, et al. Equivalence of BCR-ABL transcript levels with complete cytogenetic remission in patients with chronic myeloid leukemia in chronic phase. J Cancer Res Clin Oncol. 2014;140(11):1965-9.
98. Heather JM, Chain B. The sequence of sequencers: The history of sequencing DNA. Genomics. 2016;107(1):1-8.
99. Chan EY. Next-generation sequencing methods: impact of sequencing accuracy on SNP discovery. Methods Mol Biol. 2009;578:95-111.
100. Albitar F, Wanlong M, Diep K, De Dios I, Agersborg S, Thangavelu M, et al. Deep Sequencing of Cell-Free Peripheral Blood DNA as a Reliable Method for Confirming the Diagnosis of Myelodysplastic Syndrome. Genet Test Mol Biomarkers. 2016;20(7):341-5.
101. Dewey FE, Pan S, Wheeler MT, Quake SR, Ashley EA. DNA sequencing: clinical applications of new DNA sequencing technologies. Circulation. 2012;125(7):931-44.
102. Kurtovic-Kozaric A, Islamagic E, Komic H, Bilalovic N, Eminovic I, Burekovic A, et al. The effects of mutational profiles on phenotypic presentation of myeloproliferative neoplasm subtypes in Bosnia: 18 year follow-up. Bosn J Basic Med Sci. 2020;20(2):236-47.
103. Kang HY, Hwang JY, Kim SH, Goh HG, Kim M, Kim DW. Comparison of allele specific oligonucleotide-polymerase chain reaction and direct sequencing for high throughput screening of ABL kinase domain mutations in chronic myeloid leukemia resistant to imatinib. Haematologica. 2006;91(5):659-62.
104. Genovese G, Kähler AK, Handsaker RE, Lindberg J, Rose SA, Bakhoum SF, et al. Clonal hematopoiesis and blood-cancer risk inferred from blood DNA sequence. N Engl J Med. 2014;371(26):2477-87.
105. Jaiswal S, Fontanillas P, Flannick J, Manning A, Grauman PV, Mar BG, et al. Age-related clonal hematopoiesis associated with adverse outcomes. N Engl J Med. 2014;371(26):2488-98.
106. McKerrell T, Park N, Moreno T, Grove CS, Ponstingl H, Stephens J, et al. Leukemia-associated somatic mutations drive distinct patterns of age-related clonal hemopoiesis. Cell Rep. 2015;10(8):1239-45.
107. Zink F, Stacey SN, Norddahl GL, Frigge ML, Magnusson OT, Jonsdottir I, et al. Clonal hematopoiesis, with and without candidate driver mutations, is common in the elderly. Blood. 2017;130(6):742-52.
108. Logsdon GA, Vollger MR, Eichler EE. Long-read human genome sequencing and its applications. Nat Rev Genet. 2020;21(10):597-614.
109. Duncavage EJ, Schroeder MC, O'Laughlin M, Wilson R, MacMillan S, Bohannon A, et al. Genome Sequencing as an Alternative to Cytogenetic Analysis in Myeloid Cancers. N Engl J Med. 2021;384(10):924-35
110. Vila M, Suljovic E, Bijedic ZMV, Jamakovic M. Epidemiological analysis of leukemias in the period from 1992 to 2010 at the Hematology Clinic, Clinical Center of the University of Sarajevo. In: 1st Congress of Hematologists and Transfusiologists of Bosnia and Herzegovina; 2011 May 19-22; Association of Hematologists and Transfusiologists of Bosnia and Herzegovina; 2002. p. 46.
111. Mehinovic-Cavcic L. Molecular characterization of patients with myeloid neoplasms from the Sarajevo Canton: twenty-year follow-up [dissertation]. Sarajevo: University of Sarajevo, Faculty of Science; 2021.
112. Kurtovic-Kozaric A, Hasic A, Radich JP, Bijedic V, Nefic H, Eminovic I, et al. The reality of cancer treatment in a developing country: the effects of delayed TKI treatment on survival, cytogenetic and molecular responses in chronic myeloid leukemia patients. Br J Hematol. 2016;172(3):420-7.
113. Kurtovic-Kozaric A, Vranic S, Kurtovic S, Hasic A, Kozaric M, Granov N, et al. Lack of Access to Targeted Cancer Treatment Modalities in the Developing World in the Era of Precision Medicine: Real-Life Lessons From Bosnia. J Glob Oncol. 2018;4:1-5.
114. Malhotra H, Radich J, Garcia-Gonzalez P. Meeting the needs of CML patients in resource-poor countries. Hematol Am Soc Hematol Educ Program. 2019;2019(1):433-42.
115. Kurtovic-Kozaric A, Islamagic E, Radich JP, Hadzimesic ES, Hasic A, Kurtovic S. The Comparison of Efficacy Between Generic and Branded Imatinib in Achievement of Overall Survival and Cytogenetic Responses in CML Patients in Bosnia and Herzegovina. Blood. 2016;128(22):5451.
116. Islamagic E, Hasic A, Kurtovic S, Hadzimesic ES, Mehinovic L, Kozaric M, et al. The efficacy of generic imatinib as first- and second-line therapy: three year follow-up of

chronic myeloid leukemia patients. Clin Lymphoma Myeloma Leuk. 2017;17(4):238-40.

117. Islamagic E, Kurtovic S, Kozaric M, Hadzimesic ES, Hasic A, Mehinovic L, et al. The Three Year Follow-up of CML Patients Treated with First-line Generic and First-line Branded Imatinib in Bosnia and Herzegovina. UHOD. 2017;27(1):8-12.
118. Wang J, Shen ZX, Saglio G, Jin J, Huang H, Hu Y, et al. Phase 3 study of nilotinib vs imatinib in Chinese patients with newly diagnosed chronic myeloid leukemia in chronic phase: ENESTchina. Blood. 2015;125(18):2771-8.
119. Hochhaus A, Rosti G, Cross NC, Steegmann JL, le Coutre P, Ossenkoppele G, et al. Frontline nilotinib in patients with chronic myeloid leukemia in chronic phase: results from the European ENEST1st study. Leukemia. 2016;30(1):57-64.
120. Cortes JE, Kim DW, Kantarjian HM, Brümmendorf TH, Dyagil I, Griskevicius L, et al. Bosutinib versus imatinib in newly diagnosed chronic-phase chronic myeloid leukemia: results from the BELA trial. J Clin Oncol. 2012;30(28):3486-92.
121. Radich JP, Kopecky KJ, Appelbaum FR, Kamel-Reid S, Stock W, Malnassy G, et al. A randomized trial of dasatinib 100 mg versus imatinib 400 mg in newly diagnosed chronic-phase chronic myeloid leukemia. Blood. 2012;120(19):3898-905.
122. Islamagic E, Hasic A, Kurtovic S, Suljevic D, Kozaric M, Eminovic I, et al. Clinical Outcomes of CML Patients After Delayed Start of Nilotinib Treatment. UHOD. 2021;31(1):19-27.
123. Westerweel PE, Te Boekhorst PAW, Levin MD, Cornelissen JJ. New Approaches and Treatment Combinations for the Management of Chronic Myeloid Leukemia. Front Oncol. 2019;9:665.
124. Hughes TP, Mauro MJ, Cortes JE, Minami H, Rea D, DeAngelo DJ, et al. Asciminib in Chronic Myeloid Leukemia after ABL Kinase Inhibitor Failure. N Engl J Med. 2019;381(24):2315-26.

Narrative Review
Acta Medica Academica 2021;50(1):197-208
DOI: 10.5644/ama2006-124.335

Update on Diagnosing and Reporting Malignant Pleural Mesothelioma

Ivana Savic[1], Jeffrey Myers[2]

[1]Institute of Pathology, Faculty of Medicine, University of Belgrade, Serbia, [2]Department of Pathology, University of Michigan, Ann Arbor, Michigan, United States

Correspondence: *ivanasavic86@yahoo.com*; Tel.: + 381 11 364 33 409

Received: 6 March 2021; **Accepted:** 4 April 2021

Abstract
In this review, we summarize current approaches to diagnosis of malignant pleural mesothelioma, focusing on the distinction from benign mesothelial proliferations and other malignant tumors. Current recommendations for reporting histological subtype and tumor grade are also reviewed. Particular emphasis is placed on immunohistochemical and molecular tools that may help in establishing the diagnosis of mesothelioma with greater confidence. Immunohistochemical stains for BRCA1-associated protein (BAP1) and methylthioadenosine phosphorylase (MTAP) and homozygous deletion of *p16* using fluorescence in situ hybridization (FISH) are emphasized as important methods for distinguishing benign from malignant mesothelial proliferations. **Conclusions.** Diffuse malignant pleural mesothelioma is a heterogeneous group of aggressive pleural tumors for which histological classification plays an increasingly important role in patient management. Stage and resectability remain key drivers of therapeutic strategies and outcomes. There is an increasingly robust suite of diagnostic tools, including immunohistochemical stains for BAP1 and MTAP and *p16* FISH, for differentiating benign from malignant mesothelial proliferations in cytology and tissue specimens.

Key Words: Malignant Pleural Mesothelioma ▪ Diagnostics ▪ Immunohistochemistry ▪ Fluorescence in Situ Hybridization.

Introduction

Malignant mesothelioma originates from mesothelial cells that line serosal surfaces (*i.e.*, pleura, pericardium, peritoneum, tunica vaginalis). Pleura is the most frequently affected site, accounting for 70% to 80% of incident cases. Malignant pleural mesothelioma (MPM) is the most frequent primary malignant tumor of the pleura, and is characterized by aggressive behavior with mean survivals of 9 to 12 months.

Incidence and mortality from MPM is highly variable from one geographic region to the next, and is heavily influenced by the prevalence of mining and commercial applications of asbestos and the long latency periods between exposure and disease onset. In addition to occupational or household asbestos exposure, thoracic radiation in patients with breast carcinoma or Hodgkin lymphoma has been identified as another environmental risk factor for MPM.

Mesothelioma most commonly affects individuals 60 years of age or older, with a male predominance. MPM is very rare in the pediatric population, with fewer than 300 cases reported in children. MPM commonly presents as an otherwise unexplained persistent pleural effusion. Features that tend to favor malignant over benign pleural disease include chest wall pain, hemorrhagic effusion, circumferential pleural thickening that includes involvement of mediastinal pleura, and nodular pleural thickening on computed tomography (CT) scans of the chest (1).

Malignant mesothelioma is a locally aggressive tumor that infiltrates the chest wall and lung parenchyma. Distant metastases are common in late stage disease. Autopsy studies demonstrate extrapleural metastases in almost 90% of individuals (2). Nodal

metastases are a rare presenting manifestation of MPM and must be distinguished from benign nodal inclusions of mesothelial cells in patients with benign pleural or pericardial effusions (3).

The aim of this review article was to summarize the current approaches to diagnosis of malignant pleural mesothelioma, with a particular emphasis on its distinction from benign mesothelial proliferations and other malignant tumors using immunohistochemistry and molecular analyses.

Cytology

Cytological examination of pleural fluid is often the first, and sometimes the only, opportunity to identify patients with mesothelioma. Cytologic diagnosis alone is more limited than tissue biopsies in being able to establish specific histological subtypes or tumor grade, which may not significantly influence stage-dependent clinical management or prognosis for some patients. The sensitivity of cytology for MPM ranges from 30% to 75%, meaning that a negative cytology does not exclude the diagnosis (4). Liquid based processing and/or cell blocks can improve diagnostic performance (5). The International Mesothelioma Interest Group clusters cytology results from patients with MPM into three categories: 1. Malignant based on cytomorphological criteria, 2. Malignant on the basis of supportive ancillary studies, and 3. Nondiagnostic (6). Cytological features of MPM include hypercellularity of specimen, presence of tissue fragments, enlarged mesothelial cells with enlarged nuclei resulting in high nuclear:cytoplasmic ratios, macronucleoli, papillary three dimensional spheres, and acidophilic extracellular matrix. A "cell in a cell" phenomenon and membrane protrusions or blebs have also been described. Malignant epithelioid mesothelial cells share some cytologic features with reactive, non-neoplastic mesothelial cells such as scalloped borders of cell groups and presence of intercellular windows exhibiting lighter, dense cytoplasm edges. Effusion specimens characterized by cytologically malignant cells often require immunohistochemical studies to confirm mesothelial origin (see Table 1). Ancillary studies, such as immunohistochemistry for BRCA1-associated protein (BAP1) and methylthioadenosine phosphorylase (MTAP), and *p16* fluorescence in situ hybridization (FISH), are often required to establish a cytological diagnosis of MPM with greater confidence, and can substantially improve diagnostic sensitivity.

Histology

The 2015 WHO classification of pleural tumors divides diffuse malignant mesothelioma into three main histological subtypes: Epithelioid (60%-80%), sarcomatoid (<10%), and biphasic (10%-15%). The relative frequency is higher for biphasic subtypes and lower for sarcomatoid subtypes in surgical specimens compared to pre-resection biopsies, indicating the importance of sampling in accurate classification of malignant pleural tumors (7). It is important to distinguish between these subtypes because of stage-dependent differences in therapeutic strategies and differences in average lengths of survival. Retrospective cohorts drawn from large multi-institutional data sets consistently show the longest overall survivals in patients with epithelioid histology, the shortest survivals in those with sarcomatoid MPM, and intermediate survival in patients with biphasic MPM (8). Truly localized mesotheliomas are extremely rare, show the same range of histologic subtypes, and are affiliated with better survivals given the possibility of complete surgical excision (9).

Epithelioid Mesothelioma

Epithelioid mesothelioma, the most common form of MPM, usually comprises mildly atypical low columnar to cuboidal cells resembling reactive mesothelial cells arranged in a variety of growth patterns including most commonly a tubulopapillary architecture (Figure 1). A recent proposal from a large international multidisciplinary group suggested subclassifying epithelioid mesothelioma by specific architectural patterns and, in some variants, unique cytological features (10). The most common architectural patterns include tubu-

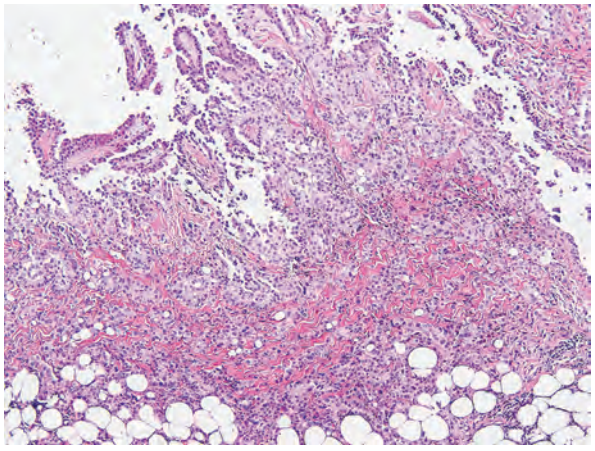

Figure 1. Epithelioid mesothelioma. Low magnification photomicrograph showing tubulopapillary mesothelioma composed of relatively bland non-mucinous cuboidal cells forming a combination of tubules (left center), papillae (upper left) and small irregularly shaped solid groups and cords (hematoxylin and eosin stain; original magnification 40×.

lopapillary, solid, and trabecular, while micropapillary, adenomatoid (microcystic), clear cell, transitional, deciduoid, small cell, and lymphohistiocytic variants are relatively rare. *Pleomorphic* subtypes are defined as epithelioid mesotheliomas in which more than 10% of tumor cells show marked nuclear pleomorphism; this subtype is associated with the worst overall survival (8.1 months) among epithelioid MPM (11). The international proposal includes recommendations for reporting percentages of the various architectural patterns and cell types for extrapleural pneumonectomy and extended pleurectomy/decortication surgical specimens, a reporting practice for which there is no evidence regarding its value and therefore not widely adopted outside of a research setting.

Grading of Epithelioid Mesothelioma

Histological subtype and TNM stage drive therapeutic strategies in patients with MPM. Several retrospective case series have demonstrated limited utility of histologic grading for epithelioid mesotheliomas, usually based on some combination of nuclear grade, mitotic rate, and necrosis. Grading of MPM has not yet been adopted in routine practice and is not included in current cancer reporting templates from the College of American Pathologists. In their previously referenced proposal, an international multidisciplinary group recommended a two-tier system of grading based on nuclear grade and necrosis. In this proposed system, low-grade MPM comprises nuclear grade 1 with or without necrosis and nuclear grade 2 without necrosis; high-grade is reserved for tumors with nuclear grade 2 and necrosis or nuclear grade 3 with or without necrosis (10). In making a recommendation for a practice not yet widely adopted the authors suggest that tumor grading may be of benefit in stratifying patients for clinical trials or adding greater precision to the risk stratification currently provided by histological subtyping. While this may eventually emerge as a standard reporting element, in our view it should be optional for pathology reporting given the absence of compelling evidence regarding its value outside of a research setting. It also should be emphasized that this proposed grading system was recommended only for epithelioid mesothelioma; other types of MM (sarcomatoid MM, and sarcomatoid parts in biphasic MM) are inherently more aggressive and therefore high grade by definition.

Sarcomatoid Mesothelioma

Sarcomatoid mesothelioma is less frequent but more aggressive than epithelioid mesothelioma, with mean survivals of 3.5-8 months (12). Differentiating between epithelioid and sarcomatoid MM is important because of stage-dependent differences in treatment approach (13). Sarcomatoid mesothelioma is characterized by neoplastic spindle cells exhibiting variable numbers of mitoses and degrees of cytologic atypia (Figure 2). The cells are typically arranged in vaguely fascicular growth patterns thus resembling soft tissue sarcomas ("sarcomatoid"). Histological subtypes of sarcomatoid MPM include conventional (44%), desmoplastic (34%), sarcomatoid with desmoplastic areas (21%), sarcomatoid with heterologous elements (1%), and lymphohistocytoid mesotheliomas (<1%) (14).

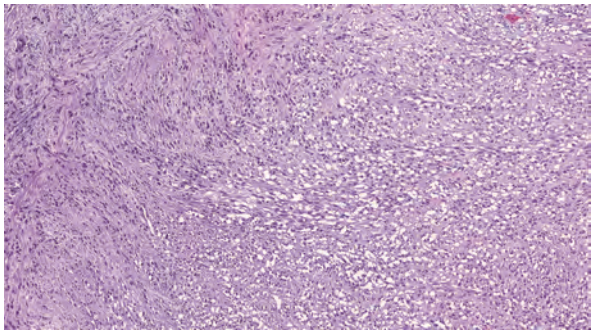

Figure 2. Sarcomatoid mesothelioma. Intermediate magnification photomicrograph showing neoplastic spindles cells arranged in a loosely organized fascicular growth pattern with invasion into chest wall soft tissue at upper left (hematoxylin and eosin stain; original magnification 132×).

Desmoplastic mesothelioma is a common subtype and is the most challenging to distinguish from benign fibrosing pleuritis, sometimes referred to as fibrous pleurisy. Desmoplastic MPM is paucicellular, with random variation in cellularity across a relatively narrow range. The areas showing an abrupt increase in cellularity comprise mildly atypical spindle cells with enlarged hyperchromatic nuclei arranged in a "patternless pattern of Stout" with abundant collagenous stroma (Figure 3). Keys to diagnosis are a combination of this distinctive storiform histology, invasion of chest wall soft tissue and/or lung parenchyma, bland necrosis characterized by dropout of basophilic nuclei, focal areas with frankly malignant sarcomatoid histology, and/or distant metastases (15). Immunohistochemical stains for cytokeratins are of limited value since non-neoplastic reactive spindled mesothelial cells are also positive, but can be helpful in identifying areas of chest wall invasion (16).

Transitional mesothelioma, traditionally considered a rare architectural and cytological subtype of epithelioid MPM, comprises cohesive plump spindle cells with elongated ambiguous cytomorphology. Recent studies indicate that transitional mesothelioma is genetically more closely related to sarcomatoid MPM, and recommend that it be considered a subgroup of sarcomatoid mesothelioma (17, 18).

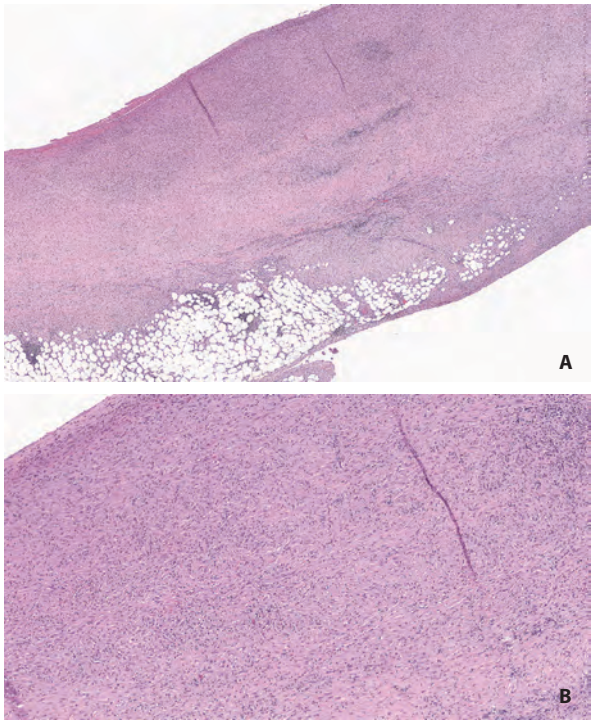

Figure 3. Desmoplastic mesothelioma. A) Low magnification photomicrograph showing thickened parietal pleura with random variation in cellularity and invasion of chest wall fat (hematoxylin and eosin stain; original magnification 27×). B) Intermediate magnification photomicrograph showing more cellular zone in which neoplastic spindle cells are arranged in the vaguely storiform "patternless pattern of Stout" (hematoxylin and eosin stain; original magnification 100×).

Biphasic Mesothelioma

Biphasic mesothelioma is defined as showing a combination of epithelioid and sarcomatoid histologies, with each component comprising more than 10% of the tumor (Figure 4). A sarcomatoid component of less than 80% in biphasic MM has been linked to improved survival. Interobserver agreement in diagnosis of biphasic mesothelioma is moderate (Kappa = 0.45), suggesting that updating the definition of biphasic MPM is needed to support more consistent risk stratification (19). Although fibrous stroma in epithelioid MPM is typically scant, it is sometimes florid and thus can mimic biphasic MPM. Cases in which it is uncertain whether the sarcomatoid component represents a benign florid stromal reaction or a prolif-

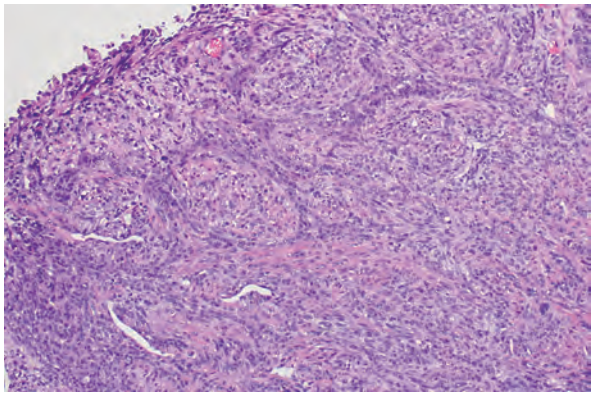

Figure 4. Biphasic mesothelioma. Photomicrograph showing a glandular epithelial component and a less differentiated stromal component comprising spindle cells (hematoxylin and eosin stain; original magnification 100×).

eration of neoplastic mesothelial cells may be resolved by demonstrating homozygous deletion of *p16* using a FISH technique (20).

Immunohistochemical Stains for Diagnosis

Histopathological diagnosis of MPM begins with careful examination of routinely stained sections in an appropriate clinical and radiological context. Immunohistochemical stains can be extremely helpful in distinguishing MPM from other malignancies capable of diffuse pleural involvement that may mimic mesothelioma ("pseudomesotheliomatous"), and in separating MPM from benign mesothelial proliferations. Pancytokeratin stains may be useful in separating MPM from other non-epithelial mimics, such as metastatic melanoma or diffuse high-grade lymphomas confined to the pleura and pleural space. They should be interpreted with caution, given that reactive spindle cells of mesothelial origin are also keratin and calretinin positive (Figure 5). A small minority of sarcomatoid MPM may be keratin negative. Epithelioid MPM is typically positive for cytokeratin 7 as are many of the entities frequently considered in the differential diagnosis, which may limit its utility. Epithelioid MPMs are also frequently positive for high molecular weight cytokeratins using antibodies directed against cytokeratins 5 and 6; staining for high molecular cytokeratins is less common in sarcomatoid types (21).

It is important to first establish a working diagnosis based on routinely stained sections and knowledge of the clinical and radiological findings before deciding on immunohistochemical stains likely to be of value. Choice of immunohistochemical markers to distinguish MPM from other entities with epithelioid phenotypes depends heavily on the histologic subtype being considered (epithelioid or sarcomatoid), location of the neoplasm (pleura or peritoneum), and the types of tumors included in the differential diagnosis (e.g., squamous cell carcinoma, adenocarcinoma, epithelioid hemangioendothelioma, melanoma). Given that none of the markers have 100% specificity, a limited panel that includes antibodies with sensitivity or specificity of at least 80% is recommended (22). An immunohistochemical panel should contain at least two mesothelial markers and two markers appropriate to the working diagnoses established on the basis of routinely stained sections and any pertinent history including previously diagnosed malignancies. For confirmation of mesothelial origin in patients suspected of having epithelioid or biphasic MPM, calretinin, WT-1 (nuclear staining only), cytokeratin 5/6, and D2-40 (podoplanin) are useful markers (23). Markers useful for tumors in which metastatic carcinoma is a diagnostic possibility include MOC31, BG8, CEA, claudin 4, and BerEP4. MOC31 and BerEP4 target the same transmembrane glycoprotein (EpCAM), and therefore the final choice of markers should include one, rather than both of them. In addition to two general carcinoma markers, immunostains that are specific for certain carcinoma subtypes may be helpful. This is dependent not only on the histologic findings but also on relevant clinical and radiological information (*i.e.*, previous malignancies or suspicion of other primary sites at presentation). In patients suspected of having metastatic adenocarcinoma for which no primary is known, TTF-1 may be helpful since lung is the most frequent source for metastatic adenocarcinomas with a pseudomesotheliomatous growth pattern (24). Major differential diagnoses and immunohistochemical markers useful for differentiating MPM from other malignant neoplasms are summarized

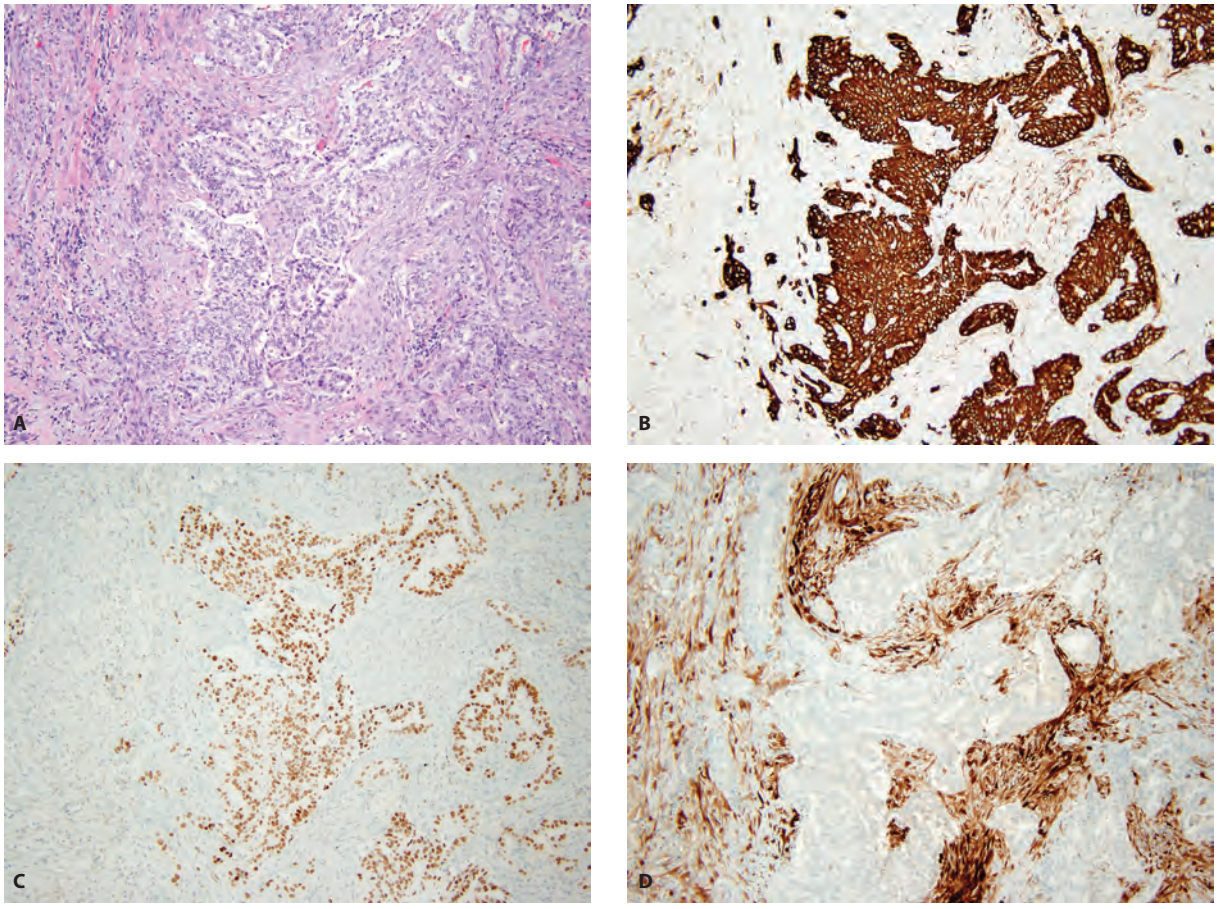

Figure 5. Metastatic adenocarcinoma of the lung. A) Photomicrograph showing glandular neoplasm infiltrating the parietal pleura with a variably cellular stromal response resembling biphasic MPM (hematoxylin and eosin stain; original magnification 100x). B-D) Photomicrographs showing immunostains performed on this pleural biopsy. Both the metastatic adenocarcinoma and the stromal cells, which include non-neoplastic spindle cells of mesothelial origin, are positive for cytokeratin 7 (B). Staining for TTF-1 (C) is limited to the adenocarcinoma, and calretinin (D) to non-neoplastic mesothelial cells (original magnification 100×).

in the Table 1. Immunohistochemistry for BAP1 is used primarily to separate benign from malignant mesothelial proliferations (see following section, Separating malignant from benign mesothelial proliferations), but can also be helpful in selected circumstances for distinguishing MPM from carcinomas in malignant pleural effusion cytology specimens, with high sensitivity (87%) and specificity (98%) (25).

Immunohistochemistry for sarcomatoid MPM often begins with cytokeratin stains to establish an epithelioid phenotype and exclude soft tissue sarcomas. In a large retrospective case series of over 300 cases, 93% of sarcomatoid mesotheliomas expressed cytokeratins; sensitivity increased with use of an antibody cocktail (*e.g.*, AE1/AE3 ± CAM5.2), more extensive tumor sampling, and adequate tissue fixation (14). Keratin staining may be negative in the osteosarcomatous or chondrosarcomatous components of sarcomatoid MPM with heterologous elements (22). Immunohistochemical markers are less useful for distinguishing sarcomatoid MPM from sarcomatoid carcinomas. Calretinin is negative in >50% of sarcomatoid mesotheliomas, as is nuclear staining for WT-1 (21). Strong diffuse staining for GATA-3 is nearly universal in sarcomatoid MPM and, along with radiological distribution of disease (*i.e.*, localized versus diffuse),

Table 1. Immunohistochemical Stains Useful for Separating MPM from Malignant Mimics

Histologic MPM type	Mesothelial markers	Markers more commonly expressed in non-mesothelial neoplasms
Epithelioid	CK AE1/3 +, calretinin +, WT-1 +, CK5/6 +, mesothelin +, D2-40 +	Lung adenocarcinoma (TTF-1 +, napsin A +)
		Adenocarcinoma, NOS (CEA+, claudin 4+, MOC31/Ber-EP4+, BG8+)
		Squamous cell lung carcinoma (p40 + MOC-31/Ber-EP4+)
		Renal cell carcinoma (PAX8 +, CAIX +)
		Breast carcinoma (ER +, PR+, GCDFP-15+, mammaglobin +, GATA3 +)
		Epithelioid hemangioendothelioma (CD31 +, CD34 +, FLI-1 +, ERG +)
Sarcomatoid	CK AE1/3 +, CAM5.2 +, D2-40 +, calretinin +, WT-1 +, GATA3 +	Sarcomatoid carcinoma (CK AE1/3 + CAM 5.2 +, GATA3 -).
		Angiosarcoma (CD31 +, CD34 +, ERG +)
		Synovial sarcoma (CD99 +, TLE-1 +)

MPM=Malignant pleural mesothelioma.

can be especially helpful for this frequently challenging differential diagnosis (26).

Separating Malignant from Benign Mesothelial Proliferations

There are a number of histological features helpful in separating MPM from benign mesothelial proliferations. Invasion of chest wall soft tissues and/or pulmonary parenchyma is the single most helpful finding in establishing a diagnosis of MPM (Figure 6) (1, 16). Cytokeratin stains may be helpful in demonstrating invasion not otherwise easily observed with routinely stained sections alone. Reactive mesothelial cells do not invade the surrounding tissues, but "pseudo invasion" may occur when benign mesothelial cells are entrapped in the fibrosis characteristic of fibrosing pleuritis resulting in a distinctive pattern of layering resembling the annual growth rings in trees (Figure 7). Inflammation of the pleura with associated mesothelial hyperplasia tends to have a predictably zonal distribution of cellularity in which the cellularity is greatest adjacent to the pleural space and gradually or abruptly diminishes as it approaches the chest wall interface. Benign mesothelial proliferations may include papillary structures but they lack the complex stratification characteristic of MPM and instead comprise simple, non-arborizing structures lined by a single layer of cells. In addition, reactive proliferations often are accompanied by surface fibrin and granulation tissue in which capillary sized vascular spaces are arranged in parallel perpendicular to the pleural surface.

Loss of BAP1 expression and homozygous deletion of *p16* have become diagnostic methods for separating benign from malignant mesothelial proliferations with greater frequency and accuracy, thus increasing diagnostic sensitivity for MM. A growing number of studies attest to their practical value in the diagnostic process (27).

BAP1 is a cellular enzyme with tumor suppressor functions. It is involved in cycle-cell progression, repairing ionizing radiation-induced DNA damage, regulation of gene expression and chromatin remodeling. Early studies showed lack of BAP1 immunoreactivity due to somatic *BAP1* genetic alterations, such as deletions or point mutations, in more than 40% of MPMs (28). More recent studies show loss of BAP1 expression in nearly 75% of epi-

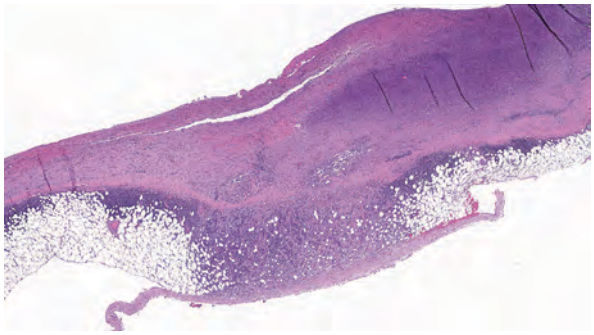

Figure 6. Epithelioid mesothelioma with chest wall invasion (hematoxylin and eosin stain; original magnification 19×).

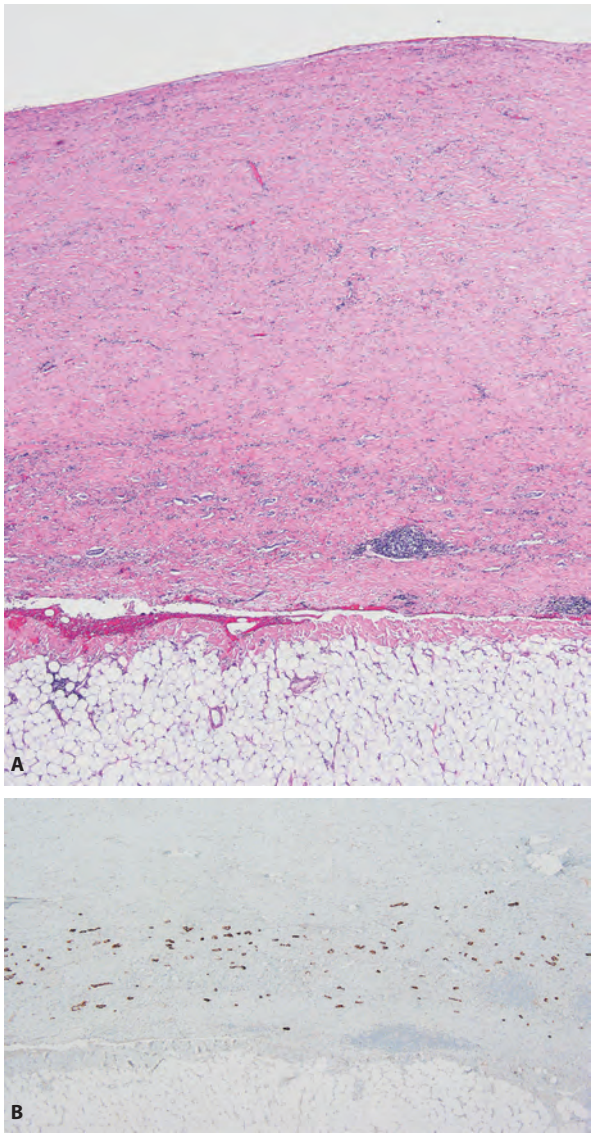

Figure 7. Fibrosing pleuritis ("fibrous pleurisy") with layering of entrapped mesothelial cells. A) Low magnification photomicrograph showing fibrous thickening of parietal pleura and a sharp interface with chest wall adipose tissue. Entrapped mesothelial cells are arranged in a linear fashion in the lower third without the random variation in cellularity and invasive growth patterns more characteristic of mesothelioma (hematoxylin and eosin stain; original magnification 20×). B) Photomicrograph of immunohistochemical stain for cytokeratins (AE1/AE3 and CAM5.2 cocktail) showing the layering of entrapped mesothelial cells and the absence of chest wall invasion (original magnification 40×).

thelioid MPM with lower sensitivities on the order of 50% for biphasic and 10% or less for sarcomatoid MPM. Loss of BAP1 expression has been associated with younger age at onset and improved median survival in MPM, although BAP1 expression as a prognostic biomarker remains controversial (29). Loss of BAP1 expression is manifested as complete, and rarely partial, loss of nuclear staining in tumor cells with positive staining of internal controls (*i.e.*, inflammatory cells and stromal cells) (Figure 8). *BAP1* loss occurs in both sporadic and familial MPM, the latter linked to germline *BAP1* mutations (30, 31). BAP1 loss has consistently shown 100% specificity for distinguishing malignant from benign mesothelial proliferations; benign reactive mesothelial proliferations always retain nuclear BAP1 expression. BAP1 expression is also retained in adenomatoid tumors, a lesion that only rarely occurs in the chest although adenomatoid tumor-like histology has been well described in MPM (32). In a comparison of two retrospective cohorts, Erber showed that BAP1 loss occurred only in mesotheliomas and was retained in all 42 genital adenomatoid tumors (33). BAP1 immunohistochemistry is a powerful addition to the growing portfolio of diagnostic tools for atypical mesothelial proliferations, but it is important to remember that the variable sensitivity of BAP1 loss in MPM limits its negative predictive value: retention of BAP1 expression by itself cannot be used to exclude a diagnosis of mesothelioma.

Loss of nuclear expression of 5-hydroxymethylcytosine (5-hmC) has shown promise as an additional immunohistochemical stain for distinguishing malignant from benign mesothelial proliferations with high (92%) sensitivity and 100% specificity, although this has not yet been widely adopted (34). Several other markers, including desmin, epithelial membrane antigen (EMA), p53, IMP3, GLUT-1, CD146, and CD147, have shown only limited diagnostic value and are unlikely to be useful in individual cases (1).

Homozygous deletion of 9p21 is an important method for separating benign from malignant mesothelial proliferations. This region comprises genes for two cyclin-dependent inhibitor kinases, *CDKNA2A (p16)* and *CDKN2B*, and *MTAP*. *CDKN2A* is present in normal cells where it is involved in cell cycle regulation. Deletion of *p16* is present

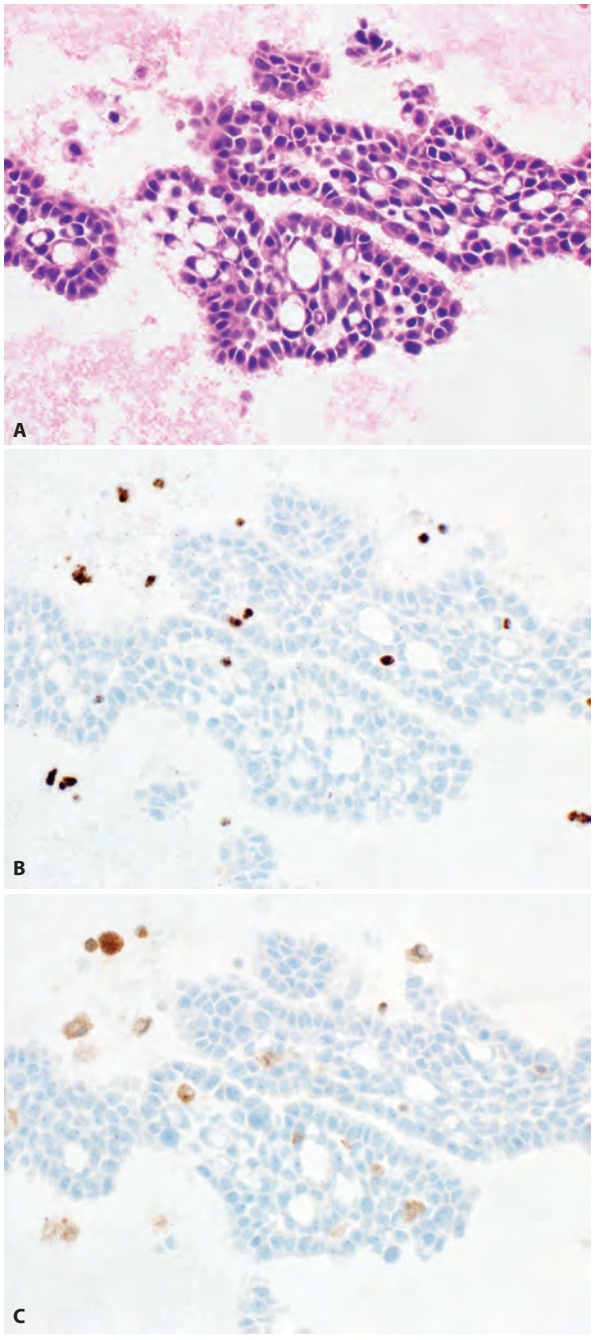

Figure 8. Immunohistochemical markers for separating mesothelioma from benign mesothelial proliferations. A) High magnification photomicrograph showing two- dimensional groups of atypical mesothelial cells in a cell block prepared from pleural fluid (hematoxylin and eosin; original magnification 400×). B-C) Immunohistochemical stains performed on the same cell block showed loss of nuclear staining for BAP1 (B) and loss of both cytoplasmic and nuclear staining for MTAP (C) with appropriately staining internal controls (original magnification 400×).

in as many as 90% of sarcomatoid mesotheliomas, and about 70% of desmoplastic subtypes, but tends to be less common in epithelioid and biphasic mesotheliomas. Practically, *p16* deletion is useful for distinguishing benign mesothelial proliferations from MPM, but cannot reliably distinguish MPM from other carcinomas in which *p16* may also be deleted (35, 36).

Homozygous *p16* deletion is demonstrated with a FISH technique using centromere 9 and *CDKN2A* probes, and can be applied to both cytology and histology specimens. Overall sensitivity of *p16* FISH in effusion cytology specimens is between 56% and 79% with a high (100%) positive predictive value given 100% specificity. False negative *p16* FISH may occur due to admixed reactive mesothelial cells that may be morphologically indistinguishable from malignant mesothelial cells (22). In histology specimens, the sensitivity of *p16* FISH for epithelioid and biphasic MM ranges between 45% and 85%. Homozygous *p16* deletion has been associated with shorter overall survival.

MTAP, a tumor suppressor gene co-located with *CDKN2A*, is often deleted with *p16*, making immunohistochemical staining for MTAP protein a reasonable surrogate for *p16* FISH (37). Negative cytoplasmic staining for MTAP in tumor cells with positive cytoplasmic and nuclear staining in positive internal controls, such as inflammatory and stromal cells, favors the diagnosis of MM with 100% specificity and a sensitivity of around 45% in tissue sections and cytology cell blocks. Combination with BAP1 immunohistochemistry increases sensitivity to around 75% to 80% (37).

Other emerging methods that are used less frequently, in part because of technological challenges that serve as barriers to access, include hemizygous deletion of neurofibromatosis type 2 *(NF2* gene) on 22q12 and gene expression arrays (38, 39). Bruno and colleagues showed that expression analysis of 117 genes using a nanoString System in a relatively small number of cases performed better than BAP1 and *p16* FISH, with overall sensitivity of 95.6% and 100% specificity (38). There are no currently recommended predictive biomarkers for patients with MPM, although that may change

as research continues with the hope of identifying more personalized treatment strategies (10). A number of clinical trials using immune checkpoint inhibitors are underway and have shown limited utility for PD-L1 testing in identifying those most likely to respond.

Malignant Mesothelioma in Situ

Malignant mesothelioma in situ is a preinvasive lesion defined as a single layer of atypical mesothelial cells lining the pleural surface and characterized by loss of BAP1 and/or MTAP expression using immunohistochemistry. Criteria for diagnosis include recurrent pleural effusions, lack of pleural thickening and nodularity on chest imaging, and either no or only incidental findings at video-assisted thoracoscopic surgery (VATS) or thoracotomy. Given these criteria, diagnosis requires a multidisciplinary approach (40). Churg et al. showed that seven of ten patients with well-defined mesothelioma in situ developed MPM during a follow-up period of 12-92 months (40).

Conclusions

Diffuse MPM is a heterogeneous group of aggressive pleural tumors for which histological classification plays an increasingly important role in patient management and survival. Update of epithelioid mesothelioma includes pleomorphic subtypes, in which more than 10% of tumor cells show marked nuclear pleomorphism; this subtype is associated with the worst overall survival among epithelioid MPM. Considering that transitional mesothelioma is genetically closely related to sarcomatoid MPM, recent studies recommend it to be within a subgroup of sarcomatoid mesotheliomas. Stage and resectability remain key drivers of therapeutic strategies and outcomes. Given that none of the immunohistochemical markers has 100% specificity, an immunohistochemical panel should contain at least two mesothelial markers and two markers appropriate to the working diagnoses established based on routinely stained sections and any pertinent history including previously diagnosed malignancies. There is an increasingly robust suite of diagnostic tools, including immunohistochemical stains for BAP1 and MTAP and *p16* FISH, for differentiating benign from malignant mesothelial proliferations in cytology and tissue specimens. Mesothelioma in situ has been recognized as a distinct clinicopathological entity for which more evidence is required to understand its natural history and treatment strategies that are proportional and targeted to the risk.

Conflict of Interest: The authors declare that they have no conflict of interest.

References

1. Churg A, Galateau-Salle F. The separation of benign and malignant mesothelial proliferations. Arch Pathol Lab Med. 2012;136(10):1217-26.
2. Finn RS, Brims FJH, Gandhi A, Olsen N, Musk AW, Maskell NA, et al. Postmortem findings of malignant pleural mesothelioma: a two-center study of 318 patients. Chest. 2012;142(5):1267-73.
3. Ogata S, Hiroi S, Tominaga A, Aida S, Kobayashi A, Tamura K, et al. Malignant pleural mesothelioma initially diagnosed on cervical lymph node biopsy. Pathol Int. 2009;59(8):592-4.
4. Henderson DW, Reid G, Kao SC, van Zandwijk N, Klebe S. Challenges and controversies in the diagnosis of mesothelioma: Part 1. Cytology-only diagnosis, biopsies, immunohistochemistry, discrimination between mesothelioma and reactive mesothelial hyperplasia, and biomarkers. J Clin Pathol. 2013;66(10):847-53.
5. Michael CW, Bedrossian CC. The implementation of liquid-based cytology for lung and pleural-based diseases. Acta Cytol. 2014;58(6):563-73.
6. Hjerpe A, Ascoli V, Bedrossian CW, Boon ME, Creaney J, Davidson B, et al. Guidelines for the cytopathologic diagnosis of epithelioid and mixed-type malignant mesothelioma. Complementary statement from the International Mesothelioma Interest Group, also endorsed by the International Academy of Cytology and the Papanicolaou Society of Cytopathology. Acta Cytol. 2015;59(1):2-16.
7. Chirieac LR, Hung YP, Foo WC, Hofer MD, VanderLaan PA, Richards WG, et al. Diagnostic value of biopsy sampling in predicting histology in patients with diffuse malignant pleural mesothelioma. Cancer. 2019;125(23):4164-71.
8. Verma V, Ahern CA, Berlind CG, Lindsay WD, Shabason J, Sharma S, et al. Survival by Histologic Subtype of Malignant Pleural Mesothelioma and the Impact of Surgical Resection on Overall Survival. Clin Lung Cancer. 2018;19(6):e901-12.

9. Marchevsky AM, Khoor A, Walts AE, Nicholson AG, Zhang YZ, Roggli V, et al. Localized malignant mesothelioma, an unusual and poorly characterized neoplasm of serosal origin: best current evidence from the literature and the International Mesothelioma Panel. Mod Pathol. 2020;33(2):281-96.
10. Nicholson AG, Sauter JL, Nowak AK, Kindler HL, Gill RR, Remy-Jardin M, et al. EURACAN/IASLC Proposals for Updating the Histologic Classification of Pleural Mesothelioma: Towards a More Multidisciplinary Approach. J Thorac Oncol. 2020;15(1):29-49.
11. Kadota K, Suzuki K, Sima CS, Rusch VW, Adusumilli PS, Travis WD. Pleomorphic epithelioid diffuse malignant pleural mesothelioma: a clinicopathological review and conceptual proposal to reclassify as biphasic or sarcomatoid mesothelioma. J Thorac Oncol. 2011;6(5):896-904.
12. Galetta D, Catino A, Misino A, Logroscino A, Fico M. Sarcomatoid mesothelioma: future advances in diagnosis, biomolecular assessment, and therapeutic options in a poor-outcome disease. Tumori. 2016;102(2):127-30.
13. Ismail-Khan R, Robinson LA, Williams CC Jr, Garrett CR, Bepler G, Simon GR. Malignant pleural mesothelioma: a comprehensive review. Cancer Control. 2006;13(4):255-63.
14. Klebe S, Brownlee NA, Mahar A, Burchette JL, Sporn TA, Vollmer RT, et al. Sarcomatoid mesothelioma: a clinical-pathologic correlation of 326 cases. Mod Pathol. 2010;23(3):470-9.
15. Mangano WE, Cagle PT, Churg A, Vollmer RT, Roggli VL. The diagnosis of desmoplastic malignant mesothelioma and its distinction from fibrous pleurisy: a histologic and immunohistochemical analysis of 31 cases including p53 immunostaining. Am J Clin Pathol. 1998;110(2):191-9.
16. Galateau-Salle F, Churg A, Roggli V, Travis WD, World Health Organization Committee for Tumors of the Pleura. The 2015 World Health Organization Classification of Tumors of the Pleura: Advances since the 2004 Classification. J Thorac Oncol. 2016;11(2):142-54.
17. Schulte JJ, Husain AN. Update on the pathologic diagnosis of malignant mesothelioma. Transl Lung Cancer Res. 2020;9(3):917-23.
18. Galateau Salle F, Le Stang N, Tirode F, Courtiol P, Nicholson AG, Tsao MS, et al. Comprehensive Molecular and Pathologic Evaluation of Transitional Mesothelioma Assisted by Deep Learning Approach: A Multi-Institutional Study of the International Mesothelioma Panel from the MESOPATH Reference Center. J Thorac Oncol. 2020;15(6):1037-53.
19. Dacic S, Le Stang N, Husain A, Weynand B, Beasley MB, Butnor K, et al. Interobserver variation in the assessment of the sarcomatoid and transitional components in biphasic mesotheliomas. Mod Pathol. 2020;33(2):255-62.
20. Wu D, Hiroshima K, Yusa T, Ozaki D, Koh E, Sekine Y, et al. Usefulness of p16/CDKN2A fluorescence in situ hybridization and BAP1 immunohistochemistry for the diagnosis of biphasic mesothelioma. Ann Diagn Pathol. 2017;26:31-7.
21. Marchevsky AM, LeStang N, Hiroshima K, Pelosi G, Attanoos R, Churg A, et al. The differential diagnosis between pleural sarcomatoid mesothelioma and spindle cell/pleomorphic (sarcomatoid) carcinomas of the lung: evidence-based guidelines from the International Mesothelioma Panel and the MESOPATH National Reference Center. Hum Pathol. 2017;67:160-8.
22. Husain AN, Colby TV, Ordonez NG, Allen TC, Attanoos RL, Beasley MB, et al. Guidelines for Pathologic Diagnosis of Malignant Mesothelioma 2017 Update of the Consensus Statement From the International Mesothelioma Interest Group. Arch Pathol Lab Med. 2018;142(1):89-108.
23. Ordonez NG. Application of immunohistochemistry in the diagnosis of epithelioid mesothelioma: a review and update. Hum Pathol. 2013;44(1):1-19.
24. Attanoos RL, Gibbs AR. 'Pseudomesotheliomatous' carcinomas of the pleura: a 10-year analysis of cases from the Environmental Lung Disease Research Group, Cardiff. Histopathology. 2003;43(5):444-52.
25. Davidson B, Totsch M, Wohlschlaeger J, Hager T, Pinamonti M. The diagnostic role of BAP1 in serous effusions. Hum Pathol. 2018;79:122-6.
26. Berg KB, Churg A. GATA3 Immunohistochemistry for Distinguishing Sarcomatoid and Desmoplastic Mesothelioma From Sarcomatoid Carcinoma of the Lung. Am J Surg Pathol. 2017;41(9):1221-5.
27. Churg A, Naso JR. The Separation of Benign and Malignant Mesothelial Proliferations: New Markers and How to Use Them. Am J Surg Pathol. 2020;44(11):e100-12.
28. Bott M, Brevet M, Taylor BS, Shimizu S, Ito T, Wang L, et al. The nuclear deubiquitinase BAP1 is commonly inactivated by somatic mutations and 3p21.1 losses in malignant pleural mesothelioma. Nat Genet. 2011;43(7):668-72.
29. Farzin M, Toon CW, Clarkson A, Sioson L, Watson N, Andrici J, et al. Loss of expression of BAP1 predicts longer survival in mesothelioma. Pathology. 2015;47(4):302-7.
30. Betti M, Casalone E, Ferrante D, Romanelli A, Grosso F, Guarrera S, et al. Inference on germline BAP1 mutations and asbestos exposure from the analysis of familial and sporadic mesothelioma in a high-risk area. Genes Chromosomes Cancer. 2015;54(1):51-62.
31. Cigognetti M, Lonardi S, Fisogni S, Balzarini P, Pellegrini V, Tironi A, et al. BAP1 (BRCA1-associated protein 1) is a highly specific marker for differentiating mesothelioma from reactive mesothelial proliferations. Mod Pathol. 2015;28(8):1043-57.
32. Weissferdt A, Kalhor N, Suster S. Malignant mesothelioma with prominent adenomatoid features: a clinicopathologic and immunohistochemical study of 10 cases. Ann Diagn Pathol. 2011;15(1):25-9.
33. Erber R, Warth A, Muley T, Hartmann A, Herpel E, Agaimy A. BAP1 Loss is a Useful Adjunct to Distinguish

Malignant Mesothelioma Including the Adenomatoid-like Variant From Benign Adenomatoid Tumors. Appl Immunohistochem Mol Morphol. 2020;28(1):67-73.

34. Chapel DB, Husain AN, Krausz T. Immunohistochemical evaluation of nuclear 5-hydroxymethylcytosine (5-hmC) accurately distinguishes malignant pleural mesothelioma from benign mesothelial proliferations. Mod Pathol. 2019;32(3):376-86.
35. Illei PB, Rusch VW, Zakowski MF, Ladanyi M. Homozygous deletion of CDKN2A and codeletion of the methylthioadenosine phosphorylase gene in the majority of pleural mesotheliomas. Clin Cancer Res. 2003;9(6):2108-13.
36. Hwang HC, Pyott S, Rodriguez S, Cindric A, Carr A, Michelsen C, et al. BAP1 Immunohistochemistry and p16 FISH in the Diagnosis of Sarcomatous and Desmoplastic Mesotheliomas. Am J Surg Pathol. 2016;40(5):714-8.
37. Hida T, Hamasaki M, Matsumoto S, Sato A, Tsujimura T, Kawahara K, et al. Immunohistochemical detection of MTAP and BAP1 protein loss for mesothelioma diagnosis: Comparison with 9p21 FISH and BAP1 immunohistochemistry. Lung Cancer. 2017;104:98-105.
38. Bruno R, Ali G, Giannini R, Proietti A, Lucchi M, Chella A, et al. Malignant pleural mesothelioma and mesothelial hyperplasia: A new molecular tool for the differential diagnosis. Oncotarget. 2017;8(2):2758-70.
39. Kinoshita Y, Hamasaki M, Yoshimura M, Matsumoto S, Iwasaki A, Nabeshima K. Hemizygous loss of NF2 detected by fluorescence in situ hybridization is useful for the diagnosis of malignant pleural mesothelioma. Mod Pathol. 2020;33(2):235-44.
40. Churg A, Galateau-Salle F, Roden AC, Attanoos R, von der Thusen JH, Tsao MS, et al. Malignant mesothelioma in situ: morphologic features and clinical outcome. Mod Pathol. 2020;33(2):297-302.

Case Report
Acta Medica Academica 2021;50(1):209-217
DOI: 10.5644/ama2006-124.336

Patient with Lobular Carcinoma of the Breast and Activating *AKT1 E17K* Variant

Harsha Trivedi[1], Omar Hamdani[2], Brittani Thomas[1], James Richard[3], Kunal Shah[2], Kira Raskina[2], Liang Zhang[2], Audrey Madigan[2], Marshall Fox[2], Seth Wander[2, 4], Matthew J Frigault[2, 4], Brian Alexander[2], Gordan Srkalovic[1]

[1]Herbert-Herman Cancer Center, E. W. Sparrow Hospital, Lansing, MI, USA, [2]FoundationMedicine, Cambridge, MA, USA, [3]Department of Pathology and Laboratory Medicine, Sparrow Hospital System, Lansing, MI, USA, [4]Massachusetts General Hospital, Boston, MS, USA

Correspondence: *gordan.srkalovic@sparrow.org*; Tel.: + 1 517 364 2182; Fax.: + 1 517 364 2886

Received: 24 February 2021; **Accepted:** 25 February 2021

Abstract

Objective. To present the characteristics of the AKT1E117K gene variant and a description of the clinical application in a patient with metastatic breast cancer. **Results.** 63 y/o woman with Stage IV Invasive lobular carcinoma at diagnosis was treated with Palbociclib and aromatase inhibitors (AI). At progression, tissue was sent for comprehensive genomic profiling to Foundation Medicine (FM) which revealed AKT1E17K mutation. In lieu of available clinical data within the patient's tumor type (HR+ HER2- breast cancer), extrapolated data from the Flatiron Health-FM (FH-FMI) Clinico-genomic Database (CGDB) was discussed at our Molecular Tumor Board (MTB). After multidisciplinary discussion, the consensus recommendation was to start treatment with the combination of mTOR inhibitor everolimus, and AI, exemestane. Patient tolerated treatment without major side effects. By the second clinical visit the patient's breast showed signs of improvement. PET/CT showed diminished left axillary uptake, decreased right paratracheal lymph node PET avidity, and stable bone disease consistent with a partial response. The most recent office visit in January 2021, breast exam revealed a normal-appearing skin with only faint erythema. All other skin lesions have resolved. Although, the role of AKT1 variant described here is not well defined and therapeutic significance of M-Tor inhibitors not established in metastatic breast cancers, comprehensive approach to this case unraveled new and successful therapeutic option in this patient. **Conclusion.** This demonstrates that applying available Precision Medicine tools like MTB and real world data sets from patient populations with similar clinical and genomic profiles may provide more options for treatment.

Key Words: AKT1 ▪ Breast Cancer ▪ Molecular Tumor Board (MTB) ▪ CGDB – Comprehensive Genomic Data Base.

Introduction

Invasive lobular carcinoma (ILC) is the most common of the breast cancer special types, accounting for up to 15% of all breast cancer cases. ILCs are noted for their lack of E-cadherin function, which results in non-cohesive growth pattern, with the knowledge from genomic profiling now there is huge amount of new data, from the genomic landscape of ILC and in particular somatic alterations associated with therapy resistance, and the evolution of several potential therapeutic avenues. Many targeted and chemotherapy options are being evaluated.

Here we present a case of ILC treated at our cancer center based on the precision medicine tools. The information provided by genomic profile is used clinically to guide treatments decisions for approved targeted therapies and in clinical trials. In this case none of that could be used. We found an effective treatment for this patient based on the MTB discussion and the real world data of the AKT1E17K variant and AKT1 WT breast cancer patients.

Results

Clinical Presentation

A 63-year-old pleasant woman with no major past medical history presented in January 2019 with a palpable left breast mass. On physical exam, besides the breast mass, the patient had palpable lymph nodes in the left axilla. She was referred for

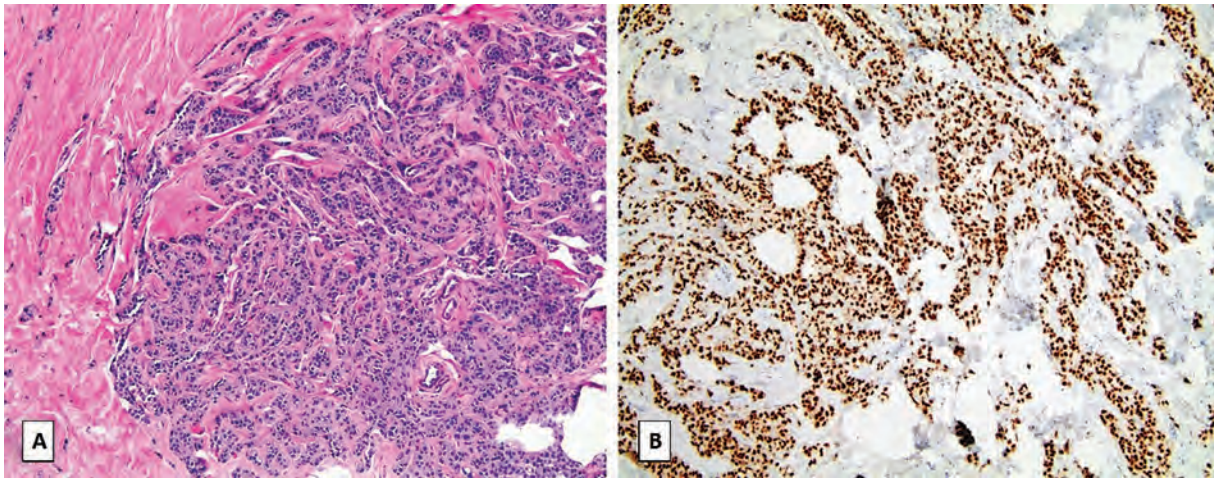

Figure 1. (A): A core needle biopsy was showing invasive lobular carcinoma infiltrating the fibrous tissue of the breast as single cells, cords, or linear strands of neoplastic cells, most often found in the desmoplastic breast stroma (Hematoxylin and Eosin stain); (B): Immunohistochemistry (IHC) of invasive lobular carcinoma patient showing diffuse and strong estrogen receptor (ER) expression. The patient's sample was PR negative and HER2 negative. Ki-67 was positive in ~50% cancer cells.

diagnostic mammography and ultrasound, which revealed a diffuse nonhomogeneous density at the site of palpable finding. A core needle biopsy was performed, and pathology revealed classic invasive lobular carcinoma infiltrating the fibrous tissue of the breast as single cells and in cords or linear strands of cells, most often found in the breast fibrous stroma (Figure 1A).

The infiltrating cells are monotonous, small in size, and possess round nuclear contours. This pattern of invasion can at times encircle benign ducts in a concentric or "targetoid" fashion. These cells can be seen infiltrating together, as in the image (Figure 1B) or in a rather insidious fashion separated by the fibrous stroma of the breast, presenting a challenge to find for even an experienced pathologist. This is especially challenging when the amount of tumor present is limited, as in needle biopsy material. The classic invasive lobular carcinoma typically expresses estrogen (ER) and progesterone receptors (PR) and is negative for HER2 expression.In this case, the cancer cells were ER-positive while PR and HER2 receptors were negative. The proliferation rate was ~50% (measured by Ki-67).

On February 5, 2019, the patient underwent a PET/CT scan, which revealed diffuse skeletal metastases and extensive left axillary lymphadenopathy (LADP) extending into the pectoralis minor muscle and the thoracic outlet. After this workup, the patient was staged as Stage IV Invasive Lobular Carcinoma of the left breast cT3N3M1, grade 2. The patient has an indeterminate right middle lobe pulmonary nodule, which was slightly fluorodeoxyglucose (FDG) avid. Genetic testing by the Invitae Panel was done on 5/7/19 and was negative for any deleterious mutations. At that time patient was treated with a combination of CDK4/6 inhibitor palbociclib and aromatase inhibitor (AI) letrozole. Zoledronic acid was also initiated as bone targeting treatment. The patient tolerated treatment with the support of growth factors for low counts and palbociclib dose reduction to 100 mg from May 2019. She tolerated further treatments without any major side effects. PET/CT scan in August 2019 showed significant positive interval response with resolution of hypermetabolic thoracic outlet and left axillary LADP, as well as decreasing left breast activity and decreasing FDG avidity of several osseous lesions. Scan in January 1/31/20 was reported as no evidence of disease (NED).

However, on a follow-up visit in February 2020, the patient complained that her left breast was feeling "heavier". She denied pain and struggled to describe the change. On physical exam, the patient had an erythematous rash involving

the medial half of the breast. The breast was not tender, and there were no palpable masses. Biopsy of the involved skin was done, and pathology confirmed lobular carcinoma with no changes in receptor status. A repeated PET/CT scan in March 2020 showed increased left anterior breast skin thickening, a mildly increased uptake within the left axillary lymph nodes, and an increased overall number and extent of osseous metastases. The patient also had several small skin lesions on the neck and chest. Biopsy of the left neck lesion confirmed metastatic lobular carcinoma with the same characteristics as previously reported. The patient continued on palbociclib, while the treatment with letrozole was changed to the ER antagonist, fulvestrant. She enjoyed a clinical response from April to August 2020. However, on her office follow-up in August, the left breast was again increasingly erythematous and swollen. The erythema involved about three-quarters of the breast, and PET/CT scan confirmed increasing osseous metastatic burden.

Genomic Analysis

To determine whether the patient was a candidate for the use of targeted therapy based on her tumor genomics, tissue from her neck skin biopsy was sent for Foundation One CDx (F1CDx) solid biopsy CGP and evaluation of PD-L1 receptor. F1CDx is a hybrid-capture-based CGP assay that baits exonic regions of 324 genes and selects intronic regions for rearrangements (FMI2021). The test can detect gene alterations (GA) in the form of short variants (SV), rearrangements (RE), and copy number alterations (CNA), including amplifications / homozygous deletions. The patient's CGP results showed detection of a previously characterized and predicted activating *AKT1 E17K* mutation. We characterize this gene variant and attempt to assign its clinical significance below.

AKT1 is an intracellular serine/threonine kinase that can phosphorylate and activate the serine/threonine kinase mTORi (1). Upon activation, the mTORi complex can stimulate cell proliferation and growth through a variety of oncogenic mechanisms. AKT1 is situated downstream of PI3K and upstream of mTORi in the PI3K-mTOR signaling pathway, which suggests inhibition of *AKT1* or downstream signaling components could be an effective treatment in *AKT1* altered cancers. It is important to note that the *AKT1* kinase phosphorylates other proteins, which may have inhibitory effects on cell growth. This diverse biology suggests that *AKT1* influences several mechanisms spanning both oncogenic and anti-oncogenic effects (2-5).

AKT1 E17K variant has been extensively characterized preclinically in a variety of cancer cell types and model systems (6-11). *AKT1 E17K* is a hotspot mutation occurring at the N-terminal of the *AKT1* protein (1, 12). In breast cancer cell line models, ectopic expression of *AKT1 E17K* leads to increased phosphorylation of *AKT1* target genes, inhibition of apoptosis, increased colony formation, and increased tumor growth in mouse xenograft models (6, 7). Furthermore, *AKT1 E17K* mutant breast cancer preclinical models demonstrate sensitivity to inhibition of the mTORi pathway using several targeted therapy agents.

AKT1 mutations occur in 4% of breast cancer patients, and *AKT1 E17K* mutations account for ~80% of those *AKT1* mutations (COSMIC database 2021). *AKT1* is still in an early stage clinical development as a biomarker for mTOR pathway targeted therapy, but clinical trials are underway (13-17). Interestingly, oncogenic properties that *AKT1 E17K* cancer cells displayed in a preclinical setting have been recapitulated in a clinical setting. The mTOR pathway activity that has been demonstrated in preclinical *AKT1 E17K* mutant breast cancer models has also been shown in breast cancer patient samples through pharmacodynamic analysis (i.e., mTORC1 activation and target gene activation). Clinical study also suggests that *AKT1 E17K* breast cancer patients may spend longer time on mTORi therapy (i.e., everolimus) than *AKT1* wild- type (WT) patients (16), and early phase clinical data suggests that *AKT1 E17K* mutant ER+ breast cancer patients may benefit from AKT inhibitors such as capivasertib (15, 17).

Collectively, these data indicate that inhibition of mTOR pathway components may be a treatment option for *AKT1 E17K* mutant breast cancer patients.

Application of Precision Medicine Tools

This report was discussed at our Molecular Tumor Board (MTB) joint activity between Sparrow Herbert-Herman Cancer Center and Foundation Medicine Inc. (FMI) (18). As an educational program, the goal of an FMI MTB program is to discuss the targetability of genomic alterations that are identified by FMI CGP. The focus of discussion during the MTB was whether mTORi pathway inhibition is a viable treatment option for *AKT1 E17K* altered breast cancer patients. As noted earlier, the available clinical data for *AKT1* targetability is still accumulating. In lieu of clinical data within the patient's tumor type (HR+ HER2- breast cancer), extrapolated data was discussed. However, this is not always appropriate or useful to ascertain treatment options for the MTB patient. One tool available to FMI cancer researchers is the Flatiron Health-Foundation Medicine (FH-FMI) Clinicgenomic Database (CGDB). Retrospective longitudinal clinical data were derived from electronic health record (EHR) data, comprising patient-level structured and unstructured data, curated via technology-enabled abstraction, and were linked to genomic data derived from FMI comprehensive genomic profiling (CGP) tests in the FH-FMI CGDB by de- identified, deterministic matching (19-22).

To better understand how the present patient may respond to mTORi treatment, a real-world data cohort consisting of HR+/HER2- breast cancer patients with *AKT1 E17K* alteration were analyzed for treatment use by a line of therapy from the CGDB. Clinical characteristics and treatment history were obtained via technology-enabled abstraction of clinician notes and radiology/pathology reports for 3155 HR+/HER2- BC patients. *AKT1 E17K* mutations were found in 143 patients while2964 patients had *AKT1* WT. Thirty-one *AKT1 E17K* and 627 of *AKT1* WT patients received mTORi (Figure 2).

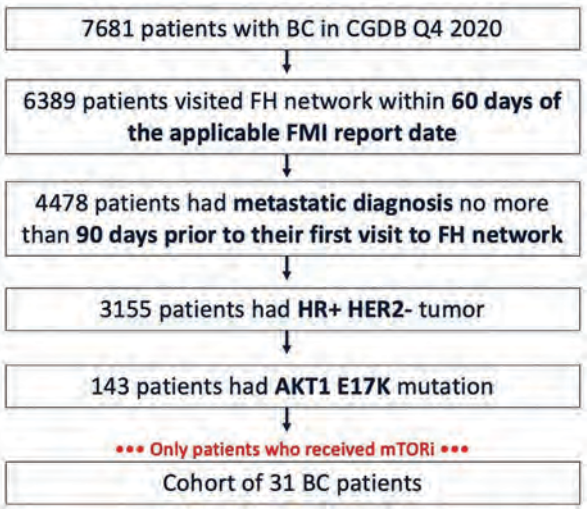

Figure 2. CGDB Cohort of HR+/HER2- Breast Cancer Patients with *AKT1 E17K* Mutation that Received mTORi.

Time to next treatment (TTNT) was also estimated with Kaplan-Meier analysis and hazard ratios from Cox proportional hazards models. Propensity-score matching (PSM) was used to account for the characteristics that predict receiving of the treatment. The cohort of patients with *AKT1 E17K* mutant BC receiving mTORi did not significantly differ on major demographic, clinical, and genetic characteristics from the *AKT1* WT cohort receiving the same treatment (Table 1). To compare TTNT on mTORi in the two cohorts, we matched the *AKT1 E17K* patients to *AKT1* WT patients on age, tumor type, ECOG, TMB, and mTORi line using PSM. The TTNT on mTORi of *AKT1 E17K* vs. *AKT1* WT patients was 6.5 months (95% CI 4.6 – n/a) and 8.7 months (95%CI 6.4 – na), respectively. The relative efficacy of receiving mTORi was not significantly higher in *AKT1 E17K* group (HR=1.2 [95%CI: 0.6 – 2.3], P=0.6). The only characteristic by which the *AKT1 E17K* cohorts receiving chemo vs. mTORi were different was the line of treatment (Table 2). A noticeably higher percentage of patients received chemotherapy in earlier lines (79.7% in lines 1-2), while mTORi was chosen in later lines of treatment (77.4% in lines 3+). To compare TTNT on mTORi vs. on chemotherapy in these cohorts, we matched the patients who received chemotherapy to the patients who received mTORi on age, tumor

Table 1. Demographic Information for HR+ HER2- Breast Cancer Patients with or without *AKT1 E17K* Mutation that Received mTORi from the CGDB

Demographics	*AKT1 E17K* (N=31)	*AKT1 WT* (N=767)	P-value	P adjusted (FDR)
Age at Dx, yrs, Median (IQR)	52.0 (46.0, 58.0)	54.0 (46.0, 62.0)	0.315	0.999
Female	31 (100.0%)	760 (99.1%)	0.593	0.999
Race			0.808	0.999
Asian	1 (3.2%)	14 (1.8%)	-	
Black or African American	1 (3.2%)	45 (5.9%)	-	-
Hispanic or Latino	0 (0.0%)	2 (0.3%)	-	-
White	25 (80.6%)	541 (70.5%)	-	-
Other Race	3 (9.7%)	134 (17.5%)	-	-
Not documented	1 (3.2%)	31 (4.0%)	-	-
Stage at Dx			0.11	0.99
I-II	18 (58.1%)	305 (39.8%)	-	-
III-IV	12 (38.7%)	399 (52.0%)	-	-
Not documented	1 (3.2%)	63 (8.2%)	-	-
Tumor Grade			0.874	0.999
Grade 1	1 (3.2%)	40 (5.2%)	-	-
Grade 2	10 (32.3%)	205 (26.7%)	-	-
Grade 3	8 (25.8%)	193 (25.2%)	-	-
Not documented	12 (38.7%)	329 (42.9%)	-	-
Tumor Type			0.954	0.999
IDC	10 (32.3%)	255 (33.2%)	-	-
ILC	2 (6.5%)	59 (7.7%)	-	-
Other	19 (61.3%)	453 (59.1%)	-	-
Community practice	28 (90.3%)	708 (92.3%)	0.686	0.999
MFI, yrs, Median (IQR)	3.7 (0.2, 7.4)	3.0 (0.0, 7.25)	0.656	0.999
Solid biopsy	27 (87.1%)	668 (87.1%)	0.999	0.999
Metastases sites			0.876	0.999
Bone-only	3 (9.7%)	62 (8.1%)	-	-
CNS	8 (25.8%)	177 (23.1%)	-	-
Visceral	20 (64.5%)	527 (68.8%)	-	-
ECOG			0.0353	0.635
1	7 (31.8%)	230 (47.3%)	-	-
2	2 (9.1%)	53 (10.9%)	-	-
3	2 (9.1%)	7 (1.4%)	-	-
PD-L1 status			0.388	0.999
Negative	2 (6.5%)	86 (11.2%)	-	-
Positive	0 (0.0%)	26 (3.4%)	-	-
Not documented	29 (93.5%)	655 (85.4%)	-	-
TMB (RUO), muts/mB, Median (IQR)	2.6 (1.3, 4.5)	2.6 (1.3, 5.2)	0.541	0.999
MSI (RAW)			0.933	0.999
MSI-H	0 (0.0%)	2 (0.3%)	-	-
MSI-I	0 (0.0%)	4 (0.5%)	-	-
MSS	21 (67.7%)	543 (70.8%)	-	-
Not documented	10 (32.3%)	218 (28.4%)	-	-
mTORi			0.727	0.999
Everolimus	31 (100.0%)	764 (99.6%)	-	-
Temsirolimus	0 (0.0%)	3 (0.4%)	-	-
Start Date, Median (Range)	2017-09-18 (2013-03-01 - 2020-06-09)	2017-08-22 (2011-12-29 - 2020-09-23)	0.84	0.999
mTORi line			0.31	0.999
1-2	7 (22.6%)	239 (31.2%)	-	-
3+	24 (77.4%)	528 (68.8%)	-	-
Deceased	22 (71.0%)	492 (64.1%)	0.437	0.999

MFI=Metastasis-free interval.

Table 2. Demographic Information for HR+ HER2- Breast Cancer Patients with *AKT1 E17K* Mutation that Received mTORi vs. Chemotherapy from the CGDB

Demographics	Chemotherapy (N=74)	mTORi (N=31)	P-value	P adjusted (FDR)	*
Age at Dx, yrs, Median (IQR)	55.0 (46.0; 62.0)	52.0 (46.0; 58.0)	0.366	0.93	
Female	74 (100.0%)	31 (100.0%)	0.932	0.932	
Race			0.932	0.932	
Asian	2 (2.7%)	1 (3.2%)	-		
Black or African American	2 (2.7%)	1 (3.2%)	-	-	
White	55 (74.3%)	25 (80.6%)	-	-	
Other Race	12 (16.2%)	3 (9.7%)	-	-	
Not documented	3 (4.1%)	1 (3.2%)	-	-	
Stage at Dx			0.678	0.93	
I-II	36 (48.6%)	18 (58.1%)	-	-	
III-IV	35 (47.3%)	12 (38.7%)	-	-	
Not documented	3 (4.1%)	1 (3.2%)	-	-	
Tumor Grade			0.652	0.93	
Grade 1	5 (6.8%)	1 (3.2%)	-	-	
Grade 2	30 (40.5%)	10 (32.3%)	-	-	
Grade 3	18 (24.3%)	8 (25.8%)	-	-	
Not documented	21 (28.4%)	12 (38.7%)	-	-	
Tumor Type			0.672	0.93	
IDC	19 (25.7%)	10 (32.3%)	-	-	
ILC	8 (10.8%)	2 (6.5%)	-	-	
Other	47 (63.5%)	19 (61.3%)	-	-	
Community practice	68 (91.9%)	28 (90.3%)	0.793	0.932	
MFI, yrs, Median (IQR)	2.9 (1.3, 7.1)	3.7 (0.2, 7.4)	0.534	0.93	
Solid biopsy	65 (87.8%)	27 (87.1%)	0.916	0.932	
Metastases sites			0.343	0.93	
Bone-only	5 (6.8%)	3 (9.7%)	-	-	
CNS	11 (15.1%)	8 (25.8%)	-	-	
Visceral	57 (78.1%)	20 (64.5%)	-		
ECOG			0.711	0.93	
0	21 (40.4%)	11 (50.0%)	-	-	
1	24 (46.2%)	7 (31.8%)	-	-	
2	3 (5.8%)	2 (9.1%)	-	-	
3	4 (7.7%)	2 (9.1%)	-	-	
PD-L1 status			0.277	0.93	
Negative	7 (9.5%)	2 (6.5%)	-	-	
Positive	5 (6.8%)	0 (0.0%)	-	-	
Not documented	62 (83.8%)	29 (93.5%)	-	-	
TMB (RUO), muts/mB, Median (IQR)	2.5 (1.3, 6.1)	2.6 (1.3, 4.5)	0.86	0.932	
MSI (RAW)			0.491	0.93	
MSS	55 (74.3%)	21 (67.7%)			
Not documented	19 (25.7%)	10 (32.3%)			
Start Date, Median (Range)	2018-01-21 (2012-02-14 – 2020-09-24)	2017-09-18 (2013-03-01 - 2020-6-09)	0.429	0.93	
Treatment Line			3.23e-08	0	*
1-2	59 (79.7%)	7 (22.6%)			
3+	15 (20.3%)	24 (77.4%)			
Deceased	47 (63.5%)	22 (71.0%)	0.463	0.93	

*Denotes a statistically significant difference.

type, ECOG, TMB, and treatment line using PSM. The TTNT on mTORi vs. chemotherapy was 6.5 months (95% CI 4.6 – n/a) and 5.8 months (95% CI 4.6 – na), respectively. The relative efficacy of receiving mTORi was not significantly higher than receiving chemo (HR=0.8 [95% CI: 0.4 – 1.5], P=0.5).

After multidisciplinary discussion, the consensus recommendation was to start treatment with the combination of mTORi, everolimus, and AI, exemestane. Treatment was initiated on 8/28/20, and the everolimus dose was decreased from 10 mg to 7.5 mg daily due to the episode of neutropenia after the first cycle. Otherwise, the patient tolerated treatment without major side effects. By the second clinical visit in October 2020, the patient's breast was less erythematous, and the density of the tissue was lessening. There was no tenderness on palpation. PET/CT showed diminished left axillary uptake, decreased right paratracheal lymph node PET avidity, and stable bone disease consistent with a partial response. The most recent office visit in January 2021, breast exam revealed a normal-appearing skin with only faint erythema. All other skin lesions have resolved. The patient feels well and reports no pain.

Discussion

Roughly 10% of all breast cancers are invasive lobular carcinomas (23, 24). Invasive lobular carcinoma is strongly associated with exposure to female hormones, and its incidence is more subject to variation. It is more strongly associated with early menarche, late menopause, and late age of first birth. Of high-penetrance genes, *BRCA1* and *TP53* are predominantly associated with invasive ductal carcinoma (IDC), *BRCA2* mutations are associated with both IDC and invasive lobular cancer (ILC), while mutations in *CDH1* (encoding E-cadherin protein) are exclusively associated with ILC (25). It is characterized by functional loss of E-cadherin, resulting in cellularadhesion defect. Besides E-cadherin loss, Ciriello et al. identified mutations targeting *PTEN*, *TBX3,* and *FOXA1* as ILC enriching features (26). PTEN loss is associated with increased AKT phosphorylation, which was highest in ILC among all breast cancer subtypes. Spatially clustered *FOXA1* mutations correlated with increased *FOXA1* expression and activity. Conversely, *GATA3*mutations and high expression characterized Luminal A IDC, suggesting differential modulation of the ER activity in ILC and IDC. The proliferation and immune-related signatures determined three ILC transcriptional subtypes associated with survival differences. Mixed IDC/ILC cases were molecularly classified as ILC-like and IDC-like revealing no true hybrid features. This points to the heterogeneity of ILC and particularly to a distinct molecular profile of ILC vs. IDC. The case presented herein, however, seems to rather represent the Luminal B category, based on PR negative status and high Ki-67 (50%) for ILC. Generally, ILC is considered as cancer with a good short-term prognosis. Metastatic ILC spreads more commonly to the ovaries, colon, omentum, and stomach. Interestingly, a high tumor mutational burden (TMB) is associated with metastatic ILC, with 8.9% of metastatic ILC classified as TMB-high (27).

The patient presented herein was treated with standard of care targeted therapy and aromatase inhibitors with some short-term success and ultimate progression. However, CGP opened another avenue of treatment that otherwise would not be one on the mind of treating physician. In addition, basic analysis of the CGP results did not directly point to the use of mTORi. The deeper up-and downstream analysis and discussion at our Molecular Tumor Board (MTB) uncovered those therapeutic options. An MTB also provides a unique setting for the application of RWD. During this MTB, RWD provided treatment information from patients in the CGDB that were genomically similar to the MTB patient. This, at least, at present, shows to be highly effective for this patient. When clinical literature for a biomarker is limited (such as *AKT1*), the CGDB can provide clinical utility through decision support. Future studies should seek to understand which controls and confounders can improve clinical decision support using RWD. Our experience with MTB showed that al-

most half of the patients (46%) presented at MTB were offered genomically matched therapy or clinical trials (18). The patient presented here is one of 22% of patients who received recommended treatment. Others did not for different reasons, including physicians and patients' preferences, poor performance status, lack of coverage, etc. In the future, more extensive use of CGP, more wide availability of MTB's to treating physicians, wider accessibility to clinical trials, better education of physicians and community, and collaboration with third-party payers will open more possibilities for effective treatment of patients with advanced malignant diseases.

Conclusion

AKT1 mutations occur in 4% of breast cancer patients, and AKT1 E17K mutations account for ~80% of those mutations (28). AKT1 E17K variants have been previously characterized as activating and oncogenic. The AKT1 E17K mutation is proposed to induce hyper activation of the mTOR pathway through constitutive AKT1 signaling and activation of the downstream components of the mTOR pathway (29, 30). Clinical study of mTOR pathway targeted therapy in AKT1 mutant breast cancer is still early in development. However, targeting AKT1 and downstream mTOR pathway components has shown efficacy in a limited number of AKT1 E17K mutant breast cancer patients (28, 31, 32).

There is no consensus model for the application of comprehensive genomic profiling (CGP) and real-world data (RWD) in the treatment of cancer patients. This case study provides an example for the use of RWD and CGP in the context of a multidisciplinary Molecular Tumor Board (MTB). Furthermore, the study adds to the growing body of clinical literature that suggests that AKT1 mutant breast cancer patients may be sensitive to mTOR pathway targeted therapy in the advanced setting.

Authors' Contributions: Conception and design: HT, OH, and GS; Acquisition, analysis and interpretation of data: OH, BT, JT, KS, KR, LZ, AM, MF, SW, MJF, and BA; Drafting the article: GS; Revising it critically for important intellectual content: HT and OH; Approved final version of the manuscript: HT, OH and GS.

Ethical (IRB) Approval: The case report was submitted to Sparrow IRB, and they have determined that this project does not meet the definition of human subject research under the purview of IRB according to federal regulations. Verbal approval of the patient was obtained by the treating physician to publish the case report.

Conflict of Interest: All authors have signed the journal's COI form. HT, BT, and JR have no conflict of interest in relation to this article. GS is on the Speaker's Bureau of Foundation Medicine, SW and MJF are consultants to Foundation Medicine; OH, KS, BA, AM, LZ, MF, and KR are employees of Foundation Medicine- Roche group.

References

1. Chen Y, Huang L, Dong Y, Tao C, Zhang R, Shao H, et al. Effect of AKT1 (p. E17K) Hotspot Mutation on Malignant Tumorigenesis and Prognosis. Front Cell Dev Biol [Internet]. 2020 [cited 2021 Jan 20]; 8. Available from: https://www.frontiersin.org/articles/10.3389/fcell.2020.573599/full#B90.
2. Khatpe AS, Adebayo AK, Herodotou CA, Kumar B, Nakshatri H. Nexus between PI3K/AKT and Estrogen Receptor Signaling in Breast Cancer. Cancers. 2021; 13(3):369.
3. Hinz N, Jücker M. Distinct functions of AKT isoforms in breast cancer: a comprehensive review. Cell Commun Signal CCS. 2019;17(1):154.
4. Alwhaibi A, Verma A, Adil MS, Somanath PR. The unconventional role of Akt1 in the advanced cancers and in diabetes-promoted carcinogenesis. Pharmacol Res. 2019;145:104270.
5. Cole PA, Chu N, Salguero AL, Bae H. AKTivation mechanisms. Curr Opin Struct Biol. 2019;59:47-53.
6. Beaver JA, Gustin JP, Yi KH, Rajpurohit A, Thomas M, Gilbert SF, et al. PIK3CA and AKT1 Mutations Have Distinct Effects on Sensitivity to Targeted Pathway Inhibitors in an Isogenic Luminal Breast Cancer Model System. Clin Cancer Res. 2013;19(19):5413-22.
7. Davies BR, Guan N, Logie A, Crafter C, Hanson L, Jacobs V, et al. Tumors with AKT1E17K Mutations Are Rational Targets for Single Agent or Combination Therapy with AKT Inhibitors. Mol Cancer Ther. 2015;14(11):2441-51.
8. Marco CD, Malanga D, Rinaldo N, Vita FD, Scrima M, Lovisa S, et al. Mutant AKT1- E17K is oncogenic in lung epithelial cells. Oncotarget. 2015;6(37):39634-50.
9. Oeck S, Al-Refae K, Riffkin H, Wiel G, Handrick R, Klein D, et al. Activating Akt1 mutations alter DNA double strand break repair and radiosensitivity. Sci Rep. 2017;7(1):42700.

10. Van Der Zwet JCG, Buijs-Gladdines JGCAM, Mollova I, Graus L, Bos FL, Rios AC, et al. The Clinical and Functional Relevance of the Transforming AKT E17K Mutation in T-ALL. Blood. 2019;134(Suppl 1):3804.
11. Wu W, Chen Y, Huang L, Li W, Tao C, Shen H. Effects of AKT1 E17K mutation hotspots on the biological behavior of breast cancer cells. Int J Clin Exp Pathol. 2020;13(3):332-46.
12. Elghazi L, Balcazar N, Bernal-Mizrachi E. Emerging role of protein kinase B/Akt signaling in pancreatic β-cell mass and function. Int J Biochem Cell Biol. 2006;38(2):157-63.
13. Hechtman JF, Sadowska J, Huse JT, Borsu L, Yaeger R, Shia J, et al. AKT1 E17K in Colorectal Carcinoma Is Associated with BRAF V600E but Not MSI-H Status: A Clinicopathologic Comparison to PIK3CA Helical and Kinase Domain Mutants. Mol Cancer Res. 2015;13(6):1003-8.
14. Hyman DM, Smyth LM, Donoghue MTA, Westin SN, Bedard PL, Dean EJ, et al. AKT Inhibition in Solid Tumors With AKT1 Mutations. J Clin Oncol. 2017;35(20):2251-9.
15. Smyth LM, Tamura K, Oliveira M, Ciruelos EM, Mayer IA, Sablin M-P, et al. Capivasertib, an AKT Kinase Inhibitor, as Monotherapy or in Combination with Fulvestrant in Patients with AKT1E17K-Mutant, ER-Positive Metastatic Breast Cancer. Clin Cancer Res. 2020;26(15):3947-57.
16. Smyth LM, Zhou Q, Nguyen B, Yu C, Lepisto EM, Arnedos M, et al. Characteristics and Outcome of AKT1E17K-Mutant Breast Cancer Defined through AACR Project GENIE, a Clinicogenomic Registry. Cancer Discov. 2020;10(4):526-35.
17. Tamura K, Hashimoto J, Tanabe Y, Kodaira M, Yonemori K, Seto T, et al. Safety and tolerability of AZD5363 in Japanese patients with advanced solid tumors. Cancer Chemother Pharmacol. 2016;77(4):787-95.
18. Trivedi H, Acharya D, Chamarthy U, Meunier J, Ali-Ahmad H, Hamdan M, et al. Implementation and Outcomes of a Molecular Tumor Board at Herbert-Herman Cancer Center, Sparrow Hospital. Acta Med Acad. 2019;48(1):105-15.
19. Singal G, Miller PG, Agarwala V, Li G, Kaushik G, Backenroth D, et al. Association of Patient Characteristics and Tumor Genomics With Clinical Outcomes Among Patients With Non-Small Cell Lung Cancer Using a Clinicogenomic Database. JAMA. 2019;321(14):1391-9.
20. Madison R, Schrock AB, Castellanos E, Gregg JP, Snider J, Ali SM, et al. Retrospective analysis of real-world data to determine clinical outcomes of patients with advanced non- small cell lung cancer following cell-free circulating tumor DNA genomic profiling. Lung Cancer Amst Neth. 2020;148:69-78.
21. Schrock AB, Lee JK, Sandhu J, Madison R, Cho-Phan C, Snider JW, et al. RAS amplification as a negative predictor of benefit from anti-EGFR containing therapy regimens in metastatic colorectal cancer. The Oncologist. 2021 January 19. Online ahead of print.
22. Yarchoan M, Albacker LA, Hopkins AC, Montesion M, Murugesan K, Vithayathil TT, et al. PD-L1 expression and tumor mutational burden are independent biomarkers in most cancers. JCI Insight [Internet]. 2019 Mar 21 [cited 2021 Feb 11];4(6). Available from: https://insight.jci.org/articles/view/126908.
23. Li CI, Anderson BO, Daling JR, Moe RE. Trends in incidence rates of invasive lobular and ductal breast carcinoma. JAMA. 2003;289(11):1421-4.
24. Li CI, Daling JR. Changes in breast cancer incidence rates in the United States by histologic subtype and race/ethnicity, 1995 to 2004. Cancer Epidemiol Biomark Prev Publ Am Assoc Cancer Res Cosponsored Am Soc Prev Oncol. 2007;16(12):2773-80.
25. Dossus L, Benusiglio PR. Lobular breast cancer: incidence and genetic and non-genetic risk factors. Breast Cancer Res BCR. 2015;17:37.
26. Ciriello G, Gatza ML, Beck AH, Wilkerson MD, Rhie SK, Pastore A, et al. Comprehensive Molecular Portraits of Invasive Lobular Breast Cancer. Cell. 2015;163(2):506-19.
27. Sokol ES, Basudan A, Lee AV, Stephens PJ, Frampton GM, Oesterreich S, et al. Abstract PD8-05: Genomic profiling of metastatic invasive lobular carcinoma reveals unique genomics and therapeutic opportunities. Cancer Res. 2018;78(4 Suppl):PD8-05-PD8-05.
28. Tamura K, Hashimoto J, Tanabe Y, Kodaira M, Yonemori K, Seto T, et al. Safety and tolerability of AZD5363 in Japanese patients with advanced solid tumors. Cancer Chemother Pharmacol. 2016;77(4):787-95.
29. Chen Y, Huang L, Dong Y, Tao C, Zhang R, Shao H, et al. Effect of AKT1 (p. E17K) Hotspot Mutation on Malignant Tumorigenesis and Prognosis. Front Cell Dev Biol. 2020;8:573599. doi: 10.3389/fcell.2020.573599.
30. Wu W, Chen Y, Huang L, Li W, Tao C, Shen H. Effects of AKT1 E17K mutation hotspots on the biological behavior of breast cancer cells. Int J Clin Exp Pathol. 2020;13(3):332-46.
31. Smyth LM, Tamura K, Oliveira M, Ciruelos EM, Mayer IA, Sablin M-P, et al. Capivasertib, an AKT Kinase Inhibitor, as Monotherapy or in Combination with Fulvestrant in Patients with AKT1E17K-Mutant, ER-Positive Metastatic Breast Cancer. Clin Cancer Res. 2020;26(15):3947-57.
32. Smyth LM, Zhou Q, Nguyen B, Yu C, Lepisto EM, Arnedos M, et al. Characteristics and Outcome of AKT1E17K-Mutant Breast Cancer Defined through AACR Project GENIE, a Clinicogenomic Registry. Cancer Discov. 2020;10(4):526-35. (Smyth 2020b)

Images in Clinical Medicine
Acta Medica Academica 2021;50(1):218-220
DOI: 10.5644/ama2006-124.337

A Giant, Complex Fibroepithelial Tumor of the Breast: Borderline Phyllodes Tumor Combined with Tubular Adenoma – a Rare Clinical Presentation of a Fibroepithelial Tumor of the Breast

Nermina Ibisevic[1], Jasmina Bajrovic[2], Ena Saranovic[1], Dijana Spiritovic[1], Faruk Skenderi[1], Semir Vranic[3, 4, a]

[1]Department of Pathology, University Clinical Center Sarajevo, Sarajevo, Bosnia and Herzegovina, [2]Department of Radiology, University Clinical Center Sarajevo, Sarajevo, Bosnia and Herzegovina, [3]College of Medicine, QU Health, Qatar University, Doha, Qatar, [4]Biomedical and Pharmaceutical Research Unit, QU Health, Qatar University, Doha, Qatar

Correspondence: *semir.vranic@gmail.com* or *svranic@qu.edu.qa*; Tel.: + 974 4403 7873; Fax.: + 974 4403 2250

Received: 5 February 2021; **Accepted:** 12 February 2021

Key Words: Breast ▪ Fibroepithelial Tumors ▪ Phyllodes Tumor ▪ Tubular Adenoma.

A 65-year-old woman with a negative family history of breast cancer presented with a palpable mass in the left breast's central portion. Mammography revealed an oval heteroechogenic, partly solid, partly cystic, sharply demarcated mass, measuring 100×90 mm in greatest diameter, classified as BI-RADS 4c, according to ACR BI-RADS Atlas Fifth Edition (Figure 1A-B). Breast MRI showed a lobulated mass with smooth margins appearing hypointense on T1WI and high signal intensity on T2WI (Figure 1C-D). A core needle biopsy revealed a cellular neoplasm, composed of small, closely packed tubules with spindle cell intervening stroma without prominent atypia and mitotic activity, classified as B3 category according to the UK National Coordinating Committee for Breast Screening Pathology (Figure 2A). The multidisciplinary tumor board discussed the case and recommended a wide surgical excision. With the patient's approval, a left mastectomy was recommended and performed. The axillary clearance was not performed. The 100×90 mm tumor was grossly well-circumscribed, grayish-white, and predominantly solid, with a smaller cystic component, without necrosis and hemorrhage (Figure 2B). Histopathologic examination revealed a well-circumscribed tumor with two distinct components (tubular adenoma and phyllodes tumor) with the transition to one another (Figure 2C). The larger portion of the tumor was composed of closely packed small round to oval tubules with little intervening spindle cell stroma consistent with tubular adenoma. The smaller component showed a biphasic fibroepithelial tumor with leaf-like projections with moderately cellular stroma (Figure 2D-E). The stromal cells exhibited mild to moderate atypia, and their mitotic activity was up to six mitoses/10 hpf (Figure 2F). Stromal overgrowth was absent, while the malignant heterologous elements were not observed despite the exhaustive tumor sampling (25 paraffin blocks). The final diagnosis was a complex fibroepithelial tumor composed of borderline phyllodes and tubular adenoma.

[a]ORCID: http://orcid.org/0000-0001-9743-7265

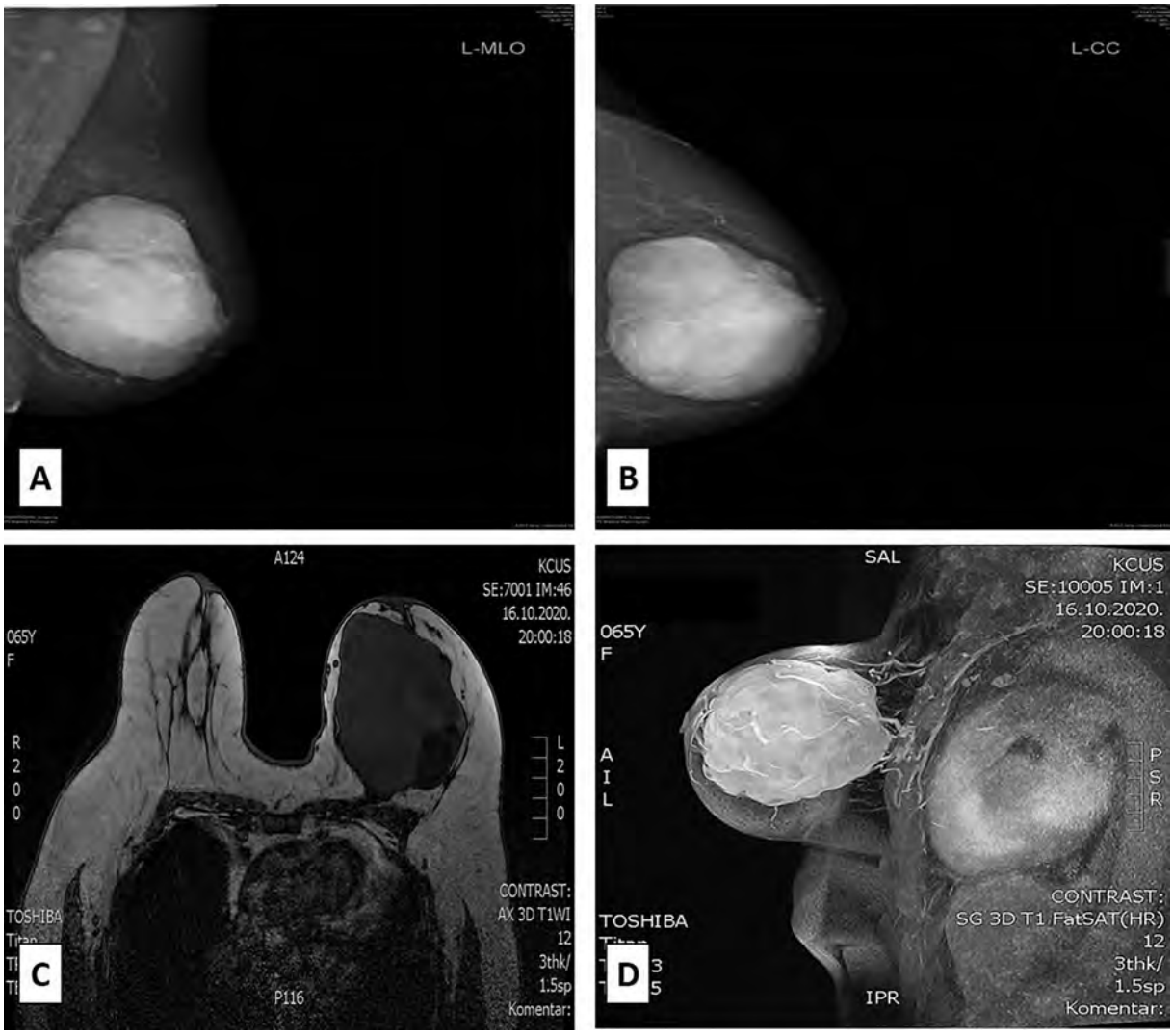

Figure 1A-D. Mammograms on the standard view (MLO and CC) revealed a round, dense mass partially surrounded by a clear halo, without any calcifications (A-B); Axial T1W1 MRI scans revealed a hypointense mass with some hyperintense foci of hemorrhage (C); Sagittal post-gadolinium subtraction image also showed intense enhancement (D).

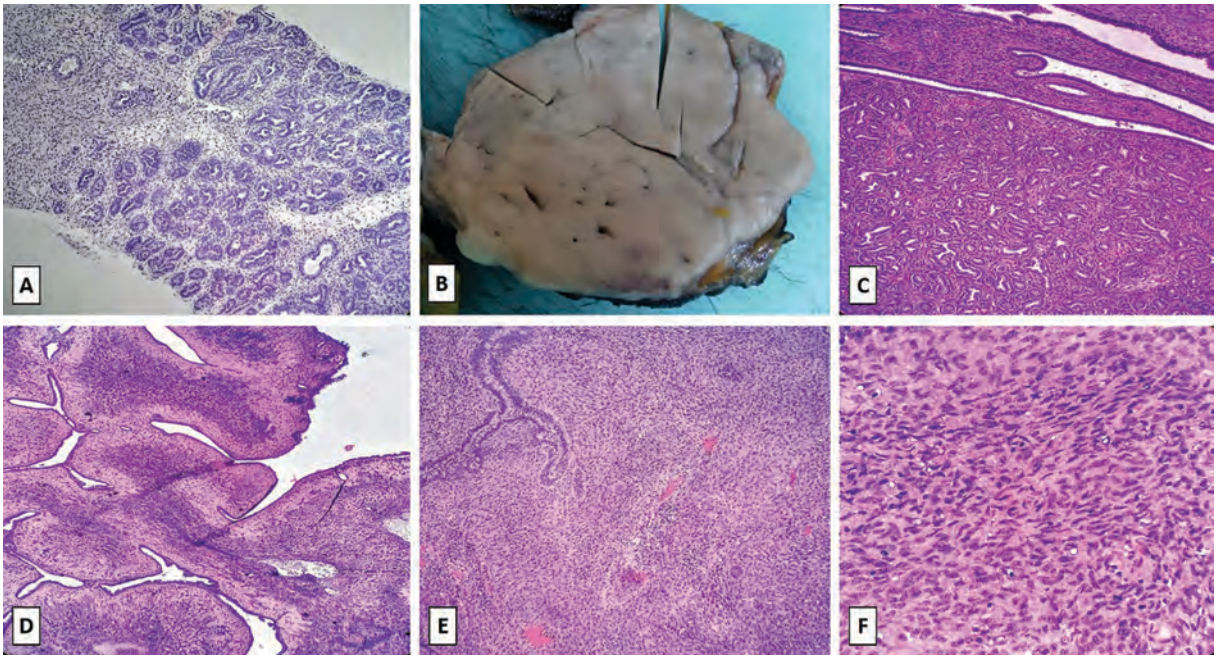

Figure 2A-F. A core biopsy specimen revealed predominantly tubular adenoma component with some spindle cell intervening stroma (Hematoxylin and Eosin, 10×) (A); A gross specimen revealed a large, (10×9 cm), well-demarcated solid mass without hemorrhage and necrosis (B); Microscopic examination revealed two distinct fibroepithelial tumors: tubular adenoma and phyllodes tumor with the abrupt transition one to another (Hematoxylin and Eosin, 10×) (C); Leaf-like projections, a hallmark of phyllodes tumor of the breast, were easily identified in the phyllodes part of the mass (Hematoxylin and Eosin, 10×) (D); The stromal component exhibited moderate cellularity without stromal overgrowth (Hematoxylin and Eosin, 10×) (E); The stromal cells showed moderate atypia with up to six mitotic figures/10 hpf (Hematoxylin and Eosin, 20×) (F).

Ethical Approval

The local institutional review board has the policy not to review the case studies. All the procedures reported in the current manuscript were performed according to the Declaration of Helsinki.

Conflict of Interest: The authors declare that they have no conflict of interest.

Historical Article

Narrative Review
Acta Medica Academica 2021;50(1):221-232
DOI: 10.5644/ama2006-124.338

Kornelija Rakić: A Woman Doctor for Women and Children in Serbia and Bosnia and Herzegovina

Husref Tahirović[1], Brigitte Fuchs[2]

[1]Department of Medical Sciences of the Academy of Sciences and Arts of Bosnia and Herzegovina, Sarajevo, Bosnia and Herzegovina [2]Department of Cultural and Social Anthropology at the University of Vienna, Vienna, Austria

Correspondence: *husref.tahirovic@untz.ba*; *brigitte.fuchs@univie.ac.at*; Tel.: + 387 61 720-740; Fax.: + 387 35 303 774

Received: 25 January 2021; **Accepted:** 30 March 2021

Abstract
This short biography focuses on the life and medical activities of Kornelija Rakić (1879–1952), a Serbian female pioneer of medicine from the then Hungarian province of Vojvodina, who acquired an MD from the University of Budapest in 1905. Rakić came from a humble background, and a Vojvodina Serbian women's organization enabled her to become a physician and pursue her social medicine mission. After a futile attempt to open a private practice as a "woman doctor for women" in Novi Sad in 1906, she successfully applied to the Austro-Hungarian provincial government in Sarajevo for the position of an official female physician in occupied Bosnia. Rakić began her career as an Austro-Hungarian (AH) official female physician in Bihać (1908–1912) and was transferred to Banja Luka in 1912 and to Mostar in 1917–1918. Kornelija Rakić stayed in Mostar after the monarchy collapsed in 1918 and continued to work as a public health officer in the service of the Kingdom of Serbs, Croats and Slovenes, founded in 1918. Subsequently, she served as the head of the "dispensary for mothers and children" at the Public Health Centre in Mostar, founded in 1929, where she practiced until her retirement in 1949. After World War II, Rakić served as Vice President of the Red Cross Society in Mostar. She received numerous awards and medals from the Austro-Hungarian Empire, the Kingdom of Yugoslavia and the Federal People's Republic of Yugoslavia. Kornelija Rakić died in Mostar in 1952 and was buried at the local Orthodox cemetery of Bjelušine. **Conclusion.** Kornelija Rakić (1879–1952) was the first Serbian female physician in Novi Sad, Vojvodina, and she was employed as an AH official female physician in Bihać (1908–1912), Banja Luka (1912–1917) and Mostar (1917–1918). After World War I, she participated in the establishment and expansion of public health institutions in Mostar and Herzegovina from 1918–1949 against the backdrop of the devastation of the two World Wars.

Key Words: (AH) Official Female Doctor ▪ Kornelija Rakić ▪ Novi Sad, Bihać, Banja Luka, Mostar ▪ Serbia ▪ Bosnia and Herzegovina.

Introduction

In 1911, a short biography of "Dr. Kornelija Rakić" appeared in the first volume of the Serbian women's magazine *Žena* (1). *Žena* was edited by Milica Tomić (1859–1944),[1] an established women's activist in Novi Sad who had been active in the Serbian women's movement in Vojvodina since the 1880s. The women's movement was closely linked to the Serbian national movement in the (at the time) Hungarian province (2, 3). Tomić herself was the author of the biography, and she explained in the first paragraph that Serbian women's health and wellbeing depended on the practice of female doctors, because many women were too "shy" to consult male doctors. This argumentation corre-

[1]Milica Tomić (1859-1944) was a writer and Serbian women's activist in Vojvodina. A daughter of the distinguished Serbian politician Svetozar Miletić, she was active for the Serbian women's organization "Dobrotvorna zadruga Srpkinja Novosatkinja" from the 1880s onwards. In 1911, she founded the women's magazine "Žena", issued 1911-1914 and 1918-1921 [cited 2021 Jan 9]. Available from: https://en.wikipedia.org/wiki/Svetozar_Mileti%C4%87; see also: Gordana Stojaković: Milica Tomić [cited 2021 Apr 12]. Available from: https://zenskimuzejns.org.rs/milica-tomic-2/.

sponds to an argument first used by Czech and Social Democrat women's activists in Austria in the 1890s. These activists used the argument to support a proposal to improve health care for women by introducing public health institutions that employed female doctors. They also argued for women's rights to academic education and particularly medical education. The second paragraph begins to provide information about Kornelija Rakić, who was among the first Serbian women in Vojvodina to acquire an MD at the University of Budapest.[2] As Tomić points out, Kornelija Rakić had worked as a "woman doctor for women" in Novi Sad before she was "invited" by the Austro-Hungarian (AH) authorities in Bosnia to work as the "first" female doctor in 1908 (1).

In fact, Kornelija Rakić was the seventh female doctor to be employed by the AH provincial government in Sarajevo. Women were admitted to medical studies starting in 1895 in Hungary and 1899 in Austria, and the governor of Bosnia, AH Finance Minister Benjamin de Kallay, created the office of "female health officer" for all districts of the "occupied territory" in 1890 primarily to serve the female Muslim population. The first AH official female doctor in Bosnia, Anna Bayerová, was a well-known Czech feminist who had studied medicine in Switzerland. Bayerová left Bosnia after one year; however, according to Nečas, she was able to shape the office into a social medicine institution "for women and children" during that year, with the governor's consent. Other AH official female doctors included Bohuslava Kecková in Mostar (1892–1911), Teodora Krajewska in Tuzla (1892–1899) and Sarajevo (1899–1918), Jadwiga Olszewska in Tuzla (1899–1918), Gisela Januszewska in Banja Luka (1899–1912) and Rosa Einhorn in Travnik (1902–1904). These doctors served predominantly as general practitioners for women and children, with a focus on Muslim women.

Kornelija Rakić filled the last vacant staff position for an AH official female doctor in Bihać in 1908. Transferred to Mostar in 1918, she stayed in the city for the rest of her life and practiced as a public health professional in the Kingdom of Serbs, Croats and Slovenes (1918–1929), the Kingdom of Yugoslavia (1929–1941), the pro-NS NDH-State (1941–1945) and the Federal People's Republic of Yugoslavia (1945-1963). Rakić's life and medical activities in Bosnia will be the subject of this review, which relies on new sources from Serbian, Hungarian, Yugoslav and Bosnian archives.

Kornelija Rakić's Short Biography

Though Kornelija Rakić is little known internationally, she is not among the forgotten women pioneers of medicine. Serbian historian Gordana Stojaković (2001) draws on Milica Tomić's portrait (3) in counting Kornelija Rakić as the first female doctor in Novi Sad, among the "famous women" of the city.

Rakić's career as an AH official female doctor in Bihać from 1908–1912, Banja Luka from 1912–1917 and Mostar in 1918 was documented by Czech historian Ctibor Nečas, author of a monograph on the AH institution of female public health officers in Bosnia (4). In the absence of preserved sources other than Rakić's personnel file, Nečas' account of her person and professional activities is poor compared to the administrative and personal records available for other official female doctors. An unpublished research paper by Barbara Martin contextualizes Rakić's activities as an AH official female doctor by referring to the better-documented careers of other AH female officers (Martin, 2017).[3] In 1918, Kornelija Rakić came to Mostar as an AH official doctor and continued her

[2]The first Serbian woman from Vojvodina (Hungary) who acquired an MD from the University of Zürich was Marija Prita, mariée Vučetić (1866-1954) in 1893; cf. Spasović Ivana B. Dr. Marija Vučetić-Prita, the first woman doctor in Southern Hungary, the second among in the Serbian people [in Serbian]. In: Godišnjak grada Beograda, book 61/62 (2014/2015 [print 2016]), p. 91-106; see also: https://sr.wikipedia.org/sr-el/%D0%9C%D0%B0%D1%80%D0%B8%D1%98%D0%B0_%D0%9F%D1%80%D0%B8%D1%82%D0%B0.

[3]We thank Barbara Martin for sharing her research with us; see also Barbara Martin: Zur Tätigkeit von Kornelika Rakić als Amtsärztin in Bosnien-Herzegowina (1908–1918) [cited 2021 Apr 12]. Available from: https://de.scribd.com/document/360574359/Zur-Tatigkeit-von-Kornelija-Raki%C4%87-als-Amtsarztin-in-Bosnien-Herzegowina.

social medicine mission in that city for more than 30 years. However, neither Serbian nor Bosnian-Herzegovinian medical historiography provides a detailed biography of her person (3, 5 -10).

Kornelija Rakić was born on August 19, 1879 in Ruma (11), a town in the region of Syrmia (Srem) in the (at the time) Hungarian province with a predominantly Serbian population. Her parents were Georgij (Đorđe) Rakić, an innkeeper at Ruma, and Ana Crnojević. In 1882, the family moved to Petrovaradin (12, 13), an historic Serbian city near Novi Sad; today, this city is part of Vojvodina's capital.

As a young woman from a modest background in Hungary's periphery, Rakić was given the opportunity to obtain higher academic education largely because of the Serbian national movement in Vojvodina. Since 1864, Novi Sad (or Újvidék in Magyar language) accommodated the "Matica Srpska", a Serbian language cultural-scientific institution founded in 1826 in Pest. In the 1860s, the city became the flourishing centre of the national and cultural "revival" of the Vojvodina Serbs. From the 1870s on, Serbian women's activists advocated for improvements in the social status of Serbian women and the introduction of higher education in Serbian language for girls. Their first success was the establishment of secondary schools for Serbian girls in Novi Sad and Pančevo in 1874, modelled on schools in the principality of Serbia (14, 15).

After completing elementary school, Kornelija Rakić attended the girls' higher school in Novi Sad. In school, she was introduced to the ideas of the "Charitable Cooperative of Serbian Women in Novi Sad" (Dobrotvorna zadruga Srpkinja Novosatkinja), which advocated for Serbian women's right to higher academic education (16). Against this background, Kornelija Rakić decided to pursue the medical profession. The only personal document left by Kornelija Rakić is a letter she sent as a student in Budapest in 1901 to her former headmaster, Arkadija Varađanin, which demonstrates that her medical aspirations were supported by the "women's club" even as a pupil (17). Rakić worked as an associate of the women's cooperative monthly magazine Ženski svet (17), and she later worked for the Serbian daily newspaper Zastava (18).

After completing Serbian girls' higher school, Kornelija Rakić had to overcome many obstacles to study medicine. Her school completion exam did not qualify her for university entrance. Women who applied to the Medical Faculty of the University of Budapest in November 1895 were required to submit a "Matura" (general qualification for university entrance) certificate from an Austrian or Hungarian gymnasium. Perhaps mediated by the "women's club", Kornelija Rakić was admitted to the Serbian-Orthodox boys' gymnasium in Novi Sad as a private pupil in 1895 (3, 5, 19). She was required to take an exam that included subject matter from the third to eighth grades of the gymnasium, and she passed her Matura exam in 1899 (20).

Funded by a scholarship from the "Charitable Cooperative of Serbian Women in Novi Sad" (Dobrotvorna zadruga Srpkinja Novosatkinja), Kornelija Rakić enrolled at the Medical Faculty of the University of Budapest in 1899 (Picture 1). Unlike at Swiss universities, the number of female students—particularly female students of medicine—remained low (21). Kornelija Rakić pursued her medical studies and was awarded her MD on 9 December 1905 (22) (Picture 2 and Picture 3) by Professor Emil Grósz[4] after less than six years of study, at the age of 26 years.

Kornelija Rakić completed her medical training by serving three months as a volunteer at the Department of Gynaecology at the university clinic in Budapest (23). Vilmos Tauffer,[5] the head of this clinic, had introduced modern obstetrics to Hungary. In early 1906, she returned to Novi Sad. In February 1906, an advertisement in Zastava announced that "Dr. Kornelija Rakić" had opened a

[4]Emil Grósz (1865–1941) was a Hungarian ophthalmologist of international reputation. He was professor of ophthalmology at the Faculty of Medicine of the University of Budapest and head of the ophthalmological university clinic from 1905–1936. [cited 2020 Dec 25]. Available from: *https://hu.wikipedia.org/wiki/Gr%C3%B3sz_Emil*.

[5]Vilmos Tauffer (1851–1934) was a Hungarian obstetrician, gynecologist, and university professor. He was a pioneer in the field in Hungary and reformed Hungarian midwife training. He was among the country's leading obstetricians [cited 2021 Feb 20]. Available from: https://www.biographien.ac.at/oebl/oebl_T/Tauffer_Vilmos_1851_1934.xml.

Picture 1. The Faculty of Medicine of the University of Budapest at the time when Kornelija Rakić started studying there. With permission of Archives of Semmelweis University, Budapest.

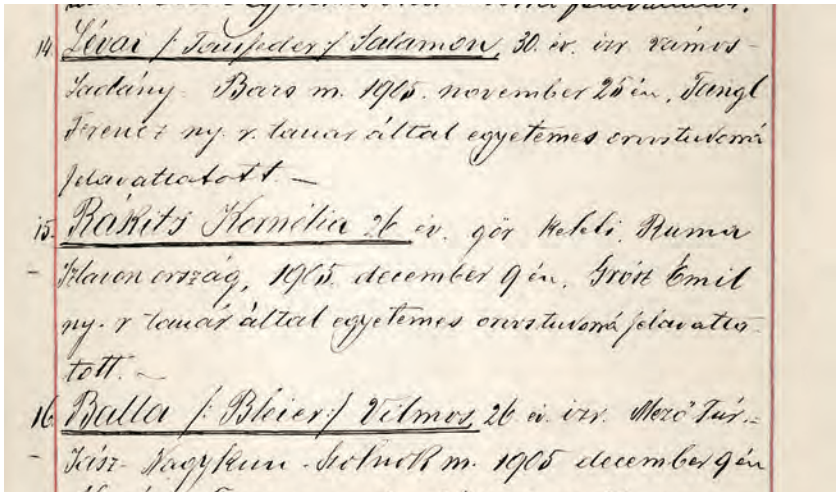

Picture 2. The page of the register of graduated students ("Golden Book") of the Medical Faculty in Budapest giving Kornelia Rakić's date of graduation. With permission of Archives of Semmelweis University, Budapest.

practice for women and children in the main street of the city (Pictures 4, 5) (3, 24). The initiative to establish herself as a local "woman doctor for women" was doubtlessly welcomed and supported by the "women's club"; however, it was premature. Data concerning Rakić's practice as a doctor in Novi Sad are not available;[6] however, it is likely that a sufficient number of female private patients failed to materialize. Forced to look elsewhere for an opportunity to practice her profession, Kornelija Rakić learned that the AH administration of Bosnia and Herzegovina (BH) had not yet staffed all positions for official female doctors in the country.

Later in 1906, Kornelija Rakić travelled to Sarajevo to introduce herself personally to the AH public health authorities. It was probably helpful to her cause that the Bihać district administration sent a letter to the provincial public health authorities in Sarajevo urging the appointment of an official female doctor for the district in October 1906. This letter was sent in reference to an intervention of the local mufti Hadži Jusuf ef. Jahić[7] and other Muslim notables in the matter and the high mortality of Muslim mothers and infants in the district (23, 25).

The evaluation process for Rakić's application as an "official female doctor with forensic medical function" (Amtsärztin mit gerichtsärz-

[6]Kornelija Rakić's "Form of personal and official data" (a form of the Ministry of Public Health of the Federal Republic of Yugoslavia that all physicians in Yugoslavia were required to complete after World War II) (24) does not contain information about her private practice in Novi Sad.

[7]Hafiz Yusuf-ef. Jahić (Zijauddin-ef), was born in Miljanovci Kalesija in 1853 and died in Tuzla, BH in 1928 (Bosnia and Herzegovina). He was the Mufti of Bihać for 26 years (1888-1914). He completed higher theological education as a cadet and state scholarship holder in Istanbul (Ottoman Empire). He was awarded the Golden Order of Merit of the Austro-Hungarian emperor Franz Joseph I. He advocated the introduction of modern education and health care for Muslim women (27).

Picture 3. Kornelija Rakić, about 1910.

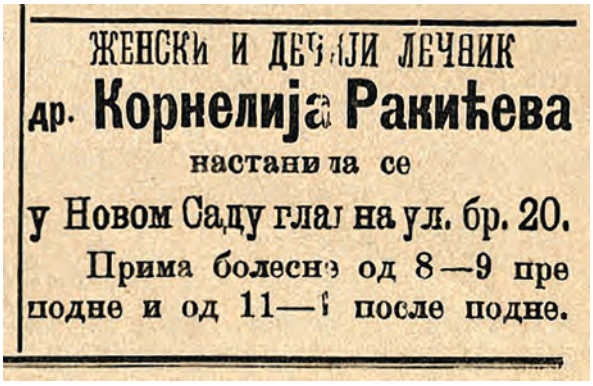

Picture 4. Advertisment for "Dr. Kornelija Rakić's" practice in Novi Sad, published in "Zastava", 1906 Feb 4; p. 4 (col. 4).

tlichen Funktionen) took more than a year, but the application was finally approved. In January 1908, the authorities decided to employ Kornelija Rakić as an official female doctor in Bihać (23). They explained their decision by pointing out that Kornelija Rakić was a native of the AHE who had acquired her MD at a domestic university and was familiar with the native "custom and language". She was also younger than any other official female doctor and "evidently of good health", which was considered a great advantage (28). Kornelija Rakić received her decree of appointment as an official female doctor in Bihać, Bosnia on 11 April 1908 (23, 26). She closed her practice "for women and children" in Novi Sad and left for Bosnia.

In Bosnia, she worked in Bihać (1908–1912), Banja Luka (1912–1918) and Mostar (1918–1949) (23, 26). She retired in 1949 at the age of 70 (29) and died on 11 July 1952 (30) in Mostar. Kornelija Rakić was buried at the Orthodox cemetery in "Bjelušine". The wooden cross with her name has since vanished and no tombstone was placed on the spot; therefore, her grave is not easily identifiable, except by a palm tree sprouting at the site (Picture 6). Kornelija Rakić received numerous AH commendations and awards as an AH official female doctor in BH. She was awarded the Order of St. Sava of the Third Degree twice: once by the Ministry of Health and once by the Ministry of Social Affairs of the Kingdom of Yugoslavia (31).

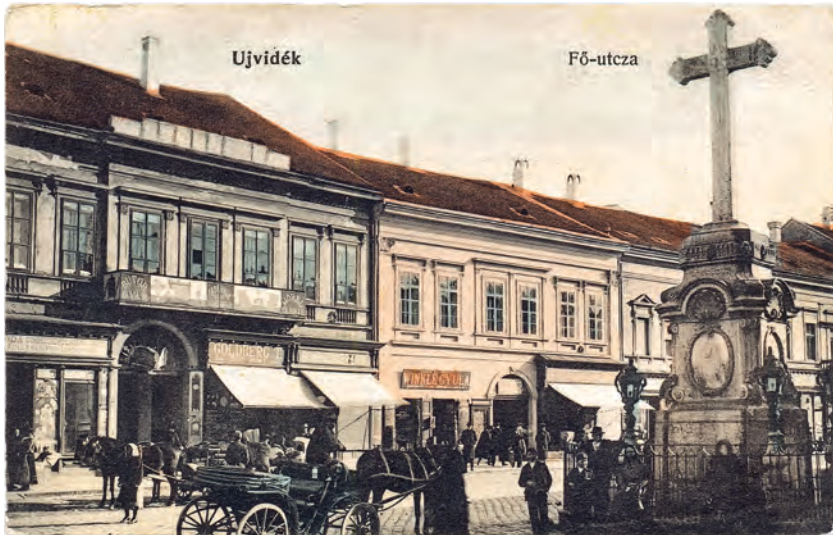

Picture 5. Novi Sad: The building (Light Pink) where Kornelija Rakic's private practice was located in 1906.

Picture 6. Kornelija Rakić's unmarked grave at the Bjelušine cemetery in Mostar, recognizable by the palm tree.

Picture 7. Bihać at the time when Kornelija Rakić started working there. Street scene with a view of the Roman Catholic Church [in German]. Signature: PCH 3.033 - C POR MAG. Available from: http://data.onb.ac.at/rec/baa13769435 and https://www.onb.ac.at/.

Kornelija Rakić's Professional Activities in Bosnia and Herzegovina

The previously employed AH female health officers were sworn into their offices at their residences. However, Kornelija Rakić took her oath of office in Sarajevo on 4 May 1908. Due to "budgetary reasons", she did not report for duty in Bihać until 1 August 1908; at that time, she was assigned to the provincial hospital in Sarajevo, where she had completed an internship (26). Rakić's position as an official female doctor of Bihać became permanent on 4 August 1909 (4, 23).

Bihać (Picture 7), located in northeast Bosnia, was the smallest and least populated district of Bosnia at the time, and most of the rural population was Serbian. The district capital counted 6,201 inhabitants in 1910, of whom 61.0% were Muslim, 27.5% were Roman Catholic and 8.5% were Serbian-Orthodox (32). The AH administration had established a community hospital with 31 beds, which was rebuilt and enlarged in 1887/1888 (33).

Presumably, Kornelija Rakić ran an outpatient ward for women and children in accordance with the instructions for AH female health officers in BH. However, there is no evidence of her practice for local women and children other than annual assessments

by her superiors. These assessments attest that Rakić was an excellent doctor who was popular with her patients and often visited by Muslim women, as well as an excellent obstetrician (23). Rakić was not able to spend much time with her outpatients, according to an assessment written by her recently appointed superior, district doctor Martin Bleicher, in 1911. Bleicher praised her participation in syphilis eradication in the subdistricts of Cazin and Krupa and remarked that she had not had many other opportunities to pursue professional work (23). Kornelija Rakić was intensively involved in the eradication of syphilis campaign in the aforementioned subdistricts from the time she took office in 1908. In 1909, she was also commissioned as a substitute to manage the community hospital in Bihać (23).

In 1905–1906, the focus of AH public health policies in BH shifted from popularizing public health utilization to campaigning for syphilis eradication. Control of the widespread endemic of syphilis was considered a priority as early as the 1880s; however, the AH public health authorities had considered it unwise to carry out an unpopular military-led syphilis eradication campaign in BH. After the turn of the century, the authorities concluded that the whole population of BH must be subject to thorough medical examinations (34, 35). All female doctors in the country, including private doctors Gisela Januszewska and Rosa Einhorn-Bloch, were ordered to examine the female Muslim population for symptoms of (endemic) syphilis. Evidently, the AH official female doctors considered syphilis eradication a great burden (36). Two petitions for equal pay in 1908 and 1912 were signed by all AH official female doctors. Among other things, these petitions argued that AH official female doctors could no longer treat private patients because they had to spend 100–200 days per year working on syphilis eradication (25). Due to these constraints, the doctors were also prevented from spending time on their outpatient practices. The burden of anti-syphilis campaigning contributed to the decision of private doctors Gisela Januszewsa (Banja Luka) and Rosa Einhorn-Bloch (Travnik) to leave the country.

By 1912, Kornelija Rakić was one of only three female doctors remaining in BH. She applied successfully for a transfer to Banja Luka (Picture 8)—then a city of about 25,000 inhabitants—after her superior had assessed her "behaviour towards colleagues in Bihać" as "uncooperative" (23).

In Banja Luka, Rakić took over from Gisela Januszewska in October 1912. Her superior in Banja Luka explicitly rejected his predecessor's criticism, attesting in 1913 that Kornelija Rakić had "won the affection of the entire population by her modest, amiable and philanthropic behaviours" (23). In addition to her work as a general practitioner for women and children, she was commissioned (like her predecessor) to provide hygiene lessons at a higher girls' school in Banja Luka (37, 25). AH sources indicate that Kornelija Rakić was also intensively involved in anti-syphilis campaigning (25) and she was commissioned repeatedly to work at the "district hospital" (Bezirksspital) of Kotor Varoš. The district hospital had about 30 beds and, like all established "district

Picture 8. Banja Luka at the time when Kornelija Rakić started working there. Published with kind permission of Museum of the Republika Srpska, Banja Luka, Bosnia and Herzegovina.

Picture 9. Mostar at the time when Kornelija Rakić started working there. With Permission from Mr. Zlatko Serdarević of Mostar.

hospitals", it was primarily dedicated to syphilis treatment (38). During the 1915 cholera epidemic in Bosnia, Kornelija Rakić was tasked with combating cholera in the districts of Banja Luka and Travnik. During World War I, she received AH awards for her commitment to combating syphilis and cholera (26).

In December 1917, Kornelija Rakić was informed that she would be transferred to Mostar in the summer of 1918. The position of official female doctor of Mostar had become vacant after the death of Bohuslava Kecková in 1911. Kecková's death likely delayed the syphilis eradication campaign in Herzegovina. On her way to Mostar in late June 1918, Rakić's health declined, and she spent several months on sick leave in Sarajevo. She finally arrived in Mostar (Picture 9) days before the monarchy collapsed in October 1918 and BH became a part of the newly established Kingdom of Serbs, Croats and Slovenes.

Kornelija Rakić decided to stay in Mostar and took her oath of allegiance to King Peter in February 1919 (Picture 10) and King Alexander in September 1921 (23). From 1918–1926, she continued her function as a public health officer of the "Mostar region"[8], and worked later, until her retirement in 1949, as the head of the "Dispensary for Mothers and Children" at the Public Health Centre in Mostar.

The new state faced problems including starvation, significant child mortality, prevalent war epidemics and spread of endemic diseases such as syphilis, malaria and trachoma in Herzegovina; therefore, the public health system relied on the development of socio-medical institutions. In Mostar, a "bacteriological ward" (Stalna bakteriološka stanica) opened in 1923 and served as a foundation for the "public health centre" founded in 1929 (39). The latter included gradually established "dispensaries" to serve patients suffering from malaria, skin and venereal diseases and tuberculosis, as well as a children's dispensary and "school policlinic" founded in 1926 and headed by the Bosnian paediatrician Berta Bergman.[9] In 1929, a "Dispensary for mothers and children" (Dispanzer za majke i djecu) was established (40) under the direction of Kornelija Rakić. She had attended the Institute for Health Care for Moth-

[8]After World War I, Mostar had become the administrative center of "Mostarka oblast" (Mostar region). As a result of the reorganization of the Yugoslavian state in 1929, Mostar region became part of the 1929-1939 existing province ("banate") Primorska banovina (Littoral Banovina), cf. Political Representation of BiH in the Kingdom of Serbs, Croats, and Slovenes / Kingdom of Yugoslavia (1918-1941) [in Bosnian]. [cited 2020 Feb 9] Available from: https://www.parlament.ba/Content/Read/180?title=Politi%C4%8DkopredstavljanjeBiHuKraljeviniSrba, HrvataiSlovenaca/KraljeviniJugoslaviji(1918.%E2%80%931941.

[9]Berta Bergman (1892–1945) was the first Bosnian woman who had qualified for university education and studied medicine in Vienna. When the Dispensary for Mothers and Children (Dispanzer za majke i djecu) was established in 1929, Kornelija Rakić was appointed as its chief. Berta Bergman became at that point the head of the newly established "School Polyclinic" (Školska poliklinika). Berta Bergman was arrested on January 14, 1945, and deported to the Jasenovac concentration camp, where she was murdered [cited 2021 Apr 8]. Available from: https://en.wikipedia.org/wiki/Berta_Bergman.

ers, Children, and Youth in Sarajevo and studied "social paediatrics and child health" with two other pioneers of Yugoslavian social medicine and hygiene, Maša Živanović[10] and Mara Kurtović.[11]

Rakić treated 907 pregnant women, 2,225 infants, and 10,429 children at the Mostar "Dispanzer za majke i djecu" in 1929; her patients were 63% Muslim, 20% Orthodox and 17% Catholic. As head and manager, Kornelija Rakić also organized and coordinated activities to educate the local women about public health and hygiene, and she was a lecturer as well (10). She also gave hygiene lessons at a higher school in Mostar (46). Kornelija Rakić's practice for women and children at the Mostar Public Health Centre was not interrupted when BH was annexed by the pro-NS NDH-state in 1941 (7). Rakić supported the local anti-fascist resistance against the pro-NS "Independent States of Croatia" (26) and the premises of the children's policlinic and the maternity and child welfare ward in Mostar provided refuge to wounded partisans, sick members of the resistance and displaced persons (10).

After World War II, the social and health situation in Herzegovina was precarious, and the public health care system in Mostar needed to be reorganized. Kornelija Rakić was employed by the public health department of the People's Committee for Herzegovina as head of a new children's and maternity dispensary (42, 43) comprised of three medical departments, a pharmacy and a kitchen that provided free meals to malnourished local children. However, she was the only doctor at the clinic, along with a dentist, two health care professionals and four auxiliary technical workers. According to Rakić's report, the maternity department was consulted by 514 pregnant women in March 1946, 136 of whom were gyne-

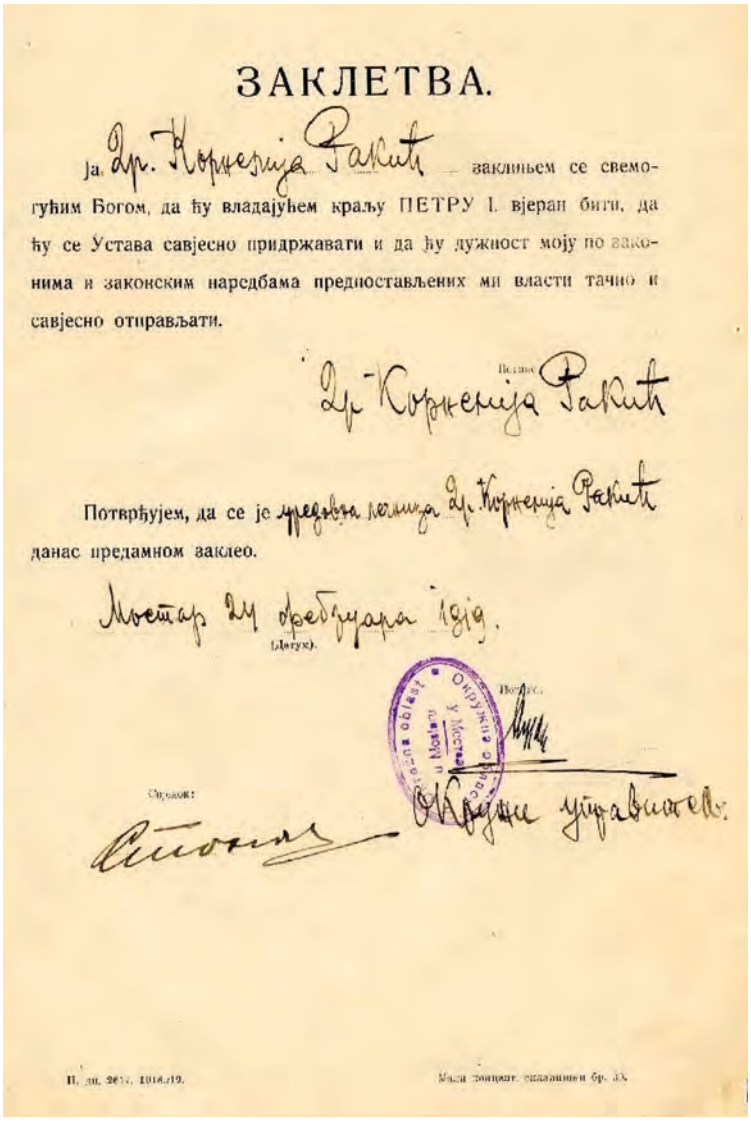
ЗАКЛЕТВА.

Ја, Др. Корнелија Ракић заклињем се свемогућим Богом, да ћу владајућем краљу ПЕТРУ I. вјеран бити, да ћу се Устава савјесно придржавати и да ћу дужност моју по законима и законским наредбама предостављених ми власти тачно и савјесно отправљати.

Потпис: Др. Корнелија Ракић

Потврђујем, да се је предњом лекница Др. Корнелија Ракић данас предамном заклео.

Мостар 24 фебруара 1919.

(Датум).

Печат: Окружна управа

Потпис:

Picture 10. Kornelija Rakić's Oath of allegiance to King Petar/Peter I. stating that she will abide by the constitution and exercise her duty according to the laws and regulations. Archives of Bosnia and Herzegovina.

[10]Maša Živanović (1898–1960) was a reputed pediatrician in Sarajevo in the interwar years. She was the head of the Children's Dispensary and the Institute for Health Care for Mothers, Children, and Youth in Skerlić's Street in Sarajevo. After World War II, she performed the same duty. Živanović was a well-known women's activist and president of the Women's Movement in Sarajevo (1924–1936).

[11]Mara Kurtović (1892– ?) was the first expert of school hygiene in Bosnia and Herzegovina. She was the head of the Children's Dispensary at the Institute for Health Care for Mothers, Children, and Youth in Skerlić's Street in Sarajevo.

cologically examined. A total of 494 children were examined in the department for mothers, infants, and young children, and 648 children were served in the "children's dispensary". The pharmacy issued prescribed medications, ointments, vitamin preparations (e.g., cod liver oil) and medical devices for children's treatment at home. The kitchen distributed 2,169 servings of cocoa and 2,333 servings of bread to 100 undernourished children, and each child had gained between 250–500 grams of body weight during the month (44).

After 1945, Kornelija Rakić served as vice president of the Red Cross Society in Mostar (30) and distributed relief supplies such as food and cod liver oil to local children and pregnant women. Despite her advanced age, she continued to practice as a doctor for women and children, and she never tired of drawing the authorities' attention to the social and medical welfare of the "new generations" (44). She was a pioneer of social medicine who dedicated her life to the welfare of women, mothers and children.

Concluding Remarks

Kornelija Rakić was the first female doctor in Novi Sad as a city that was located at Hungary's periphery but was a center of Serbian national culture and politics. Born as a Hungarian citizen in Ruma, Syrmia in 1879, Kornelija Rakić belonged to the first generation of female doctors in the AHE who were able to acquire their MDs at domestic universities. Following the completion of her medical studies in Budapest and a futile attempt to establish herself as a "woman doctor for women and children" in Novi Sad, she began her career as an AH official female doctor in occupied, then annexed, Bosnia in 1908. Kornelija Rakić was eventually transferred to Mostar, where she worked for over thirty years, first as an official doctor in the service of the AH (1918) and later as a district public health officer (1918–1926) in the service of the Kingdom of Serbs, Croats and Slovenes. A pioneer of social medicine, she became the head of the maternity and child welfare ward of the Mostar Public Health Centre, founded in 1929, where she practiced until her retirement in 1949. Kornelija Rakić died in Mostar in 1952, having dedicated her life to the welfare of women and children.

Authors' Contributions: Conception and design: HT and BF; Acquisition, analysis and interpretation of data: HT and BF; Drafting the article: HT and BF; Revising it critically for important intellectual content: HT and BF; Approved final version of the manuscript: HT and BF.

Conflict of Interest: The authors declare that they have no conflict of interest.

References

1. Tomić M. Dr. Kornelija Rakić [in Serbian]. Žena. 1911;1(1):2.
2. Kolarić A. Gender, nation, and education in the women's magazine Žena (The woman) (1911-1914). Espacio, Tiempo y Educación. 2017;4(1):1-23. doi: http://dx.doi.org/10.14516/ete.142
3. Stojaković G. Dr. Kornelija Rakić. In: Stojaković G, editor. Famous women of Novi Sad [in Serbian]. Novi Sad: Futura publikacije; 2001. p. 176-177.
4. Nečas C. Among Muslim Women. The activities of the female health officers in Bosnia and Herzegovina, 1892-1918 [in Czech]. Brno: Masaryk University; 1992.
5. Jeremić R. Contributions to the biographical dictionary of the Serbian physician of Vojvodina 1756-1940 [in Serbian]. Novi Sad; 1952. p. 119.
6. Berić BM, Sloboda L, Subotić J. The first women physicians in Vojvodina (1893-1919) [in Serbian]. Med Pregl. 1988;41(1-2):79-82.
7. Mulić S. Health conditions in Herzegovina during the Second World War with special attention to the area of Konjic [in Bosnian]. In: Kamberović H, editor. Bosna i Hercegovina 1941: Novi pogledi. Sarajevo: Institut za istoriju; 2015. p. 115-142.
8. Tolj Z. Half a century at the scene of the fight for national health [in Croatian-Serbian]. In: Tolj Z, editor. 50th anniversary of the Regional Institute for Health Care Mostar [in Croatian-Serbian]. Mostar: Regionalni zavod za zdravstvenu zaštitu Mostar; 1980. p. 11-54.
9. Šimić Lj. Memories. [in Croatian-Serbian]. In: Tolj Z, editor. 50th anniversary of the Regional Institute for Health Care Mostar [in Croatian-Serbian]. Mostar: Regionalni zavod za zdravstvenu zaštitu Mostar; 1980. p. 358-364.
10. Žurovec M. The development of the health care of mother and child. [in Croatian-Serbian]. In: Tolj Z, editor. 50th anniversary of the Regional Institute for Health Care Mostar [in Croatian-Serbian]. Mostar: Regionalni zavod za zdravstvenu zaštitu Mostar; 1980. p. 221-228.

11. Kornelija Rakić's certificate of birth from Ruma [in Serbian]. Registry office of the city of Ruma, Serbia. No. 200-00-2020; December 25, 2020.
12. Historical Archive "Srem" Sremska Mitrovica. Testimony of persons from the 'first composition' who lost their right to vote, based on the Electoral Order Act 1881 and the Order of the High Royal Government of the Department of the Interior of 1882 [in Serbian]. Fund - Ruma Market Magistrate, box 6.401-9.271.
13. Bošković Đ. Ruma in the period 1861 – 1914 [in Serbian]. Ruma: Zavičajni Muzej Ruma; 2016. p. 373; 392.
14. Stojaković G. "Women's World" (1886-1914). Serbian women's laboratory as an entrance into the public sphere. Journal of the North American Society of Serbian Studies. 2011;25(1):21-57.
15. Spasović I. Higher Schools for girls in Serbian language in the region of Banat Military Border in the period of Hungarian rule. Research in Pedagogy. 2013:3(2):61-70.
16. Women's World - Journal of Charitable Cooperative of Serbian Women in Novi Sad [in Serbian]. 1981;6(3):43.
17. Letter from Kornelija Rakić sent to Arkadije Varađanin in 1901 [in Serbian]. Matica Srpska Novi Sad; Manuscript Department. Inventory number: 15612.
18. Anonymous. Editors and Collaborators [in Serbian]. Daily newspaper Zastava in Novi Sad. 1926 Feb 23; p. 4 (col. 3).
19. Historical Archives of the City of Novi Sad, F 25 Gymnasium "Jovan Jovanović Zmaj", book 75; Register of students of I-VIII grades 1896/1897 and 1897/1898; book 76 - Register of students of I-VIII grades 1898/1899 and 1899/1900 [in Serbian].
20. Maturity exam, Kornelija Rakić, Historical Archives of the City of Novi Sad, Gymnasium "Jovan Jovanović Zmaj: The main protocol of exams maturity 1897-1905, No. 37 [in Serbian].
21. Müller I. The social composition of the female student body of the University of Budapest (1896-1914) / The social composition of female students at the Budapest University of Sciences (1896-1914) [in Hungarian]. Korall Társadalomtörténeti folyóirat. 2001;(3-4):203-20.
22. Note in the so-called "Gold book" of the graduated students at the Medical Faculty of Budapest. Budapest: Archives of Semmelweis University; 1905. p. 417.
23. Archives of Bosnia and Herzegovina. Service and qualification table of Dr. Kornelija Rakić [in German]. Collections of personal files of the Archives of Bosnia and Herzegovina. Box No. 436.
24. Advertisement: Female and pediatric physician Dr. Kornelija Rakić. Daily newspaper Zastava, Novi Sad; 1906 Feb 4; p. 4 (col. 4).
25. Martin B. About the work of Kornelija Rakić as a medical officer in Bosnia Herzegovina [in German] [cited 2002 Jul 9]. Available from: https://www.scribd.com/document/360574359/Zur-Tatigkeit-von-Kornelija-Raki%C4%87-als-Amtsarztin-in-Bosnien-Herzegowina.
26. Form of personal and official data of Dr. Kornelija Rakić [in Serbian]. Archives of Yugoslavia, fund 39, fasc. 5, dated March 6, 1922.
27. Mešić M. Bihać madrasa [in Bosnian]. Bihać: NIP "Unsko-sanske novine"; 1998. p. 80.
28. Provincial Government for Bosnia and Herzegovina Sarajevo doc. No. 149, 745 [in German]. Arhiv Bosne i Hercegovine: 1907, box No. 51, code 38-43.
29. Anonymous. Biographies [in Croatian-Serbian]. In: Tolj Z, editor. 50th anniversary of the Regional Institute for Health Care Mostar [in Croatian-Serbian]. Mostar: Regionalni zavod za zdravstvenu zaštitu Mostar; 1980. p. 383.
30. Kornelija Rakić certificate of death from Mostar [in Bosnian]. Registry office of the city of Mostar. No. 09-10-1264/2021; April 12, 2021.
31. The Order of St. Sava [in Serbian]. Glasnik lekarske komore za Bosnu, Hercegovinu, Dalmaciju i Crnu Goru. 1927;3(4):40.
32. Landesregierung für Bosnien und die Hercegovina, editor. Results of the Census from October 10, 1910 in Bosnia and Hercegovina [in German]. Sarajevo: Landesdruckerei; 1912. p. XXIII, Tafel 11; p. 226-227.
33. Landesregierung für Bosnien und die Hercegovina, editor. Public Health in Bosnia and Herzegovina 1878–1901 [in German]. Sarajevo: Landesdruckerei; 1903.
34. Syphilis eradication campaign in Bosnia and Herzegovina [in German]. Int Klin Rd. 1912;(33):519.
35. Syphilis eradication campaign in Bosnia and Herzegovina [in German]. Int Klin Rd. 1912;(34):535.
36. Krajewska z Kosmowskich T. Diary (prepared for print by Boguslawa Czajecka) [in Polish]. Cracow: Krajowa Agencja Wydawnicza; 1989. p. 136-7; 162-8.
37. Sixteenth annual report of the State Girls' High School in Banja Luka [in Bosnian]. Banjaluka: Tiskara Fon i Grgić (J. S. Wolf); 1914. p. 28.
38. Landesregierung für Bosnien und die Hercegovina (ed). Public Health in Bosnia and Herzegovina 1878–1901 [in German]. Sarajevo: Landesdruckerei; 1903. p. 324.
39. Komadina M. Construction and adaptation of the Institute [in Croatian-Serbian]. In: Tolj Z, editor. 50th anniversary of the Regional Institute for Health Care Mostar [in Croatian-Serbian]. Mostar: Regionalni zavod za zdravstvenu zaštitu Mostar; 1980. p. 287-292.
40. Babić L, Harambašić K, Ravlić S. Development of health organizations in Mostar and Herzegovina [in Croatian-Serbian]. In: Tolj Z, editor. 50th anniversary of the Regional Institute for Health Care Mostar [in Croatian-Serbian]. Mostar: Regionalni zavod za zdravstvenu zaštitu Mostar; 1980. p. 74-83.
41. Miletić KD. Great Gymnasium in Mostar [in Croatian]. Mostar: Crkva na kamenu; 2003.

42. List of staff of the Health department of the District people's committee for Herzegovina December 4, 1945. HONO Mostar 1945: Department of Health No. 1-6000 HNK Archives [in Croatian-Serbian].

43. Mulić J. The health care in Konjic from ancient time until today [in Bosnian]. Konjic: Opšta Bolnica Konjic; 2010. p. 204-205.

44. Monthly Activities Report of Maternity and child welfare dispensary Mostar for March 1946 sent to District people's committee for Herzegovina - Department of Public Health. HONO Mostar 1945: Department of Health No. 142-4884, HNK Archives [in Croatian-Serbian].

PEER REVIEWERS FOR ACTA MEDICA ACADEMICA IN 2020

The Editorial Board of Acta Medica Academica (Acta Med Acad) wishes to acknowledge and thank the reviewers who volunteered their time and expertise to read and evaluate the submissions for AMA. The following individuals provided such expert assistance to AMA in 2020:

Emmanuel Addo-Yobo, GH
Mohammed Saeed Aldossary, SA
Shahzad Ali, PK
Mehmed Taha Alpaydin, TR
Luca Ansaloni, IT
Morten Arendt Rasmussen, DK
Kenan I. Arnautović, US
Mónica Asencio Duran, ES
Irene Asouhidou, GR
Goran Augustin, HR
Phillip Bonney, US
Frederick Boop, US
Robert Boyle, GB
Michael Buchfelder, DE
Ivan Buljan, HR
Franciszek Burdan, PL
Joshua Burks, US
Carlos Carona, PT
Santiago Cepeda, ES
Letícia Chaves de Souza, US
Iwona Ciechomska, PL
Marco Confalonieri, IT
Giulia Corrao, IT
Federico Cucchiara. IT
Mojca Čižek Sajko, SI
Ivan Damjanov, US
Andrea Di Cristofori, IT
Alberto Di Somma, ES
Joyce El-Haddad, AU
Stefan Florian, RO
Márk Fráter, HU
Brigitte Fuchs, AT
Mirella Gaboli, ES
Zoran Gatalica, US
Maciej Gawęcki, PL
Tatjana Gazibara, RS
Esra Genç, TR
Jason Girkin, AU
Anna Golebiewska, LU
François Graham, CA
Richard W. Gryglewski, PL
Andrzej Grzybowski, PL
Linda Heijmen, NL
Diego Hernández, AR
Angelika Homberg, DE
Omer Ć. Ibrahimagić, BA
Manoj K. Jain, US
Jelena Jovanović Simić, RS
Husnija Kamberović, BA
Milena Karapetrović, BA
Miki Katzir, US
Aslam Khan, SA
Deepak Khatri, US
Elie S. Khoury, LB
Blaženka Kljaić Bukvić, HR
Damjana Ključevšek, SI
Fountas N. Konstantinos, GR
Peter Korošec, SI
Kristina Kralik, HR
Božo Krušlin, HR
Mladen M. Kuftinec, US
Konstantinos Laios, GR
Janice A. Layhadi, GB
James Le Duc, US
Jenni Lehtimäki, FI
Andrica Lekić, HR
Lidija Lincender-Cvijetić, BA
Gianluca Lucchese, GB
Marko Lucijanić, HR
Fergus Macbeth, GB
Melinda Madléna, HU
Gorica Marić, RS
Dubravka Matanić, HR
Davide Mattavelli, IT
Michael W. McDermott, US
Aleksandar Milojević, RS
Jasenka Mršić-Pelčić, HR
Lohendy Muñoz-Vargas, CR
B. V. Murlimanju, IN
Ilia Nadareishvili, GE
John Nicholson, GB
Katarzyna Niespodziana, AT
Ogugua Okonkwo, NG
Kadir Oktay, TR
Emine Öksüz, TR
Maja Popović, IT
Venkatesh Rangarajan, IN
Lukas Rasulić RS
Fabio Roberti, US
Juan José Rodríguez Arias, ES
Jonathan Roth, IL
Godard de Ruiter, NL
Damir Sapunar, HR
Hülya Saray Kılıç, TR
Dimitrios Schizas, GR
Bianca Maria Scicchitano, IT
Ervin Sejdić, US
Patrick W. Serruys, GB
Mohamed H. Shamji, GB
Vikas Singh, IN
Janusz Skrzat, PL
Ihsan Solaroğlu, TR
Jehuda Soleman, IL
Zdenko Sonicki, HR
Robert J. Spinner, US
Bruno Splavski, HR
Guillermo Rafael Suárez Cuartin, ES
Sergiu Susman, RO
Aida Šemić-Jusufagić, GB
Husref Tahirović, BA
Kuniaki Takahashi, NL
Silvio Luigi Taschieri, IT
Tiziano Testori, IT
Kazuo Toda, JP
Jacek Tomczyk, PL
Mirosław Topol, PL
Gianluca Trevisi, IT
Justin Ruey Tse, US
Pim van der Meer, NL
Semir Vranić, QA
Petar Vuleković, RS
Grant Waterer, AU
Mehmet Yıldız, TR
Renata Zelić, SE
Valerijan Žujo, BA

ISSN 1840-1848